

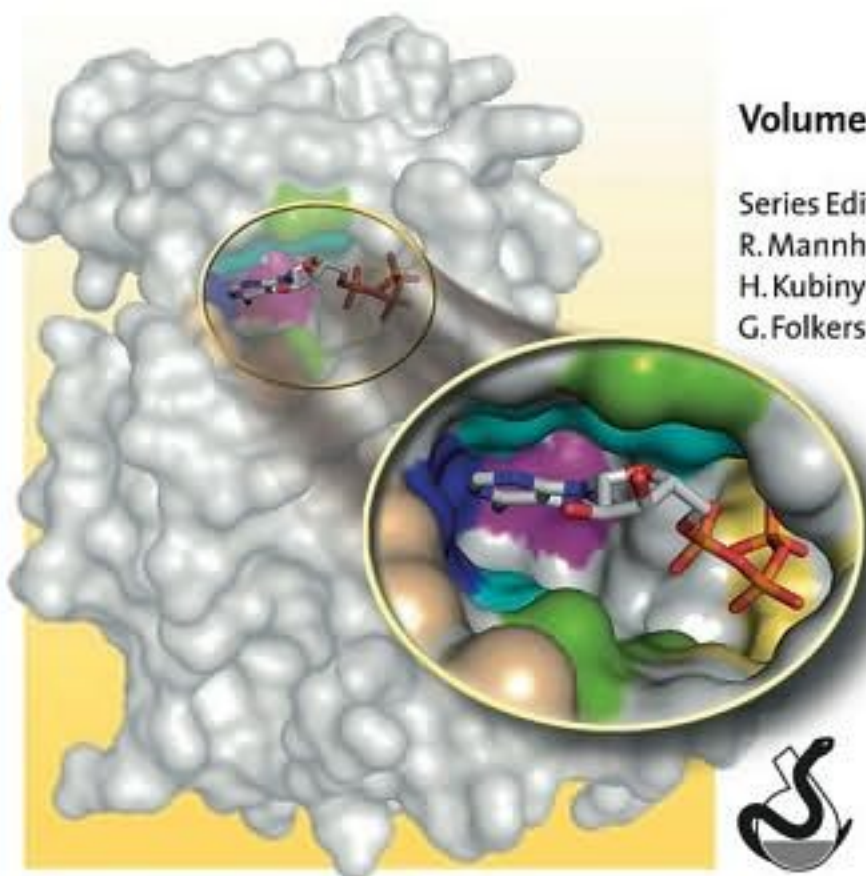
Edited by Bert Klebl, Gerhard Müller,
and Michael Hamacher

 WILEY-VCH

Protein Kinases as Drug Targets

Volume 49

Series Editors:
R. Mannhold,
H. Kubinyi,
G. Folkers



Edited by
Bert Klebl, Gerhard Müller,
and Michael Hamacher

Protein Kinases as Drug Targets

Methods and Principles in Medicinal Chemistry

Edited by R. Mannhold, H. Kubinyi, G. Folkers

Editorial Board

H. Buschmann, H. Timmerman, H. van de Waterbeemd, T. Wieland

Previous Volumes of this Series:

Sotriffer, Christopher (Ed.)

Virtual Screening

Principles, Challenges, and Practical Guidelines

2011

ISBN: 978-3-527-32636-5

Vol. 48

Faller, Bernhard / Urban, Laszlo (Eds.)

Hit and Lead Profiling

Identification and Optimization of Drug-like Molecules

2009

ISBN: 978-3-527-32331-9

Vol. 43

Rautio, Jarkko (Ed.)

Prodrugs and Targeted Delivery

Towards Better ADME Properties

2011

ISBN: 978-3-527-32603-7

Vol. 47

Sippl, Wolfgang / Jung, Manfred (Eds.)

Epigenetic Targets in Drug Discovery

2009

ISBN: 978-3-527-32355-5

Vol. 42

Smit, Martine J. / Lira, Sergio A. / Leurs, Rob (Eds.)

Chemokine Receptors as Drug Targets

2011

ISBN: 978-3-527-32118-6

Vol. 46

Todeschini, Roberto / Consonni, Viviana

Molecular Descriptors for Chemoinformatics

Volume I: Alphabetical Listing / Volume II: Appendices, References

2009

ISBN: 978-3-527-31852-0

Vol. 41

Ghosh, Arun K. (Ed.)

Aspartic Acid Proteases as Therapeutic Targets

2010

ISBN: 978-3-527-31811-7

Vol. 45

van de Waterbeemd, Han / Testa, Bernard (Eds.)

Drug Bioavailability

Estimation of Solubility, Permeability, Absorption and Bioavailability

Second, Completely Revised Edition

2008

ISBN: 978-3-527-32051-6

Vol. 40

Ecker, Gerhard F. / Chiba, Peter (Eds.)

Transporters as Drug Carriers

Structure, Function, Substrates

2009

ISBN: 978-3-527-31661-8

Vol. 44

Ottow, Eckhard / Weinmann, Hilmar (Eds.)

Nuclear Receptors as Drug Targets

2008

ISBN: 978-3-527-31872-8

Vol. 39

Edited by

Bert Klebl, Gerhard Müller, and Michael Hamacher

Protein Kinases as Drug Targets



WILEY-VCH Verlag GmbH & Co. KGaA

Series Editors

Prof. Dr. Raimund Mannhold

Molecular Drug Research Group
Heinrich-Heine-Universität
Universitätsstrasse 1
40225 Düsseldorf
Germany
mannhold@uni-duesseldorf.de

Prof. Dr. Hugo Kubinyi

Donnersbergstrasse 9
67256 Weisenheim am Sand
Germany
kubinyi@t-online.de

Prof. Dr. Gerd Folkers

Collegium Helveticum
STW/ETH Zurich
8092 Zurich
Switzerland
folkers@collegium.ethz.ch

Volume Editors

Dr. Bert Klebl

Lead Discovery Center GmbH
Emil-Figge-Straße 76 a
44227 Dortmund
Germany

Dr. Gerhard Müller

Proteros Fragments GmbH
Am Klopferspitz 19
82152 Planegg
Germany

Dr. Michael Hamacher

Lead Discovery Center GmbH
Emil-Figge-Str. 76 a
44227 Dortmund
Germany

Cover Description

ATP binding site of the Cyclin-dependent protein kinase 7 (CDK7), a member of the CDK family involved in the regulation of the cell cycle and transcription. The kinase active site is divided in sub-sites according to its interactions, varying between individual enzymes and allowing the individual design of selective inhibitors. (Photo courtesy C. McInnes)

All books published by **Wiley-VCH** are carefully produced. Nevertheless, authors, editors, and publisher do not warrant the information contained in these books, including this book, to be free of errors. Readers are advised to keep in mind that statements, data, illustrations, procedural details or other items may inadvertently be inaccurate.

Library of Congress Card No.: applied for

British Library Cataloguing-in-Publication Data

A catalogue record for this book is available from the British Library.

Bibliographic information published by the Deutsche Nationalbibliothek

The Deutsche Nationalbibliothek lists this publication in the Deutsche Nationalbibliografie; detailed bibliographic data are available on the Internet at <http://dnb.d-nb.de>.

© 2011 Wiley-VCH Verlag & Co. KGaA,
Boschstr. 12, 69469 Weinheim, Germany

All rights reserved (including those of translation into other languages). No part of this book may be reproduced in any form – by photoprinting, microfilm, or any other means – nor transmitted or translated into a machine language without written permission from the publishers. Registered names, trademarks, etc. used in this book, even when not specifically marked as such, are not to be considered unprotected by law.

Typesetting Thomson Digital, Noida, India

Printing and Binding betz-druck GmbH, Darmstadt

Cover Design Grafik-Design Schulz, Fußgönheim

Printed in the Federal Republic of Germany
Printed on acid-free paper

ISBN: 978-3-527-31790-5

Contents

List of Contributors *XI*

Preface *XV*

A Personal Foreword *XVII*

Part One Hit Finding and Profiling for Protein Kinases: Assay Development and Screening, Libraries 1

1	<i>In Vitro</i> Characterization of Small-Molecule Kinase Inhibitors	3
	<i>Doris Hafenbradl, Matthias Baumann, and Lars Neumann</i>	
1.1	Introduction	3
1.2	Optimization of a Biochemical Kinase Assay	4
1.2.1	Step 1: Identification of a Substrate and Controlling of the Linearity between Signal and Kinase Concentration	4
1.2.2	Step 2: Assay Wall and Optimization of the Reaction Buffer	6
1.2.3	Step 3: The Michaelis–Menten Constant K_m and the ATP Concentration	10
1.2.4	Step 4: Signal Linearity throughout the Reaction Time and Dependence on the Kinase Concentration	12
1.2.5	Step 5: Assay Validation by Measurement of the IC_{50} of Reference Inhibitors	15
1.3	Measuring the Binding Affinity and Residence Time of Unusual Kinase Inhibitors	15
1.3.1	Washout Experiments	18
1.3.2	Surface Plasmon Resonance	19
1.3.3	Classical Methods with Fluorescent Probes	21
1.3.4	Preincubation of Target and Inhibitor	22
1.3.5	Reporter Displacement Assay	22
1.3.6	Implications for Drug Discovery	25
1.4	Addressing ADME Issues of Protein Kinase Inhibitors in Early Drug Discovery	26

1.4.1	Introduction	26
1.4.2	Experimental Approaches to Drug Absorption	30
1.4.2.1	Measuring Solubility	30
1.4.2.2	Measuring Lipophilicity and Ionization	30
1.4.2.3	Measuring Permeability	31
1.4.2.4	Transporter Assays Addressing P-gp Interaction	33
1.4.3	Experimental Approaches to Drug Metabolism	34
1.4.3.1	Background and Concepts	34
1.4.3.2	Measuring Metabolic Stability	37
1.4.3.3	Measuring CYP450 Inhibition	39
	References	39
2	Screening for Kinase Inhibitors: From Biochemical to Cellular Assays	45
	<i>Jan Eickhoff and Axel Choidas</i>	
2.1	Introduction	45
2.1.1	Kinase Inhibitors for Dissection of Signaling Pathways	46
2.1.2	Cellular Kinase Assays for Drug Discovery Applications	46
2.2	Factors that Influence Cellular Efficacy of Kinase Inhibitors	47
2.2.1	Competition from ATP	47
2.2.2	Substrate Phosphorylation Levels	51
2.2.3	Ultrasensitivity of Kinase Signaling Cascades	51
2.2.4	Cell Permeability	52
2.2.5	Cellular Kinase Concentrations	53
2.2.6	Effects of Inhibitors Not Related to Substrate Phosphorylation	54
2.3	Assays for Measurement of Cellular Kinase Activity	55
2.3.1	Antibody-Based Detection	56
2.3.2	High-Content Screening	59
2.3.3	Use of Genetically Engineered Cell Lines	60
2.3.4	Genetically Encoded Biosensors	61
2.3.5	Label-Free Technologies	62
2.3.6	Analysis of Kinase Family Selectivity	62
2.3.7	SILAC	62
2.3.8	Affinity Chromatography with Immobilized Kinase Inhibitors	63
2.4	Outlook	63
	References	64
3	Dissecting Phosphorylation Networks: The Use of Analogue-Sensitive Kinases and More Specific Kinase Inhibitors as Tools	69
	<i>Matthias Rabiller, Jeffrey R. Simard and Daniel Rauh</i>	
3.1	Introduction	69
3.2	Chemical Genetics	71
3.2.1	Engineering ASKA Ligand–Kinase Pairs	71
3.3	The Application of ASKA Technology in Molecular Biology	76
3.3.1	Identification of Kinase Substrates	76

3.3.2	Studies on Kinase Inhibition	76
3.3.3	Alternative Approaches to Specifically Targeting Kinases of Interest	78
3.4	Conclusions and Outlook	80
	References	81

Part Two Medicinal Chemistry 85

4	Rational Drug Design of Kinase Inhibitors for Signal Transduction Therapy	87
	<i>György Kéri, László Órfi, and Gábor Németh</i>	
4.1	The Concept of Rational Drug Design	88
4.2	3D Structure-Based Drug Design	89
4.3	Ligand-Based Drug Design	92
4.3.1	Active Analogue Approach	92
4.3.2	3D Quantitative Structure–Activity Relationships	92
4.4	Target Selection and Validation	93
4.5	Personalized Therapy with Kinase Inhibitors	96
4.5.1	Target Fishing: Kinase Inhibitor-Based Affinity Chromatography	97
4.6	The NCL™ Technology and Extended Pharmacophore Modeling (Prediction-Oriented QSAR)	99
4.7	Non-ATP Binding Site-Directed or Allosteric Kinase Inhibitors	101
4.8	The Master Keys for Multiple Target Kinase Inhibitors	102
4.8.1	Application of <i>KinaTor</i> ™ for the Second-Generation Kinase Inhibitors	105
4.9	Conclusions	107
	References	109
5	Kinase Inhibitors in Signal Transduction Therapy	115
	<i>György Kéri, László Órfi, and Gábor Németh</i>	
5.1	VEGFR (Vascular Endothelial Growth Factor Receptor)	115
5.2	Flt3 (FMS-Like Tyrosine Kinase 3)	116
5.3	Bcr-Abl (Breakpoint Cluster Region–Abelson Murine Leukemia Viral Oncogene Homologue)	118
5.4	EGFR (Epidermal Growth Factor Receptor)	118
5.5	IGFR (Insulin-Like Growth Factor Receptor)	120
5.6	FGFR (Fibroblast Growth Factor Receptor)	120
5.7	PDGFR (Platelet-Derived Growth Factor Receptor)	121
5.8	c-Kit	121
5.9	Met (Mesenchymal-Epithelial Transition Factor)	122
5.10	Src	123
5.11	p38 MAPKs (Mitogen-Activated Protein Kinases)	123
5.12	ERK1/2	124
5.13	JNK (c-Jun N-Terminal Kinase, MAPK8)	126
5.14	PKC (Protein Kinase C)	126
5.15	CDKs (Cyclin-Dependent Kinases)	127

5.16	Auroras	127
5.17	Akt/PKB (Protein Kinase B)	129
5.18	Phosphoinositide 3-Kinases	129
5.19	Syk (Spleen Tyrosine Kinase)	130
5.20	JAK (Janus Kinase)	130
5.21	Kinase Inhibitors in Inflammation and Infectious Diseases	131
5.21.1	Inflammation	131
5.21.2	Infection	132
	References	134
6	Design Principles of Deep Pocket-Targeting Protein Kinase Inhibitors	145
	<i>Alexander C. Backes, Gerhard Müller, and Peter C. Sennhenn</i>	
6.1	Introduction	145
6.2	Classification of Protein Kinase Inhibitors	147
6.3	Type II Inhibitors	150
6.4	Common Features of Type II Inhibitors	154
6.5	Design Strategies for Type II Inhibitors	155
6.5.1	F2B Approach	160
6.5.2	B2F Approach	166
6.5.3	B2B Approach	169
6.5.4	Hybrid (F2B + B2F) Approach	173
6.6	Comparative Analysis of the Different Design Strategies	180
6.7	Conclusions and Outlook	187
	References	190
7	From Discovery to Clinic: Aurora Kinase Inhibitors as Novel Treatments for Cancer	195
	<i>Nicola Heron</i>	
7.1	Introduction	195
7.2	Biological Roles of the Aurora Kinases	195
7.3	Aurora Kinases and Cancer	196
7.4	<i>In Vitro</i> Phenotype of Aurora Kinase Inhibitors	197
7.5	Aurora Kinase Inhibitors	203
7.5.1	The Discovery of AZD1152	203
7.5.1.1	Anilinoquinazolines: ZM447439	203
7.5.1.2	Next-Generation Quinazolines: Heterocyclic Analogues	204
7.5.1.3	Amino-Thiazolo and Pyrazolo Acetanilide Quinazolines	208
7.5.2	MK-0457 (VX-680)	214
7.5.3	PHA-739358	215
7.5.4	MLN8054	219
7.5.5	AT9283	220
7.6	X-Ray Crystal Structures of Aurora Kinases	221
7.7	Summary	221
	References	222

Part Three Application of Kinase Inhibitors to Therapeutic Indication Areas 229

- 8 Discovery and Design of Protein Kinase Inhibitors:
Targeting the Cell cycle in Oncology 231**
Mokdad Mezna, George Kontopidis, and Campbell McInnes
 - 8.1 Protein Kinase Inhibitors in Anticancer Drug Development 231
 - 8.2 Structure-Guided Design of Small-Molecule Inhibitors of the Cyclin-Dependent Kinases 233
 - 8.3 Catalytic Site Inhibitors 234
 - 8.4 ATP Site Specificity 236
 - 8.5 Alternate Strategies for Inhibiting CDKs 239
 - 8.6 Cyclin Groove Inhibitors (CGI) 240
 - 8.7 Inhibition of CDK–Cyclin Association 242
 - 8.8 Recent Developments in the Discovery and the Development of Aurora Kinase Inhibitors 242
 - 8.9 Development of Aurora Kinase Inhibitors through Screening and Structure-Guided Design 244
 - 8.10 Aurora Kinase Inhibitors in Clinical Trials 248
 - 8.11 Progress in the Identification of Potent and Selective Polo-Like Kinase Inhibitors 250
 - 8.12 Development of Small-Molecule Inhibitors of PLK1 Kinase Activity 252
 - 8.13 Discovery of Benzthiazole PLK1 Inhibitors 254
 - 8.14 Recent Structural Studies of the Plk1 Kinase Domain 255
 - 8.15 Additional Small-Molecule PLK1 Inhibitors Reported 256
 - 8.16 The Polo-Box Domain 257
 - 8.17 Future Developments 259
- 9 Medicinal Chemistry Approaches for the Inhibition of the p38 MAPK Pathway 271**
Stefan Laufer L, Simona Margutti, Dowinik Hauser
 - 9.1 Introduction 271
 - 9.2 p38 MAP Kinase Basics 271
 - 9.3 p38 Activity and Inhibition 275
 - 9.4 First-Generation Inhibitors 278
 - 9.5 Pyridinyl-Imidazole Inhibitor: SB203580 278
 - 9.6 N-Substituted Imidazole Inhibitors 282
 - 9.7 N,N'-Diarylurea-Based Inhibitors: BIRB796 286
 - 9.8 Structurally Diverse Clinical Candidates 288
 - 9.9 Medicinal Chemistry Approach on VX-745-Like Compounds 297
 - 9.10 Conclusion and Perspective for the Future 301

References 302

10	Cellular Protein Kinases as Antiviral Targets	305
	<i>Luis M. Schang</i>	
10.1	Introduction	305
10.2	Antiviral Activities of the Pharmacological Cyclin-Dependent Kinase Inhibitors	310
10.2.1	Relevant Properties of CDKs and PCIs	310
10.2.2	Antiviral Activities of PCIs	327
10.2.2.1	Antiviral Activities of PCIs against Herpesviruses	327
10.2.2.2	Antiviral Activities of PCIs against HIV	332
10.2.2.3	Antiviral Activities of PCIs against Other Viruses	335
10.2.3	PCIs Can be Used in Combination Therapies	336
10.2.4	PCIs Inhibit Viral Pathogenesis	337
10.3	Antiviral Activities of Inhibitors of Other Cellular Protein Kinases	338
10.4	Conclusion	339
	References	341
11	Prospects for TB Therapeutics Targeting <i>Mycobacterium tuberculosis</i> Phosphosignaling Networks	349
	<i>Yossef Av-Gay and Tom Alber</i>	
11.1	Introduction	349
11.2	Rationale for Ser/Thr Protein Kinases and Protein Phosphatases as Drug Targets	350
11.3	Drug Target Validation by Genetic Inactivation	351
11.4	STPK Mechanisms, Substrates, and Functions	352
11.5	<i>M. tuberculosis</i> STPK Inhibitors	355
11.6	Conclusions and Prospects	359
	References	359
	Index	365

List of Contributors

Tom Alber

University of California
Department of Molecular and Cell
Biology
374B Stanley Hall #3220
Berkeley, CA 94720-3220
USA

Yossef Av-Gay

University of British Columbia
Department of Medicine
Division of Infectious Diseases
Vancouver, British Columbia
Canada V5Z 3J5

Alexander C. Backes

Sandoz GmbH
Sandoz Development Center
Biochemiestrasse 10
6336 Langkampfen
Austria

Matthias Baumann

Lead Discovery Center GmbH
Emil-Figge-Str 76a
44227 Dortmund
Germany

Axel Choidas

Lead-Discovery Center GmbH
Emil-Figge-Straße 76a
44227 Dortmund
Germany

Jan Eickhoff

Lead-Discovery Center GmbH
Emil-Figge-Straße 76a
44227 Dortmund
Germany

Doris Hafenbradl

BioFocus AG
Gewerbestrasse 16
4123 Allschwil
Switzerland

Nicola Heron

Devices for Dignity
Sheffield Teaching Hospitals NMS
Foundation Trust
Royal Hallamshire Hospital
Glossop Road Sheffield, S10 2YF
UK

György Kéri

Vichem Chemie Research Ltd.
Herman Ottó u. 15
1022 Budapest
Hungary

and

Semmelweis University
Hungarian Academy of Sciences
Pathobiochemical Research Group
Tüzoltó u. 37-47
1094 Budapest
Hungary

George Kontopidis

University of Thessaly
Veterinary School
Department of Biochemistry
43100 Karditsa
Greece

Stefan Laufer

Eberhard-Karls-Universität Tübingen
Pharmazeutisches Institut
Auf der Morgenstelle 8
72076 Tübingen
Germany

Campbell McInnes

South Carolina College of Pharmacy
715 Sumter St.
Columbia, SC 29208
USA

Mokdad Mezna

Beatson Institute for Cancer Research
Translational Research
Garscube Estateswitchback Road
Glasgow G61 1BD
UK

Gerhard Müller

Proteros Fragments GmbH
Fraunhoferstr. 20
82152 Martinsried
Germany

Gábor Németh

Vichem Chemie Research Ltd.
Herman Ottó u. 15
1022 Budapest
Hungary

Lars Neumann

Proteros Biostructures
Am Klopferspitz 19
82152 Martinsried
Germany

László Örfi

Vichem Chemie Research Ltd.
Herman Ottó u. 15
1022 Budapest
Hungary

and

Semmelweis University
Department of Pharmaceutical
Chemistry
Högyes Endre u. 9
1092 Budapest
Hungary

Matthias Rabiller

Chemical Genomics Centre of the
Max Planck Society
Otto-Hahn-Str. 15
44227 Dortmund
Germany

Daniel Rauh

Chemical Genomics Centre of the
Max Planck Society
Otto-Hahn-Str. 15
44227 Dortmund
Germany

Luis M. Schang

University of Alberta
Department of Biochemistry
327 Heritage Medical Research Center
Edmonton, Alberta
Canada, T6G 2S2

Jeffrey R. Simard

Chemical Genomics Centre of the
Max Planck Society
Otto-Hahn-Str. 15
44227 Dortmund
Germany

Peter C. Sennhenn

Proteros Fragments GmbH
Fraunhoferstr. 20
82152 Martinsried
Germany

Preface

Protein kinases are a huge group of evolutionary and structurally related enzymes, which by phosphorylation of certain amino acids, in first-line serine/threonine and tyrosine, activate a multitude of proteins. In this manner, they mediate signal transduction in cell growth and differentiation. The therapeutic potential of kinase inhibitors results from the crucial role kinases (as well as some kinase mutants and hybrids resulting from chromosomal translocation) play in tumor progression and in several other diseases. With a group size of more than 500 individual members, the “kinome,” that is, the sum of all kinase genes, constitutes about 2% of the human genome. Since the isolation of the first Ser/Thr-specific kinase in the muscle in 1959, it took another 20 years until tyrosine protein kinases were discovered and another 20 years before the first 3D structure of a kinase was determined. Starting with the 3D structure of protein kinase A in 1991, many more structures were elucidated in the meantime, in their active and inactive forms, without and with ligands other than ATP. These structures show not only the close structural relationship between all kinases but also the high complexity of their allosteric regulation. Today, the term “protein kinase” retrieves almost 2000 entries from the Protein Data Bank of 3D structures; most of these structures are protein–ligand complexes with about 1000 different ligands. All kinases show a highly conserved binding site for ATP, and for this reason they were for long time considered nondruggable targets. This view was supported by the fact that the natural product staurosporine inhibits a huge number of kinases in a nonspecific manner. Still today, staurosporine is the most promiscuous kinase inhibitor, despite its large size. However, with increase in structural knowledge, additional pockets were discovered in direct vicinity of the binding motif of the adenine part of ATP (the “hinge region”). Step by step, these pockets were explored and kinase inhibitors of higher specificity emerged. Finally, the optimization of a PKC inhibitor to the bcr/abl tyrosine kinase inhibitor imatinib (Gleevec[®], Novartis) marked a breakthrough in specific tumor therapy. Although initially designed for the treatment of chronic myelogenous leukemia, the drug turned out to be beneficial also for the treatment of gastrointestinal stromal tumors (GISTs). Several other kinase inhibitors followed, with significantly different specificity profiles. Even nonspecific inhibitors, such as sunitinib (Sutent[®], Pfizer), are

valuable anticancer drugs, in this case for the therapy of advanced kidney cancer and as the second-line treatment of GIST, in cases where Gleevec[®] fails. Due to the multitude of tumor forms, resulting from various mechanisms, research on kinase inhibitors is now one of the hottest topics in pharmaceutical industry. Resistance to some kinase inhibitors forces the industry to also search for analogues with a broader spectrum of inhibitory activity. As of today, nine small-molecule kinase inhibitors for the treatment of oncological diseases have reached the market and many more are in different phases of clinical development. Even the first kinase inhibitors targeted toward nononcological applications, such as inflammatory disease states, have reached late-stage clinical development.

We are very grateful to Bert Klebl, Gerhard Müller, and Michael Hamacher who assembled a team of leading scientists for discussion of various topics of protein kinase inhibitors, including assay development, hit finding and profiling, medicinal chemistry, and application of kinase inhibitors to various therapeutic areas. We are also very grateful to all chapter authors who contributed their manuscripts on time. Of course, we appreciate the ongoing support of Frank Weinreich and Nicola Oberbeckmann-Winter, Wiley-VCH, for our book series “Methods and Principles in Medicinal Chemistry” and their valuable collaboration in this project.

September 2010

Raimund Mannhold, Düsseldorf
Hugo Kubinyi, Weisenheim am Sand
Gerd Folkers, Zürich

A Personal Foreword

Kinase inhibitors are one of the fastest emerging fields in pharmaceutical research, reigning at “No. 2” in terms of overall spending for discovery and development of pharmaceuticals, when split according to target family classes. In our own professional histories, we still witnessed the dogma in pharmaceutical industry claiming that protein kinases are considered to be nondruggable targets. This dogma was all around during the 1990s of the last millennium. Some brave individuals nevertheless pursued the idea of identifying and developing kinase inhibitors for biologically highly interesting targets, such as p38 kinases [3] and protein kinase C (PKC) isoforms [4]. Although these were groundbreaking efforts in drug discovery in those early days, p38 and PKC inhibitors have never really made it beyond the status of tool compounds for biological research and chemical biology so far. At the end, a rather serendipitous finding started the race toward the competitive generation of kinase inhibitors in oncology. The introduction of a simple methyl group into a diaminopyrimidine scaffold of a known protein kinase C inhibitor led to the generation of a relatively specific Bcr-Abl inhibitor, called imatinib or Gleevec™. The fusion protein Bcr-Abl has been known as the driving oncogene in chronic myeloid leukemias (CML) with a mutation on the Philadelphia chromosome [5], which is mediated by the elevated Abl activity of the mutant. Subsequently, imatinib has shown convincing efficacy in treating CML patients [6]. A new era started when imatinib was launched in 2001 as the first specifically designed small-molecule kinase inhibitor. The second beneficial serendipity during the generation and development of imatinib was understood only slowly. Imatinib is not just a plain and simple ATP competitor as most kinase inhibitors were designed to be. It binds to the inactive form of Bcr-Abl and keeps the kinase in its inactive conformation [7]. Today, this phenomenon is not only much better understood but also considered to be an important design element when synthesizing novel kinase inhibitors. Both serendipitous features of imatinib, inhibition of Bcr-Abl and binding to the inactive kinase, paved the way for the establishment of its clinical efficacy. However, this success gave birth to another dogma that kinase inhibitors will be useful only for developing anticancer therapies. This second dogma was based on two assumptions: (1) since 2001, imatinib has been considered to be among the most selective kinase inhibitors although it potently inhibits at least a dozen other protein kinases [8]; (2) “ATP-competitive inhibitors are never going to be highly selective, because they bind

to the highly conserved active domain of kinases". Especially, the second point on the lack of selectivity was and still is highly speculative and led to the conclusion that nonselective kinase inhibitors cannot be used as treatment options in indication areas outside cancer because of their naturally invoked off-target mediated adverse effects. This assumption vice versa also led to the conclusion that nonselective but potent kinase inhibitors will be effective cancer killing agents. We would like to challenge these hypotheses for a number of reasons:

- Kinase inhibitor technologies quickly advanced, especially compound design technologies, facilitated by the development of molecular modeling and X-ray resolutions of a large number of kinase inhibitor cocrystals (www.pdb.org/pdb/home/home.do).
- Exploitation of inhibitor binding to the inactive form of a kinase (type II inhibitors) has become an accepted design strategy and leads to a number of advantages in the pharmacological development of kinase inhibitors.
- Monoselective ATP competitors (type I inhibitors) have been generated, despite the fact that they bind only to the active site of a kinase [9].
- A fair number of scaffolds are known to compete with ATP for binding to the kinase active site, allowing a quick screening effort to identify potential starting points for a subsequent optimization program on practically any kinase.
- Allosteric kinase inhibitors have been reported to be an option for further development [10].
- The correlation between kinase homology and parallel structure–activity relationship tends to be understood much better [11].
- Nowadays, kinase inhibitor design can be envisioned as the molecular game with Lego bricks – and it really works.

Over these past years, we have been able to generate highly specific kinase inhibitors [12]. Since kinases play a role not only in carcinogenesis but also in all sorts of physiologically relevant signaling pathways [13], we are convinced that both oncology and any other medical indication might represent an important playground for the application of selective and safe kinase inhibitors. Future will demonstrate that kinase inhibitors are going to be applied to treat chronic conditions and not only in life-threatening settings. Therefore, we have chosen contributions to this book that describe the generation and application of kinase inhibitors also outside the important field of anticancer drug discovery. Broadly specific kinase inhibitors, such as sunitinib, will not have a chance for development for indications other than cancer. Instead, monoselective kinase inhibitors or multikinase inhibitors with a narrow profile will turn out to be efficacious if the chosen target is critical enough in a particular pathophysiological process. It is more about the validation of the target(s) and the underlying target(s) rationale. In that respect, it remains to be seen if p38 α turns out to be a valid target for rheumatic arthritis or to be valid only for some distinct inflammatory diseases. The odds are that p38 α inhibitors will not reach the status of a general anti-inflammatory agent due to target-mediated toxicities [14]. Although all p38 α inhibitor research might then be considered a lost investment, it has nonetheless contributed enormously to the general strategies in developing kinase

inhibitors, such as the directed design of type II inhibitors and the generation of highly selective kinase inhibitors, as well as their translation into pharmacologically active substances (e.g., [15]). These efforts significantly helped to pave the way for the development of highly selective future kinase inhibitors for different kinase targets without target-mediated toxicities. The world of protein kinases consists of more than, 500 individual members, the human kinome [16], therapeutically relevant parasitic kinase targets even not considered. Therefore, our prediction is that we will see many more novel drug candidates and pharmaceutical products arising from this large and important family of enzymes.

This gives hope to millions of patients suffering not only from various cancers but also from inflammatory, metabolic, and neurological disorders and infectious diseases, where a distinct kinase is out of control and must be tamed by a highly specific and potent kinase inhibitor. But what makes a good inhibitor? Which steps have to be taken for identifying a target and successfully making a drug with, if possible, no side effects? Which kinase inhibitors have been developed so far by using which design strategy? Can we already define lessons learned?

Small molecules and their apparently endless modularity and flexibility to produce all necessary structures are the perfect source for developing kinase inhibitors. Libraries of thousands to millions of compounds can be screened easily in high-throughput screens (HTS) or even *in silico*. Detected hits can be optimized step-by-step in iterative cycles toward highly potent and specific preclinical candidates and well-tolerated drugs on the market (or toward specific probes and tools in basic research). Thus, this book is dedicated to small-molecules kinase inhibitors and their various contributions to medical application.

Literature is exploding in the kinase inhibitor field, particularly when dealing with appropriate tools and design. In order to give a comprehensive overview about this special but diverse inhibitor species, this book covers the most important criteria from assay development to profiling and from medicinal chemistry-based optimization to a potential application. This book has been arranged in a logical order in various parts to highlight

- hit finding and profiling for protein kinases, describing the Dos and Don'ts while identifying and (cellular) profiling of active small-molecule kinase inhibitors.
- chemical kinomics to detect phosphorylation networks.
- medicinal chemistry, offering a detailed summary of existing kinase inhibitors, available technologies, and design principles that might be considered.
- application to therapeutic indication areas, discussing in detail success stories and unmet needs in medical application including cancer, inflammatory diseases, and infections.

Thanks to the enthusiasm and the perseverance of the authors and the publisher of this book, we finally made it. Somehow, the genesis of this small compendium on kinase inhibitor research resembles the field of small-molecule-based kinase inhibitors itself. Some brave individuals quickly wrote and delivered their contributions within a short period of time, some others took more time to develop their chapters, and finally, some opted out of the project and were replaced by others who maybe

considered newcomers to the field. This process seemed to reflect the development of the field of kinase inhibitor research over the past 15 years in nice analogy. On purpose, we have selected contributions on kinase inhibitor drug discovery from early-stage discoveries since there have been a lot of writing and comprehensive reviews on successfully launched kinase inhibitors, such as Gleevec, Iressa, Tarceva, Sorafenib, Sutent, Dasatinib, Lapatinib, and others ([1, 2] and references therein). There is also a good body of literature available on kinase inhibitors in cancer drug discovery. So, we rather focused both on the technologies for the discovery of kinase inhibitors and on the optimization of these inhibitors, and we included novel potential therapeutic applications of kinase inhibitors, especially fields outside the cancer research. Therefore, this collection of articles is quite unique, albeit highly representative when it comes to the identification and generation of novel kinase inhibitors with biological and pharmacological activity.

In the different chapters, experts in their field summarize the historical evolution, the trends, and a good part of their own experience gained while working in their respective fields. After reading the book, it will become clear how much promise small-molecule kinase inhibitors really hold, not only for the described therapeutic indications but also beyond, when obeying basic, intrinsic rules.

We are convinced that small-molecule kinase inhibitors will become ever more important in the years to come and are going to celebrate new success stories for research and patients – despite or even because of the current dramatic changes in pharmaceutical industry. Enjoy reading!

References

- Pytel, D., Sliwinski, T., Poplawski, T., Ferriola, D., and Majsterek, I. (2009) Tyrosine kinase blockers: new hope for successful cancer therapy. *Anti-Cancer Agents in Medicinal Chemistry*, **9**, 66–76.
- Natoli, C., Perrucci, B., Perrotti, F., Falchi, L., Iacobelli, S., and Consorzio Interuniversitario Nazionale per Bio-Oncologia (CINBO) (2010) Tyrosine kinase inhibitors. *Current Cancer Drug Targets*, **10**, 462–483.
- Lee, J.C., Laydon, J.T., McDonnell, P.C., Gallagher, T.F., Kumar, S., Green, D., McNulty, D., Blumenthal, M.J., Heys, J.R., Landvatter, S.W., Strickler, J.E., McLaughlin, M.M., Siemens, I.R., Fisher, S.M., Livi, G.P., White, J.R., Adams, J.L., and Young, P.R. (1994) A protein kinase involved in the regulation of inflammatory cytokine biosynthesis. *Nature*, **372**, 739–746.
- Kawamoto, S. and Hidaka, H., (1984) 1-(5-Isoquinolinesulfonyl)-2-methylpiperazine (H-7) is a selective inhibitor of protein kinase C in rabbit platelets. *Biochemical and Biophysical Research Communications*, **125**, 258–264.
- Heisterkamp, N., Stam, K., Groffen, J., de Klein, A., and Grosveld, G. (1985) Structural organization of the bcr gene and its role in the Ph' translocation. *Nature*, **315**, 758–761.
- Druker, B.J., Talpaz, M., Resta, D.J., Peng, B., Buchdunger, E., Ford, J.M., Lydon, N.B., Kantarjian, H., Capdeville, R., Ohno-Jones, S., and Sawyers, C.L. (2001) Efficacy and safety of a specific inhibitor of the BCR-ABL tyrosine kinase in chronic myeloid leukemia. *The New England Journal of Medicine*, **344**, 1031–1037.
- Dietrich, J., Hulme, C., and Hurley, L.H. (2010) The design, synthesis, and evaluation of 8 hybrid DFG-out allosteric

- kinase inhibitors: a structural analysis of the binding interactions of Gleevec, Nexavar, and BIRB-796. *Bioorganic and Medicinal Chemistry*, **18**, 5738–5748.
- 8 Fabian, M.A., Biggs, W.H., 3rd, Treiber, D.K., Atteridge, C.E., Azimioara, M.D., Benedetti, M.G., Carter, T.A., Ciceri, P., Edeen, P.T., Floyd, M., Ford, J.M., Galvin, M., Gerlach, J.L., Grotzfeld, R.M., Herrgard, S., Insko, D.E., Insko, M.A., Lai, A.G., L  lias, J.M., Mehta, S.A., Milanov, Z.V., Velasco, A.M., Wodicka, L.M., Patel, H.K., Zarrinkar, P.P., and Lockhart, D.J. (2005) A small molecule-kinase interaction map for clinical kinase inhibitors. *Nature Biotechnology*, **23**, 329–336.
 - 9 Walburger, A., Koul, A., Ferrari, G., Nguyen, L., Prescianotto-Baschong, C., Huygen, K., Klebl, B., Thompson, C., Bacher, G., and Pieters, J. (2004) Protein kinase G from pathogenic mycobacteria promotes survival within macrophages. *Science*, **304**, 1800–1804.
 - 10 Lindsley, C.W., Zhao, Z., Leister, W.H., Robinson, R.G., Barnett, S.F., Defeo-Jones, D., Jones, R.E., Hartman, G.D., Huff, J.R., Huber, H.E., and Duggan, M.E. (2005) Allosteric Akt (PKB) inhibitors: discovery and SAR of isozyme selective inhibitors. *Bioorganic & Medicinal Chemistry Letters*, **15**, 761–764.
 - 11 Vieth, M., Higgs, R.E., Robertson, D.H., Shapiro, M., Gragg, E.A., and Hemmerle, H. (2004) Kinomics: structural biology and chemogenomics of kinase inhibitors and targets. *Biochimica et Biophysica Acta*, **1697**, 243–257.
 - 12 Wabnitz, P. *et al.* (2008) 4,6-Disubstituted aminopyrimidine derivatives as inhibitors of protein kinases. WO/2008/129080.
 - 13 Cohen, P. (2002) Protein kinases: the major drug targets of the twenty-first century? *Nature Reviews. Drug Discovery*, **1**, 309–315.
 - 14 Hammaker, D. and Firestein, G.S. (2010) “Go upstream, young man”: lessons learned from the p38 saga. *Annals of the Rheumatic Diseases*, **69** (Suppl. 1), i77–i82.
 - 15 Pargellis, C., Tong, L., Churchill, L., Cirillo, P.F., Gilmore, T., Graham, A.G., Grob, P.M., Hickey, E.R., Moss, N., Pav, S., and Regan, J. (2002) Inhibition of p38 MAP kinase by utilizing a novel allosteric binding site. *Nature Structural Biology*, **9**, 268–272.
 - 16 Manning, G., Whyte, D.B., Martinez, R., Hunter, T., and Sudarsanam, S. (2002) The protein kinase complement of the human genome. *Science*, **298**, 1912–1934.

October 2010

Bert Klebl, (Dortmund)
 Gerhard M  ller, (Planegg)
 Michael Hamacher, (Dortmund)

Part One

Hit Finding and Profiling for Protein Kinases: Assay Development and Screening, Libraries

1

In Vitro Characterization of Small-Molecule Kinase Inhibitors

Doris Hafenbradl, Matthias Baumann, and Lars Neumann

1.1

Introduction

Typically the starting point for an early-stage drug discovery project is the identification of a small-molecule entity that, among other characteristics, has inhibitory activity against a given target kinase. Kinase inhibitors are usually identified in a high-throughput screening (HTS) campaign. The identified “hits” are selected on the basis of their inhibitory potential against the target kinase, the intellectual property situation around the small-molecule inhibitor class, the potential for further chemical optimization, and other criteria. Once the optimization process has started, several parameters have to be considered and continuously monitored. In most drug discovery programs, the optimization of the inhibitory activity of the small molecules against the target kinase represents the center of activities. While this parameter seems to be a straightforward and measurable parameter, there are a variety of possibilities of how an inhibitor might be binding to a protein kinase. Potentially, these different binding modes can cause modifications of the kinetic binding behavior of the compound. For the full assessment of an inhibitor, a detailed analysis of binding modes and kinetic consequences is required.

The optimization of a specific protein kinase inhibitor requires the constant assessment of a wide range of kinases to reduce the risk of possible side effects. It is therefore important to use comparable conditions in each protein kinase assay.

A successful drug candidate also requires a balanced physicochemical profile that determines the pharmacokinetic (PK) behavior of a small-molecule inhibitor in animals. In the past 10 years, a variety of *in vitro* assays have been developed and proven to be useful for the prediction of the PK parameters of an inhibitor.

Here, we describe in detail a selection of *in vitro* assays that are critical for the optimization process of small-molecule kinase inhibitors. For an appropriate start, a thorough optimization of the biochemical kinase assay is needed. In addition, one needs to consider the mode of inhibition and should be prepared for unexpected exceptions from the general rules. Besides the rationalization of the measurement of the biochemical activity and the selectivity that influence the pharmacodynamic behavior of a small-molecule inhibitor, we will give an in-depth overview of options

for *in vitro* measurement of parameters that determine the pharmacokinetic behavior of small-molecule inhibitors.

1.2

Optimization of a Biochemical Kinase Assay

At the first glance, a biochemical kinase assay seems to be a very straightforward enterprise with only very few parameters that can be modified: the concentration of ATP, substrate, and protein kinase, the composition of the reaction buffer, and the reaction time. Nevertheless, a detailed optimization process is needed and several considerations have to be taken into account. In the following, we will give guidance for the evaluation of each step of the assay optimization and how this information is used to achieve the goal: a biochemical screening assay that yields reliable and reproducible information about the inhibitory activity of a small molecule as one of the most critical parameters throughout an entire drug discovery project. The optimization process for the AGC kinase Rock II is used as an example for describing in detail the considerations and evaluation of the results.

1.2.1

Step 1: Identification of a Substrate and Controlling of the Linearity between Signal and Kinase Concentration

Finding a substrate that is recognized and efficiently phosphorylated by the kinase of interest is the first essential step in developing a biochemical kinase assay. Equally important is the identification of the kinase concentration to start the assay optimization that guarantees a sufficiently high signal and at the same time good linearity between signal and kinase activity.

When the concentration of kinase is low, the concentration changes in ATP, ADP, and phosphorylated substrate are very small after a given reaction time. As a consequence, the associated assay signal is low and inaccurate (Figure 1.1, region of low assay signal). At moderate kinase concentrations, a sufficiently high assay signal can be detected and at the same time linearity between signal and kinase activity is observed. Thus, for example, a doubling of kinase activity is directly translated into the doubling of the assay signal (Figure 1.1, linear region). At high kinase concentrations, the bulk of ATP or substrate transforms into phosphorylated substrate after the given reaction time and the linearity between kinase activity and assay signal is lost (Figure 1.1, nonlinear region). At very high kinase concentration, all ATP or substrate is converted into ADP and phosphorylated substrate and an even higher kinase concentration cannot increase the signal further (Figure 1.1, insensitive region). Thus, as soon as the assay is depleted of either ATP or substrate, the assay is blind to changes in kinase activity. This situation is detrimental for two reasons. First, if the goal is to improve the assay conditions in order to increase the kinase activity, the assay cannot deliver an answer since changes in the kinase activity do not translate into a change in signal. A further increase in kinase activity cannot be

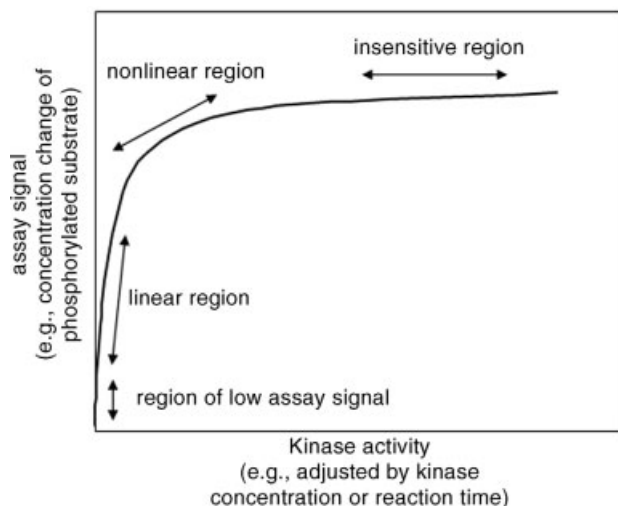


Figure 1.1 Assay signal is plotted against kinase activity. The assay signal can be derived from the concentration change of ATP, ADP, or phosphorylated substrate after the given reaction time. Kinase activity is adjustable, for example, by varying the kinase concentration or reaction time. The plot is separated in four distinct regions. (1) Region of low assay signal at very little kinase activity. In this region, the kinase activity is so low that only very little concentration changes in either educts or product have occurred. Usually, this region yields signals that are too weak to generate reliable data. (2) Linear region. At higher kinase activities, the concentration changes are larger and therefore the assay signals are generally strong enough to give robust data quality. This region is the optimal to perform kinase assays since a change in kinase activity is translated linearly in a signal change. (3) Nonlinear region.

At even higher kinase activities, most of the ATP and/or substrate is transformed into ADP and phosphorylated substrate, respectively. In this region, high assay signals can be achieved, but kinase activity and signal do not depend linearly on each other anymore. (4) Insensitive region. If all ATP or substrate is consumed after the investigated reaction time, the maximal possible change of signal has been reached. Increased kinase activity cannot modulate the signal anymore because ATP and/or substrate has been completely consumed. Thus, neither an increase nor a decrease in kinase activity can be detected. In this region, the assay is insensitive to both an improvement of kinase activity (e.g., by optimizing the buffer components) and the inhibition of kinase activity (e.g., by the presence of a kinase inhibitor) and should therefore be avoided implicitly.

detected because even less kinase activity is sufficient to consume all ATP or substrate. Second, in the opposite scenario the question is whether or not a compound reduces the activity of a kinase. If the compound blocks 50% of the kinase activity, no change of the assay signal can be detected, as even 50% kinase activity is sufficient to consume all ATP or substrate within the given reaction time. Therefore, the activity of an inhibitor would be underestimated or the inhibition would not be detected at all.

In the first assay optimization step, both the substrate that yields in the highest kinase activity and the kinase concentration that combines sufficient assay signal and signal linearity are identified. Therefore, a series of potential substrates are tested in

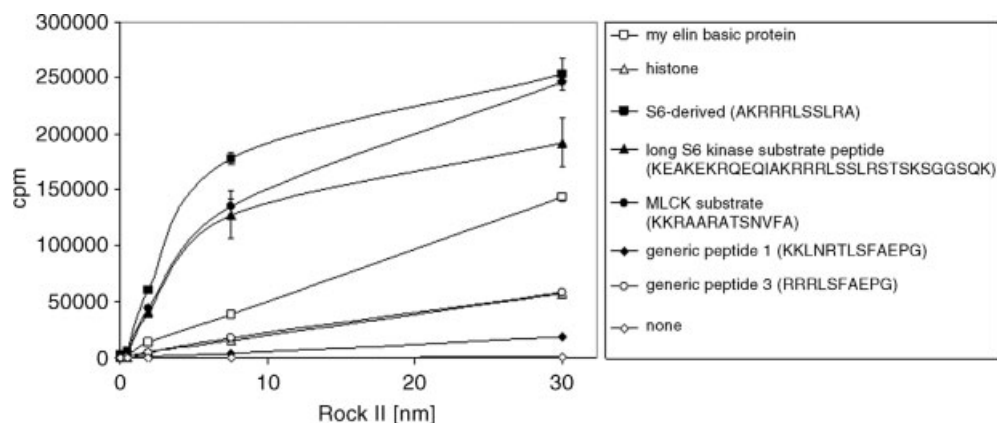


Figure 1.2 10 μ M ATP and 12.5 μ Ci/ml 33 P-y-ATP are incubated with increasing concentrations of Rock II and 10 μ M of various potential Rock II substrates in 40 μ l 20 mM Tris pH 7.5, 10 mM MgCl_2 , 1 mM DTT for 1 h at room temperature. After 1 h, the reaction was terminated by adding 10 μ l 0.5 M EDTA. The reaction mixtures are transferred to phosphor

cellulose filters and incubated with 60 μ l 0.75% H_3PO_4 for 15 min. Remaining 33 P-y-ATP was removed from the filters by three washes with 200 μ l 0.75% H_3PO_4 each. The filter-associated substrate-incorporated 33 P was quantified by scintillation counting and plotted against Rock II concentration. The error bars are given in standard deviations of duplicates.

the presence of increasing kinase concentrations. In Figure 1.2, step 1 of an assay optimization for the kinase Rock II is exemplified. Seven potential Rock II substrates were incubated with increasing concentrations of Rock II. In addition, Rock II was incubated in the absence of substrate. After 1 h, the reaction was terminated and the amount of phosphorylated substrate quantified. As shown in Figure 1.2, S6-derived peptide is phosphorylated most efficiently yielding the highest assay signal at low kinase concentrations. The generic peptide 3 was recognized with lowest efficiency. In the absence of substrate, consistently no assay signal was detected at all. In the presence of the S6-derived peptide, the linear assay region is found between 0.5 and 7 nM Rock II. Below 0.5 nM Rock II, only very small amounts of S6-derived peptide are phosphorylated and the assay signal is too small to be reliable. At Rock II concentration above 7 nM, the majority of the S6-derived peptide is phosphorylated and the assay reaches its nonlinear region. Thus, from step 1 the following information can be taken into account for the next optimization step: (1) S6-derived peptide is selected to be the substrate that is recognized most efficiently and (2) for the next optimization step, a Rock II concentration of 0.5 nM should be used to guarantee strict linearity between assay signal and kinase activity.

1.2.2

Step 2: Assay Wall and Optimization of the Reaction Buffer

In the second assay optimization step, a reaction buffer is identified that enables the kinase to work at its maximal capacity. In other words, the reaction buffer is

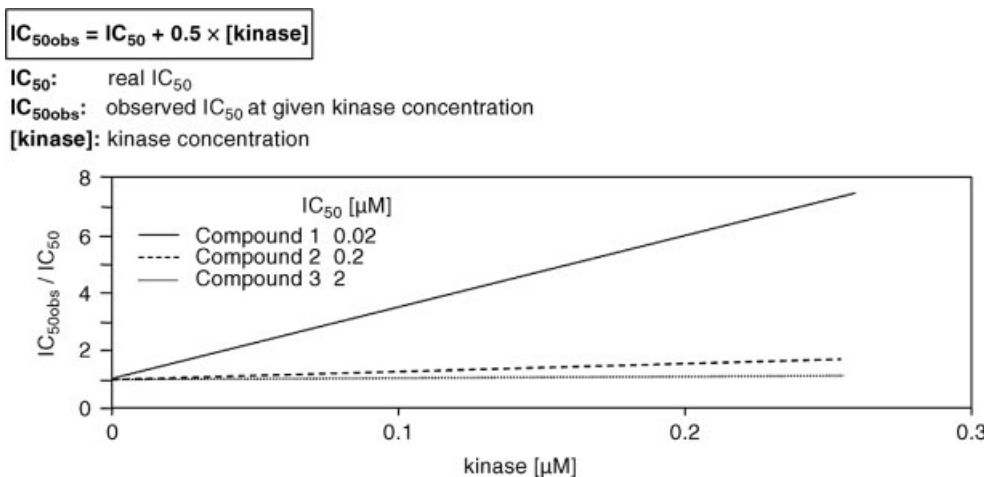


Figure 1.3 The observed IC_{50} (IC_{50obs}) is given by the sum of the real IC_{50} and 0.5-fold the kinase concentration. Consequently, the minimal IC_{50} that can be measured equals 0.5 times the kinase concentration even if the real IC_{50} value is lower. Assays requiring low kinase concentrations – lower than the IC_{50} values of the examined inhibitors – yield IC_{50} values that

are very close to the real IC_{50} . The ratio between the observed IC_{50} and the real IC_{50} (IC_{50obs}/IC_{50}) is close to 1. In contrast, assays that need high kinase concentrations – as high as or even higher than the IC_{50} values of the inhibitors – will measure IC_{50obs} larger than the real IC_{50} values. The ratio IC_{50obs}/IC_{50} is above 1 and increases with rising kinase concentrations.

optimized to obtain a sufficiently high assay signal at the lowest possible kinase concentration. Beside the cost considerations, a low kinase concentration is essential since the kinase concentration limits the lowest IC_{50} values that can be determined. The lowest IC_{50} value that can be measured equals half the kinase concentration in the assay (see Figure 1.3) [1, 2]. For example, in an assay that uses 10 nM kinase, the lowest IC_{50} value that can be measured is 5 nM. Even if the real IC_{50} value would be 0.5 nM, the observed IC_{50} revealed by the assay would be 5 nM. This phenomenon is called “assay wall.” No IC_{50} value can be measured below this wall defined by the kinase concentration. This behavior is self-evident if one considers that half the kinase molecules have to be bound by an inhibitor to reduce the kinase activity by 50%.

This assay wall can cause a severe impact on drug discovery projects. In the beginning of the project, usually the IC_{50} values are high and far above the kinase concentration. During the course of the project, the IC_{50} values typically decrease with every cycle of compound optimization. At a certain level, the IC_{50} values cannot be decreased anymore. A project course such as this is indicative of having reached the assay wall and it should be constantly monitored if the IC_{50} values have reached the kinase concentration used in the assay.

In the second optimization step, the composition of the reaction buffer is evaluated. The potential addition of detergents, the optimal pH, and ion composition are evaluated to ensure maximal kinase activity. Since kinases are most dependent on Mg^{2+} and Mn^{2+} , these ions should be investigated in great detail. In addition, the

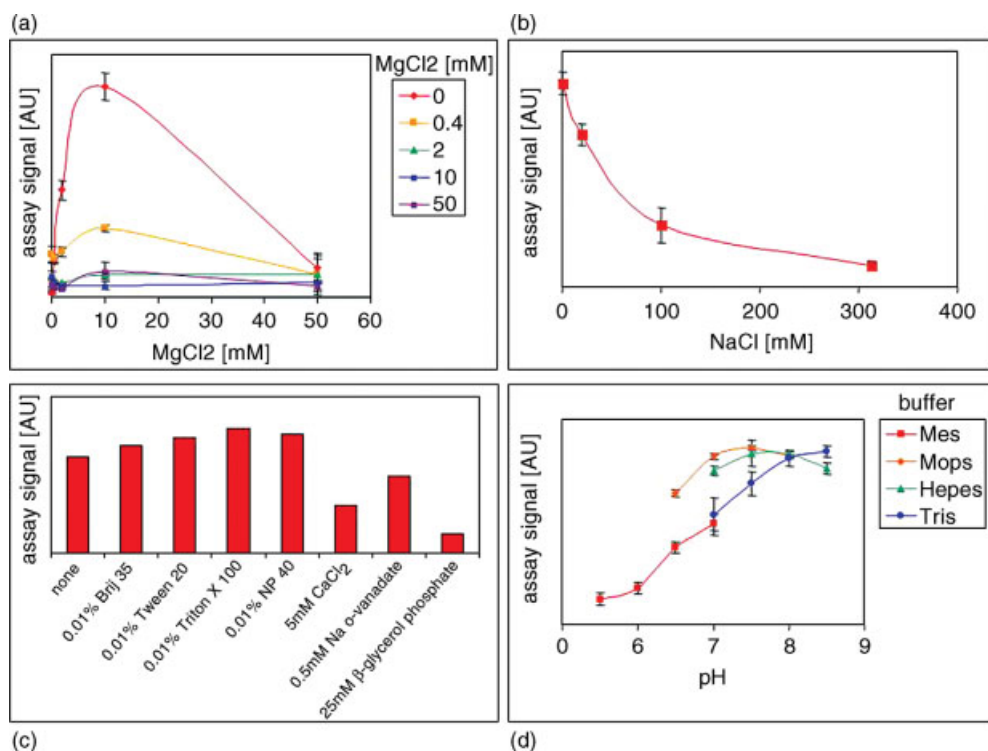


Figure 1.4 1 μ M ATP, 12.5 μ Ci/ml 33 P-Y-ATP, 10 μ M S6-derived substrate peptide are incubated with 0.5 nM Rock II for 1 h in 40 μ l (a) 20 mM Tris pH 7.5, 1 mM DTT, and the indicated amounts of MgCl₂ and MnCl₂; (b) 20 mM Tris pH 7.5, 10 mM MgCl₂, 1 mM DTT, and the indicated concentration of NaCl; (c) 20 mM Tris pH 7.5, 10 mM MgCl₂, 1 mM DTT, and the indicated concentrations of detergent, CaCl₂, or phosphate inhibitors; or (d) 10 mM MgCl₂, 1 mM DTT, and 20 mM of the

indicated buffer at the given pH values. After 1 h, the reaction was terminated by adding 10 μ l 0.5 M EDTA. The reaction mixtures were transferred to phosphor cellulose filters and incubated with 60 μ l 0.75% H₃PO₄ for 15 min. Remaining 33 P-Y-ATP, was removed from the filters by three washes with 200 μ l 0.75% H₃PO₄ each. The filter-associated substrate-incorporated 33 P was quantified by scintillation counting. Error bars are given in standard deviations of duplicates.

influence of NaCl and CaCl₂ is examined. Figure 1.4a shows how different combinations of MgCl₂ and MnCl₂ influence the Rock II activity. A clear maximum in Rock II activity is detected at 10 mM MgCl₂ in the absence of MnCl₂. Increasing or decreasing the MgCl₂ reduces the Rock II activity. Also, addition of MnCl₂ results in the loss of Rock II activity. Similarly, the presence of NaCl (Figure 1.4b), CaCl₂, and the phosphate inhibitors sodium-*o*-vanadate and β -glycerol phosphate reduces the assay signal (Figure 1.4c). In contrast, the presence of 0.01% detergent such as Brij35, Tween 20, Triton X-100, or NP40 has no significant influence on Rock II performance (Figure 1.4c). Figure 1.4d shows the pH dependence of Rock II. Various buffer systems were used to cover the pH range from 5.5 to 8.5. While Rock II is nearly

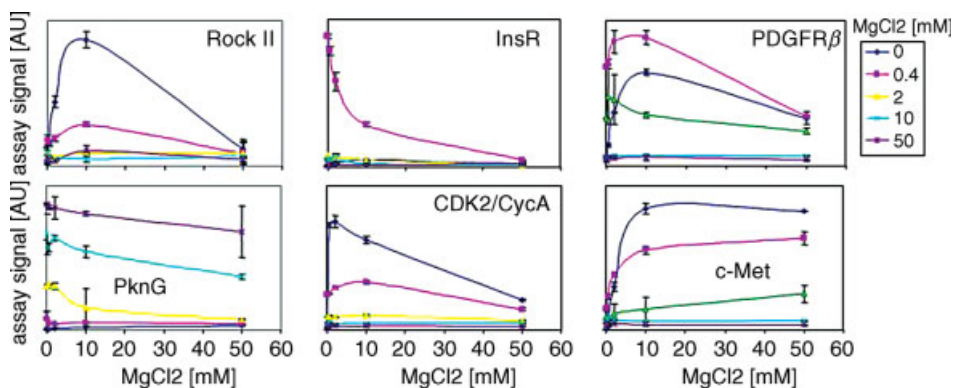


Figure 1.5 Activity of six kinases in the presence of various combinations of MgCl_2 and MnCl_2 concentrations.

inactive at acidic pH, maximal activity is reached at around pH 7.5. At pH values above 7.5, Rock II loses activity. In summary, on the basis of these results (Figure 1.4), 20 mM Mops pH 7.5, 10 mM MgCl_2 , 0.01% Triton X-100, 1 mM DTT were chosen as optimal Rock II reaction buffer and were used in the following optimization steps.

The $\text{MgCl}_2/\text{MnCl}_2$ preferences of kinases can widely vary (Figure 1.5). While Rock II prefers 10 mM MgCl_2 and the absence of MnCl_2 , the kinase PknG, for example, is almost inactive under these conditions. PknG shows maximal activity at 50 mM MnCl_2 in the absence of MgCl_2 . On the other hand, PDGFR β shows highest activity at a combination of 10 mM MgCl_2 and 0.4 mM MnCl_2 . Thus, the optimization of the MgCl_2 and MnCl_2 concentration for each kinase usually allows to dramatically reduce kinase concentrations in the assay.

In addition to the high diversity in $\text{MgCl}_2/\text{MnCl}_2$ preference, the tolerance for various detergents, CaCl_2 , and phosphatase inhibitors widely differs between kinases (Figure 1.6), so do pH optima (Figure 1.7). Thus, using a generic kinase reaction buffer for all kinases would result in significantly higher kinase assay concentrations and therefore unnecessarily high assay wall and high assay costs.

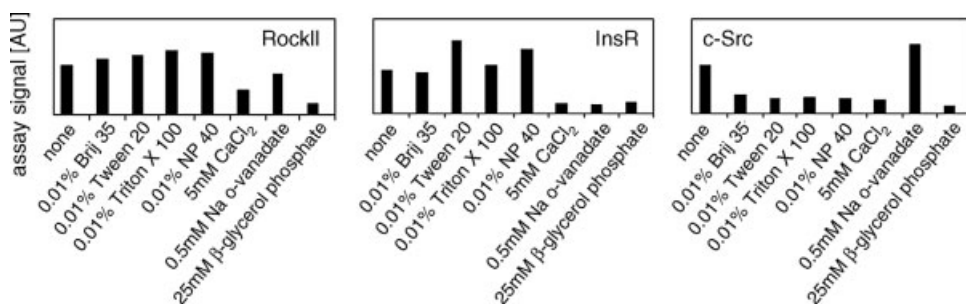


Figure 1.6 Activity of six kinases in the presence of various detergents, ions, and phosphatase inhibitors.

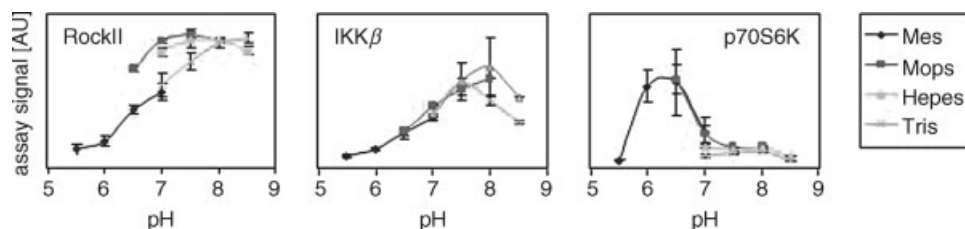


Figure 1.7 Activity of six kinases at various pH values. In order to cover a pH range from 5.5 to 8.5, different buffer systems were used.

1.2.3

Step 3: The Michaelis–Menten Constant K_m and the ATP Concentration

After the identification of a good substrate and the optimal reaction buffer, the next step is the determination of the ATP concentration that should be used. Since the majority of all kinase inhibitors are ATP competitive, the ATP concentration determines the ability of an assay to identify the potential of a given small-molecule kinase inhibitor. Generally, there are three options of choosing the ATP concentration.

The first is to use a standard ATP concentration that is identical in all different protein kinase assays. The main advantage of a standard ATP concentration is the ease of the experimental procedure, especially if a large number of different kinases are regularly screened. The main disadvantage of a kinase assay with a standard ATP concentration, for example, $30\ \mu\text{M}$ or $100\ \mu\text{M}$, is that the IC_{50} values cannot be used to rank the potency of a given inhibitor between different kinases. For ATP-competitive inhibitors, the dependencies between IC_{50} and ATP concentrations are described by the Cheng–Prusoff equation (Figure 1.8) [3]. The IC_{50} and the ATP concentration are linearly connected. The slope is given by the ratio between the inhibitor constant K_i and the Michaelis–Menten constant for ATP K_m . The y -intercept is defined by the K_i value. The K_i value describes the affinity between inhibitor and kinase, while the K_m value approximates the affinity between ATP and kinase. Since a given inhibitor has different K_i values for every kinase and since every kinase has a different K_m for ATP, slope and y -intercept are different for each kinase. As a consequence, the lines of the Cheng–Prusoff plot intersect each other. Thus, for example, at an arbitrary assay ATP standard concentration of $10\ \mu\text{M}$, a smaller IC_{50} will be measured for a given inhibitor against a theoretical kinase 1 ($K_{m\text{ATP}} = 1.5\ \mu\text{M}$, $K_i = 0.002\ \mu\text{M}$) than against kinase 2 ($K_{m\text{ATP}} = 10\ \mu\text{M}$, $K_i = 0.01\ \mu\text{M}$) (Figure 1.8). At an arbitrary ATP standard concentration of $30\ \mu\text{M}$ ATP, the opposite ranking would be observed. At $30\ \mu\text{M}$, the IC_{50} of the given inhibitor would be measured to be smaller for kinase 2 than for kinase 1 (Figure 1.8). While at one ATP concentration the given inhibitor seems to be more specific for kinase 1, it appears to be more specific for kinase 2 at another ATP concentration. Thus, selectivity ranking based on assays using standard ATP concentrations is arbitrary and therefore should be avoided.

$$IC_{50} = K_i + \frac{K_i}{K_m} \times [ATP]$$

K_m : Michaelis Menten constant

K_i : Inhibitor constant

[ATP]: ATP concentration

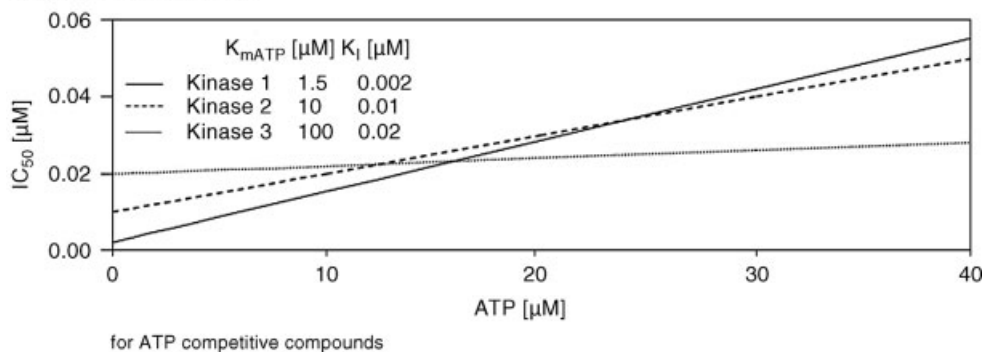


Figure 1.8 The Cheng–Prusoff equation describes the dependencies between IC_{50} value and ATP concentration for ATP-competitive inhibitors. The IC_{50} values for one inhibitor against three kinases are calculated for an ATP concentration range from 0 to 40 μM . All three kinases have different K_m values and the K_i values describing the interaction between the theoretical inhibitor and the three kinases vary from 0.002 to 0.02 μM . At ATP concentrations below 12 μM ,

kinase 1 has the lowest IC_{50} and kinase 3 has the highest IC_{50} . At ATP concentrations between 12 and 17 μM , kinase 2 has the highest and kinase 1 the lowest IC_{50} . Between 17 and 24 μM , kinase 3 has the lowest IC_{50} . Above 24 μM , the IC_{50} ranking is completely the opposite compared to the IC_{50} ranking at ATP concentrations below 12 μM . Thus, the selectivity ranking of the theoretical inhibitor depends on the selected ATP concentration.

The second option is to choose an ATP concentration at the cellular ATP level that is seen by the kinase of interest in the pathologic situation. This approach requires exact knowledge of the ATP concentration in the relevant cellular location within the patient. Unfortunately, little is known about the exact cellular ATP concentrations. Even less is known about fluctuations of ATP concentrations between different locations within a cell, between cells in different tissues, between cancer and noncancer cells, between cells in different stages of their development, and so on. As a consequence, the ATP concentration that would be assumed to mimic the cellular ATP concentration *in vivo* does most likely not reflect the reality. The chosen ATP concentration is more likely to represent another form of an arbitrary ATP standard concentration with the associated problem discussed in the beginning of this section.

The third option for choosing the ATP concentration to measure IC_{50} values for ATP-competitive inhibitors is to use ATP at a concentration that equals its K_m value for the individual kinase. The K_m value is defined by the ATP concentration that allows half maximal reaction velocity. Thus, the ATP concentration would be different for every kinase assay. In addition, the determination of the K_m value for every kinase

$$\boxed{IC_{50} = K_i + \frac{K_i}{K_m} \times [ATP]} \xrightarrow{[ATP] = K_m} \boxed{IC_{50} = K_i + \frac{K_i}{K_m} \times K_m = 2 \times K_i}$$

K_m : Michaelis Menten constant
 K_i : Inhibitor constant
 $[ATP]$: ATP concentration

Figure 1.9 The Cheng–Prusoff equation describes the relation between IC_{50} value and ATP concentration for ATP-competitive inhibitors. If the ATP concentration equals the K_m value for ATP, the IC_{50} represents twice the K_i value.

is required during the assay development, thereby complicating the assay development and screening workflow. On the other hand, IC_{50} values determined at an ATP concentration that represents its K_m value reflect $2 \times K_i$ value (Figure 1.9). Thus, the IC_{50} value is a direct measure of affinity between the inhibitor and the investigated kinase. As a consequence, the selectivity of an inhibitor against various kinases can be ranked on the basis of its binding affinity for different kinases.

Comparing the three options of choosing an ATP concentration, the K_m value for ATP represents the most advantageous choice when more than one kinase are tested. Since this situation will be found in the majority of all discovery projects, the K_m determination has to be included as the essential step in the assay development. Since the K_m value is defined by the ATP concentration that allows half maximal reaction velocity, the assay signal in the presence of increasing ATP concentrations is measured and fitted to the Michaelis–Menten equation (Figure 1.10) [4]. The ATP K_m for Rock II was determined to be 25 μ M. In further assay optimization, 25 μ M ATP will be used.

Determination of the ATP K_m of kinases is complicated by the fact that kinases have two substrates, ATP (the phosphate donor) and what we have called the substrate (the phosphate acceptor) so far. Therefore, the ATP K_m depends on the phosphate acceptor concentration. Only if the concentration of the phosphate acceptor is at least five times above its own K_m value, the ATP K_m value is independent of the phosphate acceptor concentration and can be determined precisely. At lower phosphate acceptor concentrations instead of the real ATP K_m , an apparent ATP K_m results from an ATP K_m determination experiment. Under these circumstances, the measured ATP K_m is valid only for the given phosphate acceptor (substrate) concentration.

1.2.4

Step 4: Signal Linearity throughout the Reaction Time and Dependence on the Kinase Concentration

After identifying an appropriate substrate, an optimal reaction buffer, and a meaningful ATP concentration, the selection of assay components is now complete. Step 4 of the assay optimization controls signal linearity if the optimized reaction buffer and adjusted ATP concentration have shifted the range of kinase concentration that guarantees signal linearity compared to assay optimization step 1 (Section 1.1.1). The significance of signal linearity was discussed in Section 1.1.1 (Figure 1.1). In addition,

$$v = \frac{V_{\max} [\text{ATP}]}{K_m + [\text{ATP}]}$$

v : reaction velocity; here: assay signal per 1 h
 V_{\max} : maximal reaction velocity
 K_m : Michealis Menten constant for ATP
 $[\text{ATP}]$: ATP concentration

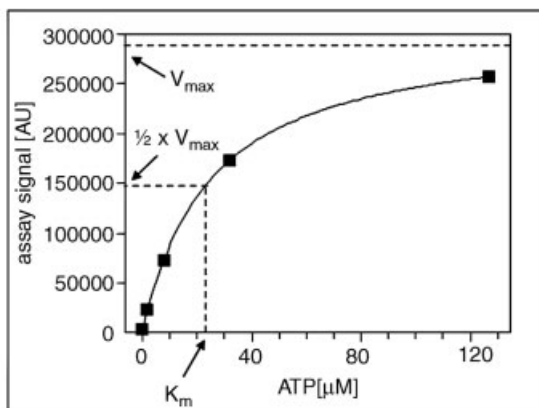


Figure 1.10 The Michaelis–Menten equation describes the dependencies between reaction velocity and ATP concentration. The K_m value is defined by the ATP concentration that results in half maximal reaction velocity. Increasing concentrations of ATP were incubated for 1 h with 0.5 nM Rock II, 2.5 $\mu\text{Ci}/\text{ml}$ ^{33}P -Y-ATP, and 10 μM S6-derived substrate peptide in 40 μl 20 mM Mops pH 7.5, 10 mM MgCl_2 , 0.01% Triton X-100, 1 mM DTT. The reaction was terminated by adding 10 μl 0.5 M EDTA and transferred to phosphor cellulose filters

followed by an incubation with 60 μl 0.75% H_3PO_4 for 15 min. Remaining ^{33}P -Y-ATP was removed from the filters by three washes with 200 μl 0.75% H_3PO_4 each. The filter-associated substrate-incorporated ^{33}P was quantified by scintillation counting. The assay signal was corrected for the dilution of ^{33}P -Y-ATP in nonradioactive ATP and plotted against the ATP concentration. The data were fitted to the given Michaelis–Menten equation, thereby determining the Rock II ATP K_m to be 25 μM .

step 4 examines the dependency between signal linearity and reaction time. Signal linearity has to be maintained regarding both kinase concentration and reaction time to ensure that the measured IC_{50} ($\text{IC}_{50\text{obs}}$) reflects the real IC_{50} (Figure 1.11) [5]. The higher the kinase activity is, regardless whether due to a high kinase concentration or due to a long reaction time, the more the substrate is converted (Figure 1.11a). At high substrate conversion, the measured IC_{50} ($\text{IC}_{50\text{obs}}$) is significantly larger than the real IC_{50} (Figure 1.11b). Thus, in order to measure meaningful IC_{50} values, it is essential to identify a combination of kinase concentration and reaction time that has a sufficiently high assay signal and minimal substrate conversion.

In order to identify the Rock II concentration and the Rock II reaction time that guarantees signal linearity, five different Rock II concentrations were incubated at six different reaction times (Figure 1.12). From this experiment, the scientist can pick the optimal combination between Rock II concentration and reaction time. If short

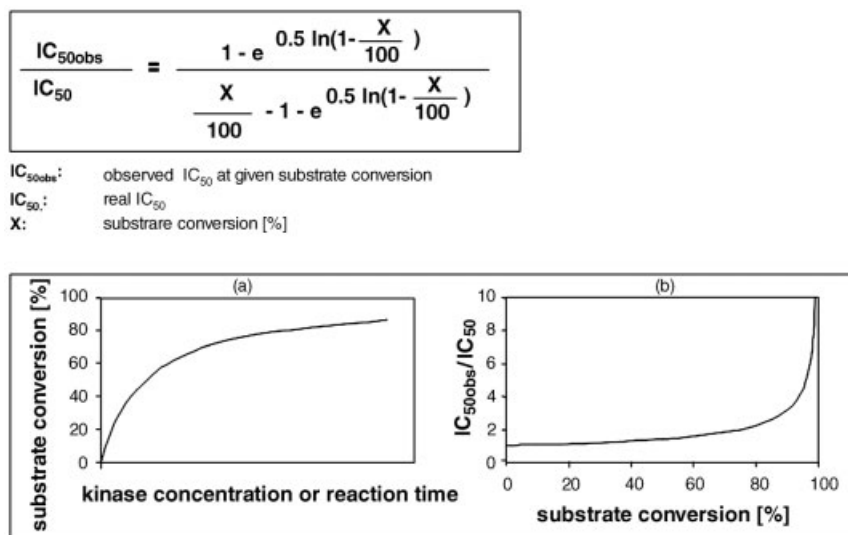


Figure 1.11 The given equation describes the dependency between measured IC_{50} (IC_{50obs}) value and substrate conversion. By increasing kinase concentration at a constant reaction time, or by increasing the reaction time at a constant kinase concentration, more and more substrate will be converted. At very high kinase

concentrations or at very long reaction times, 100% of the substrate is converted (a). Using the given equation, the ratio between observed IC_{50obs} and real IC_{50} is plotted against the substrate conversion (b). At substrate conversions above 70%, the observed IC_{50obs} becomes significantly higher than the real IC_{50} .

reaction times are needed, for example, 10 nM Rock II and a reaction time of 60 min can be selected. If low Rock II concentrations are required, for example, to shift the assay wall to lower IC_{50} values (see Section 1.1.2), a Rock II concentration of 2.5 nM and a reaction time of 240 min could be chosen without changing the intensity of the

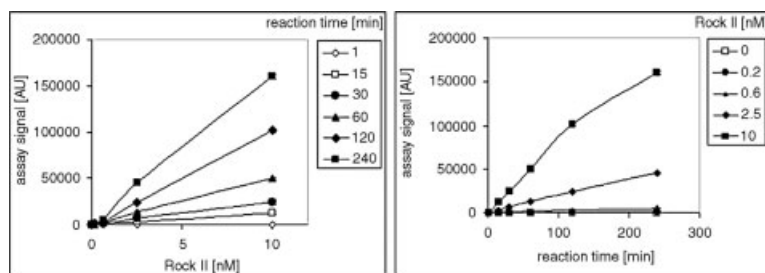


Figure 1.12 Different concentrations of Rock II were incubated for the indicated reaction time with 25 μ M ATP, 2.5 μ Ci/ml 33 P-Y-ATP, and 10 μ M S6-derived substrate peptide in 40 μ l 20 mM Mops pH 7.5, 10 mM $MgCl_2$, 0.01% Triton X-100, 1 mM DTT. Reactions were terminated by adding 10 μ l 0.5 M EDTA. The reaction mixtures were transferred to phosphor

cellulose filters and incubated with 60 μ l 0.75% H_3PO_4 for 15 min. Remaining 33 P-Y-ATP was removed from the filters by three washes with 200 μ l 0.75% H_3PO_4 each. The filter-associated substrate-incorporated 33 P was quantified by scintillation counting. Raw data were plotted either against Rock II concentration (a) or reaction time (b).

assay signal (Figure 1.12). Here, we have chosen 2.5 nM Rock II and a reaction time of 60 min for further optimization.

1.2.5

Step 5: Assay Validation by Measurement of the IC_{50} of Reference Inhibitors

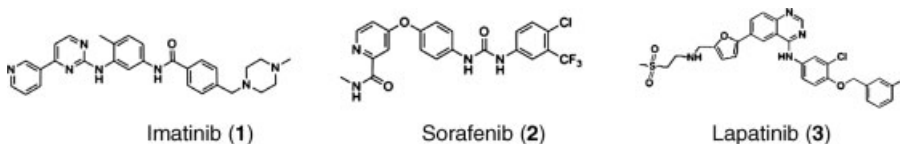
In the last step of the optimization procedure, the assay is validated by the measurement of the IC_{50} values of reference inhibitors. Besides controlling the IC_{50} values themselves, it has to be ensured that the Hill coefficients, reflecting the slope of the IC_{50} curves, are close to a value of 1 (ideally between 0.5 and 1.8). Hill coefficients deviating significantly from 1 indicate that something unexpected is occurring in the assay that in most cases will obscure the measured IC_{50} values. Phenomena such as negative or positive cooperativity of kinase, a contamination with a second kinase that has a different IC_{50} value for the inhibitor from the target kinase, and the presence of different variants of the target kinase (various phosphorylation states, dimers, splice variants, etc.) would influence the Hill coefficient.

In order to validate the optimized Rock II assay, the IC_{50} values of the reference inhibitors H-89 and Y-27632 were measured. The Rock II activity was quantified in increasing concentrations of the reference inhibitors (Figure 1.13). For H-89, an IC_{50} value of 0.18 μ M was determined that is in line with the published value of 0.27 μ M [6]. The IC_{50} value for Y-27632 was measured to be 0.22 μ M. Literature reports a K_i value of 0.14 μ M for Y-27632 against Rock II [7]. Since Y-27632 is an ATP-competitive inhibitor and an ATP concentration was used that equals the ATP K_m , the measured IC_{50} value of 0.22 μ M translates into a K_i value of 0.11 μ M (see Section 1.1.3, Figure 1.9). Thus, the value for Y-27632 was also measured correctly by the developed assay. In addition, the Hill coefficients were calculated to be 1.0 and 0.8, respectively. In conclusion, both the IC_{50} values and the Hill coefficients prove that the optimized Rock II assay is able to measure Rock II IC_{50} values in a reliable manner. Thus, the Rock II assay could be released for a potential Rock II drug discovery project.

1.3

Measuring the Binding Affinity and Residence Time of Unusual Kinase Inhibitors

Besides the classical binding mode, where small-molecule inhibitors bind into the ATP binding cleft forming H-bonds only with the hinge region, there are several known exceptions. Among these kinase inhibitors are examples such as imatinib (1), sorafenib (2), lapatinib (3), and BIRB 796 (4, see below).



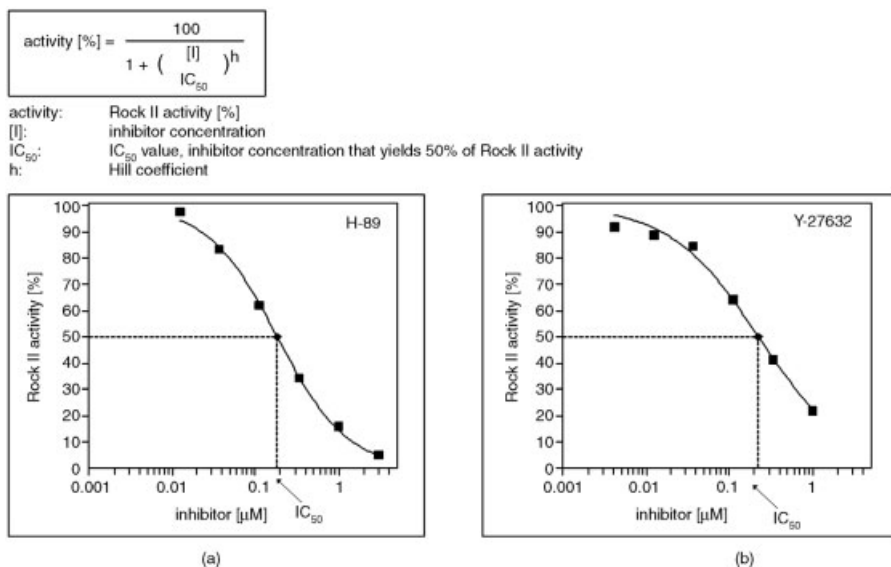


Figure 1.13 2.5 nM Rock II was incubated for 1 h with 25 μM ATP, 2.5 μCi/ml ³³P-Y-ATP, and 10 μM S6-derived substrate peptide in 40 μl 20 mM Mops pH 7.5, 10 mM MgCl₂, 0.01% Triton X-100, 1 mM DTT in the presence of the indicated concentrations of the reference inhibitor H-89 or Y-27632. Maximal Rock II activity was measured in the absence of inhibitor. Background signal was determined in the absence of Rock II. Reactions were terminated by adding 10 μl 0.5M EDTA. The reaction mixtures were transferred to phosphor cellulose filters and incubated with 60 μl 0.75% H₃PO₄ for 15 min. Remaining ³³P-Y-ATP was

removed from the filters by three washes with 200 μl 0.75% H₃PO₄ each. The filter-associated substrate-incorporated ³³P was quantified by scintillation counting. Rock II activity was expressed by calculating the ratio between the background-corrected assay signals in the absence and presence of the indicated inhibitor concentrations. The Rock II activity was plotted against the inhibitor concentration and fitted to the given equation. For H-89 (a) and Y-27632 (b), IC₅₀ values of 0.18 and 0.22 μM and Hill coefficients of 1.0 and 0.8 were calculated, respectively.

These specific inhibitors of protein kinases take advantage of the conformational differences between active and inactive forms of kinases [8]. The main determinant of these forms is the so-called activation loop that can undergo large conformational changes.

Quite often, but not always, these nonclassical inhibitors also show unusual binding characteristics that require special methods for evaluation. The classical way of IC₅₀ determination, which has been described in detail in Section 1.1, does not take into account the fact that inhibitors might also show nonclassical enzyme kinetics. Therefore, the activity of these inhibitors might be largely underestimated during the course of an optimization program or might be entirely overlooked in a high-throughput screening campaign.

Several methods have been used in the past to evaluate novel protein kinase inhibitors. To realize the full potential of these nonclassical protein kinase inhibitors,

generic and efficient tools are needed that apply the strengths of diversity-oriented chemical synthesis to the identification and optimization of lead compounds for disease-associated protein kinase targets.

Inactive conformation was first observed crystallographically for the unliganded IR kinase [9], but it was not until the structures of Abl in complex with imatinib and analogues were solved that it became clear that this conformation could be exploited by inhibitors [10] (see also Chapter 6). The so-called DFG-out conformation creates an additional hydrophobic pocket adjacent to the ATP pocket that is frequently referred to as the “allosteric site” [11] or the “deep pocket.” Because the amino acids surrounding this pocket are less conserved relative to those in the ATP binding pocket, it has been proposed that it may be easier to achieve kinase selectivity with “deep pocket” binding inhibitors [12] compared to the classical inhibitors.

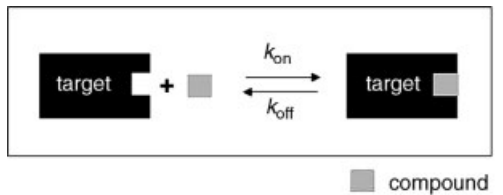
Very often these nonclassical inhibitors show remarkable cellular activity that could result from binding to the inactive conformation of kinases that may be more accessible in the cellular environment.

It has been discussed that the departure from the kinase–ligand equilibrium interaction comprises an important determinant of the *in vivo* effectiveness of small-molecule drugs. Copeland *et al.* propose that the most crucial factor for sustained drug efficacy *in vivo* is not the apparent affinity of the drug to its target *per se*, but rather the residence time of the drug molecule on its molecular target [13].

The term residence time in the field of drug target interaction is defined as the period for which the receptor is occupied by a ligand. A long dissociation half-life of an intracellular receptor would be expected to translate into sustained efficacy in cell culture after removal of the ligand supply from the extracellular medium. For the *in vivo* situation, the duration of efficacy of a ligand is no longer well described by the *in vitro* measured dissociation constant, but rather depends on the rate of receptor–ligand association (k_{on}) and, most critically, on the dissociation rate constant, or off rate (k_{off}), of the receptor–ligand complex. The off rate can be simply translated into a dissociative half-life for the receptor–ligand complex, and this half-life is a direct measure of the residence time (see Figure 1.14). As demonstrated in a simulation (Figure 1.15), the residence time becomes the driving parameter for the efficacy and the pharmacodynamic behavior of a drug candidate *in vivo*, especially when the plasma half-life is short. Over time, cKIT with *low* binding affinity but *long* compound residence time is more efficiently inhibited than DDR1 with its *high* binding affinity but *short* residence time.

Both the improvement of the metabolic stability and the residence time can be used to optimize the efficacy of an inhibitor compound. As shown in the simulation, the affinity data alone would be a misleading parameter. In addition to the efficacy, the *in vivo* selectivity is affected both by the affinity and by the residence time (Figure 1.15).

Various experimental approaches have been considered to analyze new protein kinase inhibitors. In recent years, the pharmaceutical industry has identified the need both for the discovery of inhibitors with novel modes of inhibition and for the detailed characterization of their lead compounds in preparation for clinical assess-



$$\text{residence time} = \frac{1}{k_{\text{off}}} \quad \frac{k_{\text{off}}}{k_{\text{on}}} = K_d$$

Figure 1.14 Association and dissociation of a receptor–ligand complex and calculations of the parameters residence time, k_{off} , k_{on} , and K_d .

ment. A selection of methods will be discussed and the advantages and disadvantages will be compared.

1.3.1

Washout Experiments

A recent example of the effects of ligand dissociation half-life comes from the work of Wood *et al.* on inhibitors of epidermal growth factor receptor (EGFR) tyrosine kinase activity [14]. The K_d values, off rates, and the recovery of cellular proliferation after washout for three similarly potent inhibitors of EGFR were measured: GW572016 (lapatinib (3)), ZD-1839 (Iressa), and OSI-774 (Tarceva). These compounds bind to the ATP binding pocket of the kinase, but display maximum affinity for different conformation states of the enzyme. For ZD-1839 and OSI-774, a rapid recovery of the

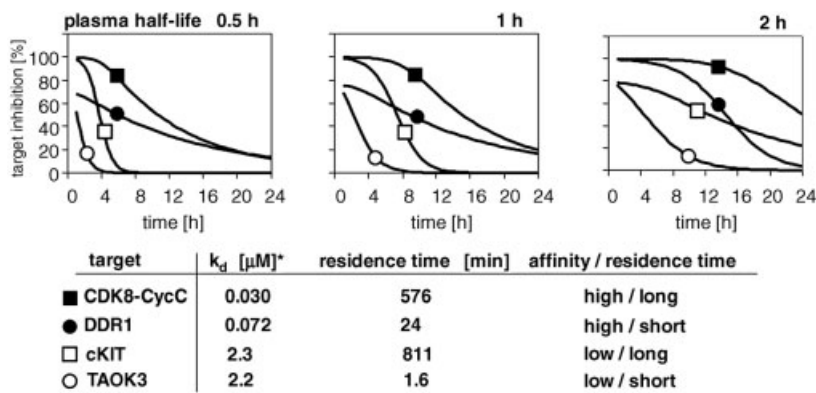


Figure 1.15 Simulation of *in vivo* inhibition of four targets of the bRaf inhibitor sorafenib: impact of residence time and K_d on pharmacodynamics for three hypothetical compound plasma half-lives ($C_{\text{max}} = 10 \mu\text{M}$).

Especially for drugs with short or medium plasma half-lives, *in vivo* target inhibition is determined by binding kinetics rather than by binding affinity.

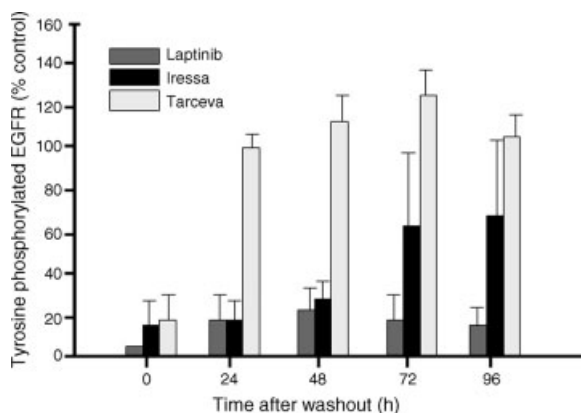


Figure 1.16 Recovery of EGFR autophosphorylation after treatment with lapatinib, Iressa, and Tarceva. Logarithmically growing HN5 cells were treated with 1 μ mol/l inhibitor in culture media for 4 h. The media was removed, cells were washed twice, and fresh compound-free media was added. The cells were lysed at the indicated time after inhibitor

washout and EGFR was isolated by immunoprecipitation. The level of tyrosine-phosphorylated EGFR was quantified for each condition and expressed as the percentage of vehicle-treated sample. The results represent the mean value of three independent experiments (adapted from Ref. [14]).

kinase activity was observed after washing out the compound. In contrast, the recovery was very slow after treatment with GW572016 (see Figure 1.16).

These data provide a clear example of the extended duration of cellular efficacy that can be achieved with drugs that have long dissociative half-lives. In addition, these data illustrate that the duration of cellular effects of slow dissociating ligands is much longer than would be predicted simply from a consideration of the dissociative half-life of the receptor–ligand complex.

1.3.2

Surface Plasmon Resonance

For the real-time and label-free determination of protein kinase inhibitor binding kinetics, surface plasmon resonance (SPR)-based biomolecular interaction analysis has been used [15, 16].

Specifically for protein kinase, mild immobilization conditions of the kinases to the surface and a carefully composed assay buffer are usually key success factors. With the SPR technology, both direct binding studies of compounds to immobilized kinase and kinase activity assays to confirm inhibitory effects can be performed. Furthermore, detailed kinetic analyses of inhibitor binding and competition assays with ATP for the identification of competitive inhibitors can be determined [16].

The SPR technology requires a sensor surface where typically the protein is immobilized. Using the flow system of the instrument, the analyte passes over the sensor surface. The interaction kinetic, that is, the rates of complex formation (k_a) and

dissociation (k_d), can be determined from the information provided by the sensorgram.

If binding occurs as the sample passes over the prepared sensor surface, the response in the sensorgram increases. If equilibrium is reached, a constant signal will be seen.

Replacing the sample with buffer causes the bound molecules to dissociate and the response decreases. On the basis of the online monitoring of the association and the dissociation process, k_{on} , k_{off} , and K_d can be determined (Figure 1.17).

Among others, p38alpha mitogen-activated protein kinase has been used as a model system. p38alpha MAP kinase has been immobilized to use it as a highly active protein surface, which is the critical and often limiting factor in the development of biosensor methods. In this specific biosensor method, a ligand-induced structural stabilization of p38alpha step was performed during the immobilization step, which should also prove useful for other kinases and ligands [15].

The SPR-based methods can also provide an efficient way to directly and reproducibly examine dissociation constants, kinetics, and even thermodynamics for small-molecule binding with the limitation that one binding partner, typically the protein, has to be bound to the surface of a chip.

Significant progress has been made in recent years in addressing some of the limitations of the SPR technology. Both the throughput and the sensitivity have been dramatically increased. The instruments, including the software, have meanwhile been adapted to a high-throughput use. Rich and Myszka [17] have summarized the most advanced instruments and approaches to higher throughput.

While SPR is the most direct method to evaluate the kinetic behavior of enzymes and inhibitors, the availability of highly pure and homogeneous protein is sometimes

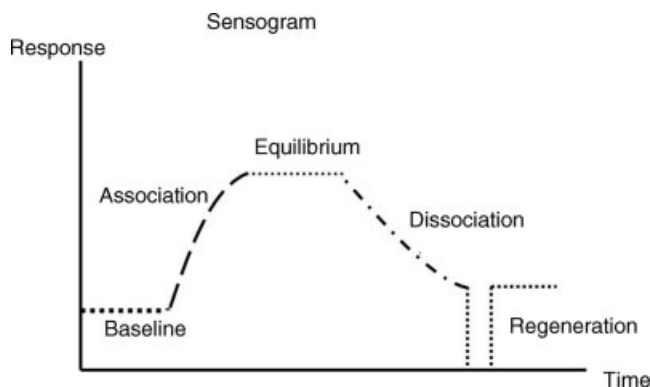


Figure 1.17 Surface plasmon resonance sensorgram. The binding of the analyte to the surface, which is typically coated with protein, is monitored online until the equilibrium is reached. Addition of the buffer causes dissociation of the analyte. When the baseline

level is reached, the surface can be regenerated and is used for the next experiment. The concentration- and time-dependent association and dissociation of the analyte allow the calculation of K_d , k_{on} , and k_{off} .

limiting. In addition, the study of full-length proteins and protein complexes is still a challenge.

1.3.3

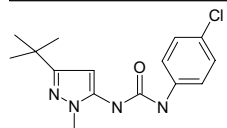
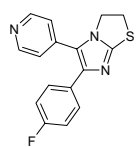
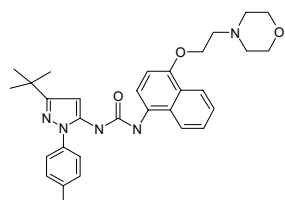
Classical Methods with Fluorescent Probes

The most widely explored slow inhibitor target interaction is that of BIRB796 with p38alpha [18–20]. The apparent IC_{50} decreases as the time of preincubation with the inhibitor increases.

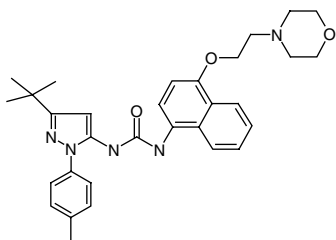
The interaction of the diaryl urea series that led to BIRB796 has been guided by a fluorescence-based assay, where the kinase in solution was studied with a fluoroprobe. The fluorescence-based assay has been established that is capable of monitoring binding in real time. The binding of the fluoroprobe of a classical inhibitor to nonactivated p38 MAP kinase was quite rapid and required the use of a stopped flow spectrophotometer to determine kinetic rate constants (Table 1.1).

Similarly, the classical ATP site binding inhibitor SB203580 has fast association and dissociation rates for the kinase. In contrast, the association of a fluorescent analogue of BIRB796 with p38MAP kinase is much slower. The calculated half-life for the dissociation of BIRB from p38MAP kinase is 23 h. BIRB796 represents one of the most potent and slowest dissociating inhibitors against human p38 MAP kinase known at present.

Table 1.1 *In vitro* data for selected p38 inhibitors.

	k_{on} ($M^{-1} s^{-1}$)	k_{off} (s^{-1})	K_d (nM)
	$1.2 \times 10^5 \pm 3.5 \times 10^4$	$1.4 \times 10^{-1} \pm 1.2 \times 10^{-2}$	1160
	$4.3 \times 10^7 \pm 2.2 \times 10^5$	$7.7 \pm 13 \times 10^{-1}$	180
	$8.5 \times 10^4 \pm 2.6 \times 10^2$	$8.3 \times 10^{-6} \pm 1.5 \times 10^{-7}$	0.1

K_d was determined at 23 °C and calculated as k_{off}/k_{on} in nM determined with a fluoroprobe assay (see Ref. [18]).

**Birb796 (4)**

The fluoroprobe assays are very easy to use, but are limited by the availability of a suitable fluoroprobe addressing the binding site of interest.

1.3.4

Preincubation of Target and Inhibitor

To further confirm the slow binding behavior, Kroe *et al.* [18] also monitored the apparent inhibitory potency of BIRB796 as a function of the preincubation time in a standard IC_{50} experiment. A decrease in the apparent IC_{50} value from 97 to 8 nM after 2 h of preincubation is consistent with the slow binding behavior. In contrast, the pyridinyl-imidazole inhibitors reached equilibrium within 30 min.

Another example where preincubation experiments have been valuable for the determination of the kinetic interaction is the inhibitor sorafenib and its interaction with the protein kinase bRaf (Figure 1.18) [21, 22] (Neumann *et al.*, unpublished data). While the activity of the enzyme remains the same, the IC_{50} significantly decreases with increased preincubation.

This type of preincubation experiments can be routinely used to determine very slow binding kinetics using the routine kinase assay as described in Section 1.1. The limitation here is that a kinetic resolution is not possible during the incubation time of the assay. Therefore, these assays are limited to extremely slow compound–target interactions.

1.3.5

Reporter Displacement Assay

A reporter displacement binding assay has been described by Neumann *et al.* [23] that allows to study the kinetic interaction in 384-well format with very little protein requirement, solving the issues of limited throughput and the need for large quantities of protein. The reporter displacement assay is based on a reporter probe that is distinctively designed to bind to the ATP binding site of the protein kinase target. The proximity between reporter and protein results in the emission of an optical signal (Figures 1.19 and 1.20). Compounds that bind to the same binding site displace the probe and cause signal loss. The reporter displacement assay is a homogeneous method that can be used both for the DFG-in and for the DFG-out conformation of the protein kinase. The displacement of the reporter is continuously

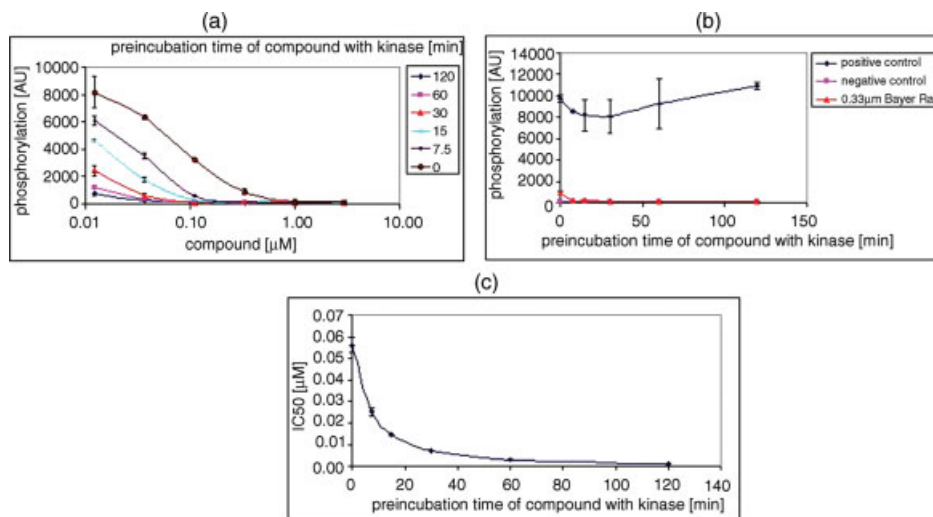


Figure 1.18 Preincubation experiments with sorafenib and bRaf were performed using the radioactive assay as described in Section 1.1. (a) The phosphorylation of the substrate peptide is monitored over a range of compound concentrations and different preincubation times; (b) to monitor the stability and the activity

of the bRaf kinase during the incubation period, the phosphorylation of the peptide substrate is monitored in parallel to the increased preincubation time; and (c) the IC_{50} values are calculated for each time point of preincubation, resulting in a significant decrease in IC_{50} over time.

measured over time. The signal for full probe binding is measured in the absence of compound and the signal for complete reporter displacement is quantified in the absence of protein kinase. The reporter probe is designed to have fast association and dissociation kinetics in order to ensure that compound binding and not reporter probe dissociation is the rate-limiting step. The signal decay describes directly the association of the compound with protein kinase. In order to calculate k_{on} and k_{off} of the protein inhibitor interaction signal, the observed association rate k_{obs} is determined for each inhibitor concentration by fitting the corresponding signal decay with a monoexponential decay equation. The exponential coefficient of each monoexponential fit equals k_{obs} for the particular inhibitor concentration. The resulting k_{obs} values were plotted against their inhibitor concentration and fitted to Equation 1.1 describing the dependency between the observed association rate k_{obs} , the association rate k_{on} , the dissociation rate k_{off} , and the inhibitor concentration. The dissociation rate k_{off} is given by the y -intercept and the association rate k_{on} by the slope of dependency between k_{obs} and [inhibitor]. Residence time is calculated by Equation 1.2.

$$k_{obs} = k_{off} + k_{on}[\text{inhibitor}] \quad (1.1)$$

$$\text{Residence time} = 1/k_{off} \quad (1.2)$$

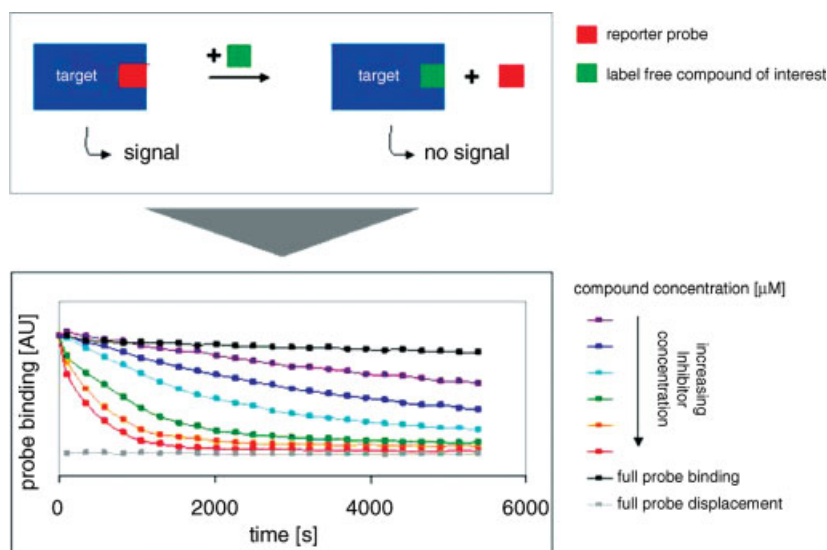


Figure 1.19 Assay principle of the reporter displacement binding assay. Binding of the reporter probe generates a specific signal. Displacement of the reporter probe by a competing compound

of interest results in signal loss. By analyzing the kinetics of signal loss at various compound concentrations, values such as K_d , k_{on} , k_{off} , and residence time can be calculated.

The reporter displacement binding assay allows the testing of entire compound series, compound collections, and specifically designed compounds and requires extremely low protein concentrations. The technology is limited by the design of a proper reporter probe addressing the binding site of the kinase of interest.

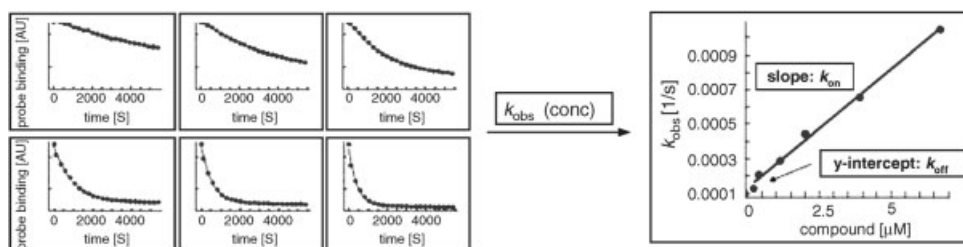


Figure 1.20 Exponential coefficient k_{obs} for each inhibitor concentration is calculated by fitting the signal decays with a monoexponential decay equation. The k_{obs} values were plotted against the corresponding inhibitor concentration and k_{on} and k_{off} were determined by fitting to Equation 1.1. For the plot, only k_{obs}

values are used that are well defined. Those k_{obs} values were omitted from analysis if signal decay for a particular inhibitor concentration was faster than the detection limit of the reporter displacement assay or if no significant reporter displacement occurred at low inhibitor concentration.

1.3.6

Implications for Drug Discovery

The lack of high-throughput technologies for measuring the residence time throughout a lead finding and optimization program has limited the number of programs where the residence time has actually been used in parallel to affinity data in the past. The increased availability of such data is inspiring the medicinal and computational chemists to design and synthesize novel compounds. Many different design principles specifically geared toward compounds with long residence times have recently been published [23–25a,b].

Besides the specific synthesis of slow interaction inhibitors, there is also need for the measurement of interaction kinetics if short residence times are required. Nonclassical inhibitors need special consideration both in the hit identification process and in the lead optimization phase. There are a number of challenges in the identification and characterization of compounds that prevent the activation of protein kinases or induce conformational changes. Understanding the relationship between compound structure and biological activity is key to drug design. The mechanism of active compounds must be deconvoluted to determine their functionality. Binding studies are often used for the kinetic analysis of inhibitors, but enzyme activity assays are equally important since only the inhibition of the enzymatic activity will typically lead to a cellular active inhibitor.

With more and more slower interaction inhibitors being characterized in detail, there are new questions arising in the field. It is not known which kinases are amenable to the so-called “deep pocket” binding inhibitors. *In silico* predictions are ongoing to determine the status of such binding capacities [26] and programs are specifically designed for their predictions. The number of deep pocket binders is still too limited to answer the question if the inhibitor is inducing the DFG-out binding or if the kinase is available for this type of binding. In addition, the selectivity profiles of most of the deep pocket binding inhibitors have been determined only in one dimension: the K_d values are available for a vast number of kinases. The question is can these K_d values be trusted, considering that preincubation with the inhibitor might significantly change the K_d value. Neumann *et al.* (submitted for publication) have determined for the first time the kinetic selectivity panel of the bRaf inhibitor sorafenib. The residence times for one inhibitor against a set of protein kinases ranges from a few seconds to 300 min significantly influencing the impact on the pharmacodynamic behavior of such a compound.

The residence time plays a major role especially in the case when the metabolic stability of the inhibitor is very short. Long residence time on the target can help introduce a better *in vivo* selectivity of an inhibitor and can help overcome the pharmacological shortcomings of an inhibitor. The challenges concerning the pharmacology of protein kinase inhibitors will be discussed in Section 1.4.

1.4

Addressing ADME Issues of Protein Kinase Inhibitors in Early Drug Discovery

1.4.1

Introduction

Ideally, the optimization process of potential hits to leads and finally to candidates suitable for preclinical and clinical trials should be guided not only by good pharmacodynamic (PD) parameters but also by satisfactory pharmacokinetic parameters in order to avoid attrition during drug development [27]. The PK behavior of an administered drug is determined by processes such as absorption, distribution, metabolism, and excretion (commonly referred to as ADME processes). Mainly during the past two decades, a toolbox of diverse *in vitro* ADME technologies has been elaborated that enables scientists to filter promising drug candidates at an early stage of drug discovery when usually only few *in vivo* data are available [28, 29].

According to the Traxler's pharmacophore model of small-molecule compounds binding to the active site of protein kinases, ATP-competitive protein kinase inhibitors need to incorporate certain structural and physicochemical specificity determinants to be able to fit into the catalytic cleft of the target protein kinase in an appropriate manner (Figure 1.21). Due to the conservation of structural features within the ATP binding cleft, the physicochemical requirements are quite similar across different classes of protein kinase compounds.

However, as much as the required determinants are crucial for the potency and selectivity of small-molecule compounds, they might translate into poor ADME/PK parameters. This especially holds true for ATP-competitive protein kinase inhibitors as they usually carry lipophilic functional groups that extend more or less deeply into

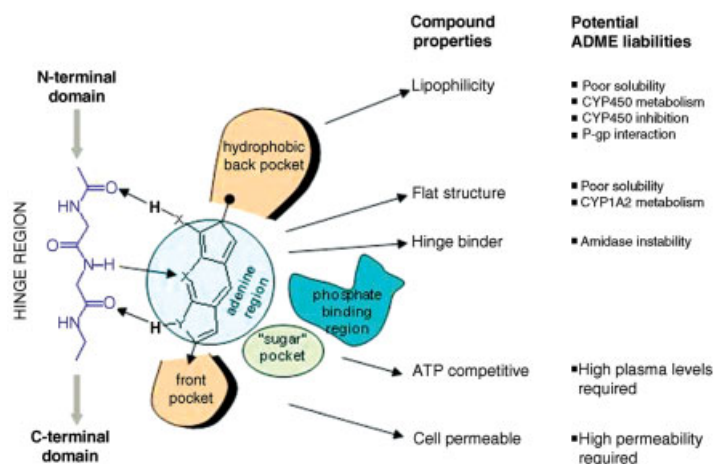


Figure 1.21 Potential ADME issues of small-molecule inhibitors binding to the catalytic cleft of protein kinases according to Traxler's pharmacophore model.

the hydrophobic backpocket of the target kinase. Common ADME liabilities associated with lipophilic moieties are poor solubility, enhanced metabolism by or inhibition of cytochrome P450 enzymes (CYP450s), and the interaction with transporter proteins such as P-glycoprotein (P-gp). Moreover, ATP-competitive protein kinase inhibitors have to efficiently penetrate cellular membranes in order to bind their target. As a consequence, both high plasma levels and high cell membrane permeability are mandatory to reach intracellular compound concentrations high enough to compete with intracellular ATP levels (Figure 1.21).

Thus, expected PK liabilities of ATP-competitive protein kinase inhibitors are likely to deal with insufficient drug absorption and increased drug metabolism raising the need for an ADME screening platform specifically adapted to protein kinase drug discovery programs. The implementation of such a kinase inhibitor-directed ADME approach should be beneficial to identify potential PK problems early in the discovery process and help circumvent these problems in parallel to the optimization of potency and selectivity of kinase inhibitor compounds.

This section will give a brief overview of *in vitro* technologies that address ADME-related characteristics of ATP-competitive protein kinase inhibitors that are most relevant for the routine screening of compounds in the drug discovery phase (Table 1.2). It will mainly focus on the context and the methodologies addressing drug absorption and drug metabolism as the two most crucial *in vitro* PK parameters for protein kinase inhibitors.

Table 1.2 Overview of *in vitro* assays relevant to address potential ADME liabilities of ATP-competitive protein kinase inhibitors in the drug discovery phase.

PK parameter	Assay	Method	Reference
Absorption	Solubility	Shake flask (solution in equilibrium)	[64]
		Turbidimetry	[33]
		Nephelometry	[65]
		Direct UV spectroscopy	[66]
Absorption/volume of distribution	Lipophilicity	Shake flask (partition in octanol versus water/buffer)	[67]
		Direct chromatography	[68]
Absorption	Ionization (pK_a)	pH-metric titration	[69]
Absorption/oral bioavailability	Permeability	PAMPA	[38]
Absorption/excretion/ CNS penetration	P-gp interaction	Caco-2	[41]
		Monolayer efflux	[45]
		ATPase	[70]
		Calcein AM	
Metabolism	Hepatocyte stability	Intrinsic clearance	[57]
	Microsomal stability		[58]
Drug–drug interaction	CYP450 inhibition	Fluorescence-based IC_{50} /	[61]
		K_i determination	

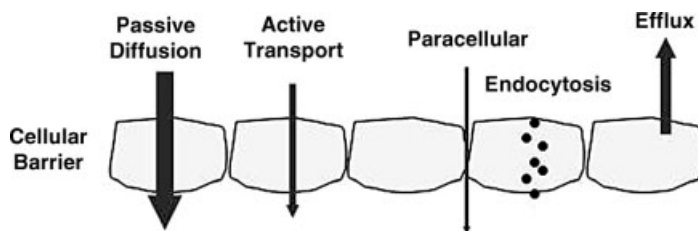


Figure 1.22 Mechanisms of membrane permeation [31]. Passive diffusion is the most common route of drug absorption through membranes and tissues. Nevertheless, other

routes of transport exist and the total percentage of the dose absorbed may be the result of a combination of several of these processes.

Primarily, the driving forces for the absorption of compounds through the gastrointestinal wall to reach systemic circulation are concentration differences, and thus, the rules of passive diffusion can be applied for both the transcellular penetration of lipophilic compounds and the paracellular diffusion of small polar compounds through and between gastrointestinal cells, respectively [30]. Other means of permeation that contribute to drug absorption are active transport by a transporter protein and endocytosis. Moreover, drugs can be effluxed by transporter proteins, such as P-gp or MRP2 (Figure 1.22).

Prior to absorption through the gastrointestinal cell walls, orally administered compounds need to dissolve in the aqueous contents of the gastrointestinal tract. This process depends on the surface area of the dissolving solid and the solubility of the drug at the surface of the dissolving solid [32]. Once the compound is dissolved, all further processes will take place in solution. Thus, solubility can be viewed as the first step to absorption. The solubility of the administered compound, in turn, depends on its physicochemical properties, for example, lipophilicity, ionization (pK_a), hydrogen bonding, molecular size, polarity, shape, and so on. Lipinski defined a widely accepted concept of druglikeness on the basis of cutoff values for key physicochemical properties known as the “rule of five” [33]. Accordingly, compounds are likely to show poor absorption when their molecular weight is >500 Da, their calculated octanol/water partition coefficient $\log P$ is >5 , the number of their H-bond donor functions is >5 , and the number of their H-bond acceptor functions is >10 . It has been suggested that drugs that fail to meet the “rule-of-five” criteria are unlikely to be absorbed and should be discontinued from development. Polar surface area (PSA) is another important parameter that is often taken into account for property-based design. It was deduced that orally active drugs that are passively transported by the transcellular route should not exceed a polar surface area of about 120 \AA^2 [34]. All these parameters can be calculated *in silico* by commercial programs that might be helpful in characterizing the physicochemical properties of a compound before it is even synthesized.

The incorporation of an ionizable moiety, such as a basic amine, into a template is a frequently employed means to improve a compound’s aqueous solubility and hence absorption (Figure 1.23). Basic drugs will have increased solubility in the acidic

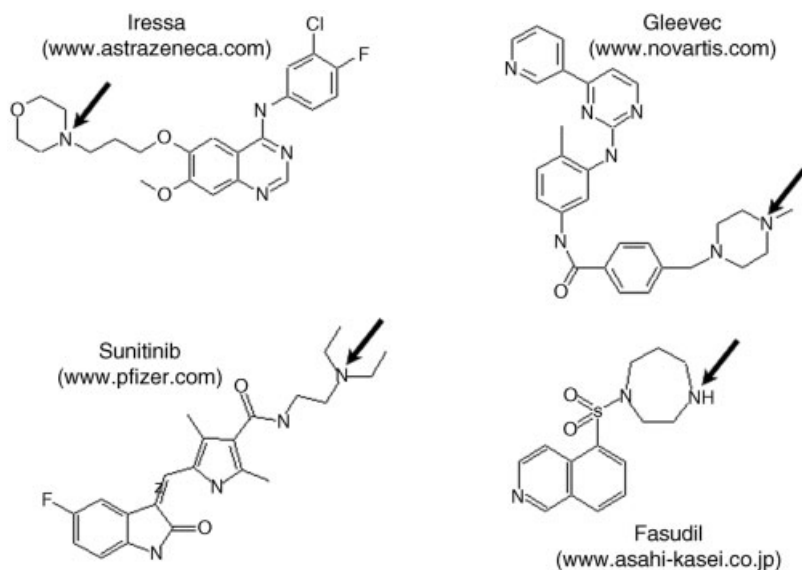


Figure 1.23 Structural formulas of approved ATP-competitive protein kinase inhibitors. Arrows point at secondary or tertiary amines that have been introduced as ionizable centers to improve aqueous solubility.

environment of the stomach where the dissolution of the compound usually takes place. In addition, if a drug has an ionizable center, then solubility can be improved by salt formation.

In contrast to the well-defined cutoff values of the rule of five, there is no generic guideline for the level of solubility sufficient to achieve oral absorption. Rather, estimates of the minimum solubility for oral absorption depend on the permeability of the compound and the required dose [35]. It has been shown that according to its permeability characteristics, the required solubility of a compound might vary between three orders of magnitude at various expected clinical potencies (Table 1.3).

To address drug absorption *in vitro*, scientists are, therefore, advised to embrace a whole set of models and methods that determine solubility, lipophilicity, ionization, permeability, and the interaction with transporters. Some of the most relevant experimental approaches and their predictive power for a potential absorption liability are reviewed below.

Table 1.3 Minimum acceptable solubility for low, medium, and high permeable compounds in $\mu\text{g/ml}$ at a projected clinical dose to achieve oral absorption.

Projected clinical dose (mg/kg)	Low permeability	Medium permeability	High permeability
0.1	21	5	1
1.0	207	52	10
10	2100	520	100

Source: Adapted from Ref. [35].

1.4.2

Experimental Approaches to Drug Absorption**1.4.2.1 Measuring Solubility**

As mentioned above, poor solubility is the key parameter to dissolution of compounds following oral administration that is likely to result in incomplete absorption. Experimentally, solubility can be determined under kinetic or thermodynamic conditions [36]. Thermodynamic solubility is the concentration of compound in a saturated solution when excess solid is present, and solution and solid are at equilibrium. Once this equilibrium has been established (24–72 h), the two phases are separated by filtration and/or centrifugation and the concentration of the compound in the dissolved phase is measured by HPLC–UV/Vis or HPLC–MS (shake flask method).

In contrast, kinetic solubility is the concentration of a compound in solution at the time when an induced precipitate first appears. Usually, kinetic solubility is measured from predissolved stocks (e.g., in DMSO) that are diluted in aqueous buffers followed by short read times in the low tens of minutes with or without filtration. The presence of a cosolvent has an impact on the apparent solubility of the compound. Since there is no crystal lattice to disrupt for compounds in DMSO solution, a compound's kinetic solubility is usually higher than the solubility value obtained from a thermodynamic experiment.

Measuring thermodynamic solubility by shake flask is thus more accurate than any apparent solubility determination by kinetic approaches. Moreover, the thermodynamic assay also provides additional information about the chemical stability and purity of the compound. However, as it is laborious and consumes larger amounts of compound, the throughput is normally far below kinetic solubility assay formats. Thus, although thermodynamic solubility measurements play only a minor role during the hit and lead generation phase of the drug discovery process, they are important during lead optimization, particularly when it comes to the selection of candidates for preclinical drug development. At this stage, the thermodynamic assay is a crucial test to conclude whether a compound has sufficient solubility to have the potential for oral activity.

In contrast, kinetic solubility assays can be viewed as early discovery formats that are most likely to predict the early drug metabolism or biology studies when the solubility assay conditions mimic the dosing schemes in early drug discovery experiments. A number of kinetic solubility assays have been developed most of which can be conducted under high-throughput conditions (Table 1.2).

1.4.2.2 Measuring Lipophilicity and Ionization

Lipophilicity is a key physicochemical parameter for the estimation of membrane permeability, distribution, and route of metabolic or renal clearance. Widely used parameters to measure lipophilicity are the partition coefficient (P) and the distribution coefficient (D):

$$P = [C]_o / [C]_w$$
$$D = \sum [C]_o / \sum [C]_w$$

where $[C]_o$ and $[C]_w$ are the concentrations of the compound in octanol (o) and in water (w), respectively.

The P value itself is a constant that defines the ratio of the concentration of the neutral form of the molecule between the two immiscible liquids, water and octanol. Substances with P values have elevated affinity for apolar solvents and are likely to show poor absorption if they exceed a P value of 10^5 (see the “rule of five”). D is the partition coefficient at a particular pH value and takes into account all the existing compound species in octanol or water/buffer. D is not constant and varies according to the protogenic nature of the molecule. It is normally convenient to use the logarithmic scale, $\log P$ and $\log D$, for P and D values, respectively.

$\log D$ at pH 7.4 is often quoted to give an indication of the lipophilicity of a drug at the pH of the blood. So, it has been suggested that $\log D_{\text{pH } 7.4}$ values between 1 and 3 are in the optimal range for orally active drugs evoking low metabolic liabilities. Above a $\log D_{\text{pH } 7.4}$ value of 3, metabolic liabilities tend to increase while poor solubility can become an issue. Clearly, $\log D_{\text{pH } 7.4}$ values above 5 should be avoided in order to minimize poor absorption, nonspecific binding, and high hepatic clearance while $\log D_{\text{pH } 7.4}$ values below 0 are associated with high renal clearance and poor permeability [37]. Lipophilicity can be increased by increasing molecular size and decreasing hydrogen-bonding capacity.

The pK_a is another important factor in drug design and development that is related to its effect on lipophilicity and solubility. This is because the majority of biologically active compounds comprise functional groups that can be ionized (see above). A high degree of ionization keeps drugs out of cells and decreases systemic toxicity. Thus, the pK_a has a high impact on both the partitioning behavior and the ligand interaction of the potential drug candidate. The pK_a is defined as the negative logarithm of the equilibrium ionization coefficient (K_a) of the neutral and charged forms of the compound.

Equilibrium ionization constants for acids : $K_a = [H^+][A^-]/[HA]$

Equilibrium ionization constants for bases : $K_a = [H^+][B]/[HB]$

Determination of the pK_a allows both to calculate the proportion of neutral and charged species at any pH and to define the basic or acidic properties of the compound. The pK_a itself is a constant and corresponds to the pH at which the concentrations of ionized and neutral forms are equal. It has been suggested that a pK_a in the range of 6–8 is advantageous for membrane penetration.

Since $\log D$ is a pK_a -dependent term for ionizable drugs, it is possible to calculate $\log D$ at any pH if $\log P$ and pK_a values are known. *In silico* tools exist for the calculation of $\log P$ and pK_a values that, although error prone for the prediction of $\log D$, *per se* are useful in the design of $\log D$ assays in order to choose appropriate experimental conditions. *In vitro* methods for lipophilicity and ionization measurements are listed in Table 1.2.

1.4.2.3 Measuring Permeability

Since the oral route is often the preferred one for drug administration, an early estimate of the absorption potential across biological membranes is highly desirable.

A number of *in vitro* models for membrane permeability have been elaborated to date that allow the prediction of the diverse routes of drug absorption *in vivo* (for details see Ref. [38]).

The parallel artificial membrane assay (PAMPA) is a robust and reproducible assay for determining passive, transcellular compound permeation through an artificial lipid membrane made of lipophilic constituents [38]. In 1998, Kansy *et al.* [39] proposed a widely accepted model membrane permeation procedure consisting of filters coated with an alkane solution of lecithin with permeation rates being expressed as % flux values according to the equation:

$$\text{Flux (\%)} = [C]_{\text{test well}}/[C]_{\text{control well}} \times 100\%$$

where $[C]_{\text{test well}}$ is the concentration of the compound in the receiver well on the sample side and $[C]_{\text{control well}}$ is the concentration of the compound in the receiver well on the reference side.

PAMPA flux rates correlate well with passive human absorption values while obviously no prediction can be made for compounds that are actively transported or absorbed by the paracellular route [38].

This method can also be used to determine the effect of pH on compound permeability by adjusting the pH of the solutions used in the analysis. It is also possible to tailor the lipophilic constituents so that they mimic specific membranes such as the blood–brain barrier. Optimization of incubation time, lipid mixture, and lipid concentration can also enhance the assay's ability to predict compound permeability. Although, due to their lipophilic nature, poor flux values are rarely observed with ATP-competitive protein kinase inhibitors, the PAMPA model is nevertheless an indispensable tool for any holistic kinase inhibitor-directed ADME approach.

In addition, several cell-based assays have been developed for permeability screening capable of predicting oral absorption such as Caco-2 and Madin-Darby canine kidney cells (MDCK) [40]. The Caco-2 concept is of particular interest as it is associated with the kinetics of intestinal drug absorption, permeation enhancement, chemical moiety structure–permeability relationships, dissolution testing, and *in vitro/in vivo* correlation (Figure 1.24). In a typical Caco-2 experiment, a monolayer of cells is grown on a filter separating two stacked microwell plates. Test compounds can be introduced to either side of the cell layer and the rate of permeability through the cells is determined from A to B or from B to A according to the formula

$$P_{\text{app}}(\text{nm/s}) = (dQ/dt)/(A \times C_{d0})$$

where P_{app} is the apparent permeability coefficient and dQ/dt is the rate of appearance of drug on the receiver side, C_{d0} is the initial drug concentration on the donor side, and A is the surface area of the filter membrane.

The assay requires that drug absorption rates be determined up to 21 days after Caco-2 cell seeding to allow monolayer formation and cell differentiation including the localization of active transporters to either side of the cell layer. Thus, the permeation observed in a fully differentiated Caco-2 monolayer is a composite of

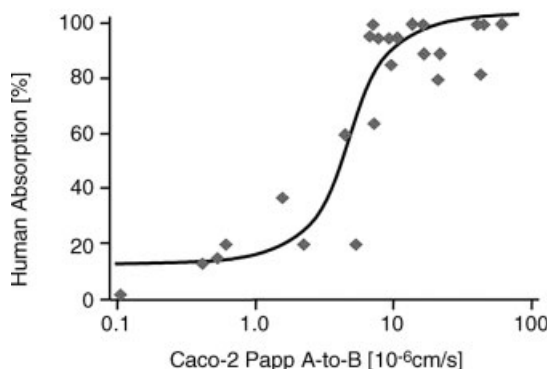


Figure 1.24 Correlation of drug transport rates with human absorption. Drug compounds representing active, passive, and efflux transporters were tested at ArQule, Inc. using the MultiScreen Caco-2 assay system. Each compound's permeability rate was plotted against their percent human absorption values [42].

multiple mechanisms of permeation such as passive transcellular diffusion, active transport through cells, paracellular diffusion, and drug efflux. Furthermore, the presence of CYP450 and phase II conjugating enzymes enables the assessment of the metabolism of a drug during intestinal passage.

Many studies have shown that human oral drug absorption and Caco-2 permeability coefficient have a good sigmoidal relationship, suggesting that human absorption can be well predicted by this *in vitro* model [41].

1.4.2.4 Transporter Assays Addressing P-gp Interaction

The family of ATP binding cassette (ABC) transporters has been identified as a potentially limiting factor in drug absorption [43, 44]. All these proteins catalyze an ATP-dependent active transport of chemically unrelated compounds. Among the many ABC transporters that are expressed in the intestinal tissue, P-gp (MDR1) is perhaps the most studied. P-gp can actively transport a wide variety of chemically diverse compounds out of cells, but preferentially extrudes large hydrophobic, positively charged molecules. Besides intestinal cells, P-gp is present in hepatocytes, epithelial cells of the kidney, and endothelial cells of the blood–brain barrier that might affect not only the absorption but also the distribution and excretion of the drug administered. Due to the significance this transporter has for *in vivo* disposition and PK, identification of compounds that are P-gp substrates can aid optimization and selection of new drug candidates.

A variety of functional *in vitro* test systems have been used to classify compounds as P-gp substrates [45]. These assays either measure the translocation of a P-gp substrate or the substrate-triggered hydrolysis of ATP by P-gp. The interaction of a compound with P-gp can be determined indirectly by measuring the competition for P-gp-mediated transport between a reporter substrate and the compound. Alternatively, the interaction can be detected by directly measuring the translocation of the compound.

As mentioned above, Caco-2 cells provide a useful monolayer efflux method since they extensively express a variety of transport systems including P-gp that is especially advantageous in studies of the interplay between P-gp and other transporter proteins. The major drawback in using Caco-2 cells is that the transporter expression pattern changes with time. Thus, transfected cells are the experimental system of choice as they harbor a well-defined and more stable expression pattern. For instance, MDCKII-MDR1 cells, a transfected version of MDCKII cells that *per se* exhibit relatively low inherent expression of transporters, overexpress P-gp and are sensitive to determining P-gp efflux substrates [46].

The ATPase is one of the most widely used membrane-based assay systems to study the interaction of test compounds with P-gp [47]. Typically, membranes are prepared from recombinant baculovirus-infected insect cells, for example, Sf9 cells. The ATPase assay can determine whether or not a drug stimulates P-gp ATPase activity that would suggest that the drug is a substrate for P-gp transport. While ATP hydrolysis is required for drug transport, the ATPase assay does not directly measure drug transport (e.g., drugs can stimulate ATPase without being transported).

Like the ATPase assay, the whole cell-based calcein AM approach offers the advantage of higher throughput and generic readout in comparison to monolayer efflux assays [48]. Calcein AM is a nonfluorescent, cell membrane-permeable compound that, once inside the cell, can be hydrolyzed to a fluorescent dye that is retained inside the cell. This reaction is efficiently reduced in the presence of functional P-gp as calcein AM is extruded by P-gp. Thus, the intracellular accumulation of fluorescent calcein can be used as a measure of the extent of P-gp inhibition by test compounds. However, similar to ATPase method, the calcein AM assay is not designed to distinguish P-gp substrates from inhibitors.

1.4.3

Experimental Approaches to Drug Metabolism

1.4.3.1 Background and Concepts

Besides excretion of unchanged compounds, drug metabolism is one of the two major pathways for elimination of xenobiotics. Drug metabolism can affect a drug's behavior in many ways. For instance, first-pass metabolism of the compound may lead to a lower oral bioavailability while prodrugs need to be metabolized first to be active. Some metabolites of the administered drug might still be active, while some might be toxic. Furthermore, drug metabolism might have an impact on drug–drug interactions [49].

Traditionally, drug metabolism is divided into phase I and II processes. Compounds are typically oxidized, reduced, or hydrolyzed by phase I enzymes, while phase II metabolism encompasses all sorts of conjugative processes such as glucuronidation, acetylation, methylation, or addition of glutathione or sulfate (Table 1.4). The basic principle of drug metabolism is the conversion of xenobiotics into more hydrophilic inactive derivatives that are readily excreted. The liver is the primary site of drug metabolism although other organs (e.g., small intestine, kidney, lung, etc.) can play an important role.

Table 1.4 Division of metabolizing enzymes into phase I and phase II.

Process	Enzymes
Phase I: oxidation and reduction	Cytochromes P450 (CYP450s), flavin monooxygenase (FMO), peroxidases, amine oxidases, dehydrogenases, azo reductase
Phase I: hydrolysis	Proteases/peptidases, esterases, glucuronidases, sulfatases, phosphatases
Phase II: conjugation	Glucuronosyl transferases, glutathione transferases, sulfotransferases, methyl transferases, acetyl transferases, kinases

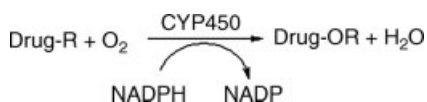
Phase I enzymes are normally oxidative and phase II conjugative.

The cytochrome P450 (CYP450) enzymes are involved in the metabolism of a wide range of drugs [50]. It has been observed that almost every drug is processed by CYP450 enzymes resulting in reduced bioavailability. CYP450s possess the unique ability to activate molecular oxygen to oxidizing species with the capacity to effect oxidation reactions extending from the hydroxylation at the unactivated carbon–hydrogen bond to the N- and S-oxidation of nitrogen and sulfur soft bases (Figure 1.25).

So far, 17 families of CYP450s representing about 50 isoforms have been characterized in the human genome, 3 of which, CYP2D6, CYP2C9, and CYP3A4, have been found to be involved in the metabolism of more than 80% of the pharmaceuticals in humans. Among other isoforms that are involved to a lesser extent CYP1A2 is especially interesting in the context of the optimization of kinase inhibitors as this CYP450 enzyme has a preference for flat molecules that is a common structural feature of ATP-competitive kinase inhibitor compounds (Figure 1.21).

Compounds that remain in the circulation after undergoing phase I metabolism often undergo phase II metabolism. In most of these reactions, a large polar group is added to the compound by transferase enzymes (see Table 1.4). Usually, this involves the interaction of the polar functional group of phase I metabolites, yet in some cases the parent compound might be a direct substrate for phase II metabolism if it provides an appropriate structural function.

One of the most important phase II conjugation reactions is that catalyzed by the UDP glucuronosyl transferase [51]. The glucuronidation reaction consists of the transfer of a glucuronosyl group from uridine 5'-diphosphoglucuronic acid (UDPGA) to substrate molecules that contain oxygen, nitrogen, sulfur, or carboxylic acid functional groups. The resulting glucuronide is ionic, more polar, frequently more water soluble, less toxic, and suitable for excretion in urine or bile.

**Figure 1.25** Overall scheme of a monooxidation reaction by CYP450s using NADPH as an electron-donating cofactor.

Ishikawa could show that after glucuronide conjugation of a drug, the adduct is recognized and transported into the bile by the hepatic transporter MRP2. Ishikawa proposed the term phase III metabolism for the canalicular export of drugs and drug metabolites from hepatocytes indicating the close connection between the oxidation and the conjugation steps of drug elimination [52, 53]. This concept has been expanded to other tissues where export pumps are present. All transporters involved in these mechanisms are members of the family of ATP binding cassette transporters (see Section 1.4.2.4), P-gp (MDR1, ABCB1), MRP2 (ABCC2), and BCRP (ABCG2) being the most prominent. All three transporters are present in the intestine and liver and therefore can reduce oral bioavailability by two mechanisms: direct inhibition of uptake out of the gut and rapid elimination of drugs and their metabolites via bile (Figure 1.26).

How efficiently xenobiotics are cleared by a given organ basically depends on three fundamental parameters: the flow of blood through the organ (Q), the intrinsic capability of the organ to clear the drug (CL_{int}), and the limitation on drug uptake into the clearing organ that in turn depends on the extent of binding of a drug to blood components (i.e., fraction unbound f_u in blood) [55].

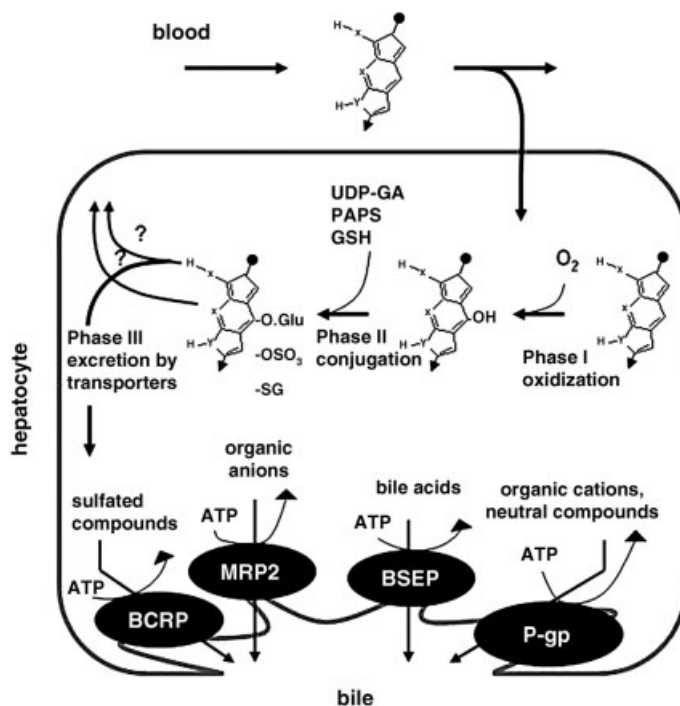


Figure 1.26 Phases of drug metabolism and biliary excretion in human hepatocytes (adapted from Ref. [54]). UDP-GA: uridine diphosphate glucuronic acid; PAPS: 3'-phosphoadenosin-5-phosphosulfate; GSH: glutathione.

Hepatic clearance (CL_H) is pharmacokinetically described by different mathematical models for the disposition of compounds in the liver such as well-stirred, parallel tube, and dispersion [56]. In their simplest forms, they all assume that the passage of a drug from blood in the liver is perfusion limited and that only unbound drug crosses the cell membrane and is available for metabolism.

For instance, under the assumption that the drug is mixed infinitely well inside the liver, the well-stirred model is applicable to the hepatic clearance (CL_H):

$$CL_H = Q_H \times f_{uB} \times CL_{uH,int} / (Q_H + f_{uB} \times CL_{uH,int})$$

where Q_H represents the hepatic blood flow, f_{uB} the fraction of drug unbound in blood, and $CL_{uH,int}$ the intrinsic metabolic clearance of the unbound drug in the liver.

Intrinsic metabolic clearance is a pure measure of enzyme activity toward a drug and is not influenced by other physiological determinants of liver clearance, that is, hepatic blood flow or drug binding within the blood matrix. There are several *in vitro* systems, such as primary hepatocytes, hepatic microsomes, or recombinantly expressed enzymes (see below) to measure the intrinsic metabolic clearance that is then used to estimate hepatic clearance in *in vitro*–*in vivo* extrapolations (Figure 1.27a).

In the absence of enzyme saturation, intrinsic metabolic clearance can be simply determined as the ratio of enzyme kinetic Michaelis–Menten parameters V_{max} and K_m (Equation 1.1). Alternatively, the *in vitro* intrinsic clearance rate can be derived from the rate of drug consumption related to the half-life of the drug in the *in vitro* system used (Equation 1.2):

- 1) $CL_{uH,int} = V_{max} / K_m$
- 2) $CL_{uH,int} = \ln 2 / (\text{in vitro } t_{1/2})$

According to the *in vitro* system used, *in vitro* $CL_{uH,int}$ is expressed per million hepatocytes, per milligram microsomal protein basis, or per unit of recombinantly expressed enzyme. Using standard scaling factors, these *in vitro* values can be extrapolated to predict *in vivo* hepatic clearance on a per-kilogram body weight basis [57, 58].

Metabolic stability rates obtained from microsomal clearance experiments in conjunction with Caco-2 transport data have been used to predict the oral bioavailability of a diverse set of compounds. This model provides a good tool to estimate human oral bioavailability solely from *in vitro* ADME data especially if the oral bioavailability of the compound predominantly depends on permeability and metabolic clearance and not on other means of elimination, for example, renal or biliary excretion (Figure 1.27b).

1.4.3.2 Measuring Metabolic Stability

Although metabolic enzymes are present in many tissues, matrices prepared from ectomized liver are most often employed to investigate the metabolic stability of a test compound. Liver microsomes that can be obtained from various species provide a useful system to measure the rate of oxidative metabolism and formation of oxidative

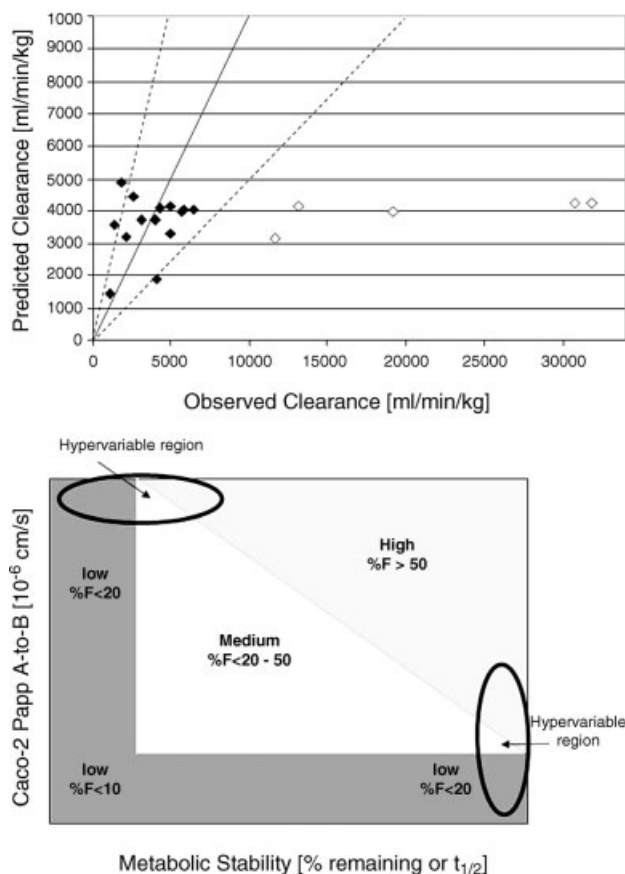


Figure 1.27 (a) Plot of mouse clearance values of diverse structural groups of kinase inhibitor compounds predicted from *in vitro* phase I intrinsic clearance data versus actual mouse clearance values. The prediction is based on the well-stirred model disregarding binding to plasma proteins or microsomal matrix. Most of the compounds fall inside

the twofold error interval (dotted line).

Outliers (indicated as white dots) are assumed to be cleared extrahepatically (Gimple *et al.*, unpublished data). (b) Graphical model for the prediction of oral bioavailability (%F) from Caco-2 Papp A to B values plotted against metabolic stability rates (adapted from Ref. [59]).

metabolites due to their high CYP450 activity [60]. However, phase II activity in liver microsomes is restricted to the conjugation of glucuronic acid by UDP glucuronosyl transferases (UGT). To study other phase II reactions, liver S9 fractions are a more appropriate system as they contain the microsomal and the cytosolic portion of liver cells. Although rather extensive and not readily available, freshly isolated hepatocytes represent the most comprehensive *in vitro* system for hepatic clearance as they encompass the full spectrum of hepatic phase I, phase II, and phase III enzymatic activities. Alternative tissues include cryopreserved hepatocytes and freshly isolated

liver slices. Finally, to exclusively study P450-mediated metabolism, higher throughput screening with human CYP450s is also available [61].

The preferred approach to metabolic stability is to incubate the compound in the matrix of choice against a control matrix containing no active CYP450 in a 96-well format. The remaining compound is detected by chromatographic analysis of the incubation medium followed by HPLC–MS/MS. Besides the determination of the clearance rate of the parental compound, this type of experiment leads to the direct identification of metabolites formed by oxidative, hydrolytic, or transferase reactions.

1.4.3.3 Measuring CYP450 Inhibition

Inhibition of CYP450s is an undesirable characteristic that may lead to drug–drug interactions [62]. *In vitro* experiments that are conducted to determine whether a drug inhibits a specific CYP450 enzyme involve incubation of the drug with probe substrates for CYP450 enzymes. Individually expressed CYP450 enzymes that can be obtained either from baculovirus-infected SF9 cells (supersomes) or from bacterial expression systems provide a convenient model to conduct P450 enzyme inhibition studies [63]. Fluorescence-based assays are available to determine CYP450 inhibition in a higher throughput. The inhibiting potential of compounds is usually tested at a wide range of concentrations on a series of probe substrates that are metabolized toward fluorescent metabolites and expressed as IC_{50} or K_i values. The assay format is in a 96-well plate that can be measured repeatedly in a fluorimeter to allow evaluation of time-dependent inhibition. In theory, significant CYP450 inhibition occurs when the concentration of the compound $[I]$ at its site of action *in vivo* is comparable to or in excess of the K_i . $[I]/K_i$ ratios have been used to predict the likelihood of inhibitory drug–drug interactions *in vivo*; however, quantitative predictions of the magnitude of an *in vivo* interaction, based on *in vitro* data, are not yet possible.

Acknowledgment

We are grateful to Drs Séverine Dedier, Marc-Nicola Sommer, Edmund Hoppe, and Friedrich Kraetzer for numerous fruitful discussions.

References

- 1 Eason, I.H. and Stedman, E. (1936) The absolute activity of choline-esterase. *Proceedings of the Royal Society of London. Series B, Biological Sciences*, **121**, 142–164.
- 2 Strauss, O.H. and Goldstein, A. (1943) Zone behaviour of enzymes. *The Journal of General Physiology*, **26**, 559–585.
- 3 Cheng, Y.C. and Prusoff, W.H. (1973) Relationship between the inhibition constant (K_i) and the concentration of inhibitor which causes 50 per cent inhibition (I_{50}) of an enzymatic reaction. *Biochemical Pharmacology*, **22**, 3099–3108.
- 4 Michaelis, L. and Menten, M.I. (1913) Die Kinetik der Invertinwirkung. *Biochemische Zeitschrift*, **49**, 333–369.
- 5 Wu, G., Yuan, Y., and Hodge, N. (2003) Determining appropriate substrate

- conversion for enzymatic assays in high throughput screening. *Journal of Biomolecular Screening*, **8**, 694–700.
- 6 Davies, S.P., Reddy, H., Caivano, M., and Cohen, P. (2000) Specificity and mechanism of action of some commonly used protein kinase inhibitors. *The Biochemical Journal*, **351**, 95–105.
 - 7 Uehata, M., Ishizaki, T., Stoh, H., Ono, T., Kawahara, T., Morishita, T., Tamakawa, H., Yamagami, K., Inui, J., Maekawa, M., and Narumiya, S. (1997) Calcium sensitization of smooth muscle mediated by a Rho-associated protein kinase in hypertension. *Nature*, **389**, 990–994.
 - 8 Huse, M. and Kuriyan, J. (2002) The conformational plasticity of protein kinases. *Cell*, **109**, 275–282.
 - 9 Hubbard, S.R., Wei, L., Ellis, L., and Hendrickson, W.A. (1994) Crystal structure of the tyrosine kinase domain of the human insulin receptor. *Nature*, **372**, 746–754.
 - 10 Schindler, T.C. *et al.* (2000) Structural mechanism for STI-571 inhibition of Abelson tyrosine kinase. *Science*, **289**, 1938–1942.
 - 11 Pargellis, C., Tong, L., Chruchill, L., Cirillo, P.F., Gilmore, T., Graham, A.G., Grob, P.M., Hickey, E.R., Moss, N., Pav, S., and Regan, J. (2002) Inhibition of p38 MAP kinase by utilizing a novel allosteric binding site. *Nature Structural Biology*, **9**, 268–272.
 - 12 Mol, C.D., Fabbro, D., and Hosfield, D.J. (2004) Structural insights into the conformational selectivity of STI-571 and related kinase inhibitors. *Current Opinion in Drug Discovery & Development*, **7**, 639–648.
 - 13 Copeland, R., Pompliano, D.L., and Meek, T.D. (2006) Drug–target residence time and its implications for lead optimization. *Nature Reviews. Drug Discovery*, **5**, 730–739.
 - 14 Wood, E.R., Truesdale, A.T., McDonald, O.B., Yuan, D., Hassell, A., Dickerson, S.H., Ellis, B., Pennisi, C., Horne, E., Lackey, K., Alligood, K.J., Rusnak, D.W., Gilmer, T.M., and Shewchul, L. (2004) A unique structure for epidermal growth factor receptor bound to GW572016 (Lapatinib): relationship among protein conformation, inhibitor off-rate, and receptor activity in tumor cells. *Cancer Research*, **64**, 6652–6659.
 - 15 Casper, D., Bukhtiyarova, M., and Springman, E.B. (2004) A Biacore biosensor method for detailed kinetic binding analysis of small molecule inhibitors of p38 α mitogen-activated protein kinase. *Analytical Biochemistry*, **325**, 126–136.
 - 16 Nordin, H., Jungnelius, M., Karlsson, R., and Karlsson, O.P. (2005) Kinetic studies of small molecule interactions with protein kinases using biosensor technology. *Analytical Biochemistry*, **340**, 359–368.
 - 17 Rich, R.L. and Myszk, D.G. (2007) Higher-throughput, label-free- real time molecular interaction studies. *Analytical Biochemistry*, **361**, 1–6.
 - 18 Kroe, R.R., Regan, J., Proto, A., Peet, G.W., Roy, T., Landro, L.D., Ruschetto, N.G., Pargellis, C.A., and Ingraham, R.H. (2003) Thermal denaturation: a method to rank slow binding, high-affinity P38 α MAP kinase inhibitors. *Journal of Medicinal Chemistry*, **46**, 4669–4675.
 - 19 Regan, J., Breitfelder, S., Cirillo, P., Gilmore, T., Graham, A.G., Hickey, E., Klaus, B., Madwed, J., Moriak, M., Moss, N., Pargellis, C., Pav, S., Proto, A., Swinamer, A., Tong, L., and Torcellini, C. (2002) Pyrazole urea-based inhibitors of p38 MAP kinase: from lead compound to clinical candidate. *Journal of Medicinal Chemistry*, **45**, 2994–3008.
 - 20 Regan, J., Pargellis, C.A., Cirillo, P.F., Gilmore, T., Hickey, E.R., Peet, G.W., Proto, A., Swinamer, A., and Moss, N. (2003) The kinetics of binding to p38 MAP kinase by analogues of BIRB 796. *Bioorganic & Medicinal Chemistry Letters*, **13**, 3101–3104.
 - 21 Wilhelm, S.M., Carter, C., Tang, L., Wilkie, D., McNabola, A., Rong, H., Chen, C., Zhang, X., Vincent, P., McHugh, M., Cao, Y., Shujath, J., Gawlak, S., Eveleigh, D., Rowley, B., Liu, L., Adnane, L., Lynch, M., Auclair, D., Taylor, I., Gedrich, R., Vzsensensky, A., Riedl, B., Post, L.E., Bollag, G., and Trail, P. (2004) BAY 43-9006 exhibits broad

- spectrum oral antitumor activity and targets the RAF/MEK/ERK pathway and receptor tyrosine kinases involved in tumor progression and angiogenesis. *Cancer Research*, **64**, 7099–7109.
- 22 Wilhelm, S., Carter, C., Lynch, M., Lowinger, T., Dumas, J., Smith, R.A., Schwartz, B., Simanotov, R., and Kelley, S. (2006) Discovery and development of sorafenib: a multikinase inhibitor for treating cancer. *Nature Reviews. Drug Discovery*, **5**, 835–844.
 - 23 Neumann, L., Ritscher, A., Mueller, G., and Hafenbradl, D. (2009) Fragment-based lead generation: identification of seed fragments by a highly efficient fragment screening technology. *Journal of Computer-Aided Molecular Design*, **23**, 501–511.
 - 24 Liu, Y. and Gray, N. (2006) Rational design of inhibitors that bind to inactive kinase conformations. *Nature Chemical Biology*, **2**, 358–364.
 - 25 (a) Backes, A.C., Zech, B., Felber, B., Klebl, B., and Mueller, G. (2008) Small-molecule inhibitors binding to protein kinases. Part I: exceptions from the traditional. *Expert Opinion on Drug Discovery*, **3** (12), 1371–1376; (b) Backes, A.C., Zech, B., Felber, B., Klebl, B., and Mueller, G. (2008) Small-molecule inhibitors binding to protein kinases. Part II: the novel pharmacophore approach of type II and type III inhibition. *Expert Opinion on Drug Discovery*, **3** (12), 1427–1449.
 - 26 Kufereva, I. and Abagyan, R. (2008) Type-II kinase inhibitor docking, screening and profiling using modified structures of active kinase states. *Journal of Medicinal Chemistry*, **51** (24), 7921–7932.
 - 27 Kola, I. and Landis, J. (2004) Can the pharmaceutical industry reduce attrition rates? *Nature Reviews. Drug Discovery*, **3** (8), 711–715.
 - 28 Balani, S.K., Miwa, G.T., Gan, L.S., Wu, J.T., and Lee, F.W. (2005) Strategy of utilizing *in vitro* and *in vivo* ADME tools for lead optimization and drug candidate selection. *Current Topics in Medicinal Chemistry*, **5** (11), 1033–1038.
 - 29 Wishart, D.S. (2007) Improving early drug discovery through ADME modelling: an overview. *Drugs in R&D*, **8** (6), 349–362, Review.
 - 30 Weiss, T.F. (1996) *Cellular Biophysics: Transport*, Vol. 1, The MIT Press, Cambridge, MA.
 - 31 Van de Waterbeemd, H. (2000) in *Oral Drug Absorption: Prediction and Assessment* (eds J.B. Dressman and H. Lennéräs), Dekker, New York, pp. 31–49.
 - 32 Horter, D. and Dressman, J.B. (2001) Influence of physicochemical properties on dissolution of drugs in the gastrointestinal tract. *Advanced Drug Delivery Reviews*, **46** (1–3), 75–87.
 - 33 Lipinski, C.A. (1997) Experimental and computational approaches to estimate solubility and permeability in drug discovery and development settings. *Advanced Drug Delivery Reviews*, **23** (1–3), 3–25.
 - 34 Clark, D.E. (1999) Rapid calculation of polar molecular surface area and its application to the prediction of transport phenomena. 1. Prediction of intestinal absorption. *Journal of Pharmaceutical Sciences*, **88**, 807–814.
 - 35 Lipinski, C.A. (2000) Drug-like properties and the cause of poor solubility and poor permeability. *Journal of Pharmacological and Toxicological Methods*, **44**, 235–249.
 - 36 Bhattachar, S.N., Deschenes, L.A., and Wesley, J.A. (2006) Solubility: it's not just for physical chemists. *Drug Discovery Today*, **11** (21–22), 1012–1018.
 - 37 Shalaeva, M. (2002) New Technologies to Increase Drug Candidate Survivability Conference, Philadelphia, PA, March 2002.
 - 38 (2006) *Drug Bioavailability*, Wiley-VCH Verlag GmbH, Weinheim.
 - 39 Kansy, M., Sennar, F., and Gebernator, K. (1998) Physicochemical high throughput screening: parallel artificial membrane permeability assay in the description of passive absorption processes. *Journal of Medicinal Chemistry*, **41**, 1007–1010.
 - 40 Press, B. and Di Grandi, D. (2008) Permeability for intestinal absorption: Caco-2 assay and related issues. *Current Drug Metabolism*, **9** (9), 893–900.
 - 41 Artursson, P., Palm, K., and Luthman, K. (2001) Caco-2 monolayers in experimental and theoretical predictions of drug

- transport. *Advanced Drug Delivery Reviews*, **46** (1–3), 27–43.
- 42 Yu, H.C. *et al.* (2002) Validation of 96-well insert plates in the Caco-2 permeability screening assay. Poster presented at the AAPS Annual Meeting and Exposition, Toronto, Canada.
 - 43 Schinkel, A.H. and Jonker, J.W. (2003) Mammalian drug efflux transporters of the ATP binding cassette (ABC) family: an overview. *Advanced Drug Delivery Reviews*, **55** (1), 3–29.
 - 44 Colabufo, N.A., Berardi, F., Contino, M., Niso, M., and Perrone, R. (2009) ABC pumps and their role in active drug transport. *Current Topics in Medicinal Chemistry*, **9** (2), 119–129.
 - 45 Glavinas, H., Krajcsi, P., Cserepes, J., and Sarkadi, B. (2004) The role of ABC transporters in drug resistance, metabolism and toxicity. *Current Drug Delivery*, **1** (1), 27–42.
 - 46 Volpe, D.A. (2008) Variability in Caco-2 and MDCK cell-based intestinal permeability assays. *Journal of Pharmaceutical Sciences*, **97** (2), 712–725.
 - 47 Sharom, F.J. (2006) Shedding light on drug transport: structure and function of the P-glycoprotein multidrug transporter (ABCB1). *Biochemistry and Cell Biology*, **84** (6), 979–992.
 - 48 Szakács, G., Jakab, K., Antal, F., and Sarkadi, B. (1998) Diagnostics of multidrug resistance in cancer. *Pathology Oncology Research*, **4** (4), 251–257.
 - 49 Korfmacher, W.A. (2009) Advances in the integration of drug metabolism into the lead optimization paradigm. *Mini-Reviews in Medicinal Chemistry*, **9** (6), 703–716.
 - 50 Venkatakrishnan, K., Von Moltke, L.L., and Greenblatt, D.J. (2001) Human drug metabolism and the cytochromes P450: application and relevance of *in vitro* models. *Journal of Clinical Pharmacology*, **41** (11), 1149–1179.
 - 51 Testa, B. and Krämer, S.D. (2008) The biochemistry of drug metabolism: an introduction. Part 4. Reactions of conjugation and their enzymes. *Chemistry & Biodiversity*, **5** (11), 2171–2336.
 - 52 Ishikawa, T. (1992) The ATP-dependent glutathione S-conjugate export pump. *Trends in Biochemical Sciences*, **7** (11), 463–468.
 - 53 Chandra, P. and Brouwer, K.L. (2004) The complexities of hepatic drug transport: current knowledge and emerging concepts. *Pharmaceutical Research*, **21** (5), 719–735.
 - 54 Ito, K., Suzuki, H., Horie, T., and Sugiyama, Y. (2005) Apical/basolateral surface expression of drug transporters and its role in vectorial drug transport. *Pharmaceutical Research*, **22** (10), 1559–1577.
 - 55 Wilkinson, G.R. and Shand, D.G. (1975) A physiological approach to hepatic drug clearance. *Clinical Pharmacology and Therapeutics*, **18**, 377–390.
 - 56 Iwatsubo, T., Hirota, N., Ooie, T., Suzuki, H., Shimada, N., Chiba, K., Ishizaki, T., Green, C.E., Tyson, C.A., and Sugiyama, Y. (1997) Prediction of *in vivo* drug metabolism in the human liver from *in vitro* metabolism data. *Pharmacology & Therapeutics*, **73**, 147.
 - 57 McGinnity, D.F., Soars, M.G., Urbanowicz, R.A., and Riley, R.J. (2004) Evaluation of fresh and cryopreserved hepatocytes as *in vitro* drug metabolism tools for the prediction of metabolic clearance. *Drug Metabolism and Disposition: The Biological Fate of Chemicals*, **32** (11), 1247–1253.
 - 58 Obach, R.S. (2001) The prediction of human clearance from hepatic microsomal metabolism data. *Current Opinion in Drug Discovery & Development*, **4** (1), 36–44.
 - 59 Mandagere, A., Thompson, T.N., and Hwang, K.K. (2002) Graphical model for estimating oral bioavailability of drugs in humans and other species from their Caco-2 permeability and *in vitro* liver enzyme metabolic stability rates. *Journal of Medicinal Chemistry*, **45** (2), 304–311.
 - 60 Rane, A., Wilkinson, G.R., and Shand, D.G. (1977) Prediction of hepatic extraction ratio from *in vitro* measurement of intrinsic clearance. *The Journal of Pharmacology and Experimental Therapeutics*, **200** (2), 420–424.
 - 61 Crespi, C.L. (1999) Higher throughput screening with human cytochrome

- P450s. *Current Opinion in Drug Discovery & Development*, **2**, 15–19.
- 62 Hutzler, M., Messing, D.M., and Wienkers, L.C. (2005) Predicting drug–drug interactions in drug discovery: where are we now and where are we going? *Current Opinion in Drug Discovery & Development*, **8** (1), 51–58.
 - 63 Crespi, C.L. and Penman, B.W. (1997) Use of cDNA-expressed human cytochrome P450 enzymes to study potential drug–drug interactions. *Advances in Pharmacology*, **43**, 171–188.
 - 64 Kabasakalian, P., Britt, E., and Yudis, M.D. (1966) Solubility of some steroids in water. *Journal of Pharmaceutical Sciences*, **55** (6), 642.
 - 65 Bevan, C.D. and Lloyd, R.S. (2000) A high-throughput screening method for the determination of aqueous drug solubility using laser nephelometry in microtiter plates. *Analytical Chemistry*, **72** (8), 1781–1787.
 - 66 Avdeef, A. (2001) Physicochemical profiling (solubility, permeability and charge state). *Current Topics in Medicinal Chemistry*, **1** (4), 277–351.
 - 67 Avdeef, A., Box, K.J., Comer, J.E., Hibbert, C., and Tam, K.Y. (1998) pH-metric log *P* 10. Determination of liposomal membrane–water partition coefficients of ionizable drugs. *Pharmaceutical Research*, **15** (2), 209–215.
 - 68 Valko, K., My Du, C., Bevan, C., Reynolds, D.P., and Abraham, M.H. (2001) Rapid method for the estimation of octanol/water partition coefficient (log *P*(oct)) from gradient RP-HPLC retention and a hydrogen bond acidity term ($\zeta\alpha(2)(H)$). *Current Medicinal Chemistry*, **8** (9), 1137–1146.
 - 69 Avdeef, A. (1993) pH-metric log *P*. II. Refinement of partition coefficients and ionization constants of multiprotic substances. *Journal of Pharmaceutical Sciences*, **82** (2), 183–190.
 - 70 Polli, J.W., Wring, S.A., and Humphreys, J.E. (2001) Rational use of *in vitro* P-glycoprotein assays in drug discovery. *The Journal of Pharmacology and Experimental Therapeutics*, **299**, 620–628.

2

Screening for Kinase Inhibitors: From Biochemical to Cellular Assays

Jan Eickhoff and Axel Choidas

2.1

Introduction

Nearly all kinase inhibitors, regardless of their origin from research institutions, drug discovery companies, or nature, have been designed or evolved with the purpose of influencing cellular processes. The information obtained from the measurement of cellular kinase inhibition enables significantly better predictability of the influence of a small molecule on biological processes in comparison to the measurement of kinase inhibition on purified enzymes under artificial conditions [1].

In contrast to biochemical kinase assays, which are performed under well-defined conditions, the outcome of cellular kinase assays greatly depends on a variety of factors that are, at least in part, difficult to control, especially when it comes to choosing the cellular system, the origin or the handling of cultured cells. Although cellular kinase assays require a much better understanding, standardization, and control of conditions than biochemical assays to get reproducible results (which does not mean that they are generally less reproducible), they are an essential part of every drug discovery program, as they integrate all factors influencing cellular kinase inhibition and are much more reliable for selection of compounds that will account for a desired *in vitro* or *in vivo* phenotype.

The choice of the system(s) to measure cellular kinase activity will very much depend on the scientific questions to be answered. For example, a cellular system for dissection of signaling pathways with kinase inhibitors within a basic research project will differ very much from a cellular system in selecting kinase inhibitors during the course of an anticancer drug discovery program with the final goal to inhibit oncogene-dependent tumors. Therefore, measurement of cellular kinase inhibition for purely academic purposes will have different requirements from those of the assessment of cellular kinase activity in a pharmaceutical drug discovery environment in regard to robustness, assay development, costs, reproducibility, and throughput.

How can one predict cellular effects from biochemical kinase inhibition? How are kinase assays embedded in the drug discovery process? Which factors determine the

cellular selectivity of kinase inhibitors? Which cellular kinase assay systems are available and when are they applied? This chapter will offer guidelines for prediction of cellular kinase activity and provide an overview of cellular kinase assays for drug discovery.

2.1.1

Kinase Inhibitors for Dissection of Signaling Pathways

In academic settings, major applications of cellular kinase assays are the dissection of signal pathways and the elucidation of physiological roles of kinases. As development of specific kinase inhibitors as tool compounds is not in the focus or not possible for most of these laboratories, many of the inhibitors used by these groups are being purchased from commercial sources, which provide only limited selectivity data. However, for proper interpretation of assay results, inhibitors need to be highly selective, or at least selectivity should be known. Comprehensive overviews of the *in vitro* selectivity profiles of commercially available inhibitors with practical recommendations for their use have been published by the group of Phil Cohen [2, 3].

2.1.2

Cellular Kinase Assays for Drug Discovery Applications

For development of kinase inhibitors in drug discovery, screening cascades traditionally begin with biochemical assays, and cellular assays are used later for more advanced substances to bridge the gap to animal studies. Here, cellular assays may serve both to estimate the cell permeability of the inhibitors coming from biochemical screening, to show that inhibition of a certain kinase target will lead to the desired phenotype, and to predict physiological inhibitor levels that have to be reached for efficacy in *in vivo* systems. Often, cellular assays with different readouts are arrayed sequentially in the screening cascade, according to the desired scientific “filter” function and throughput. A mechanistic assay monitoring direct inhibition of a (physiologically relevant) kinase target may be followed by an assay measuring the inhibition of the signaling pathway known, or expected, to be controlled by the kinase of interest. At another point of the cellular screening cascade, the desired physiological phenotype for therapeutic efficacy may be used as a third filter. The phenotype can be monitored on a cellular level (e.g., high content analysis), or in multicellular systems (e.g., angiogenesis assays in cocultures of endothelial cells and fibroblasts). The sequence of cellular assays may be varied according to the underlying scientific strategy, costs (often related to throughput), and the validation status of the kinase target.

In addition, kinase assays can be used to accompany *in vivo* studies, either by extrapolation of *in vivo* EC₅₀ values for estimation of physiological drug level to gain effects or by applying cellular substrate phosphorylation readouts to *ex vivo* material to monitor the effect of compound exposure on phosphorylation of biomarkers.

In the past, kinase drug discovery programs were based on screening campaigns directed against purified recombinant kinases, often limited to the catalytic domains. As a result, today most of the published low molecular weight kinase inhibitors bind

in an ATP-competitive fashion. In addition, hits are usually selected according to their potencies; therefore, the chance to start a kinase inhibitor discovery program with a promiscuous compound is high. In this context, the MEK inhibitors binding to a site adjacent to but different from the ATP binding pocket in a rather “nonclassical” fashion may be regarded as an exception [4].

In addition to assessment of inhibition of the target kinase, cellular kinase assays can provide data on selectivity within the kinase family, which is often problematic for kinase inhibitors (depending on the therapeutic indication for which the drug discovery program is aimed), and which, on a cellular level, depends on the kinome expressed in the target cell or tissue. In addition, undesired phenotypic effects caused by interconnection of pathways can be addressed with cellular readouts.

Another application of cellular kinase assays for drug discovery is the use in chemical validation programs. Often, target validation is limited to “genetic” approaches such as gene knockout and loss-of-function screening, downregulation with siRNAs or shRNAs, which are not able to distinguish between functions that depend on enzymatic activity and functions that are independent of the ability to transfer phosphate groups to substrate proteins, such as scaffolding. Most feasible for assessing the role of the kinase activity in the context of target validation is overexpression of kinase mutants anticipated to act in a dominant negative manner. The disadvantages of this approach are that overexpression sometimes produces artifacts and that it is not always possible or feasible to overexpress a target in the selected validation system. As an alternative strategy, tool kinase inhibitors can be used in “chemical” validation approaches to monitor if a desired phenotype can be produced by inhibition of the kinase in cells. As selective kinase inhibitors for novel target kinases are rare, data have to be interpreted with caution, and inhibitors from different chemical classes should be used to rule out off-target effects.

2.2

Factors that Influence Cellular Efficacy of Kinase Inhibitors

The effect of a kinase inhibitor on the phosphorylation of a cellular substrate does depend not only on the potency of the isolated enzyme and the ability to enter the cell but also on a multitude of factors. Some of these factors can be estimated from *in vitro* data, but others are difficult to control. Importantly, cellular selectivity within the kinase family can deviate greatly from selectivity determined in *in vitro* assays.

2.2.1

Competition from ATP

The affinity of a kinase inhibitor to its target is usually quantified as an IC_{50} value, which describes the concentration at which the activity of the kinase is reduced to 50% of its original value. The classical kinase inhibitors that inhibit the kinase in an ATP-competitive, reversible way are classified as type I inhibitors. The IC_{50} values of

these inhibitors depend on two factors: the dissociation constant K_i for the kinase, which quantifies the intrinsic affinity for the kinase, and the competition from ATP under the individual assay conditions, which depends on the ATP concentration $[ATP]$, and the affinity of ATP under the specific assay conditions ($K_{M, ATP}$). The relation of these factors is set by the Cheng–Prusoff equation [5]:

$$K_i + K_i \times [ATP] / K_{M, ATP} = IC_{50}$$

A look at the plot of the IC_{50} values against the ATP concentration according to the Cheng–Prusoff equation (Figure 2.1) illustrates that at low ATP concentrations around or below the $K_{M, ATP}$, the IC_{50} approaches the K_i as there is no significant competition from this substrate. When the ATP concentration increases above the $K_{M, ATP}$, the IC_{50} raises linear to the ATP concentration and does not plateau at high ATP. As the ATP concentrations in cells are estimated to lie between 1 and 5 mM [6, 7] and the apparent (related to the specific assay conditions) $K_{M, ATP}$ values in biochemical assays are well below these concentrations, the cellular potency of the inhibitors is determined not only by the biochemical IC_{50} values but also by the $K_{M, ATP}$ values. As the $K_{M, ATP}$ values in biochemical assays are typically in the range of 1–100 μM (Figure 2.2), the potencies of most inhibitors drop around a factor of 100 comparing cellular with biochemical IC_{50} values.

As a consequence, an inhibitor with similar affinities against different kinases in biochemical assays will bind preferentially to the cellular target with the lowest affinity to ATP. This means that kinases such as mTOR, which have $K_{M, ATP}$ values in the millimolar range, will be much easily inhibited in cells than kinase targets with $K_{M, ATP}$ values in the nanomolar range, such as PLK1. Even a selectivity panel within a kinase subfamily, such as the cyclin-dependent kinase (CDK) family, cannot be

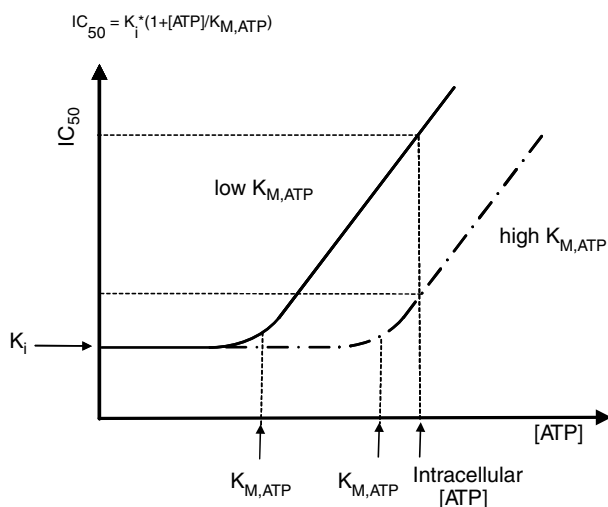


Figure 2.1 The Cheng–Prusoff equation and cellular ATP concentration.

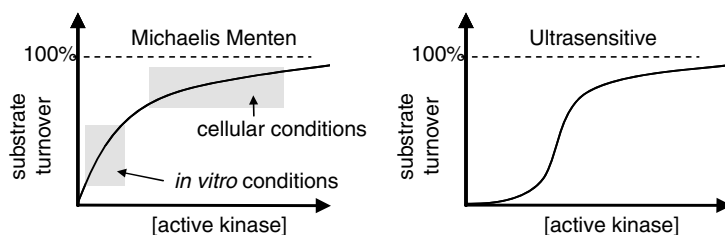


Figure 2.2 Cellular kinase reactions are not linear.

interpreted without the knowledge of the affinities for ATP of the constructs used in these assays, especially as the $K_{M, \text{ATP}}$ values of these kinases heavily depend on the type of the associated cyclin and can vary around a factor of 100 between different cyclin-dependent kinases. Finally, this situation is complicated by the fact that the apparent $K_{M, \text{ATP}}$ value depends on the specific assay condition, meaning kinase construct, substrate, counterions used, and pH values (Table 2.1).

It is assumed that most kinases can shuttle between an inactive and an active structural conformation and that phosphorylation of key residues will stabilize the active conformation by driving a flexible activation loop out of the ATP binding site, thereby increasing the affinity for ATP. In the inactive conformation, a hydrophobic pocket is created adjacent to the activation loop and the so-called C-helix of the kinase. Inhibitors binding to this pocket stabilize the kinase in an inactive conformation. These inhibitors are classified as type II, or allosteric, inhibitors, and extend very similar to type I inhibitors into the ATP binding pocket, forming hydrogen bonds to the so-called hinge region of the kinase. Examples of this type of inhibitors are imatinib (targeting Abl, PDGFR, and cKIT), sorafenib (targeting B-Raf, VEGFR, and Tie2) or BIRB-796 (targeting p38 alpha and beta). Importantly, by stabilizing the inactive conformation of the kinase, these inhibitors lower the affinity for ATP, thereby reducing competition with cellular ATP and reducing the difference between biochemical and cellular inhibition. Note that examples exist where one inhibitor can bind different kinases in either a type I or a type II fashion. For example, imatinib binds BCR-Abl in a type II fashion, whereas the kinase FAK is bound in a type I fashion [8].

Most of these inhibitors act by outcompeting ATP from the active site. In addition, their ability to prevent activation of the kinases by induction of conformations that cannot be activated may be an important component of their mode of action. The p38 inhibitor SB203580, for example, keeps p38 in a conformation that cannot be activated by phosphorylation through upstream MAPKKs [9].

Type III inhibitors bind in an allosteric way similar to type II inhibitors, but their binding is limited to the hydrophobic pocket present in the inactive form and does not extend to the ATP binding pocket. One of the rare examples of this type of inhibitor is CI-1040, an inhibitor of MEK1 and MEK2, and some pyrazolo ureas, which inhibit p38.

Inhibitors binding to a site distant from the described ATP binding or hydrophobic pockets are classified as type IV inhibitors. These are truly non-ATP-competitive

Table 2.1 Selected $K_{M, ATP}$ values for different kinases.

Y kinase	$K_{M, ATP}$ (nM)	S/T kinase	$K_{M, ATP}$ (nM)	Lipid kinase	$K_{M, ATP}$ (nM)
c-Abl	12	Akt1	132	ATM	29
Btk	29	Aurora 2	34	DNA-PK	228
Csk	15	CaMKI	110	mTOR	1000
EGFR	17	CaMKIIa	19	p110 α /p85a	62
EphA7	30	CaMKIV	27	p110 γ	7,5
ErbB-2	27	CDK1/cyclin B	2.3	PI3KC2 α	32
FAK	4.3	CDK2/cyclin E	3.6	PI3KC2 β	120
FER	7.1	CDK4/cyclin D1	418	PI4KII α	28
FGFR	70	Chk2	3.3	PI4KIIIa	300
Fyn	70	CK1a	19	PI4KIII β	1000
IGFR	107	CLK1	80	PI(4)P(5)KI	25
InsR	40	DMPK	2.3		
JAK1	15	Erk2	140		
JAK3	6	GRK1	2		
c-Kit	53.6	GSK3 β	50.2		
MuSK	380	IKK-1/IKK-2	13		
PDGFR β	15	IRAK4	600		
c-Src	80	JNK2	39		
Tie-2	73.9	MAPKAPK2	43		
TrkA	9	MEK1	5.6		
VEGF-R2	130	p38a	25		
		p90Rsk-B	35		
		PAK2	71		
		PKA- α	25		
		PKC- β I	37.2		
		PLK1	2.6		
		Raf-1	11,6		
		ROCK-I	4.5		
		TBK-1	5.9		

Source: Adapted from Ref. [22].

inhibitors and display no difference between biochemical and cellular IC_{50} values. Examples are rapamycin, an mTOR inhibitor whose binding is limited to only one of the protein complexes through which mTOR can send downstream signals, and ON012380, a BCR-Abl inhibitor competitive with peptide substrate binding [10]. The small-molecule GNF-2 is another example. It binds to a lipid binding site of the Abl kinase, inducing an inactive conformation. Interestingly, GNF-2 has been identified in a cellular screen for compounds that specifically target BCR-Abl-dependent cell lines; however, it does not inhibit the isolated Abl enzyme. This case illustrates that cellular screens can be an alternative to conventional kinase assays used predominantly in primary screening campaigns, as cellular assays allow screening of a kinase in its native conformation and thus allows the identification of inhibitors with unconventional binding modes. In addition to a superior cellular potency, type II, III, and IV inhibitors have often better pharmacokinetic properties than type I inhibitors,

as they have longer residence times on their targets, caused by the allosteric conformational changes of the kinase structures [11, 12].

Another class of kinase inhibitors forms covalent bond to the kinase active site, most frequently by reacting with a nucleophilic cysteine residue, making the binding event virtually irreversible (although at least in theory at the thermodynamic equilibrium a fraction of the inhibitor will remain unbound). The clinically most advanced covalent kinase inhibitors of the epidermal growth factor receptor, HKI-272 [13] and CL-387785 [14], were developed to target a relatively rare cysteine residue located at the lip of the ATP binding site. Like type I and type II kinase inhibitors, these compounds act by preventing ATP from binding the active site. Although standard binding equations for reversible inhibitors cannot be applied for these compounds, they still have to compete with ATP, leading to significant weaker inhibition in cells in comparison to *in vitro* assays.

2.2.2

Substrate Phosphorylation Levels

Although biochemical K_i values have some potential to predict the cellular EC_{50} of inhibitors including competition from ATP into the calculation, a number of additional factors should be taken into account that can influence inhibition of cellular substrate phosphorylation levels.

Biological effects of kinases are mediated through substrate phosphorylation. However, this substrate phosphorylation does not only depend on the action of kinases but also on the action of phosphatases that remove these modifications. The action of these phosphatases tunes the sensitivity of signal propagation for perturbations in kinase activity, as the integrated signal is the result of the netto phosphorylation through phosphate addition and removal. Therefore, a kinase inhibitor will act more efficiently on substrates with high turnover rates (Figure 2.2), as, for example, an inhibitor of the phosphatase PTEN increases the cellular IC_{50} of the PI3K inhibitor LY294002 about fivefold [15]. Indeed, some signaling pathways are being controlled by regulation of key phosphatases. An important example is the inositol polyphosphate 5-phosphatase SHIP2, which is a central regulator of insulin signaling and type 2 diabetes [16].

2.2.3

Ultrasensitivity of Kinase Signaling Cascades

In biochemical kinase assays for IC_{50} determination, substrate concentrations used are in large excess of kinase concentrations, so that only a small fraction of the substrate is consumed until the assay is stopped, so that the substrate turnover is linear to the amount of active kinase, which is the fraction of the kinase preparation not affected by the inhibitor. In cells, substrates often need to be phosphorylated nearly quantitatively to achieve biological effects. This is illustrated by the fact that a large fraction of phosphorylated ERK1 and ERK2 kinases translocates to the nucleus upon phosphorylation by MEK1 and MEK2, or the inhibitor of NF- κ B (I κ B), I κ B is

virtually undetectable in Western blots after stimulation through phosphorylation-induced degradation. When plotting the substrate turnover against the active kinase concentration, the relationship is not linear any more, but appears as a hyperbolic curve described by the Michaelis–Menten kinetics. For the translation of biochemical IC_{50} values to cellular EC_{50} values, this means that at high substrate turnover, the concentration of a substance to reduce the cellular substrate phosphorylation by half needs to be greater than the concentration of the same substance to reduce the substrate phosphorylation in a biochemical assay with substrate excess. At low substrate turnover, which can be achieved, for example, by very high inhibitor concentrations, the cellular inhibition will again approach the biochemical inhibition (Figure 2.2).

A different situation is given for signaling pathways in which kinases are arrayed in a sequential cascade or when a kinase is involved in different steps of a cascade, or if a substrate is phosphorylated by the same kinase at multiple sites. Here, the relation between a substrate phosphorylation and kinase activity can follow a sigmoidal curve, very much like cooperative binding behaviors of classical enzymes. An example is the ultrasensitivity of the MAP Kinase cascade, which has been described by Ferrell [17]. For such an ultrasensitive system, the cellular effects of an inhibitor can be better or weaker than those extrapolated from the biochemical assay, depending on the substrate turnover. At high substrate turnover, inhibitors will appear to be less sensitive, like observed at high substrate turnover in Michaelis–Menten kinetics, whereas at low substrate turnover, less inhibitor is needed to inhibit the substrate phosphorylation in comparison to the linear behavior. This kind of inhibition kinetics enables nearly quantitative inhibition of cellular substrate phosphorylation at high inhibitor concentrations, which is approached in kinase systems with Michaelis–Menten kinetics only at very high inhibitor concentrations.

2.2.4

Cell Permeability

Before a kinase inhibitor can bind to a cellular target, it must pass the cellular membrane (Figure 2.3). Inhibitors enter the cells through the membrane by passive diffusion along a concentration gradient, until a steady state is approached. In general, the membrane permeability will be a function of its lipophilicity, which accelerates entry rates from aqueous medium into the hydrophobic cell membrane, and the molecular weight, as size prevents the compounds from entering the membranes. Hydrophilic compounds with many hydrogen bond donors and acceptors, or with several charges, will find it difficult to enter the membranes (although amphiphatic compounds with both negative and positive charges resulting in no gross charge may readily enter membranes through interaction with charges in the membrane). Importantly, on the other hand, too much hydrophobicity also lowers the plasma cellular availability of inhibitors, as these compounds are readily absorbed by the membrane, but will not exit into the cytoplasm. In addition, aqueous solubility may be too low to reach significant concentrations, and these compounds often bind to plasma proteins.

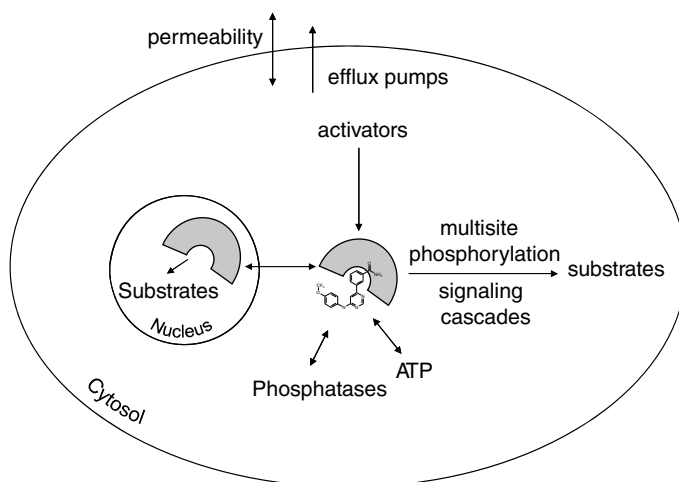


Figure 2.3 Factors that influence cellular kinase inhibition.

Molecules optimized for cell permeation enter cells often within minutes. The PI3 kinase inhibitor Wortmannin, for example, blocks the release of granule-associated mast cell mediators independent of the secretory stimulus within 2–5 min after incubation [18]. Therefore, preincubation times between 15 and 60 min, which are common in literature for kinase inhibitor studies, should be sufficient to allow the inhibitors to reach steady-state levels.

Another factor that influences the steady state of kinase inhibitor concentrations inside cells is the presence of efflux pumps, which can counteract diffusion into the cells by actively removing the compound from the cells. The efflux rates are linear to the specific pump activity, the affinity of the efflux pumps for the inhibitors, and the concentration of the inhibitor inside the cell. In most cultured cell lines, efflux pumps hardly influence the steady-state level of inhibitors; however, tumor cells often express efflux pumps such as p-glycoprotein, rendering them insensitive to otherwise effective inhibitor concentrations. Analogous to the situation in cancer cells, screening for kinase inhibitors in yeast that expresses efflux pumps leads to the removal of many compounds that are active in mammalian cells. Genetic inactivation of these transporters has been reported to restore sensitivity to most of these inhibitors [19].

2.2.5

Cellular Kinase Concentrations

In *in vitro* kinase assays, the lowest measurable IC_{50} is limited by the concentration of active kinase. According to the Cheng–Prusoff equation ([5]; also see above), the minimal IC_{50} value is equal to half the kinase concentration in the assay, as each inhibitor molecule in the reaction mixture will be bound to one kinase molecule. However, this mechanism does not apply to cellular assays, as the medium

surrounding the cell serves as a reservoir for inhibitors. Molecules depleted by binding to kinases from the unbound intracellular inhibitor pool are replenished from the much larger extracellular inhibitor pool by diffusion through the membrane; therefore, the intracellular steady-state levels of inhibitors are not influenced by the tight binder problem.

Naturally occurring variations in expression levels or activities of kinases can affect the action of cellular kinase inhibitors by influencing the absolute level of kinase activity and in turn the residual kinase activity at any effective concentration of the kinase inhibitors. Moreover, as kinase inhibitors often target essential signaling pathways, which are tightly regulated by feedback loops, cells can counteract the action of inhibitors by engaging these feedback loops. Cancer cell lines, for example, can become resistant to erlotinib, a small-molecule inhibitor of the epidermal growth factor receptor, by induction of EGFR mRNA levels [20].

Few studies have addressed the question of absolute intracellular kinase concentrations. In a study employing an epitope-tagged kinase library expressed in *Saccharomyces cerevisiae*, protein levels were determined for the majority of kinases predicted to be expressed in yeast [21]. By converting the expression levels to absolute concentrations, Knight and Shokat [22] calculated that around two-thirds of protein kinases reach cellular concentrations between 1 and 50 nM, while the most abundant are expressed at up to 38 μ M. Expression data from mammalian cells are consistent with these data. For example, cyclin-dependent kinases can reach concentrations of 1–2 μ M [23]. Although some of the expression levels of kinases relative to other cellular proteins are known, interpretation of these data in terms of inhibitor effects is difficult.

2.2.6

Effects of Inhibitors Not Related to Substrate Phosphorylation

Some examples have been described in literature where kinase inhibitors have unexpected effects different from inhibition of substrate phosphorylation. Scaltriti *et al.*, for example, have shown that lapatinib, an HER2 tyrosine kinase inhibitor, induces stabilization and accumulation of HER2, which can be exploited to potentiate anti-Her2-antibody-dependent cell cytotoxicity [24]. Another unexpected case is the protein kinase RIP2, whose activity has two functions: one is to prevent the active enzyme from degradation and the other is to downregulate the downstream signaling. Therefore, inhibition of the RIP2 kinase with either SB 203580 or PP2 leads to a fast and drastic decrease in the expression level of RIP2, which may explain why these RIP2 inhibitors inhibit both the MDP-stimulated downstream signaling and the production of interleukin-1 β and tumor necrosis factor α (Windheim *et al.* [25] and authors' own observations).

In the case of the oncogenic kinase BCR-ABL, inhibition can influence the intracellular localization. According to a study by Vigneri and Wang [26], a kinase inhibitor needs to be washed out after addition to cells to be effective. Cytosolic BCR-ABL inhibits apoptosis through activation of PI3 kinase and other pathways, whereas nuclear Abl is a positive inducer of apoptosis in response to DNA damage. BCR-Abl is

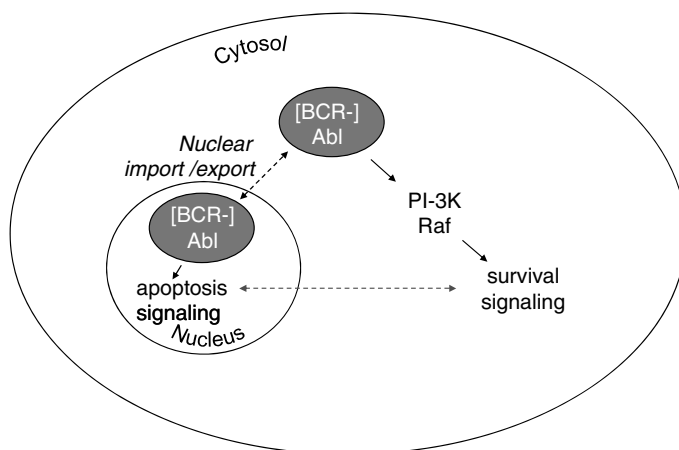


Figure 2.4 Compartmentalization of kinase signaling.

usually located in the cytoplasm. By inhibiting the kinase activity with the inhibitor STI571, the authors induced translocation of the kinase into the nucleus, where it was trapped in the next step by addition of an inhibitor of nuclear export. In the third step, the kinase inhibitor was washed out, inducing the kinase activity (limited to the nucleus), thereby inducing signals triggering the apoptotic death of leukemic cells (Figure 2.4).

For further reading on factors influencing the cellular kinase activity, the reader may refer to an excellent review written by Knight and Shokat [22].

2.3

Assays for Measurement of Cellular Kinase Activity

A broad range of assays is available for probing cellular kinase activity, from robust and cost-efficient assays applicable for industrial high-throughput screening against a distinct cellular substrate of interest to highly sophisticated assays requiring exclusive instrumentations allowing quantitative changes in the entire phosphoproteome. While cell-based assays have been traditionally used in drug discovery for assessment of the pharmacological effects of more advanced inhibitors in a relevant biological system, recent developments indicate that more primary screening campaigns will be performed on a cellular level. Assay technologies are constantly being developed further and novel assay formats are being published. The following survey on cellular assays does not aim to cover all available assay formats; instead, it intends to provide a survey of the most common ones and give an understanding of what are the main directions of current development.

Early attempts of cell-based kinase activity measurement involved monitoring of incorporation of [^{32}P] into kinase substrate in the presence of [^{32}P] ATP (or the lower energy alternative [^{33}P] ATP), which could be easily applied to a broad range of

kinases. As throughput is low, and many labs try to avoid working with radioactive reagents, these kinds of assays are rather used when no alternative is available.

2.3.1

Antibody-Based Detection

A series of assays enabling the screening of larger compound collections are based on detection of the substrate turnover by phosphospecific antibodies. Traditional assays such as Western blotting will not be featured in this chapter as they require gel electrophoresis and therefore automation is difficult.

A variant of the Western blotting allowing readout in a microtiter plate format is the in-cell Western system, which was first reported by Chen *et al.* [27]. This system is limited to adherent cells and employs near-infrared dyes, which are detected in a scanner with two near-infrared laser/detector pairs (Licor Biosciences). The assay has been validated for 96- and 384-well formats. Cells are fixed and stained with antibodies from different species for phosphorylated and, for normalization, non-phosphorylated epitopes of the substrate. Next, cells are incubated with secondary, species-specific antibodies with covalently attached near-infrared dyes. The dual wavelength readout allows normalization of substrate amounts and allows a quantitative measurement of substrate turnover. The use of near-infrared dyes reduces the autofluorescence from cell proteins or microtiter plates and allows reasonable signal-to-noise windows.

One of the first technologies used for detection of substrate phosphorylation was the ELISA (enzyme-linked immunosorbent assay) method, which achieved a reasonable throughput and signal window [28, 29]. However, automation is still difficult to achieve due to the inhomogeneous format of this assay that requires multiple washing steps. The antibodies for detection of the substrate and phosphorylation site can be arrayed in two orientations. In the first orientation, a polyclonal antibody against an epitope of the substrate distinct from the phosphorylation site is coated to the bottom of the wells of the microtiter plates. In the next step, the cell lysate of interest is incubated on the wells allowing binding of the substrate, followed by washing to remove excess and unspecifically bound protein. A monoclonal antibody from a species different from the first one is added, which recognizes only the phosphorylated substrate, followed by a secondary antibody specific for the monoclonal one. This antibody is coupled to an enzyme, which converts a chromagenic or fluorogenic substrate, enabling quantitation of phosphorylation. In another configuration, the capture antibody recognizes the phosphorylated epitope, whereas the detection antibody recognizes an epitope different from the phosphorylation site. The second array is of advantage when the phosphosubstrate constitutes only a small fraction of the total substrate and the large excess of total protein competes with binding to the phosphorylated protein to a limited number of binding places. This can significantly reduce the sensitivity of the assay. The use of a phosphospecific capture antibody ensures that a maximum of phosphorylated substrate is involved in the detection so that the sensitivity of the assay is significantly increased.

A further development in the ELISA technology is the DELFIA (dissociation-enhanced lanthanide fluorescent immunoassay) method [30], which differs from the ELISA format in the use of lanthanide-coupled antibodies for detection instead of enzyme-coupled ones. After binding of the lanthanide-coupled secondary antibody, an enhancer solution is added to the samples. The enhancer solution lowers the pH, which dissociates the lanthanide, allowing formation of a stable fluorescent chelate in the enhancer solution.

Lanthanides have fluorescence characteristics beneficial for high-throughput screening, as a large Stokes shift and a fluorescence lifetime in the millisecond range nearly eliminate the background fluorescence. DELFIA assays have a greater dynamic range and signal-to-noise ratio than traditional ELISA assays. Up to four different lanthanides with different emission spectra can be used in one assay, allowing parallel readout of different substrates by multiplexing. Lanthanides commonly used in these assays include europium (emission 613 nm), terbium (545 nm), samarium (643 nm), and dysprosium (572 nm). Like the ELISA format, the DELFIA technology (Perkin Elmer) requires removal of proteins from cell lysates through intensive washing to reduce background, which is unfavorable for screening large compound collections.

Another variant of these methods uses electrochemiluminescent labels for detection, which requires special readers and plates (e.g., from Meso Scale Discovery). Here, cell lysates with substrate proteins bind to the bottom of microplates either directly or via specific antibodies. The detection antibody is directly or indirectly coupled to an electroluminescent label containing a ruthenium chelate. These labels emit light when electrochemically stimulated. The detection process is initiated at electrodes located in the bottom of the microplates. Only labels near the electrode are excited and detected, enabling nonwashed assays. Commonly used labels emit light at 620 nm, eliminating problems with color quenching, and few compounds interfere with the electrochemiluminescence. Background signals are reduced as the stimulation (electricity) is decoupled from the signal (light). Antibodies for different protein substrates can be combined in one well allowing multiplexing. When screening larger compound collections, the consumables (plates) can become a significant cost factor.

A technology allowing more extensive multiplexing of different kinase substrates is the luminex technology (Luminex Corp.). This technology is not limited to plates and is based on detection of fluorescence-labeled particles by a flow cytometer. The polystyrene beads can be identified by unique tags of combinations between a red and a near-infrared dye. With distinct ratios of the dyes, different sets of beads can be uniquely labeled, each with a characteristic spectrum determined by the red-to-infrared ratios. The beads are coated with specific antibodies for phosphorylated targets. The cell lysates are incubated with beads that are specifically labeled with fluorescent tags and capture antibodies. A second antibody labeled with a different fluorescent tag is then added that recognizes the phosphorylated substrate on the captured kinase substrate. The mixture is subsequently analyzed with a flow cytometer. When a single bead passes the detection chamber, it is excited by two lasers. One laser is used for identification of the bead via excitation of the

red/near-infrared dyes. The other laser excites the fluorophore bound to the detection antibody, allowing quantitation of the bound protein or phosphoprotein. The advantage of this technology is that it can analyze large numbers of analytes that can be quantified from one sample in one well, allowing dissection of inhibitor specificities in cells. Although 100 different beads would allow multiplexing of up to 100 different analytes in theory, unspecific interaction between coating antibodies restrict the number of assays per well. Therefore, around 10 analytes are usually multiplexed.

Phosphorylation of substrates in the presence of kinase inhibitors can also be quantified in a homogeneous format using the AlphaScreen-based Surefire technology (Perkin Elmer). In this approach, a substrate-specific antibody is bound via a covalently attached biotin molecule to a streptavidin-coated AlphaScreen donor bead, while the AlphaScreen acceptor beads are coupled to a Protein A-Tag, to another antibody specific for the phosphorylated form or the substrate. When the substrate is phosphorylated, donor and acceptor beads are brought into close proximity by binding of both antibodies. Upon excitation, the acceptor beads release singlet oxygen that diffuses to the acceptor beads eliciting luminescence. This assay format is applicable for higher throughput screening. It has been reported to be more sensitive and to have the greatest dynamic range in comparison to other assay formats. In addition, the AlphaScreen technology requires comparably less amount of reagents due to the high signal-to-background ratio, resulting in significant cost savings in larger screening campaigns. However, interference of compound with the AlphaScreen technology has been reported to cause problems in some screening libraries.

A range of methods are available for monitoring the cellular kinase activity that does not rely on detection of protein phosphorylation by specific antibodies. Detection of processes regulated by kinase activation can allow indirect measurement of kinase activity, such as nuclear translocation of activated ERK1, induction of association of phosphoamino acid-specific binding domains such as SH2-domains to receptor tyrosine kinases, degradation (e.g., of I κ B triggered by phosphorylation through IKK γ), or activation of reporter genes. In the upstream segment of the signaling cascade, processes that lead to activation of kinases can also be exploited to measure activation of kinases, such as interaction of kinases with upstream activators. PKA (cAMP-activated protein kinase) provides an example of the successful use of a cellular protein–protein interaction assay for the identification of modulators of kinase activity. PKA consists of two subunits, a catalytic one and a regulatory one. Activation of PKA activity requires dissociation of the regulatory subunit. Prinz *et al.* [31] and Moll *et al.* [32] used the BRET (bioluminescence resonance energy transfer) technology to measure dissociation of the regulatory from the catalytic subunit. The subunits were tagged with the donor Renilla luciferase and the acceptor GFP (green fluorescent protein). When both subunits interact, the light emitted by the luciferase excites the GFP acceptor and a BRET signal can be detected. Activation of PKA leads to dissociation of both subunits and, in turn, a decrease in signal. Multiple variants of this BRET assay exist for detection of cellular protein–protein interactions. Alternatively, cellular protein–protein interactions can be

measured by enzyme fragment complementation. For this methodology, two cellular interaction partners are tagged with complementing fragments of an enzyme, which are not active alone, but can recombine to gain activity when brought into proximity by interaction of the two protein partners. Such assays have been described for various enzymes, and several companies offer ready-to-use assay systems that are useful for high-throughput screening. DiscoverRX's enzyme fragment complementation technology does not only allow detection of protein–protein interactions but has also been developed further for detection of autophosphorylation of receptor tyrosine kinase and phosphorylation of intracellular kinases. This kind of cell-based kinase assay monitors the interaction between wild type, full-length receptor proteins with SH2 phosphotyrosine binding domains. Upon activation, RTKs autophosphorylate, dimerize, and associate specifically with SH2 or PTB domains. In the PathHunter technology, two SH2 domains are coupled to two fragments of luciferase, which are brought into proximity by interaction of the two moieties leading to an activation-induced dimerization of the RTK. Upon inhibition of the RTK, autophosphorylation is inhibited, the SH2 domains do not bind any longer to the receptor dimer, and the luciferase fragments are dissociated. The assay does not require antibodies or washes and can be adapted to high-throughput screening. As an alternative to the complementation of enzyme fragments, fragments of fluorescent proteins can be used to monitor proximity of two cellular interaction partners.

Upon activation, many kinases change their intracellular location in order to get in proximity to their substrates. The kinase ERK1, for example, translocates upon activation to the nucleus, phosphorylates, and activates transcription factors. This translocation can be monitored by immunofluorescence, either via antibody staining of proteins or the expression of fluorescence-tagged proteins. Using translocation as readout for drug discovery does allow screening not only for upstream kinase inhibitors but also for compounds that interfere with the process of translocation. Traditionally, low-throughput manual confocal microscopy has been used for detection of protein translocation; therefore, the practicability for drug discovery has been limited. Recent developments in instrumentation and technology have made translocation screens available for high-throughput screening.

2.3.2

High-Content Screening

Most assays suitable for HTS enable readout of a limited number of parameters and do not provide additional information about proliferative status, morphological differences, or changes in subcellular localizations of target proteins or cell cycle. The expression high-content analysis (HCA) is referred to as multiparameter analysis of mainly fluorescent readouts to measure multiple cellular changes on a subcellular level. Traditionally, HCA is based on automated confocal microscopy and it comprises typically large numbers of comprehensive data sets. This methodology enables detailed dissection of the cellular effects and mode of action of potential drugs on a cellular level, providing a significant advantage for early assessment in drug discovery projects. High-content screens, in comparison to single- or dual-readout

screening technologies, allows an in-depth analysis of morphological changes and subcellular markers. As cells are normally fixed, they can be reanalyzed after analysis of the primary data set with additional markers or antibody staining, while stored images can be analyzed with additional algorithms retrospectively. Small numbers of cells make this assay amenable to miniaturization. One drawback of this technology is that it requires resources for intensive sample preparation, expensive instruments, and experienced personnel, especially for data interpretation, although recent advances in technology have led to methodologically sound solutions that are commercially available. However, the acquisition, storage, and interpretation of very large data sets remain the bottleneck of HCA-based screening.

HCA offers many options to analyze entire signaling cascades, for example, the PI3 kinase/Akt/mTOR pathway or the MAPK pathway. The readouts in these assays are rather called “pathway profiling” than kinase profiling [33], as most cellular HCA readouts monitor perturbations in the entire pathway, being not limited to the kinase, and extend to all perturbations upstream of the parameter that is being monitored. For this reason, compounds identified in primary HTS campaigns often require secondary assays for pathway dissection.

Detection and quantitation techniques employed in HCA for analysis of kinase signaling are versatile. Immunofluorescence can be used for detection of phosphorylated substrates, such as phospho-p38 [34] or phosphohistones [35], or for expression of inducible genes such as c-Fos, which is induced by activation of the ERK signaling cascade [36]. Redistribution of proteins fused to fluorescent tags can be used for monitoring cellular translocation events, and complementation of fragments of fluorescent proteins can be used to detect protein–protein interactions, as it has been described above.

The main technologies applied for HCA are flow cytometry, microscopic readouts, and laser scanning. Automated confocal microscopy such as the OPERA system (Perkin Elmer) or high-resolution CCD cameras such as the In Cell Analyzer from GE Healthcare have significantly expanded the throughput of HCA in comparison to the manually operated confocal microscopy. For further reading, the reader may refer to the comprehensive review by Gasparri *et al.* [37].

2.3.3

Use of Genetically Engineered Cell Lines

Cell lines can be genetically engineered to depend for proliferation on specific oncogenic kinases. This approach has been especially popular in oncology research.

The cell line Ba_F3 is of hematopoietic origin and is characterized by its dependence on IL-3 for survival and proliferation. Through transfection with known tyrosine kinase oncogenes, such as Bcr-Abl, Flt3, or NPM-Alk, it can be engineered to be IL-3-independent. Engineered Ba/F3 cell lines have often been employed to screen for differential cytotoxicity of kinase inhibitors between transformed IL-3-independent cells and parental Ba/F3 cells grown in the presence of IL-3 [38]. Melnick *et al.* transfected Ba/F3 cells with 35 different activated tyrosine kinases in order to create a robust system for screening a large number of

compounds against an extended panel of cellular RTK assays [39]. This approach identified novel cellular targets for known kinase inhibitors and proved itself as a powerful tool for screening larger compound collections, suitable for miniaturization in the 1536-well formats.

2.3.4

Genetically Encoded Biosensors

Most cellular kinase assays require fixation or lysis of cells and do not allow real-time measurement of kinase activity in living cells. Genetically engineered FRET-based reporter systems overcome this problem, as they are expressed and function within living cells. Most of these systems consist of pairs of color variants of GFP [40]. The energy transfer between the fluorophores strongly depends on proximity and orientation of both donor and acceptor. Changes in orientation of the fluorophores can be measured either as changes in donor fluorescence lifetime or as changes in emission ratios between the fluorophores [41]. The latter method is more common as a readout because collection and interpretation of fluorescence lifetime data can be challenging. A typical FRET biosensor is composed of a central element consisting of a substrate peptide fused to a phosphoamino acid binding domain and flanked by the FRET donor–acceptor pair. Phosphorylation of the substrate sequence allows the phosphoamino acid binding domain to attach, inducing a strong bending of the central part, bringing the FRET pair into close proximity. This results in a FRET signal. The simple modular design of the reporter allows variation of several parameters such as attachment points of the fluorescent proteins or swapping N- and C-terminal mutations, generating optimized selectivity, dynamic range, and sensitivity.

A series of genetically encoded biosensors have been generated with this basic design. Further variations introduced into the design include targeting sequences that direct the reporters to specific subcellular locations, as well as exploiting changes in kinase structure upon activation, which is directly fused to the FRET pair as in the case of ERK2 [42]. Here, receptor tyrosine kinase dimerization is used to bring the FRET pair into proximity [43].

The same basic design can be combined either with the technology of split fluorescence protein complementation (which has been described in this chapter for the analysis of protein–protein interaction) or with split luciferases. When fused to the central reporter module consisting of the kinase substrate and the phosphoamino acid binding sequence, the complementary parts of the split fluorescent protein combine to form a functional unit. Such reporter systems have been published for GFP, YFP, and Renilla luciferase [44].

So far, cellular reporter systems have been mainly used for monitoring dynamic changes in basic research, as reporters have been reported only for a limited number of kinases, and generation of reporters may prove difficult for many kinases. Though, once established, this kind of assay can provide a cheap and robust alternative to screen larger compound collections, enabling real-life monitoring of dynamic cellular processes and resolution of inhibition kinetics.

2.3.5

Label-Free Technologies

Label-free technologies are phenotypic assays. They do not allow direct detection of substrate phosphorylation, but rather measurement of dynamic changes of cell morphology or mass redistribution induced by signaling pathways. The readouts can be tailored more specifically for certain kinases by using overexpression systems and/or pathway-specific stimuli [45]. A common detection technology is impedance measurement that detects changes in cell shape and attachment. This technology is offered, for example, by ACEA Biosciences, Corning Biosciences, Bionas, and ibidi GmbH, and requires microtiter plates with electrodes and special reader systems.

The operating principle of the label-free Epic system (Corning Biosciences) is based on refractive waveguide grating optical biosensors, which make very sensitive measurements of the index of refraction in a detection zone approximately 150 nm above the surface of the sensor. The sensor configuration consists of a three-layered system: a glass substrate, a thin waveguide film within an embedded grating structure, and a cell/biomolecule layer. When illuminated with broadband light, the biosensor reflects a specific wavelength of light that is a sensitive function of the index of refraction close to the sensor surface. Binding events or intracellular protein movements in cells cause wavelength shifts in the reflected light that is measured with the Epic instrument. Special readers and plates are required for this system, but 384-well plates make this system suitable for HTS.

A major advantage of label-free assays is that they enable fast assay development times, as cell lines suitable for screening do not have to be generated, and readouts are already standardized. In addition, primary cells can be easily used for screening in this system. Drawbacks of this system are reader and consumable costs. In addition, data interpretation may be difficult in some cases due to very sensitive detection of general changes in cell morphology.

2.3.6

Analysis of Kinase Family Selectivity

Even with systems allowing multiplexing, for example, the Luminex system, the number of signaling pathways monitored in a given sample is limited. Recent advances in proteomic technologies have enabled the assessment of the influence of kinase inhibitors on the entire kinome expressed in a given cell or tissue, or on the entire phosphoproteome. These assays are not amenable to HTS, but can provide valuable data when applied for assessment of selectivity profiles of more advanced kinase inhibitors.

2.3.7

SILAC

Quantitative proteomics based on mass spectrometry methods has become a powerful tool for high-throughput investigation of cell signal transduction in the last few years, boosted by development of quantitative methods and appropriate instruments. With

this technology, global pattern of changes in protein phosphorylation can be monitored after different cellular treatments. SILAC (stable isotope labeling by amino acids) in cell culture opens up an avenue for very accurate quantitative proteomics. Initially, this method has been reported to provide solutions for precise mass spectrometry-based quantitative proteomics [46]. It is based on the incorporation of amino acids with substituted stable isotopic nuclei (deuterium ^2H , ^{13}C , and ^{15}N). For labeling, two groups of cells are cultured in media that are identical except that the first, for example, control group, media contains the “light” and the other, for example, the inhibitor treated, a “heavy” form of a selected amino acid. Through the use of essential amino acids that cannot be synthesized in the cell type of interest, the cells will build the labeled or unlabeled amino acids into all kinase substrates containing this particular amino acid. Therefore, in each growth phase of the cell cycle the cell population replaces at least half the unlabeled form of the amino acid, leading to nearly 100% incorporation of the “light” or “heavy” variant of the amino acid after several rounds of cell cultures. When the labeled proteins are analyzed by mass spectrometry, the origin of the sample can be easily determined by the mass difference caused through the differential labeling with light and heavy isotopes. On the basis of the intensities of the light and heavy peptides, the relative abundance of the proteins in inhibitor-treated and -untreated samples can be quantified.

2.3.8

Affinity Chromatography with Immobilized Kinase Inhibitors

An assay allowing profiling of interaction partners of kinase inhibitors covering the entire proteome expressed in a cell line of interest was developed by Daub and coworkers [47]. This technology allows the identification of small-molecule drug targets in biologically relevant systems and the estimation of binding affinities of these interactions. By combining affinity purification with an immobilized small molecule of interest under well-defined conditions with quantitative mass spectrometry and competition experiments, the platform allows calculation of the dissociation constants (K_D) for compound–target interactions. These K_D values are derived in a two-step process. In the first step, drug–protein binding partners are captured on a solid matrix-immobilized compound, and affinities of each of the protein targets for this bead-coupled compound are determined. In the second step, bound targets are displaced with free compound. Metabolic or chemical labeling of the cell line or tissue sample proteomes, combined with proprietary experimental and analytical methods, enables quantitation of the drug–protein target affinities. K_D values of the target(s) for the free compound in solution are derived by applying algorithms to the above two data sets [48].

2.4

Outlook

Screening campaigns directed against cellular kinase targets may represent an alternative to traditional biochemical assays, as they offer a higher chance to identify

small molecules targeting nonconserved binding sites in a non-ATP-competitive fashion. Cellular test systems integrate many factors necessary for a kinase inhibitor to be effective in a cellular system, which would have been overlooked by pure biochemical screens, giving early hits a “head start” over hits from classical kinase screens. Cellular screening systems may represent a bridge between “historic” pharmaceutical screening in animals or isolated organs with high predictability but low throughput, on the one hand, and pure biochemical screening with high throughput but lower selectivity and predictability on the other hand, combining the advantages of both systems.

Although cellular kinase assays are not as straightforward as enzymatic kinase assays, an investment in cellular assay may be worth not only for probing advanced compounds for the desired biological effects but also for performing primary screening campaigns. Shifting primary screening programs to cellular test systems may yield compounds with a higher probability of success in clinical trials.

References

- Nolan, G.P. (2007) What's wrong with drug screening today. *Nature Chemical Biology*, **3** (4), 187–191.
- Bain, J., Plater, L., Elliott, M., Shpiro, N., Hastie, C.J., McLauchlan, H., Klevernic, I., Arthur, J.S., Alessi, D.R., and Cohen, P. (2007) The selectivity of protein kinase inhibitors: a further update. *The Biochemical Journal*, **408** (3), 297–315.
- Bain, J., McLauchlan, H., Elliott, M., and Cohen, P. (2003) The specificities of protein kinase inhibitors: an update. *The Biochemical Journal*, **371** (Pt 1), 199–204.
- Ohren, J.F., Chen, H., Pavlovsky, A., Whitehead, C., Zhang, E., Kuffa, P., Yan, C., McConnell, P., Spessard, C., Banotai, C., Mueller, W.T., Delaney, A., Omer, C., Sebolt-Leopold, J., Dudley, D.T., Leung, I.K., Flamme, C., Warmus, J., Kaufman, M., Barrett, S., Tecle, H., and Hasemann, C.A. (2004) Structures of human MAP kinase kinase 1 (MEK1) and MEK2 describe novel noncompetitive kinase inhibition. *Nature Structural & Molecular Biology*, **11** (12), 1192–1197.
- Cheng, Y. and Prusoff, W.H. (1973) Relationship between the inhibition constant (K_i) and the concentration of inhibitor which causes 50 per cent inhibition (IC_{50}) of an enzymatic reaction. *Biochemical Pharmacology*, **22** (23), 3099–3108.
- Traut, T.W. (1994) Physiological concentrations of purines and pyrimidines. *Molecular and Cellular Biochemistry*, **140** (1), 1–22.
- Gribble, F.M., Loussouarn, G., Tucker, S.J., Zhao, C., Nichols, C.G., and Ashcroft, F.M. (2000) A novel method for measurement of submembrane ATP concentration. *The Journal of Biological Chemistry*, **275** (39), 30046–30049.
- Nowakowski, J., Sridhar, V., Thompson, D.A., Cronin, C.N., Vaughn, D.E., Gangloff, A.R., Sang, B.C., Zoa, H., Kbuth, M.W., Swanson, R.V., Snell, G., Mol, C.D., Wilson, K.P., and McRee, D.E. (2003) Insights into selectivity of STI571 (GleevecTM) from X-ray crystallography. *Cellular & Molecular Biology Letters*, **8** (2A), 556.
- Frantz, B., Klatt, T., Pang, M., Parsons, J., Rolando, A., Williams, H., Tocci, M.J., O'Keefe, S.J., and O'Neill, E.A. (1998) The activation state of p38 mitogen-activated protein kinase determines the efficiency of ATP competition for pyridinylimidazole inhibitor binding. *Biochemistry*, **37** (39), 13846–13853.
- Gumireddy, K., Baker, S.J., Cosenza, S.C., John, P., Kang, A.D., Robell, K.A., Reddy, M.V., and Reddy, E.P. (2005) A non-ATP-competitive inhibitor of BCR-ABL overrides imatinib resistance. *Proceedings*

- of the National Academy of Sciences of the United States of America, **102** (6), 1992–1997.
- 11 Copeland, R.A., Pompliano, D.L., and Meek, T.D. (2006) Drug–target residence time and its implications for lead optimization. *Nature Reviews. Drug Discovery*, **5** (9), 730–739, Epub 2006 Aug 4.
 - 12 Fabbro, D., Manley, P.W., Jahnke, W., Liebetanz, J., Szyttenholm, A., Fendrich, G., Strauss, A., Zhang, J., Gray, N.S., Adrian, F., Warmuth, M., Pelle, X., Grotzfeld, R., Berst, F., Marzinzik, A., Cowan-Jacob, S.W., Furet, P., and Mestan, J. (2010) Inhibitors of the Abl kinase directed at either the ATP- or myristate-binding site. *Biochimica et Biophysica Acta*, **1804** (3), 454–462.
 - 13 Wissner, A. and Mansour, T.S. (2008) The development of HKI-272 and related compounds for the treatment of cancer. *Archiv der Pharmazie*, **341** (8), 465–477.
 - 14 Discafani, C.M., Carroll, M.L., Floyd, M.B., Jr., Hollander, I.J., Husain, Z., Johnson, B.D., Kitchen, D., May, M.K., Malo, M.S., Minnick, A.A., Jr., Nilakantan, R., Shen, R., Wang, Y.F., Wissner, A., and Greenberger, L.M. (1999) Irreversible inhibition of epidermal growth factor receptor tyrosine kinase with *in vivo* activity by N-[4-[(3-bromophenyl)amino]-6-quinazolinyl]-2-butanamide (CL-387,785). *Biochemical Pharmacology*, **57** (8), 917–925.
 - 15 Huynh, Q.K., Boddupalli, H., Rouw, S.A., Koboldt, C.M., Hall, T., Sommers, C., Hauser, S.D., Pierce, J.L., Combs, R.G., Reitz, B.A., Diaz-Collier, J.A., Weinberg, R.A., Hood, B.L., Kilpatrick, B.F., and Tripp, C.S. (2000) Characterization of the recombinant IKK1/IKK2 heterodimer. Mechanisms regulating kinase activity. *The Journal of Biological Chemistry*, **275** (34), 25883–25891.
 - 16 Suwa, A., Kurama, T., and Shimokawa, T. (2010) SHIP2 and its involvement in various diseases. *Expert Opinion on Therapeutic Targets*, **14** (7), 727–737.
 - 17 Ferrell, J.E., Jr. (1998) How regulated protein translocation can produce switch-like responses. *Trends in Biochemical Sciences*, **23** (12), 461–465.
 - 18 Marquardt, D.L., Alongi, J.L., and Walker, L.L. (1996) The phosphatidylinositol 3-kinase inhibitor wortmannin blocks mast cell exocytosis but not IL-6 production. *Journal of Immunology*, **156** (5), 1942–1945.
 - 19 Rogers, B., Decottignies, A., Kolaczowski, M., Carvajal, E., Balzi, E., and Goffeau, A. (2001) The pleiotropic drug ABC transporters from *Saccharomyces cerevisiae*. *Journal of Molecular Microbiology and Biotechnology*, **3** (2), 207–214.
 - 20 Jimeno, A., Rubio-Viqueira, B., Amador, M.L., Oppenheimer, D., Bouraoud, N., Kulesza, P., Sebastiani, V., Maitra, A., and Hidalgo, M. (2005) Epidermal growth factor receptor dynamics influences response to epidermal growth factor receptor targeted agents. *Cancer Research*, **65** (8), 3003–3010.
 - 21 Sherman, F. (1991) Guide to yeast genetics and molecular biology. *Methods in Enzymology*, **194**, 1–863.
 - 22 Knight, Z.A. and Shokat, K.M. (2005) Features of selective kinase inhibitors. *Chemistry & Biology*, **12** (6), 621–637.
 - 23 Arooz, T., Yam, C.H., Siu, W.Y., Lau, A., Li, K.K., and Poon, R.Y. (2000) On the concentrations of cyclins and cyclin-dependent kinases in extracts of cultured human cells. *Biochemistry*, **39** (31), 9494–9501.
 - 24 Scaltriti, M., Verma, C., Guzman, M., Jimenez, J., Parra, J.L., Pedersen, K., Smith, D.J., Landolfi, S., Ramon y Cajal, S., Arribas, J., and Baselga, J. (2009) Lapatinib, a HER2 tyrosine kinase inhibitor, induces stabilization and accumulation of HER2 and potentiates trastuzumab-dependent cell cytotoxicity. *Oncogene*, **28** (6), 803–814.
 - 25 Windheim, M., Lang, C., Peggie, M., Plater, L.A., and Cohen, P. (2007) Molecular mechanisms involved in the regulation of cytokine production by muramyl dipeptide. *The Biochemical Journal*, **404** (2), 179–190.
 - 26 Vigneri, P. and Wang, J.Y. (2001) Induction of apoptosis in chronic myelogenous leukemia cells through nuclear entrapment of BCR-ABL tyrosine kinase. *Nature Medicine*, **7** (2), 228–234.

- 27 Chen, H., Kovar, J., Sissons, S., Cox, K., Matter, W., Chadwell, F., Luan, P., Vlahos, C.J., Schutz-Geschwender, A., and Olive, D.M. (2005) A cell-based immunocytochemical assay for monitoring kinase signaling pathways and drug efficacy. *Analytical Biochemistry*, **338** (1), 136–142.
- 28 King, I.C., Feng, M., and Catino, J.J. (1993) High throughput assay for inhibitors of the epidermal growth factor receptor-associated tyrosine kinase. *Life Sciences*, **53** (19), 1465–1472.
- 29 Sadick, M.D., Intintoli, A., Quarmby, V., McCoy, A., Canova-Davis, E., and Ling, V. (1999) Kinase receptor activation (KIRA): a rapid and accurate alternative to end-point bioassays. *Journal of Pharmaceutical and Biomedical Analysis*, **19** (6), 883–891.
- 30 Angeles, T.S., Lippy, J.S., and Yang, S.X. (2000) Quantitative, high-throughput cell-based assays for inhibitors of trkA receptor. *Analytical Biochemistry*, **278** (2), 93–98.
- 31 Prinz, A., Diskar, M., and Herberg, F.W. (2006) Application of bioluminescence resonance energy transfer (BRET) for biomolecular interaction studies. *Chembiochem: A European Journal of Chemical Biology*, **7** (7), 1007–1012.
- 32 Moll, D., Prinz, A., Gesellchen, F., Drewianka, S., Zimmermann, B., and Herberg, F.W. (2006) Biomolecular interaction analysis in functional proteomics. *Journal of Neural Transmission*, **113** (8), 1015–1032.
- 33 Loechel, F., Bjørn, S., Linde, V., Praestegaard, M., and Pagliaro, L. (2007) High content translocation assays for pathway profiling. *Methods in Molecular Biology*, **356**, 401–414.
- 34 Ross, S., Chen, T., Yu, V., Tudor, Y., Zhang, D., Liu, L., Tamayo, N., Dominguez, C., and Powers, D. (2006) High-content screening analysis of the p38 pathway: profiling of structurally related p38alpha kinase inhibitors using cell-based assays. *ASSAY and Drug Development Technologies*, **4** (4), 397–409.
- 35 Gasparri, F., Cappella, P., and Galvani, A. (2006) Multiparametric cell cycle analysis by automated microscopy. *Journal of Biomolecular Screening*, **11** (6), 586–598.
- 36 Curran, T., Bravo, R., and Müller, R. (1985) Transient induction of c-fos and c-myc in an immediate consequence of growth factor stimulation. *Cancer Surveys*, **4** (4), 655–681.
- 37 Gasparri, F., Sola, F., Bandiera, T., Moll, J., and Galvani, A. (2008) High-content analysis of kinase activity in cells. *Combinatorial Chemistry & High Throughput Screening*, **11** (7), 523–536.
- 38 Weisberg, E., Boulton, C., Kelly, L.M., Manley, P., Fabbro, D., Meyer, T., Gilliland, D.G., and Griffin, J.D. (2002) Inhibition of mutant FLT3 receptors in leukemia cells by the small molecule tyrosine kinase inhibitor PKC412. *Cancer Cell*, **1** (5), 433–443.
- 39 Melnick, J.S., Janes, J., Kim, S., Chang, J.Y., Sipes, D.G., Gunderson, D., James, L., Matzen, J.T., Garcia, M.E., Hood, T.L., Beigi, R., Xia, G., Harig, R.A., Asatryan, H., Yan, S.F., Zhou, Y., Gu, X.J., Saadat, A., Zhou, V., King, F.J., Shaw, C.M., Su, A.I., Downs, R., Gray, N.S., Schultz, P.G., Warmuth, M., and Caldwell, J.S. (2006) An efficient rapid system for profiling the cellular activities of molecular libraries. *Proceedings of the National Academy of Sciences of the United States of America*, **103** (9), 3153–3158.
- 40 Shaner, N.C., Patterson, G.H., and Davidson, M.W. (2007) Advances in fluorescent protein technology. *Journal of Cell Science*, **120** (Pt 24), 4247–4260.
- 41 Suhling, K., French, P.M., and Phillips, D. (2005) Time-resolved fluorescence microscopy. *Photochemical & Photobiological Sciences*, **4** (1), 13–22.
- 42 Zhang, J. and Allen, M.D. (2007) FRET-based biosensors for protein kinases: illuminating the kinome. *Molecular BioSystems*, **3** (11), 759–765.
- 43 Offterdinger, M., Georget, V., Girod, A., and Bastiaens, P.I. (2004) Imaging phosphorylation dynamics of the epidermal growth factor receptor. *The Journal of Biological Chemistry*, **279** (35), 36972–36981.
- 44 Allen, M.D. and Zhang, J. (2006) Subcellular dynamics of protein kinase A activity visualized by FRET-based reporters. *Biochemical and Biophysical Research Communications*, **348**, 716–721.

- 45 Atienza, J.M., Yu, N., Wang, X., Xu, X., and Abassi, Y. (2006) Label-free and real-time cell-based kinase assay for screening selective and potent receptor tyrosine kinase inhibitors using microelectronic sensor array. *Journal of Biomolecular Screening*, **11** (6), 634–643.
- 46 Ong, S.E., Blagoev, B., Kratchmarova, I., Kristensen, D.B., Steen, H., Pandey, A., and Mann, M. (2002) Stable isotope labeling by amino acids in cell culture, SILAC, as a simple and accurate approach to expression proteomics. *Molecular & Cellular Proteomics*, **1** (5), 376–386.
- 47 Godl, K., Wissing, J., Kurtenbach, A., Habenberger, P., Blencke, S., Gutbrod, H., Salassidis, K., Stein-Gerlach, M., Missio, A., Cotten, M., and Daub, H. (2003) An efficient proteomics method to identify the cellular targets of protein kinase inhibitors. *Proceedings of the National Academy of Sciences of the United States of America*, **100** (26), 15434–15439.
- 48 Godl, K. (2008) Chemical proteomics: small molecule selectivity testing. *European Biotechnology News*, **7** (11–12), 36–37.

3

Dissecting Phosphorylation Networks: The Use of Analogue-Sensitive Kinases and More Specific Kinase Inhibitors as Tools

Matthias Rabiller, Jeffrey R. Simard and Daniel Rauh

3.1

Introduction

In the last decades, a range of new techniques have enabled experimentalists to control the function of protein(s) of interest in cells and have brought about a significant advance in our understanding of cellular signaling processes. In most of these techniques, the protein is controlled at the transcriptional level: either the gene coding for the protein is inserted into (knock-in) or deleted (knockout) from the genome, or the mRNA coding for the protein is specifically degraded (posttranscriptional gene silencing or RNA interference). A large number of genes have been studied using these approaches and several groups are working on scaled-up methods for automated genome-wide studies [4, 5]. However, these techniques are limited by their intrinsic complexity when performing studies in living animals. In addition, these techniques physically eliminate the protein of interest from the cell and diminish the capability of the cell to reverse and tune signaling pathways, which is essential for temporal control of perturbation experiments.

The creation of knockout mice involves months of laboratory work to remove the gene of interest from the genome and breed homozygote animals. If such animals are ultimately obtained, their biology adapts to the lack of the knockout enzyme, assuming the knockout is not lethal in the first place. Interference studies have brought improvements to this situation: when trying to remove a protein of interest from the cell, specifically designed interfering RNA molecules are delivered to cells following optimization for each sequence, cell or animal type. However, although RNA interference prevents the cell from producing the protein of interest, it also has some pitfalls. RNA interference does not eliminate the protein function that is already present in the cell. The slow natural turnover rate of some proteins, which might require hours or days, dampens the desired *switch off* of protein function, thereby providing the cell with enough time to compensate for the lost function or activity using alternative pathways. Finally, a major drawback that is common to both RNA interference and the use of knockouts is that these techniques physically eliminate the target protein from the cell or organism, thereby eliminating any potential nonenzymatic functions such as scaffolding and the associated mediation

of protein–protein interactions and of the catalytic activity of other proteins. Cell biologists are therefore seeking techniques that allow the experimentalist to selectively and instantaneously inhibit the activity of enzymes in a living organism without disrupting the natural spatial and temporal distribution of the corresponding protein. Small organic molecules such as enzyme inhibitors can be used to modulate protein function within a cellular context. They are ideal reagents to rapidly and reversibly perturb catalytic activity in a dose-dependent manner at any stage of animal development, while avoiding long-term transcriptional compensation mechanisms that complicate the interpretation of knockout and RNA interference experiments. We expect that such features will prove invaluable for the elucidation of molecular network dynamics, the next great challenge in cell biology.

The systematic application of small molecules to perturb protein function in cells to better understand the dynamic composition of biological systems lies at the heart of chemical biology. However, the development of selective small molecules to “chemically knock out” an enzyme of interest is difficult and time-consuming. These inhibitors can also perturb several structurally related enzymes, leading to off-target effects: although several selective inhibitors are known, it is unlikely that any of them bind exclusively to a single protein. To deal with the extreme difficulties of designing such inhibitors, the *bump-and-hole* approach combines inhibitor design and target enzyme engineering to obtain highly specific enzyme–inhibitor pairs (Figure 3.1). Point mutations are introduced in the binding site of the target enzyme

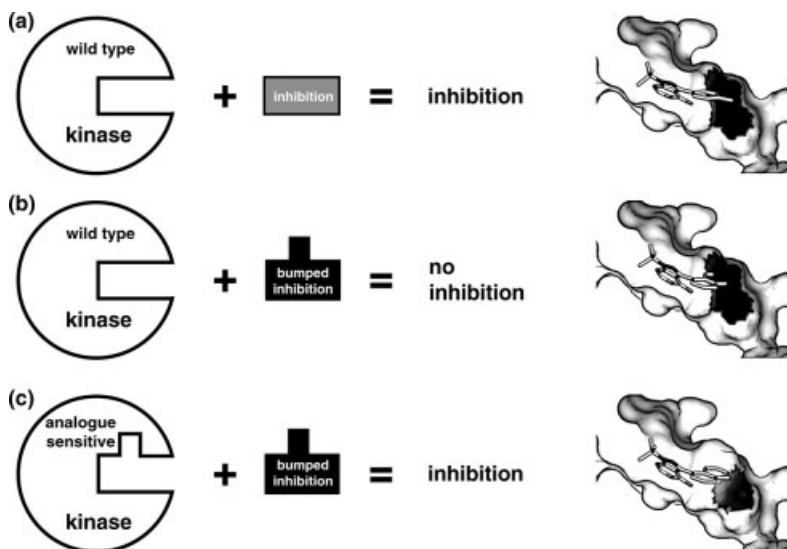


Figure 3.1 Schematic presentation of the “bump-and-hole” approach to inhibit kinases. Inhibition of a protein kinase by a broad-spectrum kinase inhibitor (a). A sterically demanding bumped inhibitor does not bind to

wild-type kinases due to steric hindrance (b). The bumped inhibitor binds to an analogue-sensitive allele of the kinase that complements the steric bulk by way of a mutated gatekeeper residue (c). The gatekeeper residue is colored black.

to accommodate an inhibitor molecule that is designed to specifically inhibit this mutated protein and not the wild-type enzyme or related family member proteins. Similarly, cofactors binding exclusively to an engineered enzyme can also be designed based on their natural counterparts.

The bump-and-hole approach was initially applied to the transcription factor EF-Tu [6] and has since then been applied to a variety of different enzymes. In the laboratory of Kevan Shokat at the University of California, San Francisco, the bump-and-hole approach was further developed into a powerful chemical genetics approach to dissect kinase function in complex systems. This technique is known under various terms, the most common ones being *orthogonal ligand* and *orthogonal receptor* pairs.

In the present chapter, we will focus on this approach and its application to protein kinases, also known as analogue-sensitive kinase allele (ASKA). We describe how ASKA ligands and kinases can be designed and functionalized for various uses in molecular and cell biology and provide brief insights into the wealth of biological information obtained from more than 60 kinases studied with ASKA. In addition, we present a few new powerful assay systems that can be used to design more specific tight binding ligands aimed at targeting less conserved binding pockets in kinases to achieve improved specificity without requiring prior mutation of the kinase gatekeeper as done for ASKA.

3.2

Chemical Genetics

Understanding the function of a particular kinase requires an understanding of its substrate proteins. Based on this knowledge, various methods have been developed to directly identify protein kinase–substrate pairs in a biologically relevant context. However, this task is made particularly difficult by the activity of a large number of kinases similar to the kinase of interest as well as overlapping substrate specificities. Many methods for target substrate identification involve the use of radioactive ATP and yield complex mixtures of hot substrate proteins, making it difficult to decipher phosphorylation by a particular kinase.

3.2.1

Engineering ASKA Ligand–Kinase Pairs

By creating an ATP analogue that can be used only by an engineered Src kinase, Shah *et al.* laid the foundation for ASKA technology [7]. The purpose of this work was to provide the proof of concept that ASKA is a straightforward method to directly identify kinase substrates by following the transfer of radioactive γ -phosphate from the ATP analogues specific for the ASKA kinase of interest. Since the three-dimensional structure of Src was not available at the time the study was initiated, the authors analyzed the crystal structures of related protein kinases such as PKA and CDK2 to identify the region of the nucleotide binding pocket where the N^6 -position of ATP binds. A Val and an Ile residue located in this area were chosen for mutation to

the smaller Ala to extend the binding pocket of Src and allow bulky N^6 -ATP derivatives to be accommodated. However, these mutations affected the catalytic efficiency, making the ASKA Src 50 times less active than the wild type. To show that the mutations have no effect on the substrate specificity of the engineered Src, SF9 insect cells, which lack endogenous tyrosine kinase activity, were transfected with either wild-type or ASKA Src. Tyrosine phosphorylation patterns of the wild-type and ASKA Src were identical, proving that the mutations did not influence substrate specificities. Several ATP analogues were designed, and one of them, N^6 -(cyclopentyl)-ATP (Figure 3.2), was chosen for its specificity and efficiency as a phosphodonor for the engineered kinase. Experiments in murine lymphocyte cell lysates showed that N^6 -cyclopentyl ATP was utilized by the ASKA Src but not by the various kinases endogenous to the lysate. The creation of an efficient analogue-sensitive Src kinase–ligand pair without complex chemistry or the benefit of detailed protein structural knowledge established ASKA as a powerful molecular biology tool that, in principle, should be easily adaptable to many kinases.

The publication of a new kinase crystal structure allowed Liu *et al.* to make a finer structural analysis and identify an amino acid position that is typically occupied by an amino acid larger than Ala in a majority of mammalian kinases [8]. This so-called

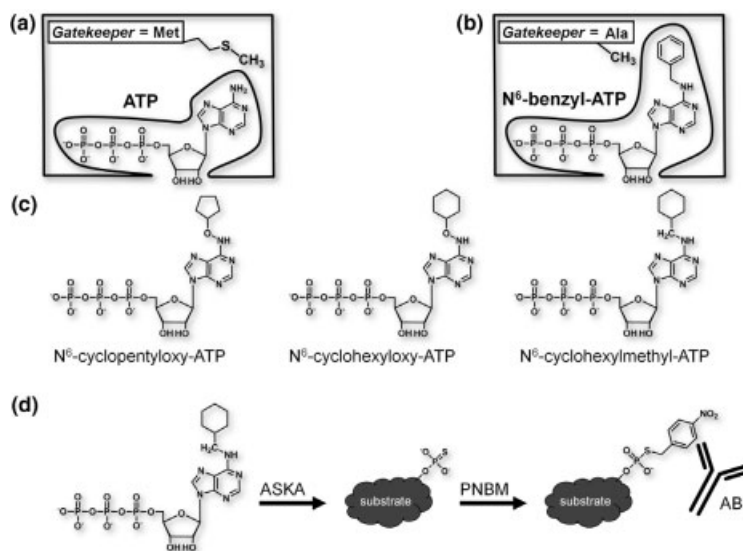


Figure 3.2 Schematic presentation of the “bump-and-hole” approach to label kinase substrates. ATP binding to the kinase domain (a). The ASKA version of a kinase complements the steric bulk of a modified ATP analogue and allows phosphate transfer to a substrate (b). ATP analogues used for substrate labeling (c).

Strategy for labeling individual kinase substrates by affinity tagging ASKA kinase substrates. N^6 -alkylated ATP γ S is used to thiophosphorylate its substrates. Subsequent alkylation with PNBM yields thiophosphate esters that are recognized by thiophosphate ester-specific antibodies (d).

gatekeeper position is situated at the back of the ATP binding pocket and adjacent to the hinge region that connects the N- and C-terminal lobes of the kinase domain. Amino acid side chains at the gatekeeper position contact the N⁶-position of ATP, but they are not essential for ATP binding. Therefore, the gatekeeper threonine of the tyrosine kinase Fyn was mutated into Ala to make it analogue sensitive for the ASKA approach. From that point onward, the Shokat group standardized the use of Ala or Gly mutations at the gatekeeper position to produce ASKA kinases. Mutations to Ala turned out to be generally most successful, yet in some cases, the Gly mutant yielded the only active kinase variant.

Having produced several “bumped” ATP derivatives for direct substrate identification, the Shokat group then applied this concept to the design of bumped kinase inhibitors to specifically inhibit ASKA kinases. The pyrazolo-pyrimidine PP1 was chosen as the basis for this approach: since it is a wide-spectrum kinase inhibitor, a bumped analogue can be expected to inhibit most ASKA kinases. Of the several candidates synthesized, two molecules named NA-PP1 and NM-PP1 (Figure 3.3) were used in nearly all follow up ASKA studies. The availability of these two compounds from commercial sources demonstrates the growing popularity of the ASKA approach. Since these pilot studies, several additional kinase inhibitors have been chemically modified for use in ASKA studies: the PI3K inhibitor LY294002 [9], pyrrolo-pyrimidines in a study of Rsk1, Rsk2, and Msk kinases [10], and quinazolines such as PD168393 that was used in a study involving ASKA EGFR and Src [11]. Interestingly, the latter two cases are examples of covalent inhibitors, carrying reactive groups capable of modifying a particular Cys residue found in the ATP binding site of the target kinase. In Refs [10] and [11], the authors exploit a Cys naturally occurring in the studied kinases as anchor points for the covalent inhibitor. In Refs [11] and [12], a reactive Cys residue was introduced into Src kinase by site-directed mutagenesis to mimic the endogenous anchor Cys of EGFR and HER2 and

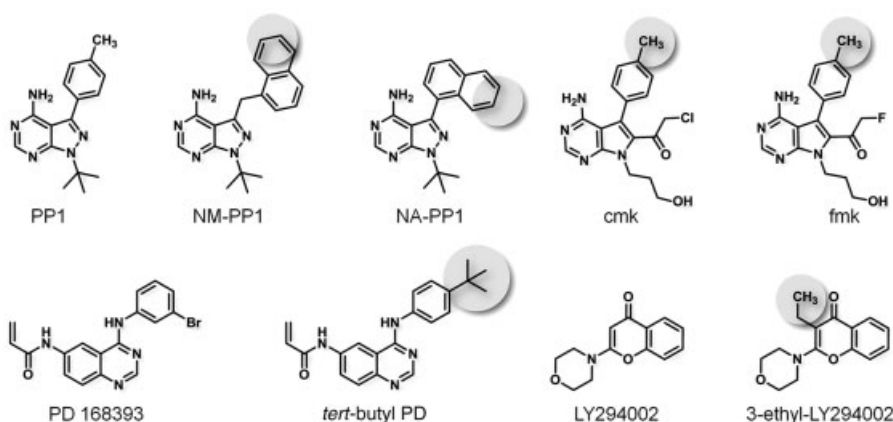


Figure 3.3 List of kinase inhibitors and their bumped counterparts. The bulky group is highlighted by a gray circle.

to serve as an anchor point for covalent inhibitor attachment. The covalent bond formed between the inhibitor and the anchor Cys of the kinase can serve as a second selectivity filter and provides a way to covalently label kinases with additional functionalities such as fluorophores to study kinase localization, compartmentalization and signaling in living cells [11]. In fact, the ASKA technology has been successfully applied *in vivo* using either NM-PP1 or NA-PP1 throughout the eukaryotic kingdom (first applications are reported in Refs [13–16] for yeast, mammalian cell cultures, plants, and mice, respectively). In all cases, cells or organisms are genetically modified to express the ASKA kinase of interest and the desired inhibitor is added to the culture medium, fed to the animal with its regular diet, or sprayed onto the plant leaves.

Like all enzymes, kinases rely on the precise spatial arrangement of their active site residues as well as on the tuning of their reactivity to stabilize transition states and thus catalyze chemical reactions. Although the gatekeeper residue of kinases is not directly involved in the phosphorylation reaction, its mutation may lead to conformational changes that adversely affect kinase activity (Box 3.1). The observation in the original ASKA paper [7] that ASKA Src (which did not rely on the gatekeeper mutation) is 50 times less active than its wild-type counterpart brought this issue into the spotlight. Such difficulties were more obvious in the case of ASKA variants of the Abelson kinase (Abl) that was unable to use natural ATP as a substrate. An enzymatically active ASKA chimera kinase retaining the protein substrate specificity of Abl was subsequently obtained by replacing the N-terminal lobe of the kinase domain of Abl by that of Src. Further research showed that ASKA kinase activity can also be rescued by subtle point mutations rather than by swapping in entire

Box 3.1

The Gatekeeper Residue

The gatekeeper residue is a conserved, large hydrophobic residue in the ATP binding pocket of protein kinases. Mutation of this naturally occurring bulky residue (Phe, Met, etc.) to smaller residues such as Ala or Gly generates a pocket not found in wild-type kinases. ATP analogue-based competitive small molecules designed to complement the extended ATP binding pocket can be used to specifically target and inhibit the analogue-sensitive kinase. The gatekeeper residue is known to be a critical determinant for selective inhibition within kinase families. Interestingly, since the kinase inhibitor Gleevec[®] was introduced into the clinic as the first targeted cancer therapeutic at the start of the millennium for chronic myelogenous leukemia (CML) and gastrointestinal stromal tumors (GISTs) [47], a single recurring mutation to a bulkier residue at the gatekeeper position that results in drug resistance of several target kinases was identified in tumor specimens [48]. It is thought that the bulkier residue at the gatekeeper position sterically impedes binding of reversible inhibitors in the active site of the kinase. At the same time however, ATP binding and kinase activity are retained.

subdomains of others kinases. Though no particular mutation could be identified as a general rescuer of ASKA kinase activity, comparing the ATP binding pocket of the kinase of interest with related kinases often provides information about the positions and nature of potential rescuing mutations. For example, the p21-activated kinase (PAK) Cla4 has a Thr in the N-terminal part of the DFG motif (an Asp–Phe–Gly sequence that is highly conserved among protein kinases and undergoes conformational changes upon activation or inactivation of the enzyme), a position occupied by an even smaller amino acid in most kinases [17]. Based on the hypothesis that the Thr side chain may not leave enough space in the active site of ASKA Cla4 to allow the bumped inhibitor to bind, Weiss *et al.* markedly improved NM-PP1 binding to ASKA Cla4 by mutating it into Ala.

Interestingly, point mutations at positions making no direct contacts with the bumped ligands can also rescue ASKA kinase activity. Although such mutations are impossible to predict with our current understanding of such structure–function relationships in kinases, the long-range effect of point mutations to rescue kinase activity was shown experimentally in a random mutagenesis study performed by Zhang *et al.* [15]. In this work, the authors took advantage of a straightforward readout (survival in presence of kanamycin) to study mutations that rescue ASKA APH(3′)-IIIa, a microbial kinase known to detoxify kanamycin and neomycin. In addition to the expected gatekeeper mutations back to larger amino acids, a second class of rescuing mutations distributed all over the nucleotide and kanamycin binding pockets of APH(3′)-IIIa were observed. At this point, it is difficult to interpret most of the rescuing mutations that are surface-exposed residues or to find direct equivalents in other protein kinases. However, since β -branched amino acids (e.g., Ile) are preferred over non- β -branched amino acids (e.g., Leu) in β -sheets, the authors interpret the rescuing mutations closest to the gatekeeper position (Asn to Thr at position 87) as compensating for the destabilizing effect of the Met to Gly gatekeeper mutation. They successfully tested this hypothesis by rescuing several nonfunctional ASKA kinases with mutations of non- β -branched amino acids in the β -sheet of the N-lobe to β -branched amino acids. In summary, three (not mutually exclusive) criteria may apply when desiring to rescue ASKA point mutations: (1) the kinase of interest can be made “more like” its relatives by domain swapping, (2) based on structural information, steric interference with the bumped ligand can be reduced, and (3) in β -sheets, non- β -branched amino acids can be replaced with β -branched ones.

Due to the use of natural ATP by ASKA kinases, experiments that rely on the transfer of radioactive phosphate from bumped ATP to kinase substrates suffer from relatively high signal-to-noise ratios, a situation that could be significantly improved by reducing the affinity of ASKA kinases for natural ATP. To this end, Ulrich *et al.* [18, 19] first produced a bumped phosphodonor small enough to be accepted by an ASKA kinase that has a shrunken ATP binding pocket. This research led to the development of first N^{\dagger} -(benzyl)-RTP (to which only ASKA Src could bind at cellular ATP concentrations but failed as a substrate) and then N^{\dagger} -(benzyl)-ACAIR triphosphate (which had better orthogonality and was used as a phosphodonor by ASKA P38, albeit less efficiently than ATP). In Ref. [20], Ulrich *et al.* describe a pair

of Leu to Met mutations that reduce catalytic efficiency of Fyn and Src with ATP as a substrate, while increasing it when bumped ATP is the substrate, eliminating the need to redesign bumped ATP. These mutations disrupt the interactions between the purine ring of ATP and the ATP binding pocket of the ASKA kinase. Alternatively, the interactions between the bulky group of bumped ATP and the “hole” in the ATP binding site allow the bumped analogue to interact better with the modified ASKA kinase.

3.3

The Application of ASKA Technology in Molecular Biology

An essential but difficult task in kinase research is the identification and characterization of kinase substrate specificities. To this end, Shokat *et al.* have proposed two basic ways to use ASKA technology to perform such studies.

3.3.1

Identification of Kinase Substrates

In biological experiments, the ASKA kinase-catalyzed transfer of radioactive phosphate from bumped ATP analogues to substrates, or the lack of substrate phosphorylation after treatment of ASKA kinases with bumped inhibitors can be monitored. These methods have allowed scientists to identify many previously unknown kinase–substrate pairs. However, the method often proves challenging due to the low natural abundance of kinase substrates. Dephoure *et al.* could circumvent this issue by investigating the phosphorylation of overexpressed TAP-tagged candidate substrates of exogenous ASKA Pho85 kinase and using radioactive bumped ATP analogues in yeast lysates [21]. TAP-tagged proteins were then isolated from the reaction mixture by immunoprecipitation and their phosphorylation status was determined by autoradiography. Recently, Allen *et al.* also presented a method to directly fish ASKA kinase substrates [22]. The method was successfully applied to the identification of an Erk2 substrate called Tpr, a nucleoporin involved in protein trafficking through the nuclear envelope. They designed and synthesized a bumped ATP γ S analogue from which the ASKA kinase of interest transfers a thiophosphate group onto its protein substrate (Figure 3.2). Treatment of the reaction mixture with *p*-nitrobenzyl-mesylate modifies the thiophosphate group to a thiophosphoester that can then be recognized by a monoclonal antibody, allowing the enrichment of ASKA kinase substrates by immunoprecipitation.

3.3.2

Studies on Kinase Inhibition

The use of bumped inhibitors opens experimental possibilities beyond the identification of kinase substrate pairs. A bumped inhibitor – classically NM-PP1 or NA-PP1 – is readily taken up from culture medium by live cells or from food by

animals. This produces a fast and dose-dependent inhibition of the ASKA kinase in otherwise undisturbed cells. Furthermore, it does not limit in any way the spectrum of methods that can be used to observe resulting phenotypes following inhibitor treatment. One particularly interesting way of monitoring phenotypical changes in bumped inhibitor treated cells is the use of microarray technology to determine gene expression profiles triggered by ASKA kinase inhibition. This information can be used to decipher pathways that are regulated by the kinase of interest or for the identification of compounds targeting the kinase of interest. The latter is done by comparing expression profiles obtained from cells treated with the compound of interest versus cells in which the ASKA kinase of interest is treated with a bumped inhibitor. Such an approach was used by Jiang *et al.* to determine the selectivity of various Btk inhibitors [23] and by Kung *et al.* to demonstrate that the effects observed following treatment of yeast cells with GW400426 are due to the simultaneous inhibition of Pho85 and Cdk1 [24].

These studies exemplify the advantage provided by the ASKA technology when compared to classical, purely biological methods. In earlier studies, Btk knockout experiments [25, 26] were impaired by the ability of cultured cells to compensate for the loss of Btk by increasing the activity of other kinases found in Btk-associated pathways. Since chemical perturbation of ASKA Btk activity does not leave the cells enough time to compensate for the loss of Btk, the ASKA method helps to provide a more precise picture of cellular processes regulated by Btk kinase activity.

A number of publications give further examples of the difficulties associated with the investigation of kinase function with conventional methods (i.e., yeast two-hybrid and temperature-sensitive alleles) that could be successfully bypassed with the use of ASKA technology. In studies of MEK1 and HOG1, ASKA helped to limit artifacts caused by cellular adaptation and allowed substrates of the kinase of interest to be more easily identified. For example, the functional relationship between the MAP kinases MEK1 and Red1 in yeast had long been unclear. Earlier studies based on MEK1 deletion mutants [27] showed that the phosphorylation of Red1 depends on the presence of MEK1, but could not conclude whether Red1 is directly phosphorylated by MEK1. Using ASKA MEK1, Wan *et al.* [28] could show that Red1 is not a direct substrate of MEK1, and proposed an alternative model in which phosphorylated Red1 recruits MEK1. They proposed that after MEK1 autophosphorylates itself, it phosphorylates proteins such as Rad51 and Rad54 thereby preventing sister chromatid recombination. The use of ASKA technology also allowed Westfall and Thorner [29] to clarify the function of HOG1 in cellular responses to hyperosmotic environments. HOG1 deletion mutants used in previous studies displayed inappropriate cross-activation of the mating pheromone pathway, but it was not known whether this resulted from long-term adaptation to the loss of HOG1, or it was the effect of the absence of HOG1 activity or the absence of the HOG1 protein itself. Using ASKA HOG1, the authors could demonstrate that HOG1 activity is indeed needed for the downregulation of the mating pheromone pathway.

The identification of hnRNP-K as a substrate of the human serine/threonine JNK kinase by Habelhah *et al.* [14] or the finding by Carroll *et al.* that yeast Pho85 controls

the expression of 250 genes not previously known to be influenced by this kinase [30] are two further examples showing that ASKA can be a potent method for the identification of kinase substrates and signaling pathway elements not readily identified by classical methods.

ASKA also offers the opportunity to greatly simplify experimental setups. For example, it may be of interest to observe the effect of different dosages of the activity of a particular kinase on an organism such as a mouse. Normally, this requires the generation of several mice lines expressing various levels of the kinase of interest. The ASKA approach cuts that effort to the production of a single mouse line in which the activity of the kinase of interest can be tuned at will by choosing concentrations of the bumped inhibitor.

Though kinases may be the class of enzymes most extensively studied by the bump-and-hole approach, they are neither the first nor the only class of enzymes studied by these methods. As mentioned earlier, Ef-TU was the first protein targeted by this approach [6], and a number of additional enzymes have been submitted to it since then. For example, the design of a retinoid X receptor (RXR) bump and hole pair by mutating RXR to bind “near drugs” – compounds synthesized during structure–activity studies that are structurally similar to an approved drug yet inactive on the wild-type receptor – was described by Doyle *et al.* [31]. In Ref. [32], Nguyen *et al.* describe the design of a peptide–peptoid orthogonal ligand binding only to the Crk SH3 domain, but not to the closely related Src and Grb2 SH3 domains.

3.3.3

Alternative Approaches to Specifically Targeting Kinases of Interest

The ASKA approach has undoubtedly led to advances in the understanding of complex kinase signaling networks and helped to validate drug targets. However, despite these recent successes in kinase inhibitor research, the lack of inhibitor selectivity, efficacy, and the emergence of kinase drug resistance remain key challenges [33] that may require alternative strategies. This can be attributed to the fact that most kinase inhibitors are ATP-competitive molecules, such as staurosporine and dasatinib, which form a critical hydrogen bond with the hinge region of the kinase domain (type I inhibitors) and often extend into the back of the ATP pocket in the vicinity of the gatekeeper residue. As described above, the gatekeeper is well known for influencing inhibitor affinity and selectivity profiles among kinases [34], thus providing the basic premise of using ASKA kinases and bumped inhibitors to elucidate signaling pathways. However, mutated gatekeeper residues also play causative roles in several types of cancer [35]. Interestingly, one of the most common kinase mutations observed in several cancer cell lines occurs at the gatekeeper position in which smaller amino acid side chains are exchanged for larger hydrophobic residues such as Ile (as in Abl) or Met (as in EGFR). Such mutations have the reverse effect as that used in the ASKA approach. They reduce the size of the ATP pocket, disrupt the binding mode of inhibitors, and can dysregulate signaling pathways in these cells by increasing the activity of the kinase variant.

To address these issues, alternative ASKA-like approaches are needed in which selectivity is enhanced through chemistry. Therefore, current medicinal chemistry endeavors seek to overcome these limitations by identifying new chemical entities that bind “around” the gatekeeper and extend into less conserved sites outside the ATP pocket [36, 37]. Such compounds (type II inhibitors) would be expected to have improved selectivity profiles, offer new opportunities for scaffold development [38], and may serve as tools for specifically inhibiting a kinase of interest in cancer cells. However, gatekeeper mutations have been shown to disrupt the binding of such inhibitors, highlighting the need to further address the allosteric pocket beyond the gatekeeper position with smaller type III inhibitors.

Two recently developed assay systems now allow the identification of molecules that bind in this pocket. The first assay employs an environmentally sensitive fluorophore that has been covalently attached to the regulatory activation loop of the kinase using a cysteine residue introduced via site-directed mutagenesis into a position that did not significantly alter the kinetic parameters of the kinase (Figure 3.4).

The activation loop is a crucial regulator of the substrate binding cleft, participating in the coordination of ATP and recognition of substrates and influencing the arrangement of the catalytic residues. In the inactive conformation, the kinase activation loop adopts a conformation that is enzymatically incompetent, thereby opening the allosteric site for ligand binding. The equilibrium between the active (DFG-in) and inactive (DFG-out) conformations can be modulated by phosphorylation of the activation loop, by protein–protein interactions, or by the binding of different inhibitor classes of type I, II, or III inhibitors. Thus, the use of fluorescent labels in kinases (FLiK) as an assay system allows the sensitive detection of ligands that address the less conserved allosteric binding site and stabilize the DFG-out conformation of the kinase. This assay system also allowed the direct measurement of dissociation constants (K_d) as well as k_{on} and k_{off} for these ligands [39]. When applied to cSrc [40], this assay approach detected the first known type III cSrc binders that were subsequently developed into potent inhibitors that can overcome bulky Met mutations at the gatekeeper position [41].

Another recently developed assay detects the binding of these types of inhibitors through the displacement of a prebound type III inhibitor probe [42]. The approach also makes use of the enzyme fragment complementation (EFC) technology originally developed for type I inhibitors (Figure 3.4) [43]. More specifically, a probe consisting of a type III inhibitor chemically conjugated to small (~5 kD) enzyme donor (ED) peptide fragment of β -galactosidase is prebound to the kinase of interest. This peptide fragment complements an inactive truncated β -galactosidase to form an active enzyme that can carry out a luminescence reaction that serves as the readout of the assay. Competitive displacement of the ED conjugate from the kinase occurs in the presence of ligands that also make use of this allosteric pocket (type II/III inhibitors). The system has been extended to additional kinases to demonstrate its broader applicability for screening of inhibitors that stabilize inactive kinase conformations.

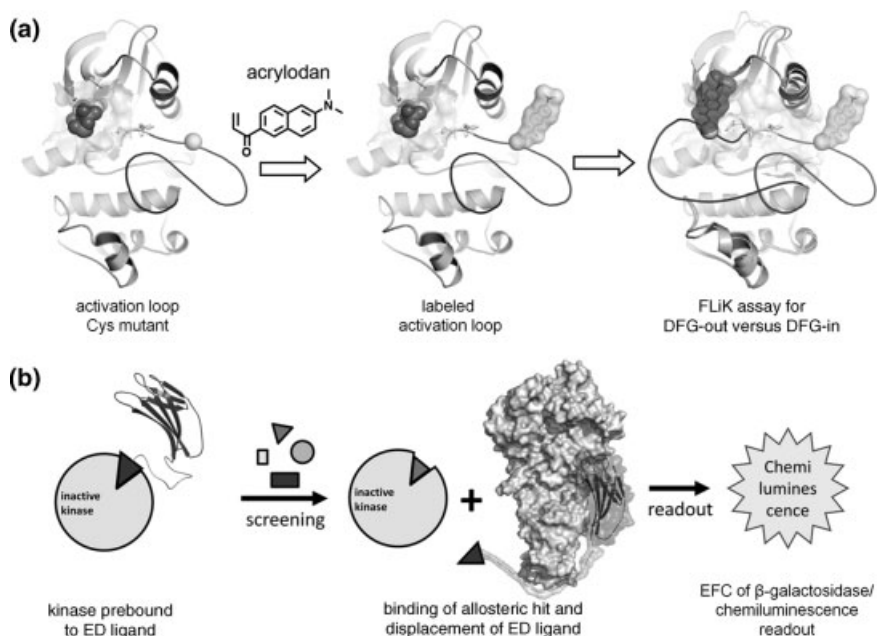


Figure 3.4 Design and development of assay systems that screen for DFG-out binding ligands. Schematic representation of the FLiK assay. The kinase of interest is labeled on the activation loop with an environmentally sensitive fluorophore such as acrylodan. The addition of DFG-out binding ligands induces a conformational change to the inactive DFG-out conformation, resulting in a fluorescence change. Using increasing concentrations of inhibitor, measurements can either be performed at an endpoint or in real-time to determine the K_d or kinetics of binding/dissociation, respectively (a).

Schematic representation of the EFC assay principle based on structure (PDB-ID: 1DPO) [42, 49]. The enzyme donor (ED) ligand is bound to the allosteric site of the inactive DFG-out conformation (b). In a screening scenario, small molecules compete with the ED ligand for binding to the kinase. The displaced peptide portion of the ED ligand binds to a truncated form of β -galactosidase that is only active when complemented by the ED ligand. The enzymatic activity of β -galactosidase is then measured via luminescence as a result of ED ligand displacement by screening hits.

3.4

Conclusions and Outlook

In this chapter, we have described the use of mutations of the gatekeeper residue of protein kinases to render them sensitive to designed ligands. Interestingly, mutations at the gatekeeper position are not only powerful cell biology tools but also have, as predicted by Blencke *et al.* [44], a high clinical relevance in kinase-targeted cancer therapy. Mutation to a large amino acid at the gatekeeper position of BCR-Abl, cKit, the platelet-derived growth factor receptor- α (PDGFR α) [45], and EGFR [46] have been observed to result in tumor drug resistance. It could be shown that these mutations prevent binding of anticancer kinase inhibitors such as imatinib, gefitinib,

and erlotinib due to steric hindrance and highlights the necessity for the development of novel strategies to design inhibitors capable of overcoming mutation-associated drug resistance in kinases [12].

The enormous wealth of knowledge on protein phosphorylation and dephosphorylation accumulated in the past years reflects the central role of these processes in the regulation of cell signaling pathways. Chemical genetic strategies in general and the ASKA technology presented here in particular are ideal tools to complement modern gene knockout and knock-in techniques and help to investigate biological phenomena with a temporal resolution unattainable by deregulating kinases at the transcriptional level. Similarly, the development of novel assay systems to address ligand binding into less conserved binding sites in kinases will address the problem of gatekeeper mutation-associated drug resistance and provide more specific inhibitors for targeting kinases of interest in cells. Eventually, these methods will help to decipher the complex dynamics of kinase signal transduction and lead to a better understanding of protein function at the cellular and organism levels to assist in the design and development of innovative new medicines.

References

- 1 Mulder, G.J. (1839) Ueber die Zusammensetzung einiger thierischen Substanzen. *Journal für praktische Chemie*, **16**, 129
- 2 Burnett, G. and Kennedy, E.P. (1954) The enzymatic phosphorylation of proteins. *The Journal of Biological Chemistry*, **211** (2), 969–980.
- 3 Krebs, E.G. (1983) Historical perspectives on protein phosphorylation and a classification system for protein kinases. *Philosophical Transactions of the Royal Society of London. Series B, Biological Sciences*, **302** (1108), 3–11.
- 4 Gwack, Y. *et al.* (2006) A genome-wide *Drosophila* RNAi screen identifies DYRK-family kinases as regulators of NFAT. *Nature*, **441** (7093), 646–650.
- 5 Pelkmans, L. *et al.* (2005) Genome-wide analysis of human kinases in clathrin- and caveolae/raft-mediated endocytosis. *Nature*, **436** (7047), 78–86.
- 6 Weijland, A. and Parmeggiani, A. (1993) Toward a model for the interaction between elongation factor Tu and the ribosome. *Science*, **259** (5099), 1311–1314.
- 7 Shah, K. *et al.* (1997) Engineering unnatural nucleotide specificity for Rous sarcoma virus tyrosine kinase to uniquely label its direct substrates. *Proceedings of the National Academy of Sciences of the United States of America*, **94** (8), 3565–3570.
- 8 Liu, Y. *et al.* (1998) Engineering Src family protein kinases with unnatural nucleotide specificity. *Chemistry & Biology*, **5** (2), 91–101.
- 9 Alaimo, P.J., Knight, Z.A., and Shokat, K.M. (2005) Targeting the gatekeeper residue in phosphoinositide 3-kinases. *Bioorganic & Medicinal Chemistry*, **13** (8), 2825–2836.
- 10 Cohen, M.S. *et al.* (2005) Structural bioinformatics-based design of selective, irreversible kinase inhibitors. *Science*, **308** (5726), 1318–1321.
- 11 Blair, J.A. *et al.* (2007) Structure-guided development of affinity probes for tyrosine kinases using chemical genetics. *Nature Chemical Biology*, **3** (4), 229–238.
- 12 Michalczyk, A. *et al.* (2008) Structural insights into how irreversible inhibitors can overcome drug resistance in EGFR. *Bioorganic & Medicinal Chemistry*, **16** (7), 3482–3488.
- 13 Bishop, A.C. *et al.* (2000) A chemical switch for inhibitor-sensitive alleles of any protein kinase. *Nature*, **407** (6802), 395–401.

- 14 Habelhah, H. *et al.* (2001) Identification of new JNK substrate using ATP pocket mutant JNK and a corresponding ATP analogue. *The Journal of Biological Chemistry*, **276** (21), 18090–18095.
- 15 Zhang, C. *et al.* (2005) A second-site suppressor strategy for chemical genetic analysis of diverse protein kinases. *Nature Methods*, **2** (6), 435–441.
- 16 Chen, X. *et al.* (2005) A chemical-genetic approach to studying neurotrophin signaling. *Neuron*, **46** (1), 13–21.
- 17 Weiss, E.L. *et al.* (2000) Chemical genetic analysis of the budding-yeast p21-activated kinase Cla4p. *Nature Cell Biology*, **2** (10), 677–685.
- 18 Ulrich, S.M. *et al.* (2000) Towards the engineering of an orthogonal protein kinase/nucleotide triphosphate pair. *Tetrahedron*, **56** (48), 9495–9502.
- 19 Ulrich, S.M., Sallee, N.A., and Shokat, K.M. (2002) Conformational restraint is a critical determinant of unnatural nucleotide recognition by protein kinases. *Bioorganic & Medicinal Chemistry Letters*, **12** (21), 3223–3227.
- 20 Ulrich, S.M., Kenski, D.M., and Shokat, K.M. (2003) Engineering a “methionine clamp” into Src family kinases enhances specificity toward unnatural ATP analogues. *Biochemistry*, **42** (26), 7915–7921.
- 21 Dephoure, N. *et al.* (2005) Combining chemical genetics and proteomics to identify protein kinase substrates. *Proceedings of the National Academy of Sciences of the United States of America*, **102** (50), 17940–17945.
- 22 Allen, J.J. *et al.* (2007) A semisynthetic epitope for kinase substrates. *Nature Methods*, **4** (6), 511–516.
- 23 Jiang, S. *et al.* (2007) Chemical genetic transcriptional fingerprinting for selectivity profiling of kinase inhibitors. *Assay and Drug Development Technologies*, **5** (1), 49–64.
- 24 Kung, C. *et al.* (2005) Chemical genomic profiling to identify intracellular targets of a multiplex kinase inhibitor. *Proceedings of the National Academy of Sciences of the United States of America*, **102** (10), 3587–3592.
- 25 Islam, T.C. *et al.* (2002) Expression profiling in transformed human B cells: influence of Btk mutations and comparison to B cell lymphomas using filter and oligonucleotide arrays. *European Journal of Immunology*, **32** (4), 982–993.
- 26 Lindvall, J.M. *et al.* (2004) Gene expression profile of B cells from Xid mice and Btk knockout mice. *European Journal of Immunology*, **34** (7), 1981–1991.
- 27 de los Santos, T. and Hollingsworth, N.M. (1999) Red1p, a MEK1-dependent phosphoprotein that physically interacts with Hop1p during meiosis in yeast. *The Journal of Biological Chemistry*, **274** (3), 1783–1790.
- 28 Wan, L. *et al.* (2004) Mek1 kinase activity functions downstream of RED1 in the regulation of meiotic double strand break repair in budding yeast. *Molecular Biology of the Cell*, **15** (1), 11–23.
- 29 Westfall, P.J. and Thorner, J. (2006) Analysis of mitogen-activated protein kinase signaling specificity in response to hyperosmotic stress: use of an analogue-sensitive HOG1 allele. *Eukaryotic Cell*, **5** (8), 1215–1228.
- 30 Carroll, A.S. *et al.* (2001) Chemical inhibition of the Pho85 cyclin-dependent kinase reveals a role in the environmental stress response. *Proceedings of the National Academy of Sciences of the United States of America*, **98** (22), 12578–12583.
- 31 Doyle, D.F. *et al.* (2001) Engineering orthogonal ligand–receptor pairs from “near drugs”. *Journal of the American Chemical Society*, **123** (46), 11367–11371.
- 32 Nguyen, J.T. *et al.* (2000) Improving SH3 domain ligand selectivity using a non-natural scaffold. *Chemistry & Biology*, **7** (7), 463–473.
- 33 Zhang, J., Yang, P.L., and Gray, N.S. (2009) Targeting cancer with small molecule kinase inhibitors. *Nature Reviews. Cancer*, **9** (1), 28–39.
- 34 Apsel, B. *et al.* (2008) Targeted polypharmacology: discovery of dual inhibitors of tyrosine and phosphoinositide kinases. *Nature Chemical Biology*, **4** (11), 691–699.
- 35 Gschwind, A., Fischer, O.M., and Ullrich, A. (2004) The discovery of receptor tyrosine kinases: targets for

- cancer therapy. *Nature Reviews. Cancer*, 4 (5), 361–370.
- 36 Backes, A.C. *et al.* (2008) Small-molecule inhibitors binding to protein kinases. Part I: exceptions from the traditional pharmacophore approach of type I inhibition. *Expert Opinion on Drug Discovery*, 3 (12), 1409–1425.
 - 37 Backes, A.C. *et al.* (2008) Small-molecule inhibitors binding to protein kinase. Part II: the novel pharmacophore approach of type II and type III inhibition. *Expert Opinion on Drug Discovery*, 3 (12), 1427–1449.
 - 38 Liu, Y. and Gray, N.S. (2006) Rational design of inhibitors that bind to inactive kinase conformations. *Nature Chemical Biology*, 2 (7), 358–364.
 - 39 Simard, J.R. *et al.* (2009) Development of a fluorescent-tagged kinase assay system for the detection and characterization of allosteric kinase inhibitors. *Journal of the American Chemical Society*, 131 (37), 13286–13296.
 - 40 Simard, J.R. *et al.* (2009) A new screening assay for allosteric inhibitors of cSrc. *Nature Chemical Biology*, 5 (6), 394–396.
 - 41 Getlik, M. *et al.* (2009) Hybrid compound design to overcome the gatekeeper T338M mutation in cSrc. *Journal of Medicinal Chemistry*, 52 (13), 3915–3926.
 - 42 Klüter, S. *et al.* (2010) Displacement assay for the detection of stabilizers of inactive kinase conformations. *Journal of Medicinal Chemistry*, 53 (1), 357–367.
 - 43 Zaman, G.J. *et al.* (2006) Enzyme fragment complementation binding assay for p38alpha mitogen-activated protein kinase to study the binding kinetics of enzyme inhibitors. *Assay and Drug Development Technologies*, 4 (4), 411–420.
 - 44 Blencke, S., Ullrich, A., and Daub, H. (2003) Mutation of threonine 766 in the epidermal growth factor receptor reveals a hotspot for resistance formation against selective tyrosine kinase inhibitors. *The Journal of Biological Chemistry*, 278 (17), 15435–15440.
 - 45 Carter, T.A. *et al.* (2005) Inhibition of drug-resistant mutants of ABL, KIT, and EGF receptor kinases. *Proceedings of the National Academy of Sciences of the United States of America*, 102 (31), 11011–11016.
 - 46 Pao, W. *et al.* (2005) Acquired resistance of lung adenocarcinomas to gefitinib or erlotinib is associated with a second mutation in the EGFR kinase domain. *PLoS Medicine*, 2 (3), e73.
 - 47 Holtz, M.S. *et al.* (2002) Imatinib mesylate (STI571) inhibits growth of primitive malignant progenitors in chronic myelogenous leukemia through reversal of abnormally increased proliferation. *Blood*, 99 (10), 3792–3800.
 - 48 Sharma, S.V. *et al.* (2007) Epidermal growth factor receptor mutations in lung cancer. *Nature Reviews. Cancer*, 7 (3), 169–181.
 - 49 Juers, D.H. *et al.* (2000) High resolution refinement of beta-galactosidase in a new crystal form reveals multiple metal-binding sites and provides a structural basis for alpha-complementation. *Protein Science*, 9 (9), 1685–1699.

Part Two

Medicinal Chemistry

4

Rational Drug Design of Kinase Inhibitors for Signal Transduction Therapy*György Kéri, László Órfi, and Gábor Németh*

It has become evident that intra- or intercellular signaling disorders represent the basis of a majority of complex pathomechanisms. Kinases play an essential role in intracellular signaling, and thus modern drug research has become increasingly focused on developing novel selective kinase inhibitors. Rational drug design aims to achieve the selective inhibition of distinct pathologically relevant signaling enzymes or receptors. In the last years, the concept of rational drug design has been expanded for a complex process including pathomechanism-based target selection, target validation, structural biology, molecular modeling, structure–activity relationships, pharmacophore-based compound selection, and pharmacological optimization. The two main branches of the chemical rational drug design are structure-based design and ligand-based design.

The normal cell has multiple independent mechanisms that regulate its growth and differentiated function, and several separate events are needed to override these control mechanisms, as well as to induce a pathological state. The processes of cellular growth and differentiation, as well as the maintenance of specialized functions show a remarkable degree of coordination. Proliferation of infected, damaged, or malfunctioning cells is very often a key factor for the generation of the pathological state in not only cancer and infectious diseases but also in inflammation or autoimmune related diseases. Inflammation has been found the ultimate cause of many chronic diseases, where the false signaling-related proliferation of immune cells turned out to be a critical factor in the pathogenesis of the disease.

The majority of molecular pathomechanisms result from intra- or intercellular communication disorders, whereas a series of genomic changes can be not only potential causes but also consequences of signaling failures. In a healthy organism, normal cells are fulfilling their duties, do not send or receive false messages, and are firmly controlled by the external messages of the communication network. In contrast, cancer cells, for example, generate a false, mimicked proliferation signal for themselves via the oncogenes and other genomic changes. Whether this communication failure is the result of environmental factors and/or external messages

(with an influence exerted at the genomic level) or whether it is encoded in the genetic program is a question that can be answered only on a case-by-case basis.

In normal cells, the regulation of cellular functions and the communication with the external world is controlled by a complex relationship between pieces of genetic information and by a large series of external factors and mediators, which provide the fine-tuning of coordinating the homeostasis of the cells. Since signaling disorders represent a major cause for the pathological states and most of the recently identified validated target molecules of drug research are signal transduction-related macromolecules, mostly kinases, developing potent kinase inhibitors has become one of the most important areas of drug research [1–4].

4.1

The Concept of Rational Drug Design

Originally, the term rational drug design was used for the planning of molecules, based on the three-dimensional structure of targets. In the meantime, however, the concept of rational drug design has been expanded and now it means the whole complex process including pathomechanism-based target selection, target validation, structural biology, molecular modeling, structure–activity relationships, pharmacophore-based compound selection, and pharmacological optimization [2]. The schematic processes of rational drug design are depicted in Figure 4.1.

Rational drug design of targeted small-molecule inhibitors of kinases might provide the basis for disease-specific therapies with a unique selectivity. The key elements of this process are identification of the pathologically relevant kinases, identification of therapeutically relevant small-molecule kinase inhibitors, and generation of kinase inhibitors with high efficacy and molecular specificity. Most of the inhibitors that are currently in development are ATP-competitive and targeted

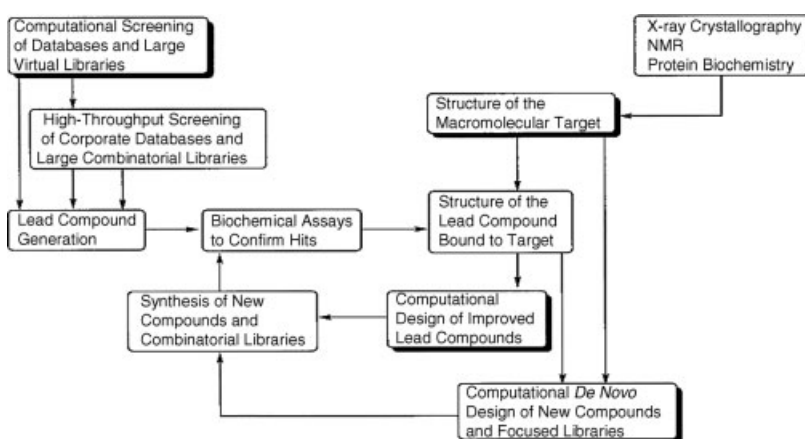


Figure 4.1 Scheme of rational drug design [5].

toward the phosphorylated high activity form of the kinase. The challenge is to develop selective inhibitors by recognizing differences in the topology and chemical and electrostatic environment of different kinases. Kinases that are in the same family have high amino acid homologies and hence similar active site topologies. Therefore, structure-based drug design (SBDD) utilizing X-ray crystallography and molecular modeling subsequent to focused library screening provides the best approach to obtain selective kinase inhibitors. This allows rational design of small molecules that have a high degree of complementarity to the target active site. Some inhibitors can target other sites on the kinase and are not ATP-competitive, while some inhibitors may target the unphosphorylated low activity form of the kinase. It might be very favorable to try to inhibit the inactive form of the kinase, which could provide enhanced specificity of an inhibitor for a particular kinase. Imatinib (Gleevec™, Novartis) is an example of such an inhibitor [6] and turns out not to be an exception, since lapatinib, BAY43-9006, BIRB-796, and others show a similar binding mode [7]. Recently, X-ray diffraction experiments with cocrystallized inhibitors like the Bcr-Abl inhibitor Gleevec [8] and p38 MAPK inhibitor BIRB-796 [9] proved the allosteric binding mode for these inhibitors.

The two main branches of rational drug design, structure-based design and ligand-based design, will be discussed in Sections 4.2 and 4.3, respectively.

4.2

3D Structure-Based Drug Design

When the 3D structure of the target molecule is known, tools of structure-based drug design can be applied. Following are the sources of the 3D structure:

- X-ray crystallography
- NMR
- Homology modeling

In order to determine the structure of the target molecule using X-ray crystallography, the protein must be isolated, purified, and crystallized. The latter is a very difficult task in the case of membrane-bound receptor tyrosine kinases, but Stamos *et al.* managed to determine the 3D structure of EGF receptor both with and without an epidermal growth factor receptor (EGFR)-specific inhibitor, Tarceva [10]. The scientific community gathers the 3D structures of proteins in the Protein Data Bank (PDB) [11] that contained 69,967 *.pdb files as of December 14, 2010, and the number is growing very fast. Vieth *et al.* summarized the kinase domains available in the PDB [1]. In 2003 they identified 164 X-ray structures for 38 different kinases. Figure 4.2 illustrates the 3D structure of BCR-ABL kinase cocrystallized with a small-molecule inhibitor; the structure file was downloaded from the Protein Data Bank [12].

The structure of relatively small proteins can also be determined with NMR, but until today there are no reports of NMR-resolved kinase structures. Given that only the primary structure of a protein is known, homology modeling can be applied. The

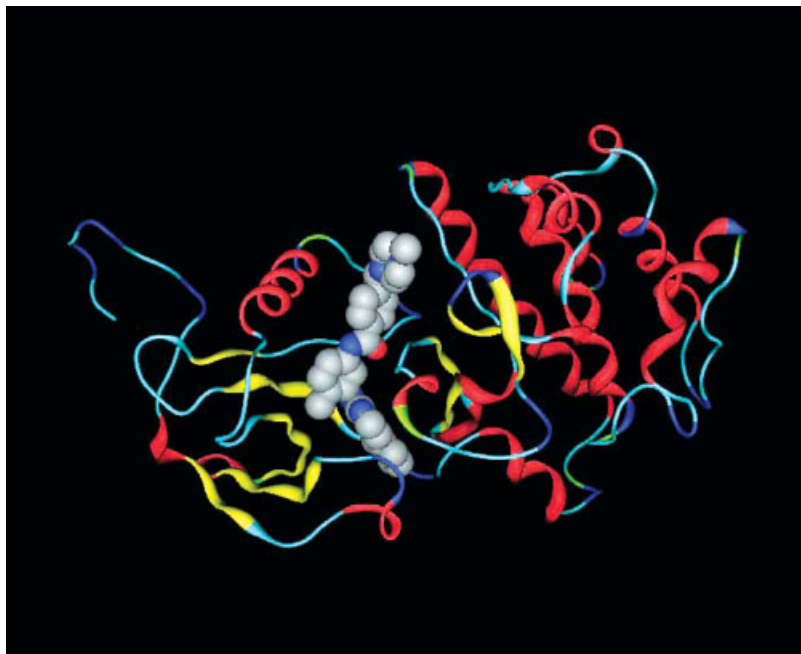


Figure 4.2 The 3D structure of BCR-ABL kinase cocrystallized with a small-molecule inhibitor.

first step in homology modeling is homology search, when the sequence of the protein is compared to sequence databases and the statistical significance of matches is calculated. A typical homology search method is the BLAST searching algorithm [13]. The 3D structure of the next neighbor in amino acid sequence can then be used as a template to predict the 3D structure of the target protein.

Today, there are a number of structure-guided drug discovery software tools available leading to the identification of potential ligands for a receptor of choice: docking software were the first binding site structure-based computer methods applied for the selection of possible starting points for medicinal chemistry. These software search for 3D ligands in databases and select possible ligands by matching them in the binding cavity using their geometry data. The ranking of molecules is based on different scoring functions. There are different types of scoring functions, using different weights for the interactions in the predictions. One example of docking software is the FlexX program [14]. In the *de novo* design, the points of interactions are calculated (electrostatic, H-bond, and hydrophobic) and bioactive molecules are built up from diverse fragment databases so that the generated molecules fit in the active site. These programs also use different scoring functions to evaluate the receptor–ligand interaction. One of the most famous *de novo* design softwares is LeapFrog [15]. The first successful drug designed by *de novo* design method was Captopryl, an ACE (angiotensin-converting enzyme) inhibitor antihypertensive drug. The 3D structural information of the closely related carboxypeptidase A inhibitor complex was used in the binding site model [16].

Kinases catalyze the transfer of the γ -phosphate group of an ATP molecule to the substrate molecule; this means that the most common region of kinases is the ATP binding site. Analysis of the amino acid sequences of kinases proved that the ATP binding site is a conservative region showing high sequence homology through all kinases. The details of the ATP binding site will be discussed later. Because of the high sequence and structural similarity of the ATP binding sites, kinases were regarded as “nondruggable” targets before the 1990s. However, in the past 15 years, it has become evident that it is possible to design selective kinase inhibitors [17]. The following features of the ATP binding site permit of designing selective inhibitors:

- 1) The hydrophobic pocket and channel are highly variable in different kinases [18].
- 2) A so-called “gatekeeper” residue flanks the hydrophobic pocket at the rear of the ATP binding site [19]. When the gatekeeper residue is a small amino acid, it allows large hydrophobic groups into the hydrophobic pocket. In contrast, when the gatekeeper is large, it forbids bulky groups to bind to the pocket.
- 3) A reactive cysteine can be located in the active site in a few kinases [20]. Cysteine is relatively rare in the active site, but it was an important feature when Bridges and coworkers developed irreversible EGFR inhibitors [21].

Until today, the most important approved and widely studied kinase inhibitors are the EGFR inhibitors Iressa (gefitinib) [22] and Tarceva (erlotinib) [23], and BCR-ABL inhibitor Gleevec (imatinib) [24]. The structures of the molecules are shown in Figure 4.3.

Analysis of the EGFR catalytic domain – Tarceva – cocrystallized structure revealed that the quinazoline group occupies the adenine region of the ATP binding site and the ligand is anchored to the receptor by forming two hydrogen bonds with N₁ and N₃ (one of the hydrogen bond donors is different from that in the case of ATP binding).

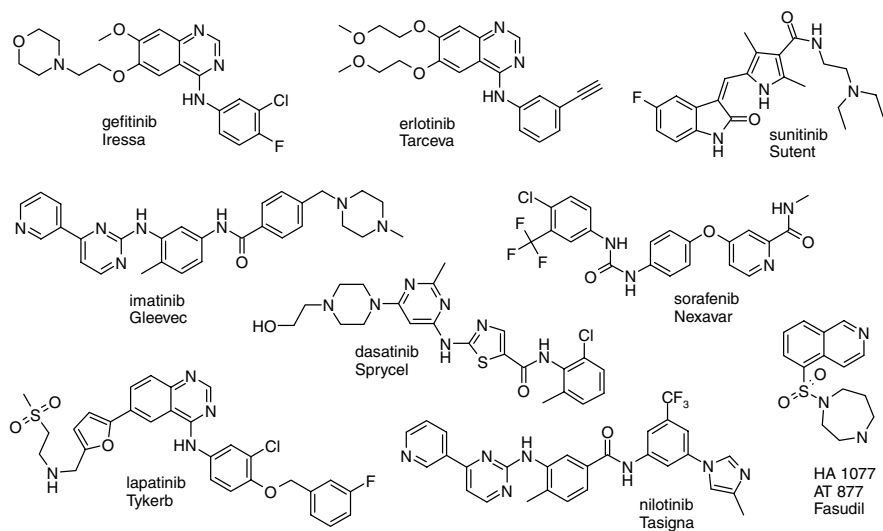


Figure 4.3 Structures of approved kinase inhibitors.

In this case, a water molecule helps the interaction between the receptor and the inhibitor). The phenylamino group occupies the hydrophobic pocket, and the methoxy–ethoxy groups stick out of the receptor, their role is to ensure proper solubility and bioavailability to the molecule [23]. The binding mode of Iressa is predicted to be similar to that of Tarceva.

Gleevec binds to the ATP binding site in a different manner [24], which might be part of the explanation why it is a relatively selective inhibitor of BCR-ABL kinase. Gleevec is very effective for the treatment of Philadelphia chromosome-positive (Ph^+) CMLs. Using rational drug design, Gumireddy *et al.* developed On012380, which is an allosteric inhibitor of BCR-ABL and active against 100% of Gleevec-resistant forms of BCR-ABL [25].

In the Protein Data Bank, there are other kinase inhibitor complexes that have been determined with X-ray crystallography, for example, the kinases FGFR (fibroblast growth factor receptor) [26], lck (lymphocyte-specific kinase) [27], PKA (cAMP-dependent protein kinase) [28], VEGFR (vascular endothelial growth factor receptor) [29], CDK2 (cyclin-dependent kinase 2) [30], Src kinase [31], and p38 MAPK [32].

Understanding the binding mode of kinase inhibitors can also help researchers to develop additional selective inhibitors for other kinases.

4.3

Ligand-Based Drug Design

When the 3D structure of the target molecule is not known, for example, for many membrane bound proteins that are extremely difficult to crystallize, one can mobilize the tools for ligand-based design.

4.3.1

Active Analogue Approach

The assumption of active analogue approach (AAA) is that all compounds that display similar activity profiles are able to adopt similar conformation [33]. The first step is searching the conformational space of a highly active compound and map its interatomic distances. The next step is searching the conformational space of other compounds to find their bioactive conformations based on the mapped interatomic distances of the first molecule. The final step is to calculate molecular volumes of the “bioactive conformations,” superpose them, and use regression analysis of the volumes to derive relationship to biological activity [34].

4.3.2

3D Quantitative Structure–Activity Relationships

Three-dimensional quantitative structure–activity relationship (QSAR) models relate the biological activity of ligands to three-dimensional fields surrounding the compounds.

One of the most popular methods is comparative molecular field analysis (CoMFA) [35]. The basic idea of CoMFA is that the intermolecular interaction energy between the receptor and the ligand correlates with the steric, electrostatic, hydrogen bonding and hydrophobic fields of the ligands. These interaction energies are calculated between the ligand and the so-called hypothetical probe atoms, which are placed on certain number of grid points. The results of the calculations can be arranged in a matrix, in which every row represents a molecule and every column represents a calculated interaction energy value in a certain grid point, and one additional column contains the biological activity data. These calculations generally generate thousands of columns (descriptors), which strongly exceed the number of rows (molecules). The QSAR model is generated by a PLS (partial least squares) analysis of the data matrix. Validated QSAR equations derived from CoMFA models can be used to predict the biological activity of new molecules.

The most difficult task in a CoMFA analysis is the superimposition of the molecules before the actual calculations. Small differences in the starting superimposed structures can lead to dramatic changes in the final QSAR equation. Finding the bioactive conformation of the molecules is another challenging issue. Several other 3D QSAR methods were developed after introducing CoMFA. Examples of 3D QSAR techniques are as follows:

- Comparative molecular similarity analysis [36] (CoMSIA) can be viewed as an extension of the CoMFA methodology. It is based on the same assumption as CoMFA: changes in binding affinities of ligands are related to changes in descriptors, represented by various fields. In CoMSIA, both steric and electrostatic features, hydrogen bond donor, hydrogen bond acceptor, and hydrophobic fields are considered. Potential energy functions are smoothed with Gaussian function. One of the major advantages of CoMSIA over CoMFA is that of less sensitivity to different ligand alignment.
- Comparative molecular moment analysis [37] (CoMMA) enables 3D QSAR analysis without the requirement of molecular superimposition using descriptors such as moments of inertia, dipole, and quadrupole moments. One drawback can be in CoMMA that the value of these descriptors equals infinity for symmetric molecules whose dipole moment is zero [38].

Four-dimensional QSAR [39] allows to use multiple conformation, orientation, and protonation state of the ligands as well as simulation of local induced fit phenomena. This technique can choose the bioactive conformation more precisely as each ligand molecule can be represented by an ensemble of conformations, orientations, and protonation states [40].

4.4

Target Selection and Validation

With a drug discovery focus on the target gene family of protein kinases, we try to raise synergies by the fact that these highly homologous enzymes comprise the

largest family of the human genome. The individual family members, approximately 530 kinases [41, 42], constitute a functional basis for basically every physiological process. Nearly all aspects of life involve cellular responses to extracellular stimulation. All cellular events are governed by signal transduction events that rely on highly coupled intracellular networks of specific protein–protein interactions, which are in turn functionally controlled by reversible phosphorylation reactions catalyzed by protein kinases. Consequently, kinases play a central role in propagation of signal transduction in every type of cell [43]. Not surprisingly, kinases are reported to be involved in a plethora of diseases. They have been found dysregulated in terms of expression levels or catalytic activity and also mutated leading to hyperactive or inactive mutants. One could argue that there is not a single therapeutic indication where protein kinases *per se* could be excluded as targets.

The common feature conserved throughout the entire protein kinase family is the catalytic domain with its associated catalytic center. Almost all protein kinases employ ATP as a cosubstrate in order to transfer the γ -phosphate of ATP onto an acceptor protein, acceptor peptide, or acceptor lipid substrate [41]. The identical catalytic mechanism together with a high degree of sequence homology, identical protein folding topologies, and the common cosubstrate ATP initially led to the assumption that protein kinases constitute a nondruggable family of protein targets. This belief dominated the majority of the pharmaceutical industry until the middle of the 1990s. This attitude drastically changed when Novartis began work on Bcr-Abl and successfully carried the corresponding inhibitor STI571 (CGP57148B, imatinib, since 2001 marketed as Gleevec) through clinical trials [44, 45]. Simultaneously, SmithKline Beecham initiated work on p38 inhibitors, yielding the lead compound SB203580 [46]. Since then, both academic research and pharmaceutical industry laboratories started a real conquest into the world of protein kinases and their small-molecule inhibitors. Currently, R&D spending for inhibitor development is highest for protein kinase-based research within the pharmaceutical and biotechnology industries [47].

Against all odds, the pharmaceutical industry began an intensive search for kinase inhibitors [47] and achieved the result of 8 FDA approved kinase inhibitors and over 100 compounds in the various stages of clinical trials [48]. The cumulated experience in kinase inhibitor drug discovery projects collected over the past 10 years teaches us that fairly selective ATP site-specific protein kinase inhibitors can be generated, despite all the functional, sequential, and structural similarities that dominate the catalytic domains of the protein kinase family [49]. Results from clinical use of kinase inhibitors of the first generation demonstrate that protein kinases are druggable enzymes. Accessibility of the ATP binding pocket for small molecule binding amenable by subsequent chemical optimization has been a major concern due to the high level of sequential, structural, and functional similarity among the kinases [54]. In contrast, it turns out that the highly conserved ATP binding site is an ideal playground for inhibitor design given the new technologies that have become available to researchers, for example, molecular inhibitor design supported by cocrystallization efforts and molecular modeling, in combination with broad panels of protein kinases available for selectivity profiling and fragment-based

high-throughput X-ray crystallography [50]. These and similar technologies were available only late into the programs for the first-generation inhibitors and could not contribute significantly. However, the success of kinase inhibitors such as imatinib, fasudil, gefitinib, and erlotinib demonstrates that even without the sophisticated technologies, a fair level of selectivity for particular kinase(s) has been achieved, sufficient to avoid general toxicity after application to cell culture systems, animals, and humans.

Given the degree of homology of the individual kinase family members on one hand and the amenability of the ATP binding site to drug design on the other hand, synergies can be defined for the design of next-generation kinase inhibitors. Selected derivatives of an identical chemical core structure frequently recognize distinct kinases with different associated therapeutic relevance. This has been shown with the imatinib-like aminopyrimidines, in which the addition of a single methyl group to the aminopyrimidine core led to an unexpected change in selectivity from PKC to Abl [12, 45, 51]. It has become clear that the specificity and selectivity for a target is a function of the derivatization pattern of an underlying core structure. Once this core structure and its derivatives meet the characteristics of drug-likeness, it might represent the starting point for more than just one development candidate in various therapeutic areas. Subsequent optimization chemistries use previously made compounds and benefits from the medicinal chemistry strategies in the first therapeutic program [52, 53]. This strategy might also be described as target hopping representing an intelligent way of recycling pharmacologically beneficial medicinal chemistry concepts, the critical parameter being the available series of molecules with associated profiles, as opposed to a proper genetically validated target [54].

In summary, large efforts are being made in the field of kinase inhibitor research and development [47]. The past 10 years of effort in this field have altered our perception of the importance of kinase inhibitors to the pharmaceutical industries. This field is now vigorously populated and the availability of new technologies, especially from the field of chemogenomics and chemoproteomics augur a tremendous potential for the next generations of kinase inhibitors.

In trying to learn from the field of kinase inhibitor drug discovery, we try to follow an opportunistic approach and repeatedly exploit the common features of all protein kinases for the target selection and validation processes. Just around the new millennium, the -omes and -omics hype started to sweep over industrial research providing companies endless lists of putative targets, unfortunately devoid of any solid validation and without associated drug discovery approaches. The expected benefits from the -omes and -omics initiatives for drug discovery and development have not yet emerged within the pharmaceutical and biotech industry [55]. Genomics typically provided a list of dysregulated genes. The process, getting from the dysregulation of a gene to a drug that targets the product of the gene, takes typically 12–15 years [42, 44]. The validation of a target through biological means requires approximately 8 years in average and is regarded as a key activity in targeted drug discovery. During the target validation period, a suite of technologies is typically exploited to gain confidence in a particular target. These technologies include gene knockout studies in mice, mode-of-action investigations in cellular and animal

models, siRNA technologies, and so on. All these technologies focus on the entire kinase gene or gene product and none really focus on the kinase activity. Nevertheless, inhibition of the kinase activity is the best that can be achieved through the application of kinase inhibitors to cellular and animal models as well as to patients. There is evidence available on the independent roles of regulatory domains of protein kinases and on the impact of protein kinase molecules on binding partners in the formation of larger complexes, as it has been recently described for the Aurora kinases [56]. Given the discrepancy of employing tools for target validation, which affect an entire protein rather than just its activity, and the subsequent generation of pharmacological agents, which modulate the activity of kinase rather than affecting the whole kinase protein, we have chosen a strategy to validate potentially novel kinase targets with tools that are as close as possible to the final product, a pharmacologically active agent (see also above). This strategy is called chemical validation and relies on a representative collection of proven kinase inhibitors, that is, a kinase-biased compound library [2, 42]. In that setting, a novel kinase target of interest is screened against this collection and the hits from one or more chemical series are determined. Subsequently, these hits are employed in a cellular model combined with a direct cellular kinase assay. Provided that the hits show activity in the cell-free and in both cellular assays, the kinase of interest is considered validated and the tool inhibitors have already proven its druggability [42].

During the subsequent compound optimization efforts, the major drivers are to conserve the properties of a privileged structure and to ensure a sufficient level of selectivity of the optimized inhibitors in a panel of more than 50 different human protein kinases.

4.5

Personalized Therapy with Kinase Inhibitors

Targeted personalized therapy has become a major issue in the recent years in drug development. For example, for quite some time, anticancer drug development has been based on the simple concept that targeting a single protein, most often an oncogene, that has an important role in tumor transformation could be effective in treating cancers that overexpress the target protein. This could be achieved by developing a specific targeted drug against a predefined target protein and everybody wanted to achieve high selectivity for that particular target in order to avoid side effects.

However, in cancer cells, hundreds of genes can be differently expressed compared to normal cells and this expression profile can significantly vary in the same kind of tumor (same kind by tissue origin) from patient to patient. From a therapeutic point of view, the key question is what are the causes and what are the causatives, in other words, which genes are the cancer-driving genes, the survival factors, and which are just accompanying signals. In personalized therapy, the aim is to identify the survival factors of cancer cells for targeted therapy and to kill them with proper inhibitors (most of the described survival factors are kinases, so kinase inhibitors are essential

for personalized targeted therapy). As it has recently become clear that most of the cancers are driven with multiple survival factors, signal transduction therapy has to aim for multiple targets and has to be accomplished on a personalized basis that needs proper molecular diagnostics. It is clear that the affectivity of a drug candidate is greatly influenced by the molecular genetic alterations of several signal transduction proteins; therefore, the final success of the drug is also determined by its “off-target” multitarget inhibitory profile. Therefore, a combination of target- and chemistry-driven approaches with the integration of iterative target reidentification and predictive marker development is required in both the preclinical and clinical phase of drug development.

Many of the first-generation molecularly targeted drugs (in particular, kinase inhibitors) were selected to be as specific as possible for the target protein, and although this turned out to be not the case, the off-target profile could not be planned or considered, while we now know that “multitargeted” drugs are often more successful anticancer agents than the more specific ones. This could be because simultaneous inhibition of multiple signal pathways is necessary for activity in most tumor types, or alternatively, perhaps a more relevant target might be among the inhibited “off-targets” of the agent.

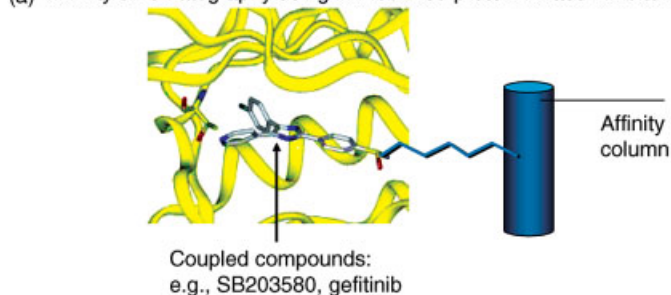
Even if the lead compound has been selected based on its activity against a validated target, for example, a kinase, several steps of iterative target validation and redefinition should be integrated into the drug discovery process with proper molecular diagnostics. In this sense, we have to combine target- and chemistry-driven drug discovery with rational drug design against a well-defined molecular target. By the term chemistry-driven drug discovery we mean preferred structures in cellular assays based drug candidate selection where selectivity profiling and off-target identification are achieved later on by a target fishing technology.

4.5.1

Target Fishing: Kinase Inhibitor-Based Affinity Chromatography

The most prominent hurdle in developing ATP-competitive inhibitors is their specificity. In addition to many proteins that use purine-based cofactors, there are ~530 kinase family members that share a highly conserved ATP binding site. Undoubtedly, selectivity testing has been one of the major drivers in kinase inhibitor optimization and kinase selectivity panels representing a selection of biochemical kinase assays have become widely used [57, 58]. It became similarly accepted that pan-kinase inhibitors, typically inhibiting a wide variety of kinase targets, would eventually become too toxic for further development. (See, for example, PD180970, a pan-tyrosine kinase inhibitor [59] or flavopiridol [60]. Kinase selectivity panels are limited to the number of available *in vitro* kinase assays and currently do not exceed 200 kinases [61]. Since the amino acid sequence of the kinase ATP binding site is not a good predictor of selectivity [1], these panels only provide limited information (200/530 or ~38% coverage.) They do provide a tendency for overall selectivity, but clearly more thorough profiling methods are required, some of which were recently developed [62–64]. Among those, the KinaTor™ technology relies on the coupling of

(a) Affinity chromatography using immobilized protein kinase inhibitors



(b)



(c)

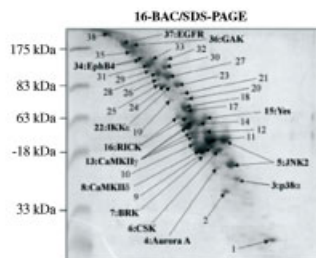


Figure 4.4 KinaTor technology. (© 2005 by The American Association of Cancer Research). Schematic representation for the immobilization of kinase inhibitors and their application to affinity chromatography (a). Immobilization strategy for gefitinib (b). Two-dimensional 16-BAC/SDS-PAGE for gefitinib binders. Each Coomassie stained spot on the gel represents a protein, which bound to the

affinity chromatography material. Spots have been excised from the gel, digested with trypsin, and analyzed via matrix-assisted laser desorption ionization mass spectrometry analysis [63]. The positions of the identified kinases are indicated (c). For experimental details, see Ref. [68]. (Figures (b) and (c) were reprinted from Ref. [68], with permission from the American Association of Cancer Research).

small-molecule kinase inhibitors via a linker to a matrix (Figure 4.4a) with the aim to generate an affinity chromatography material, which exploits the strong binding affinities between kinase inhibitors and their molecular targets. This technology is straightforward in principle, but has not delivered yet until recently, apart from a few exceptions coming from the field of the CDK inhibitors, purvalanol B, paullones, and hymenialdisines [60, 65–67].

Once coupled and proven active, immobilized ligands are processed in an affinity chromatography approach to identify all the relevant targets and off-targets from a crude extract, which bind to this matrix [63]. All binders are subsequently cloned, expressed, and purified (kinases and nonkinases). *In vitro* enzymatic assays are established for every bound protein. The affinities of the free ligands for the various enzymes are determined in these *in vitro* assays. Thus, quantitative binding can be determined and even the binding to nonkinases can be verified.

As one of the proof of concept experiments for the KinaTor technology, we used immobilized gefitinib to identify its off-targets and to obtain a better understanding of the pharmacology of gefitinib (Figure 4.4b) [68]. MS analysis of the identified protein spots and a parallel LC-MS/MS analysis not only permitted detection of the

internal control EGF-R as expected but also identified more than 20 additional gefitinib targets, such as the protein tyrosine kinases BRK, Yes, CSK, EphB4, Lyn, and Met and the serine/threonine kinases RICK (also known as RIPK2, RIP2, and CARDIAK), GAK, CaMKII, Aurora A, Jnk2, p38, and Bub1 [68]. All these kinases have been confirmed to be direct gefitinib targets. The phase III EGF-R inhibitor lapatinib and gefitinib have been tested in another kinome-wide technology, a competitive binding assay [62]. The authors identified only 4 targets for lapatinib compared to 18 kinase targets for gefitinib [62], respectively. This comparison clearly underscores the value of these novel kinome- and proteome-wide technologies.

Having raised the issue of pan-kinase inhibitors being associated with toxic side effects, these selectivity profiling technologies should become implemented as critical decision points on the way to the nomination of an investigational new drug (IND).

4.6

The NCL™ Technology and Extended Pharmacophore Modeling (Prediction-Oriented QSAR)

This rational drug design technology was developed by the authors of this chapter [69]. This is a novel hit and lead finding method based on the branded Nested Chemical Library™ (NCL) technology. The NCL relies on a systematically built knowledge base, which contains our experience accumulated during the past 18 years of kinase inhibitory chemistry. Our library is organized around 108 core structures and we have generated small focused sublibraries around each core.

The Chemical Validation Library (CVL) (~300 compounds) and the Extended Validation Library (EVL) (~1300 compounds) are built around the same 108 selected core structures with proven kinase inhibitory activity on various kinase targets. CVL and EVL are based on the following concept and take into account (1) the number of kinases against which we were able to identify inhibitors continuously increasing, (2) the possibility to include more analogues around the once proven kinase inhibitor leads (EVL), and (3) an increase in chemical diversity (currently, 108 core structures). The underlying Master Library (ML) includes novel compounds and analogue structures around CVL and EVL, extended with additional ~10 000 compounds. There is still a large series of novel compounds in the ML with space for further chemical and pharmacological optimization (Figure 4.5).

Novel kinase targets can be validated chemically using the Chemical Validation Library compounds [42, 70]. These novel kinase targets might be tested against the CVL. The resulting hits, which are typically also biologically and chemically validated, will provide sufficient input for a successful virtual screening and rational computerized design of new analogues based on the prediction-oriented QSPAR model approach using a specially developed 3DNET4W™ software [71–73]. New analogues are designed based on systematic chemical modifications using validated standard reaction schemes. New potential hit molecules are filtered by their ADMET (adsorption, distribution, metabolism, excretion, toxicity) properties, drug-likeness, and

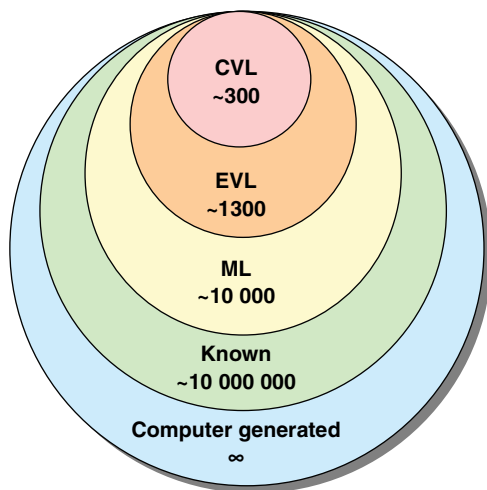


Figure 4.5 Nested Chemical Library™ (NCL). CVL, Chemical Validation Library; EVL, Extended Validation Library; ML, Master Library.

patentability. Thousands of molecular descriptors are calculated for hit compound structures and fed into 3DNET4W™ QSPAR program system. The program is able to calculate descriptors, that is, numerical representations of molecules, and build prediction-oriented QSAR models, that is, a mathematical function describing biological/physicochemical properties. Such models are achieved by selecting predictive descriptors by means of optimizing chosen statistical parameters through strict internal validation and then performing external validation, that is, verifying the predictive capability of the resulted model on a set that is not used in the process of optimization. Optimization cycle consists of four iterative steps: (1) training set/evaluation set splitting, (2) descriptor selection based on sequential or genetic algorithms, (3) applying chosen statistical method to achieve the best fitting between the training set structures represented by the selected molecular descriptors and the biological data, and (4) internal validation of fitted model with evaluation set. For internal validation, we prefer to use leave-half-out bootstrap validation instead of leave-one-out cross-validation, which can give overoptimistic results [74]. Both the models and the descriptors in optimization cycle are sorted according to their predictive ability. Enhanced MLR (multivariate linear regression), PLS, ANN (artificial neural network), and LLM (linear learning machine) methods can be used to establish relationship between activity and descriptors.

For optimization of the hit and lead molecules, we apply a focused or a diverse optimization depending on the chemical structures. We preselect the compounds to be synthesized by our prediction-oriented QSAR model and ADMET filters, and then synthesize the new compounds with solution or solid-phase synthesis, validated with HPLC-MS and NMR. Prepared compounds are tested for their biological activity and characterized for their physicochemical properties. Biological data are merged with the set used for modeling and then a new model-building phase is started in order to

improve the predictive capability of QSAR model continuously and to complete the hit and lead optimization process.

4.7

Non-ATP Binding Site-Directed or Allosteric Kinase Inhibitors

The first kinase inhibitors, tyrphostins [75] showed affinity both toward ATP binding sites of the enzymes and to their specific peptide substrate binding region. In order to optimize inhibitor selectivity, great efforts were invested into the design and development of specific “pure peptide binding site” inhibitors. High-throughput screening of corporate collections or diverse combinatorial compound libraries [76, 77] provided quite many inhibitory core structures. Unfortunately, not many peptide inhibitors have been found. On the other hand, these peptides had problems with bioavailability/ADMET properties. A possible solution was to develop more drug-like peptidomimetic compounds. Several such compounds, including some tyrphostins, tyrosine derivatives, or acyl-hydrazones, reached early-phase preclinical development but were dropped due to “lack of selectivity,” that is, acted on more kinases at the same time. [78]

Development of ATP-like or ATP binding site-directed inhibitors was opposed for a long time owing to the concern about possible lack of selectivity and side effects via various ATP binding proteins. When 4-phenylaminoquinazolines were found to have excellent and quite selective EGF inhibitory activity [79], it boosted the research in this field and almost 100 small heterocyclic cores were developed against various kinases. Although the known 530 kinases have highly conserved ATP binding site, several high affinity and selective inhibitors have been discovered and are under clinical evaluation [80].

Classifying the known kinase inhibitors by chemical structures, there are several exempts from the ATP-like structures; for example, our very first inhibitors, oxanyl-hydrazones [78, 81] showed only negligible similarity with ATP and that time the binding mode could not be explained. These compounds showed some common steric and electronic properties with some small peptide substrates; therefore, these compounds were treated like substrate binding site inhibitors. Recently, X-ray diffraction experiments with cocrystallized inhibitors like Bcr-Abl inhibitor Gleevec [8] and p38 MAPK inhibitor BIRB-796 [82] proved allosteric type binding mode for these structures. Applying our special “theoretical interactive surface” pharmacophore modeling on prefiltered “non-ATP-like” compounds, we could identify the main structural features needed for allosteric binding. Appropriate molecular shape, size, and electronic properties in suitable positions can afford selective and high-affinity binding at allosteric binding sites of kinases. For ATP-like binding, size is a principal property: the molecule must fit into the ATP binding pocket. The most potent ATP inhibitors known can be fitted into a cube of approximately 9–10 Å. In the case of several allosteric inhibitory structures, we have found that the longest distance in the molecule between two suitable electronegative (or partially positively charged) groups is around 13.6–14.5 Å. We had developed a few hundreds of allosteric inhibitor

analogues around proven allosteric type core structures to find that in certain families of allosteric inhibitors, shortening or lengthening of this characteristic distance significantly decreases kinase inhibitory activity.

Therefore, it is probable that in these cases, we have to consider two-point binding mode, and often the structure of the “middle part” of the molecule does not significantly affect the inhibitory activity. This middle spacer group can be various types of heterocycles, either amide chain or other with/without polar functional group(s).

During the construction of our allosteric inhibitory library, we considered these structural properties when combining drug-like building stones of known pharmaceuticals and kinase inhibitor structures. These compounds show inhibitory activity on several kinases in low micromolar and nanomolar concentrations.

Of course, there are various small molecular structures that can bind to different binding sites on kinases [82]. Therefore, it is difficult to establish a general strategy for allosteric kinase inhibitors. ATP competition does not necessarily mean “pure ATP-like binding” mode, but X-ray cocrystallization data can provide very important data about allosteric binding mode.

In order to develop novel non-ATP binding site or allosteric binding site-directed inhibitors, 3D structure-based drug design would probably provide a key strategy to generate promising lead compounds. It is expected that future protein kinase drug discovery will exploit a variety of high-powered *in silico* tools to computationally visualize, analyze, and probe the molecular properties and interactions of novel small-molecule inhibitors with possible allosteric binding sites. Integration of *in silico* tools (e.g., molecular modeling and virtual screening) with structural biology (e.g., X-ray and/or NMR structures of a lead compound complexed with its therapeutic target), chemical synthesis, biological screening (e.g., biochemical kinase assays with kinetic analysis, *in vitro* and *in vivo* assays), cheminformatics, and bioinformatics provides the background of novel non-ATP binding site-directed or allosteric kinase inhibitor drug discovery. For the necessary structural biological studies, the use of an allosteric inhibitory library for hit finding on various kinase targets could be a very important first step [8, 82–92].

4.8

The Master Keys for Multiple Target Kinase Inhibitors

Apart from screening efforts of either diverse chemical libraries or target family-biased compound collections within the context of lead finding, the protein family of kinases with its more than 500 distinct members qualifies for the application of target family-biased master key concept that is based on the utilization of tailor-made privileged structures [52]. Rather than following the classical approach in which a single target protein, for example, a protein kinase, is tackled at a time within a distinct disease area, the master key concept offers the opportunity to process multiple related members from a target family simultaneously across numerous therapeutic areas. The master key concept is a chemogenomics platform since it allows us to deal with a large number of potential protein targets with increased

efficiency in lead generation, delivering target-specific molecules amenable to parallel optimization toward more progressive preclinical candidates. This opportunity of systematization of drug discovery strategies follows from the acceptance that biology as well as chemistry knowledge gained from one target can be transferred to “adjacent” targets from the same gene family. Even though systematization might require significant commitment of time and resources, it allows enormous efficiencies to be gained through economies of scale, provided that the target families are of significant size, richness, and diversity in therapeutic value that is undoubtedly given for the protein kinase family. Most importantly, an accumulation of target class-specific know-how is created over time whereby past experiences allow rapid attack on new members of the target cluster of interest.

The core elements of the kinase-biased master key concept are so-called privileged structures that emerge from a sophisticated molecular design and optimization process that encode a target family-wide structural commonality in ligand binding. The combination of a kinase family-wide imprinted commonality with additional structural fragments in the molecular periphery of a once established privileged structure allows to synthesize not only highly active but, more importantly, also selective kinase inhibitors.

The novel paradigm of the target family-biased master key concept is tailor-made to fully exploit the potential of a protein family densely populated with pharmaceutically relevant and proven drug targets, such as the protein kinase family.

As a result of evolution, proteins generally cluster in, for example, receptor or enzyme families that exhibit similar, if not identical, 3D folding topologies, as well as related mechanisms of ligand or substrate binding. The key to unlock this intrinsic value of, for example, the kinase target family is the identification of these generic recognition patterns, and, subsequently, the application of this knowledge for the design of small molecular fragments, termed privileged structures, or molecular master keys.

In order to set the criteria for the design of kinase-directed privileged structures, a thorough understanding of the topological architecture of the target proteins, together with a detailed insight into the target family-wide commonalities, is mandatory. Fortunately, the advent of high-throughput technologies in structural biology provided a plethora of kinase X-ray structures over the last decade. The structural information embedded in these structures provides profound insight into kinases at a molecular level and facilitates the design of potent and selective antagonists. Furthermore, comparative studies of kinase structures in their activated versus nonactivated, liganded versus free complexation state, or ATP-bound versus inhibitor-bound state gave novel insights into those structural aspects that govern affinity on the one hand and selectivity on the other.

The two domains are connected via a so-called hinge region, which allows rotation of the two lobes that is required in the course of kinase activation. The hinge region is further involved in the binding of ATP by formation of two critical hydrogen bonds between backbone functionalities and the adenine ring of ATP.

The so-called C-helix within the N-terminal domain forms the back wall of the ATP binding site. It contains a conserved glutamic acid residue that is of key importance in the phosphotransfer forming an ion pair with a highly conserved Lys. Stabilized by

the ionic Glu–Lys interaction, deeply buried in the ATP binding cleft, the Lys side chain makes a crucial contact with the α,β -phosphate oxygen, positioning them in such a way to facilitate the γ -phosphoryl transfer. Even though most of the conserved phosphate binding residues in the ATP binding site are crucial for the catalytic process, they do not contribute significantly to the binding free energy of the ATP–kinase complex, which is nicely reflected in the equipotent affinity seen for ATP, ADP, and adenosine in PKA [93].

According to the binding model for kinase inhibitors when bound to their target enzyme proposed by Traxler and Furet at the end of the 1990s [94], five distinct subsites exist within the ATP binding site that have a distinct chemical environment and local sequence differences that enable the medicinal chemist to design potent and specific kinase inhibitors:

- 1) **Adenine binding region.** All ATP-competitive kinase inhibitors bind in this hydrophobic region and interact with the hinge domain via hydrogen bond interactions.
- 2) **Ribose binding pocket.** This region is hydrophilic in character and is often exploited to accommodate solubilizing groups. This region is not highly conserved and contains unique residues, which could be used to direct selectivity.
- 3) **Hydrophobic back pocket.** This pocket extends in the direction of the N⁶ of ATP and is not involved in the binding of ATP. This region is not conserved and is used to gain affinity as well as selectivity. Access to this region is controlled by the so-called gatekeeper residue.
- 4) **Surface-exposed front area.** This region is not addressed by ATP and could be used to gain binding affinity and selectivity.
- 5) **Triphosphate binding region.** This hydrophilic region is highly solvent exposed and seems unimportant for gaining affinity.

The majority of all inhibitor design attempts to utilize a heterocyclic core structure that is capable of forming one or more hydrogen bonds to the hinge backbone, while the core is decorated in such a way that one peripheral group reaches into the hydrophobic back pocket. Furthermore, peripheral side chains address the surface-exposed front area or the ribose pocket. It is interesting to note that the shape of the back pocket and the physicochemical properties mapped onto its surface provides the main playground for medicinal chemistry to gain intrafamily selectivity.

In order to introduce the master key concept based on kinase-directed privileged structures, common structure determinants as well as the most discriminating attributes of ATP binding sites need to be highlighted. From a medicinal chemistry perspective, the most striking commonality in molecular recognition utilized by the target family of protein kinases is the binding of ATP as a cosubstrate and phosphate source for the catalyzed phosphorylation reaction. Even though the shape, size, and physicochemical characteristics of the ATP binding site appears highly conserved throughout the entire target family of interest, close examination of crystallographically determined kinase–inhibitor complexes revealed those spatially adjacent cavities described above that are not employed by the enzymatic machinery and, thus, differ substantially from kinase to kinase in their appearance. These

observations from structural biology that on one hand the ATP binding pocket displays common structural features throughout the family and on the other hand the adenosine binding region is flanked by cavities that are aligned with residues, which from an evolutionary point of view are considerably diverged, provide the ideal precondition for a target family-biased master key concept. The conserved part of the ATP binding pocket is the negative imprint for the design of a privileged structure, while specificity-mediating peripheral groups attached to the underlying privileged structure target the flanking cavities, markedly differing in size, shape, and surface properties among different kinases (Figure 4.6).

From a thorough structural and functional analysis of kinase structures, a modular chemistry concept emerges in which specifically functionalized heterocyclic core structures account for a pronounced family-wide requirement for ATP binding, namely, the formation of a hydrogen bond duplex or triplex to the so-called hinge part present in each and every kinase, while specificity-mediating binding elements are attached to well-elaborated and positioned functional groups on the molecular scaffold of the parent privileged structure in order to gain the required selectivity profile.

Analysis of 10 years of intensive kinase inhibitor research within the pharmaceutical industry reveals recurring core structures that have been employed by different companies for targeting different kinases in different disease areas. With hindsight, the concept of a privileged structure-based lead finding and optimization strategy is proven, however, only very few examples for a proactive application of the concept exist. Definitely, AstraZeneca possesses a large collection of anilinoquinazolines, generated in the course of their early lead finding and optimization program yielding Iressa, one of the first targeted kinase inhibitors approved for the treatment of cancer. Based on this scaffolded library of quinazolines, several highly interesting starting points for novel lead optimization programs targeting different kinases emerged. The experience gained in the EGF RTK program more rapidly delivers high-quality compounds in successor programs, such as inhibition of p38 or Aurora [95], respectively.

In summary, the kinase-directed master key concept comprises an integrated and parallel drug discovery platform, including the following elements:

- Iterative cycles of protein modeling supported molecular design and synthesis of unique and proprietary privileged structures that encode a kinase family-wide commonality in ATP binding or alternatively in allosteric inhibition modes.
- Generation of lead structures and preclinical candidates for selected kinases by specific derivatization of a once generated master key.
- Launch into the entire kinase family by design and synthesis of kinase-biased compound libraries templated on a privileged structure by means of automated synthesis.

4.8.1

Application of *KinaTor*[™] for the Second-Generation Kinase Inhibitors

The kinase family-biased master key concept is intentionally designed to rigorously exploit the kinase-intrinsic potential for lead discovery and optimization in that once

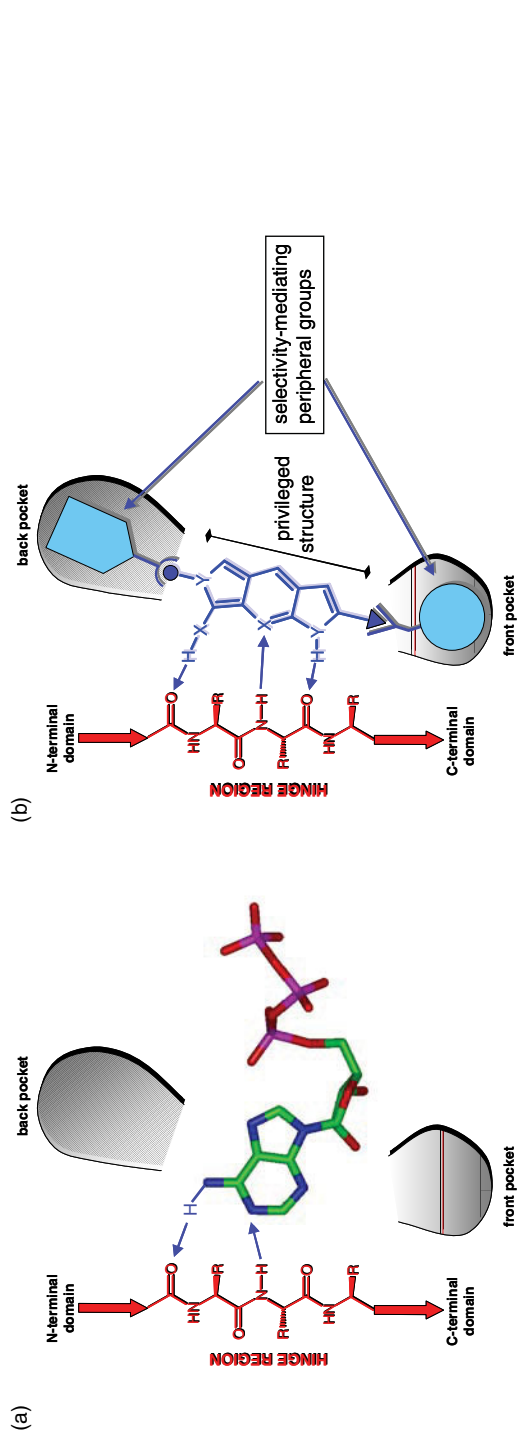


Figure 4.6 (a) Schematic presentation of the kinase family-wide conserved binding mode of ATP within the catalytically active site of a kinase. Hydrogen bonds connecting the adenine moiety with the hinge peptide backbone are shown explicitly. Cavities not utilized by the catalytic mechanism of the enzymes are denoted as front and back pockets. (b) Tailor-made master key (blue) docked into

established inhibitor concepts are repeatedly applied for various representatives of the family without compromising the required selectivity. In this context, the KinaTor technology emerges as a strategic tool for successful implementation of the corresponding research structure. The strategic relevance of the KinaTor technology in the area of lead finding and optimization is twofold. First, it provides the ultimate selectivity panel for any ongoing optimization program on distinct kinase targets, and second, more important in the context of privileged structure-based inhibitor design, it identifies novel and unexpected kinase targets for an investigated compound series templated on a privileged structure.

An immediate extrapolation of once established chemistries, structure–activity, and structure–property relationships for the primary target onto a newly identified off-target with proven validation state will give multiple opportunities for head starts, bypassing numerous iterations in early discovery chemistry. It is the conceptual combination of the proteomics tool KinaTor with an intelligent and modern medicinal chemistry concept that will elicit a cascade of drug discovery and development projects throughout the kinase family across any therapeutic boundaries.

In summary, the major gain in lead discovery and optimization efficiency is achieved by repeatedly using established and steadily growing knowledge on a target family in all involved areas of biology and chemistry. Optimized technical procedures for protein production, purification, assay development, and screening can be used for numerous members from a target family of interest. A considerable percentage of a compound collection with built-in target family bias, preferentially based on tailor-made privileged structures [52], will show activity against distinct members of the target enzyme or receptor cluster, with emerging structure–activity and structure–selectivity relationships, respectively. Multiple use of the target family-directed biology and chemistry resources is definitely more efficient than starting from scratch for each new discovery project, thus accelerating lead finding and optimization campaigns considerably.

In the chemogenomics approach, increased productivity and shorter timelines are achieved by a strict reuse of well-designed chemistry concepts, based on the mutual overlap between privileged structure-based pharmacophore space and the structural and physicochemical requirements of the ligand binding site of target family members. This overlap is the privileged structure-encoded information content that is optimized for complementarity toward the target family-wide commonality in molecular recognition. A clear structural understanding of this relation is required to leverage the intrinsic potential of a target family approach with associated multiple therapeutic scopes.

4.9 Conclusions

Signal transduction therapy has become a very important area of drug research since most of our diseases are related to intra- or intercellular signaling disorders, in other words, to systemic regulatory disorders. Deregulated protein kinase activity can

result from genetic alterations acquired early in tumorigenesis and remains an essential aspect of tumor cell physiology throughout disease progression.

Kinases are probably the most important signaling enzymes that represent about 20% of the druggable genome. Currently, more than 70 kinases are known that are validated target molecules for signal transduction therapy. Therefore in the drug discovery process, the selection of relevant, susceptible protein kinase targets, together with searches for lead drug candidates and optimization of these lead molecules for potency, selectivity and pharmacological properties have become a crucial approach.

However, we have to be aware of the fact that in the protein kinase area, it will be very much unlikely to find a unique compound that specifically inhibits a selected single protein kinase, leaving the other more than 500 protein kinases unaffected. On the other hand, with sufficient structural biology information about the binding mode and possible interactive sites and related pharmacophore modeling, we may be able to develop protein kinase inhibitors that can have a “reasonable side effect profile.” With the recently developed target fishing technology, the selectivity profile of the kinase inhibitors can be thoroughly analyzed.

To improve kinase selectivity of certain inhibitors – for example, in the area of neurodegenerative disease-related kinase targets – developing compounds that bind preferentially to the inactive forms of protein kinases or that prevent one protein kinase from activating another can represent a promising approach. Detailed understanding of the catalytic and regulatory properties of kinases can contribute significantly to develop novel kinase inhibitors, including more specific allosteric inhibitors.

A general drawback of target-specific monotherapy therefore derives from the fact that a single genetic alteration conferring target resistance to an individual tumor cell can eventually lead to relapse. The ability of kinases to mutate in response to the selective pressure created by drug treatment provides a strong rationale for hitting more than one essential target at the same time in the tumor cells. Multitargeted therapy can be achieved with either a combination of medicines or single “promiscuous” drugs that act on a set of disease-relevant proteins. Protein kinases, which share a relatively conserved ATP binding site, are amenable to the latter concept of targeted polypharmacology.

This multiple targeted compounds on the other hand can be very unselective; this might interfere with normal cellular function and result in dose-limiting toxicity. To keep potential adverse side effects to a minimum, compounds must ideally possess a multitarget selectivity that is restricted to cancer-relevant protein kinases and must be ineffective at least against the so-called untouchable kinases. This challenge might be addressed using proteomic techniques, which make use of immobilized kinase inhibitors for the affinity purification of cellular drug targets followed by sensitive mass spectrometry for subsequent protein identification.

Therefore, mechanistic and structural insights into the molecular aspects of drug-target resistance provide a rationale for the selection and design of backup compounds for drug development that show potent activity against mutant kinase alleles and might also be generally less susceptible to resistance formation.

It is essential to expand the definition of a disease-relevant target to include the whole range of functional mutant phenotypes. In this context, it might be conceivable that a set of distinct small-molecule inhibitors with complementary activities toward desensitized mutant alleles ensure effective inhibition of any resistant kinase variants that possibly emerge during targeted therapy. In this scenario, resistance formation against one targeted drug could always be therapeutically addressed with an alternative drug for the same cellular target. Moreover, the simultaneous inhibition of several cellular targets by polypharmacological intervention might have even greater potential in preventing the emergence of drug resistance in human malignancies.

Potent multitarget inhibitors with a reasonable selectivity profile can be developed by rational drug design where even possible gatekeeper or other resistance-producing mutations can be taken into account.

The challenge for rational drug design is to develop such multitarget inhibitors by recognizing differences and similarities in the topology, chemical and electrostatic environment, and specific binding modes of different kinases. Kinases that are in the same family have high amino acid homologies and hence similar active site topologies. Therefore, structure-based drug design utilizing X-ray crystallography and molecular modeling subsequent to focused library screening, provides the best approach to obtain selective kinase inhibitors. This allows rational design of small molecules that have a high degree of complementarities to the target active site.

In the ligand-based design approach, our Nested Chemical Library technology can be used to generate extended pharmacophore models.

Nevertheless, 3D structure-based drug design will continue to provide a key strategy to generate and/or optimize promising lead compounds, and it is expected that future protein kinase drug discovery will exploit a variety of high-powered *in silico* tools to computationally visualize, analyze, and probe the molecular properties and interactions of novel small-molecule inhibitors with their desired therapeutic target(s). Integration of such *in silico* tools (e.g., molecular modeling and docking approaches and virtual screening) with structural biology (e.g., X-ray and/or NMR studies, with sophisticated medicinal chemistry, chemoinformatics, and bioinformatics provides great possibility for developing novel potent kinase inhibitory drugs.

References

- 1 Vieth, M., Higgs, R.E., Robertson, D.H., Shapiro, M., Gragg, E.A., and Hemmerle, H. (2004) Kinomics-structural biology and chemogenomics of kinase inhibitors and targets. *Biochimica et Biophysica Acta*, **1697**, 243–257.
- 2 Erős, D., Órfi, L., and Kéri, G. (2004) Rational drug design and signal transduction therapy. *PharmaChem*, **3**, 27–30.
- 3 Levitzki, A. (1996) Targeting signal transduction for disease therapy. *Current Opinion in Cell Biology*, **8**, 239–244.
- 4 Levitzki, A. (1994) Signal-transduction therapy: a novel-approach to disease management. *European Journal of Biochemistry*, **226**, 1–13.
- 5 www.bmb.leeds.ac.uk (2 March 2009).
- 6 Alton, G., Schwamborn, K., Satoh, Y., and Westwick, J.K. (2002) Therapeutic

- modulation of inflammatory gene transcription by kinase inhibitors. *Expert Opinion on Biological Therapy*, **2**, 621–632.
- 7 Klebl, B.M. and Müller, G. (2005) Second-generation kinase inhibitors. *Expert Opinion on Therapeutic Targets*, **9** (5), 975–993.
 - 8 Schindler, T., Bornmann, W., Pellicena, P., Miller, W.T., Clarkson, B., and Kuriyan, J. (2000) Structural mechanism for STI-571 inhibition of Abelson tyrosine kinase. *Science*, **289**, 1938–1942.
 - 9 Pargellis, C., Tong, L. *et al.* (2002) Inhibition of p38 MAP kinase by utilizing a novel allosteric binding site. *Nature Structural Biology*, **9**, 268–272.
 - 10 Stamos, J., Silwowski, M.X., and Eigenbrot, C. (2002) Structure of the epidermal growth factor receptor kinase domain alone and in the complex with a 4-anilinoquinazoline inhibitor. *The Journal of Biological Chemistry*, **48**, 46265–46272.
 - 11 Berman, H.M., Westbrook, J., Feng, Z. *et al.* (2000) The Protein Data Bank. *Nucleic Acids Research*, **28**, 235–242.
 - 12 Nagar, B., Bornmann, W., Pellicena, P. *et al.* (2002) Crystal structures of the kinase domain of c-Abl in complex with the small molecule inhibitors PD173955 and Imatinib (STI-571). *Cancer Research*, **62**, 4236–4243.
 - 13 Altschul, S.F., Gish, W., Miller, W., Myers, E.W., and Lipman, D.J. (1990) Basic local alignment search tool. *Journal of Molecular Biology*, **215**, 403–410.
 - 14 Rarey, M., Kramer, B., Lengauer, T., and Klebe, G. (1996) A fast flexible docking method using an incremental construction algorithm. *Journal of Molecular Biology*, **261**, 470–489.
 - 15 SYBYL, Ligand-Based Design Manual, version 6.6, Tripos, Inc., St. Louis, MO (1999).
 - 16 Wermuth, C.G. (2003) Strategies in the search for new lead compounds or original working hypotheses, in *The Practice of Medicinal Chemistry*, 2nd edn (ed. C.G. Wermuth), Academic Press, London, pp. 67–89.
 - 17 Ahn, N.G. and Resing, K.A. (2005) Lessons in rational drug design for protein kinases. *Science*, **308**, 1266–1267.
 - 18 Ahn, N.G. and Resign, K.A. (2005) Lessons in rational drug design for protein kinases. *Science*, **308**, 1266–1267.
 - 19 Liu, Y., Bishop, A., Witucki, L. *et al.* (1999) Structural basis for selective inhibition of Src family kinases by PP1. *Chemistry & Biology*, **6**, 671–678.
 - 20 Cohen, M.S., Zhang, C., Shokat, K.M., and Taunton, J. (2005) Structural bioinformatics-based design of selective, irreversible kinase inhibitors. *Science*, **308**, 1318–1321.
 - 21 Bridges, A.J. (1999) The rationale and strategy used to develop a series of highly potent, irreversible, inhibitors of the epidermal growth factor receptor family of tyrosine kinases. *Current Medicinal Chemistry*, **6**, 825–843.
 - 22 Herbst, R.S., Fukuoka, M., and Baselga, J. (2004) Timeline: Gefitinib – a novel targeted approach to treating cancer. *Nature Reviews. Cancer*, **4**, 956–965.
 - 23 Stamos, J., Silwowski, M.X. *et al.* (2002) Structure of the epidermal growth factor receptor kinase domain alone and in complex with a 4-anilinoquinazoline inhibitor. *The Journal of Biological Chemistry*, **48**, 46265–46272.
 - 24 Schindler, T., Bornmann, W. *et al.* (2000) Structural mechanism for STI-571 inhibition of Abelson tyrosine kinase. *Science*, **289**, 1938–1942.
 - 25 Gumireddy, K., Baker, S.J., Cosenza, S.C. *et al.* (2005) A non-ATP-competitive inhibitor of BCR-ABL overrides imatinib resistance. *Proceedings of the National Academy of Sciences of the United States of America*, **102**, 1992–1997.
 - 26 Mohammadi, M., Froum, S., Hamby, J.M. *et al.* (1998) Crystal structure of an angiogenesis inhibitor bound to the FGF receptor tyrosine kinase domain. *The EMBO Journal*, **17**, 5896–5904.
 - 27 Zhu, X., Kim, J.L., Rose, P.E., Stover, D.R., and Toledo, L.M. (1999) Structural analysis of the lymphocyte-specific kinase Lck in complex with non-selective and Src family selective kinase inhibitors. *Structure (London, England: 1993)*, **7**, 651
 - 28 Narayana, N., Diller, T.C., Koide, K. *et al.* (1999) Crystal structure of the potent natural product inhibitor balanol in complex with the catalytic subunit of

- cAMP-dependent protein kinase. *Biochemistry*, **38**, 2367–2376.
- 29 Starovasnik, M.A., Christinger, H.W., Wiesmann, C., Champe, M.A., De Vos, A.M., and Skelton, N.J. (1999) Solution structure of the VEGF-binding domain of Flt-1: comparison of its free and bound states. *Journal of Molecular Biology*, **293**, 531–544.
 - 30 Davis, S.T., Benson, B.G., Bramson, H.N. *et al.* (2001) Prevention of chemotherapy-induced alopecia in rats by CDK inhibitors. *Science*, **291**, 134–137.
 - 31 Lamers, M.B.A.C., Antson, A.A., Hubbard, R.E., Scott, R.K., and Williams, D.H. (1999) Structure of the protein tyrosine kinase domain of C-terminal Src kinase (CSK) in complex with staurosporine. *Journal of Molecular Biology*, **285**, 713–725.
 - 32 Shewchuk, L., Hassell, A., Wisely, B. *et al.* (2000) Binding mode of the 4-anilinoquinazoline class of protein kinase inhibitor: X-ray crystallographic studies of 4-anilinoquinazolines bound to cyclin-dependent kinase 2 and p38 kinase. *Journal of Medicinal Chemistry*, **43**, 133–138.
 - 33 Marshall, G.R., Barry, C.D., Bosshard, H.E., Dammkoehler, R.A., and Dunn, D.A. (1979) Description of the active analog approach, in *Computer-Assisted Drug Design*, American Chemical Society, Symposium, vol. 112 (eds E.C. Olson and Christofferson R.E.), American Chemical Society, Washington DC, pp. 205–226.
 - 34 Richon, A.B. and Young, S.S. (2005) An introduction to QSAR methodology. <http://www.netsci.org/Science/Compchem/feature19.html> and <http://www.netsci.org/> (accessed August 15, 2005).
 - 35 Cramer, R.D., Patterson, D.E., and Bunce, J.D. (1988) Comparative molecular-field analysis (COMFA) 1. Effect of shape on binding of steroids to carrier proteins. *Journal of the American Chemical Society*, **110**, 5959–5967.
 - 36 Klebe, G., Abraham, U., and Mietzner, T. (1994) Molecular similarity indices in a comparative-analysis (CoMSIA) of drug molecules to correlate and predict their biological activity. *Journal of Medicinal Chemistry*, **37**, 4130–4146.
 - 37 Silverman, B.D. and Platt, D.E. (1996) Comparative molecular moment analysis (CoMMA): 3D-QSAR without molecular superposition. *Journal of Medicinal Chemistry*, **39**, 2129–2140.
 - 38 Perkins, R., Fang, H., Tong, W.D., and Welsh, W.J. (2003) Quantitative structure–activity relationship methods: perspectives on drug discovery and toxicology. *Environmental Toxicology and Chemistry*, **22**, 1666–1679.
 - 39 Vedani, A., Dobler, M., and Zbinden, P. (1998) Quasi-atomistic receptor surface models: a bridge between 3-D QSAR and receptor modeling. *Journal of the American Chemical Society*, **120**, 4471–4477.
 - 40 Vedani, A., Briem, H., Dobler, M., Dollinger, H., and McMasters, D.R. (2000) Multiple-conformation and protonation-state representation in 4D-QSAR: the neurokinin-1 receptor system. *Journal of Medicinal Chemistry*, **43**, 4416–4427.
 - 41 Ferrara, N. (2001) Role of vascular endothelial growth factor in regulation of physiological angiogenesis. *American Journal of Physiology. Cell Physiology*, **246**, C1358–C1366.
 - 42 Klebl, B.M., Daub, H., and Kéri, G. (2004) Chemical kinomics, in *Chemogenomics in Drug Discovery: A Medicinal Chemistry Perspective* (eds H. Kubinyi and G. Müller) Wiley-VCH Verlag GmbH, pp. 167–190.
 - 43 Cohen, P. (2000) The regulation of protein function by multisite phosphorylation: a 25 year update. *Trends in Biochemical Sciences*, **25**, 596–601.
 - 44 Li, W.Q., Favellyukis, S., Yang, J. *et al.* (2004) Inhibition of insulin-like growth factor I receptor autophosphorylation by novel 6-5 ring-fused compounds. *Biochemical Pharmacology*, **68**, 145–154.
 - 45 Capdeville, R., Buchdunger, E., Zimmermann, J., and Matter, A. (2002) Gleevec (STI571, imatinib), a rationally developed, targeted anticancer drug. *Nature Reviews. Drug Discovery*, **1**, 493–502.
 - 46 Lee, J.C., Laydon, J.T., McDonnell, P.C. *et al.* (1994) A protein kinase involved in the regulation of inflammatory cytokine biosynthesis. *Nature*, **372**, 739–746.
 - 47 Hopkins, A.L. and Groom, C.R. (2002) The druggable genome. *Nature Reviews. Drug Discovery*, **1**, 727–730.

- 48 Li, R. and Stafford, J.A. (eds) (2009) Preface, in *Kinase Inhibitor Drugs*. Hoboken, New Jersey, John Wiley & Sons, Inc., pp. ix–xii.
- 49 Fabbro, D., Ruetz, S., Buchdunger, E. *et al.* (2002) Protein kinases as targets for anticancer agents: from inhibitors to useful drugs. *Pharmacology & Therapeutics*, **93**, 79–98.
- 50 Gill, A., Cleasby, A. *et al.* (2005) The discovery of novel protein inhibitors by using fragment-based high-throughput X-ray crystallography. *Chembiochem: A European Journal of Chemical Biology*, **6**, 506–512.
- 51 Zimmermann, J., Buchdunger, E., Mett, H., Meyer, T., and Lydon, N.B. (1997) Potent and selective inhibitors of the Abl-Kinase: phenylamino-pyrimidine (PAP) derivatives. *Bioorganic & Medicinal Chemistry Letters*, **7**, pp. 187–192.
- 52 Müller, G. (2003) Medicinal chemistry of target family-directed masterkeys. *Drug Discovery Today*, **8**, 681–691.
- 53 Müller, G. (2004) *Chemogenomics in Drug Discovery: A Medicinal Chemistry Perspective* (eds H. Kubinyi and G. Müller), Wiley-VCH Verlag GmbH, Weinheim, pp. 7–41.
- 54 Klebl, B.M. (2004) Chemical kinomics: a target gene family approach in chemical biology. *Drug Discovery Today*, **1**, 25–34.
- 55 Szymkowski, D.E. (2003) Chemical genomics versus orthodox drug development. *Drug Discovery Today*, **8**, 157–159.
- 56 Keen, N. and Taylor, S. (2004) Aurora-kinase inhibitors as anticancer agents. *Nature Reviews. Cancer*, **4**, 927–936.
- 57 Davies, S.P., Reddy, H., Caivano, M., and Cohen, P. (2000) Specificity and mechanism of action of some commonly used kinase inhibitors. *The Biochemical Journal*, **351**, 95–105.
- 58 Bain, J., McLauchlan, H., Elliott, M., and Cohen, P. (2003) The specificities of protein kinase inhibitors: an update. *The Biochemical Journal*, **371**, 199–204.
- 59 Wissing, J., Godl, K., Brehmer, D. *et al.* (2004) Chemical proteomic analysis reveals alternative modes of action for pyrido[2,3-*d*]pyrimidine kinase inhibitors. *Molecular & Cellular Proteomics*, **3**, 1181–1193.
- 60 Schnier, J.B., Kaur, G., Kaiser, A. *et al.* (1999) Identification of cytosolic aldehyde dehydrogenase 1 from non-small cell lung carcinomas as a flavopiridol-binding protein. *FEBS Letters*, **454**, 100–104.
- 61 <http://www.upstate.com> (accessed May 8, 2005).
- 62 Fabian, M., Biggs, W.H., Treiber, D.K. *et al.* (2005) A small molecule–kinase interaction map for clinical kinase inhibitors. *Nature Biotechnology*, **23**, 329–336.
- 63 Godl, K., Wissing, J., Kurtenbach, A. *et al.* (2003) An efficient proteomics method to identify the cellular targets of protein kinase inhibitors. *Proceedings of the National Academy of Sciences of the United States of America*, **100**, 15434–15439.
- 64 Becker, F., Murthi, K., Smith, C. *et al.* (2004) A three-hybrid approach to scanning the proteome for targets of small molecule kinase inhibitors. *Chemistry & Biology*, **11**, 211–223.
- 65 Knockaert, M., Gray, N., Damiens, E. *et al.* (2000) Intracellular targets of cyclin-dependent kinase inhibitors: identification by affinity chromatography using immobilised inhibitors. *Chemistry & Biology*, **7**, 411–422.
- 66 Knockaert, M., Wiekling, K., Schmitt, S. *et al.* (2002) Intracellular targets of paullones. *The Journal of Biological Chemistry*, **277**, 25493–25501.
- 67 Wan, Y., Hur, W., Cho, C.Y. *et al.* (2004) Synthesis and target identification of hymenialdisine analogs. *Chemistry & Biology*, **11**, 247–259.
- 68 Brehmer, D., Greff, Z., Godl, K. *et al.* (2005) Cellular targets of gefitinib. *Cancer Research*, **65**, 379–382.
- 69 Kéri, G., Órfi, L. *et al.* (2006) Signal transduction therapy with rationally designed kinase inhibitors. *Current Signal Transduction Therapy*, **1**, 67–95.
- 70 Keri, G., Szekelyhidi, Z., Orfi, L. *et al.* (2005) Drug discovery in the kinase inhibitory field using the Nested Chemical Library™ technology. *Assay and Drug Development Technologies*, **3**, pp. 543–551.
- 71 Erős, D., Kövesdi, I., Órfi, L., Takács-Novák, K., Acsády, G., and Kéri, G. (2002) Reliability of log*P* predictions based on calculated molecular descriptors: a critical

- review. *Current Medicinal Chemistry*, **9**, 1819–1829.
- 72 Erős, D., Kéri, G., Kövesdi, I., Szántai-Kis, C., Mészáros, G., and Órfi, L. (2004) Comparison of predictive ability of water solubility QSPR models generated by MLR, PLS and ANN methods. *Mini-Reviews in Medicinal Chemistry*, **4**, 167–177.
 - 73 Kövesdi, I., Kéri, G., and Órfi, L. (2002) US Patent WO02/082329.
 - 74 Shao, J. (1993) Linear-model selection by cross-validation. *Journal of the American Statistical Association*, **88**, 486–494.
 - 75 Gazit, A., Yaish, P., Gilon, C., and Levitzki, A. (1989) Tyrphostins 1. Synthesis and biological-activity of protein tyrosine kinase inhibitors. *Journal of Medicinal Chemistry*, **32**, 2344–2352.
 - 76 Furka, Á., Sebestyén, F., Dibó, G. *et al.* (1991) General method for rapid synthesis of multicomponent peptide mixtures. *International Journal of Peptide and Protein Research*, **37**, 487–493.
 - 77 Houghten, R.A., Pinilla, C., Blondelle, S. *et al.* (1991) Generation and use of synthetic combinatorial libraries for basic research and drug discovery. *Nature*, **354**, 84–86.
 - 78 Órfi, L., Wączek, F., Kéri, G. *et al.* (1999) New antitumor leads from a peptidomimetic library. *Letters in Peptide Science*, **6**, 325–333.
 - 79 Fry, D.W., Kraker, A.J., McMichael, A. *et al.* (1994) A specific inhibitor of the epidermal growth factor receptor tyrosine kinase. *Science*, **265**, 1093–1095.
 - 80 Buijsman, R. (2004) Structural aspects of kinases and their inhibitors, in *Chemogenomics in Drug Discovery: A Medicinal Chemistry Perspective* (eds H. Kubinyi and G. Müller), Wiley-VCH Verlag GmbH, Weinheim, pp. 191–220.
 - 81 Hirth, K.P., Schwartz, D.P., Mann, E., Shawver, L.K., Kéri, G., Órfi, L. *et al.* (1997) Treatment of platelet derived growth factor related disorders such as cancers. Patent No. US5700822
 - 82 www.gsk.com and www.clinicaltrials.gov. (2 March 2009).
 - 83 Shiraishi, T., Owada, M.K., Tatsuka, M., Yamashita, T., Watanabe, K., and Kakunaga, T. (1989) Specific inhibitors of tyrosine-specific protein kinases: properties of 4-hydroxycinnamamide derivatives *in vitro*. *Cancer Research*, **49**, 2374–2378.
 - 84 Soudijn, W., van Wijngaarden, I., and Ijzerman, A.P. (2004) Allosteric modulation of G protein-coupled receptors: perspectives and recent developments. *Drug Discovery Today*, **9**, 752–758.
 - 85 Sawyer, T.K., Bohacek, R.S., Metcalf, C.A. *et al.* (2003) Novel protein kinase inhibitors: SMART drug design technology. *Biotechniques*, **34**, S2–S15.
 - 86 Pavletich, N.P. (1999) Mechanisms of cyclin-dependent kinase regulation: structures of Cdks, their cyclin activators, and Cip and INK4 inhibitors. *Journal of Molecular Biology*, **287**, 821–828.
 - 87 Huse, M. and Kuriyan, J. (2002) The conformational plasticity of protein kinases. *Cell*, **109**, 275–282.
 - 88 Peterson, J.R. and Golemis, E.A. (2004) Autoinhibited proteins as promising drug targets. *Journal of Cellular Biochemistry*, **93**, 68–73.
 - 89 Burke, J.R., Pattoli, M.A., Gregor, K.R. *et al.* (2003) Bms-345541 is a highly selective inhibitor of I kappa B kinase that binds at an allosteric site of the enzyme and blocks NF-kappa B-dependent transcription in mice. *The Journal of Biological Chemistry*, **278**, 1450–1456.
 - 90 Ohren, J.F., Chen, H.F., Pavlovsky, A. *et al.* (2004) Structures of human MAP kinase kinase 1 (MEK1) and MEK2 describe novel noncompetitive kinase inhibition. *Nature Structural & Molecular Biology*, **11**, 1192–1197.
 - 91 Corbin, A.S., Griswold, I.J., La Rosee, P. *et al.* (2004) Sensitivity of oncogenic KIT mutants to the kinase inhibitors MLN518 and PD180970. *Blood*, **104**, 3754–3757.
 - 92 Alessi, D.R., Cuenda, A., Cohen, P., Dudley, D.T., and Saltiel, A.R. (1995) PD-098059 is a specific inhibitor of the activation of mitogen activated protein kinase kinase *in-vitro* and *in-vivo*. *The Journal of Biological Chemistry*, **270**, 27489–27494.
 - 93 Hoppe, J., Freist, R., Marutzky, R., and Shaltiel, S. (1978) Mapping the

- ATP-binding site in the catalytic subunit of adenosine-3':5'-monophosphate-dependent protein kinase. Spatial relationship with the ATP site of the undissociated enzyme. *European Journal of Biochemistry*, **90**, 427–432.
- 94 Traxler, P. and Furet, P. (1999) Strategies toward the design of novel and selective protein tyrosine kinase inhibitors. *Pharmacology & Therapeutics*, **82**, 195–206.
- 95 Mortlock, A., Keen, N.J., Jung, F.H. *et al.* (2005) Progress in the development of selective inhibitors of Aurora kinases. *Current Topics in Medicinal Chemistry*, **5**, 199–213.

5

Kinase Inhibitors in Signal Transduction Therapy*György Kéri, László Órfi, and Gábor Németh*

Approximately 20–25% of the druggable genome consists of kinases involved in signal transduction. Currently, however, only 10 kinase inhibitors are used in clinical practice, which means wide perspectives for drug discovery. The first kinase inhibitor for signal transduction therapy was Gleevec – an inhibitor of BCR-ABL kinase – that has been launched in May 2002 [1, 2]. Gleevec is indicated for the treatment of chronic myeloid leukemia (CML) and has a success rate of 90% in affected patients. To our knowledge, more than 300 kinase inhibitors against more than 70 kinase targets are in the various stages of preclinical and clinical development in signal transduction therapy. This definitely underlines the significant influence of this area on drug research [3, 4]. Of the launched and late-stage clinical development compounds for cancers, the most important small-molecule synthetic tyrosine kinase inhibitors are Gleevec, the epidermal growth factor receptor tyrosine kinase inhibitors: ZD1839/gefitinib/Iressa [5] and OSI774/erlotinib/Tarceva [6], the vascular endothelial growth factor receptor (VEGFR) kinase inhibitors SU11248/sunitinib, dasatinib, and sorafenib [7].

5.1

VEGFR (Vascular Endothelial Growth Factor Receptor)

Targeting VEGFR might lead to the discovery of new anticancer agents. One of the most important processes in tumor growth is angiogenesis, by which new blood capillaries sprout from preexisting blood vessels [8–10]. Since VEGF stimulates angiogenesis, inhibition of its receptor will inhibit angiogenesis, a viable principle to inhibit tumor formation. Two small-molecule VEGF2R inhibitors have already been approved for cancer treatment. Sorafenib (VEGF2R, raf, c-KIT, and PDGFR β) has been marketed for RCC and HCC; while sunitinib (SU11248) (VEGF2R, PDGFR, c-KIT, RET, and Flt3) has been marketed for GIST and RCC.

Intrinsic and acquired resistance to antiangiogenetic drugs are clinically significant problems. Preclinical studies have begun to shed light on the mechanisms of such resistance, and to date four mechanisms of resistance have been identified:

(a) upregulation of the basic fibroblast growth factor (bFGF), (b) overexpression of matrix metalloproteinase-9 (MMP9), (c) increased levels of SDF1a (stromal cell-derived factor), and (d) hypoxia-induced factor (HIF)-1 α -induced recruitment of bone marrow-derived CD45 + myeloid cells [11]. Future studies will be required to develop strategies that will allow us to optimally exploit the potential of VEGF inhibitors to block primary tumor growth while at the same time suppressing prometastatic effects.

Other potent kinase inhibitors inhibiting VEGF signaling pathways are as follows: (a) Semaxinib (SU5416), the further development of which has been discontinued due to its inefficaciousness in clinical trials [12]. (b) Vatalanib (PTK787/ZK222584/CGP79787/CGP79787D) has already passed through clinical trials with severe side effects [13, 14]. Development of SU6668 [15, 16] and CP547632 [17] was stopped after phase I. (c) Axitinib (AG013736) is a multiple kinase inhibitor (VEGFR1, VEGFR2, VEGFR3, PDGFR, and cKIT). Pfizer reported on January 30, 2009 that phase III clinical trials of the drug when used in combination with gemcitabine showed no evidence of improved survival rates over treatments using gemcitabine alone for advanced pancreatic cancer and halted the trial [18], (Pfizer press release). (d) Cediranib (AZD2171). In February 2008, AstraZeneca announced that the use of cediranib in nonsmall cell lung cancer will not progress into phase III after failing to meet its main goal [19].

Zactima/vandetanib/ZD6474 is a potent, orally active, low molecular weight inhibitor of KDR/VEGFR2 tyrosine kinase activity and also displays inhibitory activity toward EGFR and oncogenic RET kinase. It has currently finished phase III clinical trial for NSCLC and it is still in phase II clinical development for a range of solid tumors, both as monotherapy and in combination with certain anticancer agents [20–23]. Other potent kinase inhibitors inhibiting VEGF signaling pathways are AV951 in phase II [24], CYC116, which is an Aurora A, Aurora B, and VEGF2R multiple target inhibitor in phase I (Figure 5.1) [25], and GSK1363089 (XL880), which is a c-Met, VEGF2R dual target inhibitor in phase II [26].

5.2

Flt3 (FMS-Like Tyrosine Kinase 3)

Flt3, also called CD135, is a cytokine receptor expressed on the surface of hematopoietic progenitor cells. Signaling through Flt3 plays a role in cell survival, proliferation, and differentiation. CD135 is important for lymphocyte (B cell and T cell) development. Mutations of the Flt3 receptor can lead to the development of leukemia, a cancer of bone marrow hematopoietic progenitors. Internal tandem duplications of Flt3 (Flt3-ITD) are the most common mutations associated with acute myelogenous leukemia (AML) and are a poor prognostic indicator. Flt3 inhibitors, like lestaurtinib (CEP701), showed clinical (stopped after phase II) activity in patients with acute myeloid leukemia [27, 28]. Recently, it was revealed that lestaurtinib inhibits the JAK2 kinase ($IC_{50} = 0.9$ nM) [29]. Tandutinib (MLN518) is in clinical phase II for the treatment of various cancers [30]. CHIR258/TKI258 is an orally active

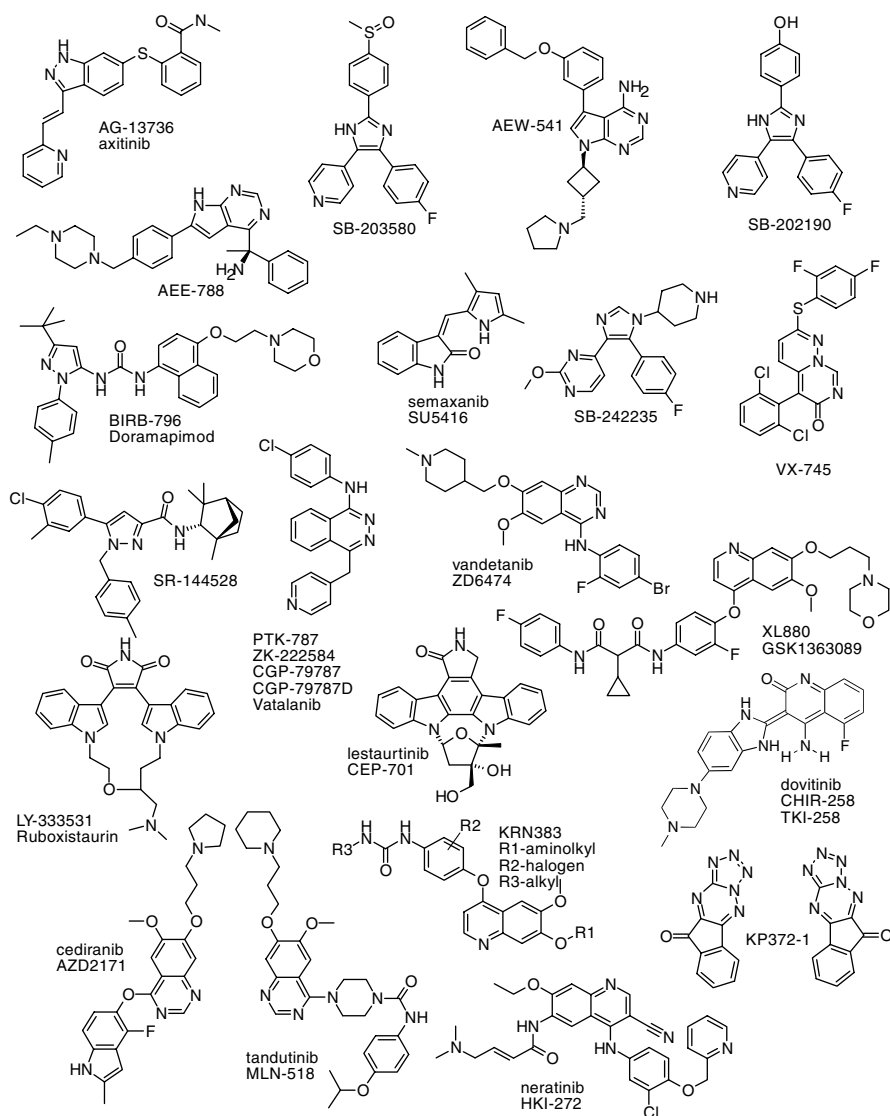


Figure 5.1 Structures of the mentioned kinase inhibitors I.

small molecule that exhibits potent inhibitory activity against multiple RTKs involved in tumor growth and angiogenesis ($IC_{50} \leq 10$ nM for VEGF, FGF, PDGF, and c-KIT receptor kinases; 37 nM for CSFR1). CHIR258 is in clinical phase II [31]. There are also some promising *Flt3* inhibitors in the preclinical development stage, such as KRN383 ($IC_{50} = 1.3$ nM) [32] and KP3721, which is an Akt/PDK-/*Flt3* multiple target inhibitor [33]. KP372-1 is a mixture of two isomers present in approximately equal amounts [34].

5.3

Bcr-Abl (Breakpoint Cluster Region–Abelson Murine Leukemia Viral Oncogene Homologue)

The Bcr-Abl tyrosine kinase inhibitor, imatinib (Gleevec) has greatly improved the outcome for patients with chronic myeloid leukemia. Unfortunately, induced mutations, which cause imatinib resistance, are leading to relapses in some patients [35]. Unlike imatinib, dasatinib (BMS354825) inhibits the active Bcr-Abl enzyme. It binds differently to the ATP binding site of Bcr-Abl. As a result, it not only inhibits wild-type Bcr-Abl but also 14 of the 15 reported Bcr-Abl mutants, leaving only the gatekeeper mutant Bcr-Abl^{T315I} unaffected. Dasatinib is sold under the trade name Sprycel [36]. Nilotinib (AMN107), another Bcr-Abl kinase inhibitor, has been approved as Tasigna in the United States and the European Union for drug-resistant chronic myelogenous leukemia [37].

In addition to dasatinib, the Aurora kinase inhibitor VX680 and the p38 inhibitor BIRB796 also inhibit the imatinib-resistant ABL^{T315I} kinase [38].

Two other receptor tyrosine kinases, c-kit and the platelet-derived growth factor receptor (PDGFR) are serendipitous, but important imatinib off-targets. Overexpression of c-kit, a tyrosine kinase is the underlying cause for the formation of gastrointestinal stromal tumors (GISTs). Some of the Gleevec treated patients, in analogy to Gleevec-induced resistance in CML, develop Gleevec-resistant GISTs, expressing the imatinib-resistant KIT^{V559D/T670I} kinase. The KIT/FLT3 inhibitor sunitinib (SU11248) shows potent activity against the imatinib-resistant KIT^{V559D/T670I} kinase, consistent with the clinical efficacy of sunitinib against imatinib-resistant GISTs. Similarly, the epidermal growth factor receptor mutant (EGFR) inhibitors EKB569 and CI1033, but not GW572016/lapatinib and ZD6474, potentially inhibit the gefitinib- and erlotinib-resistant EGFR mutant, EGFR^{L858R,T790M} [38].

5.4

EGFR (Epidermal Growth Factor Receptor)

To date, three EGFR kinase inhibitors have been approved as drugs. Despite their structural similarity, the molecules bind in different modes to the hinge domain. It was shown that lapatinib binds to the ATP binding site in a conformation that resembles an inactive kinase structure, it is just opening up the hydrophobic pocket and inducing the inactive conformation, while Tarceva binds to the active conformation [39]. The difference between the binding modes of the two molecules results in the fact that lapatinib has a slower off-rate from the active site.

The reactive cysteine situated in the ATP binding site of EGFR permits the design of selective, irreversible EGFR inhibitors, which form a covalent bond with the reactive cysteine. These types of compounds are being investigated in clinical trials [40, 41]. Wissner *et al.* [41] identified 4-anilinoquinazoline inhibitors based on modeling studies and after lead optimization, and they started the clinical trials of

inhibitor EKB569. This compound inhibits EGFR with an IC_{50} of $0.083 \mu M$ and it inhibited the growth of different carcinoma cell lines.

Anti-EGFR-targeted therapies have improved the efficacy of conventional chemotherapy in both preclinical and clinical studies. Although such therapies may lead to partial response or disease stabilization in some patients, many patients do not benefit from anti-EGFR therapy and there are some who do eventually develop resistance to that therapy. The molecular mechanisms of resistance can be attributed to several general processes: (a) resistance due to the activation of alternative tyrosine kinase receptors that bypass the EGFR pathway (e.g., c-Met and IGF1R), (b) resistance due to increased angiogenesis, (c) resistance based on constitutive activation of downstream mediators (e.g., PTEN, K-ras and others), and (d) the existence of specific EGFR mutations [11]. Interestingly, most of these resistance mechanisms (e.g., IGF1R overexpression, PTEN loss, bypassing of EGFR pathways, receptor masking, or epitope inaccessibility) are also implicated in the trastuzumab/Herceptin (it is a humanized monoclonal antibody that acts on the HER2/neu (erbB2) receptor) resistance and are reviewed elsewhere [42].

The successful kinase inhibitors (e.g., Gleevec and Iressa) are ineffective on certain mutated kinases [43]. It has been recently reported that the T790M mutations in EGFR as secondary mutations that arise in previously sensitive NSCLCs harboring an activating mutation are associated with the emergence of acquired resistance. (similar resistance and mutation have been described in the case of Gleevec in CML). However, it has been shown now that in the case of EGFR, this mutation is present only in a subset of cases and even tumors that harbor the T790M mutation may contain only a small fraction of cells with this mutation. These observations imply that multiple resistance mechanisms can coexist in recurrent tumors after an initial response to gefitinib or Gleevec. Because most of the kinase inhibitors have to reach an intracellular target, specific membrane transporters may significantly modulate their effectiveness. In addition, the hydrophobic kinase inhibitors may interact with so-called multidrug transporters and thus alter the cellular distribution of unrelated pharmacological agents. We have demonstrated recently that certain TKIs, already in the clinical phase of drug development, directly interact with the ABCG2 multidrug transporter protein with a high affinity. Low concentrations of the TKIs examined selectively modulated ABCG2-ATPase activity, inhibited ABCG2-dependent active drug extrusion, and significantly affected drug resistance patterns in cells expressing ABCG2. Our results indicated that multidrug resistance protein modulation by TKIs may be an important factor in the clinical treatment of cancer patients. These data also raised the possibility that an extrusion of TKIs by multidrug transporters, for example, ABCG2, may be involved in tumor cell TKI resistance [44, 45].

This multiple resistance problem also shows the importance of personalized therapy [46, 47], where the drug is applied after gene expression and mutation analysis.

Neratinib (HKI272) is a prospering EGFR/HER2 kinase inhibitor, currently, in phase III clinical trials [48].

One of the main targets of vandetanib is EGFR, already described under Section 5.1.

PKI166 was a promising dual inhibitor of both the EGFR and the HER2 kinases; however, its development was discontinued after phase I study [5, 49–51].

BMS599626 is an orally bioavailable inhibitor of the HER1, HER2, and HER4 tyrosine kinases (IC_{50} = 22, 32, and 190 nM, respectively); it was halted after clinical phase I [52].

The development of Her2/ErbB2 inhibitor of Pfizer, CP724714, was discontinued after phase II trials [53].

AEE788 is an anticancer agent of Novartis with various effects: it shows EGFR family tyrosine kinase receptor inhibitory, ErbB2 tyrosine kinase receptor inhibitory, and VEGF antagonist and AKT protein kinase modulatory activity. It was discontinued after clinical phase II [54].

5.5

IGFR (Insulin-Like Growth Factor Receptor)

IGF1 and its receptor play a pivotal role in many cancers; it is an attractive target for the design of inhibitors. A new family of catechol mimics has been reported to be a substrate-competitive inhibitor of IGF1 receptor (IGF1R) [55]. The ATP binding region of IGFR and insulin receptor (IR) show high similarity, as it is generally a highly conserved region of kinases. Hence, the most efficient inhibitors are monoclonal antibodies. Inhibition of IGF1R autophosphorylation by novel 6-5 ring-fused compounds (pyrrolopyrimidines and fuopyrimidines) is reported [56]. A compound from Novartis (AEW541/NPV-AEW541) inhibiting IGF1R (approximately 10-fold selectivity for IGF1R over IR) finished its clinical phase I. It is being developed against cancer and multiple myeloma [57, 58]. Another interesting IGF1R inhibitor in preclinical phase is BMS536924 [59].

5.6

FGFR (Fibroblast Growth Factor Receptor)

It has been shown that overexpression of FGFR can be detected in a population of breast cancers [60], human pancreatic cancers [61], astrocytomas [62], salivary gland adenocarcinomas [63], Kaposi's sarcomas [64], ovarian cancers [65], and prostate cancers [66]. Mohammadi et al. [67] determined the X-ray structure of FGFR cocrystallized with their oxindole (indolinone) derivatives. They have shown that the oxindole group binds to the adenine region of the ATP binding site of FGFR and the other groups interact with the residues of the hinge region. The structural information provided by this article can be used for designing novel, more potent, and selective FGFR inhibitors. For example, Hyun et al. developed a reliable CoMFA and CoMSIA models for FGFR inhibitors based on the crystal structure of the oxindole derivatives [68]. They selected their best CoMSIA model to screen a virtual library to find new inhibitors.

Another known oxindole FGFR inhibitor is SU5402. PD173074, together with SU5402, did not reach the clinical development stage. TKI258/CHIR258 and cediramib/AZD2171 both are VEGFR/FGFR inhibitors. Ki23057 is an inhibitor of FGF2R, VEGFR, PDGFR β , and cKit [69].

5.7

PDGFR (Platelet-Derived Growth Factor Receptor)

PDGFR is an important factor in regulation of cell proliferation, cellular differentiation, and cell growth and development, as well as many diseases including cancer. The extracellular region of the receptor consists of five immunoglobulin-like domains, while the intracellular part is a tyrosine kinase domain. PDGFR has two isoforms α and β . These two receptor isoforms dimerize upon binding its substrate (the PDGF dimer), leading to three possible receptor combinations ($\alpha\alpha$, $\beta\beta$, and $\alpha\beta$). Ras/mitogen-activated protein kinase (MAPK), PI3 kinase, and phospholipase- γ (PLC γ) pathways are key downstream mediators of the PDGFR signaling. This receptor tyrosin kinase is one of the most studied kinases. There are a lot of inhibitors under preclinical/clinical development, even some in the market. Imatinib, nilotinib, sorafenib, and sunitinib are PDGFR inhibitors already approved for cancer treatment. Almost all the clinically developed PDGFR inhibitors have a strong potential to inhibit other receptor tyrosine kinases, such as VEGFR, c-Kit, and FGFR. Motesanib (AMG706) inhibits, besides PDGFR, VEGFR and c-Kit kinases. Its clinical phase II studies are complete for different tumorous malignancies [70].

5.8

c-Kit

CD117, also called KIT or c-Kit receptor, is a cytokine receptor expressed on the surface of hematopoietic stem cells as well as other cell types. This receptor binds to stem cell factor (a substance that causes certain types of cells to grow). Altered forms of this receptor may be associated with some types of cancer [71]. Overexpression or mutations of c-Kit can lead to cancer. Mutations of CD117 have also been implicated in leukemia, a cancer of hematopoietic progenitors, and gastrointestinal stromal tumors (GISTs). The efficacy of imatinib, a CD117 inhibitor, is determined by the mutation status of CD117 [72]. As already said in Section 5.7, almost all the clinically developed PDGFR inhibitors have a strong potential to inhibit other receptor tyrosine kinases, such as VEGFR, c-Kit, and FGFR. Consequently, these compounds are not cited here again. There is a demand for a selective c-Kit inhibitor. As an answer, Amgen has published a series of c-Kit inhibitors. These compounds showed more than 10-fold higher activity against c-Kit than any other kinases involved in this study. However, they did not compare the c-Kit versus PDGFR and VEGFR (Figure 5.2) [73].

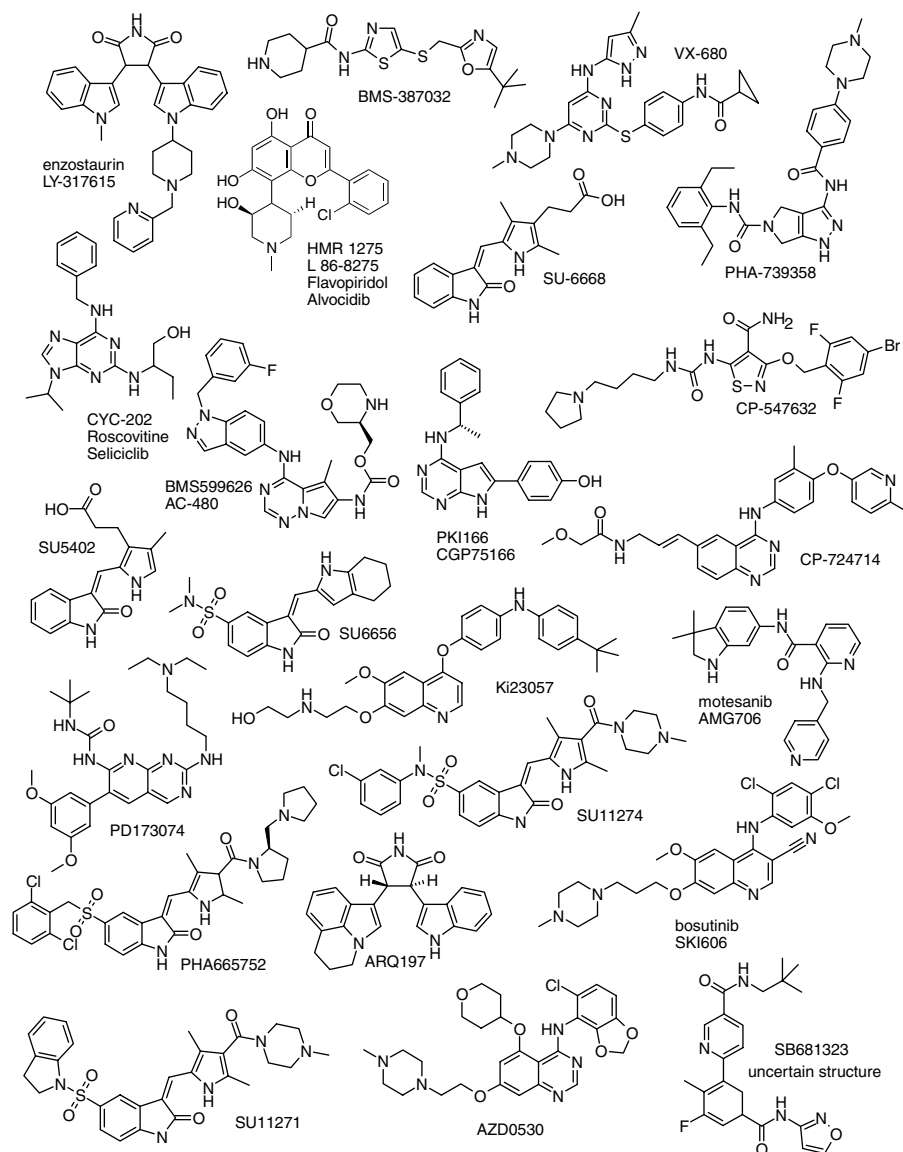


Figure 5.2 Structures of the mentioned kinase inhibitors II.

5.9

Met (Mesenchymal-Epithelial Transition Factor)

MET is a membrane receptor that is essential for embryonic development and wound healing. Hepatocyte growth factor (HGF) is the only known ligand of the MET receptor. Abnormal MET activation in cancer correlates with poor prognosis,

where aberrantly active MET triggers tumor growth, formation of new blood vessels, and cancer spread to other organs (metastasis) [74]. Met is commonly overexpressed in tumors and point mutations have been identified in hereditary and sporadic papillary renal carcinomas, gastric carcinoma, hepatocellular and head and neck carcinomas.

Several potent and selective small-molecule inhibitors of HGF/c-Met have already been reported [75]. PHA665752 [76], SU11274 [77], and SU11271 [78] are oxindoles in preclinical development. ARQ197 is specific c-Met inhibitor in phase II [79]. XL184 is a multiple kinase inhibitor (c-Met, RON, FGFR1, and FLK1), currently in phase III against medullary thyroid cancer and in phase II against NSCL and glioblastoma multiforme [80].

5.10

Src

The Src family of nonreceptor, protooncogenic tyrosine kinases has been the center of interest ever since kinases have been identified as potential therapeutic targets (Nobel Prize in Physiology or Medicine for 1989 jointly to J. Michael Bishop and Harold E. Varmus for their discovery of “the cellular origin of retroviral oncogenes.”). The widely expressed (and closely related) Src and Yes kinases are particularly attractive targets for therapeutic intervention in cancer, having been implicated in the growth and dissemination of breast and colon cancer. A major difficulty in the development of Src inhibitors for clinical development was the problem of selectivity, in particular the need to avoid targeting the Src family kinase Lck, a critical mediator of T cell development and function. First advances have been achieved by SUGEN/Pharmacia (SU6656) [81] and Novartis [82] in developing ATP-mimetics with approximately 10-fold selectivity for Src over Lck. Bosutinib (SKI606), a 4-anilino-3-quinolinecarbonitrile dual inhibitor of Src and Abl kinases, is a potent antiproliferative agent against chronic myelogenous leukemia (phase III) and breast cancer (phase II) [83, 84]. AZD0530 is a highly selective, dual-specific, orally available, small-molecule inhibitor of Src kinase and BCR-Abl. AZD0530 is in clinical phase II for the treatment of solid tumors and hematological malignancies [85].

5.11

p38 MAPKs (Mitogen-Activated Protein Kinases)

The p38 mitogen-activated protein kinase is the mammalian orthologue of the yeast HOG kinase; it plays a crucial role in regulating the production of proinflammatory cytokines. Four isoforms of p38 MAP kinase have been identified (α , β , γ , δ). Inhibiting these kinases would have an important role in treating various inflammatory diseases like rheumatoid arthritis or asthma. Several compounds have been reported to inhibit p38 kinase in nanomolar range: SB202190 [86], SB203580 [87], SB242235 [88], and SB681323 are under phase II investigation; another

GlaxoSmithKline's p38 inhibitor, losmapimod (8565533) is also in clinical phase II for cardiovascular disease (also COPD and depression) [89]. BIRB796/Doramapimod was discontinued after phase II [90], VX702 and VX745 [91]. VX745 was discontinued after phase I clinical trials, VX702 was stopped after phase II studies. The p38 MAP kinase inhibitor, SCIO323, has finished clinical phase II. It is being developed against rheumatoid arthritis, cerebrovascular ischemia, and diabetes mellitus [92]. SCIO469 is another small-molecule p38 MAP kinase inhibitor under clinical phase II development by Scios Inc. as a potential oral therapy for inflammatory disorders [93]. PS540446 is a p38 inhibitor of pharmacopeia and currently in clinical phase I for the treatment of rheumatoid arthritis [94]. TAK715 is a p38 inhibitor of Takeda, which demonstrated significant *in vitro* and *in vivo* activities and was advanced into clinical phase II trials [95]. BMS582949 is currently in phase II against inflammation, atherosclerotic plaque, and RA [96]. Ph797804 is also in phase II for RA [97]. Laufer *et al.* published a novel group of p38 MAP kinase inhibitors [98]. Recently, they have published the second generation of these molecules with enhanced pharmacological properties [99].

Gill *et al.* discovered new p38 α MAP kinase inhibitors by using fragment-based high-throughput X-ray crystallography [100]. This kinase regulates the biosynthesis of cytokines TNF α and IL1 β . Increased production of these cytokines can lead to various inflammatory diseases such as rheumatoid arthritis, Crohn's disease, and inflammatory bowel disease. Therefore, an orally active p38 α MAP kinase inhibitor would be of great therapeutic value. They used their fragment library to identify two molecular fragments as hits by using fragment-based high-throughput X-ray crystallography. These molecules were optimized, using structure-guided chemistry approaches to obtain novel, potent, and selective p38 α MAPK inhibitors. A very interesting study was published recently by GSK's researchers. They studied biphenyl amides (BPAs) that are a series of p38 α MAP kinase inhibitors. Compounds are able to bind to the kinase in either the DFG-in or DFG-out conformation, depending on substituents. DFG-out-binding compounds could be made more potent than DFG-in-binding compounds by increasing their size. Unexpectedly, compounds that bound to the DGF-out conformation showed diminished selectivity. The kinetics of binding to the isolated enzyme and the effects of compounds on cells were largely unaffected by the kinase conformation bound (Figure 5.3) [101].

5.12 ERK1/2

The MAPK pathway controls the growth and survival of a broad spectrum of human tumors. The MAPK pathways are located downstream of many growth factor receptors. There is an important link between the MAPK kinase (MEK)–ERK pathway and cell cycle machinery. Overexpression and activation of this receptor are commonly detected in various cancers, and several lines of evidence indicate that overexpression and activation of ERK play an important part in progression of cancer. The central role of RAF and MEK in transmitting signals through the

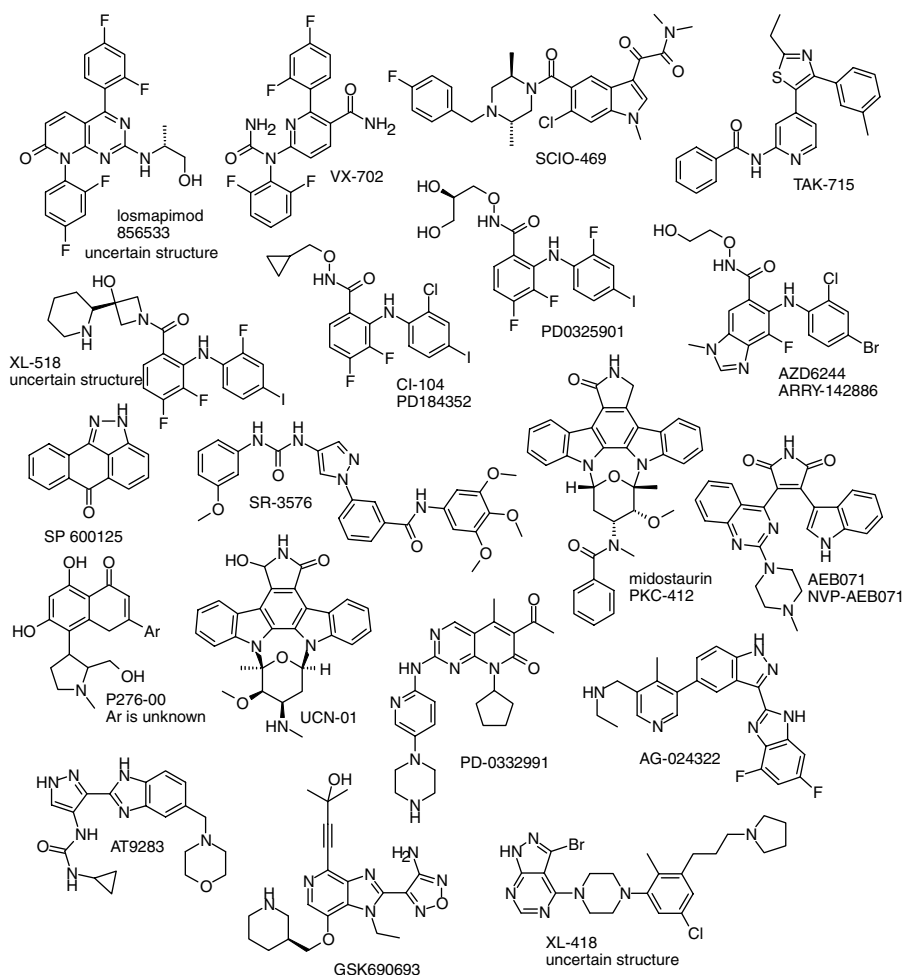


Figure 5.3 Structures of the mentioned kinase inhibitors III.

growth factors-related Ras-MAPK pathway make these kinases promising targets of anticancer drugs [102]. PD166866 [103], PD089828 [104], SR144528 [105], and conivaptan [106] inhibit MAPK in low nanomolar concentration. MEK inhibitors are the first highly selective inhibitors of the MAPK pathway to enter the clinic. Several potent MEK inhibitors have reached clinical development, like GSK1120212 in phase I [107]; ARRY438162, a MEK1/2 inhibitor, in phase II [108]; Ro5126766, a Raf/MEK dual inhibitor, in phase I [109]; RDEA119, a potent MEK inhibitor, in phase I [110], and XL518, a MEK1 inhibitor, in phase I [111]. CI1040 (PD184352) is an orally administered, selective small-molecule inhibitor of MEK. This agent significantly inhibited growth of the colon carcinoma cell lines both *in vitro* and *in vivo* models. In addition to impairing tumor cell proliferation, CI1040 blocked cell motility,

disrupted the cell–cell contact inhibition that is required for invasion, and induced dose-dependent arrest of G1. Importantly, antitumor activity was achieved without evidence of toxicity, and was correlated with a reduction in the levels of activated MAPK in excised tumors. CI1040 halted after phase I evaluation in cancer patients [112]. This agent seems to be well tolerated. PD0325901 is a follow-up project of CI1040 in phase II clinical trial [113]. It has been shown that ARRY142886 (AZD6244), a potent, selective MEK1/2 inhibitor currently in phase II trials, has demonstrated sustained inhibition of ERK1/2 phosphorylation in tumor models [114, 115].

5.13

JNK (c-Jun N-Terminal Kinase, MAPK8)

c-Jun N-terminal kinases (JNKs) are mitogen-activated protein kinases that are responsive to stress stimuli, such as cytokines, ultraviolet irradiation, heat shock, and osmotic shock, and are involved in T cell differentiation and apoptosis. It has been demonstrated that the JNK pathway plays a significant role in regulating the cellular processes that are involved in Parkinson's disease; the inhibition of JNK with SP600125, a specific inhibitor of JNK, is effective in MPTP Parkinson's disease model and in inflammatory bowel disease model [116–118]. Recently, a new family of JNK inhibitors was published. SR3576, an amino-pyrazole, was found to be very potent JNK3 inhibitor ($IC_{50} = 7$ nM) with >2800-fold selectivity over p38 ($p38 IC_{50} > 20$ μ M) and had cell-based potency ~ 1 μ M [119].

5.14

PKC (Protein Kinase C)

PKC is a family of closely related serine and threonine kinases (~ 10 isozymes). Overactivation of some PKC isozymes has been postulated to occur in several disease states, including diabetic complications. Selective inhibition of overactivated PKC isozymes may offer a unique therapeutic approach to disease states such as diabetic retinopathy. LY333531/Ruboxistaurin is a staurosporine derivative in clinical phase III [120–122]. In February 2006, Lilly submitted a New Drug Application for ruboxistaurin, and on August 18, 2006, Lilly received an “approvable” letter from the United States Food and Drug Administration for the same, with a request for an additional clinical trial, which would take 5 years to complete [123]. LY317615/enzastaurin is a PKC β 2 inhibitor with a potent antiangiogenic activity. It is in late-stage investigation (phase III) or poor prognosis in patients with diffuse large B cell lymphoma [124, 125]. Midostaurin/PKC412 is a PKC inhibitor being in clinical phase III for the treatment of leukemia [126, 127]. AEB071 is a specific inhibitor of protein kinase C (staurosporin derivative), which prevents T-lymphocyte activation. It is currently in clinical phase II to prevent islet rejection after kidney transplantation [128].

5.15

CDKs (Cyclin-Dependent Kinases)

Cyclin-dependent kinases (CDKs) play important roles in the regulation of the cell cycle [129]. Irregular activity of CDKs can often be detected in a variety of cancer cells. Several nonselective CDK inhibitors were known at that time, but the authors tried to design selective CDK4 inhibitors in order to cause cell cycle arrest in the G₁ phase, because G₁ arrest was thought to reduce the stress for healthy cells more than in other phases. This way an inhibitor with an enlarged therapeutic window could be developed. Since years, cell cycle kinases, like the cyclin-dependent kinases, have been regarded as attractive cancer targets. Cellular and xenograft models lead to the assumption that inhibition of some cell cycle and transcriptional CDKs might lead to an arrest of proliferating cells and even into apoptosis [130]. As a result, almost every large pharmaceutical company has been looking for ATP-competitors of the CDKs.

UCN01 (7-hydroxy-staurosporine) of Kyowa Hakko Kogyo Co. Ltd. is an anticancer compound that inhibits a couple of kinases such as CDKs, PKC, and checkpoint kinase 1. This compound is still in clinical phase II [131, 132]. Flavopiridol is the first potent inhibitor of cyclin-dependent kinases (cdks) to reach clinical trial. Currently, it is involved in several combination therapies (both phase I and phase II) for treating different kinds of cancers [133, 134]. BMS387032/SNS032 is a novel cyclin-dependent kinase 2 inhibitor, still in phase I clinical trials for anticancer therapy [135]. Seliciclib (CYC202 or R-roscovitine) is a potent, multiple CDK inhibitor (CDK2, CDK7, CDK9). Cyclacel is currently conducting a phase 2b, multicenter, randomized, double-blinded clinical trial to evaluate the efficacy and safety of seliciclib (CYC202) [136]. P276-00 is a potent CDK4/cycD1 (IC₅₀ = 63 nM), CDK1/cycB (IC₅₀ = 79 nM), and CDK9/cycT1 (IC₅₀ = 20 nM) inhibitor [137]. This flavopiridol derivative shows very good results in different tumor models [138, 139]. It is currently in phase II clinical development for cancer, melanoma, and squamous cell carcinoma of head and neck. P1446A-05 is another CDK4 inhibitor of Piramal Life Science that have entered into phase I trials [140]. PD0332991 and AG024322 are potent and selective CDK4/CDK6 kinase inhibitors of Pfizer in phase I clinical trials [141, 142].

5.16

Auroras

Another attractive cell cycle target is represented by the members of the Aurora family of kinases. Aurora kinase family was discovered in 1997 and closely linked to tumor genesis [143]. The Aurora kinases are overexpressed in a wide range of human tumors. Elevated expression of Aurora A has been detected in over 50% of colorectal [144, 145], ovarian [146], and gastric tumors [147] and in 94% of invasive duct adenocarcinomas of the breast [148]. Researchers from Vertex published the three-dimensional atomic structure of Aurora 2 (Aurora B) kinase in 2002 [149], a key scientific advance that enabled the design and optimization of multiple classes of

small-molecule Aurora kinase inhibitors. VX680 was advanced to preclinical development, following evaluation of the compound's activity in tumor cell lines and in animal models of tumor growth. In June 2005, Vertex and Merck initiated a phase I study of VX680 in hematological cancers. VX680 might have activity in these malignancies not only because it inhibits the Aurora kinases but also because Flt3 is an important off-target, which is potently inhibited with VX680 [38, 150]. Its follow-up molecule VX689 (MK5108) is in phase I for recurrent or nonresponsive solid tumors or cancers for which standard therapy does not currently exist [151]. A compound of Nerviano Medical Sciences, PHA739358, that inhibits Aurora A, Aurora B, and Aurora C kinases and causes significant tumor growth delay and regression in various xenograft animal models has been selected for further development and is currently being evaluated in phase II studies for leukemia and prostate cancer [152]. Cocrystallization of one of the compounds of Nerviano with Aurora A has provided useful additional information about the binding mode [153]. AT9283 is an Aurora inhibitor of Astex in phase I/II study for leukemia [154]. MLN8237 is an Aurora A inhibitor. It recently entered into phase II studies for lymphomas, leukemias, and carcinomas (Figure 5.4) [155].

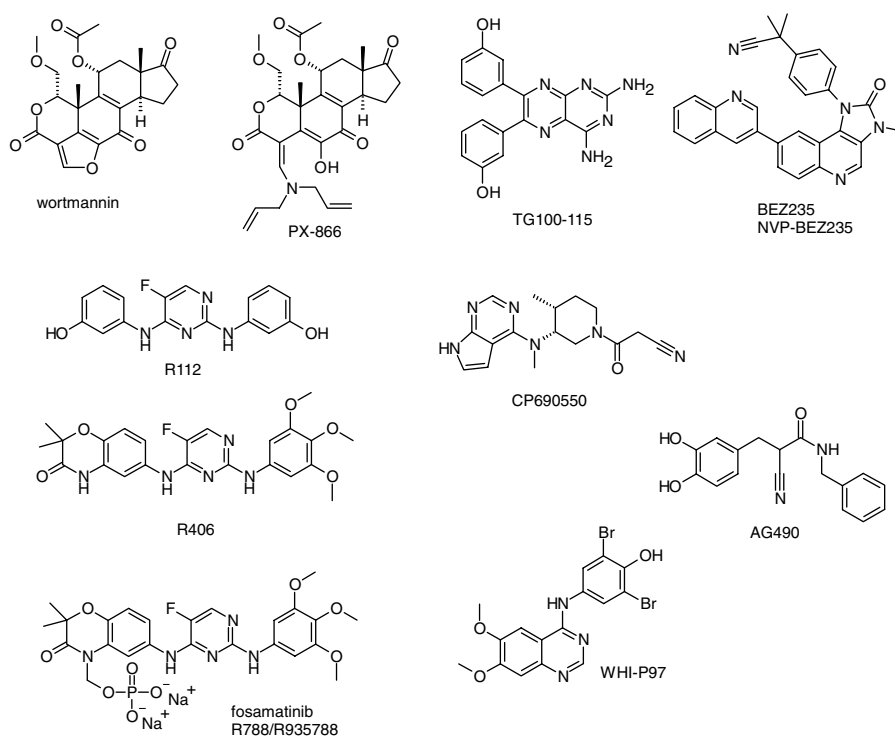


Figure 5.4 Structures of the mentioned kinase inhibitors IV.

5.17

Akt/PKB (Protein Kinase B)

AKT protein family, members of which are also called protein kinases B (PKB), plays an important role in mammalian cellular signaling. Akt (now also called Akt1) was originally identified as the oncogene in the transforming retrovirus, AKT8 [156]. Akt2 is an important signaling molecule in the insulin signaling pathway. It is required to induce glucose transport. The role of Akt3 is less clear, though it appears to be predominantly expressed in brain. Akt regulates cellular survival and metabolism by binding and regulating many downstream effectors, for example, nuclear factor- κ B, Bcl2 family proteins, and murine double minute 2 (MDM2) [157]. Overexpression of PKB can be found in prostate, breast, and ovarian carcinomas [158–160]; therefore, it is an attractive target molecule. Breitenlechner *et al.* designed selective Akt/protein kinase B inhibitors based on the crystal structure of PKA [161]. The authors used PKA as a surrogate kinase for PKB, because these kinases show 47% sequence homology in the catalytic kinase domain. The ATP binding sites of PKA and PKB differ only in three to seven residues (depending on the definitions). Azepine derivatives of the kinase inhibitor (–)-balanol were used as starting point of the design. Based upon the analysis of the crystal structures, the authors managed to develop three nanomolar inhibitors of PKB, which were selective versus PKA. A pan-Akt ATP-competitive inhibitor is GSK690693 (Akt1 IC_{50} = 2 nM, Akt2 IC_{50} = 13 nM, Akt3 IC_{50} = 9 nM). It has recently finished phase I clinical trials [162]. XL418 inhibits Akt and p70S6K kinases. Its phase I study was suspended [163]. Lindsley and coworkers have published the development of two series of potent and selective allosteric Akt kinase inhibitors that display an unprecedented level of selectivity for Akt1, Akt2, or both Akt1/Akt2. An iterative analogue library synthesis approach quickly provided a highly selective Akt1/Akt2 inhibitor that induces apoptosis in tumor cells and inhibits Akt phosphorylation *in vivo* [164].

5.18

Phosphoinositide 3-Kinases

Phosphoinositide 3-kinases (PI3Ks) are a family of related enzymes that are capable of phosphorylating the 3-position hydroxyl group of the inositol ring of phosphatidylinositol (PtdIns). They are also known as phosphatidylinositol 3-kinases. PI3Ks have been linked to an extraordinarily diverse group of cellular functions, including cell growth, proliferation, differentiation, motility, survival, and intracellular trafficking. Due to its multiple role, it is held a very promising target of drug design. Wortmannin is a natural furanosteroid that inhibits PI3Ks (IC_{50} = 5 nM) [165]. Its synthetically modified derivative PX866 is currently in phase I clinical trial [166]. TG100-115 is a selective PI3K γ and PI3K δ inhibitor, which has passed through phase II study [167]. Novartis Oncology is currently developing two novel oral PI3K/mTOR inhibitors, BEZ235 and BGT226. In preclinical studies, both BEZ235 and BGT226 showed high target specificity and demonstrated antiproliferative

activity against tumor cell lines in animal models of cancer [168]. BEZ235 and BGT226 are now being investigated in phase I clinical trials in solid tumors [169]. Two potent inhibitors of Exelixis in phase I clinical trials are XL147 (PI3K) and XL765 (PI3K/mTor) [170]. CAL101 is a specific PI3K δ inhibitor currently under phase I investigation [171]. GSK1059615 is being investigated in phase I [172].

5.19

Syk (Spleen Tyrosine Kinase)

Syk kinase is an important target in inflammation and asthma. Mast cells play important roles in both early- and late-phase allergic reactions. Syk kinase is involved in IgE signaling in mast cells, and it is a transducer of signaling through the Fc ϵ receptor of mast cells. Syk inhibitors could prevent both early- and late-phase allergic reactions blocking mast cell responses to allergic stimuli. Syk tyrosine kinase is commonly expressed by normal breast epithelial cells, that loss of Syk expression is associated with the acquisition of a malignant breast tumor phenotype, and that Syk may directly act as a tumor suppressor, presumably by controlling cell division [173]. Rigel's clinical candidate, an intranasal inhibitor of Syk kinase R112, completed a phase II clinical trial in 2004 [174–176]. In December 2004, Rigel initiated a phase I clinical trial of R406 [177]. Development of these compounds has already been halted. Currently, R788/fostamatinib (R935788) is in the first line of clinical trials (phase II) for RA and B cell lymphoma. This compound is a prodrug that loses its methylphosphonic acid disodium salt function before interfering with Syk kinase [178].

5.20

JAK (Janus Kinase)

JAK is a family of intracellular nonreceptor tyrosine kinases that transduce cytokine-mediated signals via the JAK-STAT pathway. They were initially named “just another kinase” 1 and 2, but were ultimately published as “Janus kinase” [179]. The name is taken from the two-faced Roman god of doorways, Janus, because the JAKs possess two near-identical phosphate-transferring domains. One domain exhibits the kinase activity, while the other negatively regulates the kinase activity of the first. AG490 family of tyrphostines has been shown to be a potent inhibitor of JAK2 and to a lesser extent, JAK3 [180, 181]. WHI-P97 is a JAK3 tyrosine kinase inhibitor of Wayne Hughes Institute against asthma [182]. The novel JAK3 inhibitor CP690550 is a potent immunosuppressive agent, which is in phase II clinical trials by Pfizer [183, 184]. VX509 is a JAK3 inhibitor that will enter into phase II studies in the second part of 2009 [185]. To date, there are five JAK2 inhibitors in clinic: XL019 in phase II [186]; TG101348 in phase I/II [187]; INCB018424 in phase II [188]; SB1518 in phase I/II [189], and lestaurtinib/CEP701, a staurosporin derivative that inhibits JAK2 and Flt3, in phase II [190].

5.21

Kinase Inhibitors in Inflammation and Infectious Diseases

5.21.1

Inflammation

Inflammation is controlled at different levels in a complex manner, the regulation is based on some essential cellular signaling mechanisms in immune cells like macrophages, lymphocytes, and granulocytes. The inflammatory response is characterized by coordinated activation of various signaling pathways that regulate expression of both pro- and anti-inflammatory mediators. These signaling mechanisms include the recognition of extracellular molecular pattern of microbial origin such as bacterial lipopolysaccharide (LPS) by Toll-like receptors and the subsequent synthesis and release of and signaling by proinflammatory master cytokines such as tumor necrosis factor or IL1. Receptor engagement results in recruitment of adapter proteins that possess either Toll-IL1 receptor (TIR) domains in the case of TLRs and IL1R or death domains (DD) in the case of those members of the TNFR family that control cell survival. Once recruited to oligomerized IL receptors, these adaptors engage a variety of signaling proteins. Briefly, the ILR complex signals via MyD88 (myeloid differentiation 88). The recruitment of MyD88 leads to the recruitment of IRAK1 and IRAK4, probably via their death domains. The MyD88 complex is also connected to ubiquitination processes, to NF- κ B inhibitor, and modulator kinases via TAK1 growth factor as well as to upstream kinases for p38 and JNK. The ILR/TLR receptor superfamily was recently reviewed by O'Neil [191]. These molecules, upon receptor engagement, activate several effector pathways, the most important of which include mitogen-activated protein kinases, especially JNK [192] and p38 MAPK [193], as well as I κ B kinases (IKK). The MAPKs lead to direct and indirect phosphorylation and activation of various transcription factors, for example, the IKKs are responsible for activation of NF- κ B transcription factors and have emerged as central regulators of inflammatory and immune responses [194].

MAPKs are a family of serine/threonine kinases that transduce extracellular signals to the nucleus. In mammalian cells, three major groups of MAPK that differ in their substrate specificity have been characterized: ERK, JNK, and p38 MAP kinase. Inhibiting MAPK pathways may not necessarily require direct inhibition of the MAPK themselves since these pathways are involved in processes other than inflammation.

p38 MAPK kinase is a Ser/Thr kinase involved in many processes thought to be important in lower airways' inflammatory responses and tissue remodeling.

The c-Jun NH2-terminal kinases (JNKs) phosphorylate and activate members of the proinflammatory transcription factor activator protein-1 (AP1) transcription factor family and other cellular factors implicated in regulating altered gene expression, cellular survival (apoptosis), differentiation and proliferation in response to cytokines, growth factors and oxidative stress, and cancer genesis.

NF- κ B is a key transcriptional regulator of multiple proinflammatory mediators such as TNF α and interleukins; moreover, it plays a crucial role in the regulation of

cell apoptosis/survival. NF- κ B normally resides in the cytoplasm held in an inactive state by its inhibitor chaperone, I κ B α . Phosphorylation of I κ B α results in ubiquitination and proteolysis of I κ B α , which then releases NF- κ B to promote gene transcription [195].

All these kinases play a crucial role, for example, in osteoclastogenesis in inflammatory conditions such as rheumatoid arthritis [196].

Another key signaling pathway is phosphoinositide 3-kinases (PI3K) that are important enzymes generating lipid second messengers that regulate a number of cellular responses, including cell growth/division, cell apoptosis/survival, and activation [197]. Numerous components of the PI3K pathway play an important role especially in the expression and activation of inflammatory mediators, inflammatory cell recruitment, and immune cell function [198].

Syk is also involved in antigen receptor signaling of B and T lymphocytes and in eosinophil survival in response to IL5 and GM-CSF suggesting that this might be an important potential target for the development of new antiasthma drugs [199].

It is clear that the molecular pathomechanism of inflammation is quite complex, involving, among others, a wide range of kinases; consequently, several point of applications are present to be exploited as therapeutic targets. Inhibitors or antagonists of these molecular targets in clinical trials are most monoclonal antibodies; however, some kinase inhibitors have already reached the clinical stage of development as it was discussed above (p38, JNK, JAK, Syk, and PI3K). Drugs against multiple targets may overcome the many limitations of single targets and achieve a more effective and safer control of the disease. Therefore, a multiple kinase inhibitor will be an adequate treatment for inflammation. Nevertheless, there is no significant advancing in the field of anti-inflammatory kinase inhibitors; thus, a multiple kinase inhibitor against inflammatory diseases is still to be discovered.

5.21.2

Infection

An infection is the detrimental colonization of a host organism by a foreign species. In an infection, the infecting organism seeks to utilize the host's resources to multiply (usually at the expense of the host). The infecting organism, or pathogen, interferes with the normal functioning of the host and can lead to chronic wounds, gangrene, loss of an infected limb, and even death. The host's response to infection is inflammation. A pathogen is usually considered a microscopic organism though the definition is broader, including parasites, bacteria, fungi, viruses, prions, and viroids. Mainly viral and bacterial infections are under investigation in the kinase field.

Pathogens are typically hijacking the host cell signaling machinery to ensure their propagation. Kinase inhibitors directed either against host cell kinases or against viral and bacterial kinases might help to block and prevent disease progression.

Kinases involved in inflammation, described above, are usually engaged in the process of infection. Pathogens use these signals to multiply and/or protect the host cell against the immune system. For example, activated NF- κ B is a critical mechanism by which lymphoma cells infected by Epstein-Barr virus (EBV/HHV4) and

Kaposi sarcoma herpes virus (KSHV/HHV8) are protected from apoptotic stress. A selective NF- κ B inhibitor can prevent, delay the appearance of, reduce the tumor burden of, or slow the growth of EBV- and KSHV-associated lymphoma *in vivo* [200]. *Helicobacter pylori* infection activates mitogen-activated protein kinases and modulates cell proliferation and apoptosis [201]. It was demonstrated that both host cell G-protein activity and casein kinase 2 (CK2) function are critically involved in the budding process of influenza viruses [202]. Balasubramanian and coworkers studied the effects of envelope proteins, E2 of HCV and gp120 of HIV, in model HepG2 cells. Upon costimulation with HCV-E2 and HIV-gp120, they observed a potent proinflammatory response with the induction of IL8. Furthermore, our studies revealed that HCV-E2 and HIV-gp120 act collaboratively to trigger a specific set of downstream signaling pathways that include activation of p38 MAP kinase and the tyrosine phosphatase SHP2 [203]. CDK9 is the catalytic subunit of positive transcription elongation factor b (P-TEFb). CDK9 is the kinase of the TAK complex (Tat-associated kinase complex) and it binds to Tat protein of HIV, suggesting a possible role for CDK9 in AIDS progression. CDK9 complexed with its regulatory partner cyclin T1 serves as a cellular mediator of the transactivation function of the HIV Tat protein. P-TEFb is responsible for the phosphorylation of the carboxyl-terminal domain of RNA Pol II, resulting in stimulation of transcription [204].

Bacterial pathogens also operate by attacking crucial intracellular pathways in their hosts. These pathogens usually target more than one intracellular pathway and often interact at several points in each of these pathways to commandeer them fully.

Shigella flexneri parasitism is shedding light onto a new mechanism of PI3K/Akt activation via PtdIns(5)P production that plays an important role in host cell responses such as survival. The *S. flexneri* effector IpgD is injected into the host cell, where it acts as a phosphoinositide phosphatase specifically transforming PtdIns(4,5)P₂ into PtdIns(5)P. This bacterial intracellular parasitism model revealed a novel mechanism of PI3K/Akt activation through PtdIns(5)P production via a process involving tyrosine phosphorylations. This pathway is likely to play a critical role in direct and transcriptional control of host cell survival that would benefit the bacterium [205].

One of the most severe worldwide bacterial infections is tuberculosis. The success of *Mycobacterium tuberculosis* as a pathogen is caused, in part, by its ability to survive in macrophages and establish long-term, persistent infection in the host during periods of control by the cell-mediated immunity [206]. The mycobacterial serine/threonine protein kinase, PknG, plays a key role in keeping the phagosomes intact within the macrophages. It has been demonstrated that inhibition of PknG leads to the degradation of the mycobacteria by inducing lysosomal–phagosomal fusion [207]. In case of *M. tuberculosis*, two other Ser/Thr protein kinases (PknA and PknB) were also found to be required for mycobacterial growth [208]. Székely *et al.* have proposed a method to develop a PknG/PknB dual target inhibitor that might be a very promising strategy in (a) eradicating mycobacteria from intracellular stores by inhibiting PknG and (b) killing them by targeting an essential function through the inhibition of PknB [209]. Later the authors stepped forward and they have tried to combine the above-mentioned two kinases with another two targets (PknB, PknG,

NAD kinase, and NAD synthetase). Their aim was to identify a common pharmacophore for at least two of these targets. First, a hit-finding library, consisting of ~19 000 small molecules, was virtually screened against these validated target molecules. Subsequently, the hits from the *in silico* screening were tested in enzymatic assay systems. Potent hits were then tested for biological activity in macrophages, infected with mycobacteria. Finally, they identified some promising compounds that inhibit PknG and another target from this group, which, however, require further development [210].

It is clear that inhibition of host cell kinases, probably together with bacterial or viral kinases, can eradicate the pathogens; moreover, it can decrease the host's response to infection: the inflammation. Kinase inhibition as a method of an anti-infection therapy is immature but promisingly prospering field of drug development.

References

- Deininger, M.W., Goldman, J.M., Lydon, N., and Melo, J.V. (1997) The tyrosine kinase inhibitor CGP57148B selectively inhibits the growth of BCR-ABL-positive cells. *Blood*, **90**, 3691–3698.
- Goldman, J.M. (2000) Tyrosine-kinase inhibition in treatment of chronic myeloid leukaemia. *Lancet*, **355**, 1031–1032.
- Dancey, J. and Sausville, E.A. (2003) Issues and progress with protein kinase inhibitors for cancer treatment. *Nature Reviews. Drug Discovery*, **2**, 296–313.
- Kolibaba, K.S. and Druker, B.J. (1997) Protein tyrosine kinases and cancer. *Biochimica et Biophysica Acta*, **1333**, F217–F248.
- Bennasroune, A., Gardin, A., Aunis, D., Cremel, G., and Hubert, P. (2004) Tyrosine kinase receptors as attractive targets of cancer therapy. *Critical Reviews in Oncology/Hematology*, **50**, 23–38.
- Bennasroune, A., Gardin, A. *et al.* (2004) Tyrosine kinase receptor has attractive targets of cancer therapy. *Critical Reviews in Oncology/Hematology*, **50**, 23–38.
- Laird, A.D. and Cherrington, J. (2003) Small molecule tyrosine kinase inhibitors: clinical development of anticancer agents. *Expert Opinion on Investigational Drugs*, **12**, 51–64.
- Manning, G., Whyte, D.B., Martinez, R., Hunter, T., and Sudarsanam, S. (2002) The protein kinase complement of the human genome. *Science*, **298**, 1912–1934.
- Kyriakis, J.M. and Avruch, J. (1990) pp54 Microtubule-associated protein-2 kinase: a novel serine threonine protein-kinase regulated by phosphorylation and stimulated by poly-L-lysine. *The Journal of Biological Chemistry*, **265**, 17355–17363.
- Kyriakis, J.M., Banerjee, P., Nikolakiki, T. *et al.* (1994) The stress-activated protein kinase subfamily of c-Jun kinases. *Nature*, **369**, 156–160.
- Dempke, W.C.M. and Heinemann, V. (2009) Resistance to EGF-R (erbB-1) and VEGF-R modulating agents. *European Journal of Cancer (Oxford, England: 1990)*, **45** (7), 1117–1128.
- O'Donnell, A., Padhani, A. *et al.* (2005) A phase I study of the angiogenesis inhibitor SU5416 (sunitinib) in solid tumours, incorporating dynamic contrast MR pharmacodynamic end points. *British Journal of Cancer*, **93** (8), 876–883.
- Wiedmann, M.W. and Caca, K. (2005) Molecularly targeted therapy for gastrointestinal cancer. *Current Cancer Drug Targets*, **5**, 171–193.
- Los, M., Roodhart, J.M. *et al.* (2007) Target practice: lessons from phase III trials with bevacizumab and vatalanib in the treatment of advanced colorectal cancer. *The Oncologist*, **12** (4), 443–450.
- Laird, A.D., Vajkoczy, P., Shawver, L.K. *et al.* (2000) SU6668 is a potent

- antiangiogenic and antitumor agent that induces regression of established tumors. *Cancer Research*, **60**, 4152–4162.
- 16 Godl, K., Gruss, O.J., Eickhoff, J., Órfi, L., Kéri, G., Ullrich, A. *et al.* (2005) Proteomic characterization of the angiogenesis inhibitor SU6668 reveals multiple impacts on cellular kinase signaling. *Cancer Research*, **65**, 6919–6926.
 - 17 Beebe, J.S., Jani, J.P., and Knauth, E. (2003) Pharmacological characterization of CP-547,632, a novel vascular endothelial growth factor receptor-2 tyrosine kinase inhibitor for cancer therapy. *Cancer Research*, **63**, 7301–7309.
 - 18 Wilmes, L.J., Pallavicini, M.G. *et al.* (2007) AG-013736, a novel inhibitor of VEGF receptor tyrosine kinases, inhibits breast cancer growth and decreases vascular permeability as detected by dynamic contrast-enhanced magnetic resonance imaging. *Magnetic Resonance Imaging*, **25** (3), 319–327.
 - 19 Wedge, S.R., Kendrew, J., Hennequin, L.F. *et al.* (2005) AZD2171: a highly potent, orally bioavailable, vascular endothelial growth factor receptor-2 tyrosine kinase inhibitor for the treatment of cancer. *Cancer Research*, **65**, 4389–4400.
 - 20 Holden, S.N., Eckhardt, S.G., Bassar, R. *et al.* (2005) Clinical evaluation of ZD6474, an orally active inhibitor of VEGF and EGF receptor signaling, in patients with solid, malignant tumors. *Annals of Oncology*, **16**, 1391–1397.
 - 21 Wedge, S.R., Ogilvie, D.J., Dukes, M. *et al.* (2002) ZD6474 inhibits vascular endothelial growth factor signaling, angiogenesis, and tumor growth following oral administration. *Cancer Research*, **62**, 4645–4655.
 - 22 Zareba, G., Castaner, J., and Bozzo, J. (2005) Vandetanib. *Drugs Future*, **30**, 138–146.
 - 23 National Cancer Institute, U.S. National Institutes of Health. www.cancer.gov. (2 March 2009).
 - 24 www.aveopharma.com and www.clinicaltrials.gov. (2 March 2009).
 - 25 www.cyclacel.com and www.clinicaltrials.gov. (2 March 2009).
 - 26 Bean, J., Brennan, C. *et al.* (2007) MET amplification occurs with or without T790M mutations in EGFR mutant lung tumors with acquired resistance to gefitinib or erlotinib. *Proceedings of the National Academy of Sciences of the United States of America*, **104** (52), 20932–20937; also available at www.clinicaltrials.gov.
 - 27 Smith, B.D., Levis, M., and Beran, M. (2004) Single-agent CEP-701, a novel FLT3 inhibitor, shows biologic and clinical activity in patients with relapsed or refractory acute myeloid leukemia. *Blood*, **103**, 3669–3676.
 - 28 Knapper, S., Burnett, A.K. *et al.* (2006) A phase 2 trial of the FLT3 inhibitor lestaurtinib (CEP701) as first-line treatment for older patients with acute myeloid leukemia not considered fit for intensive chemotherapy. *Blood*, **108** (10), 3262–3270.
 - 29 Hexner, E.O., Serdikoff, C. *et al.* (2008) Lestaurtinib (CEP701) is a JAK2 inhibitor that suppresses JAK2/STAT5 signaling and the proliferation of primary erythroid cells from patients with myeloproliferative disorders. *Blood*, **111** (12), 5663–5671.
 - 30 Walters, D.K., Stoffregen, E.P., and Heinrich, M.C. (2005) RNAi-induced down-regulation of FLT3 expression in AML cell lines increases sensitivity to MLN518. *Blood*, **105**, 2952–2954.
 - 31 Sarker, D., Evans, J., Judson, I. *et al.* (2005) CHIR-258: first-in-human phase 1 dose escalating trial of an oral, selectively targeted tyrosine kinase inhibitor in patients with solid tumors. *Journal of Clinical Oncology*, **23**, 3044.
 - 32 Nishiyama, U., Yoshino, T. *et al.* (2006) Antineoplastic effect of a single oral dose of the novel Flt3 inhibitor KRN383 on xenografted human leukemic cells harboring Flt3-activating mutations. *Leukemia Research*, **30**, 1541–1546.
 - 33 Zeng, Z., Samudio, I.J. *et al.* (2006) Simultaneous inhibition of PDK1/AKT and Fms-like tyrosine kinase 3 signaling by a small-molecule KP372-1 induces mitochondrial dysfunction and apoptosis in acute myelogenous leukemia. *Cancer Research*, **66** (7), 3737–3746.

- 34 Mandal, M., Kim, S. *et al.* (2005) The Akt inhibitor KP372-1 suppresses Akt activity and cell proliferation and induces apoptosis in thyroid cancer cells. *British Journal of Cancer*, **92**, 1899–1905.
- 35 Daub, H., Specht, K., and Ullrich, A. (2004) Strategies to overcome resistance to targeted protein kinase inhibitors. *Nature Reviews. Drug Discovery*, **3**, 1001–1010.
- 36 Shah, N.P., Tran, C., Lee, F.Y. *et al.* (2005) BMS-354825: a novel drug with potential for the treatment of imatinib-resistant chronic myeloid leukaemia. *Expert Opinion on Investigational Drugs*, **14**, 89–91.
- 37 Weisberg, E., Manley, P. *et al.* (2006) AMN107 (nilotinib): a novel and selective inhibitor of BCR-ABL. *British Journal of Cancer*, **94** (12), 1765–1769.
- 38 Carter, T.A., Wodicka, L.M., Shah, N.P. *et al.* (2005) Inhibition of drug-resistant mutants of ABL, KIT, and EGF receptor kinases. *Proceedings of the National Academy of Sciences of the United States of America*, **102**, 11011–11016.
- 39 Wood, E.R., Truesdale, A.T., McDonald, O.B. *et al.* (2004) A unique structure for the epidermal growth factor receptor bound to GW572016 (lapatinib): relationships among protein conformation, inhibitor off-rate, and receptor activity in tumor cells. *Cancer Research*, **64**, 6652–6659.
- 40 Baselga, J. and Hammond, L.A. (2002) HER-targeted tyrosine-kinase inhibitors. *Oncology*, **63** (Suppl. 1), 6–16.
- 41 Wissner, A., Floyd, M.B., Rabindran, S.K. *et al.* (2002) Syntheses and EGFR and HER-2 kinase inhibitory activities of 4-anilinoquinoline-3-carbonitriles: analogues of three important 4-anilinoquinazolines currently undergoing clinical evaluation as therapeutic antitumor agents. *Bioorganic & Medicinal Chemistry Letters*, **12**, 2893–2897.
- 42 Valabrega, G., Montemurro, F. *et al.* (2007) Trastuzumab: mechanism of action, resistance and future perspectives in HER2-overexpressing breast cancer. *Annals of Oncology*, **18**, 977–984.
- 43 Pao, W., Miller, V.A., Politi, K.A. *et al.* (2005) Acquired resistance of lung adenocarcinomas to gefitinib or erlotinib is associated with a second mutation in the EGFR kinase domain. *PLoS Medicine*, **2**, 225–235.
- 44 Özvegy-Latczka, C., Hegedűs, T., Várady, G., Kéri, G., Órfi, L., Sarkadi, B. *et al.* (2004) High-affinity interaction of tyrosine kinase inhibitors with the ABCG2 multidrug transporter. *Molecular Pharmacology*, **65**, 1485–1495.
- 45 Elkind, N.B., Szentpétery, Z., Apáti, Á., Özvegy-Latczka, C., Kéri, G., Sarkadi, B. *et al.* (2005) Multidrug transporter ABCG2 prevents tumor cell death induced by the epidermal growth factor receptor inhibitor Iressa (ZD1839, Gefitinib). *Cancer Research*, **65**, 1770–1777.
- 46 Kaneta, Y., Kagami, Y., Katagiri, T. *et al.* (2002) Prediction of sensitivity to STI571 among chronic myeloid leukemia patients by genome-wide cDNA microarray analysis. *Japanese Journal of Cancer Research: Gann*, **93**, 849–856.
- 47 Kakiuchi, S., Daigo, Y., Ishikawa, N. *et al.* (2004) Prediction of sensitivity of advanced non-small cell lung cancers to gefitinib (Iressa, ZD1839). *Human Molecular Genetics*, **13**, 3029–3043.
- 48 Minami, Y., Shimamura, T. *et al.* (2007) The major lung cancer-derived mutants of ERBB2 are oncogenic and are associated with sensitivity to the irreversible EGFR/ERBB2 inhibitor HKI-272. *Oncogene*, **26** (34), 5023–5027.
- 49 Traxler, P., Bold, G., Buchdunger, E. *et al.* (2001) Tyrosine kinase inhibitors: from rational design to clinical trials. *Medicinal Research Reviews*, **21**, 499–512.
- 50 Hoekstra, R., Dumez, H. *et al.* (2005) Phase I and pharmacologic study of PKI166, an epidermal growth factor receptor tyrosine kinase inhibitor, in patients with advanced solid malignancies. *Clinical Cancer Research*, **11**, 6908–6915.
- 51 Onn, A., Isobe, T. *et al.* (2004) Epidermal growth factor receptor tyrosine kinase inhibitor does not improve paclitaxel effect in an orthotopic mouse model of

- lung cancer. *Clinical Cancer Research*, **10**, 8613–8619.
- 52 Garland, L.L., Pegram, M., and Song, S. (2005) Phase I study of BMS-599626, an oral pan-HER tyrosine kinase inhibitor, in patients with advanced solid tumors. *Journal of Clinical Oncology*, **23**, 3152.
 - 53 <http://www.invitrogen.com/content.cfm?pageid=10561> (accessed August 24, 2005).
 - 54 Traxler, P., Allegrini, P.R., Brandt, R. *et al.* (2004) AEE788: a dual family epidermal growth factor receptor/ErbB2 and vascular endothelial growth factor receptor tyrosine kinase inhibitor with antitumor and antiangiogenic activity. *Cancer Research*, **64**, 4931–4941.
 - 55 Blum, G., Gazit, A., and Levitzki, A. (2003) Development of new insulin-like growth factor-1 receptor kinase inhibitors using catechol mimics. *The Journal of Biological Chemistry*, **278**, 40442–40454.
 - 56 Li, W.Q., Favellyukis, S., Yang, J. *et al.* (2004) Inhibition of insulin-like growth factor I receptor autophosphorylation by novel 6-5 ring-fused compounds. *Biochemical Pharmacology*, **68**, 145–154.
 - 57 Scotlandi, K., Manara, M.C., Nicoletti, G. *et al.* (2005) Antitumor activity of the insulin-like growth factor-I receptor kinase inhibitor NVP-AEW541 in musculoskeletal tumors. *Cancer Research*, **65**, 3868–3876.
 - 58 Moser, C., Schachtschneider, P. *et al.* (2008) Inhibition of insulin-like growth factor-I receptor (IGF-IR) using NVP-AEW541, a small molecule kinase inhibitor, reduces orthotopic pancreatic cancer growth and angiogenesis. *European Journal of Cancer*, **44**, 1577–1586.
 - 59 Huang, F., Greer, A. *et al.* (2009) The mechanisms of differential sensitivity to an insulin-like growth factor-1 receptor inhibitor (BMS-536924) and rationale for combining with EGFR/HER2 inhibitors. *Cancer Research*, **69**, 161–170.
 - 60 Adnane, J., Gaudray, P., Dionne, C.A. *et al.* (1991) BEK and FLG, 2 receptors to members of the FGF family, are amplified in subsets of human breast cancers. *Oncogene*, **6**, 659–663.
 - 61 Leung, H.Y., Gullick, W.J., and Lemoine, N.R. (1994) Expression and functional-activity of fibroblast growth factors and their receptors in human pancreatic-cancer. *International Journal of Cancer*, **59**, 667–675.
 - 62 Yamaguchi, F., Saya, H., Bruner, J.M., and Morrison, R.S. (1994) Differential expression of 2 fibroblast growth factor-receptor genes is associated with malignant progression in human astrocytomas. *Proceedings of the National Academy of Sciences of the United States of America*, **91**, 484–488.
 - 63 Myoken, Y., Myoken, Y., Okamoto, T. *et al.* (1996) Expression of fibroblast growth factor-1 (FGF-1), FGF-2 and FGF receptor-1 in a human salivary-gland adenocarcinoma cell line: evidence of autocrine growth. *International Journal of Cancer*, **65**, 650–657.
 - 64 Li, J.J., Huang, Y.Q., Moscatelli, D. *et al.* (1993) Expression of fibroblast growth-factors and their receptors in acquired-immunodeficiency-syndrome associated kaposi-sarcoma tissue and derived cells. *Cancer*, **72**, 2253–2259.
 - 65 Theillet, C., Adelaide, J., Louason, G. *et al.* (1993) FGFR1 and plat genes and DNA amplification at 8P12 in breast and ovarian cancers. *Genes, Chromosomes & Cancer*, **7**, 219–226.
 - 66 Story, M.T. (1995) Regulation of prostate growth by fibroblast growth-factors. *World Journal of Urology*, **13**, 297–305.
 - 67 Mohammadi, M., McMahon, G., Sun, L. *et al.* (1997) Structures of the tyrosine kinase domain of fibroblast growth factor receptor in complex with inhibitors. *Science*, **276**, 955–960.
 - 68 Hyun, K.H., Kwack, I.Y., Lee, D.Y., Park, H.Y., Lee, B.S., and Kim, C.K. (2004) Ligand-based QSAR studies on the indolinones derivatives as inhibitors of the protein tyrosine kinase of fibroblast growth factor receptor by CoMFA and CoMSIA. *Bulletin of the Korean Chemical Society*, **25**, 1801–1806.
 - 69 Sakurai, K., Yamada, Y. *et al.* (2007) A novel angiogenesis inhibitor, Ki23057, is useful for preventing the progression of colon cancer and the spreading of cancer

- cells to the liver. *European Journal of Cancer*, **43**, 2612–2620.
- 70 Sherman, S.I., Wirth, L.J. *et al.* (2008) Motesanib diphosphate in progressive differentiated thyroid cancer. *The New England Journal of Medicine*, **359**, 2727.
 - 71 Edling, C.E. and Hallberg, B. (2007) c-Kit-a hematopoietic cell essential receptor tyrosine kinase. *The International Journal of Biochemistry & Cell Biology*, **39** (11), 1995–1998.
 - 72 Miettinen, M. and Lasota, J. (2005) KIT (CD117): a review on expression in normal and neoplastic tissues, and mutations and their clinicopathologic correlation. *Applied Immunohistochemistry & Molecular Morphology*, **13** (3), 205–220.
 - 73 Chen, N., Bürli, R.W. *et al.* (2008) Discovery of a potent and selective c-Kit inhibitor for the treatment of inflammatory diseases. *Bioorganic & Medicinal Chemistry Letters*, **18**, 4137–4141.
 - 74 Gentile, A., Trusolino, L. *et al.* (2008) The Met tyrosine kinase receptor in development and cancer. *Cancer Metastasis Reviews*, **27** (1), 85–94.
 - 75 Stelrecht, C.M. and Gandhi, V. (2008) MET receptor tyrosine kinase as a therapeutic anticancer target. *Cancer Letters*, **280** (1), 1–14.
 - 76 Chattopadhyay, C., El-Naggar, A.K. *et al.* (2008) Small molecule c-MET inhibitor PHA665752: effect on cell growth and motility in papillary thyroid carcinoma. *Head & Neck*, **30** (8), 991–1000.
 - 77 Koon, E.C., Ma, P.C. *et al.* (2008) Effect of a c-Met-specific ATP-competitive small-molecule inhibitor SU11274 on human ovarian carcinoma cell growth motility and invasion. *International Journal of Gynecological Cancer*, **18**, 976–984.
 - 78 Wang, X., Le, P. *et al.* (2003) Potent and selective inhibitors of the Met [hepatocyte growth factor/scatter factor (HGF/SF) receptor] tyrosine kinase block HGF/SF-induced tumor cell growth and invasion. *Molecular Cancer Therapeutics*, **2**, 1085–1092.
 - 79 Yap, T.A., Harris, D. *et al.* (2008) Phase I trial to determine the dose range for the c-Met inhibitor ARQ 197 that inhibits c-Met and FAK phosphorylation, when administered by an oral twice-a-day schedule. *Journal of Clinical Oncology*, **26**, 3584.
 - 80 Salgia, R., Sherman, S. *et al.* (2008) A phase I study of XL184, a RET, VEGFR2, and MET kinase inhibitor, in patients (pts) with advanced malignancies, including pts with medullary thyroid cancer (MTC). *Journal of Clinical Oncology*, **26**, 3522.
 - 81 Blake, R.A., Broome, M.A. *et al.* (2000) SU6656, a selective Src family kinase inhibitor, used to probe growth factor signaling. *Molecular and Cellular Biology*, **20** (23), 9018–9027.
 - 82 Recchia, I., Ruccia, N. *et al.* (2003) Pyrrolopyrimidine c-Src inhibitors reduce growth, adhesion, motility and invasion of prostate cancer cells *in vitro*. *European Journal of Cancer*, **39**, 1927–1935.
 - 83 Vultur, A., Buettner, R. *et al.* (2008) SKI-606 (bosutinib), a novel Src kinase inhibitor, suppresses migration and invasion of human breast cancer cells. *Molecular Cancer Therapeutics*, **7** (5), 1185–1194.
 - 84 www.veyth.com and www.clinicaltrials.gov. (2 March 2009).
 - 85 Lockton, J.A., Smethurst, D., Macpherson, M. *et al.* (2005) Phase I ascending single and multiple dose studies to assess the safety, tolerability and pharmacokinetics of AZD0530, a highly selective, dual-specific Src-Abl inhibitor. *Journal of Clinical Oncology*, **23**, 223S.
 - 86 Gallagher, T.F., Fierthompson, S.M., Garigipati, R.S. *et al.* (1995) 2, 4, 5-Triarylimidazole inhibitors of Il-1 biosynthesis. *Bioorganic & Medicinal Chemistry Letters*, **5**, 1171–1176.
 - 87 Regan, J., Breitfelder, S., Cirillo, P. *et al.* (2002) Pyrazole urea-based inhibitors of p38 MAP kinase: from lead compound to clinical candidate. *Journal of Medicinal Chemistry*, **45**, 2994–3008.
 - 88 Adams, J.L., Boehm, J.C., Gallagher, T.F. *et al.* (2001) Pyrimidinylimidazole inhibitors of p38: cyclic N-1 imidazole substituents enhance p38 kinase inhibition and oral activity. *Bioorganic &*

- Medicinal Chemistry Letters*, **11**, 2867–2870.
- 89 http://science.gsk.com/pipeline/product_pipeline_netscape.htm (accessed August 24, 2005).
 - 90 Pargellis, C., Tong, L., Churchill, L. *et al.* (2002) Inhibition of p38 MAP kinase by utilizing a novel allosteric binding site. *Nature Structural Biology*, **9**, 268–272.
 - 91 Haddad, J.J. (2001) VX-745 (Vertex Pharmaceuticals). *Current Opinion in Investigational Drugs*, **2**, 1070–1076.
 - 92 Dominguez, C., Powers, D.A., and Tamayo, N. (2005) p38 MAP kinase inhibitors: many are made, but few are chosen. *Current Opinion in Drug Discovery & Development*, **8**, 421–430.
 - 93 Laufer, S. and Lehmann, F. (2009) Investigations of SCIO-469-like compounds for the inhibition of p38 MAP kinase. *Bioorganic & Medicinal Chemistry Letters*, **19** (5), 1461–1464.
 - 94 <http://www.pharmacopeia.com/wt/page/pipeline> (accessed August 24, 2005).
 - 95 Miwatashi, S., Arikawa, Y., Kotani, E. *et al.* (2005) Novel inhibitor of p38 MAP kinase as an anti-TNF- α drug: discovery of *N*-[4-[2-ethyl-4-(3-methylphenyl)-1,3-thiazol-5-yl]-2-pyridyl]benzamide (TAK-715) as a potent and orally active anti-rheumatoid arthritis agent. *Journal of Medicinal Chemistry*, **48**, 5966–5979.
 - 96 www.bms.com and www.clinicaltrials.gov. (2 March 2009).
 - 97 www.bms.com and www.clinicaltrials.gov. (2 March 2009).
 - 98 Laufer, S.A., Ahrens, G.M. *et al.* (2006) Design, synthesis, and biological evaluation of phenylamino-substituted 6,11-dihydro-dibenzo[*b,e*]oxepin-11-ones and dibenzo[*a,d*]cycloheptan-5-ones: novel p38 MAP kinase inhibitors. *Journal of Medicinal Chemistry*, **49** (26), 7912–7915.
 - 99 Karcher, S.C. and Laufer, S.A. (2009) Aza-analogue dibenzepinone scaffolds as p38 mitogen-activated protein kinase inhibitors: design, synthesis, and biological data of inhibitors with improved physicochemical properties. *Journal of Medicinal Chemistry*, **52** (6), 1778–1782.
 - 100 Gill, A., Cleasby, A., and Jhoti, H. (2005) The discovery of novel protein kinase inhibitors by using fragment-based high-throughput X-ray crystallography. *Chembiochem: a European Journal of Chemical Biology*, **6**, 506–512.
 - 101 Angell, R.M., Angell, T.D. *et al.* (2008) Biphenyl amide p38 kinase inhibitors 4: DFG-in and DFG-out binding modes. *Bioorganic & Medicinal Chemistry Letters*, **18**, 4433–4437.
 - 102 Fang, J. and Richardson, B. (2005) The MAPK signalling pathways and colorectal cancer. *The Lancet Oncology*, **6**, 322–327.
 - 103 Panek, R.L., Lu, G.H., Dahringer, T.K. *et al.* (1998) *In vitro* biological characterization and antiangiogenic effects of PD 166866, a selective inhibitor of the FGF-1 receptor tyrosine kinase. *The Journal of Pharmacology and Experimental Therapeutics*, **286**, 569–577.
 - 104 Panek, R.L., Lu, G.H., Klutcho, S.R. *et al.* (1997) *In vitro* pharmacological characterization of PD 166285, a new nanomolar potent and broadly active protein tyrosine kinase inhibitor. *The Journal of Pharmacology and Experimental Therapeutics*, **283**, 1433–1444.
 - 105 Rinaldi-Carmona, M., Barth, F., Millan, J. *et al.* (1998) SR 144528, the first potent and selective antagonist of the CB2 cannabinoid receptor. *The Journal of Pharmacology and Experimental Therapeutics*, **284**, 644–650.
 - 106 Tahara, A., Tomura, Y., Wada, K. *et al.* (1998) Effect of YM087, a potent nonpeptide vasopressin antagonist, on vasopressin-induced protein synthesis in neonatal rat cardiomyocyte. *Cardiovascular Research*, **38**, 198–205.
 - 107 www.gsk.com and www.clinicaltrials.gov. (2 March 2009).
 - 108 Engelman, J.A., Chen, L. *et al.* (2008) Effective use of PI3K and MEK inhibitors to treat mutant Kras G12D and PIK3CA H1047R murine lung cancers. *Nature Medicine*, **14** (12), 1351–1356; also available at www.clinicaltrials.gov.
 - 109 www.roch.com and www.clinicaltrials.gov. (2 March 2009).
 - 110 www.ardeabiosciences.com and www.clinicaltrial.gov. (2 March 2009).

- 111 Johnston, S. *et al.* (2007) XL518, a potent, selective orally bioavailable MEK1 inhibitor, down-regulates the Ras/Raf/MEK/ERK pathway *in vivo*, resulting in tumor growth inhibition and regression in preclinical models. 19th AACR-NCI-EORTC International Conference on Molecular Targets and Cancer Therapeutics, San Francisco, CA, October 22–26, 2007, Abstract C209. Also available at www.exelixis.com; www.clinicaltrials.gov.
- 112 Allen, L.F., Sebolt-Leopold, J., and Meyer, M.B. (2003) CI-1040 (PD184352), a targeted signal transduction inhibitor of MEK (MAPKK). *Seminars in Oncology*, **30**, 105–116.
- 113 Brown, A.P., Carlson, T.C. *et al.* (2007) Pharmacodynamic and toxicokinetic evaluation of the novel MEK inhibitor, PD0325901, in the rat following oral and intravenous administration. *Cancer Chemotherapy and Pharmacology*, **59** (5), 671–679.
- 114 Doyle, M.P., Yeh, T.C., Suzy, B. *et al.* (2005) Validation and use of a biomarker for clinical development of the MEK1/2 inhibitor ARRY-142886 (AZD6244). *Journal of Clinical Oncology*, **23**, 210S.
- 115 Wickenden, J.A., Jin, H. *et al.* (2008) Colorectal cancer cells with the BRAF (V600E) mutation are addicted to the ERK1/2 pathway for growth factor-independent survival and repression of BIM. *Oncogene*, **27** (57), 7150–7161.
- 116 Scapin, G., Patel, S.B., Lisnock, J., Becker, J.W., and LoGrasso, P.V. (2003) The structure of JNK3 in complex with small molecule inhibitors: structural basis for potency and selectivity. *Chemistry & Biology*, **10**, 705–712.
- 117 Wang, W., Ma, C., Mao, Z., and Li, M. (2004) JNK inhibition as a potential strategy in treating Parkinson's disease. *Drug News and Perspectives*, **17**, 646–654.
- 118 Assi, K., Pillai, R. *et al.* (2006) The specific JNK inhibitor SP600125 targets tumour necrosis factor- α production and epithelial cell apoptosis in acute murine colitis. *Immunology*, **118** (1), 112–121.
- 119 Kamenecka, T., Habel, J. *et al.* (2009) Structure–activity relationships and X-ray structures describing the selectivity of amino-pyrazole inhibitors for c-Jun-N-terminal kinase 3 (JNK3) over p38. *The Journal of Biological Chemistry*, **284** (19), 12853–12861.
- 120 Jirousek, M.R., Gillig, J.R., Gonzalez, C.M. *et al.* (1996) (S)-13-[(dimethylamino)methyl]-10,11,14,15-tetrahydro-4,9:16,21-dimetheno-1H,13H-dibenzo[*e,k*]pyrrolo[3,4-*h*][1,4,13]oxadiazacyclohexadecene-1,3(2H)-dione (LY333531) and related analogues: isozyme selective inhibitors of protein kinase C β . *Journal of Medicinal Chemistry*, **39**, 2664–2671.
- 121 Wheeler, G.D. (2003) Ruboxistaurin (Eli Lilly). *IDrugs*, **6**, 159–163.
- 122 Ziegler, D. (2004) Polyneuropathy in the diabetic patient: update on pathogenesis and management. *Nephrology, Dialysis, Transplantation*, **19**, 2170–2175.
- 123 www.lilly.com and www.drugs.com. (2 March 2009).
- 124 Fine, H.A., Kim, L., and Royce, C. (2005) Results from phase II trial of enzastaurin (LY317615) in patients with recurrent high grade gliomas. *Journal of Clinical Oncology*, **23**, 1504.
- 125 Mina, L., Krop, I. *et al.* (2009) A phase II study of oral enzastaurin in patients with metastatic breast cancer previously treated with an anthracycline and a taxane containing regimen. *Investigational New Drugs*, **27** (6), 565–570.
- 126 Force, T., Kuida, K., and Namchuk, M. (2004) Inhibitors of protein kinase signaling pathways. *Circulation*, **109**, 1196–1205.
- 127 Wang, Y., Yin, O.Q. *et al.* (2008) Dose- and time-dependent pharmacokinetics of midostaurin in patients with diabetes mellitus. *Journal of Clinical Pharmacology*, **48** (6), 763–775.
- 128 Merani, S., Pawlick, R.L. *et al.* (2009) Protein kinase C inhibitor, AEB-071, acts complementarily with cyclosporine to prevent islet rejection in rats. *Transplantation*, **87** (1), 59–65.
- 129 Pines, J. (1993) Cyclins and cyclin dependent kinases: take your partners. *Trends in Biochemical Sciences*, **18**, 195–197.
- 130 Hirai, H., Kawanishi, N., and Iwasawa, Y. (2005) Recent advances in the

- development of selective small molecule inhibitors for cyclin-dependent kinases. *Current Topics in Medicinal Chemistry*, **5**, 167–179.
- 131 Syljuasen, R.G., Sorensen, C.S., Hansen, L.T. *et al.* (2005) Inhibition of human Chk1 causes increased initiation of DNA replication, phosphorylation of ATR targets, and DNA breakage. *Molecular and Cellular Biology*, **25**, 3553–3562.
 - 132 Levesque, A.A., Kohn, E.A., Bresnick, E., and Eastman, A. (2005) Distinct roles for p53 transactivation and repression in preventing UCN-01-mediated abrogation of DNA damage-induced arrest at S and G2 cell cycle checkpoints. *Oncogene*, **24**, 3786–3796.
 - 133 Shapiro, G.I. (2004) Preclinical and clinical development of the cyclin-dependent kinase inhibitor flavopiridol. *Clinical Cancer Research*, **10**, 4270s–4275s.
 - 134 Christian, B.A., Grever, M.R. *et al.* (2007) Flavopiridol in the treatment of chronic lymphocytic leukemia. *Current Opinion in Oncology*, **19** (6), 573–578.
 - 135 Kamath, A.V., Chong, S., Chang, M., and Marathe, P.H. (2005) P-glycoprotein plays a role in the oral absorption of BMS-387032, a potent cyclin-dependent kinase 2 inhibitor, in rats. *Cancer Chemotherapy and Pharmacology*, **55**, 110–116.
 - 136 Raje, N., Kumar, S., Hideshima, T. *et al.* (2005) Seliciclib (CYC202 or R-roscovitine), a small-molecule cyclin-dependent kinase inhibitor, mediates activity via down-regulation of Mcl-1 in multiple myeloma. *Blood*, **106**, 1042–1047.
 - 137 Joshi, K.S., Rathos, M.J. *et al.* (2007) *In vitro* antitumor properties of a novel cyclin-dependent kinase inhibitor, P276-00. *Molecular Cancer Therapeutics*, **6** (3), 918–925.
 - 138 Joshi, K.S., Rathos, M.J. *et al.* (2007) P276-00, a novel cyclin-dependent inhibitor induces G1–G2 arrest, shows antitumor activity on cisplatin-resistant cells and significant *in vivo* efficacy in tumor models. *Molecular Cancer Therapeutics*, **6** (3), 926–934.
 - 139 Raje, N., Hideshima, T. *et al.* (2009) Preclinical activity of P276-00, a novel small-molecule cyclin-dependent kinase inhibitor in the therapy of multiple myeloma. *Leukemia*, **23** (5), 961–970.
 - 140 www.piramallifesciences.com and www.clinicaltrials.gov. (2 March 2009).
 - 141 Fry1, D.W., Harvey, P.J. *et al.* (2004) Specific inhibition of cyclin-dependent kinase 4/6 by PD 0332991 and associated antitumor activity in human tumor xenografts. *Molecular Cancer Therapeutics*, **3**, 1427–1438.
 - 142 Brown, A.P., Courtney, C.L. *et al.* (2008) Toxicity and toxicokinetics of the cyclin-dependent kinase inhibitor AG-024322 in cynomolgus monkeys following intravenous infusion. *Cancer Chemotherapy and Pharmacology*, **62**, 1091–1101.
 - 143 Andrews, P.D. (2005) Aurora kinases: shining lights on the therapeutic horizon? *Oncogene*, **24**, 5005–5015.
 - 144 Bischoff, J.R., Anderson, L., Zhu, Y.F. *et al.* (1998) A homologue of *Drosophila* Aurora kinase is oncogenic and amplified in human colorectal cancers. *The EMBO Journal*, **17**, 3052–3065.
 - 145 Takahashi, T., Futamura, M., Yoshimi, N. *et al.* (2000) Centrosomal kinases, HsAIRk1 and HsAIRK3, are overexpressed in primary colorectal cancers. *Japanese Journal of Cancer Research: Gann*, **91**, 1007–1014.
 - 146 Gritsko, T.M., Coppola, D., Paciga, J.E. *et al.* (2003) Activation and overexpression of centrosome kinase BTAK/Aurora-A in human ovarian cancer. *Clinical Cancer Research*, **9**, 1420–1426.
 - 147 Sakakura, C., Hagiwara, A., Yasuoka, R. *et al.* (2001) Tumor-amplified kinase BTAK is amplified and overexpressed in gastric cancers with possible involvement in aneuploid formation. *British Journal of Cancer*, **84**, 824–831.
 - 148 Tanaka, T., Kimura, M., Matsunaga, K. *et al.* (1999) Centrosomal kinase AIK1 is overexpressed in invasive ductal carcinoma of the breast. *Cancer Research*, **59**, 2041–2044.
 - 149 Cheetham, G.M., Knegt, R.M., Coll, J.T. *et al.* (2002) Crystal structure of Aurora-2, an oncogenic serine/threonine kinase. *The Journal of Biological Chemistry*, **277**, 42419–42422.

- 150 Harrington, E.A., Bebbington, D., Moore, J. *et al.* (2004) VX-680, a potent and selective small-molecule inhibitor of the Aurora kinases, suppresses tumor growth *in vivo*. *Nature Medicine*, **10**, 262–267.
- 151 www.vpharm.com and www.clinicaltrials.gov. (2 March 2009).
- 152 Carpinelli, P., Ceruti, R. *et al.* (2007) PHA-739358, a potent inhibitor of Aurora kinases with a selective target inhibition profile relevant to cancer. *Molecular Cancer Therapeutics*, **6**, 3158.
- 153 Fancelli, D., Berta, D., Bindi, S. *et al.* (2005) Potent and selective Aurora inhibitors identified by the expansion of a novel scaffold for protein kinase inhibition. *Journal of Medicinal Chemistry*, **48**, 3080–3084.
- 154 Howard, S., Berdini, V. *et al.* (2009) Fragment-based discovery of the pyrazol-4-yl urea (AT9283), a multitargeted kinase inhibitor with potent Aurora kinase activity. *Journal of Medicinal Chemistry*, **52** (2), 379–388.
- 155 Gorgun, G., Calabrese, E. *et al.* (2008) A novel Aurora-A kinase inhibitor MLN8237 induces cytotoxicity and cell cycle arrest in experimental multiple myeloma models. 50th ASH Annual Meeting and Exposition, abstract, December 6–9, 2008, San Francisco, CA.
- 156 Staal, S.P., Hartley, J.W. *et al.* (1997) Isolation of transforming murine leukemia viruses from mice with a high incidence of spontaneous lymphoma. *Proceedings of the National Academy of Sciences of the United States of America*, **74** (7), 3065–3067.
- 157 Song, G., Ouyang, G. *et al.* (2005) The activation of Akt/PKB signaling pathway and cell survival. *Journal of Cellular and Molecular Medicine*, **9** (1), 59–71.
- 158 Thakkar, H., Chen, X., Tyan, F. *et al.* (2001) Pro-survival function of Akt/protein kinase B in prostate cancer cells. Relationship with TRAIL resistance. *The Journal of Biological Chemistry*, **276**, 38361–38369.
- 159 Malik, S.N., Brattain, M., Ghosh, P.M. *et al.* (2002) Immunohistochemical demonstration of phospho-Akt in high Gleason grade prostate cancer. *Clinical Cancer Research*, **8**, 1168–1171.
- 160 Stal, O., Perez-Tenorio, G., Akerberg, L. *et al.* (2003) Akt kinases in breast cancer and the results of adjuvant therapy. *Breast Cancer Research*, **5**, R37–R44.
- 161 Breitenlechner, C.B., Friebe, W.G. *et al.* (2005) Design and crystal structures of protein kinase B-selective inhibitors in complex with protein kinase A and mutants. *Journal of Medicinal Chemistry*, **48**, 163–170.
- 162 Rhodes, N., Heerding, D.A. *et al.* (2008) Characterization of an Akt kinase inhibitor with potent pharmacodynamic and antitumor activity. *Cancer Research*, **68** (7), 2366–2374.
- 163 www.ir.exelixis.com and www.clinicaltrials.gov. (2 March 2009).
- 164 Lindsley, C.W., Zhao, Z. *et al.* (2005) Allosteric Akt (PKB) inhibitors: discovery and SAR of isozyme selective inhibitors. *Bioorganic & Medicinal Chemistry Letters*, **15**, 761–764.
- 165 Nakanishi, S., Kakita, S. *et al.* (1992) Wortmannin, a microbial product inhibitor of myosin light chain kinase. *The Journal of Biological Chemistry*, **267**, 2157–2163.
- 166 Ihle, N.T., Williams, R. *et al.* (2004) Molecular pharmacology and antitumor activity of PX-866, a novel inhibitor of phosphoinositide-3-kinase signaling. *Molecular Cancer Therapeutics*, **3**, 763–772.
- 167 Doukas, J., Eide, L. *et al.* (2009) Aerosolized phosphoinositide 3-kinase gamma/delta inhibitor TG100-115 [3-[2,4-diamino-6-(3-hydroxyphenyl)pteridin-7-yl]phenol] as a therapeutic candidate for asthma and chronic obstructive pulmonary disease. *The Journal of Pharmacology and Experimental Therapeutics*, **328**, 758–765.
- 168 Stauffer, F., Garcia-Echeverria, C., Furet, P. *et al.* (2007) Biochemical, cellular, and *in vivo* profiling of a new PI3K inhibitor from the imidazoquinoline series. Proceedings/Annual Meeting of the American Association for Cancer Research, April 14–18, 2007, Los Angeles, CA and Philadelphia, PA, Abstract 269.

- 169 www.novartis oncology.com and www.clinicaltrials.gov. (2 March 2009).
- 170 www.exelixis.com and www.clinicaltrials.gov. (2 March 2009).
- 171 www.calistogapharma.com and www.clinicaltrials.gov. (2 March 2009).
- 172 www.gsk-clinicalstudyregister.com and www.clinicaltrials.gov. (2 March 2009).
- 173 Coopman, P.J.P., Do, M.T.H., Barth, M. *et al.* (2000) The Syk tyrosine kinase suppresses malignant growth of human breast cancer cells. *Nature*, **406**, 742–747.
- 174 Allergy/asthma – R112. <http://www.rigel.com/rigel/R112> (accessed August 23, 2005).
- 175 Meltzer, E., Berkowitz, R., and Grossbard, E. (2005) An intranasal Syk-kinase inhibitor (R112) improves the symptoms of seasonal allergic rhinitis in a park environment. *The Journal of Allergy and Clinical Immunology*, **115**, 791–796.
- 176 Ruschel, A. and Ullrich, A. (2004) Protein tyrosine kinase Syk modulates EGFR signalling in human mammary epithelial cells. *Cellular Signalling*, **16**, 1249–1261.
- 177 Rheumatoid arthritis – R406/788. http://www.rigel.com/rigel/rheumatoid_arthritis (accessed August 24, 2005).
- 178 Weinblatt, M.E., Kavanaugh, A. *et al.* (2008) Treatment of rheumatoid arthritis with a Syk kinase inhibitor: a twelve-week, randomized, placebo-controlled trial. *Arthritis and Rheumatism*, **58** (11), 3309–3318.
- 179 Wilks, A.F. (1989) Two putative protein-tyrosine kinases identified by application of the polymerase chain reaction. *Proceedings of the National Academy of Sciences of the United States of America*, **86** (5), 1603–1607.
- 180 Levitzki, A. (1999) Protein tyrosine kinase inhibitors as novel therapeutic agents. *Pharmacology & Therapeutics*, **82**, 231–239.
- 181 Meydan, N., Grunberger, T., Dadi, H. *et al.* (1996) Inhibition of recurrent human pre-B acute lymphoblastic leukemia by Jak-2 tyrosine kinase inhibitor. *Nature*, **379**, 645–648.
- 182 Wong, W.S., Leong, F., and Pang, K. (2004) Tyrosine kinase inhibitors: a new approach for asthma. *Biochimica et Biophysica Acta*, **1697**, 53–69.
- 183 Kudlacz, E., Perry, B., Sawyer, P. *et al.* (2004) The novel JAK-3 inhibitor CP-690550 is a potent immunosuppressive agent in various murine models. *American Journal of Transplantation*, **4**, 51–57.
- 184 van Gurp, E.A., Schoordijk-Verschoor, W. *et al.* (2009) The effect of the JAK inhibitor CP-690, 550 on peripheral immune parameters in stable kidney allograft patients. *Transplantation*, **87** (1), 79–86.
- 185 www.vpharm.com. (2 March 2009).
- 186 www.exelixis.com and www.clinicaltrials.gov. (2 March 2009).
- 187 Lasho, T.L., Tefferi, A. *et al.* (2008) TG101348, a JAK2-selective antagonist, inhibits primary hematopoietic cells derived from myeloproliferative disorder patients with JAK2V617F, MPLW515K or JAK2 exon 12 mutations as well as mutation negative patients. *Leukemia*, **22** (9), 1790–1792.
- 188 Mesa, R.A., Verstovsek, S. *et al.* (2008) 1760 INCB018424, a selective JAK1/2 inhibitor, significantly improves the compromised nutritional status and frank cachexia in patients with myelofibrosis (MF). 50th ASH Annual Meeting and Exposition, abstract, December 6–9, 2008, San Francisco, CA.
- 189 www.sbio.com and www.clinicaltrials.gov. (2 March 2009).
- 190 Hexner, E.O., Serdikoff, C. *et al.* (2008) Lestaurinib (CEP701) is a JAK2 inhibitor that suppresses JAK2/STAT5 signaling and the proliferation of primary erythroid cells from patients with myeloproliferative disorders. *Blood*, **111** (12), 5663–5671.
- 191 O'Neil, L.A.J. (2008) The interleukin-1 receptor/Toll-like receptor superfamily: 10 years of progress. *Immunological Reviews*, **226**, 10–18.
- 192 Karin, M. and Gallagher, E. (2005) From JNK to pay dirt: Jun kinases, their biochemistry, physiology and clinical importance. *IUBMB Life*, **57** (4–5), 283–295.
- 193 Zarubin, T. and Han, J. (2005) Activation and signaling of the p38 MAP kinase pathway. *Cell Research*, **15** (1), 11–18.

- 194 Bonizzi, G. and Karin, M. (2004) The two NF-kappaB activation pathways and their role in innate and adaptive immunity. *Trends in Immunology*, **25** (6), 280–288.
- 195 Adcock, I.M. and Chung, K.F. (2006) Kinase inhibitors and airway inflammation. *European Journal of Pharmacology*, **533**, 118–132.
- 196 Wei, S. and Siegal, G.P. (2008) Mechanisms modulating inflammatory osteolysis: a review with insights into therapeutic targets. *Pathology: Research and Practice*, **204**, 695–706.
- 197 Condcliffe, A.M. and Cadwallader, K.A. (2000) Phosphoinositide 3-kinase: a critical signalling event in pulmonary cells. *Respiratory Research*, **1**, 24–29.
- 198 Park, S.J., Min, K.H., and Lee, Y.C. (2008) Phosphoinositide 3-kinase δ inhibitor as a novel therapeutic agent in asthma. *Respirology (Carlton, Vic.)*, **13** (6), 764–771.
- 199 Yousefi, S. and Hoessli, D.C. (1996) Requirement of Lyn and Syk tyrosine kinases for the prevention of apoptosis by cytokines in human eosinophils. *The Journal of Experimental Medicine*, **183**, 1407–1414.
- 200 Keller, S.A. and Hernandez-Hopkins, D. (2006) NF- κ B is essential for the progression of KSHV- and EBV-infected lymphomas *in vivo*. *Blood*, **107**, 3295–3302.
- 201 Ding, S.Z., Smith, M.F., and Goldberg, J.B. (2007) *Helicobacter pylori* and mitogen-activated protein kinases regulate the cell cycle, proliferation and apoptosis in gastric epithelial cells. *Journal of gastroenterology and hepatology*, **23**, 67–78.
- 202 Hui, E.K.-W. and Nayak, D.P. (2002) Role of G protein and protein kinase signalling in influenza virus budding in MDCK cells. *Journal of General Virology*, **83**, 3055–3066.
- 203 Balasubramanian, A. *et al.* (2003) Hepatitis C virus and HIV envelope proteins collaboratively mediate interleukin-8 secretion through activation of p38 MAP kinase and SHP2 in hepatocytes. *The Journal of Biological Chemistry*, **278**, 35755–35766.
- 204 Canduri, F. and Perez, P.C. (2008) CDK9 a potential target for drug development. *Journal of Medicinal Chemistry*, **4** (3), 210–218.
- 205 Pendaries, C. and Tronchère, H. (2006) PtdIns(5)P activates the host cell PI3-kinase/Akt pathway during *Shigella flexneri* infection. *The EMBO Journal*, **25** (5), 1024–1034.
- 206 Zahrt, T.C. and Deretic, V. (2001) Mycobacterium tuberculosis signal transduction system required for persistent infections. *Proceedings of the National Academy of Sciences of the United States of America*, **98**, 12706–12711.
- 207 Walburger, A., Koul, A. *et al.* (2004) Protein kinase G from pathogenic mycobacteria promotes survival within macrophages. *Science*, **304**, 1800–1804.
- 208 Sassetti, C.M., Boyd, D.H., and Rubin, E.J. (2003) Genes required for mycobacterial growth defined by high density mutagenesis. *Molecular Microbiology*, **48**, 77–84.
- 209 Székely, R., Wączek, F. *et al.* (2008) A novel drug discovery concept for tuberculosis: inhibition of bacterial and host cell signalling. *Immunology Letters*, **116**, 225–231.
- 210 Hegymegi-Barakonyi, B., Székely, R. *et al.* (2008) Signalling inhibitors against *Mycobacterium tuberculosis*: early days of a new therapeutic concept in tuberculosis. *Current Medicinal Chemistry*, **15**, 2760–2770.

6

Design Principles of Deep Pocket-Targeting Protein Kinase Inhibitors

Alexander C. Backes, Gerhard Müller, and Peter C. Sennhenn

6.1

Introduction

The design of selective protein kinase inhibitors is a serious challenge for the medicinal chemist. As all protein kinases share the same protein fold, have high sequence identities, utilize the same ubiquitous cellular cofactor adenosine triphosphate (ATP), use the same catalytic mechanism, and are closely associated with each other in signal transductions cascades, selective inhibition of a given kinase is a difficult task. The success of the small-molecule kinase inhibitors imatinib (Gleevec™; **1**), gefitinib (Iressa™; **2**), erlotinib (Tarceva™; **3**), sorafenib (Nexavar™; **4**), sunitinib (Sutent™; **5**), dasatinib (Sprycel™; **6**), lapatinib (Tykerb™; **7**), and nilotinib (Tasigna™; **8**) as anticancer drugs show that these difficulties can be overcome (Figure 6.1).

However, the question remains how selective a kinase inhibitor indeed needs to be. Compound **7** is a highly selective dual-kinase inhibitor of the ErbB-1 (EGF) and ErbB-2 receptors that was very recently approved for the treatment of breast cancer; **1** and **8** are selective inhibitors of the Abelson protein tyrosine kinase (Abl) and c-Kit, used to treat patients suffering from chronic myelogenous leukemia (CML) and gastrointestinal tumors (GISTs), respectively; and both **3** and **2** (although its use has been restricted by the FDA) are selective inhibitors of the EGF receptor applied in the treatment of patients suffering from nonsmall-cell lung cancer (NSCLC). The selectivity of these inhibitors is a useful tool in probing the role of a given protein kinase in driving the phenotype of individual tumors and provides a highly customized therapy to cancer patients. On the other hand, **4** and **5** are multitargeted inhibitors that block the function of a large number of different cancer-relevant protein kinases, such as the VEGF and the PDGF receptor tyrosine kinase families, Flt-3, the Raf kinases, and c-Kit [1, 2]. Nevertheless, they are successfully used in the clinical treatment of renal cancers as well as, in the case of **5**, of patients diagnosed with Gleevec-resistant GIST. The development of both compounds initially started with the intention to hit one specific protein kinase family, the Raf kinases in the case of **4**, and the split kinase domain superfamily of receptor tyrosine kinases (RTK) in

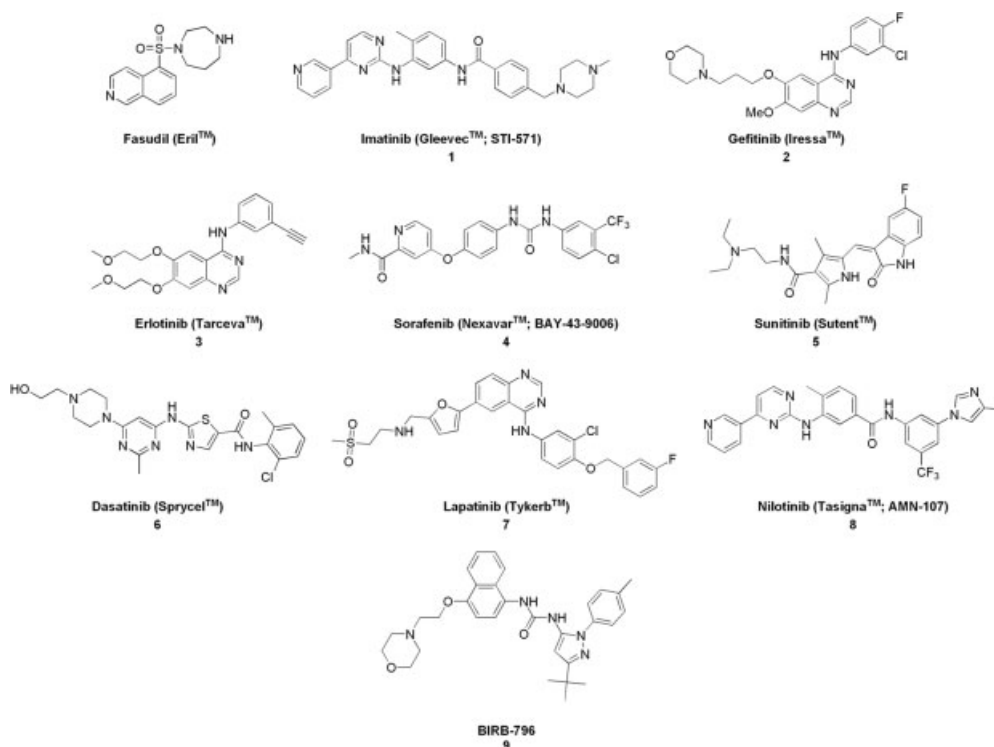


Figure 6.1 Marketed protein kinase inhibitors and drug-like compound BIRB-796 (9); 1, 4, and 7–9 are type II inhibitors.

the case of 5. As it turned out, the multitarget profile of both compounds for RTKs has been advantageous especially in the treatment of renal tumors in a clinical setting. Therefore, as cancer is a consequence of deregulation of protein kinase function, one should be receptive to the need of multitargeted, as well as single-targeted, kinase inhibitors. In a therapeutic setting, both kinds of inhibitors have their value, and more often than not the distinction between the two classes is ambiguous [3, 4].

One strategy to gain selective inhibition is target the protein kinase in its inactive state. The majority of kinase inhibitors act against the active form of the protein, that is, the phosphorylated form, and target the ATP binding site via hinge binding motifs. Selectivity can be gained here by addressing the hydrophobic *back pocket*, also called the *selectivity pocket* or the *BR-I* in Traxler's pharmacophore model (see further below), which is part of the ATP binding site of an active kinase but has no obvious function in the catalytic reaction. It is not conserved among the kinases and can accordingly be addressed by an inhibitor to gain selectivity. An example is 3 whose alkynyl side chain reaches the *back pocket* and is responsible for the drug's high selectivity toward the EGF receptor [5]. However, a number of inhibitors are known to address a different ATP binding site in a so far limited number of protein kinases. This extended binding pocket that we term the *deep pocket* (DP), sometimes also called the *Phe pocket* or

allosteric pocket, is accessible only in the inactive state of the kinase. Inactivation not only does stem from the phosphorylation state of the activation loop but can also be due to other conformational changes in the protein, such as from a shift of the α C helix, from breakage of the highly conserved glutamate-lysine ion pair that is essential for catalytic function, and from other mechanisms such as domain binding or posttranslational modification. The deep pocket is of unpolar nature and extends toward the back of the protein opposite to the hinge region, and rational design of a small molecule can lead to compounds that exhibit a good shape complementarity with the protein surface in the deep pocket. Accordingly, both high selectivity and high activity can be obtained from this mode of inhibition. A number of approaches have, therefore, been undertaken to design compounds that specifically address the inactive state of kinases. Kinases that are targeted with this approach include representatives from the receptor tyrosine kinase family, such as the EGF receptor, the VEGF and the PDGF receptor kinases, Flt-3 kinase, and Tie-2 kinase; the nonreceptor tyrosine kinases, such as the c-Src kinase family, including Lck and Hck, the Raf kinases, and the Abelson tyrosine kinase; and the serine/threonine kinases, such as the Aurora kinase family and the p38 MAP kinases. For other kinases, the inactive state has not yet been observed in the crystal structure, but one can assume that with the continuously increasing number of available structures other examples will emerge.

In this chapter, we attempt to classify various approaches to specifically design deep pocket binders according to a pharmacophore model, on the basis of an analysis of the binding modes of deep pocket binders, and underline the strategies with examples of inhibitors whose crystal structures in complex with their respective protein kinases are available. An analysis of changes in various properties that occur when going from the initial starting points to the final inhibitors will provide ideas about the principles underlying the design and assist in the development of new selective drugs.

6.2

Classification of Protein Kinase Inhibitors

Small-molecule protein kinase inhibitors can be categorized into three classes according to their binding mode: *type I*, *type II*, and *type III* (Table 6.1) [6, 7]. *Type I inhibitors* are ATP-competitive compounds that bind to the *active (phosphorylated)* form of a kinase. They target the ATP binding site according to the pharmacophore model developed by Traxler (Figure 6.2a) [8]. All type I inhibitors contain at least one hydrogen bond donor or acceptor that enables binding to the hinge region. It is usually difficult to achieve high selectivity with type I inhibitors. However, examples are known where selectivity is gained by specifically addressing the hydrophobic back pocket. Access to the back pocket is controlled by the *gatekeeper residue*. The majority of known kinase inhibitors fall into the type I category, and the marketed drugs gefitinib (2), erlotinib (3), sunitinib (5), and dasatinib (6) are examples of this category.

Table 6.1 Classification of protein kinase inhibitors.

Type I	Type II	Type III
ATP competitive	ATP competitive	Non-ATP competitive
Binding to the ATP site	Binding to an extended ATP site (deep pocket)	Binding to allosteric sites
Hydrogen bond to hinge	Hydrogen bond to hinge not necessarily required	No hinge binding
Kinase in active or inactive state	Kinase in inactive state	Kinase in active or inactive state
Little conformational changes in the protein	Significant changes in the protein conformation	Possible conformational changes in the protein
Address all kinases	Address only few kinases	Address very few kinases
Moderate selectivity	High selectivity	High selectivity
Many examples	Some examples	Only very few examples
IP situation unfavorable	IP situation favorable, new chemical entities	IP situation favorable, new chemical entities

Type II inhibitors, in contrast, bind to the *inactive* form of a protein kinase. They are ATP competitive, as well, and also target the ATP binding site. Often a hinge binding motif is present, although there are type II compounds that do not contain hinge binding motifs [9]. However, all type II compounds address an extended ATP binding site by extending into the hydrophobic *deep pocket* that is not available in an activated kinase (Figure 6.2b). The deep pocket is created by conformational changes in the protein and is available only in the catalytically inactive form of the protein (see below). As a consequence, as an alternative we name compounds that bind in the type II mode *deep pocket binders*. It is generally more straightforward to achieve high selectivity with type II inhibitors than with type I compounds, as only few kinases are known so far that have the deep pocket. On the other hand, a type II inhibitor can also bind in type I mode in another kinase, as it is known from **1** that binds to the inactive form of Abl kinase as a type II inhibitor, but adopts a type I binding mode in the ATP binding site of Syk [10]. A fair number of examples of deep pocket binders are described in the discussion that follows. BIRB-796 (**9**) as well as the marketed drugs Gleevec (**1**), sorafenib (**4**), and nilotinib (**8**) are representative examples of type II inhibitors (Figure 6.1). They are often denoted as allosteric inhibitors for historic reasons, as the DFG-out conformation was first observed in the complex of p38 α MAP kinase with a urea-based scaffold that did not reach the hinge binding region of the ATP binding site [11]. However, in the strict sense of the enzymological definition they are not allosteric inhibitors. An allosteric inhibitor is non-ATP competitive as it binds to a binding site that is distant to the ATP pocket. As all type II inhibitors known so far are ATP competitive, they are not allosteric.

Type III inhibitors are *non-ATP competitive*. They do not target the ATP binding site of a kinase, but bind to allosteric sites of the protein distant from the ATP pocket. Type III compounds, therefore, do not address the hinge region. They do not require any typical hinge binding motifs and can target the kinase regardless of its activation state.

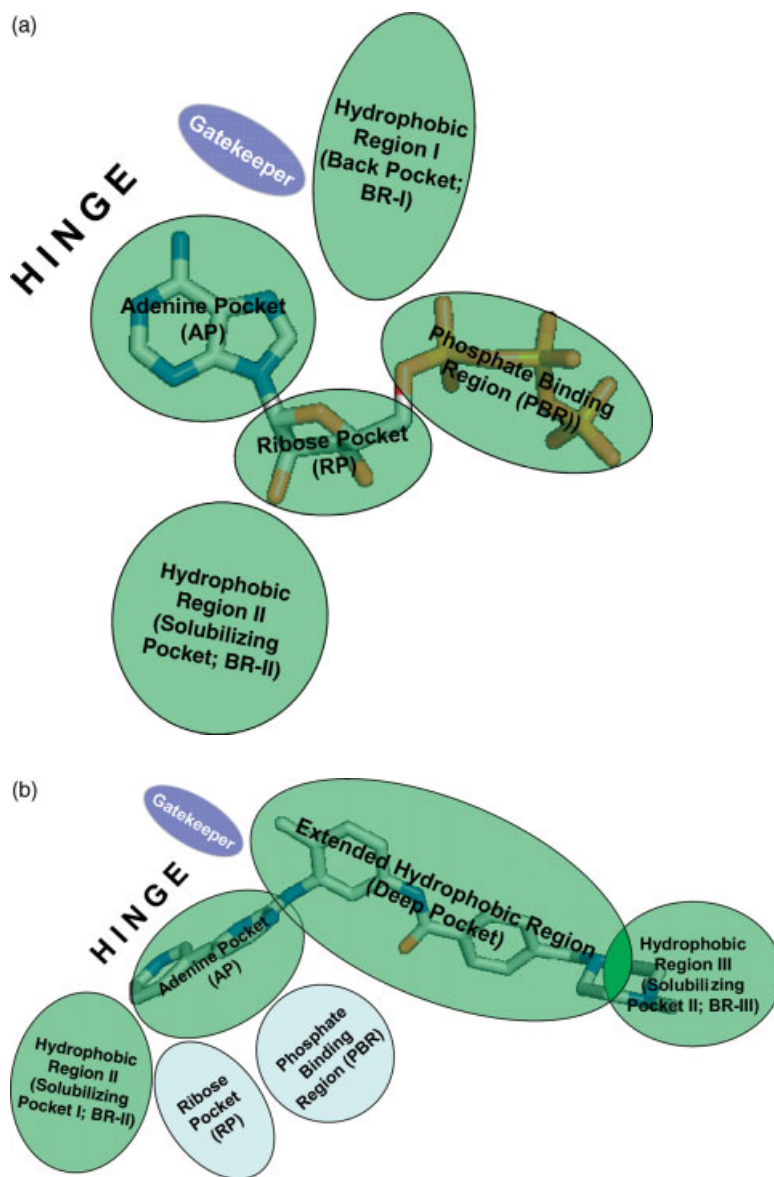


Figure 6.2 Pharmacophore models.

(a) Pharmacophore model for type I inhibitors (adapted from Ref. [8]); ATP is shown in the PKA binding site as reference (PDB entry code 1ATP). (b) Pharmacophore model for type II inhibitors [7]; Gleevec (**1**) is shown in the binding site of Abl kinase as reference

(PDB entry code 1IEP). The approximate positions of the hinge region and the gatekeeper residues are indicated. Carbon atoms are colored in gray, nitrogen atoms in blue, oxygen atoms in red, and phosphorus atoms in orange.

As allosteric sites are highly specific for a given kinase, type III compounds can be expected to exert high selectivity and potency. On the other hand, only few kinases may have allosteric binding sites and consequently few examples of this type are known so far, and none of them has made it into clinical trials yet (see Table 6.1) [12–16].

6.3

Type II Inhibitors

In this overview, we focus on the development of type II inhibitors by different design strategies. All type II inhibitors occupy a deep pocket that is formed by conformational changes of different nature. In most cases, the conformation of the activation loop (the A-loop) of the protein kinase changes. Phosphorylation and dephosphorylation of residues in the A-loop result in a conformational switch between the active and the inactive form of a kinase (see below). A deep pocket can also be formed with the movement of the α C helix containing the glutamate residue of the conserved Glu–Lys ion pair that is essential in the catalytic mechanism, in effect disrupting the salt bridge and rendering the kinase inactive. Hydrogen bond acceptors or donors in the inhibitor at a specific position may also lead to binding of the lysine or glutamate residue, thereby breaking the Glu–Lys ion pair and rendering the kinase inactive [7]. Gleevec (**1**) in complex with the kinase domain of the Abelson protein tyrosine kinase is a typical example for type II binding to an inactive A-loop conformation (Figure 6.3) [17–19].

Inhibitor **1** adopts an elongated conformation in the extended ATP binding pocket, effectively spanning through the entire interlobal space of the Abl kinase (Figure 6.3). The 4-pyridin-3-yl-2-aminopyrimidine moiety of **1** occupies the adenine pocket, and one hydrogen bond contact is formed between the nitrogen atom of the terminal pyridine substituent and the backbone NH of Met318 in the hinge region. Other crucial hydrogen bond contacts exist between the NH of the 2-aminopyrimidine ring and the backbone oxygen atom of the gatekeeper Thr315; between the central amide bond and the terminal carboxylate group of Glu286 of the conserved Glu286–Lys271 pair; and between the amide bond and the carboxylate group of Asp381. The orthogonal tolyl and *N*-methylpiperazinylphenyl moieties of **1** penetrate the deep pocket past the small gatekeeper Thr315 and wedge themselves between the activation loop (residues 381–402) and the α C helix, locking the protein kinase in the inactive conformation. The beginning of the A-loop is characterized by the conserved sequence Asp–Phe–Gly (the *DFG*-motif). In the complex of **1** with Abl, Phe382 of the *DFG*-motif is flipped toward the ATP binding site due to folding of the A-loop. As a result, access to the nucleotide binding site is blocked and a π -stacking interaction of Phe382 with the pyrimidine moiety of **1** is enabled. Unphosphorylated Tyr393 in the A-loop, which is the major site of phosphorylation in Abl, forms a hydrogen bond with the catalytic base Asp363, locking the A-loop in an inactive conformation. The conformation of the *DFG*-motif is *out*, as defined by a flip of the *DFG* residues of about 180°, resulting in the phenylalanine side chain pointing outward to the surface of the protein kinase. In the *in* conformation of an active kinase, the phenylalanine side chain is buried inside the protein and oriented toward

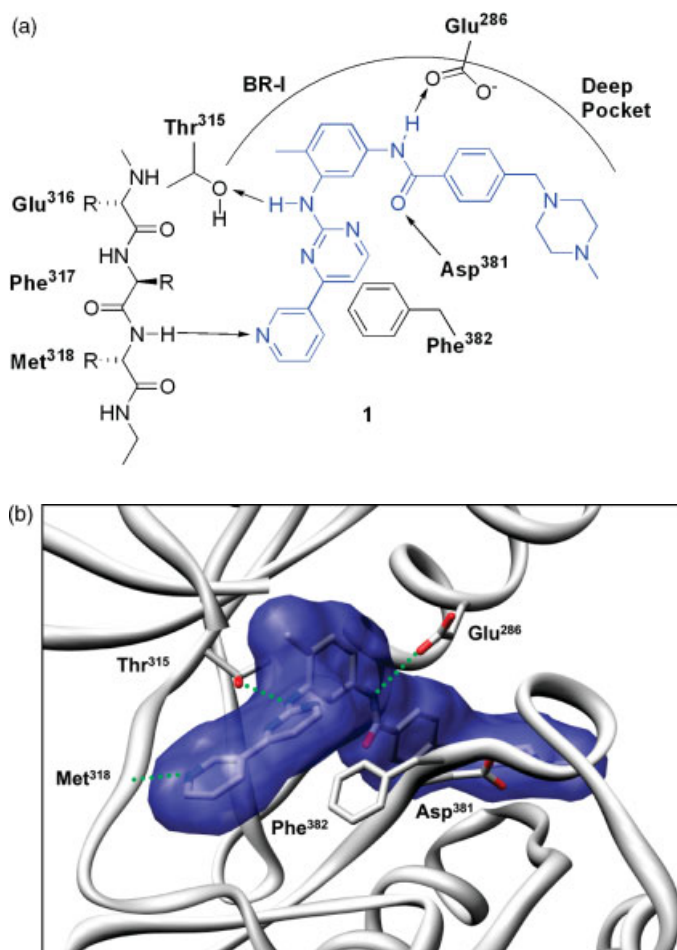


Figure 6.3 Binding of Gleevec to the Abelson protein tyrosine kinase. (a) Schematic binding interactions. (b) ATP binding site of Abl with bound **1** (PDB entry code 1IEP). Important residues and hydrogen bonds are indicated. Carbon atoms are colored in gray, nitrogen

atoms in blue, and oxygen atoms in red; the protein backbone is depicted as gray ribbons; regular hydrogen bonds are shown as dotted green lines; and the van der Waals surface of **1** is shown in transparent blue. Residues 248–256 of the P-loop are omitted for clarity.

the α C helix. The movement of the DFG-motif covers approximately a 10 Å distance between the residues. A clear definition of the conformations of DFG-in and DFG-out is described via the backbone torsion angle of the Asp [20]. The DFG-out conformation was first reported for the inactive conformation of the insulin receptor kinase IRK [21] and has so far been observed in the crystal structures of Abl kinase, p38 α MAP kinase (MAPK14), B-Raf, Flt-3, c-Kit, Lck, KDR, Tie-2, AurKA, Fms/CSFR, and CDK6. To illustrate the significant conformational changes between the active and the inactive state of the Abl kinase, Figure 6.4 shows the crystal structures of both

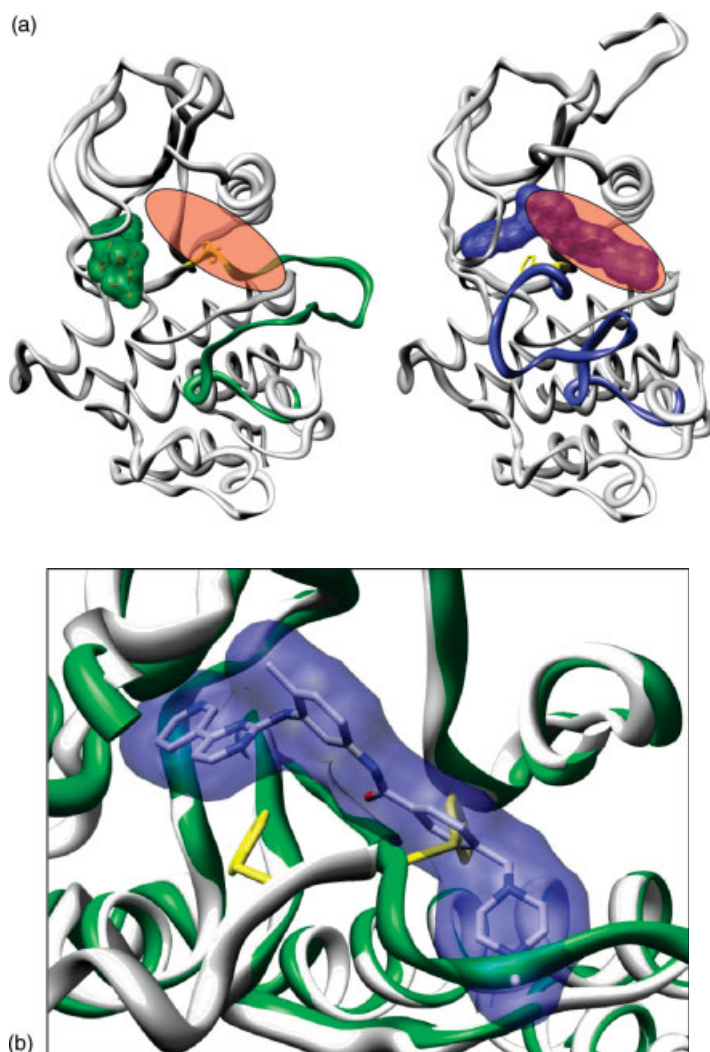


Figure 6.4 Abl protein kinase in the active and inactive state. (a) Crystal structure of Abl kinase in complex with ADP (PDB code 2G2I), left, and in complex with **1** (PDB code 1IEP), right. (b) Overlay of the ATP binding sites of Abl kinase in the active (green) and inactive (gray) conformation. The distance between the centers of both phenyl rings of Phe382 is 8.8 Å. The protein backbone is shown in gray ribbons.

Both the activation loop (residues 381–409) and the ligand surface are colored in green for ADP and in blue for **1**, respectively. The DFG-motif is colored in yellow, and the phenylalanine side chain of Phe382 is shown. The deep pocket accessible in the **1**–Abl complex upon conformational rearrangement of the activation loop is emphasized in red.

ADP and **1** bound to Abl [20]. ADP binds in the type I mode to the active form of Abl. The deep pocket of Abl cannot be addressed by ADP as Phe382 of the DFG-motif in the *in* conformation occupies the corresponding space in the protein, the deep pocket is therefore not present. Binding of **1** in Abl, on the other hand, is possible only in the *out* conformation of the DFG-motif, where the flip of Phe382 toward the nucleotide binding site opens the deep pocket that is addressed by the inhibitor, and the A-loop (residues 381–402) is shifted about 33 Å toward the ATP binding site.

For some time, it has been discussed whether the inactive and the active forms of a given protein kinase are in a conformational equilibrium and if a type II inhibitor is selecting from the preexisting equilibrium preferably for the inactive state of the protein, or whether binding of the inhibitor induces the conformational shift from active to inactive state. Recent kinetic, NMR, and crystallographic studies with p38 α MAP kinase show that under cellular conditions the active and inactive state of p38 α MAP kinase are in a complex equilibrium, with the active (DFG-*in*) form being favored [22]. The deep pocket binder BIRB-796 (**9**) has been shown to select for the DFG-*out* conformation from the preexisting equilibrium rather than inducing the conformation. A type I inhibitor was utilized to trap p38 α MAP kinase in both the DFG-*out* and the DFG-*in* conformation in the solid state, showing that the conformational equilibrium is present even in the crystal structure [23].

To understand the fact that crystal structures of kinases with bound inhibitors are known where the DFG-motif can adopt various other conformational arrangements except for *in* and *out*, an in-house survey of all crystal structures of protein kinases available in the Protein Data Bank (PDB) was performed. All kinases were superimposed at the hinge region, and the center of the phenylalanine residue of the DFG-motif was plotted in three-dimensional space (Figure 6.5).

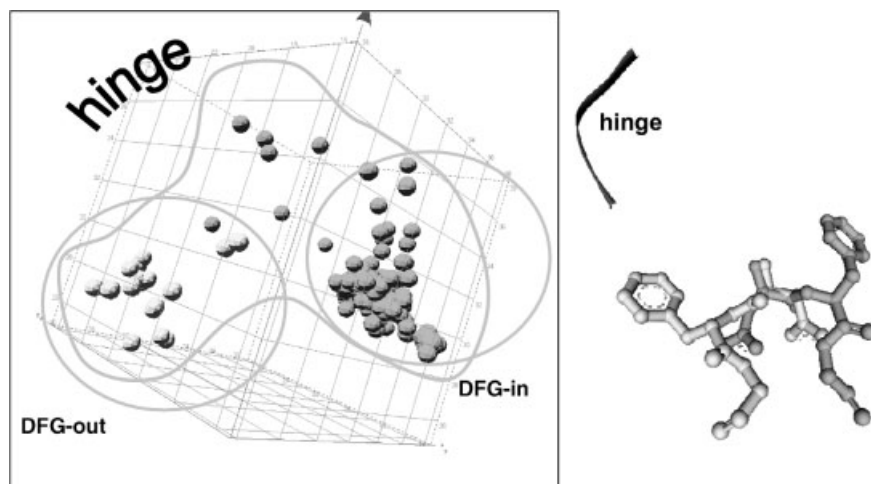


Figure 6.5 Conformational space of the DFG-motif. The center of the phenylalanine benzene ring has been plotted in three-dimensional space for all protein kinases with structures available in the Protein Data Bank.

As it turns out, not surprisingly, the *in* and the *out* conformations of the DFG-motif are only two extremes of a broad spectrum of possible conformations. As a consequence, the often-used classification of inhibitor binding solely according to DFG-in and DFG-out is arbitrary and inappropriate. Furthermore, inhibitors such as lapatinib (7) bind to an inactive form of a protein kinase and address a newly formed deep pocket *without* influencing the conformation of the DFG-motif [7]. We therefore suggest better to talk about the active or inactive state of a protein kinase with regard to the conformational state of the A-loop or the α C helix.

6.4

Common Features of Type II Inhibitors

A comparison of all deep pocket binders for which crystal structures with their respective kinases are available resulted in the development of a pharmacophore model that summarizes the structural requirements for a compound to be a type II inhibitor [6, 7]. The features required for a type II inhibitor ranked according to their significance are as follows:

- A *central urea or amide, or a corresponding bioisosteric core*, facilitating essential hydrogen-bond interactions with the α C helix glutamate side chain of the Glu–Lys ion pair and with the backbone amide of aspartate of the DFG-motif; an additional hydrogen bond may be formed to the catalytic lysine.
- *Hydrophobic moieties* to exploit unpolar interactions within the deep pocket, typically with halogen-substituted phenyl rings and heterocycles; polar groups can also be incorporated to capture additional hydrogen-bond interactions with residues located at the exit of the pocket or with water molecules at the protein–solvent interface.
- An *orthogonally arranged (hetero)aromatic scaffold* that ensures an extended conformation of the molecule in combination with enhancement of affinity by unpolar interactions; often a “magic methyl” or sterically demanding substituents, such as 2,6-dihalo-substituted phenyl groups or larger aromatic moieties, such as naphthyl, are used.
- A *hinge binding group* that makes one or two hydrogen bond contacts with the hinge backbone as an additional anchor. This is an optional requirement, as deep pocket binding molecules are known that have no hinge-addressing residues.

These requirements are fulfilled by all deep pocket binders to various extent and can be summarized in a pharmacophore model (Figure 6.6). A special case of a deep pocket binder is lapatinib (7) that does not make any hydrogen bonds with either the α C helical Glu or the Asp of the DFG-motif, but only with the hinge region and water molecules within the binding site, employing mainly unpolar interactions within the deep pocket to gain affinity (see further below).

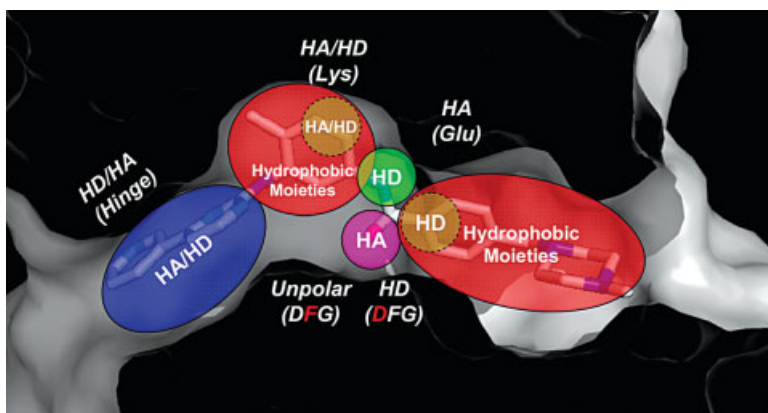


Figure 6.6 Pharmacophore model of deep pocket binders. Gleevec (**1**) is shown for orientation; carbon atoms are colored in gray, nitrogen atoms in blue, and oxygen atoms in red. The van der Waals surface of the protein is

depicted in gray. HD: hydrogen bond donor; HA: hydrogen bond acceptor. The approximate locations of the hinge region, the DFG-motif, the catalytic lysine, and the α C helical glutamate are indicated.

6.5

Design Strategies for Type II Inhibitors

Utilizing the deep pocket of protein kinases for inhibitor binding offers new possibilities in selective inhibition, which is desirable in molecular targeted therapy [3]. Inhibitors with high selectivity for a specific kinase target serve as useful clinical tools to probe the role of this target in the phenotype of an individual tumor and as such affords the possibility to provide highly customized therapy to cancer patients [4].

The deep pocket is unique for each kinase. However, so far only 12 out of all 518 human kinases are known to bind a type II inhibitor. Consequently, efforts have been undertaken to design type II inhibitors using different approaches. We classify the current design strategies into four categories: *front-to-back* (F2B), *back-to-front* (B2F), *hybrid* (F2B + B2F), and *back-to-back* (B2B) (Table 6.2, Figure 6.7). This classification derives from the analysis of type II inhibitors that have been crystallized in complex with their respective protein kinases. More molecules are published in the literature that are very likely type II inhibitors. This is based on the one hand on experimental data in agreement with deep pocket binding, such as low nanomolar or even picomolar affinity of a protein kinase, especially if the kinase is known to be inhibited in an inactive state, or slow binding kinetics, that is, the decrease in inhibitory constant over time, although not every type II inhibitor necessarily exhibits slow binding kinetics. On the other hand, the pharmacophore model for deep pocket binders can be applied and if the inhibitor contains structural features that satisfy the model there is a good chance that it is indeed a deep pocket binder. However, as long as no unambiguous structural data are available, a clear statement of an inhibitor

Table 6.2 Classification of deep pocket binder design strategies.

Type	Characteristics
Front-to-back	“Classical” design strategy, starts with a previously optimized type I lead structure; predefined linking direction toward the deep pocket; Increases the complexity of the design; leads to moieties that may not be essential for function; creates a molecular weight problem
Back-to-front	“Retro-design” approach; starts with fragments rather than leads; predefined linking direction toward hinge; no prior optimization of a type I core required; no hinge-anchoring residues implicitly required; avoids unnecessary moieties; requires structural methods for characterization
Hybrid	Previously optimized type I or type II core; nonrational optimization at two positions required; increases complexity of the problem; generates a molecular weight problem
Back-to-back	Subtle changes in an existing type II core; combines parts of previously optimized type II structures; modifies in the deep pocket to gain selectivity and affinity; rational optimization strategy of type II inhibitors; may generate a molecular weight problem

being type II or not is not possible. Recent studies suggest that even crystal structure data alone may not be sufficient for characterization of type II inhibitors, but that kinetic as well as structural data, both in the solid state and in the solution, may be necessary for an unambiguous characterization of a type II inhibitor [22, 23].

Figure 6.7 schematically depicts the different approaches to specifically design type II inhibitors according to our classification. The pharmacophore model for type II inhibitors (Figure 6.2b) is used as a basis for the schematics. In green are indicated the solubilizing pocket (BR-II), the adenine pocket (AP), and the deep pocket; in gray are shown the ribose pocket (RP) and the phosphate binding region (PBR) that are usually not or only partially accessible in type II inhibition. In our terminology, the “front” of the protein kinase is comprised of the AP and the BR-II, the “back” is the deep pocket. The location of the hinge region is indicated by a short peptide chain with the typical hydrogen bond acceptor–donor–acceptor pattern. The pharmacophore of the initial starting structure for each design strategy is indicated in blue. Pharmacophores occupying different regions of the model can be connected, as indicated by a black line. The pharmacophores that are created in the design approach are shown as red ovals, with both numbers and arrows indicating the design sequence.

In the F2B approach (Figure 6.7a), type II inhibitors are generated by using a known type I inhibitor as the starting point that contains a classical hinge binding motif and addresses the adenine and the solubilizing pockets of an active protein kinase (blue; no. 1). Both pockets are usually targeted, but it is conceivable that a smaller structure occupying only the adenine pocket can be a sufficient starting point. Substituting or extending the type I inhibitor with unpolar moieties that specifically address the deep pocket and provide crucial hydrogen-bonding residues to address the α C helical Glu and the Asp of the DFG-motif, according to the general

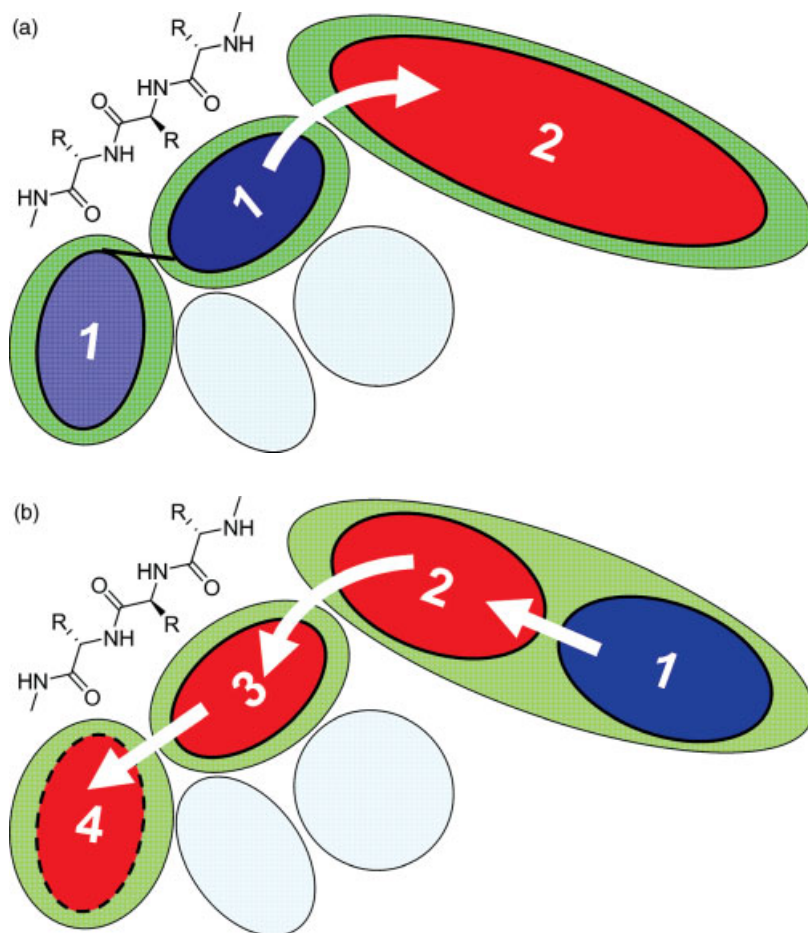


Figure 6.7 Design principles for deep pocket binders based on the pharmacophore model for type II inhibition (see also Table 6.2). (a) F2B; (b) B2F; (c) hybrid; (d) B2B. The pharmacophores BR-II, AP, and deep pocket for type II inhibitors are indicated in green, the pharmacophores RP and PBR in gray, based on

Figure 6.6. The initial pharmacophores of the design are indicated in blue, and a black line indicates connectivity. The pharmacophores created in the design are indicated in red, and the design sequence is indicated both by numbers and by arrows. For orientation, the hinge region is shown.

requirements (Figure 6.6), generates a new type II inhibitor. The added moieties are indicated as red ovals (no. 2) in Figure 6.7a and can vary in size to either fill the deep pocket or to address it only partially. The direction of the design is clearly defined as going from the hinge binding region toward the back of the protein. It was explicitly put into practice first by Liu and Gray and was referred to by the authors as “hybrid design approach” since the design combines parts of a hinge binding type I inhibitor with motifs from a type II inhibitor [6, 24]. However, in our terminology this would be a F2B approach, and we classify a different strategy as a hybrid design approach. The

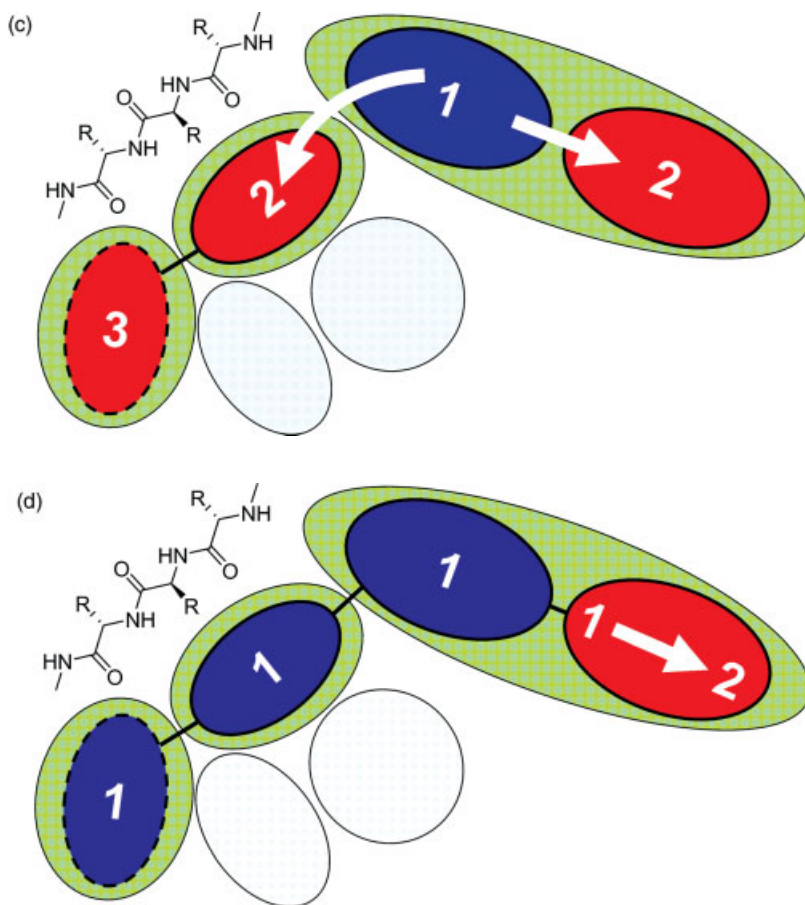


Figure 6.7 (Continued)

F2B strategy offers the advantage of starting with a previously optimized core that is a known protein kinase inhibitor. The design can be initiated either with lead structures or with fragments (compounds of a molecular weight between 100 and 300 Da, of limited functionality, and of weak affinity). As with all design approaches, a subsequent synthetic modification with moieties derived from known deep pocket binders obviously needs to be possible. The F2B strategy has several disadvantages. Introduction of mainly unpolar deep pocket-targeting moieties usually leads to unfavorable physicochemical properties as it decreases aqueous solubility. However, it is possible to modify the moieties with additional solubilizing groups, and a subsequent hybrid or B2B design may follow the initial F2B approach. Introduction of solubilizing functions may not necessarily maintain the desired activity or selectivity, and a compromise has to be found to have both favorable physicochemical and binding properties. This may increase the complexity of the design problem and

lead to a nonrational and lengthy optimization procedure. The F2B approach also leads to a significant increase in molecular weight (MW), which is undesirable from a physicochemical point of view but may be counterbalanced by introduction of suitable functionalities.

The B2F design (Figure 6.7b) can be regarded as a novel “retrodesign” approach. A type II inhibitor is designed by first addressing the deep pocket of the protein kinase (the “back”) with a suitable scaffold that contains the necessary pharmacophores, as indicated by the blue oval (no. 1), followed by a subsequent stepwise construction of the inhibitor directed toward the hinge region (the “front”) to increase affinity and solubility, as indicated in red (nos 2–4). The solubilizing pocket may also be addressed as the last step. However, if the design starts with a molecule that already contains a solubilizing group that extends out of the deep pocket, such as Gleevec (**1**), where the *N*-methylpiperazine group extends toward the solvent-accessible site in the back of the protein, this addition may not be necessary (indicated by the dotted red oval). Most importantly, the B2F approach starts directly with deep pocket-targeting fragments rather than with lead structures. This avoids unnecessary decoration of the final inhibitor as it is possible to introduce substituents in a stepwise and minimalist fashion, and the linking direction is clearly defined. The scaffold is not required to be a known type I inhibitor. This has advantages from an intellectual property point of view, as it allows the design of novel protein kinase inhibitors from small fragments that have not been used as kinase-targeting ligands so far. Furthermore, as hinge binding residues are not required, the typical kinase inhibitor motifs can be omitted. On the other hand, it also presents an unbiased approach for the design of novel inhibitors. In contrast to the F2B design, the focus in the B2F approach is on the protein target rather than on the inhibitor. The B2F approach *a priori* requires a protein kinase that is known to adopt a conformation that opens a deep pocket. A disadvantage of the B2F design resides in the fact that fragments have very weak affinity, typically in the micromolar to millimolar range, and unfavorable physicochemical parameters, especially regarding aqueous solubility. This affinity range is beyond the normal sensitivity range and the fragments therefore cannot be routinely identified in standard bioassays due to high concentration of the compound that would be required, which is often not accessible due to low solubility, and the fragments can also interfere with other proteins or biochemical compounds in the assay and lead to false positives. Structural methods, such as protein crystallography or NMR spectroscopy, are therefore required in a routine fashion to confirm the correct type II binding mode and the intended spatial direction of the design [25].

The hybrid or F2B + B2F approach (Figure 6.7c) according to our definition can be regarded as an extension of the F2B design. A core lead structure, as indicated by the blue oval (no. 1), is modified both toward the deep pocket (red ovals, no. 2) and toward the hinge region (red oval, no. 2), to generate a new hybrid structure. Position 2 can be present in the initial structure and subsequently be exchanged by other residues. The solubilizing pocket (red oval, no. 3) may optionally be addressed. As both the F2B and the hybrid approaches share common motifs, the classification of an inhibitor according to either design is not strict and compounds categorized into the hybrid approach can also be viewed as extended F2B designs. However, in contrast to the F2B

approach, the changes in the inhibitor at the hinge-addressing and the deep pocket-targeting ends are not subtle, for example, the substitution of a hydrogen atom with a methoxy group, but rather large, and as such lead to the introduction of larger moieties on both ends of the compound. The hybrid design does not necessarily have to be carried out in a concerted fashion, but can be done successively. As in the F2B approach, introduction of a solubilizing group while retaining a specific deep pocket-targeting moiety may not necessarily maintain the desired activity or selectivity, and vice versa. Again, this generally increases the complexity of the design problem and may lead to a nonrational and lengthy optimization procedure. Furthermore, the introduction of larger substituents creates a clear molecular weight problem similar to the F2B approach. This may not be significant when starting from a small drug-like structure.

In the B2B approach, as outlined in Figure 6.7d, a known type II inhibitor, either a optimized lead or a final drug, is modified with regard to the deep pocket-targeting residues in order to enhance activity or selectivity, or to improve physicochemistry and pharmacokinetics. In Figure 6.7d, the retained inhibitor structure is schematically indicated in blue (no. 1), with the solubilizing pocket optionally addressed (indicated by the dotted line). Modification of the deep pocket-targeting moiety (red oval, no. 1) leads to a different group addressing the deep pocket (no. 2). The essential type II features of the inhibitor remain, but different arrangement of substituents, such as the switch from an amide to an inverse amide, or introduction of rigidity, leads to high affinity compounds while retaining the binding mode. As only subtle changes are made to the molecule, this is a fast and rational strategy for optimization of an existing deep pocket binder and is most advantageously applied to increase the potency and the selectivity of a second-generation drug. The only disadvantage of this approach may be an increase in molecular weight by introduction of larger moieties.

In the following sections, we will exemplify the different strategies in designing new type II inhibitors, perform an analysis of molecular features that accompany the design, and finally discuss our conclusions and recommendations.

6.5.1

F2B Approach

Several inhibitors are known that we classify according to the F2B strategy, as shown in Figure 6.8: Gleevec (**1**), the dihydropyrimidopyrimidinone **11**, the pyridodiazines **14** and **15**, the pyridotriazine **16**, the furopyrimidine **18**, MPAQ (**19**), and the pyridylethers **22** and **23**.

The first and foremost example of an F2B design is Gleevec (**1**). The starting point of **1** was phenylaminopyrimidine **10** (PAP), which was the initial hit in a discovery program for inhibitors of protein kinase C (PKC), but showed no notable activity toward Abl. Phenylaminopyrimidine **10** was subjected to an optimization program in the course of which it was discovered that an amide function and introduction of a methyl group in the central diaminophenyl moiety enhanced activity against Abl. The lead optimization finally resulted in the discovery of **1** with an IC_{50} of 38 nM toward Abl [26]. Although no structural data are available for **10**, the missing activity toward

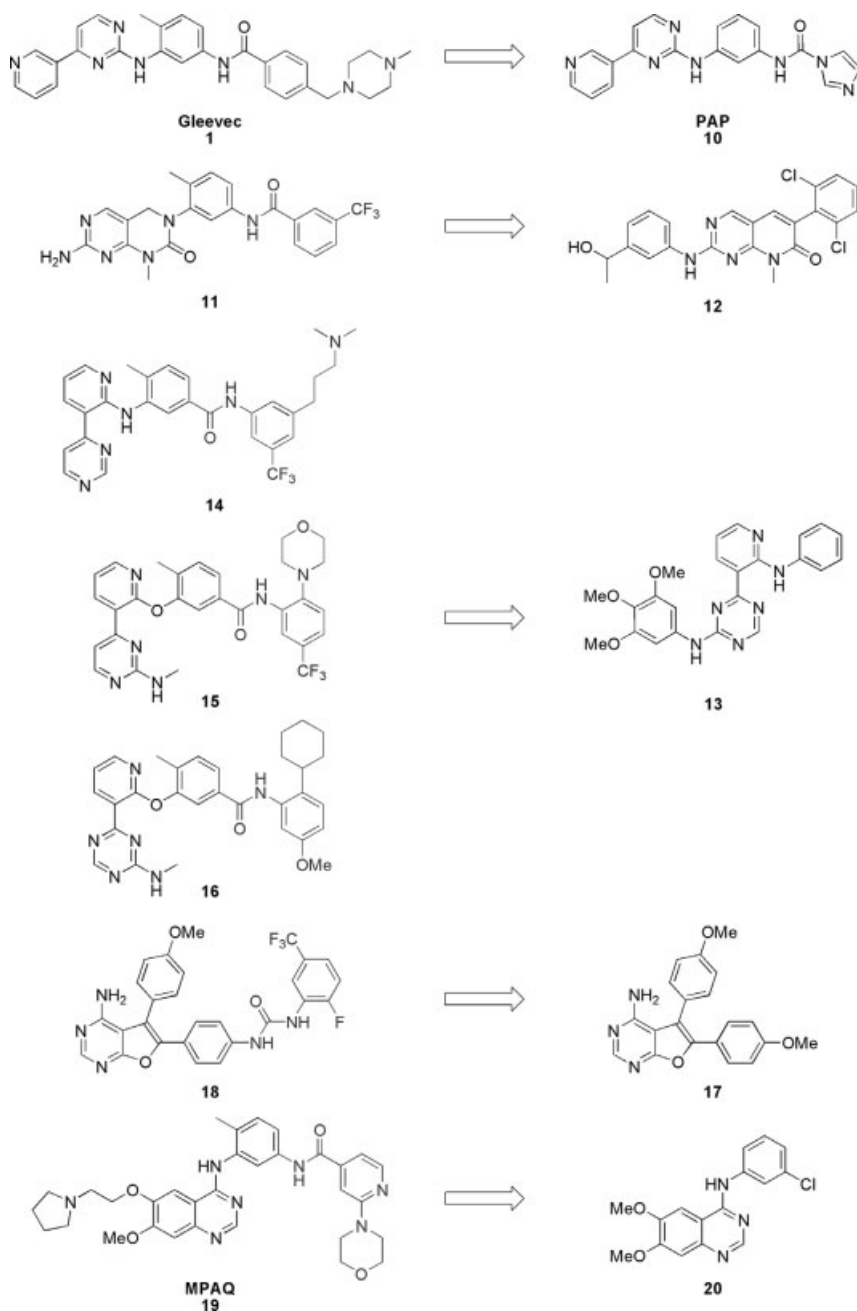


Figure 6.8 Type II inhibitors designed according to the F2B strategy.

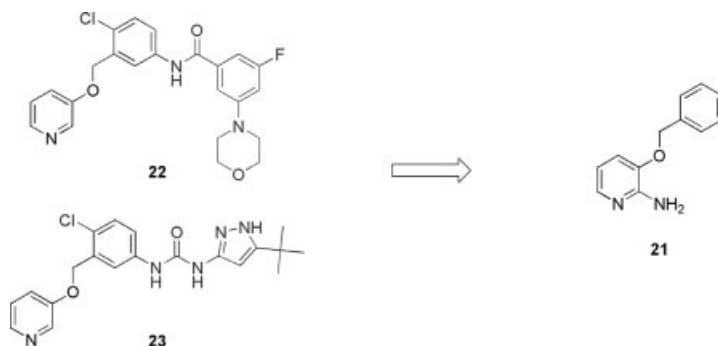


Figure 6.8 (Continued)

Abl suggests that the inhibitor binds to PKC in a type I mode with a binding mode that is probably analogous to the demethylated variant of **1** in c-Src [27] or **1** in Syk [10]. The crucial changes that generated type II inhibitor **1** out of type I compound **10** were the introduction of the “magic methyl” that leads to a perpendicular orientation of the two halves of the molecule and therefore to an extended conformation, and the attachment of a large deep pocket-targeting moiety with an amide motif suitable to establish the required hydrogen bond interactions with the DFG-motif and the α C helical glutamate.

Okram *et al.* described the design of a type II Abl inhibitor (**11**) by combining features from a known type I inhibitor of Abl, a derivative of PD173955 (**12**), with deep pocket-targeting moieties derived both from **1** and from the Raf-inhibitor **4** [24]. The conformation of **11** in Abl is analogous to **1** in Abl and to **4** in B-Raf, with the trifluoromethylphenyl moiety penetrating into the deep pocket (Figure 6.8). A superimposition of the three inhibitors **1**, **4**, and **11** shows a very good alignment of the structures. The central amide core of **11** makes hydrogen bond contact with the backbone amide of Asp399 of the DFG-motif and with the side-chain carboxylate of Glu304 of the α C helix. The trifluoromethylphenyl group penetrates the deep pocket that has opened by displacement of the activation loop into an inactive conformation, and the hinge-directed part of **11** is fixed by two hydrogen bonds from the exocyclic amine and one of the ring nitrogen atoms to Met336 and Phe335 of the hinge region (Figure 6.9). However, in contrast to **1**, compound **11** does not make any hydrogen bond contact with the gatekeeper Thr315 and therefore may be active against the clinically important Gleevec-resistant T315I mutant of Abl where the hydrogen bond between the exocyclic amine of the aminopyrimidine and the side-chain hydroxyl of Thr315 is crucial for inhibitory activity. Compound **11** binds to the unphosphorylated form of Abl with an IC_{50} of 8 nM. However, **11** also binds to the phosphorylated form of Abl with 11 nM activity. The result is explained by the authors with the exceptional potency of the inhibitor that may drive the equilibrium between active and inactive A-loop conformation of Abl toward the inactive form, regardless of its phosphorylation state [24].

A similar case of an inhibitor binding to a protein kinase regardless of its phosphorylation state with similar affinities is the p38 α MAP kinase-specific type

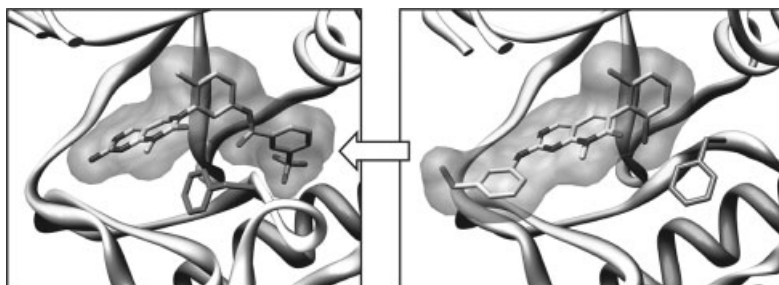


Figure 6.9 Example of a F2B design approach. *Left:* Crystal structure of Abl kinase in complex with **11** (PDB code 2HIW); *right:* in complex with **12** (PDB code 1OLP). The protein backbone is shown as ribbon, carbon atoms are

depicted in light gray, and oxygen and nitrogen atoms in dark gray. The ligand surface is emphasized as a transparent Connolly surface. Residues 248–256 of the P-loop are omitted for clarity.

I inhibitor SB203580. However, in this case the conformational change in the activation loop between activated and inactive (phosphorylated and nonphosphorylated) state does not significantly influence the binding mode of the inhibitor, as both NMR spectroscopic and X-ray crystallographic studies showed [23].

Amgen Inc. has developed several new inhibitors of KDR and the Tie-2 receptor tyrosine kinases that were designed starting from an aminotriazine scaffold **13** that binds to the active form of KDR in the type I binding mode with an IC_{50} of 57 nM but displays only 25 μ M affinity for Tie-2 kinase. An optimization program toward the specific design of Tie-2 kinase inhibitors led to pyrimidine **14**, 2-methylaminopyrimidine **15**, and 3-methylaminotriazine **16**, that all have been crystallized with Tie-2 kinase [28–30]. Compound **14** exhibits low nanomolar biochemical activity both toward KDR (IC_{50} = 2 nM) and Tie-2 kinase (IC_{50} = 1 nM). The crystal structure of **14** is known in complex with KDR and with Tie-2 kinase and binds in both kinases in the type II binding mode: the activation loop in both KDR and Tie-2 kinase adopts an inactive conformation, and the central inverse amide core makes hydrogen bond contact with the α C helical glutamate and the backbone amide of aspartate of the DFG-motif. The two halves of **14** are orthogonally arranged to each other, induced by the methyl group analogous to Gleevec (**1**), and the trifluoromethyl group is buried in the respective deep pockets of KDR and Tie-2 kinase. Analogously to **14**, the **15**–Tie-2 kinase and the **16**–Tie-2 kinase complexes are known and show that the inhibitors also bind in the type II binding mode. In the **15**–Tie-2 kinase complex, the hydrogen bond to Glu872 of the α C helix is absent, compared to the **14**–Tie-2 kinase complex, due to a steric clash with the bulky morpholino group. This leads to a 3.5 Å shift of the α C helix from its regular position and forces the trifluoromethyl group of **15** to be buried deeper into the deep pocket, compared to the **14**–Tie-2 kinase complex. As a result, **15** shows better selectivity for Tie-2 kinase (IC_{50} = 10 nM) over KDR (IC_{50} = 310 nM), as the corresponding binding region may be more flexible in Tie-2 kinase than in KDR. Interestingly, variations in the hinge-directed part of the molecules resulted in the triazine derivative **16** that has much higher selectivity for

Tie-2 kinase ($IC_{50} = 22$ nM) over KDR ($IC_{50} > 25$ μ M) and favorable pharmacokinetic properties. Compound **16** also binds to the Tie-2 kinase as a type II inhibitor [28]. All three inhibitors **14**, **15**, and **16** bind to Tie-2 kinase in a similar fashion. The strategy employed in the design of **14**, **15**, and **16**, starting from **13**, was the introduction of a central benzamide core that enables hydrogen bonding to the α C helix glutamate and to the aspartate of the DFG-motif; the incorporation of a “magic methyl” into the benzamide core to ensure a perpendicular orientation of the two halves of the compounds, in analogy to **1**; and the substitution with mainly unpolar residues to address the hydrophobic deep pocket. A subsequent optimization program based on the crystal structure information finally afforded a potent pyridinyl triazine inhibitor of Tie-2 kinase with good pharmacokinetic properties and potency in a mouse model [29].

Another F2B strategy has been applied by GlaxoSmithKline in the development of dual inhibitors of both KDR and Tie-2 kinase, based on the type I binding aminofur-pyrimidine scaffold **17**. Compound **17** is a 1.25 μ M inhibitor of KDR and a 1 μ M inhibitor of Tie-2 kinase [31]. By replacing one of the methoxy functions with a central urea core and introducing a deep pocket-targeting side chain derived from the Raf inhibitor **4**, the type II inhibitor **18** was designed that shows an IC_{50} of 3 nM for KDR and of 2 nM for Tie-2 kinase. The crystal structure with KDR demonstrates the type II binding mode of **18**. The urea core is hydrogen-bonded to the α C helical Glu883 and to the backbone amide of Asp1044 of the DFG-motif. Due to a gap in the crystal structure, Phe1045 is not visible. The furo-pyrimidine scaffold is additionally hydrogen bonded via the exocyclic nitrogen and one of the ring nitrogen atoms to the backbone amides of Glu915 and Phe916 of the hinge region [31].

AstraZeneca reported the development of the p38 α MAP kinase-specific type II inhibitor MPAQ (**19**), starting from the generic 4-aminoquinazoline **20** [32]. Compound **20** has an IC_{50} of 560 nM for p38 α MAP kinase and of 5 nM for the EGF receptor. As **20** is closely related to the marketed drug Erlotinib (**3**) where the chlorine atom is substituted by an ethinyl moiety, and **3** binds to the EGF receptor kinase domain in the type I binding mode as the crystal structure demonstrates, it can be assumed that **20** also binds in the type I mode [5]. By introducing deep pocket-targeting side chains and the “magic methyl,” **19** was developed that shows an IC_{50} of 39 nM for p38 α MAP kinase and no activity toward the EGF receptor. The crystal structure of p38 α MAP kinase in complex with **19** demonstrates the type II binding mode. The morpholinopyridyl moiety penetrates into the deep pocket. The central amide core is hydrogen bonded to Glu71 and to the backbone amide of Asp168 of the DFG-motif with the activation loop being in an inactive conformation. The quinazoline scaffold is hydrogen bonded via both ring nitrogen atoms to the backbone amide of Met109 of the hinge region and to the side chain of the gatekeeper Thr106 [32]. Compound **19** is an example of the undesirable effect of the F2B design of increasing the molecular weight: the inhibitor has a molecular weight of 584 Da.

An interesting and promising F2B strategy is the fragment-based approach of Astex to generate new lead compounds as p38 α MAP kinase inhibitors [33–35]. The pyridine-based fragment **21** binds to p38 α MAP kinase with low affinity ($IC_{50} = 1.3$ mM). The crystal structure of **21** in complex with p38 α MAP kinase shows that the fragment occupies the ATP binding site as a type I inhibitor, with the pyridine making

hydrogen bond contact with the backbone amide of Met109 and the benzyloxy side chain occupying the back pocket. The fragment offered good synthetic tractability and a clearly defined direction for further optimization toward the development of more potent inhibitors. Subsequently, the substitution of the benzyloxy side chain with unpolar moieties of increasing size led ultimately to the amide **22** and the urea **23**. Both **22** and **23** showed a significant improvement in the *in vitro* activity against p38 α MAP kinase with IC₅₀ values of 65 nM and 350 nM, respectively, and have the necessary requirements for the type II binding mode. The crystal structures of both inhibitor–p38 α MAP kinase complexes have been solved and indeed show that the compounds bind in the type II mode. The A-loop of the protein adopts an inactive conformation. The structures of **22** and **23** superimpose very nicely and share essentially the same interactions with the protein. Both the central amide core of **22** and the central urea core of **23** are hydrogen bonded to the backbone amide of Asp168 of the DFG-motif and to the side chain of Glu71 in the α C helix, with the Glu71–Lys53 ion pair kept intact. The fluoromorpholino benzamide moiety in **22** and the *tert*-butylpyrazole group in **23** occupy the deep pocket that has opened by displacement of Phe169 of the DFG-motif. The pyridine moieties in both compounds still make hydrogen bond contact with the backbone of Met109 of the hinge region, as does the precursor fragment **21**. Figure 6.10 shows the structures of the precursor fragment **21** and inhibitors **22** and **23** in p38 α MAP kinase.

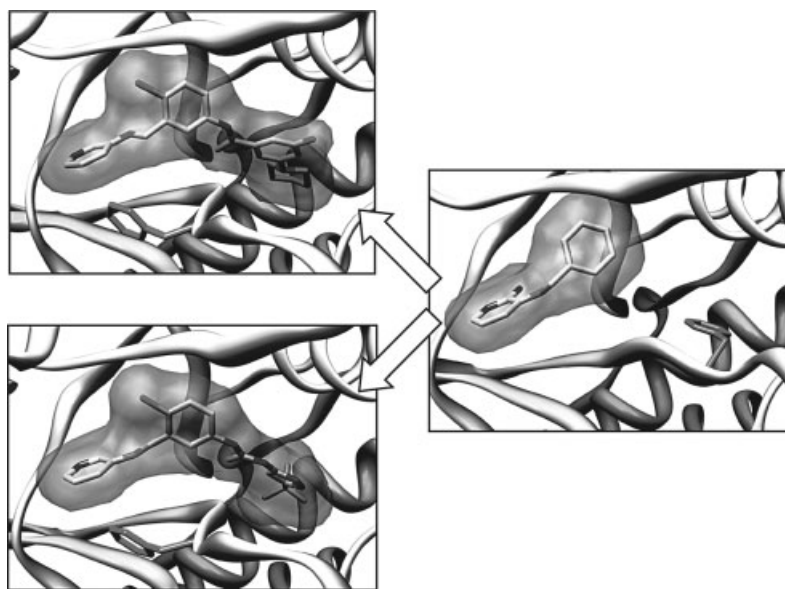


Figure 6.10 Example of a F2B design approach. *Top left:* Crystal structure of p38 α MAP kinase in complex with **22** (PDB code 1W83); *top right:* in complex with **23** (PDB code 1WBN); *right:* in complex with **21** (PDB code 1W7H). The protein backbone is shown as

ribbon, carbon atoms are depicted in light gray and oxygen, nitrogen, and halogen atoms in dark gray. The ligand surface is emphasized as a transparent Connolly surface. The phenylalanine side chain of Phe169 of the DFG-motif is shown.

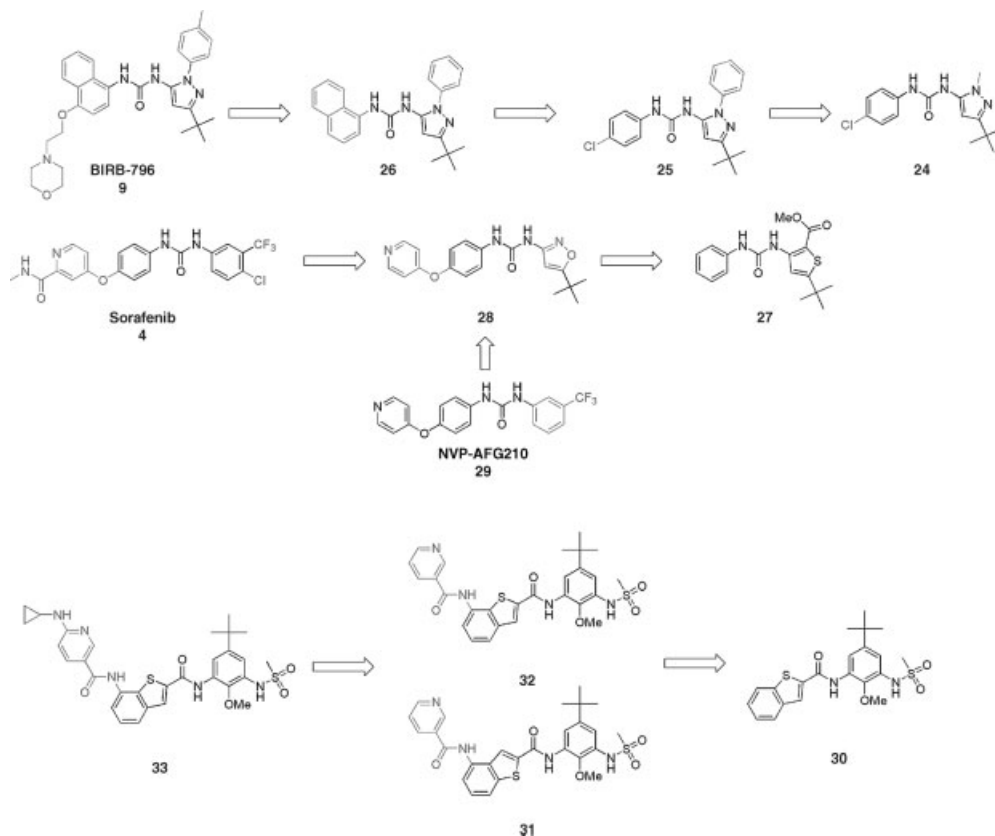


Figure 6.11 Type II inhibitors designed according to the B2F strategy.

6.5.2

B2F Approach

So far, three examples of this type of design approach are known: BIRB-796 (9), the marketed kinase inhibitor sorafenib (4), and the p38 α MAP kinase benzothiophene inhibitors 30–33 (Figure 6.11).

In a rational design-driven and X-ray structure-based B2F approach, Boehringer-Ingelheim US identified the generic *N*-pyrazole-*N'*-aryl-urea screening hit 24 as an inhibitor of p38 α MAP kinase ($K_D = 350$ nM). The 24–p38 α MAP kinase cocrystal structure unambiguously revealed a 10 Å conformational shift of the DFG-motif of the activation loop that opens up a large hydrophobic deep pocket that is occupied by the *tert*-butyl group of 24 [9]. SAR studies showed that the *tert*-butyl group was best suited to utilize the hydrophobic interactions relevant to this new binding pocket that has been observed for the first time in a serine/threonine protein kinase. The nitrogen atoms of the central urea core of 24 make a bidentate hydrogen bond to the side chain of Glu71 located in the α C helix, and the carbonyl oxygen atom makes

hydrogen-bond contact with the backbone amide of Asp168 of the DFG-motif. The *p*-chlorophenyl group is oriented toward the former back pocket that has merged into the deep pocket in the inactive conformation, and has no directionality toward the hinge region. Since none of the pyrazole nitrogen atoms is involved in specific hydrogen-bonding interactions, either, the pyrazole moiety of **24** serves only as a scaffold for correct positioning of the *tert*-butyl group and the urea pharmacophore. Replacement of the methyl group at N2 of the pyrazole by a phenyl ring resulted in compound **25** that shows a 40-fold improved binding affinity for p38 α MAP kinase as measured in a fluorescent binding assay ($K_D = 8$ nM). The X-ray crystal structure of the **25**–p38 α MAP kinase complex again emphasizes the crucial hydrogen-bond network between the urea core of **25** and the residues Glu71 and Asp168. In contrast to **24**, however, the *N*-phenyl derivative **25** initiates a conformational shift of the Glu71 side chain due to the steric requirements of the phenyl ring, resulting in only one hydrogen bond of the urea core to Glu71. The **25**–p38 α MAP kinase complex underlines the crucial contribution of the 3-urea motif to the binding with the protein kinase through extensive hydrogen bonding and established the correct geometric relationships of the other pharmacophores of the inhibitor. Subsequently, the phenyl substituent at the urea that addresses the former back pocket, analogous to the methyl group in **24**, was replaced by a naphthyl substituent, leading to **26** with a 15-fold improved affinity toward p38 α MAP kinase ($K_D = 5$ nM) that is probably due to favorable edge-to- π hydrophobic interactions of the naphthalene ring with the phenyl side chain of Phe169 of the DFG-motif. The crystal structure of the **26**–p38 α MAP kinase complex shows that the naphthyl group is buried deeper in the former back pocket than the phenyl group in **25** and that the 4-position is pointing toward the hinge region and the solvent-accessible region, giving now a directionality for further substitution. Pharmacokinetic studies suggested to replace the *N*-phenyl moiety by an *N*-tolyl substituent, which resulted in a significant improvement of both oral bioavailability and potency ($K_D = 1$ nM). Finally, further extension toward the hinge region by introduction of a solubilizing ethoxymorpholine residue in 4-position of the naphthalene moiety resulted in **9** (BIRB-796) that showed extraordinary potency toward p38 α MAP kinase ($K_D = 0.01$ nM). The crystal structure of the **9**–p38 α MAP kinase complex shows that BIRB-796 binds, analogously to Gleevec (**1**), as a type II inhibitor (Figure 6.12) [9, 11]. The DFG-motif is flipped into the *out* conformation due to the inactive state of the A-loop, with the side chain of Phe169 making a side-on hydrophobic interaction with the naphthyl moiety of **9**. One of the nitrogen atoms of the urea core makes hydrogen bond contact with the side chain of the α C helical Glu71, with the Glu71–Lys53 ion pair still remaining intact, and the carbonyl oxygen atom forms a hydrogen bond to the backbone amide of Asp168 of the DFG-motif, as has been observed previously in the crystal structures of **25** and **26** bound to p38 α MAP kinase. In addition, **9** forms one hydrogen bond to the backbone amide of Met109 in the hinge region. The development of **9** is an elegant example of how a structure-guided design leads to a final drug-like compound with favorable pharmacokinetic properties and both high *in vitro* and high *in vivo* affinity. Although **9** has been under phase III clinical development for some time, it is not being pursued further.

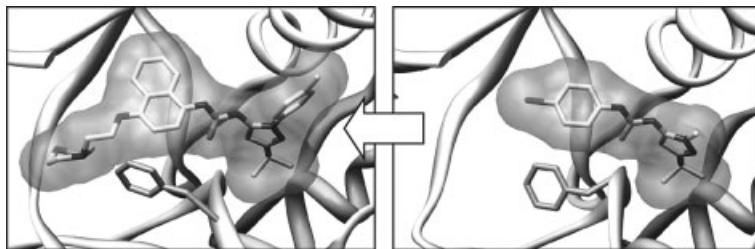


Figure 6.12 Example of a B2F design approach. *Left:* Crystal structure of p38 α MAP kinase in complex with **9** (PDB code 1KV2); *right:* in complex with **24** (PDB code 1KV1). The protein backbone is shown as ribbon; carbon

atoms are depicted in light gray and oxygen and nitrogen atoms in dark gray. The ligand surface is emphasized as a transparent Connolly surface. Residues 30–38 of the P-loop are omitted for clarity.

In another B2F approach solely driven by classical compound analoguing, Bayer and Onyx identified deep pocket binder **4** (sorafenib), the first orally bioavailable multikinase inhibitor that targets the C-Raf and wild-type B-Raf kinases as well as the oncogenic B-Raf V600E kinase. Compound **4** also potently inhibits the VEGF and the PDGF receptor tyrosine kinase families, as well as the FGFR1, Flt-3, c-Kit, and RET kinases, and affects tumor signaling and tumor vasculature. During the whole chemical structure optimization process that ultimately culminated in the discovery of **4**, no X-ray crystal structural information was available for any given compound in complex with the target kinases B-Raf or C-Raf [36]. The initial starting point of the optimization was the 3-thienyl urea hit GK00687 (**27**) that was identified in a high-throughput screen of 200 000 compounds against C-Raf (Raf1) and exhibited an IC_{50} of 17 μ M. In-depth SAR investigation of the parent hit **27** by employing not only sequential analoguing but also parallel synthesis techniques led to replacement of the thiophene moiety by a trifluoromethyl-chlorophenyl residue. Further extension of the structure into the ATP binding site via introduction of a pyridylether linkage on the phenyl urea resulted in the discovery of the 5-*tert*-butylisoxazole derivative **28** that exhibits high biochemical potency toward C-Raf (IC_{50} = 46 nM). Finally, further structural extension to the hinge region by introduction of a solubilizing *N*-methyl amide function in *ortho*-position to the pyridyl nitrogen yielded **4** that has an IC_{50} of 12 nM on C-Raf, 25 nM on B-Raf wild type, and 38 nM on oncogenic B-Raf V600E, as well as high cellular potency and favorable pharmacokinetic properties. At the end of phase II clinical development of **4**, X-ray crystallographic studies of the **4**–C-Raf complex, followed by **4**–B-Raf(wt) and **4**–B-Raf(V600E), finally provided a structurally based rationale for the earlier SAR observations. Compound **4** binds, analogously to **1** and **9**, as a type II inhibitor with the activation loop of B-Raf being in an inactive conformation. The central urea core makes two crucial hydrogen-bond interactions, analogous to **9**: one between one nitrogen atom and the side chain of Glu500, with the ion pair Glu500–Lys482 still being intact, and one between the carbonyl oxygen atom and the backbone amide of Asp593 of the DFG-motif. The 3-trifluoromethyl-4-chloro-phenyl moiety inserts into the hydrophobic deep pocket and makes numerous

hydrophobic contacts. Compound **4** interacts with the hinge region in a bidentate fashion: the backbone of Cys531 makes two hydrogen bonds to the amide nitrogen atom and to the pyridyl nitrogen of the inhibitor [37]. The SAR compound NPV-AFG210 (**29**) can be regarded a direct precursor of **4** and has been crystallized with the Abelson protein kinase [19, 38]. The **29**–Abl complex shows binding of the compound as a type II inhibitor, analogous to **4** in B-Raf, both forming the same crucial interactions between the central urea motif and the protein kinase and anchoring the inhibitor with one hydrogen bond from the pyridyl moiety toward the hinge region [19].

Boehringer-Ingelheim US optimized a new series of potent p38 MAP kinase inhibitors by combining computer-assisted drug design, X-ray crystallography, and chemical design [39]. The design started with an analysis of the ATP binding site of p38 MAP kinase in the inactive conformation and subsequent assembly of an inhibitor that addresses the key interactions of the deep pocket. The generic benzothiophene amide **30** was the initial starting fragment. The crystal structure with p38 MAP kinase shows binding of the ligand to the protein in the inactive state. The amide NH group of **30** makes a hydrogen bond contact with the α C helical Glu71, and the carbonyl oxygen atom forms a hydrogen bond to the backbone NH of Asp168 of the DFG motif. The *tert*-butyl group of the phenylsulfonamide moiety binds into the deep pocket. The benzothiophene moiety does not reach the hinge region, and no hydrogen bond contacts are made with the hinge. Subsequent modification of **30** with a hinge-directed head group led to compound **31**. Compound **31** binds to the DFG-out state of the protein, as well. In contrast to **30**, **31** is less potent. The crystal structure with p38 MAP kinase shows that the benzothiophene is in an energetically less favored conformation. Repositioning of the amide attachment of the hinge-directed pyridyl carboxamide led to compound **32** with higher potency. Both **31** and **32** bind with the amide core in the same manner as generic **30**. The pyridyl head group makes hydrogen bond contact with the backbone NH of Met109 in the hinge region, and the pyridyl carboxamide forms two additional hydrogen bonds: one between the NH and the side-chain hydroxyl group of the gatekeeper Thr106 and the other one between the carbonyl oxygen and a water molecule that connects with the catalytic Lys53 and with Tyr35. Further design to improve potency toward p38 MAP kinase led to the substituted pyridyl **33**. Compound **33** also binds to p38 MAP kinase in an inactive conformation. An additional hydrogen bond contact is made between the cyclopropylamine NH and the backbone carbonyl oxygen of Met109 in the hinge region.

6.5.3

B2B Approach

We find six examples for this type of design: the Abl protein kinase inhibitor nilotinib (AMN107; **8**), the KDR-targeting naphthoylamide **39**, the 2-aminoquinazoline **41** as an inhibitor of Lck, the KDR- and Tie-2-binding urea **34**, the KDR-targeting 2-aminobenzimidazole **34**, and the KDR binding 2-aminobenzoxazole **36** (Figure 6.13).

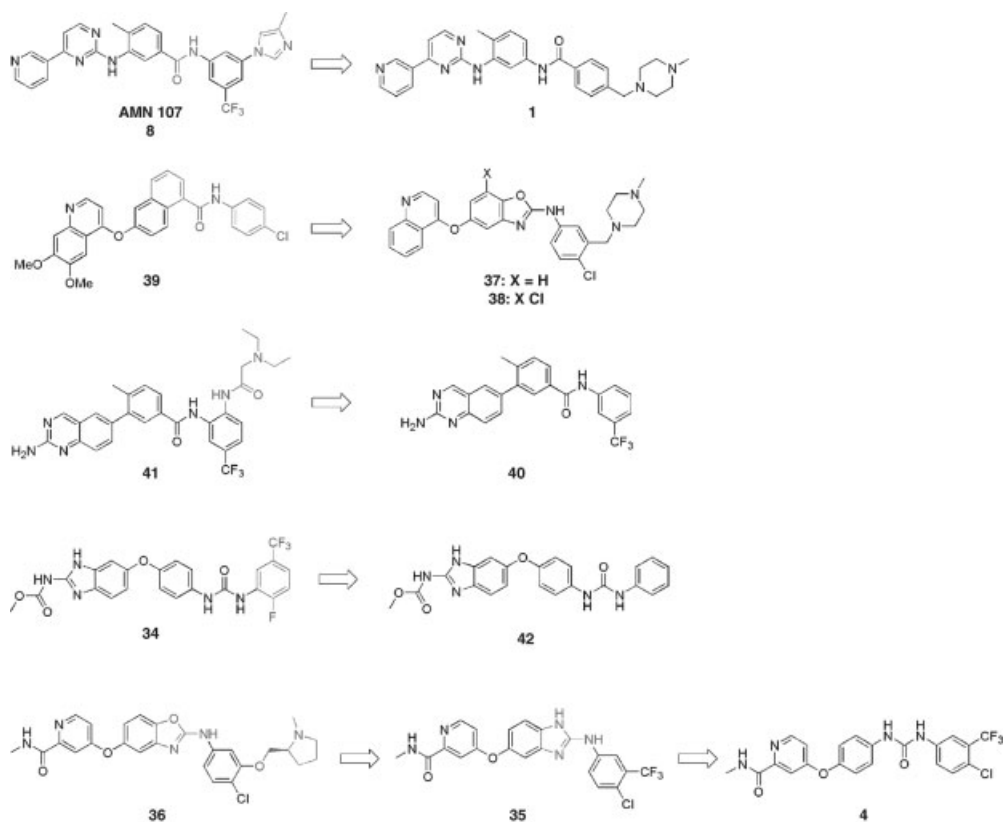


Figure 6.13 Type II inhibitors designed according to the B2B strategy.

Nilotinib (AMN107; **8**) was designed from **1** as a starting point with the intention to gain a more selective and more potent Abl inhibitor with efficacy against Gleevec-resistant Abl mutants [40]. Changing the amide in **1** to the reverse amide and replacing the *N*-methylpiperazinemethyl moiety with a methylimidazole and a trifluoromethyl group yields **8** as a type II inhibitor of Abl. A superimposition of the crystal structures of Abl in complex with **8** and **1** shows that the deep pocket binding portion of **8** is slightly shifted, compared to **1**, resulting in a better hydrophobic contact of the methylimidazole group with the protein. The orthogonal tolyl moiety is tilted slightly, compared to **1**, resulting in the nitrogen atom and the carbonyl oxygen atom of the inverse amide core of **8** to superimpose nicely with the amide of **1**. The hydrogen bond contacts between the inverse amide core and the α C helical Glu286 as well as Asp381 of the DFG-motif are retained, so are the hydrogen bonds to the gatekeeper Thr315 and to Met318 of the hinge region, analogous to **1**. Compound **8** has an IC_{50} of 15 nM toward Abl and is 18-fold more potent than **1** that exhibits an IC_{50} of 280 nM under identical assay conditions. In addition, nilotinib shows high cellular activity against several clinically relevant Gleevec-resistant

mutants of Abl, albeit not against the most prominent mutant T315I, and has been approved in 2007 for the treatment of Gleevec-resistant CML [40].

Amgen Inc. has designed a new class of KDR inhibitors, starting from the previously optimized naphthoylamide **37** that is a 4 nM type I inhibitor of KDR. The chlorine-substituted variant **38** is a putative type II inhibitor of KDR, as suggested by docking studies. Consequently, **37** was subjected to an optimization program that resulted in the development of **39** as a lead compound with a K_i of 0.5 nM toward KDR. The crystal structure of the **39**–KDR complex shows that the inhibitor binds in the type II mode, with the A-loop adopting an inactive conformation. The *p*-chloro substituent occupies the deep pocket, and the amide core is hydrogen bonded to Glu885 in the α C helix and to the backbone amide of Asp1046 of the DFG-motif. Interestingly, simple inversion of the amide function and replacement of the *p*-chloro substituent with hydrogen in **39** leads to a type I inhibitor of KDR (K_i = 6 nM). The hydrogen bond of the amide nitrogen to Glu885 is retained in this compound, but while in **39** the carbonyl oxygen is hydrogen-bonded to the backbone amide of Asp1046 of the DFG-motif, the corresponding hydrogen bond in the type I inhibitor is indirectly facilitated by insertion of a water molecule to bridge the increased distance between the donor and the acceptor. The spatial requirements of the chlorine substituent in **39** are responsible for the conformational shift of the A-loop and an impressive example of how small changes in a molecule may completely change the binding mode [41, 42].

Amgen Inc. has also identified the 2-aminoquinazoline **40** as a highly potent (0.2 nM) but unselective inhibitor of Lck. Optimization of **40** with regard to selectivity and pharmacokinetic properties led to the highly selective Lck-inhibitor **41** with an IC_{50} of 0.5 nM. Crystallographic studies show that both compounds **40** and **41** bind in the same type II mode, with the trifluoromethyl group occupying the deep pocket and the A-loop in an inactive conformation (Figure 6.14). The amide cores are hydrogen bonded to Glu288 of the Glu–Lys ion pair and to the backbone amide of Asp382 of the DFG-motif. The 2-aminoquinazoline scaffold of each compound is fixed at the hinge region by hydrogen bonds of the exocyclic nitrogen atom to the backbone amide of Met319 and of one of the ring nitrogen atoms to the backbone amide of Tyr318.

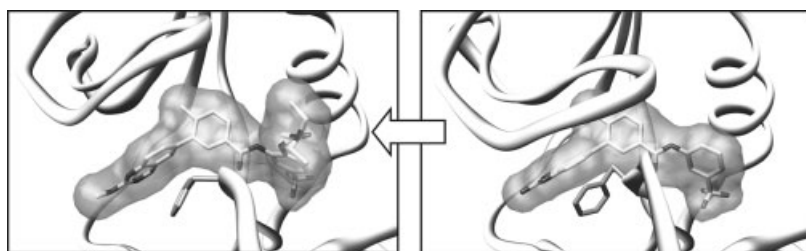


Figure 6.14 Example of a B2B design approach. *Left:* Crystal structure of Lck in complex with **41** (PDB code 2OG8); *right:* in complex with **40** (PDB code 2OFV). The protein

backbone is shown as ribbon; carbon atoms are depicted in light gray and oxygen and nitrogen atoms in dark gray. The ligand surface is emphasized as a transparent Connolly surface.

Introduction of a solubilizing group into **40**, resulting in **41**, not only leads to enhanced oral bioavailability and favorable pharmacokinetic properties but also selectivity toward Lck over KDR is greatly enhanced due to the forced conformational out-of-plane twist of the 2-carboxamide-substituted aryl ring with respect to the central amide [43].

The benzimidazolo-substituted bisaryl urea **42** from GlaxoSmithKline was found to exhibit moderate KDR and weak Tie-2 inhibitory affinity ($IC_{50} = 32$ nM and 3.2 μ M, respectively) [44]. On the basis of the comparison of structural congruencies of **42** with BIRB-796 (**9**) the crystal structure of which in complex with p38 α is known, a binding model of **42** in KDR was established that consists of six subsites. Subsequent modification of these subsites finally resulted in the design of **34** that is a 3.5 nM inhibitor of KDR, and a 6.9 nM inhibitor of Tie-2. **34** designed by the B2B approach that can be regarded as modification of the deep pocket-targeting aryl urea moiety in **42** leads to improved affinity. The crystal structure of **34** in complex with KDR has been solved and shows that the compound binds as a type II inhibitor. The urea core makes hydrogen bond contact with the α C helical Glu885 and the backbone amide of Asp1046 of the DFG-motif. The benzimidazole group acts as a handle for the hinge region, where one of the ring nitrogen atoms makes hydrogen bond contact with the backbone of Cys919.

Amgen Inc. published the first crystal structures of the bioisosteric deep pocket binders **35** and **36** [45]. Although the Raf and KDR inhibitor RAF-265 (formerly CHIR-265) is the first compound to mimic the central urea core of sorafenib (**4**) with a 2-aminobenzimidazole moiety, no crystal structure of RAF-265 has been made public yet that would unambiguously identify it as a type II inhibitor, although docking studies strongly suggest so. Compound **35** was designed using sorafenib (**4**) as template by cyclization and replacing the urea motif of **4** with the bioisosteric 2-aminobenzimidazole core [45]. The crystal structure of **35** in KDR shows that the compound binds as a type II inhibitor with a K_i of 9 nM. The 2-amino function of the benzimidazole core makes hydrogen bond contact with the α C helical Glu885, so does one of the benzimidazole ring nitrogen atoms. The catalytic Glu885–Lys868 salt bridge is kept intact. The second ring nitrogen atom forms a hydrogen bond to the backbone NH of Asp1046 of the DFG-motif. The A-loop is in an inactive conformation, which allows the 3-trifluoromethyl 4-chloro phenyl moiety to occupy the deep pocket. The pyridyl group and the *N*-methylacetamido substituent form hydrogen bonds to the backbone of Cys919 in the hinge region. The overall structure of **35** in KDR very closely resembles the structure of **4** in B-Raf (see Figure 6.15) [37]. Subsequent replacement of the benzimidazole core with a benzoxazole motif and optimization toward cellular potency yielded 2-aminobenzoxazole **36** that has a K_i of 3 nM against KDR and more than 100-fold improved cellular potency [45]. Compound **36** also binds to KDR as a type II inhibitor, as the crystal structure shows (Figure 6.15). Analogous to **35**, the benzoxazole nitrogen atom makes hydrogen bond contact with the backbone amide of Asp1046 of the DFG-motif, and the exocyclic 2-amino group forms a hydrogen bond to the α C helical Glu885. The Glu885–Lys868 remains intact, and the DFG-motif is again in the *out* conformation. The pyridyl head group forms hydrogen bonds to Cys919 in the hinge region. The aryl substituent

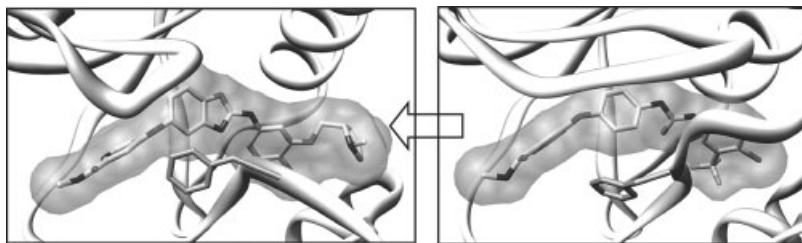


Figure 6.15 Example of a B2B design approach using the bioisosteric principle. *Left*: Crystal structure of KDR in complex with **36** (PDB code 2QU6); *right*: B-Raf in complex with **4** (PDB code 1UWH). The protein backbone is shown as

ribbon; carbon atoms are depicted in light gray and oxygen and nitrogen atoms in dark gray. The ligand surface is emphasized as a transparent Connolly surface.

occupies the deep pocket, with the *N*-methyl pyrrolidine side chain directed toward the solvent-exposed side of the protein.

6.5.4

Hybrid (F2B + B2F) Approach

Although the hybrid approach is the most prominent one, it is also the most difficult approach to categorize compounds. Figure 6.16 shows the protein kinase inhibitors we classify according to this design strategy.

The foremost and also most interesting example of a hybrid design is the dual ErbB-1 (EGF)/ErbB-2 receptor inhibitor lapatinib (**7**). Compound **7** can be regarded as a derivative of erlotinib (**3**), which is a 0.7 nM type I inhibitor (K_i) of the EGF receptor. The core scaffold of both inhibitors is 4-aminoquinazoline. Addition of a *p*-fluorobenzyloxy side chain to the benzamide moiety and replacement of the ethinyl group of **3** with a chlorine atom, as well as replacement of erlotinib's polyether solubilizing groups by one large solubilizing group, led to **7** that is a 3 nM inhibitor (K_i) of the EGF receptor kinase domain and a 13 nM inhibitor (K_i) of ErbB-2 [5]. Compound **7** is a highly selective compound and inhibits only two other protein kinases in the μ M range [1, 2]. The compound binds in the type II mode, but in contrast to the type II inhibitors discussed previously, the A-loop of the EGF receptor kinase domain is not shifted to an inactive conformation and the DFG-motif remains in the *in* conformation (Figure 6.17). The deep pocket is created by a large 7 Å shift of the α C helix in the back of the protein, where the fluorobenzyloxy moiety is binding. The A-loop is not completely in the typical loop-like active state, as observed in the 3-EGF receptor kinase domain complex, but residues 857–863 of the A-loop adopt a semihelical conformation that is tightly packing against the α C helix. Numerous hydrophobic interactions of Phe856 of the DFG-motif, of Leu858, Leu862, and Leu861 with Phe723 in the P-loop, and unpolar residues in the β 3-strand and the α C helix stabilize this conformation and fix the A-loop in an inactive state. The P-loop of the EGF receptor kinase domain is shifted significantly downward to the nucle-

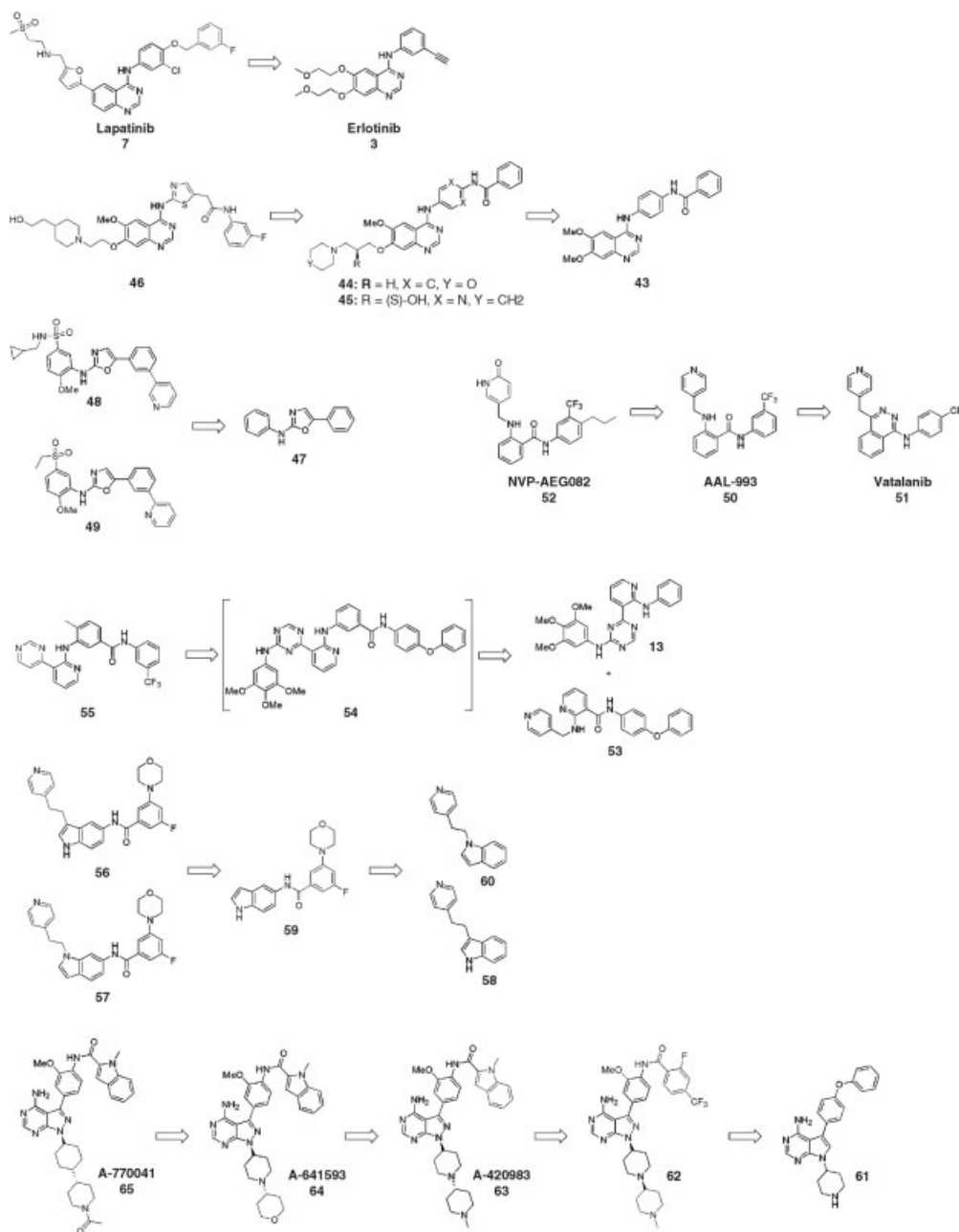


Figure 6.16 Type II inhibitors designed according to the hybrid strategy.

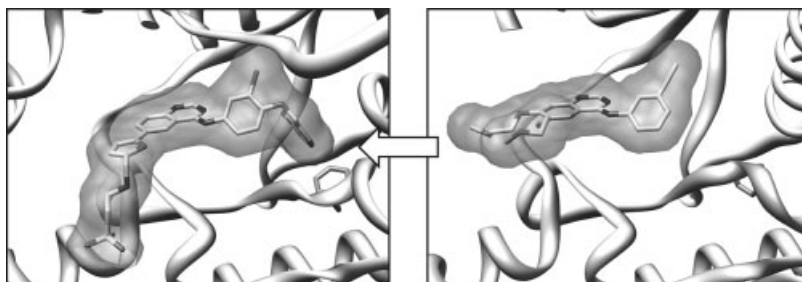


Figure 6.17 Example of a hybrid design approach. *Left:* Crystal structure of the EGF receptor kinase domain in complex with **7** (PDB code 1XKK); *right:* in complex with **3** (PDB code 1M17). The protein backbone is shown as

ribbon; carbon atoms are depicted in light gray and oxygen and nitrogen atoms in dark gray. The ligand surface is emphasized as a transparent Connolly surface. The P-loop is omitted for clarity.

otide binding site, compared to the **3**–EGF receptor kinase domain complex, and prevents access to the ATP binding site. As a consequence of the α C helix shift, the conserved Glu762–Lys745 ion pair is broken and the EGF receptor kinase domain adopts an inactive state. Glu762 is flipped away 9.7 Å from the binding site, pointing outward to the solvent, and the catalytic Lys745 makes a hydrogen bond contact with the side chain of Asp855 of the DFG-motif. The quinazoline core of **7** is anchored to the hinge region by a hydrogen bond of one of the ring nitrogen atoms to the backbone amide of Met793 region, and the second ring nitrogen is indirectly hydrogen bonded to the side chain of the gatekeeper Thr790 via a network of water molecules. The second ring nitrogen atom is hydrogen bonded via a water molecule to Thr854 in the activation loop that precedes the DFG-motif. The solubilizing substituent contributes unpolar interactions and no hydrogen bonds, and the methylsulfone points to the solvent. The binding mechanism of **7** results in an extremely slow dissociation rate of the inhibitor from the kinase: the cellular half-life of the **7**–EGF receptor complex is 300 min, which makes the inhibitor practically irreversible. In contrast, the cellular half-life of the type I inhibitor **3** with the EGF receptor is below 10 min [46]. Due to its high selectivity and exceptional cellular potency, **7** has been approved by the FDA for the treatment of advanced HER-2-positive breast cancer in combination with capecitabine (Xelodal™).

AstraZeneca developed selective Aurora kinase A and B (AurKA/B) inhibitors also based on a 4-aminoquinazoline scaffold, starting from compound **43** that has an IC_{50} of 393 nM toward AurKA [47]. The binding mode of **43** is not known. However, the compound partially fulfils the requirements of a type II pharmacophore model: it has a central amide core and a hydrophobic substituent pointing toward the back of the protein. The introduction of a large solubilizing moiety led to the development of 4-aminoquinazoline **44** that is a 110 nM inhibitor of AurKA. Compared to **44**, the derivative **45** has improved solubility and was used in crystallographic studies with AurKA, but no inhibitory data are reported. The **45**–AurKA complex shows that the inhibitor binds in the type II mode with the benzamide moiety penetrating a newly

created deep pocket. The activation loop of AurKA adopts an inactive conformation. The phenyl ring of Phe274 of the DFG-motif is flipped toward the inhibitor and makes a π -stacking interaction with the pyrimidine ring. The steric demand of the almost linear arrangement of pyrimidine and aryl amide results in a conformational switch of Glu180 in the α C helix away from the binding site outward to the solvent. As a consequence, the conserved Glu180–Lys161 ion pair is broken, and the Lys161 side chain makes hydrogen bond contact with the oxygen atom of the amide and with one of the pyrimidine nitrogen atoms of **45**. Binding of the inhibitor therefore leads to inactivation of AurKA both by a conformational change in the A-loop and by breaking of the Glu–Lys pair. This is similar to the previously discussed 7–EGF receptor kinase domain complex where inactivation results from both the shift of the α C helix and the semihelical structure of the A-loop. Further development of 4-aminoquinazoline **44** with regard to affinity and pharmacokinetic properties led to thiazole **46** that shows an IC_{50} below 1 nM toward AurKA. The binding mode of **46** is not known, as no structural data are available. However, modeling studies as well as the very low affinity and the structural similarity to **45** suggest it to be a type II inhibitor [48]. Compound **46** is a good example of the molecular weight problem arising from the hybrid approach. The compound has a very high molecular weight of 580 Da. Nevertheless, in this case the physicochemical properties are excellent and **46** has entered preclinical development.

The generic oxazole **47** was discovered by GlaxoSmithKline, as a screening hit in a campaign to find inhibitors for the VEGF receptor, and is a 1.2 μ M inhibitor of KDR (VEGF-R2) [49]. The introduction of a pyridine ring for solubility reasons and modification of the anilino moiety with sulphonamide and sulphone groups in **47** led to the derivatives **48** and **49**. From the structures, one would expect both compounds to bind to KDR in the type I mode, with the pyridyl group occupying the solubilizing pocket and the sulphone and sulphonamide reaching the back pocket due to their bent geometry. Crystal structures of the complexes of both compounds with the kinase domain of KDR have been solved and show that **48** and **49** surprisingly address the inactive state of KDR. The aminooxazole core, which can be regarded a bioisosteric replacement for the urea motif, makes hydrogen bond contact with the backbone of Cys917 in the hinge region. The activation loop adopts an inactive conformation, and the DFG-motif is flipped into the *out* conformation. This enables the phenyl ring of Phe1045 of the DFG-motif to make a π -stacking interaction with the pyridyl group that is bound at the entrance to the deep pocket but does not address it. The gatekeeper Val914 is additionally making favorable unpolar interactions with the phenyl ring at the oxazole moiety. In the **48**–KDR kinase domain complex, the Glu883–Lys866 ion pair is retained. In **49**, however, the 2-pyridiyl moiety is disordered in the crystal structure and adopts another orientation toward the solvent. A superimposition of **1** in Abl with **48** in KDR shows that the pyridyl ring in **48** is approximately at the same position as the tolyl group of **1**. The disordered conformation of **49** and the very similar IC_{50} values of both **48** and **49** suggest that hydrophobic interactions of the deep pocket with the compounds do not make significant contributions to the affinity. It may well be that under the crystallization conditions that were applied, both inhibitors may have trapped the DFG-out conformation from an equilibrium between DFG-in and DFG-out, and the crystal

structure accordingly provides a frozen snapshot of this equilibrium. Therefore, **48** and **49** would have to be regarded type I inhibitors. As they are lead structures, further substitution with direction toward the back pocket could lead to type II inhibitors that target the deep pocket and may gain additional affinity. A similar case of freezing out different equilibrium states of different activation loop conformations in the solid state has also been observed for the p38 α MAP kinase [22, 23].

In the search for highly specific second-generation antiangiogenesis inhibitors with improved pharmacokinetic properties and toxicity profile, Novartis developed the amide AAL-993 (**50**) as an inhibitor of KDR (VEGF-R2; IC_{50} = 23 nM), as well as of Flt-1 (VEGF-R1; IC_{50} = 130 nM) and Flt-4 (VEGF-R3; IC_{50} = 18 nM) [50]. The compound was designed by scaffold morphing and subsequent lead optimization from the phthalazine vatalanib (**51**) as starting point. Compound **51** is an inhibitor of all VEGF-R isoforms (IC_{50} (KDR) = 32 nM) and is in phase III clinical trials for the treatment of colorectal cancer [51]. The binding mode of **51** is not known, but the crystal structure of **50** in complex with the KDR kinase domain shows that **50** binds analogously to other deep pocket binders. The trifluoromethyl group penetrates into the deep pocket that has opened up by conformational change of the A-loop into the inactive state. The central inverse amide (compared to **1**) core is hydrogen bonded both to Glu885 of the α C helix, retaining the Glu–Lys ion pair, and to the backbone amide of Asp1046 of the DFG-motif. The inhibitor is anchored to the hinge region via a hydrogen bond between the pyridine nitrogen and the backbone amide of Met919. A slight modification of **50** led to NVP-AEG082 (**52**) that is a 330 nM inhibitor of the Abl kinase, while the activity against KDR is not reported. The crystal structure of Abl in complex with **52** is available and shows that the inhibitor binds analogously to Gleevec (**1**). The A-loop is in an inactive conformation, but in comparison to the **1**–Abl complex adopts a slightly different conformation in the **52**–Abl complex, resulting in a shift of the P-loop, preventing access to the nucleotide binding pocket [19].

In the course of the development of Tie-2 kinase inhibitors **14**, **15**, and **16** (see Figure 6.8), the structure of the initial precursor trimethoxyaminotriazine **13** was combined with the structure of nicotinamide **53**. Compound **53** is a 38 nM type II inhibitor of KDR (IC_{50} for Tie-2 kinase > 25 μ M) and has been crystallized within the KDR kinase domain. The inhibitor binds in the type II binding mode [29]. The two halves of the molecule adopt a perpendicular orientation in the ATP binding site of the KDR kinase domain, with the diphenyl ether moiety penetrating the deep pocket. The pyridine group is oriented toward the hinge region, and the central amide core is in hydrogen bond distance to the DFG-motif. As the **53**–KDR kinase domain structure is not publicly available and in the publication no details are described, it is not clear how the central amide core interacts with the protein. Possibly hydrogen bonds are formed to Asp1044 of the DFG-motif and to the α C helical Glu883, although it is unclear whether the Glu883–Lys866 ion pair is being kept intact. However, the superimposition of both type I inhibitor **13** and type II inhibitor **53** in the KDR kinase domain resulted in the development of an initial hybrid compound **54** that combines the features of both inhibitors and has a molecular weight of 642 Da. Although the designed inhibitor **54** has now considerable activity both against

Tie-2 kinase ($IC_{50} = 85$ nM) and against KDR ($IC_{50} = 38$ nM), the high molecular weight leads to unfavorable pharmacokinetic properties. Trimming **54** with respect to minimizing molecular weight finally yielded the hybrid pyrimidine **55** as a new general type II scaffold of Tie-2 kinase inhibitors. Compound **55** is a multikinase inhibitor with most prominent activity against KDR ($IC_{50} = 4$ nM) and Tie-2 kinase ($IC_{50} = 4$ nM), as well as against Lck, Syk, c-Src, EphB4, c-Kit, and p38 α MAPK kinase with IC_{50} values below 25 nM [29, 52]. The Tie-2 kinase inhibitors **14**, **15**, and **16** can also be regarded as derivatives of **55** in a B2B or hybrid design. However, we classified the design as F2B because the initial starting scaffold for the development was the type I inhibitor **13** [28].

Another example of the hybrid approach are the indoleamides **56** and **57** that have been developed by Astex using a fragment-based approach by an initial F2B design and subsequent B2F modification (Figure 6.16). Compounds **56** and **57** were identified as a novel indole-derived lead series of p38 α MAP kinase inhibitors in an X-ray crystallography fragment-based approach [33, 35]. The generic indole-based fragment hit **58** binds to the ATP binding site of p38 α MAP kinase as a type I inhibitor with very low affinity ($IC_{50} = 35$ μ M). The pyridyl nitrogen makes a hydrogen bond contact with the backbone amide of Met109 in the hinge region, while the indole moiety is accommodated within the unpolar back pocket. The X-ray structure of a second indole-based fragment hit, **59** ($IC_{50} = 162$ μ M), that was generated by rationally elaborating SAR and structural knowledge around **58** with the intention of addressing the DFG-segment of the activation loop, revealed the indole moiety of **59** to be also bound in the hydrophobic back pocket. However, in contrast to generic **58**, the higher decorated **59** lacks the pyridyl group and as such makes no contact with the hinge region. Instead, the inhibitor forms two hydrogen bonds from the central amide core to the backbone amide of Asp168 of the DFG-motif and to the side chain carboxylate of the α C helical Glu171. The activation loop of the kinase is in an inactive conformation, and Phe169 of the DFG-motif moves 11.6 Å toward the nucleotide binding site. The fluoromorpholinophenyl moiety occupies the created deep pocket.

Superimposition of the two crystal structures of the **58**–p38 α and the **59**–p38 α MAP kinase complex showed that the indole moieties of both inhibitors are essentially overlapping and that the indole nitrogen atom of **59** is not directed toward the deep pocket but toward the solvent-accessible front of the kinase, thus offering a vector to address the hinge region. This is supported by the crystal structure of the **60**–p38 α MAP kinase complex where the pyridylethyl moiety that addresses the hinge region is directly attached at the indole nitrogen atom. Consequently, in a B2F strategy the indoleamides **56** and **57** were prepared by conjoining the fragments **58** and **60**, respectively, with the overlapping fragment **59**. The combination of both hinge-addressing moieties and deep pocket-targeting substituents resulted in >100-fold increase in potency (**56**, $IC_{50} = 630$ nM; **57**, $IC_{50} = 340$ nM), compared to the generic fragments, and thus provided a novel lead series of potent type II inhibitors of p38 α MAP kinase. Figure 6.18 shows the crystal structures of **56**–**59** in p38 α MAP kinase.

Another example of a hybrid approach are the pyrazolopyrimidines **62**–**65** from Abbott that were designed as selective inhibitors of Lck [53–56]. Pyrrolopyrimidine **61**

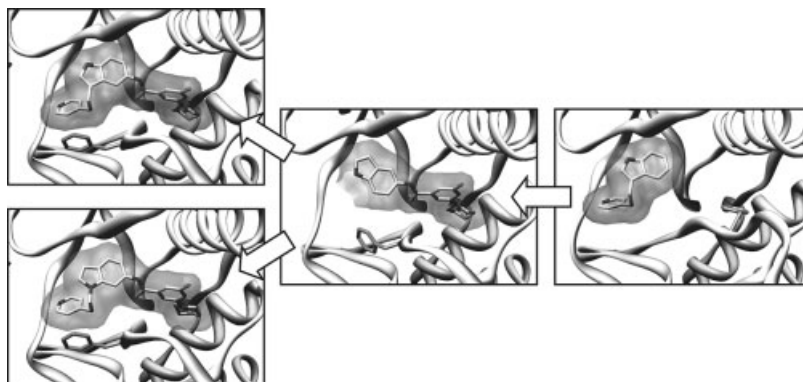


Figure 6.18 Example of hybrid design approach. *Top left:* Crystal structure of p38 α MAP kinase in complex with **56** (PDB code 1WBS); *bottom left:* in complex with **57** (PDB code 1WBT); *middle:* in complex with **59** (PDB code 1WBV); *right:* in complex with **58** (PDB

code 1W84). The protein backbone is shown as ribbon; carbon atoms are depicted in light gray and oxygen and nitrogen atoms in dark gray. The ligand surface is emphasized as a transparent Connolly surface.

is a 141 nM and pyrazolopyrimidine **62** is a 196 nM inhibitor of Lck, respectively. Both compounds show more than 15-fold selectivity for Lck over the related kinases Fyn and c-Src. Both the unpolar phenyl side chains in **61** and **62** and the piperidine moiety in **61** are crucial for selectivity toward Lck. A subsequent development program to further increase selectivity for Lck and to gain *in vivo* potency by improving both affinity and pharmacokinetic properties yielded the indoleamides A-420983 (**63**), A-641593 (**64**), and A-770041 (**65**) that are highly efficacious inhibitors of Lck with IC₅₀ values of 37 nM, 107 nM, and 147 nM, respectively, and show a more than 500-fold selectivity toward Lck over Fyn kinase [53]. The design of the compounds started as a hybrid design with the replacement of the phenoxy group in **61** by an unpolar substituted benzamide and introduction of an additional methoxy group. Furthermore, the pyrrolopyrimidine core was changed to a pyrazolopyrimidine, and the solubilizing piperidine was extended by introducing an additional *N*-methylpiperidine group to yield **62**. In a subsequent B2B approach, benzamide was changed to a *N*-methylindole moiety, resulting in compound **63** that shows a high oral bioavailability and increased *in vivo* potency. Further subtle changes with regard to the solubilizing groups (a kind of “F2F” approach) resulted in **64** and **65** with very high Lck selectivity, high *in vivo* potency, and improved oral bioavailability [53]. Compounds **62–65** fulfill the requirements for a deep pocket binder. They have a central amide core for providing hydrogen bonds to the DFG-motif; the benzamide is methoxy substituted to ensure an orthogonal orientation of the deep pocket-targeting residues, the deep pocket is addressed by a large unpolar group, and the purine ring provides a handle by offering hydrogen bond donors and acceptors toward the hinge region. Compounds **63**, **64**, and **65** have all been crystallized in human Hck, and the structures of the complexes show that the inhibitors indeed bind to the protein kinase in the type II mode. Most interestingly, the binding mode of all three inhibitors in

Hck is analogous to lapatinib (**7**) in the EGF receptor. A superimposition of the structures of the 7-EGF receptor kinase domain complex with the three Hck complexes shows a very good structural agreement. The orthogonally arranged benzamide makes only one hydrogen bond contact with the backbone amide of Asp378 of the DFG-motif, which remains in the *in* conformation. The side chain of Asp378 forms an ion pair with the catalytic Lys269 in the structures of **63** and **65** with Hck. In the structure of **64** with Hck, Lys269 adopts a different conformation to point away from the binding site and makes no ionic contact with Asp378. The *N*-methylindole moieties reaches deep into the back of the protein, leading to a shift in the α C helix toward the back of the protein, as it is also observed in the 7-EGF receptor kinase domain complex. The α C helical Glu284 is flipped away from the binding site. A comparison between the structure of Hck in complex with a type I inhibitor (PG-1009247) and in complex with **65** shows that the α C helix, referenced to the backbone C α of Glu284, is shifted 5.62 Å toward the back of the protein kinase, and the side chain carboxylate moves 9.27 Å away from the binding site. In addition, the helix movement and the DFG-in conformation induces residues 378–385 of the activation loop to adopt a semihelical inactive conformation that is making unpolar interactions with the P-loop as well as the β 2-strand and the α C helix. No structural data are available for **62**, but the structural similarity with the successor compounds of known type II inhibition suggests that **62** is also a deep pocket binder.

6.6

Comparative Analysis of the Different Design Strategies

The different types of design approaches can be expected to have different outcomes for the properties of the resulting inhibitors. The “rule of five” provides a framework to estimate the oral bioavailability for a small-molecule inhibitor [57]. It states that the likelihood of a small molecule to show oral absorption is high if the *molecular weight* does not exceed 500 Da; the number of *hydrogen bond donors* (HBDs) as the sum of amino and hydroxyl groups does not exceed 5; the number of *hydrogen bond acceptors* (HBAs) as the sum of nitrogen and oxygen atoms does not exceed 10; and the partition coefficient water–octanol *clog P* is below 5. This has been further extended by introducing the *number of rotatable bonds* (NROTs) that should not exceed 7 [58]. Furthermore, the *polar surface area* (PSA) is an important property of a compound that is defined as the sum of surfaces of polar atoms in a compound and provides good correlation with oral bioavailability. PSA values larger than 100–140 Å² are reported likely to have low oral bioavailabilities [59, 60]. As another important parameter, the *ligand efficiency* (LE) has been introduced. It states the binding energy per nonhydrogen atom of a ligand and normalizes the potency and molecular mass of a compound to provide a comparison between different inhibitors of varying molecular masses and potencies. Optimization of a compound series to maximize ligand efficiency instead of affinity is more useful, as it maximizes potency while keeping the number of nonhydrogen atoms and therefore the molecular weight as low as possible [61, 62].

It is instructive to analyze the changes in selected properties for different types of designs when transgressing from the initial compound to the final inhibitor). The properties we find useful to analyze in this respect are as follows:

- **Molecular weight:** A large molecular weight decreases the possibility of passive transport through the cellular membrane; a value of up to 550 Da is still reasonable.
- **PSA:** We define values between 50 and 80 Å² as the range for a lead-like structure and values between 80 and 100 Å² as desirable for a drug-like compound or final drug.
- **Alog P:** Although most drugs and drug-like compounds contain at least one ionizable functionality, we regard the Alog *P* of an uncharged molecule as a better and more comparable measure for the lipophilicity of a compound in our analysis. Some compounds are developed for oral administration where a pH of 5.5 is found for gastrointestinal absorption, while others are intended for intravenous administration for which the blood pH of 7.4 is relevant. Therefore, calculation of the more relevant log *D* at different pH values makes it difficult to compare the compounds discussed in this chapter.
- **LE:** Expressed as the binding energy per atom $\Delta g = -RT \ln K_d / N_{\text{nonhydrogen atom}}$ in kcal/mol. This directly relates to the maximum achievable binding energy from burying the surface area per single heavy atom and is a chemical scaffold-independent measure for the fit of a compound in the protein binding site [62].

The following section provides a comparison of aforementioned properties within the different design approaches. We find it to be instructive to compare the relative percentile changes in properties between the precursor and the final compounds. Figures 6.19–6.22 show the relative changes in molecular weight, Alog *P*, polar surface area, and ligand efficiency in percentage.

The relative changes in molecular weight are prominently different for the design approaches (Figure 6.19). For compounds designed according to the B2B approach, the changes are small and the values are clustered, ranging from 3% for benzimidazole **35** to 30% **41** (Figure 6.16). The absolute values range between 461.8 Da for **35** and 550.6 Da for **41**, respectively (Table 6.3). This is understandable as only subtle changes are introduced in the deep pocket-targeting moieties. A different picture emerges from the B2F, F2B, and hybrid approaches, where more significant and widely distributed changes are observed. In the B2F approach, the changes range from 12% for NVP-AFG210 (**29**) to 72% for BIRB-796 (**9**). The absolute values range between 41 Da for **29** and 175 Da for benzothiophene **33**. The largest change is observed for **9**. The F2B approach shows changes ranging from 3% for **11** to 120% for amide **22**. The absolute values range from 400 Da for urea **23** to 583 for MPAQ (**19**). The hybrid approach leads to similarly distributed changes in molecular weight from 7% for AAL-993 (**50**) to 102% for oxazole **48**. Absolute values are in the range from 339 Da for **59** to 627 Da for pyrazolopyrimidine **62** (Table 6.3). The introduction of additional substituents, either of unpolar nature to address the deep pocket or polar groups to address the hinge region and to improve physicochemical properties, leads to larger changes in molecular weight. In the B2F design, **9** is an exception as all other

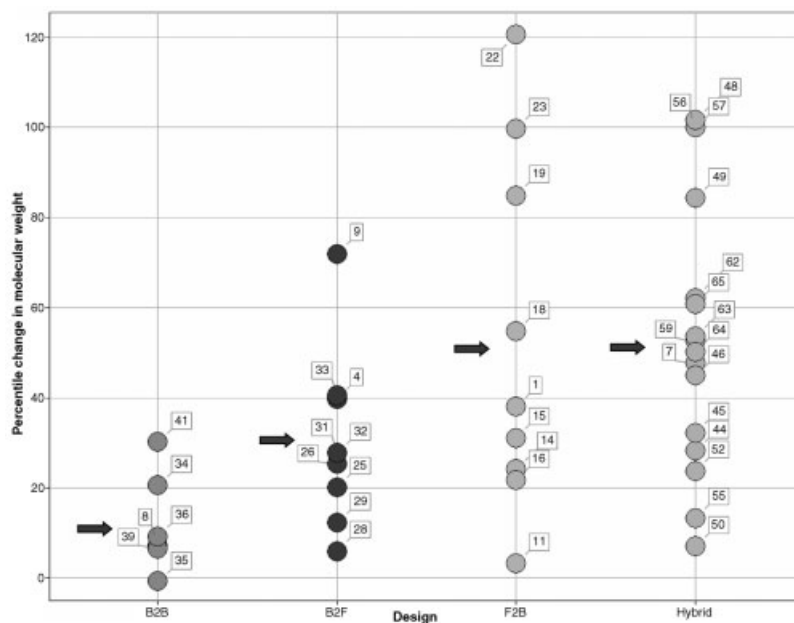


Figure 6.19 Comparative analysis of molecular weight for the different design strategies. Percentile changes in molecular weight of precursors and final type II inhibitors are shown, grouped according to the design principle.

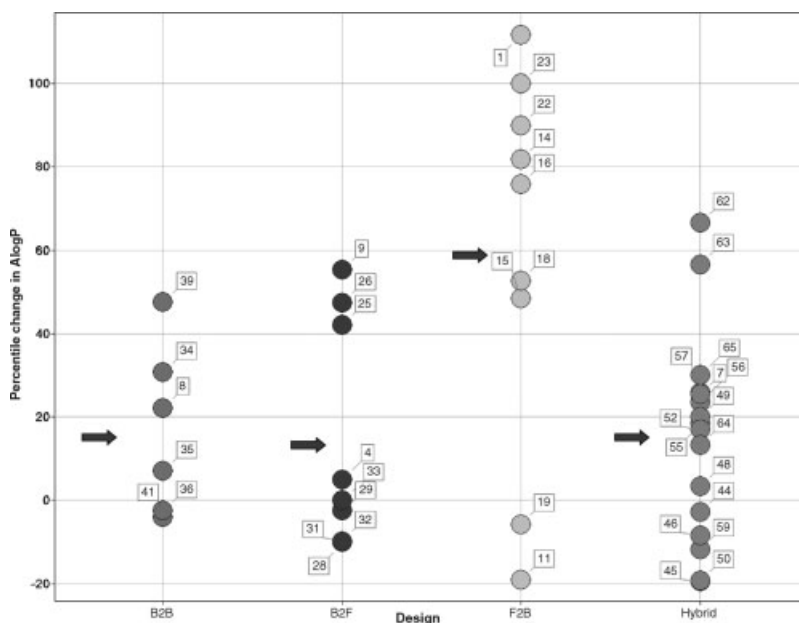


Figure 6.20 Comparative analysis of Alog P for the different design strategies. Percentile changes in calculated Alog P of precursors and final type II inhibitors are shown, grouped according to the design principle.

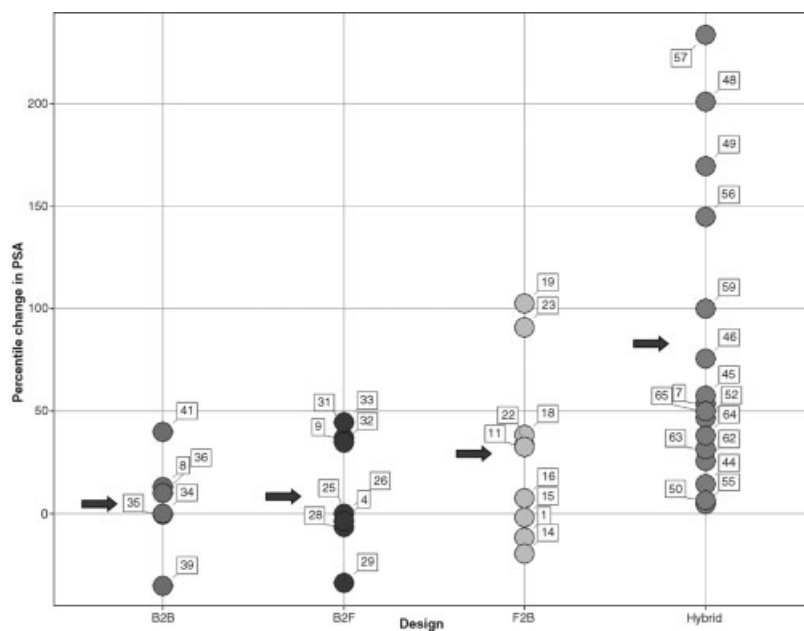


Figure 6.21 Comparative Analysis of polar surface area for the different design strategies. Percentile changes in calculated PSA of precursors and final type II inhibitors are shown, grouped according to the design principle.

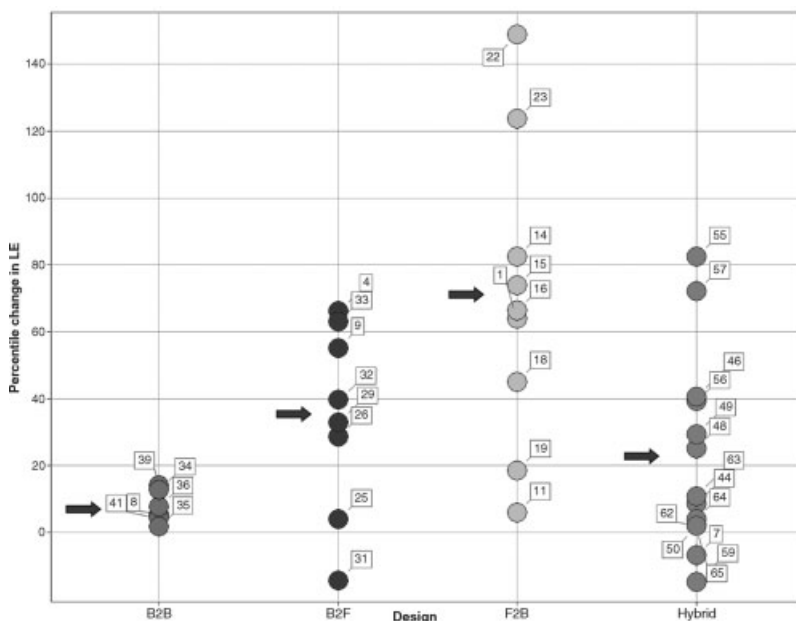


Figure 6.22 Comparative analysis of ligand efficiency for the different design strategies. Percentile changes in LE of precursors and final type II inhibitors are shown, grouped according to the design principle.

Table 6.3 Selected properties for precursor compounds and final type II inhibitors.

No.	Name	MW (Da)	Change in MW (%)	Alog P	Change in Alog P (%)	PSA (Å ²)	Change in PSA (%)	LE (kcal/ mol)	Change in LE (%)	Design
1	Gleevec	493.61		3.60		86.30		0.237		
3	Erlotinib	393.44		4.30		74.70		0.292		
4	Sorafenib	464.83	39.8	4.20	5.00	92.40	−3.45	0.253	66.071	B2F
7	Lapatinib	581.07	47.7	5.40	25.58	114.70	53.55	0.272	−6.904	Hybrid
8	AMN107	529.53	7.3	4.40	22.22	97.60	13.09	0.250	5.440	B2B
9	BIRB-796	527.67	72.0	5.90	55.26	80.70	36.78	0.319	55.101	B2F
10	PAP	357.38		1.70		97.60		0.144		
11		456.43	3.4	3.40	−19.05	104.40	33.16	0.258	6.004	F2B
12		441.32		4.20		78.40		0.244		
13		430.47		3.30		103.30		0.147		
14		534.59	24.2	6.00	81.82	83.00	−19.65	0.268	82.482	F2B
15		564.57	31.2	4.90	48.48	101.50	−1.74	0.255	73.835	F2B
16		524.62	21.9	5.80	75.76	111.20	7.65	0.244	66.395	F2B
17		347.37		3.60		83.40		0.191		
18		537.47	54.7	5.50	52.78	115.30	38.25	0.277	44.983	F2B
19	MPAQ	583.69	84.9	3.30	−5.71	114.00	102.49	0.236	18.509	F2B
20		315.76		3.50		56.30		0.199		
21		200.24		2.00		48.10		0.092		
22		441.89	120.7	3.80	90.00	63.70	32.43	0.229	149.028	F2B
23		399.88	99.7	4.00	100.00	91.90	91.06	0.206	123.694	F2B
24		306.80		3.80		59.00		0.206		
25		368.87	20.2	5.40	42.11	59.00	0.00	0.214	3.900	B2F
26		384.48	25.3	5.60	47.37	59.00	0.00	0.265	28.580	B2F
27		332.42		4.00		95.70		0.152		
28		352.39	6.0	3.60	−10.00	89.30	−6.69			B2F
29	NVP- AFG210	373.33	12.3	3.90	−2.50	63.30	−33.86	0.202	32.869	B2F
30		432.56		4.10		121.10		0.209		
31		552.67	27.8	3.70	−9.76	163.10	34.68	0.179	−14.321	B2F
32		552.67	27.8	3.70	−9.76	163.10	34.68	0.292	39.576	B2F
33		607.75	40.5	4.10	0.00	175.10	44.59	0.341	63.117	B2F
34		503.41	20.6	5.10	30.77	117.40	0.00	0.270	12.823	B2B
35		461.83	−0.6	4.50	7.14	91.90	−0.54	0.257	1.763	B2B
36		507.98	9.3	4.10	−2.38	101.80	10.17	0.272	7.601	B2B
38		454.87		4.00		107.70		0.260		
39		484.94	6.6	5.90	47.50	69.70	−35.28	0.297	14.054	B2B
40		422.41		4.90		80.90		0.285		
41		550.58	30.3	4.70	−4.08	113.20	39.93	0.297	4.262	B2B
42		417.42		3.90		117.40		0.239		
43		400.44		3.60		85.40		0.204		
44	ZM447439	513.60	28.3	3.50	−2.78	97.80	14.52	0.222	8.633	Hybrid
45	HPM	529.60	32.3	2.90	−19.44	134.60	57.61			Hybrid
47		236.27		3.00		38.10		0.189		
48		476.55	101.7	3.10	3.33	114.70	201.05	0.236	25.134	Hybrid

Table 6.3 (Continued)

No.	Name	MW (Da)	Change in MW (%)	Alog P	Change in Alog P (%)	PSA (Å ²)	Change in PSA (%)	LE (kcal/ mol)	Change in LE (%)	Design
49		435.50	84.3	3.60	20.00	102.70	169.55	0.244	29.333	Hybrid
50	AAL-993	371.36	7.1	3.80	−19.15	54.00	6.51	0.244	1.914	Hybrid
51	Vatalanib	346.82		4.70		50.70		0.239		
52	NVP- AEG082	429.44	23.8	5.50	17.02	74.30	46.55			Hybrid
53		396.45		3.80		76.10		0.147		
55		449.44	13.4	4.50	18.42	79.80	4.86	0.268	82.482	Hybrid
56		444.51	100.0	4.20	23.53	70.30	144.95	0.198	39.155	Hybrid
57		444.51	100.0	3.90	25.81	59.40	233.71	0.206	72.174	Hybrid
58		222.29		3.40		28.70		0.142		
59		339.37	52.7	3.00	−11.76	57.40	100.00	0.121	−14.934	Hybrid
60		222.29		3.10		17.80		0.120		
61		386.46		3.00		90.90		0.214		
62		626.66	62.2	5.00	66.67	114.40	25.85	0.219	2.132	Hybrid
63	A-420983	593.74	53.6	4.70	56.67	119.40	31.35	0.237	10.794	Hybrid
64	A-641593	580.69	50.3	3.40	13.33	125.40	37.95	0.222	3.919	Hybrid
65	A-770041	621.75	60.9	3.90	30.00	136.40	50.06	0.218	1.863	Hybrid

compounds exhibit small changes. The introduction of the morpholino-ethoxy function in **9** leads to a large increase in molecular weight. A comparison of the mean values shows that the B2B design changes the molecular weight on average only 5%, the B2F approach 12%, the F2B design 30%, and the hybrid approach 78% (see Table 6.4).

The changes in Alog *P* are also distinctively different for the various design strategies. Changes are moderate for the B2B design and range from −4% for the diethylamino-functionalized aminoquinazoline **41** to 49% for naphthoylamide **39** (Figure 6.20). The absolute values for Alog *P* range from 4.1 for benzoxazole **36** to 5.9 for **39** (Table 6.3). The B2F design shows a very similar picture. However, two distinct clusters can be identified. Only small changes are observed for sorafenib (**4**) and its precursors **27** and **28**, and for thiophenes **30–33**, ranging from −10% for **28** as well

Table 6.4 Comparison of mean percentile changes in molecular weight, Alog *P*, PSA, and LE for the discussed design principles.

	B2B	B2F	F2B	Hybrid
Molecular weight	12%	30%	53%	54%
Alog <i>P</i>	17%	13%	60%	15%
PSA	5%	12%	30%	78%
LE	8%	34%	70%	21%

as **31** and **32**, up to 5% for **4**. The other cluster consists of BIRB-769 (**9**) and its precursor compounds **25** and **26**, where changes range from 42% for **25** to 55% for **9**. The total change in Alog *P* for the B2F design is very similar to the B2B approach, ranging from –10% to 55%. Absolute Alog *P* values are in between 3.6 for **28** and 5.9 for **9**. Also, the hybrid design leads to rather moderate changes in Alog *P*, ranging from a decrease of –19% for the Aurora inhibitor **45** to an increase of 66% for pyrazolopyrimidine **62**. Absolute values are in the range of 3 for indoleamide **59** to 5.5 for NVP-AEG082 (**52**). The B2B design makes changes only in the deep pocket-targeting moieties. As these changes are mainly of lipophilic nature, the Alog *P* generally increases, albeit moderately, as the precursor compounds are previously optimized structures with intrinsic high lipophilicity. Analogously, the B2F design starts from highly lipophilic molecules binding in the deep pocket that are modified with small polar hinge binding head groups compared to the lipophilic scaffold. These do not contribute much change in Alog *P*. The hybrid design includes both unpolar groups that increase Alog *P* and polar functionalities that roughly compensate the change. Therefore, changes in Alog *P* are moderate and clustered. In contrast, the F2B design results in large changes in Alog *P*. Two groups can be distinguished. The Abl inhibitor **11** and MPAQ (**19**) show improvement of Alog *P* by –20% and –6%, respectively. The values in the upper group range from 48% for **15** to 112% for Gleevec (**1**). In general, the changes in the F2B approach are more prominent than in the other three approaches. The introduction of large lipophilic moieties to address the deep pocket, starting from precursors that include polar hinge binding, increase the Alog *P*. This is reflected in the comparison of the mean values for the four approaches: 17% for B2B, 13% for B2F, 15% for the hybrid design, but 50% for the F2B approach (see Table 6.4).

Changes in polar surface area are more clustered for the B2B, the B2F, and the F2B approaches, while here the hybrid design stands out (Figure 6.21). The B2B design changes PSA in a range from –35% for **39** to 40% for **41**. Absolute values range from 70 Å² for **41** to 117 Å² for **34**. The B2F approach shows the same picture: changes are in the range from –34% for **29** to 45% for **33**. Absolute values range from 59 Å² for **25** and **26** to 175 Å² for **33**. In these approaches, either lipophilic scaffolds are modified with small polar hinge binding groups or unpolar functionalities are added to drug-like molecules, which in both cases lead to an increase in molecular surface area and only subtle increases in PSA. For the F2B design, the changes are more widely distributed and the increase in PSA is larger, ranging from –20% for **14** to 103% for MPAQ (**19**). As a separate group, **23** and **19** show a 100% increase in PSA compared to their precursors. The other group is more clustered and shows smaller changes ranging up to 50% increase. Absolute values are calculated from 64 Å² for **22** to 115 Å² for **18**. In contrast to these approaches, the hybrid design shows much more distributed changes and generally strong increase in the PSA. The changes range from 5% for Tie-2 inhibitor **55** to 234% for indole **57**. Absolute values are calculated to be in the range from 54 Å² for AAL-993 (**50**) to 136 Å² for A-770041 (**65**). The hybrid design utilizes changes at both ends of the molecule, in the hinge region and in the deep pocket. These changes lead to a general increase in molecular surface area, and introduction of polar atoms by solubilizing groups, and mainly by amide functions or

heterocyclic moieties, leads to significant increases in the PSA. The mean values for all four strategies reflect the differences: 5% for B2B, 12% for B2F, 30% for F2B, but 78% for the hybrid design (see Table 6.4).

The three parameters of molecular weight, Alog *P*, and PSA are important for physicochemical properties of a drug. However, a comparison of the ligand efficiencies (LE) for the four design strategies gives a direct measure of the improvement (or decline) in the affinity of a compound for its target, related to the molecular weight (Figure 6.22). Also, this plot has to be read differently from the others. In this case, an increase in percentile LE is advantageous, as it means that affinity of the compound for the target increases. The ligand efficiencies for the B2B design are observed in a very narrow range, from 2% for **35** to 14% for **39**. The B2B approach changes only very little the affinities and the molecular weight of the designed compound, compared to the precursor that is already a drug-like molecule, reflecting the intention of mainly improving both selectivity and cellular potency. The B2F approach shows a wider distribution in LE, ranging from –14% for **31** to 66% for sorafenib (**4**). These compounds already gain much affinity by the good fit of unpolar moieties inside the deep pocket. The introduction of hinge-directed groups that provide hydrogen bonds additionally improves affinity. Since the introduced groups are small, molecular weight does not change very much, leading to a high LE. A very similar picture can be seen in the hybrid approach. Here, the differences in LE range from –15% for **59** to 83% for **55**. Changes in hinge- and deep pocket-targeting residues lead both to an increase in molecular weight and to an increase in affinity, resulting in generally improved LE. In contrast, the F2B design leads to a wide distribution of percentile LE, as well as very high LE. They range from 6% for **11** to 149% for **22**. The latter, as well as **23** with 124% change, are impressive examples of how the fragment-based design approach by Astex led to a significant improvement in affinity. Generally, the F2B design always leads to an improvement in LE.

Again, these observations are supported by the mean values of changes in LE: 8% for B2B, 34% for B2F, 21% for hybrid design, and 70% for F2B (see Table 6.4).

6.7

Conclusions and Outlook

In the past 5 years, an increasing number of protein kinase inhibitors have emerged that target the inactive form of a kinase. For many of these type II inhibitors, structural information is available through the crystal structures of their complexes with protein kinases. So far, a limited number of compounds are available and 12 kinases have been identified that are inhibited in the inactive state, notably the Abelson protein kinase, the VEGF receptor, p38 MAP kinase, B-Raf, and Tie-2, among others. As the number of structures in the Protein Data Bank increases, more type II inhibitors will be identified, so will be other protein kinases that can be inhibited in the inactive state. Since the marketing of Gleevec, the hallmark example

of type II inhibitors, other compounds have been designed by various approaches that specifically target the inactive state. In this chapter, we have worked out for the first time a classification of design strategies to generate type II inhibitors, on the basis of the crystal structures of known deep pocket binders. These four design strategies – the front-to-back, the back-to-front, the and the hybrid back-to-back approach – are a useful tool to understand and characterize the underlying principles of design and to install new ideas for assembling type II inhibitors. As the wealth of structural data increases, a reevaluation of the current classification will follow in a few years to address the upcoming results.

Both from the analysis of important molecular properties such as molecular weight, polar surface area, and lipophilicity and from the experimental ligand efficiency, we draw conclusions and recommendations that we hope to have an impact on the future design of protein kinase inhibitors. The “classical” design approach of building a kinase inhibitor from the “front” (the hinge region) of the protein toward the “back” (the deep pocket), the front-to-back approach, and modification of a compound at both these ends at the same time in the hybrid approach, both seem to be flawed. Large increases in molecular weight are observed, so are significant increases in polar surface area, which lead to unfavorable physicochemical properties. However, ligand efficiency is increasing, which is definitely a positive result, but this in itself may not be sufficient to counter the physicochemical problems in later development. Building an inhibitor by starting from the deep pocket (the back-to-front design) and by changing the fit of a compound in the deep pocket (the back-to-back approach) seems to us a more promising strategy in designing type II inhibitors. Changes in molecular weight, PSA, and also Alog *P* are small to moderate, thus avoiding physicochemical problems. Ligand efficiency is also increasing, although moderately in the case of the B2B approach. Yet we do not necessarily see this as a disadvantage, as the B2B approach starts from optimized structures and dramatic changes in affinity are not expected.

Each of the approaches discussed herein resulted in one drug each on the market so far: the F2B approach yielded Gleevec (1); the B2F approach resulted in sorafenib (4); lapatinib (7) came from an hybrid design; and nilotinib (8) resulted from a B2B approach. Obviously, each approach has had its own merits, resulting in the successful design of clinically relevant inhibitors. Nevertheless, the number of examples of marketed drugs and that of deep pocket binders in general is rather limited at present. The future will show which of these approaches is indeed successful in an industrial setting.

On the basis of our analysis, we suggest initiating the design of a deep pocket binder from fragments or small lead-like structures in a B2F approach to generate molecules with high ligand efficiency, selectivity, and reasonable physicochemical properties. This is subsequently followed by a fine-tuning in a B2B design to improve the ligand efficiency and, more importantly, the selectivity of the initial inhibitor to a lead structure by adjusting the fit of the molecule into the deep pocket of the desired target kinase. This strategy has also another advantage: the repurposing of the deep pocket-targeting scaffold. By varying only the deep pocket binding moieties, it is possible to change the selectivity of the same compound class

from one kinase target to the other, without having to go through the tedious process of starting with a hit structure.

We believe that one tends to oversimplify the binding of a protein kinase inhibitor if focusing solely on the ATP binding site, as described in the classical pharmacophore model, and considering hinge binding as the primary important feature of a ligand. The type II inhibitor class indicates that hinge-addressing residues act more as an anchor to direct the compound into a bioactive conformation, and they may not even be required at all for a reasonably potent inhibitor. Affinity and selectivity in type II inhibition almost exclusively result from fulfilling the requirements of the deep pocket pharmacophore and rely on the fit in the deep pocket of a given kinase target. As more and more type II inhibitors become known that all target the inactive state of kinases and bind in an extended ATP binding site, one is prone to a certain reductionism when focusing on hinge-directed binding and as such may lose sight of new opportunities in inhibitor design. Our deeper understanding of protein kinases and inhibition principles is just beginning.

We are convinced that a sound interplay of creative design, that is, the application of medicinal chemistry knowledge and intellect, biological target profiling by modern methods, and structure-based techniques both in solid state and in solution, that is, X-ray crystallography and NMR-spectroscopy, are the essential tools to discover and design new clinically relevant protein kinase inhibitors.

Abbreviations

ErbB	erythroblastoma virus gene B/human epidermal growth factor receptor kinase
EGFR	epidermal growth factor receptor
ATP	adenosine triphosphate
ADP	adenosine diphosphate
Abl	Abelson tyrosine kinase
Bcr-Abl	protein encoded by breakpoint cluster region–Abelson fusion gene (tyrosine kinase)
c-Kit	stem cell factor receptor tyrosine kinase
c-Src	tyrosine kinase oncogene product of Schmidt–Ruppin avian sarcoma virus
Lck	lymphocyte-specific kinase
Hck	member of the Src-family of cytoplasmic tyrosine kinases
Tie-2	tunic internal endothelial cell receptor (ligand: angiopoietin) kinase
p38 α MAP kinase	p38 α mitogen-activated protein kinase
CML	chronic myelogenous leukemia
GIST	gastrointestinal tumor
NSCLC	nonsmall-cell lung cancer
RCC	renal cell carcinoma
RTK	receptor tyrosine kinase

VEGF-R	vascular endothelial growth factor receptor tyrosine kinase
PDGF-R	platelet-derived growth factor receptor tyrosine kinase
Flt-3	fms-like tyrosine kinase
AurK	Aurora kinase family of serine/threonine kinases
PKA	protein kinase A
Fms/CSFR	colony-stimulating factor-1 receptor
CDK	cyclin-dependent kinases
FGFR1	fibroblast growth factor receptor tyrosine kinase
PKC	protein kinase C
PAP	phenylaminopyrimidine
SAR	structure–activity relationship
Syk	spleen tyrosine kinase
EphB4	ephrin receptor
Fyn	member of the Src-family of cytoplasmic tyrosine kinases
TK	tyrosine kinase

Acknowledgments

The authors highly appreciate the support from Dr. Heiko Walch for the survey displayed in Figure 6.5 and Dr. Joachim Vogt for various discussions on protein kinase structures and additional computational support.

References

- 1 Fabian, M.A., Biggs, W.H., III, Treiber, D.K. *et al.* (2005) A small molecule–kinase interaction map for clinical kinase inhibitors. *Nature Biotechnology*, **23** (3), 329–336.
- 2 Karaman, M.W., Herrgard, S., Treiber, D.K. *et al.* (2008) A quantitative analysis of kinase inhibitor selectivity. *Nature Biotechnology*, **26** (1), 127–132.
- 3 Collins, I. and Workman, P. (2006) New approaches to molecular cancer therapeutics. *Nature Chemical Biology*, **2** (12), 689–700.
- 4 Sebolt-Leopold, J.S. and English, J.M. (2006) Mechanisms of drug inhibition of signalling molecules. *Nature*, **441**, 457–462.
- 5 Stamos, J., Sliwkowski, M.X., and Eigenbrot, C. (2002) Structure of the epidermal growth factor receptor kinase domain alone and in complex with a 4-anilinoquinazoline inhibitor. *The Journal of Biological Chemistry*, **277** (48), 46265–46272.
- 6 Liu, Y. and Gray, N.S. (2006) Rational design of inhibitors that bind to inactive kinase conformations. *Nature Chemical Biology*, **2** (7), 358–364.
- 7 Backes, A.C., Zech, B., Felber, B., Klebl, B., and Müller, G. (2008) Small-molecule inhibitors binding to protein kinases. Part I. Exceptions from the traditional pharmacophore approach of type I inhibition. *Expert Opinion on Drug Discovery*, **3** (12), 1409–1425; Backes, A.C., Zech, B., Felber, B., Klebl, B., and Müller, G. (2008) Small-molecule inhibitors binding to protein kinases. Part II. The novel pharmacophore approach of type II and type III inhibition. *Expert Opinion on Drug Discovery*, **3** (12), 1427–1449.
- 8 Traxler, P.M. (1997) Protein tyrosine kinase inhibitors in cancer treatment.

- Expert Opinion on Therapeutic Patents*, 7 (6), 571–588.
- 9 Regan, J., Breitfelder, S., Cirillo, P. *et al.* (2002) Pyrazole urea-based inhibitors of p38 MAP kinase: from lead compound to clinical candidate. *Journal of Medicinal Chemistry*, 45 (14), 2994–3008.
 - 10 Atwell, S., Adams, J.M., Badger, J. *et al.* (2004) A novel mode of Gleevec binding is revealed by the structure of spleen tyrosine kinase. *The Journal of Biological Chemistry*, 279 (53), 55827–55832.
 - 11 Pargellis, C., Tong, L., Churchill, L. *et al.* (2002) Inhibition of p38 MAP kinase by utilizing a novel allosteric binding site. *Nature Structural & Molecular Biology*, 9 (4), 268–272.
 - 12 Davidson, W., Frego, L., Peet, G.W. *et al.* (2004) Discovery and characterization of a substrate selective p38 α inhibitor. *Biochemistry*, 43 (37), 11658–11671.
 - 13 Ohren, J.F., Chen, H., Pavlovsky, A. *et al.* (2004) Structures of human MAP kinase kinase 1 (MEK1) and MEK2 describe novel noncompetitive kinase inhibition. *Nature Structural & Molecular Biology*, 11 (12), 1192–1197.
 - 14 Adrian, F.J., Ding, Q., Sim, T. *et al.* (2006) Allosteric inhibitors of Bcr-Abl-dependent cell proliferation. *Nature Chemical Biology*, 2 (2), 95–102.
 - 15 Lindsley, C.W., Zhao, Z., Leister, W.H. *et al.* (2005) Allosteric Akt (PKB) inhibitors: discovery and SAR of isozyme selective inhibitors. *Bioorganic & Medicinal Chemistry Letters*, 15, 761–764.
 - 16 Gumireddy, K., Baker, S.J., Cosenza, S.C. *et al.* (2005) A non-ATP-competitive inhibitor of BCR-ABL overrides imatinib resistance. *Proceedings of the National Academy of Sciences of the United States of America*, 102 (6), 1992–1997.
 - 17 Nagar, B., Bornmann, W.G., Pellicena, P. *et al.* (2002) Crystal structures of the kinase domain of c-Abl in complex with the small molecule inhibitors PD173955 and imatinib (STI-571). *Cancer Research*, 62 (15), 4236–4243.
 - 18 Schindler, T., Bornmann, W., Pellicena, P. *et al.* (2000) Structural mechanism for STI-571 inhibition of Abelson tyrosine kinase. *Science*, 289, 1938–1942.
 - 19 Cowan-Jacob, S.W., Fendrich, G., Floersheimer, A. *et al.* (2007) Structural biology contributions to the discovery of drugs to treat chronic myelogenous leukaemia. *Acta Crystallographica, Section D: Biological Crystallography*, D63, 80–93.
 - 20 Levinson, N.M., Kuchment, O., Shen, K. *et al.* (2006) A src-like inactive conformation in the Abl tyrosine kinase domain. *PLoS Biology*, 4 (5), 753–767.
 - 21 Hubbard, S.R., Wei, L., Ellis, L., and Hendrickson, W.A. (1994) Crystal structure of the tyrosine kinase domain of the human insulin receptor. *Nature*, 372 (6508), 746–754.
 - 22 Sullivan, J.E., Holdgate, G.A., Campbell, D. *et al.* (2005) Prevention of MKK6-dependent activation by binding to p38 α MAP kinase. *Biochemistry*, 44 (50), 16475–16490.
 - 23 Vogtherr, M., Saxena, K., Hoelder, S. *et al.* (2006) NMR characterization of kinase p38 dynamics in free and ligand-bound forms. *Angewandte Chemie – International Edition*, 45, 993–997.
 - 24 Okram, B., Nagle, A., Adrian, F.J. *et al.* (2006) A general strategy for creating “inactive-conformation” Abl inhibitors. *Chemistry & Biology*, 13, 779–786.
 - 25 Sharff, A. and Jhoti, H. (2003) High-throughput crystallography to enhance drug discovery. *Current Opinion in Chemical Biology*, 7 (3), 340–345.
 - 26 Zimmermann, J., Buchdunger, E., Mett, H., Meyer, T., and Lydon, N.B. (1997) Potent and selective inhibitors of the Abl-kinase: phenylaminopyrimidine (PAP) derivatives. *Bioorganic & Medicinal Chemistry Letters*, 7 (2), 187–192.
 - 27 Cowan-Jacob, S.W., Fendrich, G., Manley, P.W. *et al.* (2005) The crystal structure of a c-Src complex in an active conformation suggests possible steps in c-Src activation. *Structure (London, England: 1993)*, 13 (6), 861–871.
 - 28 Hodous, B.L., Geuns-Meyer, S., Patel, V.F. *et al.* (2006) Discovery of a potent, highly selective, and efficacious pyridinyl triazine Tie-2 kinase inhibitor. AACR Annual Meeting, April 1–April 5, 2006, Washington DC, USA
 - 29 Hodous, B.L., Geuns-Meyer, S.D., Hughes, P.E. *et al.* (2007) Evolution of a

- highly selective and potent 2-(pyridin-2-yl)-1,3,5-triazine Tie-2 kinase inhibitor. *Journal of Medicinal Chemistry*, **50** (4), 611–626.
- 30 Cee, V.J., Albrecht, B.K., Geuns-Meyer, S. *et al.* (2007) Alkynylpyrimidine amide derivatives as potent, selective, and orally active inhibitors of Tie-2 kinase. *Journal of Medicinal Chemistry*, **50** (4), 627–640.
 - 31 Miyazaki, Y., Matsunaga, S., Tang, J. *et al.* (2005) Novel 4-amino-furo[2,3-d]pyrimidines as Tie-2 and VEGFR2 dual inhibitors. *Bioorganic & Medicinal Chemistry Letters*, **15** (9), 2203–2207.
 - 32 Cumming, J.G., Mckenzie, C.L., Bowden, S.G. *et al.* (2004) Novel, potent and selective anilinoquinazoline and anilinoypyrimidine inhibitors of p38 MAP kinase. *Bioorganic & Medicinal Chemistry Letters*, **14** (21), 5389–5394.
 - 33 Gill, A.L., Frederickson, M., Cleasby, A. *et al.* (2005) Identification of novel p38a MAP kinase inhibitors using fragment-based lead generation. *Journal of Medicinal Chemistry*, **48** (2), 414–426.
 - 34 Gill, A., Cleasby, A., and Jhoti, H. (2005) The discovery of novel protein kinase inhibitors by using fragment-based high-throughput X-ray crystallography. *ChemBioChem*, **6** (3), 506–512.
 - 35 Congreve, M.S., Murray, C.W., Carr, R.A.E., and Rees, D.C. (2007) Fragment-based lead discovery. *Annual Reports in Medicinal Chemistry*, **42**, 431–448.
 - 36 Wilhelm, S., Carter, C., Lynch, M. *et al.* (2006) Discovery and development of sorafenib: a multikinase inhibitor for treating cancer. *Nature Reviews. Drug Discovery*, **5**, 835–844.
 - 37 Wan, P.T.C., Garnett, M.J., Roe, S.M. *et al.* (2004) Mechanism of activation of the RAF-ERK signaling pathway by oncogenic mutations of B-RAF. *Cell*, **116**, 855–867.
 - 38 Thaimattam, R., Daga, P., Rajjak, S.A., Banerjee, R., and Iqbal, J. (2004) 3D-QSAR CoMFA, CoMSIA studies on substituted ureas as Raf-1 kinase inhibitors and its confirmation with structure-based studies. *Bioorganic and Medicinal Chemistry*, **12**, 6415–6425.
 - 39 Goldberg, D.R., Hao, M.H., Qian, K.C. *et al.* (2007) Discovery and optimization of p38 inhibitors via computer-assisted drug design. *Journal of Medicinal Chemistry*, **50** (17), 4016–4026.
 - 40 Weisberg, E., Manley, P.W., Breitenstein, W. *et al.* (2005) Characterization of AMN107, a selective inhibitor of native and mutant Bcr-Abl. *Cancer Cell*, **7**, 127–141.
 - 41 Weiss, M., Bajpaj, M., Bauer, D. *et al.* (2006) Discovery, synthesis and optimization of a new class of potent KDR inhibitors: naphthoylamides. AACR Annual Meeting, April 1–April 5, 2006, Washington DC, USA
 - 42 Potashman, M., Bajpaj, M., Bauer, D. *et al.* (2006) 1,6-Naphthyls as a new class of potent KDR inhibitors. AACR Annual Meeting, April 1–April 5, 2006, Washington DC, USA
 - 43 Dimauro, E.F., Newcomb, J., Nunes, J.J. *et al.* (2006) Discovery of aminoquinazolines as potent, orally bioavailable inhibitors of Lck: synthesis, SAR, and *in vivo* anti-inflammatory activity. *Journal of Medicinal Chemistry*, **49** (19), 5671–5686.
 - 44 Hasegawa, M., Nishigaki, N., Washio, Y. *et al.* (2007) Discovery of novel benzimidazoles as potent inhibitors of TIE-2 and VEGFR-2 tyrosine kinase receptors. *Journal of Medicinal Chemistry*, **50** (18), 4453–4470.
 - 45 Potashman, M.H., Bready, J., Coxon, A. *et al.* (2007) Design, synthesis, and evaluation of orally active benzimidazoles and benzoxazoles as vascular endothelial growth factor-2 receptor tyrosine kinase inhibitors. *Journal of Medicinal Chemistry*, **50** (18), 4351–4373.
 - 46 Wood, E.R., Truesdale, A.T., McDonald, O.B. *et al.* (2004) A unique structure for epidermal growth factor receptor bound to GW572016 (lapatinib): relationships among protein conformation, inhibitor off-rate, and receptor activity in tumor cells. *Cancer Research*, **64**, 6652–6659.
 - 47 Heron, N.M., Anderson, M., Blowers, D.P. *et al.* (2006) SAR and inhibitor complex structure determination of a novel class of potent and specific Aurora kinase inhibitors. *Bioorganic & Medicinal Chemistry Letters*, **16**, 1320–1323.
 - 48 Jung, F.H., Pasquet, G., Brempt, C.L.-V.D. *et al.* (2006) Discovery of novel and potent

- thiazoloquinazolines as selective Aurora A and B kinase inhibitors. *Journal of Medicinal Chemistry*, **49** (3), 955–970.
- 49 Harris, P.A., Cheung, M., Hunter, R.N., III *et al.* (2005) Discovery and evaluation of 2-anilino-5-aryloxazoles as a novel class of VEGFR2 kinase inhibitors. *Journal of Medicinal Chemistry*, **48**, 1610–1619.
 - 50 Manley, P.W., Bold, G., Brueggen, J. *et al.* (2004) Advances in the structural biology, design and clinical development of VEGF-R kinase inhibitors for the treatment of angiogenesis. *Biochimica et Biophysica Acta*, **1697** (1–2), 17–27.
 - 51 Bold, G., Altmann, K.-H., Frei, J. *et al.* (2000) New anilinophthalazines as potent and orally well absorbed inhibitors of the VEGF receptor tyrosine kinases useful as antagonists of tumor-driven angiogenesis. *Journal of Medicinal Chemistry*, **43** (12), 2310–2323.
 - 52 Manley, P.W., Furet, P., Bold, G. *et al.* (2002) Anthranilic acid amides: a novel class of antiangiogenic VEGF receptor kinase inhibitors. *Journal of Medicinal Chemistry*, **45**, 5687–5693.
 - 53 Burchat, A., Borhani, D.W., Calderwood, D.J. *et al.* (2006) Discovery of A-770041, a Src-family selective orally active lck inhibitor that prevents organ allograft rejection. *Bioorganic & Medicinal Chemistry Letters*, **16**, 118–122.
 - 54 Borhani, D.W., Calderwood, D.J., Friedman, M.M. *et al.* (2004) A-420983: a potent, orally active inhibitor of lck with efficacy in a model of transplant rejection. *Bioorganic & Medicinal Chemistry Letters*, **14**, 2613–2616.
 - 55 Burchat, A.F., Calderwood, D.J., Friedman, M.M. *et al.* (2002) Pyrazolo[3,4-d]pyrimidines containing an extended 3-substituent as potent inhibitors of Lck: a selectivity insight. *Bioorganic & Medicinal Chemistry Letters*, **12**, 1687–1690.
 - 56 Calderwood, D.J., Johnston, D.N., Munschauer, R., and Rafferty, P. (2002) Pyrrolo[2,3-d]pyrimidines containing diverse N-7 substituents as potent inhibitors of Lck. *Bioorganic & Medicinal Chemistry Letters*, **12**, 1683–1686.
 - 57 Lipinski, C.A., Lombardo, F., Dominy, B.W., and Feeney, P.J. (2001) Experimental and computational approaches to estimate solubility and permeability in drug discovery and development settings. *Advanced Drug Delivery Reviews*, **46**, 3–26.
 - 58 Veber, D.F., Johnson, S.R., Cheng, H.-Y. *et al.* (2002) Molecular properties that influence the oral bioavailability of drug candidates. *Journal of Medicinal Chemistry*, **45** (12), 2615–2623.
 - 59 Ertl, P., Rohde, B., and Selzer, P. (2000) Fast calculation of molecular polar surface area as a sum of fragment-based contributions and its application to the prediction of drug transport properties. *Journal of Medicinal Chemistry*, **43**, 3714–3717.
 - 60 Clark, D.E. and Pickett, S.D. (2000) Computational methods for the prediction of “drug-likeness.” *Drug Discovery Today*, **5** (2), 49–58.
 - 61 Abad-Zapatero, C. and Metz, J.T. (2005) Ligand efficiency indices as guideposts for drug discovery. *Drug Discovery Today*, **10** (7), 464–469.
 - 62 Hopkins, A.L., Groom, C.R., and Alex, A. (2004) Ligand efficiency: a useful metric for lead selection. *Drug Discovery Today*, **9** (10), 430–431.

7

From Discovery to Clinic: Aurora Kinase Inhibitors as Novel Treatments for Cancer

Nicola Heron

7.1

Introduction

The process of mitosis is highly complex biological system, whereby a complete copy of the duplicated genome is precisely segregated into two daughter cells. The current generation of clinically successful drugs that target mitosis, such as those derived from the taxanes and vinca alkaloids, bind to tubulin stabilizing or depolymerizing the microtubules (which form the mitotic spindle) causing cells to arrest in mitosis and subsequently undergo apoptosis. These agents suffer from undesired side effects such as neurotoxicity as a consequence of the physiological roles played by microtubules outside of mitosis. Therefore new targets, which are mitosis-specific and for which novel anticancer drugs with reduced toxicity to nondividing or normally dividing cells can be developed, have been the subject of intense interest [1–3].

The Aurora kinases are a family of serine/threonine protein kinases, critical for the proper regulation of mitosis. Mammals express three Aurora kinase paralogues, Aurora A, Aurora B, and Aurora C of which at least two (Aurora A and Aurora B) are commonly overexpressed in human tumors [4, 5]. The Aurora kinases are known to be critical for the most important steps in mitosis including centrosome duplication, formation of a bipolar mitotic spindle, and chromosome alignment on the mitotic spindle [5]. They are also essential for cell spindle checkpoint systems that have evolved to monitor the fidelity of mitosis and if necessary arrest the cell cycle to allow errors to be resolved [6–8]. As kinases, they should be amenable to small-molecule inhibition and they have been highlighted as attractive targets for anticancer drug development [5, 9, 10].

7.2

Biological Roles of the Aurora Kinases

The first member of the Aurora kinase family was identified in 1995 by Glover *et al.* in *Drosophila* mutants that were defective in the centrosome duplication–separation

cycle [11]. Since this initial discovery, members of the Aurora kinase family have emerged as key mitotic regulators required for genome stability. Aurora A, Aurora B, and Aurora C are only expressed during mitosis, and despite a high degree of sequence homology in the catalytic domains, the Aurora kinases exhibit strikingly different subcellular localization and functions ([12–14]; reviewed in Ref. [5]).

Aurora A localizes to the centrosomes and poles of the mitotic spindle and is required to establish a bipolar mitotic spindle. The kinase activity of Aurora A is regulated by binding to the protein TPX2, which is also required for mitotic spindle assembly. Repression of Aurora A activity in human cells by genetic techniques delays their entry into mitosis [15], increases the mitotic index and induces monopolar spindle defects [16]. Further, overexpression of Aurora A can inhibit cytokinesis [17] and also compromise the spindle checkpoint [6].

Aurora B is a chromosomal passenger protein. It localizes to the centromeric regions of chromosomes in the early stages of mitosis. Later in mitosis, Aurora B undergoes a dramatic relocation from the centromeres to the microtubules at the spindle equator. As the spindle elongates and the cell undergoes cytokinesis, Aurora B accumulates in the spindle midzone before finally concentrating at the midbody [14]. Aurora B complexes with at least three other proteins at the centromere: INCENP, survivin, and borealin [5]. Proper localization and function of any one of these four proteins is dependent on the function of the other three, suggesting that complex formation is required to target Aurora B to both the centromeres and the spindle. Aurora B is required for phosphorylation of Histone H3 on serine 10 in mitosis. This is thought to be important for chromosome condensation and sister chromatid cohesion. Aurora B plays a key role in kinetochore function and it is required for accurate chromosome alignment and segregation during mitosis. Similar to Aurora A, Aurora B is also important for spindle checkpoint function and cytokinesis [18].

Aurora C localizes to spindle poles, but only in late mitosis [19] and appears to be a chromosome passenger [20, 21]. Little is known about the functional role of Aurora C but it may play a specific role in meiosis [19, 22].

7.3

Aurora Kinases and Cancer

The first indication that Aurora kinases may be implicated in cancer came with the observation that Aurora A and Aurora B were overexpressed in primary colon tumor samples [4] when compared with adjacent normal tissue. The Aurora A gene was also amplified in a subset of these tumors. Many subsequent studies have identified overexpression and gene amplification of Aurora A and Aurora B in other tumor types including breast, pancreas, ovarian, gastric, and prostate tumors [23–25]. In a systematic analysis of Aurora A, Aurora B, and Aurora C, mRNA expression levels in multiple primary tumor samples of different stage and diverse origin, Aurora A and Aurora B were found to be significantly overexpressed in parallel when compared with normal controls [5]. In contrast, Aurora C was found not to be overexpressed

compared with normal tissue. Aurora A in particular has been identified as a drug target, given the observation that it can act as an oncogene and transform cells when ectopically expressed [4]. In addition, the Aurora A gene localizes to an amplicon known to associate with poor prognosis in breast tumors (20q13) [4].

It is hypothesized that abnormal expression of Aurora A may contribute to genetic instability and hence tumorigenesis through either abnormal centrosome duplication or defects in the spindle checkpoint [6, 24, 26–28]. Abnormal expression of Aurora B may similarly contribute to genetic instability by inducing abnormalities in chromosome attachment or alignment to the spindle during mitosis, or by affecting the spindle checkpoint [8, 18, 29]. Furthermore, it is interesting that Aurora B complexes with survivin, since survivin is commonly overexpressed in tumors and rarely expressed in normal tissue. It has been suggested that survivin functions to prevent apoptosis on the basis of its similarity to other proteins with this function (reviewed in Ref. [30]). The loss of survivin leads to an increase in apoptosis and a failure of cytokinesis. A similar phenotype is observed upon treatment with Aurora kinase inhibitors (see above) suggesting that Aurora B and survivin are part of the same functional complex, and that overexpression of Aurora B may help protect tumor cells from apoptosis.

7.4

In Vitro Phenotype of Aurora Kinase Inhibitors

A number of small-molecule inhibitors of Aurora kinases have been explored in both *in vitro* and *in vivo* systems and have helped to increase the understanding of their biological roles [7, 8, 31–33]. In two early reports, the cellular effects of inhibiting Aurora kinase with Hesperadin (1) [7] and ZM447439 (2) [8] (Figure 7.1) were described, setting the scene for future inhibitors. Hesperadin is a novel indolinone that inhibits Aurora B and several other kinases *in vitro*. Its potency against Aurora A was not reported. Hesperadin has an IC_{50} value of $0.25\ \mu\text{M}$ when assayed against Aurora B immunoprecipitated from mitotic cells [7]. Hesperadin appears more

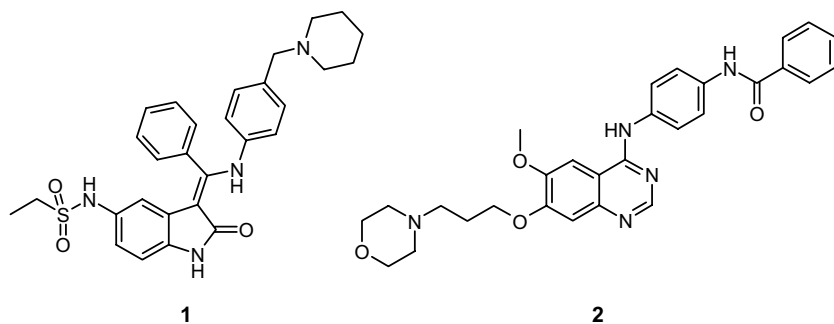


Figure 7.1 Structures of Hesperadin (1) and ZM447439 (2).

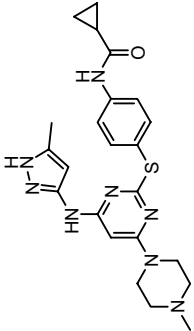
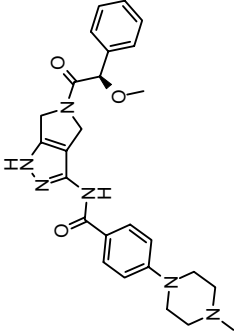
potent in cell-based assays, with 0.02–0.1 μM sufficient to reduce mitotic Histone H3 phosphorylation.

ZM447439, a quinazoline derivative, is an ATP-competitive inhibitor that, in *in vitro* kinase assays, was shown to inhibit both Aurora A and Aurora B kinase activity with IC_{50} values of approximately 0.1 μM [8]. This inhibition is relatively specific with ZM447439 showing no inhibition ($\text{IC}_{50} > 10 \mu\text{M}$) of a range of kinases including other kinases involved in regulating the cell cycle such as CDK1 and PLK1 [8].

Both Hesperadin and ZM447439 induce similar phenotypic changes in cell-based systems [7, 8]. Both compounds inhibit phosphorylation of Histone H3 on serine 10 and inhibit cytokinesis. However, the cells do not undergo a simple mitotic arrest. Rather, the cell cycle proceeds with normal timing, and entry and exit from mitosis are unaffected [7, 8]. This cell cycle progression without resulting cytokinesis induces tetraploid cells. Longer exposures reveal cell line-dependent effects. Treated cells either continue to cycle without cytokinesis and become highly polyploid (and ultimately die) or alternatively undergo a G1-like cell cycle arrest [8]. When cells that are passing through mitosis are treated with either ZM447439 or Hesperadin, the chromosomes fail to align properly during metaphase, but do attach to the microtubule spindle correctly. Analysis of Hesperadin-treated cells shows that many of the chromosomes are oriented with both kinetochores attached to the same pole (known as syntelic attachment [7]). Thus, Aurora kinase activity may be required for correct chromosome orientation during mitosis. However, these cells exit mitosis even though they have not aligned their chromosomes correctly. Since cells have evolved a spindle checkpoint system to prevent this catastrophic event happening, this indicates that Aurora kinase activity is necessary for the activity of this checkpoint. This was further demonstrated by the failure of cells treated with either Hesperadin or ZM447439 to arrest in mitosis in response to additional treatment with Paclitaxel, a potent activator of the spindle checkpoint. Furthermore, a number of checkpoint proteins, including the kinases Bub1 and BubR1, do not localize correctly to kinetochores in mitotic cells treated with the inhibitors. ZM447439 inhibits phosphorylation of BubR1 suggesting that it may be a substrate of one of the Aurora kinases, and given its proximity at the kinetochore one could speculate that BubR1 phosphorylation may be an activity of Aurora B. In summary, Aurora kinase activity is required for spindle checkpoint function, as well as having roles in cytokinesis and in chromosome alignment.

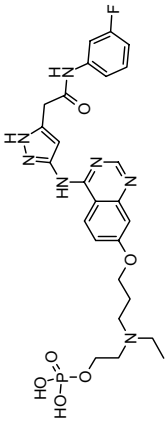
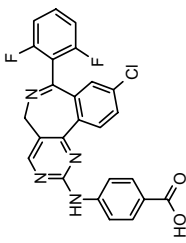
A number of inhibitors (see Table 7.1) have subsequently been reported with greater potency against the Aurora kinases and have demonstrated inhibition of tumor growth in rodent xenograft models. The first of these compounds to be published was VX-680 (MK-0457) [31]. VX-680 potently inhibits all three Aurora kinases (A, B, and C) *in vitro* with inhibition constants of 0.0006, 0.018, and 0.0046 μM , respectively [31]. More recently, Nerviano Medical Sciences have published data on two related inhibitors, PHA-680632 [32] and PHA-739358 [33]. PHA-739358 is also a potent inhibitor of all three human Aurora kinase paralogues ($\text{IC}_{50} = 0.013$, 0.079, and 0.061 μM against Aurora A, Aurora B, and Aurora C, respectively). The profiles of VX-680 (MK-0457), PHA-680632, and PHA-739358 are

Table 7.1 Aurora kinase inhibitors in clinical development.

Drug name/company	Chemical structure	Aurora kinase selectivity	Kinase specificity	Route/schedule	Development stage/tumor type
MK-0457 (VX-680) Vertex/Merck		K_i (μM): Aurora A: 0.0006 Aurora B: 0.018 Aurora C: 0.0046	>1000-fold against 50 other kinases FLT-3: 0.030 μM ABL: 0.010 μM ABL (T315I): 0.030 μM JAK-2 JAK-2 (V617F)	5-day i.v. infusion every 2–4 weeks [4, 7–12]	Phase II Leukemias and solid tumors
PHA-739358 Nerviano		IC_{50} (μM): Aurora A: 0.013 Aurora B: 0.079 Aurora C: 0.061	From 10- to >100-fold against 28 other kinases ABL: 0.025 μM TRKA: 0.030 μM RET: 0.031 μM FGFR1: 0.047 μM	24 h i.v. infusion every 14 days [17]	Phase II Leukemias and solid tumors

(Continued)

Table 7.1 (Continued)

Drug name/company	Chemical structure	Aurora kinase selectivity	Kinase specificity	Route/schedule	Development stage/tumor type
AZD1152 AstraZeneca		K_i (μM): Aurora A: 1.4 Aurora B: 0.0004 Aurora C: 0.017	$\text{IC}_{50} > 1 \mu\text{M}$ against 50 kinases	2 h i.v. infusion every week [56]	Phase I Leukemias and solid tumors
MLN8054 Millennium		IC_{50} (μM): Aurora A: 0.004 Aurora B: 0.172	> 1000 -fold against 10 other kinases	Oral	Phase I Solid tumors
AT9283 Astex	Structure not reported	Aurora A and Aurora B	JAK-2 BCR-ABL (T3151)	i.v. infusion/Oral	Phase I/II Leukemias and solid tumors
R-763 Rigel/Serono	Structure not reported	Aurora A and Aurora B		Oral	Phase I Solid tumors

CYC-116 Cyclacel	Structure not reported	Aurora A and Aurora B	Oral	IND filed
SNS-314 Sunesis	Structure not reported	Aurora A and Aurora B	i.v. infusion	IND filed

Schellens, J.H., Boss, D., Witteveen, P.O., Zandvliet, A., Beijnen, J.H., Voogel-Fuchs, M., Morris, C., Wilson, D., Voest, E.E. (2006) Phase I and pharmacological study of the novel Aurora kinase inhibitor AZD1152. *Journal of Clinical Oncology*, 24, 3008.

described in detail in Sections 7.5.2 and 7.5.3, respectively. Interestingly, these compounds, despite possessing more potent Aurora A than Aurora B kinase inhibitory activity, produce analogous cellular phenotypes to Hesperadin and ZM447439. Both compounds inhibit phosphorylation of Histone H3 at serine 10 and inhibit cytokinesis leading to an accumulation of cells with $\geq 4N$ DNA content [31–33]. The effects observed *in vitro* are replicated *in vivo* and lead to potent tumor growth inhibitory activity in a range of human tumor xenograft models [31–33]. VX-680 (MK-0457) and PHA-739358 have advanced into clinical studies (see above).

While none of the inhibitors described are selective for the different Aurora kinase paralogues, the phenotypes reported most strongly resemble those reported for inhibition of Aurora B using molecular genetic approaches [8, 34]. In contrast, none of the effects described for genetic ablation of Aurora A in human cells are manifest in these experiments. However, an inhibition of Aurora A autophosphorylation is reported following treatment with PHA-680632, consistent with inhibition of Aurora A in cells [32]. Girdler *et al.* have demonstrated that Aurora A kinase activity is required for bipolar spindle assembly in human cells [34]. Importantly, they have also shown that it is possible to inhibit Aurora A kinase activity in cells with a small-molecule producing cells with monopolar spindles (note, this was only in the presence of the proteasome inhibitor MG32, which prevented premature exit from mitosis) [34]. However, inhibition of Aurora B at the same time causes a suppression of the spindle checkpoint system leading to the characteristic Aurora B derived phenotype [16, 34].

Inhibitors that are selective for either Aurora A or Aurora B have now started to emerge. AZD1152 is a potent inhibitor of Aurora B-INCENP kinase activity ($K_i = 0.0004 \mu\text{M}$), while being a weaker inhibitor of Aurora A ($K_i = 1.4 \mu\text{M}$) [35, 57]. In contrast, MLN8054 is reported to inhibit potently the kinase activity of Aurora A in cells ($\text{IC}_{50} = 0.030 \mu\text{M}$) but is a weaker inhibitor of Aurora B in cells ($\text{IC}_{50} = 5.7 \mu\text{M}$) [36]. AZD1152 produces a phenotype identical to the inhibitors already described while MLN8054 caused cells to accumulate in mitosis (with a concomitant increase in Histone H3 phosphorylation) and increased the incidence of monopolar and tripolar spindles [37] a phenotype analogous to that produced by inhibition of Aurora A using genetic approaches. Both AZD1152 and MLN8054 have demonstrated potent tumor growth inhibitory activity in a range of human tumor xenograft rodent models at tolerated doses (described in Sections 7.5.1 and 7.5.4, respectively) and both compounds have advanced into clinical trials.

Inhibition of Aurora A and/or Aurora B induces profound mitotic phenotypes [5, 9, 14]. The Aurora B phenotype is unique – chromosomes fail to align properly during mitosis, the spindle checkpoint system is abrogated and cytokinesis fails. Multiple rounds of the cell cycle occur in this context, which renders the cells nonviable and has proven an effective way to halt the proliferation of tumor cells [5]. In contrast, similar to microtubule toxins, selective inhibition of Aurora A results in prolonged mitotic arrest and subsequent tumor cell apoptosis thus offering an alternative avenue for anticancer therapy [34]. It is not clear if inhibiting Aurora A and/or Aurora B will yield tumor cell selective killing, but it is encouraging from a therapeutic

standpoint that Aurora kinase inhibitors display potent antitumor activity in rodent tumor xenograft models and are well tolerated preclinically.

7.5

Aurora Kinase Inhibitors

The identification of the Aurora kinases as important regulators of the cell cycle has generated intense interest in developing small-molecule inhibitors as novel anti-cancer drugs [38–40]. A number of inhibitors have now been developed with differing Aurora kinase selectivity, kinase specificity, and pharmacokinetic profiles. These compounds have demonstrated potent tumor growth inhibitory activity in preclinical models and have entered clinical evaluation (Table 7.1). In Section 7.5.1, we will first describe the discovery of AZD1152 – a novel, highly potent, and selective inhibitor of Aurora B kinase, and then present comparative preclinical and clinical data for the other inhibitors currently undergoing clinical evaluation, comparing, and contrasting the characteristics of each compound.

7.5.1

The Discovery of AZD1152

7.5.1.1 Anilinoquinazolines: ZM447439

Our approach to identifying a starting point for medicinal chemistry was to run a high-throughput screen on the company compound collection. A series of anilinoquinazolines [41–43], exemplified by compound **3** (Figure 7.2), stood out in terms of both potency and selectivity for Aurora kinases. Clear SAR was evident from the primary screening data and suggested that compounds where the aniline group contained a large *para*-substituent showed good potency toward Aurora kinases [44]. Knowledge from other quinazoline-based kinase inhibitors, such as Iressa™, suggested that the quinazoline should bind into the adenine site (with N-1 making a critical interaction with the protein backbone), and indicated that the extended benzamido group should occupy the selectivity pocket.

During the initial exploration of SAR, ZM447439 (**2**), where the methoxy group at the C7-position of the quinazoline has been replaced by a 3-(1-morpholino)propoxy

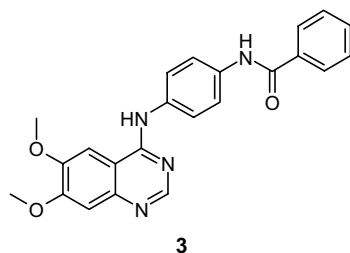


Figure 7.2 Structure of anilinoquinazoline lead **3**.

group was prepared and showed much improved cellular potency, making it an attractive tool to probe further the mechanism and cellular phenotype of an Aurora kinase inhibitor. Evaluation of ZM447439 in a panel of *in vitro* kinase inhibition assays demonstrated good activity against the Aurora kinases (Aurora A $IC_{50} = 0.11 \mu M$ and Aurora B $IC_{50} = 0.13 \mu M$). In contrast, there was some modest activity against a few other kinases (MEK1 $IC_{50} = 1.79 \mu M$; Src $IC_{50} = 1.03 \mu M$; and Lck $IC_{50} = 0.88 \mu M$) whereas ZM447439 was inactive ($>10 \mu M$) against CDK1, CDK2, CDK4, PLK1, CHK1, KDR, IKK1, IKK2, and FAK [8, 44]. Published studies with ZM447439 [8] show that it causes a dose-dependent increase in 4N DNA, due to a failure of cytokinesis, that is consistent with the proposed mechanism of action. Furthermore, ZM447439 selectively induced apoptosis in cycling cells but had relatively little effect on G1-arrested MCF-7 cells when profiled in *in vitro* clonogenicity assays, consistent with the proposed mechanism of action.

ZM447439 demonstrates good activity against the Aurora kinases, shows reasonable cellular potency, and is selective over a range of other kinases making it an attractive tool to probe further the mechanism and cellular phenotype of an Aurora kinase inhibitor. However, despite the utility of ZM447439 as a tool for exploring Aurora kinase function, it has relatively low aqueous solubility (10 μM in pH 7.4 phosphate buffer) and is also highly protein bound (0.3% free drug in rat plasma).

In an effort to improve physical properties, we investigated strategies to lower lipophilicity by replacing the central aniline with heterocycles.

7.5.1.2 Next-Generation Quinazolines: Heterocyclic Analogues

A number of analogues were made where the core aniline was replaced with a range of six-membered heterocycles such as pyrimidine and pyridine [45–47]. We were pleased to find that heterocycles that significantly reduced lipophilicity also, as shown in Table 7.2, increased potency for the Aurora kinases. Interestingly, the improved potency over the parent aniline (compound 3) has been shown to be highly sensitive to which isomer of the pyridine or the pyrimidine employed. Thus, the 5-pyrimidinyl isomer (compound 7) is approximately 100 times more potent against Aurora A than the 2-pyrimidyl isomer (compound 6).

Introduction of the 3-(1-morpholino)propoxy group at the C7-position of the quinazoline resulted in compound 8 (Figure 7.3), which showed an increase in potency when compared to compound 7. This compound also showed excellent levels of potency in an MCF7 cellular proliferation assay [44]. The reduction in lipophilicity arising from introduction of the pyrimidine ring has a significant effect on the physical properties of this quinazoline series as illustrated by comparing compound 8 with its direct aniline analogue ZM447439. While the percentage of unbound compound ZM447439 in rat plasma is 0.3%, the corresponding value for compound 8 is 4.5%.

Using the 5-amino-pyrimidinyl analogue (compound 8) as our new lead, we investigated the effect of substitution on the phenyl ring of the benzamido group. As illustrated in Table 7.3, Aurora A enzyme potency data suggested a strong preference for small, lipophilic substituents. Thus, the 3-chloro and the 3-chloro-4-fluoro analogues (compounds 9 and 10) gave excellent levels of enzyme potency,

Table 7.2 *In vitro* SAR for six-membered-ring heterocyclic analogues of compound 3.

Compound	Ar	Aurora A ^{a)} IC ₅₀ (μM)	Aurora B ^{b)} IC ₅₀ (μM)
3		0.310	0.240
4		0.165	>1
5		0.099	0.122
6		1.18	>1
7		0.011	0.025

a) For a description of the Aurora A enzyme assay, see Ref. [41].

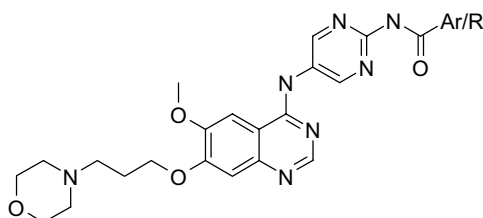
b) For a description of the Aurora B enzyme assay, see Ref. [54].

which also resulted in a significant improvement in cell activity (80 and 20 nM, respectively). The introduction of larger groups (compounds 11 and 12) had a detrimental effect on potency while introduction of a very large sulfonamido group (compound 13) resulted in a 1000-fold drop in activity when compared with

8

Aurora A IC ₅₀ (μM)	Aurora B IC ₅₀ (μM)	MCF7 IC ₅₀ (μM)
0.003	0.001	0.210

Figure 7.3 Lead pyrimidinoquinazoline (**8**).

Table 7.3 *In vitro* SAR of benzamide substitution.

Compound	Ar/R	Aurora A IC ₅₀ (μM) ^{a)}
9	3-Chlorophenyl	<0.0001
10	3-Chloro-4-fluorophenyl	0.00015
11	3-Bromo-4-methylphenyl	0.070
12	4-Ethylphenyl	0.085
13	(4-Dipropylaminosulfonyl)phenyl	3.9
14	4-Pyridyl	0.69
15	<i>n</i> -Butyl	0.017

a) For a description of the Aurora A enzyme assay, see Ref. [41].

compound **8**. Replacement of the phenyl ring with either a heterocyclic group (e.g., 4-pyridyl, compound **14**) or an alkyl substituent (e.g., *n*-butyl, compound **15**) gave compounds with much improved aqueous solubility but the drop in potency against both enzyme and cell assays was unacceptable.

Although beneficial for potency, the introduction of the halogens on the pendant phenyl ring resulted in increasingly lipophilic molecules displaying disappointing levels of aqueous solubility and plasma protein binding (e.g., compound **10** showed 1.4 μM solubility and only 0.4% free drug in rat plasma). Early modeling studies, later supported by the X-ray structure of the enzyme: inhibitor complex, indicated that the C7-substituent on the quinazoline lay in a channel that placed the morpholine in a solvent-accessible region. Modification of this position of the aniline-quinazoline series is known to influence potency and selectivity [48–51]. In addition, the physicochemical properties of quinazoline compounds can largely be influenced by the introduction of hydrophilic and basic groups at this position. The hydrophilic group must be attached to a suitable linear spacer. A three-carbon linker is generally optimal although two-carbon linkers are also tolerated. We observed that compound **16** (Figure 7.4), where the morpholine group had been replaced with the more basic piperidine moiety has a dramatically improved level of aqueous solubility (3600 μM, compared to compound **9**: 0.4 μM). Neither the excellent levels of Aurora A enzyme potency (0.8 nM) nor the activity of this compound in the MCF7 antiproliferative assay (24 nM) were affected by these modifications. The introduction of more polar hydroxyl groups also gave very soluble compounds (compound **17**, aqueous solubility: 1500 μM).

At this point in our program, we were successful in obtaining a crystal structure for Aurora A in complex with compound **17** [47, 52]. This complex indicated that Aurora

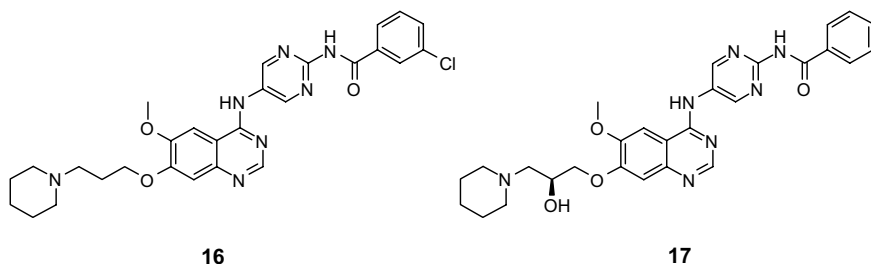


Figure 7.4 Examples of pyrimidinoquinazolines with improved solubility.

A is typical of other protein kinases and displays a bilobal kinase catalytic domain with the ATP binding site at the interface between an alpha-helical C-terminal lobe and a beta-sheet N-terminal lobe. Compound **17** binds in the ATP binding site in the cleft between the two domains (or hinge region) (Figure 7.5). A classical kinase (adenine-mimetic) inhibitor hydrogen-bond interaction with the main chain peptide is made between N (**17**) in the inhibitor and the amide of Ala212 (Figure 7.5a). The inhibitor adopts an extended conformation, demonstrating the extent of the available binding pocket. This may explain the early SAR observed on our screening output, that a large *para*-substituent on the aniline was required for potency and specificity. The piperidine moiety of the inhibitor extends into solvent. The C4-amino-pyrimidine ring is nearly coplanar with the benzoyl group but tilted with respect to the quinazoline. The amide carboxyl between the pyrimidine and the benzoyl rings shows a hydrogen bond to the conserved Lys161 while there are water-mediated contacts between the protein and the amide nitrogen. The benzoyl moiety fits into a hydrophobic pocket, which is occupied by Phe274 in the conserved DFG motif in an in-house ADPNP structure [47, 52]. The inhibitor stabilizes a “DFG-out”

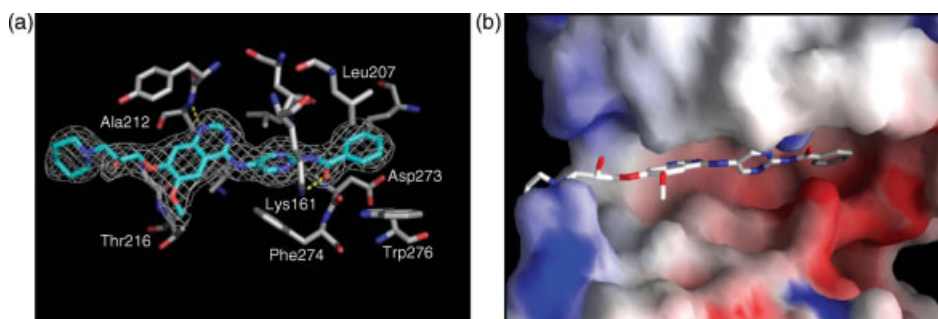


Figure 7.5 Crystal structure of pyrimidinoquinazoline **17** with Aurora A. (a) The inhibitor in final 2Fo-Fc electron density, indicating hydrogen bonds with Ala212 and Lys161. The conserved DFG motif in the

activation loop adopts a “DFG-out” conformation. (b) Surface diagram indicating the extent of the cleft between the N- and C-terminal lobes and the fit of the elongated inhibitor molecule.

conformation of the kinase [53]. This typically prevents the activation loop adopting a productive conformation for activation by phosphorylation and may contribute to the inhibitory mechanism of this series of compounds.

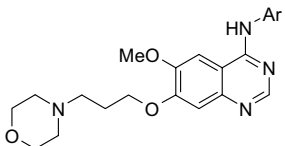
The observation that six-membered heterocyclic replacements could be found for the aniline group in ZM447439 suggested that the analogous compounds containing five-membered-ring heterocycles were worthy of study [54]. A number of quinazolines with five-membered rings of various structures (compounds **18–26**) were made and evaluated as illustrated in Table 7.4. Although many of these changes resulted in a loss of Aurora enzyme potency, 5-thiophene **20** and the 2-thiazole **26** analogues showed excellent affinity for the Aurora kinases.

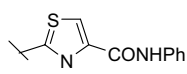
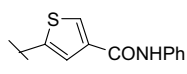
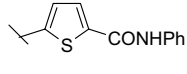
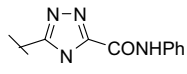
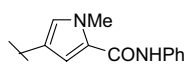
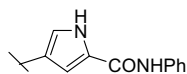
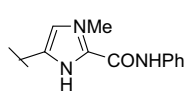
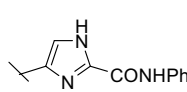
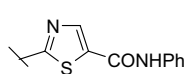
Again, we observed that employing the correct isomer of the heterocycle played a critical part in the potency of these compounds. The high levels of potency observed in this series suggested that the kinase has some flexibility in the selectivity pocket as it is clear that the five-membered ring in compounds **20** and **26** must change the conformational relationship between the quinazoline system and the benzamido phenyl group that exists in the earlier pyrimidinoquinazolines such as compound **17**. This observation suggested to us that further improvements in selectivity and potency might be achievable by introducing further conformational change [54].

7.5.1.3 Amino-Thiazolo and Pyrazolo Acetanilide Quinazolines

An exciting discovery was made when optimizing the amide linker group between particular five-membered-ring heterocycles and the terminal benzamide group (pertinent SAR is summarized in Table 7.5). By introducing an extra methylene unit between the amide carbonyl and the five-membered heterocyclic ring, significant increases in cellular potency were observed. Thus, while compound **27** showed a cellular potency of 0.6 μM , the addition of the extra methylene unit improved the potency to <0.001 μM (compound **29**). This favorable effect of the linker was not observed for all heterocycles and whereas the amino-pyrazole (compound **31**) showed a similar increase in potency, the amino-oxazole (compound **30**) did not. In addition, there is a clear preference for the position of the substituent on the five-membered ring. The C4-substituted thiazole **28** shows a 100-fold decrease in cellular activity compared with the C5-substituted thiazole **29**.

We have attempted to explain this very particular requirement for a C5 acetanilide substituent by looking at a conformational analysis of the thiazole series [54]. *Ab initio* molecular orbital calculations indicate that the thiazole and the quinazoline adopt a coplanar orientation with the sulfur placed on the same side as the quinazoline N3 (as drawn in Figure 7.5). Thus, positions C4 and C5 are not equivalent and it appears that only the C5-substituted thiazole can access a low energy conformation that orientates the substituent into the correct position in the enzyme. Furthermore, docking studies have shown that the flexible acetanilide side chain adopts a near perpendicular orientation relative to the thiazole (very different to the more planar conformation of compound **17**) placing the aryl group deep into a hydrophobic pocket of the enzyme. In order to accommodate this binding mode, the protein must adopt a DFG-out inactive conformation. The excellent levels of cellular activity seen would support this hypothesis [54].

Table 7.4 *In vitro* SAR for five-membered-ring heterocyclic quinazolines.


Compound	Ar	Aurora A IC ₅₀ (μM) ^{a)}	Aurora B IC ₅₀ (μM) ^{a)}
18		0.18	0.53
19		0.46	0.048
20		0.011	0.057
21		5.2	ND
22		0.78	1
23		0.37	0.12
24		0.57	>1
25		4.9	>1
26		0.004	0.042

a) For a description of the Aurora A and B enzyme assays, see Ref. [54].

Knowledge of the SAR from earlier series suggested that small and lipophilic groups are particularly favored in the terminal lipophilic binding pocket. SAR in the thiazole acetanilide series follows the same broad trends [44, 47, 54]. Thus, introduction of small lipophilic groups (such as 3-chloro or fluoro) into the terminal phenyl group was advantageous in terms of potency. At the other end of the molecule,

Table 7.5 *In vitro* SAR for acetanilide substituted heterocycles.

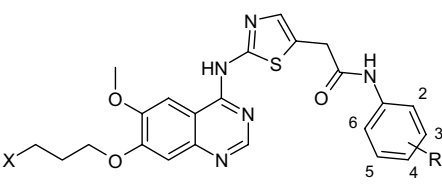
Compound	Ar	MCF7 Cell IC ₅₀ (μM) ^{a)}
27		0.6
28		0.2
29		<0.001
30		1
31		0.024 ^{b)}

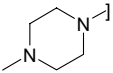
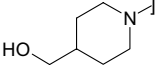
a) Inhibition of cellular proliferation.

b) Inhibition of cellular proliferation in SW620 cells.

hydrophilic groups on the end of the propoxy side chain allowed the retention of excellent cellular potency at the same time keeping solubility and plasma protein binding in the desired range [44, 54].

Compounds **32** and **33** (Table 7.6) have very potent antiproliferative effects in both MCF7 and SW620 cells. Further *in vitro* studies showed that SW620 cells exposed to compound **33** at a 1 μM concentration for 24 h showed both an accumulation of 4N cells (consistent with a failure of cytokinesis) and a complete inhibition of phosphorylation of Histone H3. When compound **32** was dosed (25–50 mg/kg i.p.) to nude mice inoculated with SW620 tumors there is a 25–45% inhibition of Histone H3 phosphorylation that occurs in a dose-dependent manner. To explore longer term exposure of an Aurora kinase inhibitor, we prepared phosphate analogues of

Table 7.6 Thiazole-acetanilide inhibitors.


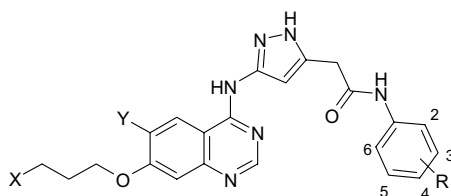
Compound	X	R	Aurora A IC ₅₀ (μ M) ^{a)}	Aurora B IC ₅₀ (μ M) ^{a)}	MCF7 IC ₅₀ (μ M) ^{a),b)}	SW620 IC ₅₀ (μ M) ^{a),b)}
32		3-Cl	<0.001		0.006	0.012
33		3-F	<0.001	0.007	0.004	0.002

a) For a description of enzyme and cellular assays, see Ref. [54].

b) Inhibition of cell proliferation.

compounds such as **33** [44, 54, 55]. The phosphate derivatives are highly soluble in simple pH-adjusted vehicles making them ideal for mini-pump dosing [54]. Compound **33** (dosed as a phosphate derivative via subcutaneous mini pump) demonstrated a reduction in phospho-Histone H3 in subcutaneously implanted SW620 human colorectal carcinoma xenografts. Significant inhibition of Histone H3 phosphorylation was demonstrated in tumor sections immunostained for phospho-Histone H3 expression. Analysis of phospho-Histone H3 stained cells using a scanning microscope indicated a ~30% reduction in phospho-Histone H3 positive cells in the compound-treated sections versus vehicle control [54].

In parallel with work in the thiazole series, we were also evaluating alternative starting points. The related pyrazole acetanilide series (e.g., compound **31**, Table 7.5) were also found to be potent inhibitors of Aurora kinase activity in cells. Important roles for the quinazoline C7 side chain and the lipophilic pocket binding group had been established in the earlier series, and these roles and the associated SAR also broadly applied to the pyrazole series; compounds **34–38** (Table 7.7) are representative of the compounds made in this series [35]. Surprisingly, it was found that removal of the quinazoline C6-methoxy group (e.g., compound **37** and **38**, Table 7.7) retains very high potency against Aurora B kinase (and excellent cellular activity) but reduces the potency against Aurora A kinase. Compounds such as **38** show 1000-fold greater potency for Aurora B than for Aurora A in the recombinant enzyme assays. In cells, the Aurora B selective inhibitors, such as **38**, induce chromosome

Table 7.7 Pyrazole acetanilide inhibitors.

Compound	X	Y	R	Aurora A K_i (μM) ^{a)}	Aurora B-INCEP K_i (μM) ^{a)}	SW620 IC ₅₀ (μM) ^{a),b)}
34		MeO	3-F	0.45	0.002	0.68
35		MeO	2,3-di-F	0.094	<0.001	0.042
36		MeO	2,3-di-F	0.087	<0.001	0.018
37		H	2,3-di-F	0.95	<0.001	0.005
38		H	3-F	1.4	<0.001	0.017

a) For a description of enzyme and cellular assays, see Ref. [35].

b) Inhibition of phospho-Histone H3 following 24 h incubation.

misalignment and prevent cell division thus inducing a polyploid phenotype and resultant apoptosis in tumor cells [35]. Compounds such as **38** also have high specificity for Aurora B kinase showing very little other kinase activity in a panel of serine/threonine and tyrosine kinases [35].

The pyrazole compounds are less lipophilic than the analogous thiazoles (giving rise to reduced plasma protein binding), shows no significant inhibition of any of the five major cytochrome P450 isoforms and despite the presence of a basic side chain, do not inhibit the hERG ion-channel at concentrations of up to 30 μM [35]. The phosphate prodrugs of compounds **35–38** are soluble at concentrations of up to 25 mg/ml in Tris buffer at pH9 and undergo rapid and complete cleavage to give the active drug species when dosed parentally to rodents [35].

In contrast to the thiazole series, the pyrazole compounds demonstrate robust pharmacodynamic activity that translates into potent tumor growth inhibitory activity [35, 56]. Significant suppression of phospho-Histone H3 was evident following 48 h administration of the phosphate derivative of compound **38** (AZD1152) at doses as low as 0.5 mg/kg/day while doses of 10–150 mg/kg/day resulted in >75% inhibition [56]. Flow cytometric analysis of the DNA content of the tumors indicated an increased proportion of cells with a 4N and >4N DNA content compared to vehicle-treated controls. In addition, histological analysis showed an increase in large multinucleated cells [56]. The accumulation of cells with $\geq 4N$ DNA content is consistent with failed cytokinesis and continued cell cycle progression following inhibition of Aurora B kinase activity [56].

AZD1152 shows significant and dose-dependant inhibition of growth in a range of human tumor xenografts with AZD1152 (summarized in Table 7.8) [56]. At doses of 10–150 mg/kg/day (dosed in a single cycle for 48 h), AZD1152 inhibits tumor growth ranging from 28% to $\geq 100\%$ in colorectal (SW620, HCT116, and Colo205), lung (A549 and Calu-6), and hematological (HL-60) tumors grown in nude mice [56]. HL-60 tumors were most responsive to AZD1152, with complete tumor regression at the end of the study in 8/11 animals. Significant antitumor activity was also observed when AZD1152 was dosed episodically. Four consecutive daily injections of AZD1152 at 25 mg/kg to nude rats bearing established SW620 tumor xenografts resulted in 93% inhibition of tumor size 8 days after the final dose [56]. AZD1152 was well tolerated at doses where antitumor efficacy was observed. AZD1152-treated athymic rats had a mean maximal body weight loss of 5%, 24 h following 4 days of

Table 7.8 Summary of *in vivo* studies with AZD1152 from Ref. [56].

Tumor	Treatment schedule	Efficacy: Percent inhibition of tumor volume
Mouse efficacy studies: human tumor cell xenografts		
SW620	10 mg/kg/day for 2 days s.c. infusion.	28 ^{a)}
	25 mg/kg/day for 2 days s.c. infusion.	49 ^{a)}
	150 mg/kg/day for 2 days s.c. infusion.	87 ^{a)}
Colo205	150 mg/kg/day for 2 days s.c. infusion.	94 ^{b)}
A549	25 mg/kg/day for 2 days s.c. infusion.	36 ^{c)}
	150 mg/kg/day for 2 days s.c. infusion.	69 ^{c)}
Calu-6	150 mg/kg/day for 2 days s.c. infusion.	55 ^{d)}
HL-60	150 mg/kg/day for 2 days s.c. infusion.	>100. Complete tumor regression in 8/11 animals ^{e)}
Rat efficacy studies: human tumor cell xenografts		
SW620	25 mg/kg i.v. Q1Dx4	93 ^{f)}

a) 15 days after drug withdrawal.

b) 17 days after drug withdrawal.

c) 16 days after drug withdrawal.

d) 20 days after drug withdrawal.

e) 18 days after drug withdrawal.

f) 8 days after final dose.

treatment (25 mg/kg/day i.v. Q1Dx4) and regained weight thereafter. These data suggest targeting of Aurora B has profound effects on tumor growth and may be a promising therapeutic approach for the treatment of a range of malignancies. AZD1152 is currently in Phase I clinical trials.

7.5.2

MK-0457 (VX-680)

MK-0457 (VX-680) is a 4,6-di-amino-pyrimidine compound resulting from a program to identify inhibitors of the Aurora kinases by targeting the ATP-binding site [31]. MK-0457 is a potent inhibitor of all three Aurora kinase enzymes with K_i values of 0.0006, 0.018, and 0.0046 μM (Aurora A, Aurora B, and Aurora C, respectively) [31]. This series of kinase inhibitors was shown to be generally selective with MK-0457 showing an $\text{IC}_{50} > 1 \mu\text{M}$ against 50 kinases with additional inhibitory activity versus FLT-3 ($\text{IC}_{50} = 0.030 \mu\text{M}$) [31]. In other studies, MK-0457 was discovered to bind to 37 out of 119 kinases tested at a concentration of 10 μM , including 19 kinases with K_d values $< 0.20 \mu\text{M}$ [57]. Interestingly, MK-0457 has also been shown to potently bind to wild-type ABL and most of the imatinib-resistant ABL variants, including ABL (T315I) [57]. The BCR-ABL (T315I) mutant accounts for $\sim 15\%$ of cases of acquired resistance to imatinib. MK-0457 inhibits the kinase activity of wild-type ABL and ABL (T315I) with an IC_{50} of 0.010 and 0.030 μM , respectively [57]. In cells expressing the BCR-ABL (T315I) mutant, MK-0457 has shown significant inhibitory activity [57, 58]. In T315I expressing Ba/F3 cells, BCR-ABL autophosphorylation was inhibited with an IC_{50} of $\sim 5 \mu\text{M}$ [57] while in peripheral blood mononuclear cells from patients with the T315I mutation, inhibition of phosphorylation of CrkL (a BCR-ABL substrate) was observed at concentrations of 10 μM [58]. A crystal structure of MK-0457 bound to an imatinib-resistant mutant form of ABL tyrosine kinase (H396P) has been published and appears to explain the ability of MK-0457 to accommodate the substitution of threonine with isoleucine at the gatekeeper position [58]. In addition to its inhibitory activity toward FLT-3 and BCR-ABL, MK-0457 has been shown to inhibit both the wild-type and the V617F activating mutation of Janus kinase 2 (JAK2) [59], a potentially important target for CML and other myeloproliferative diseases [60].

Harrington *et al.* have published data demonstrating *in vitro* and *in vivo* antitumor activity with MK-0457 [31]. Consistent with a mechanism of inhibiting Aurora B, in MCF7 cells MK-0457 induces accumulation of cells with 4N DNA content and in HeLa cells MK-0457 causes a failure of cell division resulting in polyploidy. The phosphorylation of Histone-H3 in MCF7 cells is inhibited at concentrations of 0.003–0.3 μM and MK-0457 blocks tumor cell proliferation in a panel of tumor cell lines (colorectal, leukemia, breast, prostate, pancreatic, melanoma, and cervical) with EC_{50} of 0.015–0.113 μM after 96 h treatment. MK-0457 induces cell death in multiple tumor cell types and in COLO205 cells MK-0457 was shown to induce apoptosis. MK-0457 has no effect on the viability of noncycling cells (peripheral blood mononuclear cells) at concentrations of 10 μM an observation consistent with the fact that the expression and the activity of Aurora proteins is low in noncycling cells. MK-0457

ablated colony formation of primary leukemic cells from patients with AML who were refractory to standard therapies, with IC_{50} values in the range 0.035–0.1 μ M. MK-0457 also abolished colony formation of primary leukemic cells possessing internal tandem duplication mutations of FLT-3 [31]. Recent studies suggest the differing sensitivity of different cell types to MK-0457 could be the result of impaired checkpoint function [61]. In particular, the integrity of the p53-p21^{Waf1/Cip1} pathway governs the response to MK-0457. While cells with intact checkpoint function arrest with 4N DNA content, those cells with compromised checkpoint function rapidly undergo endoreduplication followed by apoptosis [61].

In vivo human xenograft rodent studies reported by Harrington *et al.* [31] are summarized in Table 7.9. MK-0457 causes significant inhibition of tumor growth at well-tolerated doses. Tumor regression was observed in three tumor types – leukemia (AML: HL-60), pancreatic (MIA PaCa-2), and colon (HCT-116) following either intraperitoneal (i.p.) or intravenous (i.v.) administration to nude mice or rats [31]. Histological evaluation in tumor sections of the Aurora B substrate Histone H3, indicated a marked reduction in Histone H3 phosphorylation in MK-0457-treated HCT-116 bearing rats compared with matched vehicle controls. In the same study, MK-0457-treated sections exhibited a higher incident of apoptosis as determined by TUNEL immunohistochemical staining compared with control-treated tumor [31].

While MK-0457 was well tolerated in the mouse, toxicity was more evident in the rat models [31]. The main toxicity encountered was neutropenia with no sign of mechanism-independent toxicity. At the 1 mg/kg/h dose level, neutrophil counts were suppressed by 54% at the nadir, which returned to normal following cessation of dosing [31].

MK-0457 is in Phase I/II clinical studies in both solid [63] and hematological tumor settings [59, 63–67]. Reports of significant efficacy with MK-0457 in patients with chronic myeloid leukemia or acute lymphocytic leukemia with the BCR-ABL (T315I) mutation has been published [67]. This report is the first observed clinical activity of a kinase inhibitor against the T315I phenotype. While the relative contributions of Aurora kinase, BCR-ABL and JAK2 inhibitory activity of MK-0457 have yet to be established [67], these early signs of clinical efficacy are very encouraging.

7.5.3

PHA-739358

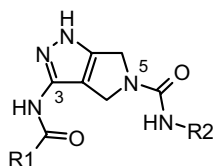
Nerviano Medical Sciences have described an elegant use of combinatorial chemistry to synthesize a series of 3-amino-tetrahydropyrrolo[3,4-*c*]pyrazoles to target the ATP pocket of protein kinases [68, 69]. A 3-phenylacetamide substituent, for example, in compound **39** (Table 7.10), affords selectivity for CDK2 over Aurora A [69] whereas a benzamido group at position 3, for example, in compound **40** (Table 7.10), is selective for Aurora A over CDK2 [68]. This difference in kinase activity is believed to be due to the differing protein conformation between the hinge region and the beginning of the C-terminal domain disfavoring nonplanar inhibitors in Aurora A [69].

Compound **40** (PHA-680632) is a potent inhibitor of all three human Aurora kinase paralogues (IC_{50} = 0.027, 0.135, and 0.120 μ M against Aurora A, Aurora B, and

Table 7.9 Summary of reported *in vivo* studies with MK-0457 from Ref. [31].

Nude mouse efficacy studies		
Tumor	Treatment schedule [b.i.d.; i.p. for 13 days] dose (mg/kg)	Efficacy
HL-60	12.5	% T/C = 78
HL-60	25	% T/C = 71
HL-60	50	% T/C = 17
HL-60	75	98% reduction in mean tumor volume relative to controls. Regression in 4/10 animals.
MIA PaCa-2	50	22% decrease in mean tumor volume relative to the initial tumor size before treatment. Regression in 7/10 animals.
Nude rat efficacy studies		
Tumor	Treatment schedule [i.v. infusion for 3 days per week] dose (mg/kg/h)	Efficacy
HCT-116	0.5	% T/C = 73
HCT-116	1	Tumor regression in 4/7 animals. Mean % T/C = 3.
HCT-116	2	56% decrease in mean tumor volume relative to initial tumor size before treatment.
Nude rat pharmacodynamic studies		
Tumor	Treatment schedule [50 mg/kg, u.i.d., i.p.] duration (days)	% Reduction H3 phosphorylation % Increase apoptosis (TUNEL)
HCT-116	3	51 84
HCT-116	4	67 171

% T/C = Percent change in mean tumor volume for treatment group/change in mean tumor volume for control group.

Table 7.10 3-Amino-tetrahydropyrrolo[3,4-*c*]pyrazole CDK and Aurora kinase inhibitors from Refs [68, 69].

Compound	R1	R2	CDK2/ cyclin A IC ₅₀ (μ M)	Aurora A IC ₅₀ (μ M)	HCT116 cells IC ₅₀ (μ M)
39			0.033	4.2	0.90
40			>10	0.027	0.045

Aurora C, respectively) [68, 32]. In a panel of other serine-threonine and tyrosine kinases, PHA-680632 was found to be inactive ($IC_{50} > 10 \mu M$) against 22 other kinases but to have some moderate activity ($IC_{50} < 1 \mu M$) against FGFR1, PLK-1, FLT-3, and ABL [32]. In cells, PHA-680632 has potent antiproliferative activity (EC_{50} ranging from 0.06–7.15 μM) and leads to an accumulation of cells with $\geq 4N$ DNA content and an inhibition of phosphorylation of Histone H3 at serine 10 [32]. While the phenotype observed in cells is dominated by inactivation of Aurora B, an induction of active caspase-9 and caspase-3 together with an inhibition of Aurora A autophosphorylation is reported, consistent with the inhibition of Aurora A in cells [70]. Similar to MK-0457, different cell lines respond in differing ways to PHA-680632. Human colon carcinoma HCT-116 cells are highly sensitive to PHA-680632 and rapidly undergo endoreduplication following drug treatment whereas primary NHDF cells do not become polyploid even at high dose and after long exposure to the drug. NHDF cells remain blocked in the G2-M phase of the cell cycle and after drug washout, are able to return to normal ($\sim 90\%$ cell number compared with untreated cells by day 6 after replating) [32]. In contrast, a large proportion of HCT116 cells treated with PHA-680632 become polyploid and following drug washout and replating only a small proportion of these cells recover ($\sim 3\%$ cell number compared with untreated cells) [32].

PHA-680632 inhibited the phosphorylation of Histone-H3 in A2780 xenografts (grown in athymic mice) within 30 min in both tumor and bone marrow tissue following a 60 mg/kg i.v. bolus dose [32]. By 8 h after dosing, the effect of the compound had reduced, which is compatible with the half-life of the compound in

Table 7.11 Summary of reported in-vivo studies with PHA-680632 from Ref. [32]

Mouse efficacy studies: human tumor cell xenografts		
Tumor	Treatment schedule	Efficacy
HL-60	45 mg/kg i.v. bolus b.i.d for 5 days.	85% TGI
A2780	60 mg/kg i.v. bolus b.i.d for 5 days.	78% TGI
HCT-116	30 mg/kg i.p. t.i.d for 12 days	75% TGI
Mouse efficacy studies: syngeneic models		
MMTV-H-ras	45 mg/kg i.p. t.i.d for 5 days followed by 2 days off repeated for four cycles.	Complete tumor stabilization and partial regression

% TGI = $100 - (\text{mean tumor weight of treated group} / \text{mean tumor weight of control group}) \times 100$.

mouse. Histological analysis of A2780 xenografts showed an increase in both cellular size and nuclear size, the appearance of multinucleated cells and a significant reduction of cell proliferation (measured using bromodeoxyuridine incorporation). In HL60 xenografts, a threefold increase in apoptosis was observed as measured using caspase-3 staining. PHA-680632 showed potent antitumor activity in leukemia (HL-60), ovarian (A2780), and colon (HCT-116) human tumor xenograft models utilizing a number of treatment schedules (Table 7.11) [32]. PHA-680632 also showed tumor stabilization and partial regression in a syngeneic breast cancer model (mouse mammary tumor virus v-Ha-ras mammary carcinoma – MMTV-H-ras) [32]. Toxicity was evaluated on the basis of body weight loss and PHA-680632 appears to be well tolerated in these mouse models [32].

Fancelli *et al.* have described a related 5-amidopyrrolopyrazole subclass, exemplified by PHA-739358 (Table 7.1) [33]. Interestingly, PHA-739358 not only retains potent activity against the Aurora kinases (IC_{50} = 0.013, 0.079, and 0.061 μ M against Aurora A, Aurora B, and Aurora C, respectively) but also inhibits additional protein kinases, in particular, ABL, RET, TRKA, and FGFR1 (IC_{50} = 0.025, 0.031, 0.030, and 0.047 μ M, respectively) [33]. The difference in selectivity between PHA-680632 and PHA-739358 is presumably a result of introducing the angular 5-phenylacetyl group in PHA-739358 relative to the more planar urea moiety in PHA-680632. PHA-739358 has potent antiproliferative activity in four human tumor cell lines (HeLa, MCF7, HCT-116, and A2780) with EC_{50} ranging from 0.028–0.140 μ M. The cell phenotype appears identical to that described for PHA-680632 [32, 33].

PHA-739358 has high aqueous solubility (>15 mg/ml at pH 5.5) and good stability making it well suited for development as an injectable therapeutic agent [33]. PHA-739358 has efficacy in the HL-60 xenograft model in SCID mice. At doses of 7.5, 15, and 30 mg/kg (i.v. bolus b.i.d. for 5 days) PHA-739358 showed dose-dependant tumor growth inhibition of up to 98% at the highest dose. At the same dose, PHA-739358 demonstrated evidence of tumor regression and cures in 2/8 animals with a maximal and reversible body weight loss of 16% [33]. PHA-739358 is currently in phase I

clinical trials in patients with advanced/metastatic solid tumors [70] and hematological malignancies and Phase II in patients with CML.

7.5.4

MLN8054

MLN8054 is a novel fused amino-pyrimidine-benzazepine-based inhibitor with an aryl carboxylic acid which, in contrast to the previously described Aurora kinase inhibitors, is selective for Aurora A over Aurora B and is orally bioavailable [36, 71, 72].

MLN8054 is a potent inhibitor of Aurora A kinase activity ($IC_{50} = 0.004 \mu M$), but less potent against Aurora B ($IC_{50} = 0.172 \mu M$) as measured in recombinant enzyme assays [36, 72]. The Aurora A selectivity appears to be enhanced in cell-based assays ($IC_{50} = 0.034$ and $5.7 \mu M$ against Aurora A and Aurora B, respectively) [36, 72]. MLN8054 is >100-fold selective for Aurora A compared with a panel of 10 other kinases. In addition, when MLN8054 was tested in a panel of 226 kinases at a concentration of $1 \mu M$, only 7 were inhibited by >50% [72]. In cells at low concentrations, MLN8054 caused cells to accumulate in mitosis and increased the incidence of monopolar and tripolar spindles [37, 72] a phenotype consistent with inhibiting Aurora A kinase activity. Despite the mitotic delay, however, and in contrast to inhibitors of Aurora B kinase, MLN8054-treated cells were able to complete mitosis and undergo cytokinesis [37]. Interestingly, in combination with microtubule disorganizers, MLN8054 causes cells to rapidly exit mitosis without undergoing cell division resulting in the formation of multinucleated cells [37]. At high concentrations, MLN8054 results in an inhibition of Histone-H3 phosphorylation and causes an increase in multinucleated cells consistent with inhibition of Aurora B kinase activity.

MLN8054 dosed orally at 30 mg/kg to nude mice generates high plasma exposure with a peak total plasma concentration of $>30 \mu M$, which remains over $1 \mu M$ for 24 h [36]. Tissue penetration appears to be good with compound levels in HCT-116 xenografts closely following plasma levels. Following a single oral dose of MLN8054 at 30 mg/kg to HCT-116 bearing nude mice, inhibition of Aurora A (T288) phosphorylation was observed with recovery by 24 h mirroring the PK profile [36]. At the same dose, a fourfold increase in phospho-Histone H3 (serine 10) was observed, peaking at 6–8 h after dosing and remained elevated for 24 h [71]. An increase in phospho-Histone H3 with MLN8054 is in contrast to the inhibition of Histone H3 phosphorylation at serine 10 seen with MK-0457, PHA-739358, and AZD1152, and is the same phenotype observed with Aurora A siRNA [16].

MLN8054 inhibits tumor growth with both continuous and noncontinuous dosing schedules [36, 71, 72]. The *in vivo* human xenograft mouse studies reported by Millennium are summarized in Table 7.12. Continuous once daily (u.i.d) oral dosing of MLN8054 at 3–30 mg/kg for 21 days to HCT-116 bearing nude mice inhibited tumor growth in a dose-dependant manner with a maximum tumor growth inhibition (TGI) of 84% and tumor growth delay (TGD) of 25 days at the highest dose. A twice daily (b.i.d) dose of 30 mg/kg for 20 days was more efficacious with a TGI = 103% and TGD = 31 days in the same model. Multiple noncontinuous dosing

Table 7.12 Summary of reported *in vivo* studies with MLN8054 from Refs [36, 71, 72]

Mouse efficacy studies: human tumor cell xenografts		
Tumor	Treatment schedule	Efficacy
HCT116	3 mg/kg u.i.d for 21 days	26% TGI, 4 days TGD
	10 mg/kg u.i.d for 21 days	76% TGI, 14 days TGD
	30 mg/kg u.i.d for 21 days	84% TGI, 25 days TGD
	30 mg/kg b.i.d for 20 days	103% TGI, 31 days TGD
	60 mg/kg b.i.d, 3 days on/7 days off × 2	73% TGI, 11 days TGD
	30 mg/kg b.i.d, 5 days on/5 days off × 2	77% TGI, 14 days TGD
	30 mg/kg b.i.d, 10 days on/10 days off × 1	83% TGI, 15 days TGD
PC-3	30 mg/kg b.i.d 40 days continuous	119% TGI
	30 mg/kg b.i.d 5 days on/5 days off × 4	100% TGI
	30 mg/kg b.i.d 10 days on/10 days off × 2	94% TGI
	60 mg/kg u.i.d 3 days on/7 days off × 4	82% TGI
Calu-6	30 mg/kg b.i.d for 21 days	84.5% TGI
	30 mg/kg b.i.d 4 days on/3 days off × 3	55.4% TGI
	60 mg/kg u.i.d 4 days on/3 days off × 3	31.7% TGI

% TGI (tumor growth inhibition) = $100 - (\text{mean tumor volume of treated group} / \text{mean tumor volume of control group}) \times 100$ and was calculated on the last day of treatment. TGD calculated when the average tumor volume reached 1000 mm³ (from an initial treatment volume of ~200 mm³).

schedules (Table 7.12) were efficacious but less so than the continuous dosing schedule [71]. An initial drop in body weight was seen in the 60 mg/kg treatment group (15% on day 6) but less than 5% body weight loss was observed in all other groups [71]. Similar schedules were shown to be efficacious in PC-3 (prostate) and Calu-6 (lung) xenograft mouse models (Table 7.12) with continuous dosing schedules again giving the highest tumor growth inhibitions. MLN8054 is currently in Phase I clinical trials in advanced solid tumors.

7.5.5

AT9283

Astex have developed AT9283 from a fragment-based chemical series [73]. AT9283 is a potent inhibitor of both Aurora A and Aurora B (52% inhibition and 58% inhibition at 0.003 μM against Aurora A and Aurora B, respectively) [73]. AT9283 potently inhibits cell colony formation in a panel of tumor lines (colon, ovarian, lung, breast, and pancreatic) with IC₅₀ of 0.0077–0.020 μM [73]. AT9283 inhibits the phosphorylation of Histone-H3 (serine 10) in HCT-116 cells in a dose-dependant manner. The same cell line treated with 0.10 μM AT9283 results in endoreduplication and a large polyploid cell population. Normal HMEC epithelial cells appear less sensitive to AT9283. Interestingly, HCT-116 cells treated with 0.10 μM AT9283 over a period of eight days have increased p53-p21^{Waf1/Cip1} protein expression. A single 10 mg/kg i.v. bolus dose of AT9283 suppressed Histone-H3 levels for up to 6 h in HCT-116 xenografts grown in nude mice. Tumor growth inhibitory activity was demonstrated

at doses of 7.5–20 mg/kg dosed intermittently i.p. b.i.d in HCT-116 and A2780 human tumor xenograft models in nude mice. AT9283 is currently in Phase I/II trials in patients with leukemia and solid tumors.

7.6

X-Ray Crystal Structures of Aurora Kinases

In addition to the AstraZeneca Aurora A/inhibitor complex [47, 52], there have been a number of other recent publications documenting both Aurora A [68, 74–77] and Aurora B [78] X-ray structures in complex with ADP [74, 76], adenosine [47, 75], small-molecule inhibitors [47, 68, 77, 78], and activating proteins [76, 78].

The availability of these structures has shed light onto the activation and regulation of these important kinases highlighting the difference in activation mechanisms for Aurora A [76] and Aurora B [77]. The EMBL structures [76] indicate that in Aurora A, the activation segment is completely ordered and includes two phosphorylated threonine residues (Thr-287 and Thr-288). In the absence of TPX2, the phosphorylated Thr-288 is exposed to solvent whereas the binding of TPX2, although not triggering a global conformational change in the kinase, results in a “buried” position for the phosphorylated threonine thus locking the active conformation. This is in contrast to the AstraZeneca structures, where the activation loop is disordered.

The structures from Sessa *et al.* [78] provide an insight into the mechanism of activation of Aurora B suggesting a two-stage activation process involving an INCENP induced allosteric activation of the T loop to form an intermediate stage of activation. Phosphorylation of two serines in the carboxy terminus of INCENP generates the fully active kinase. The X-ray structure of Aurora B bound to Hesperadin and INCENP show the kinase to be in an active DFG-in conformation.

As active kinases have been shown to be structurally similar in the catalytic binding cleft [78], inhibitors that bind to this DFG-in active conformation of Aurora might be expected to show limited kinase specificity. Indeed, Hesperadin shows activity across a range of kinases [7]. A similar conclusion is made by Swanson *et al.* [77] when discussing the binding mode of their series of Aurora inhibitors. In contrast, inhibitors that stabilize a DGF-out inactive conformation might be expected to show high specificity for the Aurora kinases as demonstrated by AstraZeneca’s series of quinazolines [47, 52]. However, a recent article by Gray *et al.* demonstrates that this is not a general conclusion and describes the design and synthesis of a set of compounds that do stabilize a DGF-out inactive conformation that are potent and *nonselective* kinase inhibitors [79]. No X-ray structures of Aurora C have been reported to date.

7.7

Summary

The Aurora kinase inhibitors described are members of an exciting new class of targeted anticancer agents that have demonstrated potent tumor growth inhibitory

activity in preclinical models. It is already apparent from these preclinical studies that the dose, schedule, and genetic makeup of the tumor are likely to be important factors in the ongoing clinical development of these agents. Studies have revealed potential mechanisms by which some tumor cells are rendered hypersensitive to Aurora kinase inhibitors compared with normal cycling cells. Drugs that possess increased selectivity toward tumor cells are of great interest but given the important role of Aurora kinases in cell cycle regulation, some toxicity in rapidly dividing tissues such as the bone marrow is expected. It is not yet known whether the concentrations of Aurora kinase inhibitors achievable in man with acceptable side effect profiles will be sufficient to result in significant tumor cell death. Compounds have been developed for delivery via intravenous infusion and/or oral ingestion. Both continuous and intermittent dosing schedules have been shown to be efficacious and generally well tolerated in preclinical studies giving confidence that an efficacious and tolerated schedule can be found in patients. The compounds that are currently in clinical trials (MK-0457, PHA-739358, and AT9283) have pan-Aurora kinase activity, while others are selective for either Aurora B (AZD1152) or Aurora A (MLN8054) kinase activity. It is not yet clear whether inhibition of Aurora A and/or Aurora B could be the more advantageous in terms of providing a therapeutic benefit; definitive answers on the roles of the individual Aurora family members in cancer may well come from patient studies. The Aurora kinase inhibitors described have a range of kinase specificity profiles and while additional activities could provide enhanced efficacy in particular settings they may also result in reduced tolerance. Further, the myelosuppressive nature of Aurora kinase inhibitors means that the schedule required to balance Aurora-led efficacy and tolerability may not be one that allows add-on activities to contribute to an antitumor effect.

The relative importance of the route of administration, Aurora kinase selectivity profile, kinase specificity, and other subtle differences between the compounds described and others that are beginning to emerge will be established by ongoing clinical studies.

References

- Garber, K. (2005) Divide and conquer: new generation of drugs target mitosis. *Journal of the National Cancer Institute*, 97 (12), 874–876.
- Jiang, N., Wang, X., Yang, Y., and Dai, W. (2006) Advances in mitotic inhibitors for cancer treatment. *Mini Reviews in Medicinal Chemistry*, 6, 885–895.
- Jackson, J.R., Patrick, D.R., Dar, M.M., and Huang, P.S. (2007) Targeted anti-mitotic therapies: can we improve on tubulin agents? *Nature Reviews. Cancer*, 7, 107–117.
- Bischoff, J.R., Anderson, L., Zhu, Y., Mossie, K., Ng, L., Souza, B., Schryver, B., Flanagan, P., Clairvoyant, F., Ginther, C., Chan, C.S.M., Novotny, M., Slamon, D.J., and Plowman, G.D. (1998) A homologue of *Drosophila* Aurora kinase is oncogenic and amplified in human colorectal cancers. *The EMBO Journal*, 17 3052–3065.
- Keen, N. and Taylor, S. (2004) Aurora-kinase inhibitors as anticancer agents. *Nature Reviews. Cancer*, 4, 927–936.
- Anand, S., Penrhyn-Lowe, S., and Venkitaraman, A.R. (2003) AURORA-A

- amplification overrides the mitotic spindle assembly checkpoint, inducing resistance to Taxol. *Cancer Cell*, **3**, 51–62.
- 7 Hauf, S., Cole, R.W., LaTerra, S., Zimmer, C., Schnapp, G., Walter, R., Heckel, A., van Meel, J., Rieder, C.L., and Peters, J.-M. (2003) The small molecule Hesperadin reveals a role for Aurora B in correcting kinetochore-microtubule attachment and in maintaining the spindle assembly checkpoint. *The Journal of Cell Biology*, **161**, 281–294.
 - 8 Ditchfield, C., Johnson, V.L., Tighe, A., Ellston, R., Haworth, C., Johnson, T., Mortlock, A., Keen, N., and Taylor, S.S. (2003) Aurora B couples chromosome alignment with anaphase by targeting BubR1, Mad2, and Cenp-E to kinetochores. *The Journal of Cell Biology*, **161**, 267–280.
 - 9 Andrews, P.D. (2005) Aurora kinases: shining lights on the therapeutic horizon? *Oncogene*, **24**, 5005–5015.
 - 10 Matthews, N., Visintin, C., Hartzoulakis, B., Jarvis, A., and Selwood, D.L. (2006) Aurora A and B kinases as targets for cancer: will they be selective for tumours? *Expert Review of Anticancer Therapy*, **6** (1), 109–120.
 - 11 Glover, D.M., Leibowitz, M.H., McLean, D.A., and Parry, H. (1995) Mutations in Aurora prevent centrosome separation leading to the formation of monopolar spindles. *Cell*, **81**, 95–105.
 - 12 Adams, R.R., Carmena, M., and Earnshaw, W.C. (2001) Chromosomal passengers and the (Aurora) ABCs of mitosis. *Trends in Cell Biology*, **11**, 49–54.
 - 13 Nigg, E.A. (2001) Mitotic kinases as regulators of cell division and its checkpoints. *Nature Reviews. Molecular Cell Biology*, **2**, 21–32.
 - 14 Carmena, M. and Earnshaw, W.C. (2003) The cellular geography of Aurora kinases. *Nature Reviews. Molecular Cell Biology*, **4**, 842–854.
 - 15 Hirota, T., Kunitoku, N., Sasayama, T., Marumoto, T., Zhang, D., Nitta, M., Hatakeyama, K., and Saya, H. (2003) Aurora-A and an interacting activator, the LIM protein Ajuba, are required for mitotic commitment in human cells. *Cell*, **114**, 585–598.
 - 16 Yang, H., Burke, T., Dempsey, J., Diaz, B., Collins, E., Toth, J., Beckmann, R., and Ye, X. (2005) Mitotic requirement for Aurora A kinase is bypassed in the absence of Aurora B kinase. *FEBS Letters*, **579**, 3385–3391.
 - 17 Meraldi, P., Honda, R., and Nigg, E.A. (2002) Aurora-A overexpression reveals tetraploidization as a major route to centrosome amplification in p53^{-/-} cells. *The EMBO Journal*, **21**, 483–492.
 - 18 Kallio, M.J., McClelland, M.L., Stukenberg, P.T., and Gorbisky, G.J. (2002) Inhibition of Aurora B kinase blocks chromosome segregation, overrides the spindle checkpoint, and perturbs microtubule dynamics in mitosis. *Current Biology*, **12**, 900–905.
 - 19 Kimura, M., Matsuda, Y., Yoshioka, T., and Okano, Y. (1999) Cell cycle-dependent expression and centrosome localization of a third human Aurora/Ipl1-related protein kinase, AIK3. *The Journal of Biological Chemistry*, **274**, 7334–7340.
 - 20 Li, X., Sakashita, G., Matsuzaki, H., Sugimoto, K., Kimura, K., Hanaoka, F. *et al.* (2004) Direct association with inner centromere protein (INCENP) activates the novel chromosomal passenger protein, Aurora-C. *The Journal of Biological Chemistry*, **279**, 47201–47211.
 - 21 Sasai, K., Katayama, H., Stenoién, D.L., Fujii, S., Honda, R., Kimura, M. *et al.* (2004) Aurora-C kinase is a novel chromosomal passenger protein that can complement Aurora-B kinase function in mitotic cells. *Cell Motility and the Cytoskeleton*, **59** (4), 249–263.
 - 22 Tang, C.J., Lin, C.Y., and Tang, T.K. (2006) Dynamic Localization and functional implications of Aurora-C kinase during male mouse meiosis. *Developmental Biology*, **290**, 398–410.
 - 23 Royce, M.E., Xia, W., Sahin, A.A., Katayama, H., Johnston, D.A., Hortobagyi, G., Sen, S., and Hung, M.C. (2004) STK15/Aurora-A expression in primary breast tumors is correlated with nuclear grade but not with prognosis. *Cancer*, **100**, 12–19.

- 24 Miyoshi, Y., Iwao, K., Egawa, C., and Noguchi, S. (2001) Association of centrosomal kinase STK15/BTAK mRNA expression with chromosomal instability in human breast cancers. *International Journal of Cancer*, **92**, 370–373.
- 25 Lee, E.C.Y., Frolov, A., Li, R., Ayala, G., and Greenberg, N.M. (2006) Targeting Aurora kinases for the treatment of prostate cancer. *Cancer Research*, **66** (10), 4996–5002.
- 26 Sakakura, C., Hagiwara, A., Yasuoka, R., Fujita, Y., Nakanishi, M., Masuda, K., Shimomura, K., Nakamura, Y., Inazawa, J., Abe, T., and Yamagishi, H. (2001) Tumour-amplified kinase BTAK is amplified and overexpressed in gastric cancers with possible involvement in aneuploid formation. *British Journal of Cancer*, **84**, 824–831.
- 27 Ewart-Toland, A., Briassouli, P., de Koning, J.P., Mao, J.H., Yuan, J., Chan, F., MacCarthy-Morrogh, L., Ponder, B.A., Nagase, H., Burn, J., Ball, S., Almeida, M., Linardopoulos, S., and Balmain, A. (2003) Identification of Stk6/STK15 as a candidate low-penetrance tumor-susceptibility gene in mouse and human. *Nature Genetics*, **34**, 403–412.
- 28 Zhou, H., Kuang, J., Zhong, L., Kuo, W.L., Gray, J.W., Sahin, B.R., Brinkley, B.R., and Sen, S. (1998) Tumour amplified kinase STK15/BTAK induces centrosome amplification, aneuploidy and transformation. *Nature Genetics*, **20**, 189–193.
- 29 MurataHori, M. and Wang, Y.L. (2002) The kinase activity of Aurora B is required for kinetochore-microtubule interactions during mitosis. *Current Biology*, **12**, 894–899.
- 30 Li, F. (2003) Survivin study: what is the next wave? *Journal of Cellular Physiology*, **197**, 8–29.
- 31 Harrington, E.A., Bebbington, D., Moore, J., Rasmussen, R.K., Ajose-Adeogun, A.O., Nakayama, T., Graham, J.A., Demur, C., Hercend, T., Diu-Hercend, A., Su, M., Golec, J.M.C., and Miller, K.M. (2004) VX-680, a potent and selective small-molecule inhibitor of the Aurora kinases, suppresses tumour growth *in vivo*. *Nature Medicine*, **10**, 262–267.
- 32 Soncini, C., Carpinelli, P., Gianellini, L., Fancelli, D., Vianello, P., Rusconi, L., Storici, P., Zugnoni, P., Pesenti, E., Croci, V., Ceruti, R., Giorgini, M.L., Cappella, P., Ballinari, D., Sola, F., Varasi, M., Bravo, R., and Moll, J. (2006) PHA-680632, a novel Aurora kinase inhibitor with potent antitumoural activity. *Clinical Cancer Research*, **12** (13), 4080–4089.
- 33 Fancelli, D., Moll, J., Varasi, M., Bravo, R., Artico, R., Berta, D., Bindi, S., Cameron, A., Candiani, I., Cappella, P., Carpinelli, P., Croci, W., Forte, B., Giorgini, M.L., Klapwijk, J., Marsiglio, A., Pesenti, E., Rocchetti, M., Roletto, F., Severino, D., Soncini, C., Storici, P., Tonani, R., Zugnoni, P., and Vianello, P. (2006) 1,4,5,6-Tetrahydropyrrolo[3,4-c]pyrazoles: identification of a potent Aurora kinase inhibitor with a favorable antitumour kinase inhibition profile. *Journal of Medicinal Chemistry*, **49**, 7247–7251.
- 34 Girdler, F., Gascoigne, K.E., Evers, P.A., Hartmuth, S., Crafter, C., Foote, K.M., Keen, N.J., and Taylor, S.S. (2006) Validating Aurora B as an anti-cancer drug target. *Journal of Cell Science*, **119**, 3664–3675.
- 35 Mortlock, A.A., Foote, K.M., Heron, N.M., Jung, F.H., Pasquet, G., Lohmann, J.-J.M., Warin, N., Renaud, F., De Savi, C., Roberts, N.J., Johnson, T., Dousson, C.B., Hill, G.B., Perkins, D., Hatter, G., Wilkinson, R.W., Wedge, S.R., Heaton, S., Odedra, R., Keen, N.J., Crafter, C., Brown, E., Thompson, K., Brightwell, S., Khatri, L., Brady, M.C., Kearney, S., McKillop, D., Rhead, S., Parry, T., Green, S. *et al.* (2007) Discovery, synthesis, and *in vivo* activity of a new class of pyrazoloquinazolines as selective inhibitors of Aurora B kinase. *Journal of Medicinal Chemistry*, **50**, 2213–2224.
- 36 Manfredi, M., Ecsedy, J., Meetze, K., Balani, S., Burenkova, O., Chen, W., Galvin, K., Hoar, K., Huck, J., LeRoy, P., Ray, E., Sells, T., Stringer, B., Stroud, S., Vos, T., Weatherhead, G., Wysong, D., Zhang, M., and Claiborne, C. (2006)

- MLN8054, an orally active Aurora A kinase small molecule inhibitor in phase I clinical trials. *Proceedings of the American Association for Cancer Research*, **47**, 1110, Abstract 4724.
- 37 Ecsedy, J.A., Hoar, K., Wysong, D.R., Rabino, C., Bowman, D.S., Chakravarty, A., and Roy, N. (2006) Effect of Aurora A inhibition in cultured human tumor cells using the selective small molecule inhibitor MLN8054. *Proceedings of the American Association for Cancer Research*, **47**, 488, Abstract 2066.
 - 38 Gautschi, O., Mack, P.C., Davies, A.M., Lara, P.N., and Gandara, D.R. (2006) Aurora kinase inhibitors: a new class of targeted drugs in cancer. *Clinical Lung Cancer*, **8** (2), 93–98.
 - 39 Carvajal, R.D., Tse, A., and Schwartz, G.K. (2006) Aurora kinases: new targets for cancer therapy. *Clinical Cancer Research*, **12** (23), 6869–6875.
 - 40 Naruganahalli, K.S., Lakshmanan, M., Dastidar, S.G., and Ray, A. (2006) Therapeutic potential of Aurora kinase inhibitors in cancer. *Current Opinion in Investigational Drugs*, **7** (12), 1044–1051.
 - 41 Mortlock, A.A., Keen, N.J., Jung, F.H., and Brewster, A.G. (2001) Preparation of quinazolines as Aurora 2 kinase inhibitors. US Patent WO2001021596, A1 20010329, CAN 134:266317, AN 2001:228866.
 - 42 Mortlock, A.A. and Keen, N.J. (2001) Preparation of quinazoline derivatives, method of preparation and use in inhibiting Aurora 2 kinase. US Patent WO2001021595, A1 20010329, CAN 134:266316, AN 2001:228865.
 - 43 Mortlock, A.A. and Keen, N.J. (2001) Preparation of quinazolines as Aurora 2 kinase inhibitors. US Patent WO2001021594, A1 20010329, CAN 134:252355.
 - 44 Mortlock, A.A., Keen, N.J., Jung, F.H., Heron, N.M., Foote, K.M., Wilkinson, R., and Green, S. (2005) Progress in the development of selective inhibitors of Aurora kinases. *Current Topics in Medicinal Chemistry*, **5**, 199–213.
 - 45 Mortlock, A.A. and Keen, N.J. (2001) Preparation of quinazoline derivatives, method of preparation and use in inhibiting Aurora 2 kinase. US Patent WO2001021597, A1 20010329, CAN 134:266318, AN 2001:228867.
 - 46 Mortlock, A.A. (2001) Preparation of phosphonoxy quinazoline derivatives as therapeutic agents. US Patent WO 2004058782, A1 20040715, CAN 141:123758, AN 2004:566625.
 - 47 Heron, N.M., Anderson, M., Blowers, D.P., Breed, J., Eden, J.M., Green, S., Hill, G.B., Johnson, T., Jung, F.H., McMiken, H.H.J., Mortlock, A.A., Pannifer, A.D., Pauptit, R.A., Pink, J., Roberts, N.J., and Rowsell, S. (2006) SAR and inhibitor complex structure determination of a novel class of potent and specific Aurora kinase inhibitors. *Bioorganic & Medicinal Chemistry Letters*, **16** (5), 1320–1323.
 - 48 Hennequin, L.F., Thomas, A.P., Johnstone, C., Stokes, E.S.E., Plé, P.A., Lohmann, J.J.M., Ogilvie, D.J., Dukes, M., Wedge, S.R., Curven, J.O., Kendrew, J., and Lambert-van der Brempt, C. (1999) Design and structure–activity relationship of a new class of potent VEGF receptor tyrosine kinase inhibitors. *Journal of Medicinal Chemistry*, **42**, 5369–5389.
 - 49 Hennequin, L.F., Stokes, E.S.E., Thomas, A.P., Johnstone, C., Plé, P.A., Ogilvie, D.J., Dukes, M., Wedge, S.R., Kendrew, J., and Curven, J.O. (2002) Novel 4-anilinoquinazolines with C-7 basic side chains: design and structure activity relationship of a series of potent, orally active, VEGF receptor tyrosine kinase inhibitors. *Journal of Medicinal Chemistry*, **45**, 1300–1312.
 - 50 Pandey, A., Volkots, D.L., Seroogy, J.M., Rose, J.W., Yu, J.C., Lambing, J.L., Hutchaleelaka, A., Hollenbach, S.J., Abe, K., Giese, N.A., and Scarborough, R.M. (2002) Identification of orally active, potent and selective 4-piperazinylquinazolines as antagonists of the platelet-derived growth factor receptor tyrosine kinase family. *Journal of Medicinal Chemistry*, **45**, 3772–3793.
 - 51 Smaill, J.B., Rewcastle, G.W., Loo, J.A., Greis, K.D., Chan, O.H., Reyner, E.L., Lipka, E., Showalter, H.D.H., Vincent, P.W., Elliot, W.L., and Denny,

- W.A. (2000) Tyrosine kinase inhibitors. 17. Irreversible inhibitors of epidermal growth factor receptor. 4-(phenyl-amino)quinazoline- and 4-(phenyl amino)pyrido [3,2-d]pyrimidine-6-acrylamides bearing additional solubilizing functions. *Journal of Medicinal Chemistry*, **43**, 1380–1397.
- 52 Anderson, M., Keen, N.J., Pannifer, A.D.B., Paupit, R.A., and Rowsell, S. (2003) Crystal structure of human Aurora A kinase catalytic domain complexed with ATP analog and inhibitor and applications to structure-based drug design. US Patent WO2003031606, A2 20030417, CAN 138:316772, AN 2003:301212.
- 53 Breitenlechner, C.B., Bossemeyer, D., and Engh, R.A. (2005) Crystallography for protein kinase drug design: PKA and SRC case studies. *Biochimica et Biophysica Acta*, **1745**, 38–49.
- 54 Jung, F.H., Pasquet, G., Lambert-van der Brempt, C., Lohmann, J.-J.M., Warin, N., Renaud, F., Germain, H., De Savi, C., Roberts, N., Johnston, T., Dousson, C., Hill, G.B., Mortlock, A.A., Heron, N., Wilkinson, R.W., Wedge, S.R., Heaton, S.P., Odedra, R., Keen, N.J., Green, S., Brown, E., Thompson, K., and Brightwell, S. (2006) Discovery of novel and potent thiazoloquinazolines as selective Aurora A and B kinase inhibitors. *Journal of Medicinal Chemistry*, **49**, 955–970.
- 55 Heron, N.M., Jung, F.H., Pasquet, G.H., and Mortlock, A.A. (2004) Preparation of phosphonoxy quinazoline derivatives and their pharmaceutical use. US Patent WO2004058781.
- 56 Wilkinson, R.W., Odedra, R., Heaton, S., Wedge, S.R., Keen, N.J., Crafter, C., Foster, J.R., Brady, M.C., Bigley, A., Brown, E., Byth, K., Barrass, N.C., Mundt, K., Foote, K.M., Heron, N.M., Jung, F., Mortlock, A.A., Boyle, F.T., and Green, S. (2007) AZD1152, a selective inhibitor of Aurora B kinase, inhibits human tumor xenograft growth by inducing apoptosis. *Clinical Cancer Research*, **13**, 3682–3688.
- 57 Carter, T.A., Wodicka, L.M., Shah, N.P., Velasco, A.M., Fabian, M.A., Treiber, D.K., Milanov, Z.V., Atteridge, C.E., Biggs, W.H. III, Edeen, P.T., Floyd, M., Ford, J.M., Grotzfeld, R.M., Herrgard, S., Insko, D.E., Mehta, S.A., Patel, H.K., Pao, W., Sawyers, C.L., Varmus, H., Zarrinkar, P.P., and Lockhart, D.J. (2005) Inhibition of drug-resistant mutants of ABL, KIT, and EGF receptor kinases. *PNAS*, **102** (31), 11011–11016.
- 58 Young, M.A., Shah, N.P., Chao, L.H., Seeliger, M., Milanov, Z.V., Biggs, W.H. III, Treiber, D.K., Patel, H.K., Zarrinkar, P.P., Lockhart, D.J., Sawyers, C.L., and Kuriyan, J. (2006) Structure of the kinase domain of an imatinib-resistant abl mutant in complex with the Aurora kinase inhibitor VX-680. *Cancer Research*, **66** (2), 1007–1014.
- 59 Giles, F., Bergstrom, D.A., Garcia-Manero, G., Kornblau, S., Andreeff, M., Kantarjian, H., Jones, D., Freedman, S.J., and Verstovsek, S. (2006) MK-0457 is a novel Aurora kinase and janus kinase 2 (JAK2) inhibitor with activity in transformed JAK2-positive myeloproliferative disease (MPD). ASH Annual Meeting Abstracts, 108, Abstract 4893.
- 60 Samanta, A.K., Lin, H., Sun, T., Kantarjian, H., and Arlinghaus, R.B. (2006) Janus kinase 2: a critical target in chronic myelogenous leukemia. *Cancer Research*, **66** (13), 6468–6472.
- 61 Gizatullin, F., Yao, Y., Kung, V., Harding, M.W., Loda, M., and Shapiro, G.I. (2006) The Aurora kinase inhibitor VX-680 induces endoreduplication and apoptosis preferentially in cells with compromised p53-Dependent postmitotic checkpoint function. *Cancer Research*, **66** (15), 7668–7677.
- 62 Rubin, E.H., Shapiro, G.I., Stein, M.N., Watson, P., Bergstrom, D., Xiao, A., Clark, J.B., Freedman, S.J., and Eder, J.P. (2006) A phase I clinical and pharmacokinetic (PK) trial of the Aurora kinase (AK) inhibitor MK-0457 in cancer patients. *Proceedings of the American Journal of Clinical Oncology*, **24**, 123s, Abstract 3009.
- 63 Bergstrom, D.A., Clark, J.B., Xiao, A., Griffiths, M., Falcon, S., Pollard, J., Freedman, S.J., and Giles, F. (2006) MK-0457, a novel multikinase inhibitor, inhibits BCR-ABL activity in patients with chronic myeloid leukemia (CML) and

- acute lymphocytic leukemia (ALL) with the T315I BCR-ABL mutation. ASH Annual Meeting Abstracts, 108, Abstract 637.
- 64 Giles, F., Freedman, S.J., Xiao, A., Borthakur, G., Garcia-Manero, G., Wierda, W., Kornblau, S.M., O'Brien, S., Bergstrom, D.A., and Rizzieri, D.A. (2006) MK-0457, a novel multikinase inhibitor, has activity in refractory AML, including transformed JAK2 positive myeloproliferative disease (MPD), and in philadelphia-positive ALL. ASH Annual Meeting Abstracts, 108, Abstract 1967.
 - 65 Giles, F., Cortes, J., Bergstrom, D.A., Xiao, A., Bristow, P., Jones, D., Verstovsek, S., Thomas, D., Kantarjian, H., and Freedman, S.J. (2006) MK-0457, a novel Aurora kinase and BCR-ABL inhibitor, is active against BCR-ABL T315I mutant chronic myelogenous leukemia (CML). ASH Annual Meeting Abstracts, 108, Abstract 163.
 - 66 Giles, F., Cortes, J., Bergstrom, D.A., Xiao, A., Jones, D., Verstovsek, S., Thomas, D., Kantarjian, H., and Freedman, S.J. (2006) MK-0457, a novel multikinase inhibitor, is active in patients with chronic myeloid leukemia (CML) and acute lymphocytic leukemia (ALL) with the T315I BCR-ABL resistance mutation and patients with refractory JAK-2 positive myeloproliferative diseases (MPD). ASH Annual Meeting Abstracts, 108, Abstract 253.
 - 67 Giles, F.J., Cortes, J., Jones, D., Bergstrom, D., Kantarjian, H., and Freedman, S.J. (2007) MK-0457, a novel kinase inhibitor, is active in patients with chronic myeloid leukemia or acute lymphocytic leukemia with the T315I BCR-ABL mutation. *Blood*, **109** (2), 500–502.
 - 68 Fancelli, D., Berta, D., Bindi, S., Cameron, A., Cappella, P., Carpinelli, P., Catana, C., Forte, B., Giordano, P., Giorgini, M.L., Mantegani, S., Marsiglio, A., Meroni, M., Moll, J., Pittala, V., Roletto, F., Severino, D., Soncini, C., Storici, P., Tonani, R., Varasi, M., Vulpetti, A., and Vianello, P. (2005) Potent and selective Aurora inhibitors identified by the expansion of a novel scaffold for protein kinase inhibition. *Journal of Medicinal Chemistry*, **48** (8), 3080–3084.
 - 69 Pevarello, P., Fancelli, D., Vulpetti, A., Amici, R., Villa, M., Pittala, V., Vianello, P., Cameron, A., Ciomei, M., Mercurio, C., Bischoff, J.R., Roletto, F., Varasi, M., and Brasca, M.G. (2006) 3-Amino-1,4,5,6-tetrahydropyrrolo[3,4-c]pyrazoles: a new class of CDK2 inhibitors. *Bioorganic & Medicinal Chemistry Letters*, **16** (4), 1084–1090.
 - 70 Burris, H.A. III, Hudes, G., Jones, S., Cheng, J., Spiegel, D., Mariani, M., Macdonald, H., Rocchetti, M., Laffranchi, B., and Cohen, R.B. (2006) A Phase I dose-escalation study of the Aurora kinases inhibitor PHA-739358 administered as a 24hours infusion in a 14-day cycle in patients with advanced/metastatic solid tumors. AACR-NCI-EORTC International Conference, Molecular Targets and Cancer Therapeutics, Prague, Czech Republic, Abstract C271.
 - 71 Huck, J., Zhang, M., Burenkova, O., Connolly, K., Manfredi, M., and Meetze, K. (2006) Preclinical anti-tumor activity with MLN8054, A small molecule Aurora A kinase inhibitor. *Proceedings of the American Association for Cancer Research*, **47**, 1104, Abstract 4698.
 - 72 Manfredi, M.G., Ecsedy, J.A., Meetze, K.A., Balani, S.K., Burenkova, O., Chen, W., Galvin, K.M., Hoar, K.M., Huck, J.J., LeRoy, P.J., Ray, E.T., Sells, T.B., Stringer, B., Stroud, S.G., Vos, T.J., Weatherhead, G.S., Wysong, D.R., Zhang, M., Bolen, J.B., and Claiborne, C.F. (2007) Antitumor activity of MLN8054, an orally active small-molecule inhibitor of Aurora A kinase. *PNAS*, **104** (10), 4106–4111.
 - 73 Gallagher, N., Angove, H., Berdini, V., Carr, M., Curry, J., Fazal, L., Howard, S., Lyons, J., Maman, S., Reule, M., Tisi, D., and Gill, A. (2006) Inhibitors of Aurora kinase derived from fragment based lead discovery. *Proceedings of the American Association for Cancer Research*, **47**, 1155, Abstract 4915.
 - 74 Nowakowski, J., Cronin, C.N., McRee, D.E. *et al.* (2002) Structures of the cancer-related Aurora A, FAK, and EphA2

- protein kinases from nanovolume crystallography. *Structure*, **10** (12), 1659.
- 75 Cheetham, G.M., Knegt, R.M., Coll, J.T. *et al.* (2002) Crystal structure of Aurora-2, an oncogenic serine/threonine kinase. *The Journal of Biological Chemistry*, **277** (45), 42419.
- 76 Bayliss, R., Sardon, T., Vernos, I. *et al.* (2003) Structural basis of Aurora-A activation by TPX2 at the mitotic spindle. *Molecular Cell*, **12** (4), 851.
- 77 Tari, L.W., Hoffman, I.D., Benson, D.C., Hunter, M.J., Nix, J., Nelson, K.J., McRee, D.E., and Swanson, R.V. (2007) Structural basis for the inhibition of Aurora A kinase by a novel class of high affinity disubstituted pyrimidine inhibitors. *Bioorganic & Medicinal Chemistry Letters*, **17**, 688.
- 78 Sessa, F., Mapelli, M., Ciferri, C. *et al.* (2005) Mechanism of Aurora B activation by INCENP and inhibition by Hesperadin. *Molecular Cell*, **18** (3), 379.
- 79 Okram, B., Nagle, A., Adrian, F.J., Lee, C., Ren, P., Wang, X., Sim, T., Xie, Y., Wang, X., Xia, G., Spraggon, G., Warmuth, M., Liu, Y., and Gray, N.S. (2006) A general strategy for creating "inactive conformation" Abl inhibitors. *Chemistry and Biology*, **13**, 779.

Part Three

Application of Kinase Inhibitors to Therapeutic Indication Areas

8

Discovery and Design of Protein Kinase Inhibitors: Targeting the Cell cycle in Oncology

Mokdad Mezna, George Kontopidis, and Campbell McInnes

8.1

Protein Kinase Inhibitors in Anticancer Drug Development

A number of therapeutic targets from the 518 genes comprising the human kinome [1, 2] are currently being pursued, with the search for inhibitors comprising approximately 30% of pharmaceutical discovery programs. Genes encoding protein kinases constitute almost 2% of the human genome making this enzyme class the second largest group of drug targets after GPCRs. As a result of this interest, nine protein kinase inhibitor drugs (as of early 2010) have been approved for use in oncology by the FDA in addition to several biologics targeting extracellular domains of growth factor receptor kinases. As many kinases have been implicated in the etiology of cancer, it is not surprising that these are highly sought-after antitumor drug targets. In particular, tyrosine kinases have been extensively investigated and the efforts on BCR-ABL, EGFR, and VEGFR kinases have resulted in successful drug launches in oncology. Other tyrosine kinases being investigated currently include the c-met (metastasis and angiogenesis) and the FGFR (fibroblast growth factor receptor).

Due to the complexity of structural mechanisms that regulate kinases, there are several potential ways that protein kinase activity can be modulated. The most common, and to date, the most successful approach in drug discovery has been to focus on the ATP binding cleft and to block the catalytic site. A multitude of compounds have resulted from this strategy and several compounds either are in late-stage clinical trials or have been approved as drugs [3]. As mentioned, the first successful approval was imatinib (Figure 8.1; Glivec®/Gleevec®) [4], having revolutionized the treatment of chronic myelogenous leukemia (CML) by dramatically improving survival rates [5–7]. Inhibition of c-Kit, also a tyrosine kinase targeted by imatinib has resulted in approval of treatments for gastrointestinal stromal tumors (GIST) [8, 9], which were largely untreatable until recently, having a survival rate of <5% after chemotherapy. Treatment with imatinib, however, leads to a 40–70% response rate in metastatic or inoperable cases of GIST. Sunitinib (Figure 8.1; Sutent®), has recently been approved by the FDA and shown to be effective against

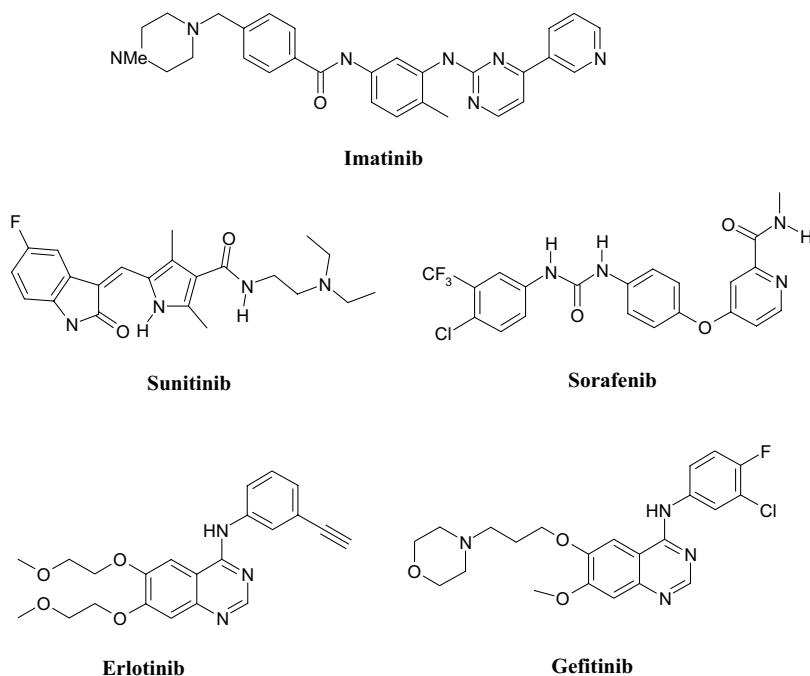


Figure 8.1 The chemical structures of several kinase inhibitors approved for clinical use in oncology. Proof of concept in targeting the ATP binding site as a viable strategy for drug development has been achieved with these compounds.

GIST in cases where imatinib fails, with patients surviving up to four times longer without progressive disease [8, 9].

The epidermal growth factor receptor (EGFR) family are signal transduction receptors that have successfully been targeted in drug discovery in the first instance with monoclonal antibodies. Gefitinib (Figure 8.1; Iressa[®]), an orally active tyrosine kinase inhibitor of the EGFR showed early promise in shrinking lung tumors [10], however, subsequent clinical trials with monotherapy of gefitinib and in combination with approved chemotherapeutics did not produce a survival benefit in several multicenter Phase III trials [11]. A second EGFR inhibitor, erlotinib (Figure 8.1; Tarceva[®]), after extensive testing in Phase III clinical trials, showed an overall survival benefit compared with placebo and now has full FDA approval for treatment of patients with NSCLC who have progressed after treatment with chemotherapy [12]. The success of erlotinib demonstrated that lack of efficacy may be compound and not necessarily target specific.

Another class of tyrosine kinases, the VEGF receptor kinases are implicated in tumor growth and metastasis through angiogenesis and two inhibitors has been approved as cancer therapeutics. Sunitinib and sorafenib (Figure 8.1; Nexavar[®]) have been approved for solid tumors including colorectal cancer, gastrointestinal stromal tumors, and renal cell carcinoma [13]. Sorafenib development took roughly 11 years,

with approval obtained 5 years after the initiation of the first Phase I trial [14, 15]. The approval of these compounds effective against several different anticancer targets described demonstrate that inhibiting protein kinases is a viable and effective therapeutic strategy in oncology. At the same time, failures of some kinase inhibitors in clinical oncology trials show that there is scope for improvement in target selection, and in compound efficacy. Besides the tyrosine kinases described, which have resulted in approved drugs, other kinase targets being pursued include the ser/thr protein kinases. The purpose of this chapter is to discuss about the approaches that have resulted in the successful identification of promising inhibitors directed toward cell cycle protein kinases and to discuss some of the work that is ongoing in promoting these compounds as future therapeutic agents in oncology. Targeting cell cycle regulatory kinases in oncology research have yet to result in a successful approval of a clinically validated drug, however, many compounds are in advanced stages of clinical testing. Three targets for which this is true include the mitotic Aurora, the polo-like kinases, and the cyclin-dependent kinases that are implicated in regulating many stages of the eukaryotic cell cycle.

8.2

Structure-Guided Design of Small-Molecule Inhibitors of the Cyclin-Dependent Kinases

The first 3D structure of a protein kinase was that of cyclic AMP-dependent kinase (protein kinase A) (PKA) [16] and since then significant advances have been made in understanding the structural basis for protein kinase regulation. There are currently in excess of 300 structures of approximately 40 unique kinase domains that have been deposited in the Protein Data Bank (PDB). The catalytic domain of protein kinases is highly conserved structurally and is comprised of two subdomains [2, 17] with ATP binding in a hydrophobic cleft formed by the intersection of two lobes (the N-lobe – predominantly β -sheet – and the C-lobe (primarily α -helical)) and H-bonding to a flexible hinge segment connecting these. Protein kinase activity is precisely regulated through conformation changes induced by binding of regulatory domains or proteins and/or through phosphorylation/dephosphorylation events [18, 19]. Phosphorylation of the activation loop by another kinase is a frequent event required to induce conformational changes necessary to open the substrate binding site and enable alignment of the residues for catalysis [20, 21]. The majority of kinase inhibitors developed so far are ATP-competitive due to the druggability of the catalytic site, however, other potential strategies include preventing substrate docking (where required prior to phosphorylation); and stabilization of conformations, which cannot productively bind ATP or are not catalytically competent. The latter success has been achieved through identifying “allosteric pockets” distinct from the catalytic site or in locking kinases into inactive conformations that do not bind ATP.

At least 11 genes encoding Cdk_s and 9 other genes encoding Cdk-like proteins with conserved primary structure [22] have been discovered so far in the human and the

mouse genomes. They have long been known to control the various phases of the cell cycle (CDK1, entry into mitosis; CDK4/6, progression through G1; CDK2/A, E, progression through G1, entry into S phase, respectively) and their deregulation is frequently associated with cancer and have therefore been widely investigated as antitumor drug targets. Recently, it was also found that CDKs play an important roles in the regulation of transcription by phosphorylation of the C-terminal domain of RNA polymerase II [23, 24] and CDK7 and CDK9 inhibitors specifically been shown to downregulate the transcription of antiapoptotic genes [25].

In terms of the structural basis for regulation and inhibition, the CDKs are among the most extensively characterized. Crystal structures of CDK2 [26–28], CDK5 [29], CDK6 [30], CDK7 [31], CDK9 [32], and CDK4 [33] have been obtained recently and among these, CDK2 has the most information with more than 200 structures available (EC 2.7.11.22 cyclin-dependent kinase, 225 PDB entries, October 2010) in <http://www.ebi.ac.uk/thornton-srv/databases/enzymes/>). Numerous complexes have been solved in monomeric, cyclin-activated, and inhibitor-bound forms [28, 34, 35] and the resulting information has enabled the discovery and the optimization of highly potent ATP inhibitors of CDK2 [36]. CDKs are essentially inactive in monomeric form; which are being partially activated after binding of cyclins and fully after phosphorylation of the T-loop. CDKs remain the focus of intense efforts in drug development and many inhibitors with activity against CDKs are under preclinical and clinical examinations in cancer research [37]. To date, several inhibitors including flavopirodol and roscovitine have been investigated in Phase I and Phase II trials; however, none have been approved to date as therapeutics in oncology. Despite this, the biological rationale for targeting the cell cycle and transcription regulation provides the impetus for continued development of inhibitory compounds including those that target alternate mechanisms of kinase inhibition.

8.3

Catalytic Site Inhibitors

The majority of effort directed toward the discovery of kinase inhibitors useful as therapeutics has focused on blocking the ATP binding site in the catalytic domain [38]. As the majority of CDK inhibitors in clinical and preclinical trials [37] are ATP competitive, it is apparent that this site is druggable. The distinct features [39] allowing this include an appropriate balance between available H-bond donor–acceptors [40] and hydrophobic residues presented in the cleft (Figure 8.2) and the large buried surface that can efficiently bind a small molecule [40].

The ATP binding site of CDKs has been described in detail [3, 41, 42] from the variety of X-ray structures available in the PDB (Figures 8.2 and 8.3). Kinases can generally bind ATP in catalytically inactive forms, for example, in monomeric CDKs where the residues of the active site are improperly aligned for catalysis. An overlay of active and inactive CDK2, the only CDK protein structure available in both forms, shows significant differences in the kinase domain. Comparison of the ATP binding site and its interactions with a series of related pyrimidine inhibitors was recently

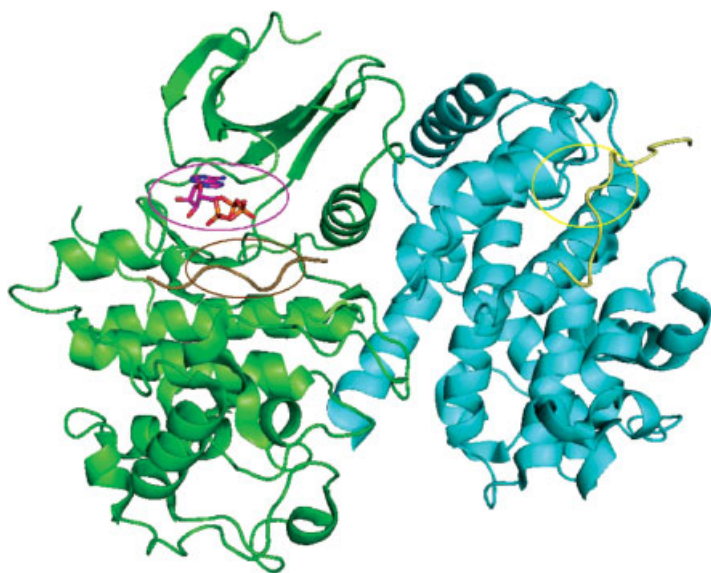


Figure 8.2 Sites for potential inhibitor design in the CDK/cyclin complex. The ATP and substrate binding sites on the CDK monomer are highlighted in magenta and brown,

respectively, and the cyclin binding groove circled on the cyclin positive regulatory subunit (ribbon structure from PDB entry: 2CCI).

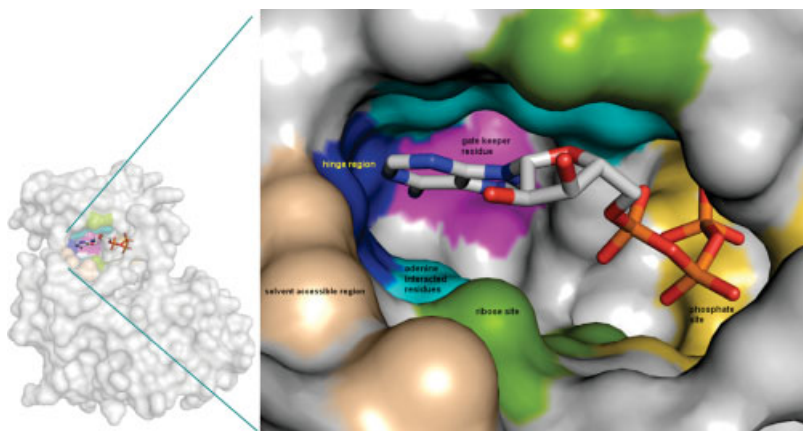


Figure 8.3 ATP binding site of CDK7. The kinase active site is divided into subsites according to its interactions (vdW contacts, H-bonding, and electrostatic) with ATP, solvent, and established nomenclature. In general, the active site of protein kinases is

comprised of subsites that vary between individual enzymes. The gatekeeper residue and the solvent accessible surface are key determinants for the design of selective inhibitors.

conducted [43]. The results obtained from rigorous comparison indicate that while dramatic differences are not observed between monomeric and cyclin-bound inhibitor complexes, at least for the adenine and the ribose pockets (Figure 8.2), these differences are nevertheless sufficient in some instances to significantly alter inhibitor binding mode and/or result in substantial changes in binding affinity between the two states of the same ligand [44]. This became apparent only after a number of CDK2-inhibitor structures were solved and the energetics and the binding modes of inhibitors compared in both forms [45–48]. This study illustrated that complex structures can identify flexible residues that should be considered in docking or design studies [44, 49].

The observed conformations of the CDK ATP binding site indicate a comparatively rigid scaffold when compared to other members of kinase family. In protein–ligand complex structures of other kinases such as Aurora and c-Abl, the ATP site undergoes significant changes and particularly in the case of c-Abl, ligands can induce dramatic differences. Inhibitors STI-571 and PD173955 bind in the ATP site with buried surface area 913–1251 Å², respectively, and the large difference observed is the result of dynamic plasticity of c-Abl and its ATP cleft [7]. The DGF-out (inactive) conformation observed with these kinases has not been found in CDK inhibitor complexes.

8.4

ATP Site Specificity

Currently, there are crystal structures available for six CDK isoforms, CDK2 [50], CDK5 [29], CDK6 [51], CDK7 [31], CDK9 [32], and CDK4 [33]. Many of these structures have been solved in complex with inhibitors [32, 44, 48, 52] and/or partner protein [29, 53]. Comparison of the ATP binding sites of CDK2 (PDB entry: 1JSV), CDK5 (1UNG), CDK6 (2F2C), CDK7 (1UA2), CDK9 (3BLR), and CDK4 (2W96) reveals structural similarity with the adenine and the ribose pockets having almost identical primary and tertiary structure and where the gatekeeper residue is Phe in all cases (Figure 8.3). Differences between CDKs can be found mainly in the solvent accessible region where Lys⁸⁹ in CDK5 and CDK2 changes to Thr¹⁰² and Thr¹⁰⁷ in CDK4 and CDK6, respectively, and Val¹⁰⁰ in CDK7. In the phosphate binding site, only one residue difference is observed where residue Asn¹⁴⁴ in CDK5 changes to Asp in CDK2, CDK6, and CDK7 and its conformation altered similar to what has seen in active to inactive CDK2 [44].

As the observed differences are relatively minor, it is not surprising that the identified inhibitors are not absolutely selective for a single CDK [54]. On the other hand, they are significant enough for designing a highly selective CDK6/CDK4-specific inhibitor [55]. The most specific inhibitor reported to date [37] (but not for a single CDK) has a low-nanomolar IC₅₀ for CDK4 and CDK6 compared to >10 μM for CDK1, CDK2, and CDK5 (4, Figure 8.4). The structural explanation for CDK4 and CDK6 selectivity apparently derives from differences in the interactions with the solvent accessible region. Both CDK4 and CDK6, unlike the rest of CDKs family, have hydrogen acceptor groups (Thr¹⁰⁷ in CDK6 and Glu¹⁴⁴ in CDK4) in this region.

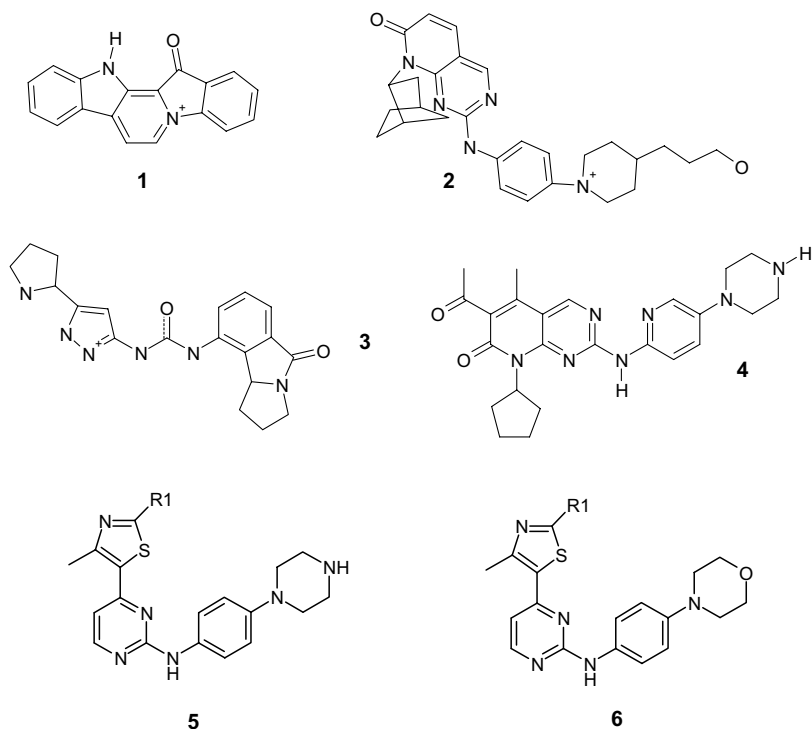


Figure 8.4 Chemical structures of CDK4 selective inhibitors. A common determinant for selectivity is the presence of a positively charged nitrogen that forms electrostatic interactions with unique residues in the CDK4 ATP binding site.

The particular region of the ATP site has been used before for the design of selective CDK4 inhibitors [56] where electrostatic interactions between Glu¹⁴⁴, in solvent accessible region, and ionizable nitrogens of the inhibitor were exploited to increase selectivity. Significantly, both of the above CDK4-selective ligands share a piperazine ring containing this determinant.

With most CDK inhibitors described to date, it has been observed that CDK2 selectivity is predominant over other isoforms. Recently, however, significant progress has been achieved in elucidating the structural basis of selective CDK inhibition and these results have enabled the design and optimization of isoform-specific compounds. As might be expected from similarities in their ATP binding sites, CDK1 inhibition tracks closely with that of CDK2, although some partially selective compounds have been synthesized [57–59]. Inhibitors of CDK2 are, in general, less potent against CDK4, however, recent advances have been made in generating very potent and selective for this isoform. Inhibitors reported in the literature as being highly specific for CDK4 over CDK2 include fascaplysin (1) [60]; PD0183812 (2) [61]; and the urea-based inhibitor series 3 [62–64] (Figure 8.4). The use of a homology structure for CDK4 and a CDK4 mimic construct in which the ATP binding residues of CDK2 were replaced with those of CDK4, attempted to generate surrogate

structures that facilitate the structural basis for observed potency and selectivity information [62, 63].

Using a homology structure for CDK4, an in-depth computational study of inhibitors that bind preferentially to CDK4 was performed [65]. The model structure generated highlighted key differences in the active site of CDK4 that could potentially be exploited in the design of selective inhibitors. In particular, T¹⁰² (CDK4) compared to K⁸⁹ (CDK2) results in a relative decrease in volume of the ATP pocket and enables larger functional groups adjacent to the hinge region H-bond contacting groups. Through docking studies, the observation was made that the majority of CDK4-selective inhibitors contain a positively charged nitrogen at physiological pH and that these inhibitors bind to CDK4 with significantly more favorable calculated interaction energies relative to CDK2. Subsequent analysis of the CDK4 binding pocket suggests that the formal charge differences between the two isoforms (CDK4 ATP binding site has a formal charge of -2 units relative to CDK2), is the primary reason for the increase in complementarity with the protonated inhibitors.

This study also demonstrated that an otherwise CDK2-selective pharmacophore could be converted to a CDK4-specific one by appropriate introduction of an ionizable nitrogen (piperazine (5), Figure 8.4) and replacement of this with a neutral functional group (morpholine(6), Figure 8.4) resulted in loss of favorable binding to CDK4 [36, 65]. This showed conclusively how determinants could be incorporated into CDK inhibitors based on structural information to generate selective ATP-competitive molecules. The CDK4 selectivity determinants identified were somewhat validated structurally by investigators who generated site-specific mutants in the context of CDK2 crystal structures [66]. The CDK2 K89T mutant (CDK4 residue) was crystallized in complex with a CDK4-selective inhibitor. A bisanilinopyrimidine compound had a similar IC₅₀ to native CDK4 in the mutant enzyme and is 18-fold more potent than on wild-type CDK2. In structural terms, the selectivity of this analogue was attributed to electrostatic repulsion with K⁸⁹ in CDK2 and a favorable electrostatic potential in the CDK4 mimic [66].

Recently, several other studies have contributed to understanding of additional determinants of CDK4 selectivity. A major advance resulted in the synthesis and the characterization of an inhibitor, which was completely selective for CDK4/cyclin D1 and CDK6/cyclin D2, cyclin D3 versus studied members of the CDK family and against a wide panel of other protein kinases. It was found that simple addition of a methyl group to the C5-position of a pyrido[2,3-*d*] pyrimidine-7-one core structure resulted in the discovery of a highly selective compound (PD0332991 (4), Figure 8.4) [55, 67, 68]. In addition, substitution of the N8-position of this series with phenylpiperazine resulted in an increase in potency relative to the unsubstituted phenyl group. The structural basis for these discoveries was highlighted in a recent publication of the complex structures of CDK6 with the selective analogues [69]. In this work, the CDK6 interactions of PD0332991 (4, Figure 8.4) were compared with its CDK2/cyclin A contacts. The model generated for CDK2-PD0332991 identified several unfavorable contacts of F⁸⁰ with the C5 methyl group and the C6 acetyl group, therefore explaining the very low affinity of the inhibitor to CDK2. The clashes observed in CDK2 were not seen in CDK6 as a result of conformational

adaptations in the hinge region (F^{80} - H^{84} CDK2 numbering) suggesting that favorable H-bonds to this region and favorable F^{80} interactions are mutually exclusive in the CDK2 context. These results indicate that the hinge region conformation is kinase specific since it plays a significant role in the specificity of PD0332991.

Interestingly, PD0332991 (CDK4 IC_{50} , 0.011 $\mu\text{mol/l}$; Cdk6 IC_{50} , 0.016 $\mu\text{mol/l}$; no activity against 36 other protein kinases) is a potent antiproliferative agent against retinoblastoma (Rb)-positive tumor cells and induces a G1 arrest, with concomitant reduction of phospho-Ser780/Ser795 on the pRb itself [67]. Oral administration of this compound to mice bearing the Colo-205 human colon carcinoma xenografts resulted in marked tumor regression suggesting that it has significant therapeutic potential and that targeting CDK4 selectively is a viable strategy.

Recently, other concepts that have gained support in kinase inhibitor design include targeting the inactive form of a kinase [70] and specifically exploiting the structural differences between active and inactive forms of CDKs [44, 71] in order to design more specific inhibitors. Structural differences have been reported in detail for CDK2, which comprises the largest set of CDK and possibly kinase crystal structures available. As mentioned, CDK2 undergoes extensive conformational changes upon activation by cyclin binding and phosphorylation [28], however, the most significant of these can not be exploited as they are not localized to the ATP pocket where known inhibitors bound. The recent comparison described above showed that the differences in the ATP-site between monomeric/active forms can potentially be utilized for the design of more specific CDK2 inhibitors [44]. To further enable design, structural information for other members of the CDK family in different activation states would be necessary in order to incorporate selectivity determinants.

8.5

Alternate Strategies for Inhibiting CDKs

Other strategies for inhibiting CDKs, although significantly more challenging, involve targeting alternate binding sites. The ternary complex structure of CDK2/cyclin A together with $p27^{KIP1}$ peptide [28] provides information on the most promising sites for ligand design and includes the substrate and the cyclin binding groove. The substrate groove is located adjacent to the ATP binding site (Figure 8.1) and from recent X-ray structures it is apparent that this is a shallow groove forming numerous diffuse contacts with the polypeptide substrate [72]. In comparison with the CBG, this site lacks a well-defined hydrophobic cleft able to interact with a lipophilic peptide motif. Substrate-competitive inhibitors of the insulin-like growth factor receptor [73] (IGF-1R) and CDK1 [74] have been identified with these being among the few examples of kinase substrate-competitive inhibitors and giving precedent for further studies. Combination of the substrate inhibitor with an ATP antagonist to gain potency while binding in the substrate site to provide specificity may result in highly effective and selective kinase inhibitors.

8.6

Cyclin Groove Inhibitors (CGI)

Many protein kinases possess a substrate-docking site through which a binding and recognition event must occur before transfer of phosphate from ATP to the substrate. Targeting these binding interactions has considerable potential for designing compounds with high selectivity as they tend to differ substantially among kinases [75] in contrast to the ATP binding site. Several reports have described the identification and the design of inhibitors of kinase substrate-docking sites [75, 76].

The G1 and S phase CDKs (CDK2/cyclin A, cyclin E and CDK4/cyclin D1) phosphorylate substrates containing the cyclin binding motif (CBM) [77–79] including members of the pRb and the E2F1 families as well as p53 itself. Interestingly, substrate recruitment through the cyclin groove is kept in check with natural CDKs inhibitory mechanisms in addition to those targeting the ATP cleft. A striking observation revealed by the CDK2/cyclin A/p27 crystal structure is the folding of p27 into both the ATP and the CBG sites on the CDK2 and the cyclin monomers, respectively. Inactivation of endogenous CDK inhibitors, such as p16^{INK4a}, p21^{WAF1}, p27^{KIP1}, and p57^{KIP2}, provides a means for cells to override the G1 checkpoint and is a common tumorigenic event. Synthetic peptides comprising the CBM are able to potentially inhibit CDK2/cyclin A activity and in cell permeable forms to induce cytotoxic effects in tumor cells grown *in vitro*.

The CBG (Figure 8.1) is comprised of three subsites that form interactions with the pharmacophoric elements for substrate and peptide inhibitor complex formation. These include (a) a hydrophobic pocket that contacts two lipophilic peptide side chains, (b) an adjacent site providing polar and ionic complementarity with basic residues of the peptide, (c) a secondary hydrophobic pocket (Figure 8.5). Currently, only cyclins A, D, and E have been demonstrated to have a functional cyclin groove [80] suggesting therefore a possible mechanism through which only the CDKs forming substrate complexes could be specific targeted.

Peptidomimetic approaches to the development of CGIs have been pursued by a number of groups [81–84]. The outcome of this work has resulted in the discovery of the peptide-small-molecule hybrid inhibitors [85, 86] and supports the approach for generating potent and specific inhibitors of a single CDK isoform. The determination of structure–activity relationships for a series of octapeptides through substitution and truncation studies resulted in the characterization of smaller less potent tetrapeptide inhibitors of CDK2/cyclin A [86]. An optimization and rigidification strategy resulted in the identification of noncharged small molecules bypassing arginine residues in the peptide motif important for binding. An optimized compound (IC₅₀, 8 nM) was identified consisting of only one natural amino acid residue and thus is significantly more drug-like than the peptide derivatives.

A drug discovery strategy for protein–protein interactions (REPLACE) was applied to identify replacements for amino acid and peptide determinants in another approach to generate nonpeptidic molecules [87]. Validation was obtained in the discovery of fragment-like molecules that when ligated to the N- and C-terminal portions of a tetrapeptide resulted in comparable activities to an optimized

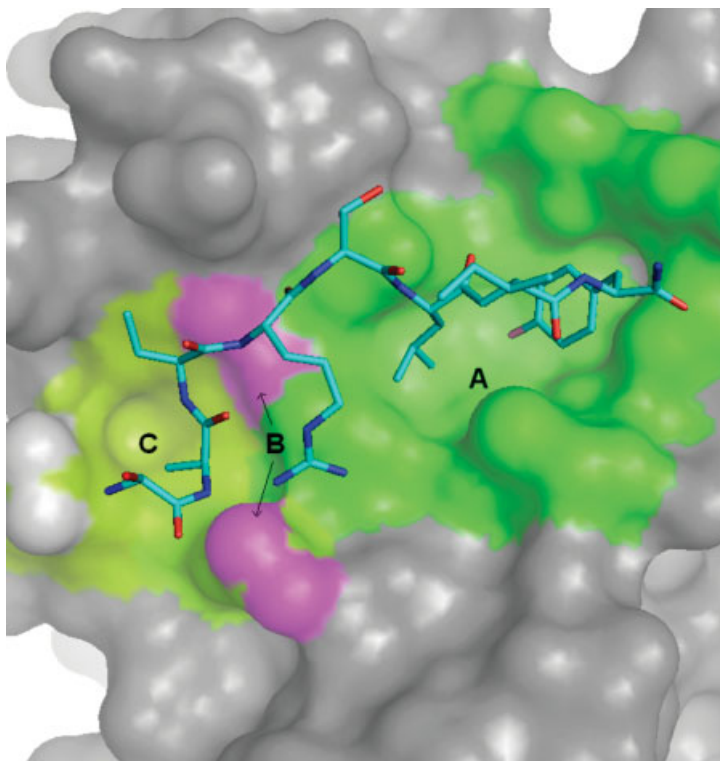


Figure 8.5 The cyclin groove consists of two hydrophobic pockets A (green) and C (lime) separated by site B (magenta) that provides polar and ionic interactions to substrate and

inhibitory molecules. Arginine, Leucine, and Phenylalanine side chains represent the key binding determinants and main chain atoms contribute H-bonding interactions.

pentapeptide. The N-terminal arginine of p21 peptides was replaced with a phenyl-triazole substructure interacting with the secondary hydrophobic subsite while a biphenyl ether system replaced the interactions of the C-terminal phenylalanine residues that make critical contacts with the primary lipophilic pocket. Another strategy to make more drug-like peptidomimetic molecules targeting the cyclin groove employed the synthesis of cyclic peptides mimicking a naturally occurring intramolecular H-bond observed in the p27-CDK2/cyclin A crystal structure [88]. Cyclization through a lysine residue to the C-terminus of the molecule resulted in significant potency enhancement relative to the linear peptide as a result of lowering the entropic cost of binding. Subsequent structural analysis confirmed the cyclic structure and provided further insights for design of enhanced molecules. Together, these studies validate the concept of targeting substrate binding as a viable strategy for kinase inhibition and for the design of selective compounds. Nevertheless, the true potential of such inhibitors remains to be determined as these compounds remain in early discovery and they have not yet moved to preclinical and clinical stages.

8.7

Inhibition of CDK–Cyclin Association

Since activation of the CDKs requires binding of the cyclin positively regulatory subunit and thus formation of CDK–cyclin complex, it is at least in theory possible to inhibit CDK activities by blocking this association and potentially achieving similar results as the one seen from inhibition of ATP and CGI sites. Protein complexes that exist as homo- or heterodimers generally bind strongly with K_{ds} in the range from 1 nM to 1 pM and often cannot be separated without denaturation of the individual monomer structures. Proteins can also exist as monomers and associate or disassociate in response to their environment and therefore have much higher K_{ds} (from 1 μ M to 1 nM) [89]. CDKs and cyclins belong to the second group. The CDK2–cyclin A complex with a dissociation constant around 50 nM [90] is in a range that makes the task of small-molecule-induced complex dissociation challenging but still feasible. Work in this area has resulted in the identification of peptides [91] that bind to a surface pocket in cyclin A and disrupt its interaction with CDK2 and as might be expected, the hexapeptide NBI1 competes neither with ATP nor with CDK2 substrates.

8.8

Recent Developments in the Discovery and the Development of Aurora Kinase Inhibitors

Aurora kinases were discovered by Glover *et al.* when it was reported that *Drosophila* mutants possessing monopolar spindles and circular chromosomes, lacked a ser/thr kinase essential for the proper execution of mitosis and maintenance of genome integrity [92]. This kinase was named Aurora (referring to Aurora Borealis) and later on was shown existing in Aurora A, Aurora B, and Aurora C isoforms. They are important for the mitotic functions of spindle assembly, chromosome maturation, segregation, and also cytokinesis. It has been shown that Aurora kinases are frequently overexpressed in many human cancers indicating their involvement in tumorigenesis and although the exact mechanism in tumorigenesis is still not completely understood, they nonetheless represent plausible drug targets for cancer therapy. Currently, the main focus of drug discovery efforts are on Aurora A and Aurora B [93, 94] whereas Aurora C (Figure 8.6) has been reported to be a chromosomal passenger protein and its expression is exclusive to testis. In humans, the Aurora A gene is commonly amplified and both mRNA and protein levels increase in breast, colon, bladder, ovarian, and pancreatic tumors. While the Aurora B gene is not associated with tumorigenesis through amplification, the mRNA and protein levels increase considerably in transformed cells implicating the role of these two proteins in tumor formation. The functions of Aurora C and its role in tumorigenesis remain to be fully determined.

Aurora A is a ubiquitous protein and acts as a key regulator of the cell cycle. The protein level is undetectable in G1 and increases in late S phase and G2 as the cell

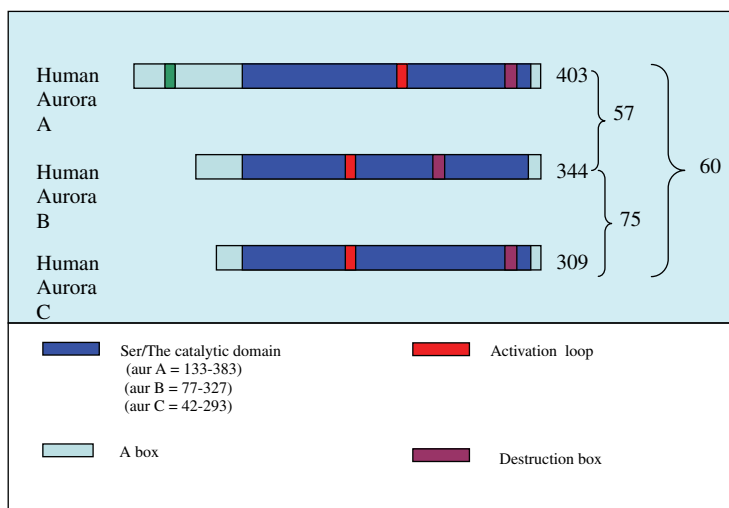


Figure 8.6 Schematic representation of the functional domains of the most significant isoforms of Aurora kinase.

prepares for division as the centrosome reaches maturity. AKA at this stage is localized at the centrosome in duplicated chromosomes and orchestrates centrosomal maturation, a process that requires its phosphorylation of the transforming acidic coiled coil protein. This results in complex formation with the microtubule-associated protein, XMAP215, which then promotes the growth of microtubules from both ends. Further regulation of mitotic entry by AKA occurs when both protein levels and activity peak in prometaphase through binding and activation by LIM protein Ajuba resulting in AKA autophosphorylation. Upon execution of mitotic entry, various proteins including γ -tubulin are recruited to the pericentriolar material thus increasing the nucleation of microtubules. At this stage, AKA is further activated by the spindle protein and Aurora substrate, Ran-TPX2 rendering itself resistant to dephosphorylation and therefore maintaining activity. Maintenance of kinase activity regulates the separation of the centrosomes and allows localization to the spindle poles where it promotes bipolar spindle assembly and the alignment of chromosomes on the metaphase plate. There is also evidence that in anaphase and metaphase, AKA localizes to the midzone and centrosomes to initiate and to regulate cytokinesis.

Aurora B (AKB) is thought to be a chromosomal passenger protein and also plays a number of roles in various cell cycle stages [95]. The enzyme was identified using a degenerative primer-based PCR and a cDNA encoding STK2, later named Aurora related kinase 2, was isolated [96]. At the onset of mitosis, AKB relocates from centromeres to microtubules that interdigitate the spindle midzone and in prophase, AKB is localized to the chromosomes where it controls their accurate segregation. Its binding partners in mitosis include the inner centrosome protein (INCEP), survivin and borealin where these complexes work in synchrony to progress the cell cycle. One

of the key substrates of AKB in mitosis is Histone H3 and phosphorylation at S10 and S28 in mammalian cells is reported to play a fundamental role in chromosome condensation in mitosis and initiation in the heterochromatin at G2 phase [97]. Other functions of AKB include chromosome alignment and spindle checkpoint control in addition to cytokinesis [98].

The third member of the Aurora family Aurora C (AKC), similar to AKB, is a chromosomal passenger protein; however, it is less extensively characterized than the A and the B isoforms. The highest levels of AKC have been reported in the testis in contrast to much lower expression in other tissues, suggesting that its role in meiosis and in spermatogenesis. Further experiments examining AKC expression suggest that levels peak in G2/M phase. Indirect immunofluorescence studies indicated that AKC localizes to the centrosomes from anaphase to telophase interacting with INCEP in a similar manner to AKB [99] suggesting that activity of AKC may complement and overlap that of AKB.

As mentioned, AKA and AKB have been shown to be overexpressed in many human tumors including breast, colon, and lung cancers with the expression profiles implicating both kinases in cancers. The levels of AKC, on the other hand, appear not to be elevated in tumors suggesting limited involvement of this isoform in tumorigenesis and proliferation [93].

8.9

Development of Aurora Kinase Inhibitors through Screening and Structure-Guided Design

Initial studies performed to examine the cellular implications of downregulating Aurora activity used RNAi and determined its mechanism and localization of Aurora kinase and interacting partners [93, 100–104]. This approach is not ideal since silencing Aurora at the RNA level leads to the lack of protein complex formation and thus also prevents kinase-independent functions. These studies did, however, further demonstrate the critical role this family plays in regulating mitotic functions and also alludes to its potential in antitumor therapy. In addition to the development of AK inhibitors for antitumor drug development, in order to further probe the functions of the Aurora Kinases, it is necessary to develop selective inhibitors of the catalytic activity of the Aurora family and potentially of the individual isoforms. As structural information on the Aurora kinases has been available for some time, its use has greatly facilitated the search for and optimization of novel inhibitor chemotypes. Numerous studies have pursued an understanding of the structural determinants of the Aurora kinases and sought to use this information in structure-guided discovery and design of novel inhibitors.

The crystal structure of Aurora in complex with adenosine derivatives was first solved by two independent groups simultaneously [105–107]. Despite similar protein constructs comprising the Aurora A kinase domain, comparison of these structures indicates dramatic differences in the ATP binding region. Closer examination of these structures suggests that the DFG loop of the Aurora A can adopt a number of

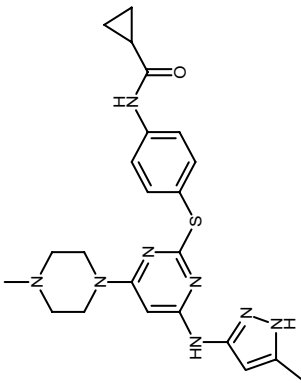
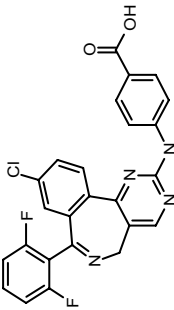
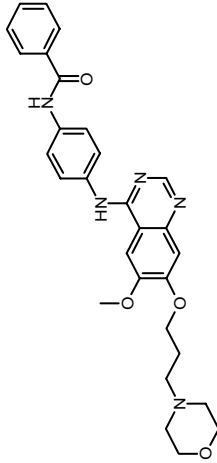
conformational states and that these depend on the nature of the ligand occupying the ATP cleft. While the ATP-bound AKA adopts a “normal” state of the activation loop, the adenosine conformation reveals a P-loop position that is incompatible with ATP binding as W177 occupies the phosphate binding domain. These results suggest that when ATP binds, the triphosphate group destabilizes this conformation and pushes the loop away from the ligand. It also suggests the possibility that design of an appropriate ligand could exploit interactions with the tryptophan and induce an inactive conformation of Aurora. Subsequent to the initial structural solutions, numerous crystal structures have been obtained indicating further conformational variability of the W277 loop and other ATP binding residues including E177 and F275. These residues and the loops containing them, adopt a variety of positions that is highly dependant on the bound ligand. The first inhibitor to be solved in complex with Aurora A through X-ray crystallography was the pyrrolo[3,4-*c*]pyrazole bicyclic compound (PHA-680632, Table 8.1) [108]. The structure revealed that PHA680632 binds with the aminopyrazole ring H-bonding to the hinge region and the activation loop rotated into the ATP cleft. In this structure, both F275 and W277 contacting the ligand and form a hydrophobic cleft allowing additional ligand contact sites (Figure 8.7c). Another molecule from this series (PHA-680626) was also crystallized in complex with Aurora A and despite having an identical core structure stabilized a different conformation of the activation loop in which neither F275 nor W277 make intermolecular contacts with the ligand.

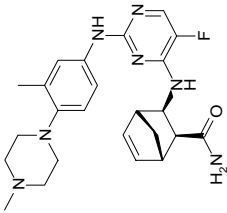
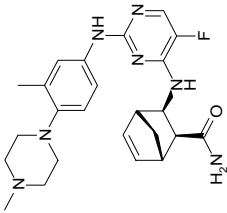
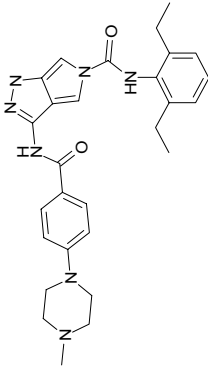
Subsequent to this initial crystallographic analysis, the structure of an analogue of ZM447439 (Table 8.1, Figure 8.7d), which resulted in a highly potent (on AKA and AKB) thiazoloquinazoline series, revealed yet another conformation of the Aurora active site. In this conformation, H-bonds from an inhibitor amide or urea group of the inhibitor, to the main chain D274 and to the catalytic residue E181 stabilize an inactive AKA. The DFG out conformation rendered by the inhibitor is similar to that previously observed in crystal structures of c-Abl (STI-571 (Gleevec)), P38 (BIRB-796), and c-RAF (BAY43-9006) protein kinases. This conformation is stabilized by a network of van der Waals contacts from aromatic portions of the inhibitor to the side chains of F275 and W277 therefore contributing to the subnanomolar inhibition of AKA and AKB showing that significant ligand induced conformational changes can be induced. Since the thiazoloquinazoline inhibitors are among the most potent compounds reported to date, both in the *in vitro* kinase assay and in the cytotoxicity assays, these results suggest that stabilization of the inactive AKA (and probably AKB) through F275 and W277 are important determinants of the biological profile of the inhibitors.

The recent structure of a bisamino-pyrimidine AKA inhibitor bound in the active site revealed an active conformation and the first reported nonadenosine derivative complex with the DFG in conformation (active Aurora) [109]. As a whole, the collection of Aurora A structures solved to date indicate how the nature of the ligand and its substitution pattern can induce variations in the loop configuration and demonstrate the large degree of plasticity in the AKA active site cleft.

The crystal structure of AKB was recently solved in complex with INCENP and Hesperadin (BI1489 (7); derived from the word Hespera, goddess of dusk, opponent of

Table 8.1 Structure and activity table for Aurora kinase inhibitors currently being developed.

Company	Inhibitor	Structure/Class	Target	Administration	Current status
Vertex/Merck	VX680/MK0457		Aurora A, B, and C/Flt3	Intravenous infusion	Phase I (refractory AML), Phase II (NSCLC)
Millennium Pharma	MLN8054		Aurora A	Oral	Phase I (advanced solid tumors)
AstraZeneca	AZD1152 (ZM 447439)		Aurora A and B	Intravenous	Phase I

Astex Therapeutics	AT9283	Not disclosed		Aurora B, JAK2, Abl	Intravenous/ oral	Phase I (CML)
Rigel Pharmaceutical/ Serono	R763			Aurora A, B, and C	NA	Phase I (solid tumors)
Nerviano Medical Sciences (NCI)	PHA680632			Aurora A, B, and C, Flt3	Intravenous	Phase II (CML)

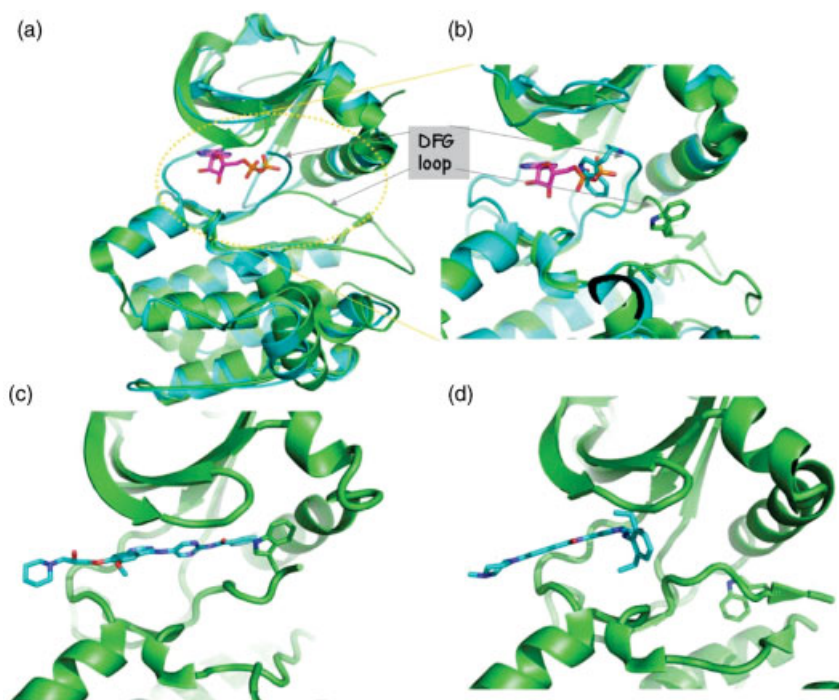


Figure 8.7 Superposition of the 3D structures of Aurora-inhibitor complexes determined crystallographically and illustrating the conformational variability in the DFG loop and

ATP binding site: (a) and (b) illustrate the ADP and adenosine-bound conformations of Aurora A, respectively, whereas (c) and (d) show PHA680632 and ZM447439, respectively.

Aurora, goddess of dawn), a selective indolinone Aurora B inhibitor [110]. The O and N atoms of the main ring system of the inhibitor H-bond to the main chain of E171 and A173, while the central phenyl ring make contacts with L99, V107, and E177 of the ATP binding site. Hesperidin induces an ordered conformation of the glycine loop and binds in an active AKB conformation with the structures of the apo and holo AKB: INCENP being essentially identical. This structure contains a DFG in conformation similar to the AKA: TPX2 complex. The solution of the AKB structure also allows comparison with the AKA conformation and therefore shedding light on the structural basis for selectivity of inhibitors.

8.10

Aurora Kinase Inhibitors in Clinical Trials

Through a combination of high-throughput screening, structure-guided discovery and optimization of potent and selective compounds mentioned above, several potent Aurora inhibitors including those mentioned above are being developed as antitumor

therapeutics. These compounds are currently in Phase I and Phase II clinical trials for various tumor types. One of the first reported clinical candidate Aurora inhibitors was VX680, Tozasertib (Table 8.1; Vertex, now in joint development with Merck as MK0457). This compound was also recently crystallized in complex with AKA [111] and potently inhibits all three Aurora isoforms with reported inhibition constants of 0.6, 18, and 4.6 nM for A, B, and C, respectively [112]. MK 0457 not only is completely selective for the Aurora kinases but also inhibits the receptor tyrosine kinase Flt3 (Fms-like tyrosine kinase 3) and C-Abl and other Src related Kinase [94, 111]. This protein was identified in a proportion of acute myelogenous leukemia (AML) patients, and was reported to be the most commonly mutated gene in AML. MK0547 was also found to be effective against imatinib (Gleevec) and dasatinib (BMS 354825) acquired resistant and intolerant tumors inducing tetraploidy and apoptosis in cultured cells [111]. These effects were shown in patients to result in inhibition of tumor growth. In preclinical studies, MK0547 showed very strong antitumor activity and in some cases including acute myelogenous leukemia (HL60) nude mice achieves over 90% tumor reduction [113]. Other preclinical studies that include human colon cancer (HCT116) nude rat xenografts showed a significant tumor reduction in over 50% of the animals, while indicating minimal toxicity with neutropenia being the only observed toxicity. The biomarker readout in these studies was the inhibition of Histone H3 phosphorylation indicative of Aurora B inhibition. The impressive preclinical results led Merck and Co to sponsor a number of trials of MK0457. This compound was tested in a Phase I trial in patients with refractory or relapsed AML (by inhibition of Flt3), one Phase II in patients with advanced nonsmall-cell lung cancer (NSCLC) and two Phase II trials in patients with advanced cancer. The results, in general, are encouraging and show a good tolerability with neutropenia being the dose-limiting toxicity. As of January 2010, further trials with this compound were suspended and discontinued based on preliminary safety data in which a clinical safety finding of QTc prolongation was observed in one patient.

Another Aurora kinase inhibitor, VX689 again in collaboration with Merck (MK5108) has recently entered Phase I clinical trials as a single agent as well as in combination with docetaxel in patients with advanced and/or refractory solid tumors.

PHA680632 (Table 8.1; Nerviano Medical Sciences) exhibits a nanomolar activity against AKA, AKB, and AKC and some activity against FGFR. This drug is currently in NCI sponsored Phase II clinical trials to study its effects in patients with relapsed chronic myelogenous leukemia resistant to imatinib mesylate (Gleevec) therapy and in solid tumors.

ZM447439 (also known as AZD1152 and abbreviated as ZM) (Table 8.1) was one of the first inhibitors to be developed and to be phenotypically characterized for Aurora inhibition. Treatment of human somatic cells with this compound led to an incorrect spindle formation and that phosphorylation of Histone H3 (AKB substrate) was markedly reduced despite the fact that AZD inhibits both A and B isoforms *in vitro*. Treatment of cells with ZM results in either apoptosis of the cells harboring the misaligned chromosomes leading to mitotic catastrophe or arrest in G1 consistent with the P53-dependent checkpoint control. ZM was reported to be selective for

Aurora B over aurora A hence the phenotype observed. This inhibitor is a prodrug cleaved in human plasma to yield the active molecule and is currently being evaluated in Phase I clinical trials. Data from a European trial with ZM administered by infusion for 2 h weekly indicated a maximum tolerated dose of 200 mg with neutropenia being reported at this dose. Further trials are ongoing in the United States.

CYC116 (Table 8.1; Cyclacel Pharmaceuticals) emerged from an in-house kinase discovery program and is an orally available drug reported to inhibit both Aurora A and Aurora B kinases in addition to VEGFR2. The compound entered the clinic recently in a Phase I multicenter trial in patients with advanced solid tumors. Several other Aurora inhibitors are in clinical trials including MLN8054 (Table 8.1; Millenium), AT9283 (Table 8.1; Astex Therapeutics) and R763 (Table 8.1; Rigel Pharmaceuticals). The status of Aurora kinase targeted inhibitors is summarized in Table 8.1.

As mentioned above, Hesperidin (Table 8.1) is an AKB-selective compound and the cellular consequences of this were examined and shown to induce a dramatic increase in cell size (up to sevenfold) as the inhibitor stopped the proliferation but not the cell growth. Analysis of the mitotic marker Histone H3 Ser 10 phosphorylation showed a marked decrease in cells treated with Hesperidin compared to control. This was correlated with polyploidization. The results obtained were similar to those seen with AZD1152, which led to the suggestion that Hesperadin causes chromosome defects and failure of cytokinesis. Further studies established that Hesperadin functions by inhibiting AKB leading to the inhibition of Histone H3 phosphorylation. In terms of the specificity and the selectivity of Hesperadin, a counter screen of 25 kinases in the presence of 1 μ M compound showed that six kinases were inhibited (Chk1, AMPK, Lck, MKK1, MAPKAP-K1, and PHK). Multiple kinase inhibition complicates interpretation of the observed phenotypes as they may be attributed to the inhibition of kinases in addition to/other than AKB. No information was available for Hesperadin entering clinical trials during the time of publication of this book.

8.11

Progress in the Identification of Potent and Selective Polo-Like Kinase Inhibitors

Polo kinases are a family of Ser/Thr protein kinases identified in mammals subsequent to the initial characterization of *polo* kinase in *Drosophila melanogaster* [114]. The PLKs function primarily in mitosis [115–117] and possess two conserved domains, the N-terminal catalytic kinase domain and the C-terminal region containing the polo boxes [117]. PLK1 is the best characterized of the four members of the PLK family identified thus far. Plk1 activity has been shown to peak at the G2/M transition [118, 119] and upon mitotic exit, PLK1 levels decrease through ubiquitin-dependent proteolysis [120]. A primary function of PLK1 is believed to be in the initiation of mitosis through activation of the dual-specificity phosphatase CDC25C [121]. CDC25c activity relieves MYT1- and WEE1-mediated [122, 123] suppression of CDK1/cyclin B activity through dephosphorylation at the CDK1 pThr¹⁴ and pTyr¹⁵ sites [124, 125] resulting in progression through mitosis [126]. An amplification loop

whereby CDK1/cyclin B activity results in activation of PLK1, in turn activates additional MPF complexes further [127]. MPF activity is also regulated through nuclear import and export by phosphorylations in the cytoplasmic retention sequence present in cyclin B [128, 129]. At least some of these phosphorylations are due to the action of PLK1 and result in activation of CDK1/cyclin B complexes at the centrosome [130].

PLK1 has additional roles in regulating progression through mitosis with its involvement in bipolar spindle formation [131–133] and subsequently in sister chromatid separation [134–138], and cytokinesis [139, 140]. The role of PLK1 in regulating the APC [141] is also thought to result in degradation of cyclin B, and event necessary for a cell to exit from mitosis [142, 143]. Expression of constitutively active PLK1 has been shown to override G2 arrest induced by DNA damage where blocks to both mitotic entry and mitotic exit as a result of the activation of the ATM- and the ATR-regulated DNA-damage checkpoints converge on PLK1 (resulting in its inhibition) therefore preventing MPF activation [144, 145].

With regard to the other Plks, Plk2 is expressed primarily in G1 phase [146] in contrast to Plk3, the kinase activity of which appears to peak during late S and G2 phase. Plk3 is activated during DNA-damage checkpoint activation and severe oxidative stress [147], which plays a significant role in the regulation of microtubule dynamics and the centrosome function in the cell, and when deregulated results in cell cycle arrest and apoptosis [148, 149]. Both PLK2 and PLK3 may have additional important postmitotic functions [150].

Overexpression of PLK1 is frequently observed in human tumors and PLK1 expression has been shown to be of prognostic value for patients suffering from various types of tumors including nonsmall-cell lung cancer [151], breast tumors [152], and in esophageal and in gastric carcinomas [153]. Other studies suggested that the majority of colorectal tumors (73%) produced high levels of PLK relative to the normal cell samples examined [154]. Therapeutic potential for PLK1 inhibition has been demonstrated using antisense oligonucleotides to downregulate PLK1 at the mRNA level. In several studies, this strategy was shown to induce growth inhibition in cancer cells both *in vitro* and *in vivo* [155–158] and thus confirming the role of PLK1 and suggesting its significance as an antitumor drug target.

PLKs, like other Ser/Thr kinases, remain inactive until a Thr residue in the activation T-loop, Thr²¹⁰ in PLK1 [159], is phosphorylated [160, 161]. In several inactive kinases, this loop occludes the ATP binding site of the catalytic domain until phosphorylation unmask the enzymatic activity. Studies on Thr²¹⁰ in PLK1 show that introduction of an Asp residue, which mimics pThr, at this site elevates kinase activity [159, 162]. Furthermore, phosphatase treatment of mitotic PLK1 reduces its kinase activity [163], and although the upstream activating kinase(s) of PLKs in human cells remain to be identified, some candidates have been suggested [164–168]. Deletion of the C-terminal domain substantially increases the kinase activity, suggesting involvement of the polo-box domain (PBD) in regulation of Plk1 activity [163]. This was also suggested by the ability of constructs lacking the kinase domain to bind to both full-length and catalytic domains and inhibit kinase activity, but only when Thr¹²⁰ is unphosphorylated [169]. The activation model indicated from these

results involves priming kinases destabilizing an autoinhibitory conformation involving interactions between the N- and the C-terminal domains. This enables the catalytic activity of the kinase domain and also allows recruitment of PLKs to their physiological substrates [117].

8.12

Development of Small-Molecule Inhibitors of PLK1 Kinase Activity

As discussed, the four human PLKs have divergent and potentially apposing biological functions with PLK1 being the most closely associated with tumor proliferation. For this reason, it may be advantageous although challenging (due to similarities in ATP binding sites) to generate isoform-selective inhibitors. Success in generating selective inhibitors for other protein kinase isoforms suggests that the differences in flexibility and volume of similar ATP binding sites can be exploited to achieve this aim. Recently, considerable progress has been made in the development and also clinical application of polo kinase inhibitors, primarily characterized on Plk1. Although, the Plks have been considered as targets for antitumor therapeutics for a number of years, it is only recently that potent and selective inhibitory compounds have been identified [170–172].

One of the first systematic studies to examine potential PLK1 inhibitory compounds and to understand the structural basis for inhibition looked at a number of generic kinase inhibitors. Unsurprisingly, staurosporine (**7**, Figure 8.8) [173] was found to be a potent inhibitor ($IC_{50} = 0.8 \pm 0.2 \mu M$), however, more discerning inhibitors such as wortmannin (**8**), a phosphatidylinositol-3-kinase (PI3K) inhibitor (PI3K $IC_{50} = 4.2 nM$), and purvalanol A (**9**), a comparatively selective cyclin-dependent kinase (CDK) inhibitor (CDK2 $IC_{50} = 1 nM$) [174, 175], were found to inhibit PLK1 with low micromolar to submicromolar potency ($IC_{50} = 0.07$ and $5 \mu M$, respectively). Kinetic analysis revealed the inhibition of PLK1 by compound **8** was independent of ATP concentration suggesting irreversible covalent modification of the catalytic lysine (as observed with Lys⁸³³ in the ATP binding site of PI3K with the reactive lactone function) [176].

Subsequent to the generation of the *in vitro* data, a homology model for the Plk1 kinase domain was generated and provided significant insights into the nature of the ATP binding pocket and into the interactions of the characterized inhibitors. The model structure revealed some unique features uncommon in other protein kinases. The residue at position 67 (Plk1 numbering), which is valine in most kinases, is cysteine in PLK1 and suggests that this feature can be exploited in generated covalently binding inhibitors. Previously, the concept of irreversible inhibition with ATP antagonists possessing an electrophilic group appended in such a way as to react with a Cys thiol in the active site has been demonstrated in the context of the erbB2 tyrosine kinase. Reactive functionality, when introduced into a potent inhibitor, resulted in covalent modification of the enzyme [177, 178] and resulted in exquisite selectivity. In Plk1, the free Cys residue located on the opposite face of the active site compared to the erbB2 kinase precedent and therefore would

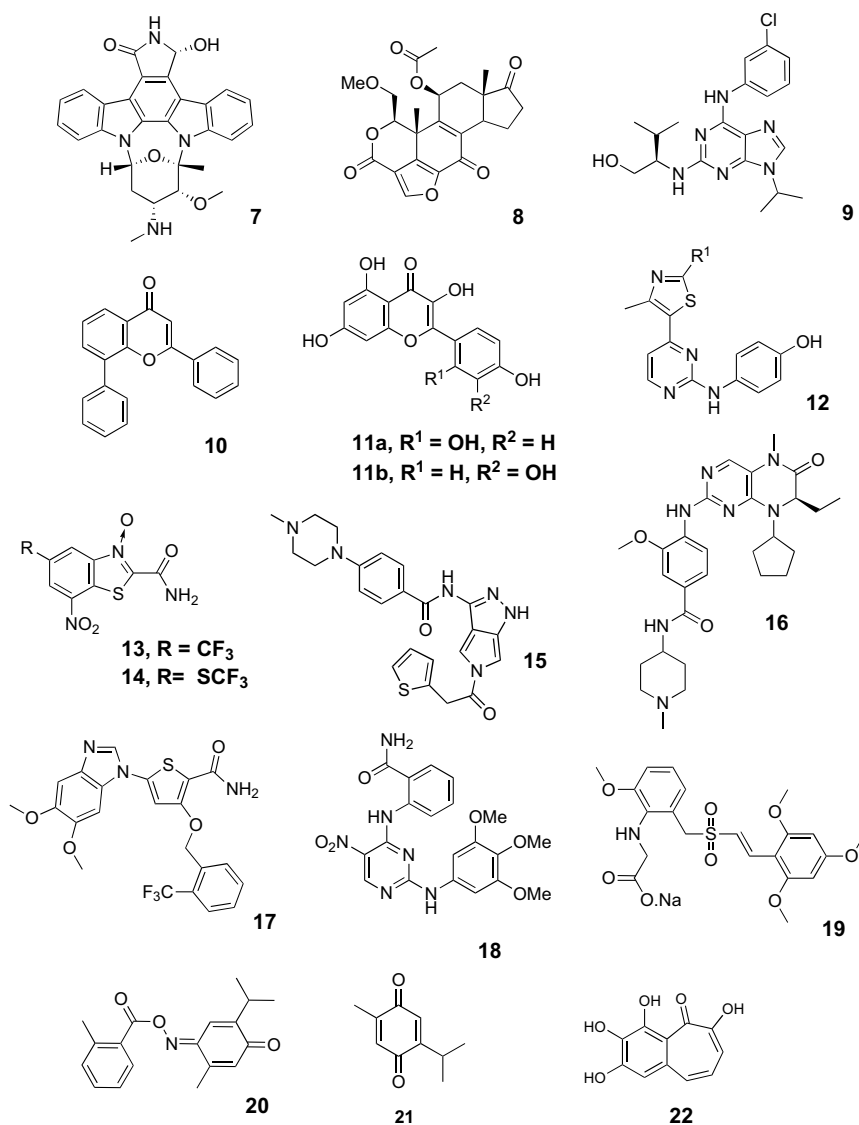


Figure 8.8 Chemical structures of ATP-competitive inhibitors of the polo-like kinases.

require careful design to introduce the appropriate functionality. Other key residues in the ATP binding pocket of PLK1 that can potentially be utilized to generate selective inhibitors include Leu¹³⁰ (corresponding to the so-called gate-keeper residue), Arg¹³⁵, and Phe¹⁸³.

Using the Plk1 model structure, docking simulations of compound **8** with the ATP binding site indicate a similar inhibition mechanism to that reported previously for PI3K, where compound **8** forms a covalent adduct with Lys⁸³³ [176]. A docking pose generated for the intact structure of compound **8** with PLK1 indicated positioning of the reactive lactone group in close proximity to Lys⁸² (mutations of which abolished the kinase activity of PLK1 [179]) and further modeling indicated that the covalent link to this lysine could be made without significantly perturbing this binding mode.

Since the PI3K inhibitor, compound **8**, also potently inhibited PLK1, a series of flavonoid compounds, many of which are known to inhibit PI3K [180, 181] were examined. LY294002 (**10**) (IC₅₀ = 9.3 μM) [182], morin (**11a**) (12.6 μM), and quercetin (**11b**) (64 μM) inhibited PLK1, whereas other related compounds were inactive (PLK1 IC₅₀ > 100 μM). Molecular docking of (**11a**) with the PLK1 homology model suggests a pose consistent with the observed structure–activity relationship [170]. The importance of the hydroxyls suggested by the structure–activity relationship is confirmed by the energetic contributions of H-bond interactions of these groups with PLK1.

The discovery of a series of 2-anilino-4-heteroaryl-pyrimidine CDK inhibitors has previously been reported [47, 183, 184]. Of several hundred diverse analogues with varying selectivity profiles, tested against recombinant human PLK1, only three compounds emerged that possessed significant activity against PLK1 (PLK1 IC₅₀ 5–50 μM; CDK2 IC₅₀ < 100 nM). A determinant for PLK1 inhibition of these compounds was the *para*-hydroxyl group in the aniline portion as shown in the example (**12**, Figure 8.8). Methylation of the bridge aniline N confirmed the role of the aniline NH group in the binding modes in a similar fashion to CDK2 (hinge region H-bonds) and docking of these compounds with the homology structure provided further insight into the interactions of these compounds with PLK1.

8.13

Discovery of Benzthiazole PLK1 Inhibitors

After validation of the model structure that involved docking of the characterized Plk1 inhibitors and correlation of SAR with observed interaction, it was further used in high-throughput docking calculations for the discovery of new Plk1 pharmacophores [185]. By using the program LIDAEUS, which previously has been successfully applied to discover novel CDK2 inhibitors [47], a database of commercially available compounds were docked in high-throughput fashion. After ranking of the predicted hits based on energetic scoring, compounds were screened biochemically against human recombinant PLK1 [121]. The most potent confirmed *in silico* hit to emerge was the highly selective benzthiazole N-oxide (**13**). This compound has *in vitro* antiproliferative properties against human tumor cell lines consistent with cellular PLK1 inhibition [185] and optimization of this series through introduction of a thioether functionality (**14**, Figure 8.8) significantly increased potency while maintaining selectivity. Use of this compound as a mechanistic tool enabled previously unidentified functions of Plk1 to be identified and provided further insight into the role of the polo kinases in spindle pole maintenance [186]. This

series is currently undergoing lead optimization and further studies will be described [187].

8.14

Recent Structural Studies of the Plk1 Kinase Domain

Recently, the X-ray crystal structure of the Plk1 kinase domain was solved to 2.1 Å resolution. This success required specific mutations in the sequence (T210D) and came after many failed attempts in a number of kinase research groups. The complex structures of AMPPNP (nonhydrolyzable ATP analogue) and a pyrrolo-pyrazole inhibitor were obtained. Overlay of the experimental structure with the previously generated homology model confirmed many of the predicted features including the presence of C67 on the C-lobe of Plk1. The two liganded crystal structures of Plk1 described are essentially identical when the alpha carbons were superimposed and the P-loop was found to exist predominantly in an active configuration. The AMPPNP molecule makes similar interactions to those of nucleotide derivatives in other kinases where H-bonds are formed to the hinge region (E131 and C133). The purine ring stacks against F183, a residue infrequently observed at this position, however, found in PKA (the template structure on which the model of Plk1 was based) (Figure 8.9). The pyrazole analogue (PHA-680626 (15)) binds to Plk1 in a similar mode with conservation of the hinge region H-bonds (an additional H-bond from the linker NH to the C133 carbonyl group is observed). In this study, the presence of F183 was

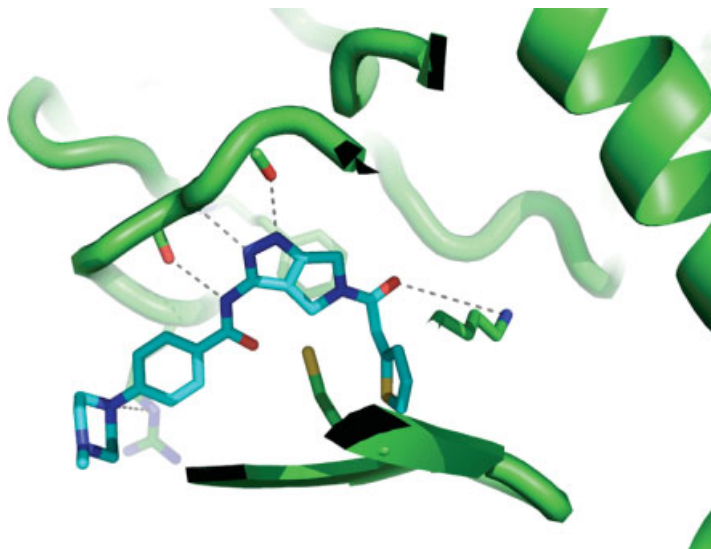


Figure 8.9 The inhibitor–complex structure of the Plk1 kinase domain was recently solved and highlights the unique nature of the ATP binding site including the residues C67 and F183 that have been proposed as key contributors to selectivity.

postulated to result in the selectivity for this inhibitor for Aurora A over Plk1 by restricting the available conformations of the thiophene substituent. The investigators used the crystal structure of Plk1 to generate a binding model of BI2536 (**16**) (Figure 8.8), the highly selective Plk1 inhibitor and to rationalize its selectivity. The ortho-methoxyphenyl group, which occupies a pocket possibly unique to Plk1 was described as a key selectivity determinant. This unique pocket is created by the smaller volume of L132, which is generally conserved as a Tyr or a Phe residue in other kinases; therefore, leaving less room for this substituent. Also the presence of C67 created additional space to accommodate an ethyl substitution and V114 may not be tolerated in other kinases that have larger residues.

Another recent study examined the structure–activity relationships for the most reported Plk1 inhibitors compounds that were tested across all four members of the Plk family. The investigators also undertook a structural comparison of polo kinase ATP binding sites through sequence alignment and homology modeling. The resulting data showed that staurosporine is selective for Plk4 (<3 nM), the isoform most divergent in sequence from Plks 1–3. Although markedly less potent on Plks 1–3, selectivity for Plk2 is apparent from these results. LY294002 is equipotent on Plks 1–3 but much less so on Plk4, as is wortmannin. The highly potent thiophene (**17**, Figure 8.8) and dihydropteridinone (BI2536 (**16**)) compounds have similar nanomolar activity on Plk 1–3 but are much less significant inhibitors of Plk4. Overall, this study provides valuable insight into Plk isoform potency and selectivity and will undoubtedly be significant for the interpretation of preclinical and clinical results obtained with these compounds.

8.15

Additional Small-Molecule PLK1 Inhibitors Reported

A series of trisubstituted diamino-pyrimidine PLK1 inhibitors were recently described with the most potent analogue having a reported IC_{50} value of 0.33 μ M [188]. Active compounds generally contain either a tetrazole group or a nitrile function at the pyrimidine C5-position and a number of (hetero)aralkylamino groups are tolerated at C2-position. A related set of congeners, 5-nitro- N^2,N^4 -diaryl-pyrimidine-2,4-diamines, was discovered by GlaxoSmithKline [189]. The most potent compound was **18**, with submicromolar potency reported against PLK1 and against a tumor cell line panel. Compounds with a variety of pyrimidine C2 and C4 arylamine substituents were active and the C5 nitro group was required. GSK has also reported on a series of 5-benzimidazol-1-yl-3-aryloxy-thiophene-2-carboxamides [190]. Numerous potent compounds were described in the patent literature, including analogue **17** (submicromolar potency against PLK1 and antiproliferative activity). Mechanistic studies on this compound that has dual potency on Plk1 and Plk3 (2 and 9 nM, respectively) have recently been reported with this molecule significantly inhibiting the proliferation of a variety of tumor cell lines [191]. It was shown to induce a transient G2-M arrest, mitotic spindle defects, and apoptosis in a lung adenocarcinoma cell line (NCI-H460). Contrasting studies using normal human fibroblasts

indicated that this inhibitor induces a G2-M arrest, however, does not lead to high levels of apoptosis.

Onconova are developing the benzyl-styrylsulfone ON 01910.Na (**19**, Figure 8.8) [192] as a cell cycle agent with CDK inhibitory properties. This agent has been reported to act as an ATP noncompetitive kinase inhibitor and although it inhibits CDK1 activity, the relevant tumor cell target appears to be PLK1, which it also inhibits potently (reported $IC_{50} = 9$ nM). ON 01910.Na has shown broad activity against a number of solid tumors types as well as in hematological malignancies in preclinical studies. The company is planning multiple Phase II and combination Phase I clinical trials (synergistic activity observed when combined with conventional chemotherapeutic agents) with leading investigators at major oncology clinical centers.

Currently, the most advanced potent and selective Plk inhibitor is the Boehringer Ingelheim compound, BI2536 (**16**), which is currently entering Phase II clinical trials. As mentioned above, this compound is extremely potent on all three Plk isoforms (subnanomolar against Plk1) and is exquisitely selective against a large panel of protein kinases tested to date (more than 1000-fold selective). Among the two major studies published using this compound, the first examined the consequences blocking Plk1 activity with high potency and selectivity, which in turn enabled controversial and unknown functions of Plk1 to be elucidated. BI2536 treated cells were shown to exhibit a delay in exiting prophase in mitosis but to eventually import Cdk1–cyclin B into the nucleus, and enter prometaphase, resulting in degradation of cyclin A. Cells treated with this compound lack prophase microtubule asters and form monopolar spindles that do not stably attach to kinetochores. BI2536 was also shown to induce detachment of microtubules from kinetochores and treatment leads to spindle collapse when added to cells in metaphase.

A second study published with this compound demonstrated in a panel of diverse human tumor cell lines, that BI2536 potently induces mitotic arrest and apoptosis in human cancer cell lines. Studies of this compound examining its *in vivo* anticancer activity demonstrated significant inhibition of the growth of human tumor xenografts in nude mice and elicited regression of large tumors when the drug was administered intravenously. Mechanistic experiments on cells extracted from the *in vivo* tumor models indicated mitotic arrest in prometaphase and exhibited aberrant mitotic spindles and high levels of apoptosis. The high potency and bioavailability observed in preclinical studies warranted further investigation in humans and resultantly, BI2536 has progressed into clinical studies in patients with locally advanced or metastatic cancers.

8.16

The Polo-Box Domain

Apart from the N-terminal catalytic domain, PLKs also have C-terminal extensions, the PBDs, which contain the polo boxes (PBs) shown to be critical for the regulation of the subcellular localization and biological function [193, 194]. The importance of the PBs in the function of PLK1 has been indicated in several studies including one

report that application to tumor cell cultures of a cell permeabilized PB1 fragment, produces phenotypes similar to those observed upon PLK1 knockdown including mitotic arrest, misaligned chromosomes, and multiple centrosomes [195]. These and additional observations including induction of apoptosis presumably arise through competition between the PB peptide and the native PLK1 for binding to target proteins [196–198]. The PBD of PLK1 has been described as a pSer/pThr binding module where it was demonstrated that a clone expressing a C-terminal portion of PLK1 (95–603) interacts with a phosphopeptide consensus sequence. Further analysis of deletion constructs based on this PLK1 clone revealed that the two PBs, and the linker between them, are requisite for phosphopeptide binding and where the recognition domain consists of residues 326–603. Application of an oriented peptide library screens showed that a number of important mitotic proteins, including the Plk1 substrate, CDC25C contain this motif and bind to the PLK1 PBD.

Several X-ray crystal structures of the human PLK1 PBD in apo form and in complex with phosphopeptides have been solved recently [199–201]. The two PBs are each contained in a $\beta_6\alpha$ region within the PBD (Figure 8.7) and although of low comparative sequence identity both have an almost identical fold, packing together to form a 12-stranded β -sandwich flanked by three α -helices. The phosphopeptide binding site is formed by a shallow groove occurring at the interface of the PBs and the phosphopeptide is bound through a number of electrostatic (Gln², Ser³, and Thr⁴) and van der Waals contacts (Met¹ and Leu⁶). Many of the polar interactions are mediated through bridging water molecules between the atoms of the peptide and those of the PBD.

The insight provided into the interaction of the PBD and its ligands, as well as the significance of these interfaces to the biological function of PLKs, suggest the feasibility of designing mimetic inhibitors of PLKs. Similar approaches are being applied in the case of several Tyr kinases that contain subunits or adapter proteins that also recognize phosphopeptide motifs [202]. In the case of Src-homology (SH2 and SH3) domains, which recognize pTyr motifs, peptidomimetic design of drug candidates is fairly advanced [177, 203].

Initial studies of the PBD binding motif suggested that it is highly specific for pThr-peptides with a Ser at the –1-position and this Ser residue forms complementarity with Trp⁴¹⁴ in the binding groove and indicates that the Ser-pThr dipeptide could be used as a template for inhibitor design. However, the absence of a deep lipophilic pocket and the requirement for the phosphorylated threonine residue in these structures indicates that small-molecule development would be difficult. A more recent set of crystal structures and binding activity results for PBD peptide interactions with the C-terminal and full-length Plk1 constructs has been described [204]. These results provide further insights into PBD binding determinants and suggest equal affinities of the phospho plus and minus peptides for the PBD construct alone. Interactions with the full-length Plk1 indicate a higher affinity for the phosphorylated peptide in the full-length context. The observation in this study suggesting a potentially decreased importance of the phosphate determinant indicates that the PBD may be inhibited with a noncharged molecule and is therefore more attractive from a drug development standpoint.

To this end, Reindl *et al.* [205] screened a library of 22,461 small molecules for their potential to interfere with the binding of a fluorescently tagged PBD binding peptide. This library screening led to the identification of compounds **20** (Poloxin, IC₅₀ of $4.8 \pm 1.3 \mu\text{M}$) and **21** (thymoquinone), inhibitors of PLK1 PDB [205, 206]. Poloxin is a synthetic derivative of the natural product thymoquinone **21**, a constituent of the volatile oil of black seed (*Nigella sativa*) and well known for its anti-inflammatory, antioxidant, and antineoplastic properties [207]. Thymoquinone (apparent IC₅₀ of $1.14 \pm 0.04 \mu\text{M}$) was found to inhibit PLK1 PDB more potently than does Poloxin [205], however, thymoquinone also inhibited other phosphothreonine/phosphoserine binding domains and therefore has lower selectivity. The redox potential of these compounds may limit their usefulness as drugs, however. More recently, two additional PBD inhibitory compounds, purpurogallin [208] (**22**, IC₅₀ = 500 nM) and poloxipan [206], have been identified. While compounds **20** and **22** are reasonably selective for the PBD of Plk1, compound **21** inhibits phosphopeptide binding with roughly equal potency for Plk1, Plk2, and Plk3. The identification of low molecular weight inhibitors of the PBD binding site provides significant impetus for further investigation of these analogues as potential antitumor therapeutics based on inhibiting the protein–protein regulation of the polo-like kinases.

8.17

Future Developments

Some significant advances in the development of protein kinase inhibitors have been described in this chapter. In a short time frame, the inhibition of kinase activity through the ATP binding site has been validated as a viable therapeutic approach. After the initial clinical success, the second-generation kinase inhibitor therapeutics are currently being evaluated preclinically and clinically with some of the latest compounds targeting unique mechanisms of protein kinase inhibition. Structure-guided design has facilitated many advances in drug development of compounds inhibiting cell cycle protein kinases and these in addition to signaling kinases show tremendous promise in drug design and development, specifically within the field of antitumor therapeutics.

References

- 1 Manning, G., Whyte, D.B., Martinez, R. *et al.* (2002) The protein kinase complement of the human genome. *Science*, **298**, 1912–1934.
- 2 Niedner, R.H., Buzko, O.V., Haste, N.M. *et al.* (2006) Protein kinase resource: an integrated environment for phosphorylation research. *Proteins*, **63**, 78–86.
- 3 Noble, M.E.M., Endicott, J.A., and Johnson, L.N. (2004) Protein kinase inhibitors: insights into drug design from structure. *Science*, **303**, 1800–1805.
- 4 Ross, D.M. and Hughes, T.P. (2004) Cancer treatment with kinase inhibitors: what have we learnt from imatinib? *British Journal of Cancer*, **90**, 12–19.

- 5 Nagar, B., Hantschel, O., Young, M.A. *et al.* (2003) Structural basis for the autoinhibition of c-Abl tyrosine kinase. *Cell*, **112**, 859–871.
- 6 Nagar, B., Bornmann, W.G., Pellicena, P. *et al.* (2002) Crystal structures of the kinase domain of c-Abl in complex with the small molecule inhibitors PD173955 and imatinib (STI-571). *Cancer Research*, **62**, 4236–4243.
- 7 Schindler, T., Bornmann, W., Pellicena, P. *et al.* (2000) Structural mechanism for STI-571 inhibition of abelson tyrosine kinase. *Science*, **289**, 1938–1942.
- 8 Kubota, T. (2006) Gastrointestinal stromal tumor (GIST) and imatinib. *International Journal of Clinical Oncology/Japan Society of Clinical Oncology*, **11**, 184–189.
- 9 Schnadig, I.D. and Blanke, C.D. (2006) Gastrointestinal stromal tumors: imatinib and beyond. *Current Treatment Options in Oncology*, **7**, 427–437.
- 10 Herbst, R.S., Fukuoka, M., and Baselga, J. (2004) Gefitinib: a novel targeted approach to treating cancer. *Nature Reviews. Cancer*, **4**, 956–965.
- 11 Blackhall, F., Ranson, M., and Thatcher, N. (2006) Where next for gefitinib in patients with lung cancer? *The Lancet Oncology*, **7**, 499–507.
- 12 Minna, J.D. and Dowell, J. (2005) Erlotinib hydrochloride. *Nature Reviews. Drug Discovery*, (Suppl.), S14–S15.
- 13 Herbst, R.S. (2006) Therapeutic options to target angiogenesis in human malignancies. *Expert Opinion on Emerging Drugs*, **11**, 635–650.
- 14 Schreck, R. and Rapp, U.R. (2006) Raf kinases: oncogenesis and drug discovery. *International Journal of Cancer*, **119**, 2261–2271.
- 15 Smith, R.A., Dumas, J., Adnane, L., and Wilhelm, S.M. (2006) Recent advances in the research and development of RAF kinase inhibitors. *Current Topics in Medicinal Chemistry*, **6**, 1071–1089.
- 16 Madhusudan, M., Trafny, E.A., Xuong, N.H. *et al.* (1994) cAMP-dependent protein kinase: crystallographic insights into substrate recognition and phosphotransfer. *Protein Science: A Publication of the Protein Society*, **3**, 176–187.
- 17 Hanks, S.K. and Hunter, T. (1995) Protein kinases. 6. The eukaryotic protein kinase superfamily: kinase (catalytic) domain structure and classification. *The FASEB Journal*, **9**, 576–596.
- 18 Huse, M. and Kuriyan, J. (2002) The conformational plasticity of protein kinases. *Cell*, **109**, 275–282.
- 19 Engh, R.A. and Bossemeyer, D. (2002) Structural aspects of protein kinase control-role of conformational flexibility. *Pharmacology & Therapeutics*, **93**, 99–111.
- 20 Lew, D.J. and Kornbluth, S. (1996) Regulatory roles of cyclin dependent kinase phosphorylation in cell cycle control. *Current Opinion in Cell Biology*, **8**, 795–804.
- 21 Brown, N.R., Noble, M.E.M., Lawrie, A.M. *et al.* (1999) Effects of phosphorylation of threonine 160 on cyclin-dependent kinase 2 structure and activity. *Journal of Biological Chemistry*, **274**, 8746–8756.
- 22 Malumbres, M. and Barbacid, M. (2005) Mammalian cyclin-dependent kinases. *Trends in Biochemical Sciences*, **30**, 630–641.
- 23 Palancade, B. and Bensaude, O. (2003) Investigating RNA polymerase II carboxyl-terminal domain (CTD) phosphorylation. *European Journal of Biochemistry*, **270**, 3859–3870.
- 24 Romano, G. and Giordano, A. (2008) Role of the cyclin-dependent kinase 9-related pathway in mammalian gene expression and human diseases. *Cell Cycle Abstract*, **7**, 3664–3668.
- 25 Fischer, P.M. and Gianella-Borradori, A. (2005) Recent progress in the discovery and development of cyclin-dependent kinase inhibitors. *Expert Opinion on Investigational Drugs*, **14**, 457–477.
- 26 Jeffrey, P.D., Russo, A.A., Polyak, K. *et al.* (1995) Mechanism of CDK activation revealed by the structure of a cyclin A-CDK2 complex. *Nature*, **376**, 313–320.
- 27 Russo, A.A., Jeffrey, P.D., and Pavletich, N.P. (1996) Structural basis of cyclin-dependent kinase activation by phosphorylation. *Nature Structural Biology*, **3**, 696–700.

- 28 Russo, A.A., Jeffrey, P.D., Patten, A.K. *et al.* (1996) Crystal structure of the p27Kip1 cyclin-dependent-kinase inhibitor bound to the cyclin A-Cdk2 complex. *Nature*, **382**, 325–331.
- 29 Tarricone, C., Dhavan, R., Peng, J. *et al.* (2001) Structure and regulation of the CDK5–p25(ncK5a) complex. *Molecular Cell*, **8**, 657–669.
- 30 Russo, A.A., Tong, L., Lee, J.-O.D. *et al.* (1998) Structural basis for inhibition of the cyclin-dependent kinase Cdk6 by the tumour suppressor p16^{INK4a}. *Nature*, **395**, 237–243.
- 31 Lolli, G., Lowe, E.D., Brown, N.R., and Johnson, L.N. (2004) The crystal structure of human CDK7 and its protein recognition properties. *Structure*, **12**, 2067–2079.
- 32 Baumli, S., Lolli, G., Lowe, E.D. *et al.* (2008) The structure of P-TEFb (CDK9/cyclin T1), its complex with flavopiridol and regulation by phosphorylation. *EMBO Journal*, **27**, 1907–1918.
- 33 Day, P.J., Cleasby, A., Tickle, I.J. *et al.* (2009) Crystal structure of human CDK4 in complex with a D-type cyclin. *Proceedings of the National Academy of Sciences of the United States of America*, **106**, 4166–4170.
- 34 Vulpetti, A. and Pevarello, P. (2005) An analysis of the binding modes of ATP-competitive CDK2 inhibitors as revealed by X-ray structures of protein–inhibitor complexes. *Current Medicinal Chemistry. Anti-Cancer Agents*, **5**, 561–573.
- 35 Kontopidis, G., McInnes, C., Pandalaneni, S.R. *et al.* (2006) Differential binding of inhibitors to active and inactive CDK2 provides insights for drug design. *Chemistry & Biology*, **13**, 201–211.
- 36 Wang, S., Meades, C., Wood, G. *et al.* (2004) 2-Anilino-4-(thiazol-5-yl) pyrimidine CDK inhibitors: synthesis, SAR analysis, X-ray crystallography, and biological activity. *Journal of Medicinal Chemistry*, **47**, 1662–1675.
- 37 McInnes, C. (2008) Progress in the evaluation of CDK inhibitors as anti-tumor agents. *Drug Discovery Today Abstract*, **13**, 875–881.
- 38 Fischer, P.M. (2004) The use of CDK inhibitors in oncology a pharmaceutical perspective. *Cell Cycle*, **3**, 742–746.
- 39 McInnes, C. and Fischer, P.M. (2005) Strategies for the design of potent and selective kinase inhibitors. *Current Pharmaceutical Design*, **11**, 1845–1863.
- 40 Lipinski, C. and Hopkins, A. (2004) Navigating chemical space for biology and medicine. *Nature*, **432**, 855–861.
- 41 Noble, M., Barrett, P., Endicott, J. *et al.* (2005) Exploiting structural principles to design cyclin-dependent kinase inhibitors. *Biochimica et Biophysica Acta. Proteins and Proteomics*, **1754**, 58–64.
- 42 Fischer, P.M. (2005) Cyclin-dependent kinase inhibitors: Discovery, development and target rationale for different therapeutic applications. *Drugs of the Future*, **30**, 911–929.
- 43 McInnes, C. and Fischer, P.M. (2005) Strategies for the design of potent and selective kinase inhibitors. *Current Pharmaceutical Design*, **11**, 1845–1863.
- 44 Kontopidis, G., McInnes, C., Pandalaneni, S.R. *et al.* (2006) Differential binding of inhibitors to active and inactive CDK2 provides insights for drug design. *Chemistry and Biology*, **13**, 201–211.
- 45 Pevarello, P., Fancelli, D., Vulpetti, A. *et al.* (2004) 3-Amino-pyrrolo[3,4-*c*] pyrazoles: a new class of CDK2 inhibitors. *Proceedings of the American Association for Cancer Research*, **45**, Abstract 2479.
- 46 Tang, J., Shewchuk, L.M., Sato, H. *et al.* (2003) Anilinopyrazole as selective CDK2 inhibitors: design, synthesis, biological evaluation, and X-ray crystallographic analysis. *Bioorganic & Medicinal Chemistry Letters*, **13**, 2985–2988.
- 47 Wu, S.Y., McNae, I., Kontopidis, G. *et al.* (2003) Discovery of a novel family of CDK inhibitors with the program LIDAEUS: structural basis for ligand-induced disordering of the activation loop. *Structure*, **11**, 399–410.
- 48 Mapelli, M., Massimiliano, L., Crovace, C. *et al.* (2005) Mechanism of CDK5/p25 binding by CDK inhibitors. *Journal of Medicinal Chemistry*, **48**, 671–679.

- 49 Thomas, M.P., McInnes, C., and Fischer, P.M. (2006) Protein structures in virtual screening: a case study with CDK2. *Journal of Medicinal Chemistry*, **49**, 92–104.
- 50 Toledo, L.M. and Lydon, N.B. (1997) Structures of staurosporine bound to CDK2 and cAPK: new tools for structure-based design of protein kinase inhibitors. *Structure*, **5**, 1551–1556.
- 51 Brotherton, D.H., Dhanaraj, V., Wick, S. *et al.* (1998) Crystal structure of the complex of the cyclin D-dependent kinase Cdk6 bound to the cell-cycle inhibitor p19^{INK4d}. *Nature*, **395**, 244–250.
- 52 Lolli, G., Lowe, E.D., Brown, N.R., and Johnson, L.N. (2004) The crystal structure of human CDK7 and its protein recognition properties. *Structure*, **12**, 2067–2079.
- 53 Honda, R., Lowe, E.D., Dubinina, E. *et al.* (2005) The structure of cyclin E1/CDK2: implications for CDK2 activation and CDK2-independent roles. *EMBO Journal*, **24**, 452–463.
- 54 Shah, M.A. and Schwartz, G.K. (2006) Cyclin dependent kinases as targets for cancer therapy. *Update on Cancer Therapeutics*, **1**, 311–332.
- 55 Fry, D.W., Harvey, P.J., Keller, P.R. *et al.* (2004) Specific inhibition of cyclin-dependent kinase 4/6 by PD0332991 and associated antitumor activity in human tumor xenografts. *Molecular Cancer Therapeutics*, **3**, 1427–1438.
- 56 McInnes, C., Wang, S., Anderson, S. *et al.* (2004) Structural determinants of CDK4 inhibition and design of selective ATP competitive inhibitors. *Chemistry & Biology*, **11**, 525–534.
- 57 Seong, Y.S., Min, C., Li, L. *et al.* (2003) Characterization of a novel cyclin-dependent kinase 1 inhibitor, BMI-1026. *Cancer Research*, **63**, 7384–7391.
- 58 Imbach, P., Capraro, H.G., Furet, P. *et al.* (1999) 2,6,9-Trisubstituted purines: optimization towards highly potent and selective CDK1 inhibitors. *Bioorganic & Medicinal Chemistry Letters*, **9**, 91–96.
- 59 Senderowicz, A.M. (2003) Small-molecule cyclin-dependent kinase modulators. *Oncogene*, **22**, 6609–6620.
- 60 Soni, R., Muller, L., Furet, P. *et al.* (2000) Inhibition of cyclin-dependent kinase 4 (Cdk4) by fascaplysin, a marine natural product. *Biochemical and Biophysical Research Communications*, **275**, 877–884.
- 61 Barvian, M., Boschelli, D.H., Crossrow, J. *et al.* (2000) Pyrido[2,3-*d*]pyrimidin-7-one inhibitors of cyclin-dependent kinases. *Journal of Medicinal Chemistry*, **43**, 4606–4616.
- 62 Ikuta, M., Kamata, K., Fukasawa, K. *et al.* (2001) Crystallographic approach to identification of cyclin-dependent kinase 4 (CDK4)-specific inhibitors by using CDK4 mimic CDK2 protein. *The Journal of Biological Chemistry*, **276**, 27548–27554.
- 63 Honma, T., Yoshizumi, T., Hashimoto, N. *et al.* (2001) A novel approach for the development of selective Cdk4 inhibitors: library design based on locations of Cdk4 specific amino acid residues. *Journal of Medicinal Chemistry*, **44**, 4628–4640.
- 64 Honma, T., Hayashi, K., Aoyama, T. *et al.* (2001) Structure-based generation of a new class of potent cdk4 inhibitors: new *de novo* design strategy and library design. *Journal of Medicinal Chemistry*, **44**, 4615–4627.
- 65 McInnes, C., Wang, S., Sian Anderson, S. *et al.* (2004) Structural determinants of CDK4 inhibition and design of selective ATP competitive inhibitors. *Chemistry and Biology*, **11**, 525–534.
- 66 Pratt, D.J., Bentley, J., Jewsbury, P. *et al.* (2006) Dissecting the determinants of cyclin-dependent kinase 2 and cyclin-dependent kinase 4 inhibitor selectivity. *Journal of Medicinal Chemistry*, **49**, 5470–5477.
- 67 Baughn, L.B., Di Liberto, M., Wu, K. *et al.* (2006) A novel orally active small molecule potentially induces G1 arrest in primary myeloma cells and prevents tumor growth by specific inhibition of cyclin-dependent kinase 4/6. *Cancer Research*, **66**, 7661–7667.
- 68 Toogood, P.L., Harvey, P.J., Repine, J.T. *et al.* (2005) Discovery of a potent and selective inhibitor of cyclin-dependent kinase 4/6. *Journal of Medicinal Chemistry*, **48**, 2388–2406.
- 69 Lu, H. and Schulze-Gahmen, U. (2006) Toward understanding the structural basis of cyclin-dependent kinase 6

- specific inhibition. *Journal of Medicinal Chemistry*, **49**, 3826–3831.
- 70 Okram, B., Nagle, A., Adrian, F.J. *et al.* (2006) A general strategy for creating “inactive-conformation” abl inhibitors. *Chemistry and Biology*, **13**, 779–786.
 - 71 McInnes, C., Mezna, M., and Kontopidis, G. (2006) Catch the kinase conformer. *Chemistry and Biology*, **13**, 693–694.
 - 72 Cheng, K.Y., Noble, M.E.M., Skamnaki, V. *et al.* (2006) The role of the phospho-CDK2/cyclin A recruitment site in substrate recognition. *Journal of Biological Chemistry*, **281**, 23167–23179.
 - 73 Blum, G., Gazit, A., and Levitzki, A. (2003) Development of new insulin-like growth factor-1 receptor kinase inhibitors using catechol mimics. *Journal of Biological Chemistry*, **278**, 40442–40454.
 - 74 Gumireddy, K., Reddy, M.V.R., Cosenza, S.C. *et al.* (2005) ON01910, a non-ATP-competitive small molecule inhibitor of Plk1, is a potent anticancer agent. *Cancer Cell*, **7**, 275–286.
 - 75 Biondi, R.M. and Nebreda, A.R. (2003) Signalling specificity of Ser/Thr protein kinases through docking-site-mediated interactions. *The Biochemical Journal*, **372**, 1–13.
 - 76 Kirkland, L.O. and McInnes, C. (2009) Non-ATP competitive protein kinase inhibitors as anti-tumor therapeutics. *Biochemical Pharmacology*, **77**, 1561–1571.
 - 77 McInnes, C., Andrews, M.J., Zheleva, D.I. *et al.* (2003) Peptidomimetic design of CDK inhibitors targeting the recruitment site of the cyclin subunit. *Current Medicinal Chemistry. Anti-Cancer Agents*, **3**, 57–69.
 - 78 Kontopidis, G., Andrews, M.J.I., McInnes, C. *et al.* (2003) Insights into cyclin groove recognition: complex crystal structures and inhibitor design through ligand exchange. *Structure*, **11**, 1537–1546.
 - 79 Zheleva, D.I., McInnes, C., Gavine, A.L. *et al.* (2002) Highly potent p21^{WAF1}-derived peptide inhibitors of CDK-mediated pRb phosphorylation: delineation and structural insight into their interactions with cyclin A. *The Journal of Peptide Research*, **60**, 257–270.
 - 80 Zheleva, D.I., McInnes, C., Gavine, A.L. *et al.* (2002) Highly potent p21^{WAF1}-derived peptide inhibitors of CDK-mediated pRb phosphorylation: delineation and structural insight into their interactions with cyclin A. *Journal of Peptide Research*, **60**, 257–270.
 - 81 Kontopidis, G., Andrews, M.J.I., McInnes, C. *et al.* (2003) Structural understanding of cyclin groove inhibition: complex crystal structures through ligand exchange. 5th International Conference on Molecular Structural Biology, September 3–7, 2003; Vienna, Austria.
 - 82 Atkinson, G.E., Cowan, A., McInnes, C. *et al.* (2002) Peptide inhibitors of CDK2-cyclin a that target the cyclin recruitment-site: structural variants of the C-terminal Phe. *Bioorganic & Medicinal Chemistry Letters*, **12**, 2501–2505.
 - 83 Mendoza, N., Fong, S., Marsters, J. *et al.* (2003) Selective cyclin-dependent kinase 2/cyclin a antagonists that differ from ATP Site inhibitors block tumor growth. *Cancer Research*, **63**, 1020–1024.
 - 84 Lowe, E.D., Tews, I., Cheng, K.Y. *et al.* (2002) Specificity determinants of recruitment peptides bound to phospho-CDK2/Cyclin A. *Biochemistry*, **41**, 15625–15634.
 - 85 Andrews, M.J.I., Kontopidis, G., McInnes, C. *et al.* (2006) REPLACE: a strategy for iterative design of cyclin-binding groove inhibitors. *ChemBioChem*, **7**, 1909–1915.
 - 86 Castanedo, G., Clark, K., Wang, S. *et al.* (2006) CDK2/cyclin A inhibitors: targeting the cyclin A recruitment site with small molecules derived from peptide leads. *Bioorganic & Medicinal Chemistry Letters*, **16**, 1716–1720.
 - 87 Andrews, M.J., Kontopidis, G., McInnes, C. *et al.* (2006) REPLACE: a strategy for iterative design of cyclin-binding groove inhibitors. *Chembiochem: A European Journal of Chemical Biology*, **7**, 1909–1915.
 - 88 Andrews, M.J.I., McInnes, C., Kontopidis, G. *et al.* (2004) Design, synthesis, biological activity and structural analysis of cyclic peptide inhibitors targeting the substrate recruitment site of cyclin-dependent

- kinase complexes. *Organic & Biomolecular Chemistry*, **2**, 2735–2341.
- 89 Larsen, T.A., Olson, A.J., and Goodsell, D.S. (1998) Morphology of protein–protein interfaces. *Structure*, **6**, 421–427.
 - 90 Heitz, F., Morris, M.C., Fesquet, D. *et al.* (1997) Interactions of cyclins with cyclin-dependent kinases: a common interactive mechanism. *Biochemistry*, **36**, 4995–5003.
 - 91 Canela, N., Orzaez, M., Fucho, R. *et al.* (2006) Identification of an hexapeptide that binds to a surface pocket in cyclin A and inhibits the catalytic activity of the complex cyclin-dependent kinase 2–cyclin A. *The Journal of Biological Chemistry*, **281**, 35942–35953.
 - 92 Glover, D.M., Leibowitz, M.H., McLean, D.A., and Parry, H. (1995) Mutations in Aurora prevent centrosome separation leading to the formation of monopolar spindles. *Cell*, **81**, 95–105.
 - 93 Keen, N. and Taylor, S. (2004) Aurora-kinase inhibitors as anticancer agents. *Nature Reviews Cancer*, **4**, 927–936.
 - 94 Mortlock, A., Keen, N.J., Jung, F.H. *et al.* (2005) Progress in the development of selective inhibitors of Aurora kinases. *Current Topics in Medicinal Chemistry*, **5**, 199–213.
 - 95 Bischoff, J.R., Anderson, L., Zhu, Y. *et al.* (1998) A homologue of *Drosophila* Aurora kinase is oncogenic and amplified in human colorectal cancers. *EMBO Journal*, **17**, 3052–3065.
 - 96 Shindo, M., Nakano, H., Kuroyanagi, H. *et al.* (1998) cDNA cloning, expression, subcellular localization, and chromosomal assignment of mammalian Aurora homologues, Aurora-related kinase (ARK) 1 and 2. *Biochemical and Biophysical Research Communications*, **244**, 285–292.
 - 97 Goto, H., Yasui, Y., Nigg, E.A., and Inagaki, M. (2002) Aurora-B phosphorylates Histone H3 at serine 28 with regard to the mitotic chromosome condensation. *Genes to Cells*, **7**, 11–17.
 - 98 Schumacher, J.M., Golden, A., and Donovan, P.J. (1998) AIR-2: an Aurora/Ipl1-related protein kinase associated with chromosomes and midbody microtubules is required for polar body extrusion and cytokinesis in *Caenorhabditis elegans* embryos. *The Journal of Cell Biology*, **143**, 1635–1646.
 - 99 Sasai, K., Katayama, H., Stenoiien, D.L. *et al.* (2004) Aurora-C kinase is a novel chromosomal passenger protein that can complement Aurora-B kinase function in mitotic cells. *Cell Motility and the Cytoskeleton*, **59**, 249–263.
 - 100 Gassmann, R., Carvalho, A., Henzing, A.J. *et al.* (2004) Borealin: a novel chromosomal passenger required for stability of the bipolar mitotic spindle. *The Journal of Cell Biology*, **166**, 179–191.
 - 101 Meraldi, P., Honda, R., and Nigg, E.A. (2004) Aurora kinases link chromosome segregation and cell division to cancer susceptibility. *Current Opinion in Genetics & Development*, **14**, 29–36.
 - 102 Klein, U.R., Nigg, E.A., and Gruneberg, U. (2006) Centromere targeting of the chromosomal passenger complex requires a ternary subcomplex of borealin, survivin, and the N-terminal domain of INCENP. *Molecular Biology of the Cell*, **17**, 2547–2558.
 - 103 Marumoto, T., Zhang, D., and Saya, H. (2005) Aurora-A: a guardian of poles. *Nature Reviews Cancer*, **5**, 42–50.
 - 104 Girdler, F., Gascoigne, K.E., Evers, P.A. *et al.* (2006) Validating Aurora B as an anti-cancer drug target. *Journal of Cell Science*, **119**, 3664–3675.
 - 105 Nowakowski, J., Cronin, C.N., McRee, D.E. *et al.* (2002) Structures of the cancer-related Aurora-A, FAK, and EphA2 protein kinases from nanovolume crystallography. *Structure*, **10**, 1659–1667.
 - 106 Cheetham, G.M., Knegetel, R.M., Coll, J.T. *et al.* (2002) Crystal structure of Aurora-2, an oncogenic serine/threonine kinase. *The Journal of Biological Chemistry*, **277**, 42419–42422.
 - 107 Vankayalapati, H., Mahadevan, D., Rojanala, S. *et al.* (2002) Structure-based design of Aurora kinase-2 inhibitors: homology modeling and molecular dynamics docking simulation studies. *Proceedings of the American Association for Cancer Research*, **43**, 4209.
 - 108 Fancelli, D., Berta, D., Bindi, S. *et al.* (2005) Potent and selective Aurora

- inhibitors identified by the expansion of a novel scaffold for protein kinase inhibition. *Journal of Medicinal Chemistry*, **48**, 3080–3084.
- 109 Tari, L.W., Hoffman, I.D., Bensen, D.C. *et al.* (2007) Structural basis for the inhibition of Aurora A kinase by a novel class of high affinity disubstituted pyrimidine inhibitors. *Bioorganic & Medicinal Chemistry Letters*, **17**, 688–691.
 - 110 Sessa, F., Mapelli, M., Ciferri, C. *et al.* (2005) Mechanism of Aurora B activation by INCENP and inhibition by Hesperadin. *Molecular Cell*, **18**, 379–391.
 - 111 Cheetham, G.M., Charlton, P.A., Golec, J.M., and Pollard, J.R. (2007) Structural basis for potent inhibition of the Aurora kinases and a T315I multi-drug resistant mutant form of Abl kinase by VX-680. *Cancer Letters*, **251**, 323–329.
 - 112 Harrington, E.A., Bebbington, D., Moore, J. *et al.* (2004) VX-680, a potent and selective small-molecule inhibitor of the Aurora kinases, suppresses tumor growth *in vivo*. *Nature Medicine*, **10**, 262–267.
 - 113 Carvajal, R.D., Tse, A., and Schwartz, G.K. (2006) Aurora kinases: new targets for cancer therapy. *Clinical Cancer Research*, **12**, 6869–6875.
 - 114 Llamazares, S., Moreira, A., Tavares, A. *et al.* (1991) Polo encodes a protein kinase homolog required for mitosis in *Drosophila*. *Genes and Development*, **5**, 2153–2165.
 - 115 Glover, D.M., Hagan, I.M., and Tavares, A.A. (1998) Polo-like kinases: a team that plays throughout mitosis. *Genes and Development*, **12**, 3777–3787.
 - 116 Nigg, E.A. (2001) Mitotic kinases as regulators of cell division and its checkpoints. *Nature Reviews Molecular Cell Biology*, **2**, 21–32.
 - 117 Barr, F.A., Sillje, H.H.W., and Nigg, E.A. (2004) Polo-like kinases and the orchestration of cell division. *Nature Reviews Molecular Cell Biology*, **5**, 429–441.
 - 118 Lee, K.S., Yuan, Y.-L.O., Kuriyama, R., and Erikson, R.L. (1995) Plk is an M-phase-specific protein kinase and interacts with a kinesin-like protein, CHO1/MKLP-1. *Molecular and Cellular Biology*, **15**, 7143–7151.
 - 119 Hamanaka, R., Smith, M.R., O'Connor, P.M. *et al.* (1995) Polo-like kinase is a cell cycle-regulated kinase activated during mitosis. *Journal of Biological Chemistry*, **270**, 21086–21091.
 - 120 Ferris, D.K., Maloid, S.C., and Li, C.-C.H. (1998) Ubiquitination and proteasome mediated degradation of polo-like kinase. *Biochemical and Biophysical Research Communications*, **252**, 340–344.
 - 121 Roshak, A.K., Capper, E.A., Imburgia, C. *et al.* (2000) The human polo-like kinase, PLK, regulates cdc2/cyclin B through phosphorylation and activation of the cdc25C phosphatase. *Cell Signalling*, **12**, 405–411.
 - 122 Liu, F., Stanton, J.J., Wu, Z., and Piwnicka-Worms, H. (1997) The human Myt1 kinase preferentially phosphorylates Cdc2 on threonine 14 and localizes to the endoplasmic reticulum and Golgi complex. *Molecular and Cellular Biology*, **17**, 571–583.
 - 123 Parker, L.L., Atherton-Fessler, S., and Piwnicka-Worms, H. (1992) The p107wee1 is a dual-specificity kinase that phosphorylates p34cdc2 on tyrosine 15. *Proceedings of the National Academy of Sciences of the United States of America*, **89**, 2917–2921.
 - 124 Gautier, J., Solomon, M.J., Booher, R.N. *et al.* (1991) cdc25 is a specific tyrosine phosphatase that directly activates p34cdc2. *Cell*, **67**, 197–211.
 - 125 Sebastian, B., Kakizuka, A., and Hunter, T. (1993) Cdc25M2 activation of cyclin-dependent kinases by dephosphorylation of threonine-14 and tyrosine-15. *Proceedings of the National Academy of Sciences of the United States of America*, **90**, 3521–3524.
 - 126 Nurse, P. (1990) Universal control mechanism regulating onset of M-phase. *Nature*, **344**, 503–508.
 - 127 Abrieu, A., Brassac, T., Galas, S. *et al.* (1998) The polo-like kinase Plx1 is a component of the MPF amplification loop at the G2/M-phase transition of the cell cycle in *Xenopus* eggs. *Journal of Cell Science*, **111**, 1751–1757.
 - 128 Hagting, A., Karlsson, C., Clute, P. *et al.* (1998) MPF localization is controlled

- by nuclear export. *EMBO Journal*, **17**, 4127–4138.
- 129 Hagting, A., Jackman, M., Simpson, K., and Pines, J. (1999) Translocation of cyclin B1 to the nucleus at prophase requires a phosphorylation-dependent nuclear import signal. *Current Biology*, **9**, 680–689.
 - 130 Jackman, M., Lindon, C., Nigg, E.A., and Pines, J. (2003) Active cyclin B1-Cdk1 first appears on centrosomes in prophase. *Nature Cell Biology*, **5**, 143–148.
 - 131 Casenghi, M., Meraldi, P., Weinhart, U. *et al.* (2003) Polo-like kinase 1 regulates Nlp, a centrosome protein involved in microtubule nucleation. *Developmental Cell*, **5**, 113–125.
 - 132 Dai, W., Wang, Q., and Traganos, F. (2002) Polo-like kinases and centrosome regulation. *Oncogene*, **21**, 6195–6200.
 - 133 Dai, W. and Cogswell, J.P. (2003) Polo-like kinases and the microtubule organization center: targets for cancer therapies. *Progress in Cell Cycle Research*, **5**, 327–334.
 - 134 Weitzer, S. and Uhlmann, F. (2002) Chromosome segregation: playing polo in prophase. *Developmental Cell*, **2**, 381–382.
 - 135 Alexandru, G., Uhlmann, F., Mechtler, K. *et al.* (2001) Phosphorylation of the cohesin subunit Scc1 by Polo/Cdc5 kinase regulates sister chromatid separation in yeast. *Cell*, **105**, 459–472.
 - 136 Sumara, I., Vorlaufer, E., Stukenberg, P.T. *et al.* (2002) The dissociation of cohesin from chromosomes in prophase is regulated by polo-like kinase. *Molecular Cell*, **9**, 515–525.
 - 137 Kraft, C., Herzog, F., Gieffers, C. *et al.* (2003) Mitotic regulation of the human anaphase-promoting complex by phosphorylation. *EMBO Journal*, **22**, 6598–6609.
 - 138 Musacchio, A. and Hardwick, K.G. (2002) The spindle checkpoint: structural insights into dynamic signalling. *Nature Reviews Molecular Cell Biology*, **3**, 731–741.
 - 139 Adams, R.R., Tavares, A.A.M., Salzberg, A. *et al.* (1998) pavarotti encodes a kinesin-like protein required to organize the central spindle and contractile ring for cytokinesis. *Genes & Development*, **12**, 1483–1494.
 - 140 Zhou, T., Aumais, J.P., Liu, X. *et al.* (2003) A role for Plk1 phosphorylation of NudC in cytokinesis. *Developmental Cell*, **5**, 127–138.
 - 141 Moshe, Y., Boulaire, J., Pagano, M., and Hershko, A. (2004) Role of polo-like kinase in the degradation of early mitotic inhibitor 1, a regulator of the anaphase promoting complex/cyclosome. *Proceedings of the National Academy of Sciences of the United States of America*, **101**, 7937–7942.
 - 142 Golan, A., Yudkovsky, Y., and Hershko, A. (2002) The cyclin-ubiquitin ligase activity of cyclosome/APC is jointly activated by protein kinases Cdk1-cyclin B and Plk. *Journal of Biological Chemistry*, **277**, 15552–15557.
 - 143 Kotani, S., Tugendreich, S., Fujii, M. *et al.* (1998) PKA and MPF-activated polo-like kinase regulate anaphase-promoting complex activity and mitosis progression. *Molecular Cell*, **1**, 371–380.
 - 144 Smits, V.A.J., Klompmaier, R., Arnaud, L. *et al.* (2000) Polo-like kinase-1 is a target of the DNA damage checkpoint. *Nature Cell Biology*, **2**, 672–676.
 - 145 van Vugt, M.A., Smits, V.A., Klompmaier, R., and Medema, R.H. (2001) Inhibition of polo-like kinase-1 by DNA damage occurs in an ATM- or ATR-dependent fashion. *Journal Of Biological Chemistry*, **276**, 41656–41660.
 - 146 Ma, S., Charron, J., and Erikson, R.L. (2003) Role of Plk2 (Snk) in mouse development and cell proliferation. *Molecular and Cellular Biology*, **23**, 6936–6943.
 - 147 Bahassi, E.M., Conn, C.W., Myer, D.L. *et al.* (2002) Mammalian polo-like kinase 3 (Plk3) is a multifunctional protein involved in stress response pathways. *Oncogene*, **21**, 6633–6640.
 - 148 Wang, Q., Xie, S., Chen, J. *et al.* (2002) Cell cycle arrest and apoptosis induced by human polo-like kinase 3 mediated through perturbation of microtubule integrity. *Molecular and Cellular Biology*, **22**, 3450–3459.
 - 149 Conn, C.W., Hennigan, R.F., Dai, W. *et al.* (2000) Incomplete cytokinesis and induction of apoptosis by overexpression

- of the mammalian polo-like kinase, Plk3. *Cancer Research*, **60**, 6826–6831.
- 150 Kauselmann, G., Weiler, M., Wulff, P. *et al.* (1999) The polo-like protein kinases Fnk and Snk associate with a Ca^{2+} - and integrin-binding protein and are regulated dynamically with synaptic plasticity. *EMBO Journal*, **18**, 5528–5539.
 - 151 Wolf, G., Elez, R., Doermer, A. *et al.* (1997) Prognostic significance of polo-like kinase (PLK) expression in non-small cell lung cancer. *Oncogene*, **14**, 543–549.
 - 152 Yuan, J., Hoerlin, A., Hock, B. *et al.* (1997) Polo-like kinase, a novel marker for cellular proliferation. *American Journal of Pathology*, **150**, 1165–1172.
 - 153 Tokumitsu, Y., Mori, M., Tanaka, S. *et al.* (1999) Prognostic significance of polo-like kinase expression in esophageal carcinoma. *International Journal of Oncology*, **15**, 687–692.
 - 154 Takahashi, T., Sano, B., Nagata, T. *et al.* (2003) Polo-like kinase 1 (PLK1) is overexpressed in primary colorectal cancers. *Cancer Science*, **94**, 148–152.
 - 155 Spankuch-Schmitt, B., Wolf, G., Solbach, C. *et al.* (2002) Downregulation of human polo-like kinase activity by antisense oligonucleotides induces growth inhibition in cancer cells. *Oncogene*, **21**, 3162–3171.
 - 156 Elez, R., Piiper, A., Giannini, C.D. *et al.* (2000) Polo-like kinase 1, a new target for antisense tumor therapy. *Biochemical and Biophysical Research Communications*, **269**, 352–356.
 - 157 Elez, R., Piiper, A., Kronenberger, B. *et al.* (2003) Tumor regression by combination antisense therapy against Plk1 and Bcl-2. *Oncogene*, **22**, 69–80.
 - 158 Cory, S., Huang, D.C.S., and Adams, J.M. (2003) The Bcl-2 family: roles in cell survival and oncogenesis. *Oncogene*, **22**, 8590–8607.
 - 159 Lee, K.S. and Erikson, R.L. (1997) Plk is a functional homolog of *Saccharomyces cerevisiae* Cdc5, and elevated Plk activity induces multiple septation structures. *Molecular and Cellular Biology*, **17**, 3408–3417.
 - 160 Morgan, D.O. (1995) Principles of CDK regulation. *Nature*, **374**, 131–134.
 - 161 Huang, W. and Erikson, R.L. (1994) Constitutive activation of Mek1 by mutation of serine phosphorylation sites. *Proceedings of the National Academy of Sciences of the United States of America*, **91**, 8960–8963.
 - 162 Jang, Y.-J., Ma, S., Terada, Y., and Erikson, R.L. (2002) Phosphorylation of threonine 210 and the role of serine 137 in the regulation of mammalian polo-like kinase. *Journal of Biological Chemistry*, **277**, 44115–44120.
 - 163 Mundt, K.E., Golsteyn, R.M., Lane, H.A., and Nigg, E.A. (1997) On the regulation and function of human polo-like kinase 1 (PLK1): effects of overexpression on cell cycle progression. *Biochemical and Biophysical Research Communications*, **239**, 377–385.
 - 164 Qian, Y.-W., Erikson, E., and Maller, J.L. (1998) Purification and cloning of a protein kinase that phosphorylates and activates the polo-like kinase Plx1. *Science*, **282**, 1701–1704.
 - 165 Erikson, E., Haystead, T.A.J., Qian, Y.-W., and Maller, J.L. (2004) A feedback loop in the polo-like kinase activation pathway. *Journal of Biological Chemistry*, **279**, 32219–32224.
 - 166 Kuramochi, S., Moriguchi, T., Kuida, K. *et al.* (1997) LOK is a novel mouse STE20-like protein kinase that is expressed predominantly in lymphocytes. *Journal of Biological Chemistry*, **272**, 22679–22684.
 - 167 Ellinger-Ziegelbauer, H., Karasuyama, H., Yamada, E. *et al.* (2000) Ste20-like kinase (SLK), a regulatory kinase for polo-like kinase (Plk) during the G2/M transition in somatic cells. *Genes to Cells*, **5**, 491–498.
 - 168 Kelm, O., Wind, M., Lehmann Wolf, D., and Nigg, E.A. (2002) Cell cycle-regulated phosphorylation of the xenopus polo-like kinase Plx1. *Journal of Biological Chemistry*, **277**, 25247–25256.
 - 169 Jang, Y.-J., Lin, C.-Y., Ma, S., and Erikson, R.L. (2002) Functional studies on the role of the C-terminal domain of mammalian polo-like kinase. *Proceedings of the National Academy of Sciences of the United States of America*, **99**, 1984–1989.
 - 170 McInnes, C., Mezna, M., and Fischer, P.M. (2005) Progress in the discovery of

- polo-like kinase inhibitors. *Current Topics in Medicinal Chemistry*, **5**, 181–197.
- 171 Strebhardt, K. and Ullrich, A. (2006) Targeting polo-like kinase 1 for cancer therapy. *Nature Reviews. Cancer*, **6**, 321–330.
 - 172 Strebhardt, K. (2006) Small molecules keep mitotic kinases in check. *ACS Chemical Biology*, **1**, 683–686.
 - 173 Fischer, P.M. and Lane, D.P. (2000) Inhibitors of cyclin-dependent kinases as anti-cancer therapeutics. *Current Medicinal Chemistry*, **7**, 1213–1245.
 - 174 Bain, J., McLauchlan, H., Elliott, M., and Cohen, P. (2003) The specificities of protein kinase inhibitors: an update. *The Biochemical Journal*, **371**, 199–204.
 - 175 Davies, S.P., Reddy, H., Caivano, M., and Cohen, P. (2000) Specificity and mechanism of action of some commonly used protein kinase inhibitors. *The Biochemical Journal*, **351**, 95–105.
 - 176 Walker, E.H., Pacold, M.E., Perisic, O. *et al.* (2000) Structural determinants of phosphoinositide 3-kinase inhibition by wortmannin, LY294002, quercetin, myricetin, and staurosporine. *Molecular Cell*, **6**, 909–919.
 - 177 Fischer, P.M. (2004) The design of drug candidate molecules as selective inhibitors of therapeutically relevant kinases. *Current Medicinal Chemistry*, **11**, 1563–1583.
 - 178 Singh, J., Dobrusin, E.M., Fry, D.W. *et al.* (1997) Structure-based design of a potent, selective, and irreversible inhibitor of the catalytic domain of the erbB receptor subfamily of protein tyrosine kinases. *Journal of Medicinal Chemistry*, **40**, 1130–1135.
 - 179 Cogswell, J.P., Brown, C.E., Bisi, J.E., and Neill, S.D. (2000) Dominant-negative polo-like kinase 1 induces mitotic catastrophe independent of cdc25C function. *Cell Growth and Differentiation*, **11**, 615–623.
 - 180 Agullo, G., Gamet-Payraastre, L., Manenti, S. *et al.* (1997) Relationship between flavonoid structure and inhibition of phosphatidylinositol 3-kinase: a comparison with tyrosine kinase and protein kinase C inhibition. *Biochemical Pharmacology*, **53**, 1649–1657.
 - 181 Gamet-Payraastre, L., Manenti, S., Gratacap, M.-P. *et al.* (1999) Flavonoids and the inhibition of PKC and PI 3-kinase. *General Pharmacology*, **32**, 279–286.
 - 182 Vlahos, C.J., Matter, W.F., Hui, K.Y., and Brown, R.F. (1994) A specific inhibitor of phosphatidylinositol 3-kinase, 2-(4-morpholinyl)-8-phenyl-4H-1-benzopyran-4-one (LY294002). *Journal of Biological Chemistry*, **269**, 5241–5248.
 - 183 Wang, S., Wood, G., Meades, C. *et al.* (2004) Synthesis and biological activity of 2-Anilino-4-(1H-pyrrol-3-yl)pyrimidine CDK inhibitors. *Bioorganic & Medicinal Chemistry Letters*, **14**, 4237–4240.
 - 184 Wang, S., Meades, C., Wood, G. *et al.* (2004) 2-Anilino-4-(thiazol-5-yl)pyrimidine CDK inhibitors: synthesis, SAR analysis, X-ray crystallography, and biological activity. *Journal of Medicinal Chemistry*, **47**, 1662–1675.
 - 185 McInnes, C., Mezna, M., Griffiths, G. *et al.* (2003) Structure-based ligand discovery and anti-tumor effects of polo-like kinase-1 ATP-competitive inhibitors. *Clinical Cancer Research*, **9** (Suppl. 16), Abstract A191.
 - 186 McInnes, C., Mazumdar, A., Mezna, M. *et al.* (2006) Inhibitors of polo-like kinase reveal roles in spindle-pole maintenance. *Nature Chemical Biology*, **2**, 608–617.
 - 187 McInnes, C., Meades, C., Mezna, M., and Fischer, P. (2004) Benzthiazole-3 oxides useful for the treatment of proliferative disorders. US Patent, WO2004067000, A1 20040812, WO2004-GB327 20040127, GB 2003-2220 A 20030130.
 - 188 Umehara, H., Yamashita, Y., Tsujita, T. *et al.* (2004) Preparation of 2-aminopyrimidine derivatives as polo-like kinase inhibitors for treatment of tumor. US Patent WO2004043936, A1 20040527, WO2003-JP14518 20031114, JP 2002-331141, A 20021114.
 - 189 Davis-Ward, R., Mook, R.A. Jr., Neeb, M.J., and Salovich, J.M. (2004) Preparation of pyrimidine derivatives as polo-like kinases inhibitors for treatment of cancers. US Patent WO2004074244, A2 20040902, WO2004-US4197 20040211, US 2003-448795P P 20030220.

- 190 Andrews, C.W. III, Cheung, M., Davis-Ward, R.G. *et al.* (2004) Preparation of benzimidazolyl substituted thiophenes as polo like kinases (PLK) inhibitors for treating cancer. US Patent WO2004014899, A1 20040219, WO2003-US24272 20030804, US 2002-402008P P 20020808.
- 191 Lansing, T.J., McConnell, R.T., Duckett, D.R. *et al.* (2007) *In vitro* biological activity of a novel small-molecule inhibitor of polo-like kinase 1. *Molecular Cancer Therapeutics*, **6**, 450–459.
- 192 Reddy, P.E., Reddy, R.M.V., and Bell, S.C. (2003) Preparation of amino-substituted 1 (E)-2,6-diakoxystyryl 4-substituted benzyl sulfones for treating proliferative disorders. US Patent WO2003072062, A2 20030904, WO2003-US6357 20030228, WO2003072062, A3 20031204, US 2002-360697P P 20020228.
- 193 Lee, K.S., Grenfell, T.Z., Yarm, F.R., and Erikson, R.L. (1998) Mutation of the polo-box disrupts localization and mitotic functions of the mammalian polo kinase Plk. *Proceedings of the National Academy of Sciences of the United States of America*, **95**, 9301–9306.
- 194 Lee, K.S., Song, S., and Erikson, R.L. (1999) The polo-box-dependent induction of ectopic septal structures by a mammalian polo kinase, Plk, in *Saccharomyces cerevisiae*. *Proceedings of the National Academy of Sciences of the United States of America*, **96**, 14360–14365.
- 195 Yuan, J., Kramer, A., Eckerdt, F. *et al.* (2002) Efficient internalization of the polo-box of polo-like kinase 1 fused to an antennapedia peptide results in inhibition of cancer cell proliferation. *Cancer Research*, **62**, 4186–4190.
- 196 May, K.M., Reynolds, N., Cullen, C.F. *et al.* (2002) Polo boxes and Cut23 (Apc8) mediate an interaction between polo kinase and the anaphase-promoting complex for fission yeast mitosis. *Journal of Cell Biology*, **156**, 23–28.
- 197 Nakajima, H., Toyoshima-Morimoto, F., Taniguchi, E., and Nishida, E. (2003) Identification of a consensus motif for Plk (polo-like kinase) phosphorylation reveals Myt1 as a Plk1 substrate. *Journal of Biological Chemistry*, **278**, 25277–25280.
- 198 Neef, R., Preisinger, C., Sutcliffe, J. *et al.* (2003) Phosphorylation of mitotic kinesin-like protein 2 by polo-like kinase 1 is required for cytokinesis. *Journal of Cell Biology*, **162**, 863–875.
- 199 Cheng, K.-Y., Lowe, E.D., Sinclair, J. *et al.* (2003) The crystal structure of the human polo-like kinase-1 polo box domain and its phospho-peptide complex. *EMBO Journal*, **22**, 5757–5768.
- 200 Elia, A.E.H., Rellos, P., Haire, L.F. *et al.* (2003) The molecular basis for phosphodependent substrate targeting and regulation of plks by the polo-box domain. *Cell*, **115**, 83–95.
- 201 Leung, G.C., Hudson, J.W., Kozarova, A. *et al.* (2002) The Sak polo-box comprises a structural domain sufficient for mitotic subcellular localization. *Nature Structural Biology*, **9**, 719–724.
- 202 Pawson, T. and Scott, J.D. (1997) Signaling through scaffold, anchoring, and adaptor proteins. *Science*, **278**, 2075–2080.
- 203 Sawyer, T.K., Bohacek, R.S., Dalgarno, D.C. *et al.* (2002) SRC homology-2 inhibitors: peptidomimetic and nonpeptide. *Mini-Reviews in Medicinal Chemistry*, **2**, 475–488.
- 204 Garcia-Alvarez, B., de Carcer, G., Ibanez, S. *et al.* (2007) Molecular and structural basis of polo-like kinase 1 substrate recognition: implications in centrosomal localization. *Proceedings of the National Academy of Sciences of the United States of America*, **104**, 3107–3112.
- 205 Reindl, W., Yuan, J., Kramer, A. *et al.* (2008) Inhibition of polo-like kinase 1 by blocking polo-box domain-dependent protein–protein interactions. *Chemistry & Biology*, **15**, 459–466.
- 206 Reindl, W., Yuan, J., Kramer, A. *et al.* (2009) A pan-specific inhibitor of the polo-box domains of polo-like kinases arrests cancer cells in mitosis. *Chembiochem: A European Journal of Chemical Biology*, **10**, 1145–1148.
- 207 Gali-Muhtasib, H., Roessner, A., and Schneider-Stock, R. (2006) Thymoquinone: a promising anti-cancer drug from natural sources. *The*

International Journal of Biochemistry & Cell Biology, **38**, 1249–1253.

- 208** Watanabe, N., Sekine, T., Takagi, M. *et al.* (2009) Deficiency in chromosome

congression by the inhibition of Plk1 polo box domain-dependent recognition. *The Journal of Biological Chemistry*, **284**, 2344–2353.

9

Medicinal Chemistry Approaches for the Inhibition of the p38 MAPK Pathway

Stefan Laufer L, Simona Margutti, Dowinik Hauser

9.1

Introduction

The MAP kinases are a family of enzymes that participate in many cellular activities and are divided into three subfamilies: (1) The extracellular signal-related kinases (ERKs) that are widely expressed and that typically regulate cellular proliferation and differentiation. (2) The c-Jun-N-terminal kinases (JNKs) play a major role in extracellular matrix regulation through the production of metalloproteinases [1]. (3) p38 MAP kinase has four isoforms (α , β , γ , and δ) and plays an especially important role in the production of cytokines such as interleukin-1 (IL-1), tumor necrosis factor alpha (TNF- α), and IL-6 [2]. p38 MAP kinase, its central role in numerous proinflammatory cellular responses and the approaches of its inhibition by “small-molecule” chemical entities is the subject of this chapter.

The p38 mitogen-activated protein kinase (p38 MAPK) is known under several other names such as cytokine suppressive anti-inflammatory drug binding protein (CSPB) [3], stress-activated protein kinase 2 (SAPK2), and mHOG1 protein which is a yeast analogue encoded by the budding yeast HOG1 gene that is activated in response to hyperosmolarity.

9.2

p38 MAP Kinase Basics

The p38 MAP kinases are widely expressed in many cell types, including immune, inflammatory, and endothelial cells. Originally described as a 38 kDa polypeptide that underwent Tyr phosphorylation in response to endotoxin treatment and osmotic shock [4], p38 (the α -isoform) was purified by anti-phosphotyrosine immunoaffinity chromatography; p38 α is 50% identical to ERK2 and bears significant identity to the yeast kinase Hog1p involved in the response to hyperosmolarity [5, 6].

The p38 α -isoform has been associated most closely to inflammatory responses. A variety of factors, including stress, endotoxin, cytokines such as TNF- α and

interleukin-1 beta (IL-1 β), and cigarette smoke, activate the p38 kinases. Once activated, p38 phosphorylates downstream substrates to initiate a signal cascade that regulates synthesis of a variety of proinflammatory mediators. TNF- α , IL-1 β , and COX-2 are among the most important ones regulated by p38. The inhibition of each of these inflammatory mediators has been demonstrated to lead to clinical benefit in rheumatoid arthritis (RA), based on approved biologics and NSAIDs. In addition to regulating the production of mediators such as TNF- α and IL-1 β , p38 is activated following the binding of TNF- α , IL-1 β , and RANKL to their receptors and is responsible for some of their effects. p38 inhibition therefore offers opportunities to intervene in processes involving these cytokines. In addition to inhibiting production of the cytokines themselves, p38 inhibition has the potential to block subsequent deleterious effects caused by the cytokines.

Three additional p38 family members, p38 β [7–9], p38 γ [10, 11], and p38 δ [7–9], share 47–42% sequence identity to ERK2, but are 75, 62, and 64% identical to p38 α , respectively. In mammalian cells, the p38 isoforms are strongly activated by environmental stresses and inflammatory cytokines, but not appreciably by mitogenic stimuli. The expression of the four different isoforms is reported in Table 9.1.

Both p38 γ and p38 δ , with 67% identity to each other, have distinct expression patterns. p38 γ is primarily expressed in skeletal muscle, and its expression is upregulated during muscle differentiation [10]. p38 δ expression is also developmentally regulated and is most highly detected in lung, kidney, endocrine organs, and small intestine [13]. Within the p38 family, the ubiquitously expressed p38 α and p38 β are inhibited by pyridinyl-imidazole “drugs,” while the other two p38 kinases, p38 γ and p38 δ , are insensitive to these drugs [14]. Most stimuli that activate p38 also activate JNK (Figure 9.1), are also inhibited by the anti-inflammatory drug SB203580, which has been extremely useful in delineating the function of p38 α [5].

Activation of p38 in cells is mainly mediated by MEK3 and MEK6. MEK4 also displays activity toward p38 *in vitro* [15]. In MEK4^{−/−} fibroblasts, both JNK and p38 lost their responsiveness to TNF- α , interleukin-1, and hyperosmotic stress, suggesting that crosstalk exists between these two stress-sensitive pathways [16]. Activation

Table 9.1 p38 isoforms’ expression in cells of the immune system and endothelium [12].

p38 isoforms	Tissues expression	Cellular expression
p38 α	Ubiquitous. Mainly spleen, bone marrow, heart, brain, pancreas, liver, lung skeletal muscle, kidney, and placenta.	All cell types. Mainly peripheral leukocytes.
p38 β	Ubiquitous. Mainly brain and heart.	Endothelial cells, T cells.
p38 γ	Skeletal muscles, heart.	Little or no expression in immune system.
p38 δ	Lung, kidney, endocrine organs, and small intestine	Macrophages, neutrophils, T cells, monocytes.

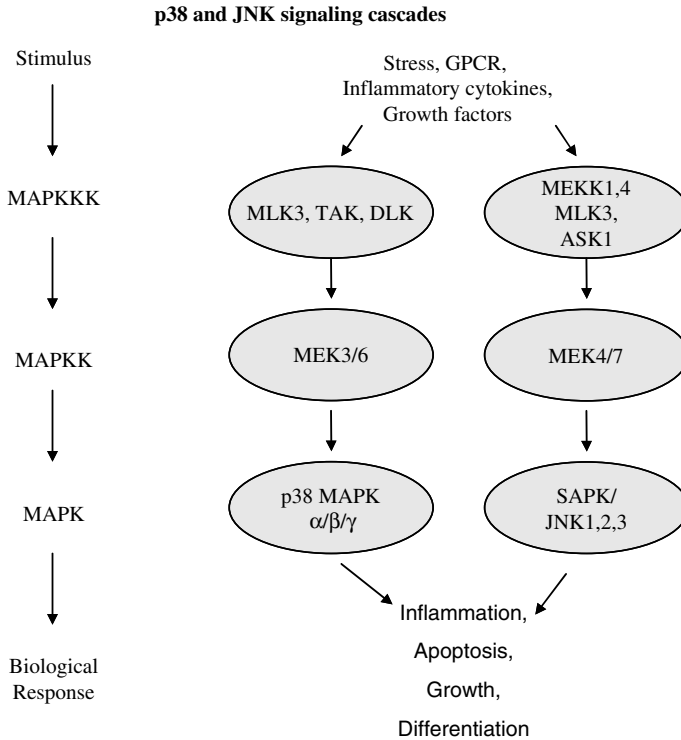


Figure 9.1 p38 and JNK signaling cascades. Although each MAPK has unique characteristics, a number of features are shared by the MAPK pathways. Each family of MAPKs is composed of a set of three evolutionarily conserved, sequentially acting kinases: a MAPK, a MAPK kinase (MAPKK), and a MAPKK kinase (MAPKKK). The MAPKKKs, which are serine/threonine kinases, are often activated through phosphorylation and/or as a result of their interaction with a small GTP binding protein of the Ras/Rho family in response to extracellular

stimuli. MAPKKK activation leads to the phosphorylation and activation of a MAPKK, which then stimulates MAPK activity through dual phosphorylation on threonine and tyrosine residues located in the activation loop of the kinase. Once activated, MAPKs phosphorylate target substrates on serine or threonine residues followed by a proline; however, substrate selectivity is often conferred by a specific interaction motif located on the physiological substrate.

of the p38 isoforms results from the MEK3/6-catalyzed phosphorylation of a conserved Thr-Gly-Tyr (TGY) motif in their activation loop.

The structures of inactive and active (phosphorylated) p38 α have been solved by X-ray crystallography. The most prominent PDB entry is the cocrystal 1a9u with SB203580 [17]. The phosphorylated TGY motif and the length of the activation loop were found to differ in ERK2 and JNK, which likely contribute to the substrate specificity of p38 [18, 19].

Owing to the specificity of MEKs and the relatively low sequence identity among the p38 isoforms, selective activation of different p38 isoforms by distinct MEKs was

observed. This signaling specificity is crucial for the generation of appropriate biological responses by the p38 pathway.

MEKs are activated by a plethora of MAPKKs, typically a MEKK or a mixed lineage kinase (MLK), which becomes activated in response to various physical and chemical stresses such as oxidative stress, UV irradiation, hypoxia, ischemia, and various cytokines including IL-1 and TNF- α (Figure 9.1). Details regarding the contributions of MEKKs and MLKs to the p38 pathway remain poorly understood. MEKKs 1–3 have been implicated in p38 activation, although they preferentially regulate JNKs and ERKs.

Members of the MLK family contain a SH3 domain, leucine zippers, and a small GTPase binding domain [20]. Protein–protein interaction through these domains facilitates integration of signals by MLKs from upstream regulators to the downstream MAP kinases. Other kinases that may regulate p38 include TPL2, ASK1, and TAK1 (Figure 9.2).

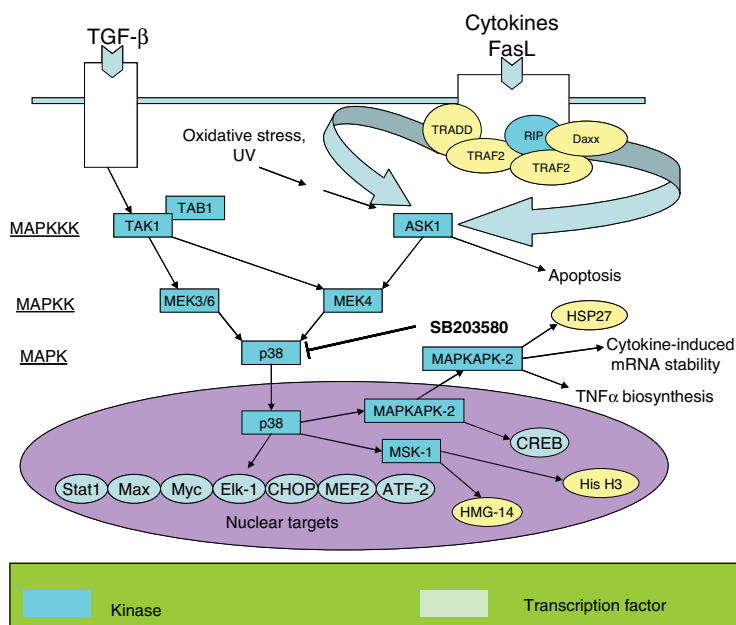


Figure 9.2 p38 MAPK Signaling Pathways. p38 MAPKs are members of the MAPK family that are activated by a variety of environmental stresses and inflammatory cytokines. As with other MAPK cascades, the membrane-proximal component is a MAPKKK, typically a MEKK or a MLK. The MAPKKK phosphorylates and activates MKK3/6, the p38 apoptotic stimuli. p38 MAPK is involved in regulation of HSP27 and MAPKAP-2 as well as several transcription factors including ATF-2, Stat1, the Max/Myc

complex, MEF-2, Elk-1, and, indirectly, CREB via activation of MSK1. Localization of p38 is controversial; in fact, p38 has been shown to be present in both the nucleus and the cytoplasm of quiescent cells, but upon cell stimulation, the cellular localization of p38 is not well understood. Some evidence suggests that, following activation, p38 translocates from the cytoplasm to the nucleus, but other data indicate that activated p38 is also present in the cytoplasm of stimulated cells.

9.3

p38 Activity and Inhibition

A large body of evidence indicates that p38 activity is critical for normal immune and inflammatory responses. p38 is activated in macrophages, neutrophils, and T cells by numerous extracellular mediators of inflammation, including chemoattractants, cytokines, chemokines, and bacterial lipopolysaccharides [21]. p38 participates in macrophage and neutrophil functional responses, including respiratory burst activity, chemotaxis, granular exocytosis, adherence, apoptosis, and also mediates T cell differentiation and apoptosis by regulating gamma interferon production.

The requirement for p38 activation in cellular responses has been defined largely through the use of experimental pyridinyl-imidazole anti-inflammatory drugs, the cytokine-suppressive anti-inflammatory drugs (CSAIDs), the most extensively characterized of which is the compound SB203580.

p38 inhibitors are potent inhibitors of LPS-mediated TNF- α production in macrophages [5]. The ability of p38 inhibitors to block TNF- α synthesis can be exploited in the treatment of inflammatory diseases.

Taking into consideration the kinase inhibition principles, it is possible to distinguish four types of inhibitors: substrate-competitive inhibitors, ATP-competitive inhibitors, activation inhibitors/allosteric modulators, and irreversible inhibitors.

The substrate binding site seems to have obvious advantages over the ATP binding site as a target for inhibiting kinase activity. First, substrate binding inhibitors are not affected by the high ATP concentration [22–24] found in cells. Second, the substrate binding site of a kinase controls selectivity, whereas the ATP binding site is highly conserved throughout all kinase family members. While substrate-competitive inhibition has been applied successfully in enzyme classes such as the proteases, its use for kinase inhibition has not been successful thus far. Because of their large substrate binding sites, kinases [25] lack the specific, compact hydrophobic pockets that could serve as targets for small-molecule inhibitors. Irreversible inhibitors are not usually used in the pharmaceutical industry due to the possible toxicity they could incur. Example of this type of inhibitors is Canertinib, an irreversible small-molecule tyrosine kinase inhibitor that blocks signal transduction through all four members of the ErbB (or epidermal growth factor (EGF)) family and is in development for the treatment of advanced nonhematological cancers [26].

Of higher relevance are ATP-competitive inhibitors. For a long time, the development of a potent and a selective ATP-competitive inhibitor was considered as impossible. The main concerns are selectivity, due to the shared highly conserved ATP binding site, and potency, as a consequence of intracellular ATP concentrations up to 2–10 mM [22–24]. Thus, the concentrations required for an inhibitor to reach 50% inhibition are two or three orders of magnitude higher than the inhibition constant itself. Experience collected over the last 10 years shows that fairly selective ATP-site-specific kinase inhibitors can be generated, due to the suitability of the binding site to drug design, with different examples showing that specificity and selectivity can be achieved by the derivatization pattern of an underlying core

structure [27]. On the other hand, it must be underscored that many specific protein kinase inhibitors, such as PD98059 and SB203580 are not developable due to toxicity or ADME problems. Nevertheless, from a chemical biology perspective, these compounds could be extremely useful research agents.

Selectivity of an inhibitor can theoretically be explored by a kinase profile assay. The standard biochemical approach to addressing this problem relies on the specificity screens with an *in vitro* inhibition assay against panels of purified kinases [28].

To further prove that specificity could be achieved by ATP-competitive inhibitors, crucial experimental data were published by researchers at Merck [29]. Comparison of the crystal structures of p38 bound to different compounds showed that binding of more specific molecules is characterized by a peptide flip between Met109 and Gly110 with Gly110 being a residue specific to the α -, β -, and γ -isoforms of p38. The δ -isoform and the other MAP kinases have bulkier residues in this position. These larger residues would likely make the peptide flip energetically unfavorable, thus explaining the selectivity of binding. This stabilized peptide flip is caused by a switching of the hydrogen-bond donor and acceptor distribution around the peptide plane.

Researchers at Merck compared cocrystal structures with p38 α of compound 1 (PDB entry: 1OUK) and compound 2 (PDB entry: 1M7Q) (Figure 9.3). Comparison of the structures of the pyrimidine-imidazole compound 1 [30] and the dihydroquinazolinone compound 2 [31] shows that N6 in compound 1, a hydrogen-bond donor, is replaced by O1 in compound 2, a hydrogen-bond acceptor.

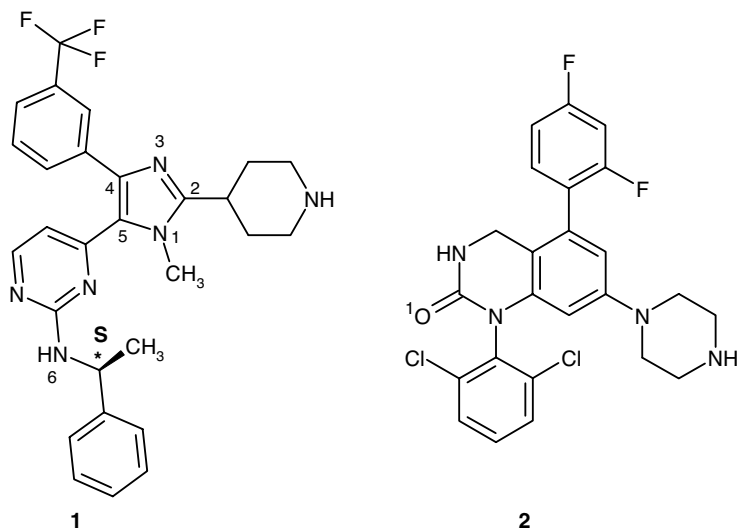


Figure 9.3 Structure of Merck compounds [29] that inhibit p38 kinase.

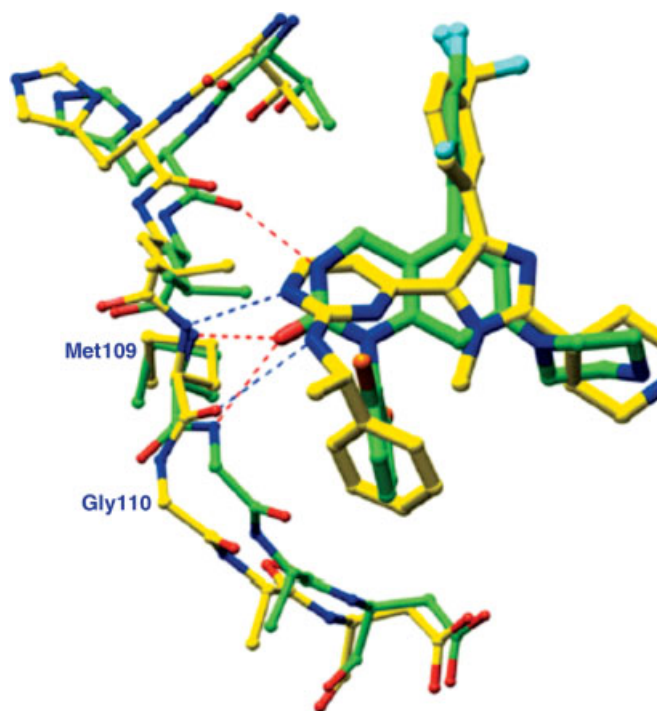


Figure 9.4 Compound-induced peptide flip in the linker region. Overlay of p38 α -bound compounds **1** (yellow) and **2** (green) [29].

This change in polarity is accommodated by a peptide flip at the Met109-Gly110 bond, so that in complex containing compound **2**, the carbonyl is interacting with two hydrogen-bond donors (the main chain nitrogens of Met109 and Gly110) (Figure 9.4).

In p38 α , the peptide flip changes the (Φ , ψ) peptide bond angles of Met109 (i residue) and Gly110 ($i + 1$ residue) from a (β , α_R) conformation to a (α_R , α_L) conformation, without affecting the orientation of adjacent peptide planes or side chains. This flip belongs to the group 2 flips, which are characterized by having $\psi(i)$ values that are in the α_R or α_L regions when $\Phi(i + 1)$ is positive. As $\Phi(i + 1)$ must take on positive values if peptide-plane flipping is to occur, the residue at position $i + 1$ is often a glycine; the X-Gly motif seems to be quite common among different cases. If the residue $i + 1$ is not a glycine, the presence of a residue other than glycine would probably reduce the likelihood that the peptide flip would occur.

Relevant and interesting are the allosteric modulators, which as previously pointed out, could potentially solve the selectivity issues related to protein kinase inhibition [32]. Example of this allosteric type of binding mode is the Boehringer Ingelheim compound BIRB-796, which was reported as allosteric inhibitor and has been discussed earlier (see Chapter 6).

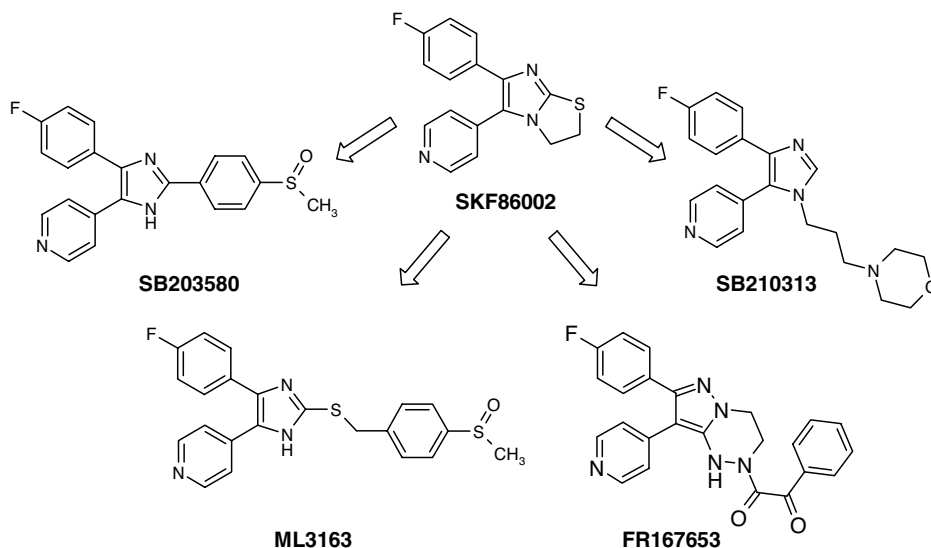


Figure 9.5 Prototypical inhibitors of p38 derived from the early lead SKF86002.

9.4

First-Generation Inhibitors

Similar to the other structurally related first-generation p38 inhibitors, the prototypical pyridinyl-imidazole SB203580 had been derived from the early lead SKF86002 (Figure 9.5). Without knowledge of its precise mode of action, the anti-inflammatory properties of SKF86002 in turn had been described in a seminal publication by Lantos *et al.* as early as 1984 [33]. The compound FR167653 was already patented in 1994 by Fujisawa as an inhibitor of interleukin-1 and tumor necrosis factor inhibitory activity [34]. The mechanism of action of FR167653 remained unclear until 1999/2000 when it was assigned to p38 MAPK inhibition [35–38]. For a series of 2-alkylsulfanyl-imidazoles exemplified by ML3163, scientists at Merckle described SAR around the 4-fluorophenyl- and pyridin-4-yl-moieties similar to those of SB203580 and its analogs [39]. Some of the related 2-sulfanyl-imidazoles showed a favorable interaction profile with CYP450 isoenzymes compared to SB203580 [40]. The identification of p38 as the molecular target for anticytokine agents such as SB203580, SKF86002, and FR167653 triggered a vibrant search for more potent and less toxic inhibitors of p38.

9.5

Pyridinyl-Imidazole Inhibitor: SB203580

The basis for p38 inhibition was revealed in the crystal structure of p38 α in complex with SB203580 (PDB entry: 1a9u) [17]. As previously discussed, *in vitro* assays

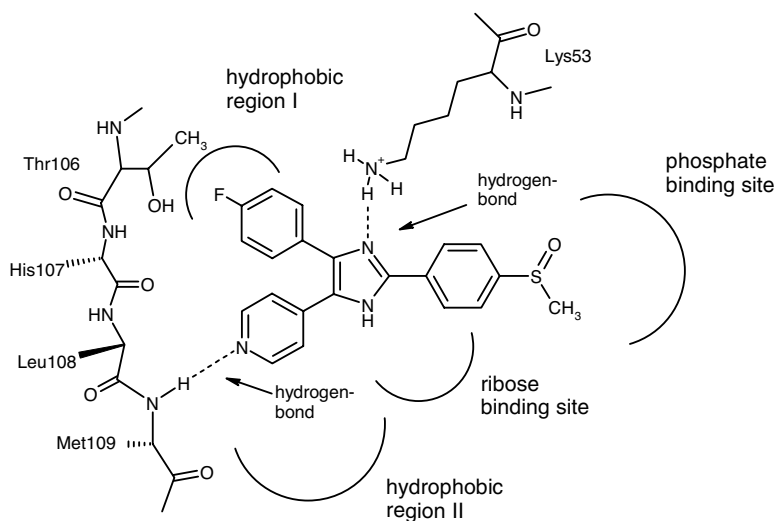


Figure 9.6 Important interactions between the prototypical pyridine-4-yl-imidazole inhibitor SB203580 and the ATP binding site of p38 α : The 4-fluorophenyl moiety penetrates deeply into the selectivity pocket (hydrophobic region I), the backbone N—H of

Met109 forms the essential H-bond with the pyridine N, an additional H-bond is formed between Lys53 and imidazole N1. The hydrophobic region II is not occupied by SB203580.

demonstrated that only p38 α and p38 β are inhibited by CSAIDs; p38 δ and p38 γ are completely unaffected by this class of drugs *in vitro* or in transfected cells [8]. Davies *et al.* [28] published a study on specificities of different commercially available compounds with relatively selective inhibition of particular serine/threonine-specific protein kinases, describing the preferential inhibition of the α - and β -isoforms over the γ - and σ -isoforms by SB203580.

Crystallographic [17, 41, 42], mutational [43, 44], and biochemical [45] studies demonstrated that SB203580 binds in the ATP binding site of p38. The 4-fluorophenyl ring of the inhibitor is located in a hydrophobic pocket with walls formed by the N-terminal domain core at the back of the active site (Figure 9.6).

Thr106 in the hinge of the p38 α ATP binding pocket is the factor determining the nature of the residue that can be accommodated in the hydrophobic region. The selectivity of compounds as SB203580 for p38 α has been attributed to the presence of Thr106 in the ATP binding site. Therefore, Thr106 is often referred to as a gatekeeper. Groups such as *p*-fluorophenyl, *m,p*-difluorophenyl, and *m*-trifluoromethylphenyl substituents on either imidazole or pyrrole scaffolds can occupy a space near Thr106 (Figure 9.6). The structures reported in Figure 9.7 were used by Lisnock *et al.* [44] to assess how mutations at the amino acids 106, 109, and 157 in p38-affected inhibitor binding.

Other MAP kinases (Table 9.2), except p38 β , have either a Met or a Gln residue in position 106 and the larger side chains of these residues prevent the binding of the fluorophenyl ring of the inhibitors. A site-direct mutagenesis study undertaken by

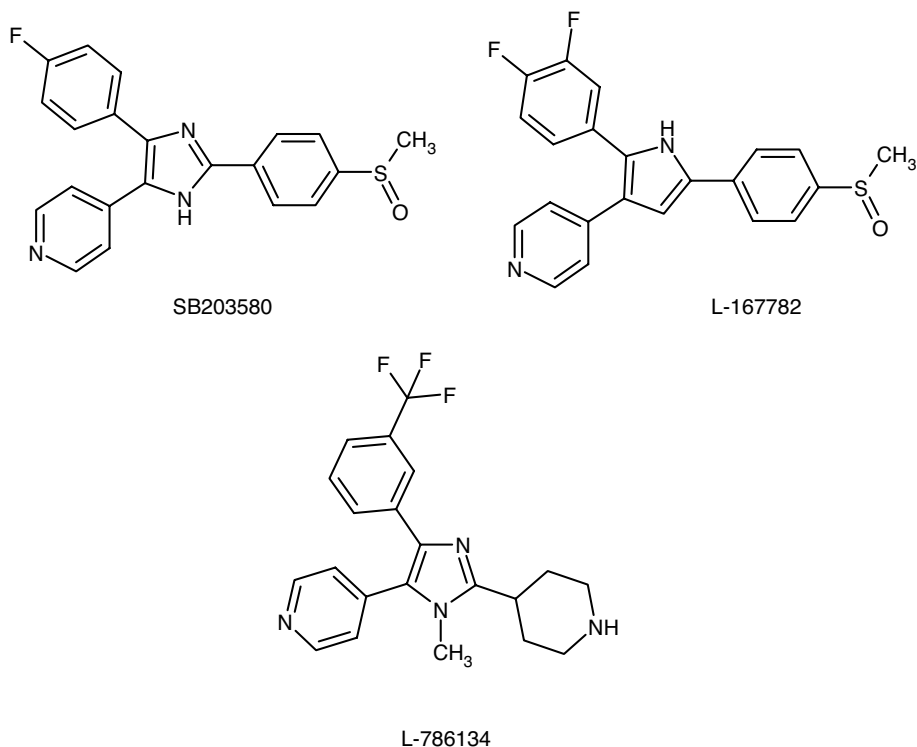


Figure 9.7 Structures of triaryl-imidazole SB203580, triarylpyrrole L-167782, and diaryl-imidazole L-786134.

Table 9.2 Amino acid comparison between residues in p38 α and homologous Ser/Thr kinases.

	35	38	51	53	75	84	86	104	106	107	108	109	155	157	168
p38 α	Y	V	A	K	L	I	L	L	T	H	L	M	N	A	D
p38 β	Y	V	A	K	L	I	L	L	T	T	L	M	N	A	D
p38 γ	Y	V	A	K	L	I	L	L	M	P	F	M	N	A	D
p38 δ	Y	V	A	K	L	I	L	L	M	P	F	M	N	A	D
JNK2 β	Q	V	A	K	L	I	L	L	M	E	L	M	N	V	D
JNK2 α	Q	V	A	K	L	I	L	L	M	E	L	M	N	V	D
ERK-2	Y	V	A	K	L	I	I	I	Q	D	L	M	N	L	D
cAPK	F	V	A	K	L	V	L	L	M	E	Y	V	N	L	D

Bold residues represent amino acids different from those in p38 α . Sequence differences at the primary level are most prominent at residues 106, 107, 108, and 157. Even though residue 109 is highly conserved, it has been suggested that Met109 is a key contributor to inhibitor specificity. Site-direct mutagenesis studies [44] show that mutation of Ala157 in p38 α caused diaryl-imidazoles to be more potent as compared to wild-type p38.

Lisnock *et al.* [44] showed that mutation of Thr106 to Gln, the residue present at the corresponding position in ERK-2, or Met, the corresponding residue in p38 γ , p38 δ , and JNKs, renders the inhibitor ineffective. Thr106 orients the drug to interact with His107 and Leu108 of the ATP binding pocket. Substitution of Thr106, alone or in combination with His107 or Leu108, with the corresponding, more bulky residues from p38 γ or p38 δ (Met, and Pro or Phe, respectively, in both cases) abolishes SB203580 binding. Conversely, if the amino acid of p38 γ , p38 δ , or even SAPK γ (which corresponds to p38 α) Thr106 is replaced with Thr, the resulting mutants display at least partial sensitivity to SB203580 [43, 46].

In addition to the interaction with Thr106, the binding mode of SB203580 shares a common set of features with various described pyridin-4-yl-imidazole derivatives: notably, the formation of a hydrogen bond between the backbone NH group of Met109 in the linker region and the 4-pyridine nitrogen atom of the inhibitor (Figure 9.6) [17, 19, 41]. As observed with various inhibitors of p38 MAP kinase [47, 48], replacement of the pyridin-4-yl moiety with a pyridin-3-yl ring results in a 500-fold decrease in the inhibition of cytokine release. This loss of potency could be explained by an unfavorable geometry of the pivotal hydrogen bond with Met109, thus underscoring the crucial importance of this pyridine ring for biological activity. Furthermore, according to Lisnock's data [44], mutation of Met109 to Ala caused the inhibitor to be less potent compared to wild-type p38. Still open to debate is the relevance of the hydrogen bond between N3 of the imidazole ring and Lys53 of p38 MAP kinase. Although several studies indicate the imidazole as a critical determinant for the binding of pyridinyl-imidazoles to p38 MAP kinase [2, 17, 41, 43], some authors [29, 43, 49] suggest a sole role for the imidazole as a scaffold for positioning the fluorophenyl and pyridine rings.

For ATP-competitive inhibitors to show *in vivo* efficacy, they must maintain their bioactivity in the presence of millimolar levels of ATP [22–24]. To understand how exactly this is accomplished, several studies were undertaken [50]. Crystallographic and kinetic experiments have shown that all pyridinyl-imidazole p38 inhibitors bind at the ATP binding site of p38 and compete with ATP for binding to active, phosphorylated p38. In crystal structures of kinases solved with bound ATP, the N-terminal and the C-terminal domains work together to form a catalytic pocket capable of binding all substrates in the proper orientation. In the crystal structure of inactivated p38, however, the two domains of the kinase are misaligned, suggesting that ATP cannot bind to inactivated p38. It has also been shown that p38 inhibitors like SB203580 bind equally well to both the activated and the inactivated forms of the enzyme. Therefore, when p38 is in its inactivated form, ATP is noncompetitive with those inhibitors. This fact leads to a thermodynamic advantage for the inhibitor *in vivo*, where the high ATP concentration would require very high inhibitor concentrations to effectively compete with ATP. Experimental data suggest a mechanism by which a kinase inhibitor that competes with ATP can function *in vivo* at concentrations approximately equal to its value of K_i (see also Chapter 1). The inhibitor may bind to a form of the enzyme that is inaccessible to ATP and thereby prevents the enzyme's transformation into its ATP accessible form.

SB203580 is a reasonably selective and cell permeable inhibitor that inhibits p38 α kinase activity *in vitro* with an IC_{50} of 50 nM against 100 μ M ATP. Using

SB203580, several SAR studies leading to selectivity and potency improvements and novel p38 chemotypes discovery programs have been undertaken and recently reviewed [51–53].

The development of SB203580, and of first-generation p38 inhibitors in general, into anti-inflammatory drugs was obstructed by its severe liver toxicity, as the pyridinyl-imidazoles were found to interact with hepatic cytochrome P450 (CYP450) enzymes involved in drug metabolism [54]. It remains unclear whether this unwanted side effect is caused by the pyridine or the imidazole ring. Strategies to dissect inhibition of p38 from interference with cytochrome P450 have included the replacement of the pyridine ring with other hydrogen-bond acceptors [54, 55], the introduction of sterically demanding substituents at the 2-position of the pyridine ring [55, 56], the introduction of substituents at the imidazole ring nitrogen adjacent to the pyridine ring [55, 56], and the replacement of the imidazole ring with other five- or six-membered heterocycles [48, 49, 57–59].

9.6

N-Substituted Imidazole Inhibitors

In addition to 2,4,5-triaryl-imidazoles, well represented by SB203580, the group at GlaxoSmithKline (GSK) has also prepared a vast number of 1,4,5-substituted imidazole inhibitors of p38 MAP kinase and cytokine release [47, 60]. Originally, it had been observed with bicyclic imidazoles such as SKF86002 and its analogues that the correct regiochemistry at the core heterocycle is crucial for efficient binding to p38 (Figure 9.8) [60]. For various N-substituted imidazole inhibitors of p38 it was confirmed that only at the imidazole ring nitrogen adjacent to the pyridine ring are substituents tolerated without loss of activity [47, 55, 60]. Initially N-substituted imidazoles were mainly prepared to reduce interaction with CYP450 enzymes; however, appropriate substituents at this position were found to contribute to enhanced p38 α binding [42, 61] and oral anticytokine activity [61].

Boehm and Gallagher have reported that N-substituted pyridinyl-imidazoles bind to p38 MAP kinase with generally lower affinity than their N-unsubstituted counterparts [47, 60] (Figure 9.9). The lower binding affinity also translated into weaker inhibition of IL-1 β release from PBMC (peripheral blood mononuclear cells), although the more potent compounds (i.e., SB216995 and SB210313) still displayed anti-TNF- α activity *in vivo*.

SB210313, furthermore, interferes slightly less with most of the CYP450 enzymes than either SKF86002 or SB203580 [54] (Table 9.3).

The basic piperidine substituent of SB235699 = VK19911 = HEP689) [42] interacts with Asp168 of p38 MAP kinase, and this additional interaction may account for the outstanding bioactivity observed for SB235699 compared to other N-substituted pyridinyl-imidazoles (Figure 9.9).

Several groups have investigated the properties of this compound. Vertex investigators have reported the cocrystallization of p38 MAP kinase with SB235699 [42]. GSK and Leo Pharmaceuticals have jointly developed SB235699 as a topical anti-

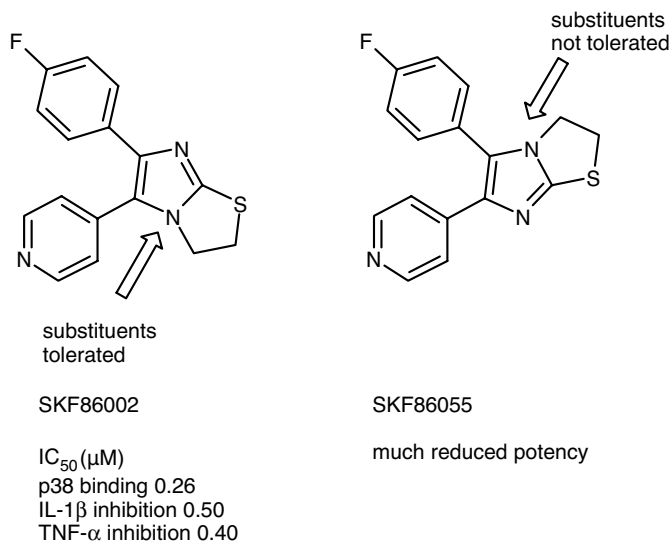


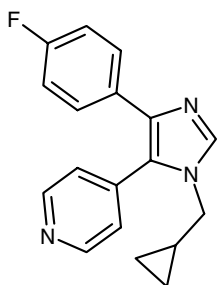
Figure 9.8 The correct regiochemistry is required at the imidazole nucleus for bioactivity of SKF86002.

inflammatory agent and have advanced this drug candidate into Phase I clinical trials for the treatment of psoriasis, contact eczema, and atopic dermatitis.

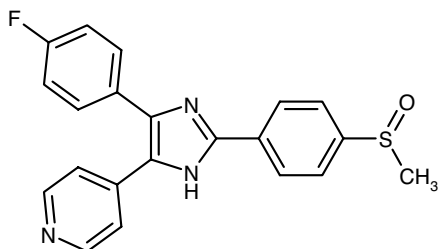
Several groups have undertaken studies on other N-substituted pyridinyl-imidazoles. A series of piperidin-4-yl-imidazoles and N-methylpiperidinyl-imidazole were realized by researchers at Smith-Kline Beecham [61]; those investigations showed that substitution on the 2-aminopyrimidine nitrogen in some cases reduced p38 inhibition, but simultaneously improved oral activity. The 2-alkoxypyrimidine SB242235 [62] (Figure 9.10) has been used as a pharmacological tool in various models of inflammation and it was selected as a clinical development candidate.

Studies probing substituents at the N1-position to enhance inhibitory effects on p38 MAPK and to minimize its interference with the CYP450 pathway were undertaken at the University of Tübingen [40]. In a previous work [39], the authors reported the identification of a methylsulfanyl residue as a favorable substituent at the imidazole C2-position. This group contributes low steric hindrance, thus allowing deep penetration of the inhibitor into the ATP pocket and thereby leading to tighter binding. Novel substituents at the N1-position were combined with the optimized C2 residue, leading to the identification of a methoxyethyl moiety as the optimal N1 substituent. This methoxyethyl group is assumed to build a hydrogen bond to Asp168, yielding an inhibitor that combines significantly decreased CYP450 interference and highly efficient inhibition of p38 MAPK activity regardless of its C2 substituent (Figure 9.11).

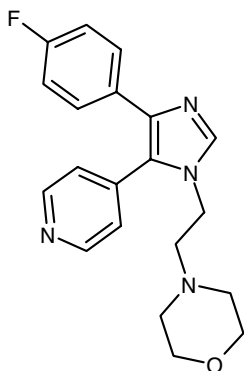
Beside SB242235 and SB235699, another N-substituted imidazole is at present in clinical development: RWJ67657. Workers at the R.W. Johnson Pharmaceutical Research Institute investigated the binding kinetics to p38 in a series of 1,2,4,5-tetrasubstituted imidazoles exemplified by the above-mentioned RWJ67657 and

**SB216995**

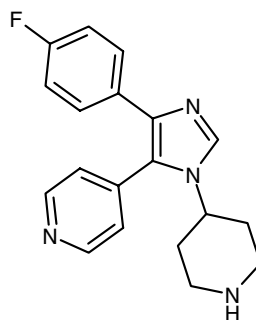
p38 binding $IC_{50}(\mu M)$: 0.09
 p38 inhibition $IC_{50}(\mu M)$: 0.16
 IL-1 β $IC_{50}(\mu M)$: nd¹

**SB203580**

p38 binding $IC_{50}(\mu M)$: 0.042
 p38 inhibition $IC_{50}(\mu M)$: 0.074
 IL-1 β $IC_{50}(\mu M)$: 0.08

**SB210313**

p38 binding $IC_{50}(\mu M)$: 0.12
 p38 inhibition $IC_{50}(\mu M)$: 1.3
 IL-1 β $IC_{50}(\mu M)$: 0.60

**SB235699**

p38 inhibition $IC_{50}(\mu M)$: 0.060
 p38 binding $IC_{50}(\mu M)$: nd¹
 IL-1 β $IC_{50}(\mu M)$: nd¹

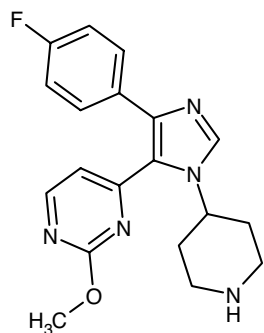
Figure 9.9 N-substituted pyridinyl-imidazoles: SB216995, SB235699, and SB210313; nd¹ not determined.

RWJ67671 [63]. For these compounds, the same rank order of potency was found in the isolated p38 α assay and in the cell-based TNF- α release assay (Table 9.4). The weaker binding inhibitors (cf. RWJ67671) differ from the more potent ones, such as RWJ67657 and SB203580, mostly in their association rates. The difference between the most potent inhibitors, in turn, is determined by their dissociation rate (RWJ67657 versus SB203580), that is, the strength of protein–inhibitor interactions. Interestingly, the binding characteristics of ATP are similar to those of the weak inhibitors. With regard to the correlation between K_d and IC_{50} values in the cell-based assay, the authors conclude that these imidazoles bind to the unactivated form of the

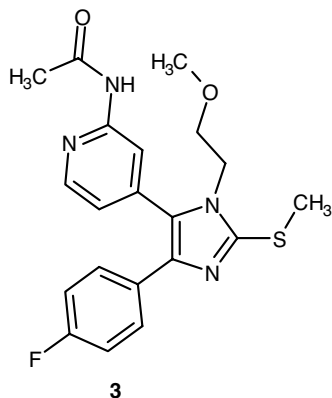
Table 9.3 Reduced inhibition of human CYP450 isoforms by the N1-substituted pyridinyl-imidazole SB210313.

Code	Inhibition of CYP450 isoforms (%) ^{a)}				
	1A2	2C9	2C19	3A4	2D6
SKF86002	85	80	64	19	22
SB203580	61	75	85	61	67
SB210313	<50	<50	<50	<50	86

a) Inhibition (%) of CYP450 isoforms at test compound concentration of 10 μ M.

**SB242235**

p38 inhibition IC_{50} (μ M): 0.019

Figure 9.10 Structure of SB242235.

p38 inhibition IC_{50} (μ M): 0.205

Relative potency (IC_{50} SB203580/ IC_{50} test compound): 2.2

Figure 9.11 Experimental compound and p38 inhibition data.

Table 9.4 Binding kinetics of SB203580, ATP, and 1,2,4,5-tetrasubstituted imidazoles developed at R.W. Johnson Pharmaceutical Research Institute.

		IC ₅₀ (nM)		K _d (s ⁻¹) ^c	K _a (m ⁻¹ · s ⁻¹) ^d	K _d (nM) ^e
Code	R	p38α ^a	TNF-α ^b			
SB203580	na	79 ± 12	23 ± 1	0.017	8.05 × 10 ⁵	21
RWJ67657	CH ₂ OH	30 ± 3	3.2 ± 0.1	0.003	7.12 × 10 ⁵	5
RWJ67671	C ₅ H ₁₁	1700 ± 222	81 ± 6	0.010	1.09 × 10 ⁵	89
ATP	na	na	na	0.016	1.24 × 10 ⁴	1280

a) Inhibition of activated p38α MAP kinase.

b) Inhibition of LPS-stimulated TNF-α release from human PBMC.

c) Dissociation rate.

d) Association rate.

e) Dissociation constant.

na: not applicable.

enzyme. ATP, on the other hand, has only weak affinity for unactivated p38 [63], and this crucial difference may explain why inhibitors binding in the ATP cleft of p38 are able to maintain their efficacy in cell-based assays. The pharmacology of RWJ67657 as the most potent inhibitor from this series was further evaluated and the compound was advanced into early clinical trials with indications as an antiarthritic drug and agent for inflammatory bowel disease [64].

9.7

N,N'-Diaryllurea-Based Inhibitors: BIRB796

Research groups at Vertex [65, 66], Bayer, and Boehringer have independently described N,N'-diaryllureas as inhibitors of p38 induced cytokine release [67–69]. While binding to the ATP cleft of p38, inhibitors of this class adopt a binding mode distinct from that of both the ATP-competitive and the diaryl heterocycles-based inhibitors.

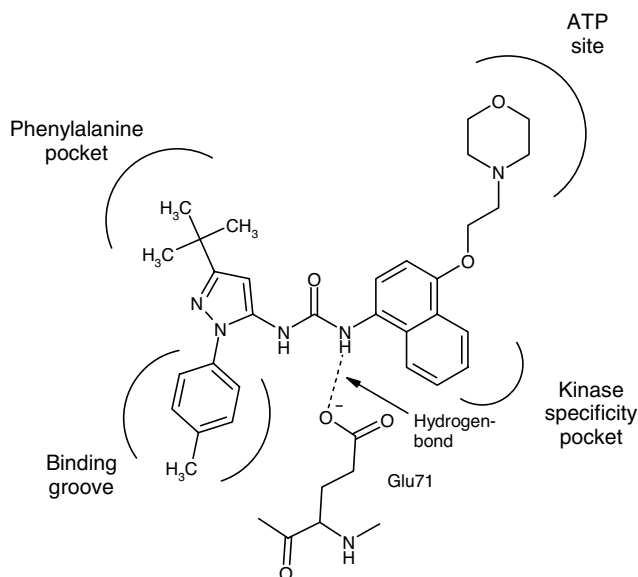


Figure 9.12 Structure of BIRB796 and its main interaction with p38 α .

The group at Boehringer has demonstrated that the potent *N*-aryl-*N'*-pyrazolylurea BIRB796 (Figure 9.12) stabilizes a conformation of p38 that cannot be accessed by ATP; the compound was originally described as allosteric modulator of p38 α , even though it occupies partially the ATP binding site.

Upon binding of BIRB796 to p38, a considerable conformational change takes place in the conserved Asp168/Phe169/Gly170 (DFG) region. The switch from the “DFG-in” to the “DFG-out” conformation arranges the side chain of Phe169 in a way that leads to a steric clash with the phosphate groups of ATP. At the same time, a large hydrophobic pocket is revealed, which is capable of accommodating the *tert*-butyl group characteristic for potent *N,N'*-diarylurea inhibitors. The tolyl substituent on the pyrazole ring has favorable interactions with the hydrophobic portions of the side chain of the conserved Glu 71 in helix α C. This tolyl group also causes a conformational change in the Glu 71 side chain such that only one of the urea NH groups can form a hydrogen bond with this residue (Figure 9.12). As previously pointed out, it has been speculated that this conformational rearrangement of the protein is the rate determining step responsible for the slow binding kinetic observed for these allosteric p38 inhibitors. The morpholino ether oxygen makes a hydrogen bond with the backbone NH of residue 109, equivalent to that made by the N1 atom of the adenine base of ATP. In addition to establishing interactions in the ATP pocket, the morpholino group also improves the physicochemical properties of the otherwise lipophilic inhibitor [67].

BIRB796 is in development by Boehringer Ingelheim as a treatment for rheumatoid arthritis and other inflammatory conditions such as Crohn's Disease and psoriasis. BIRB796 has a picomolar affinity for p38 α ($K_d = 0.1$ nM) and inhibits the enzyme with an $IC_{50} = 63$ nM.

By September 2001, the *in vivo* effects of BIRB796 on neutrophil activation had been tested in Phase I clinical trials. In a single-escalating dose, randomized, placebo-controlled, double-blind, 64-patient trial, BIRB796 was well tolerated at all dosages.

In 2001, a randomized, parallel-group, double-blind, placebo-controlled study into the efficacy and the safety of different doses (5, 10, 20, and 30 mg) of BIRB796, taken orally twice daily during 4 weeks in patients with active rheumatoid arthritis in whom at least one DMARD has not been effective was initiated. A potentially dose-limiting side effect, liver transaminase values above the upper limit of normal, has been reported.

9.8

Structurally Diverse Clinical Candidates

Apart from the imidazole nucleus, a multitude of other monocyclic and fused heterocycles was employed as scaffolds for the essential diaryl pharmacophore. The trisubstituted pyrazole developed at Pfizer, SD06 (Table 9.5, Figure 9.13), is an example. Pfizer recently presented data [70] on the synthesis and the development of this orally active p38 inhibitor. The compound exhibits significant functional selectivity for p38 α (IC_{50} = 80 nM) over p38 β (IC_{50} = 26.000 nM). The binding modus of SD06 has been described. As the substituent at the 3-position of the pyrazole ring approaches the ATP binding site of p38 kinase, a hydrophobic cavity in the p38 kinase develops around the 3-position substituent at the binding site. This hydrophobic cavity is believed to form as the 3-position substituent binds to a specific peptide sequence of the enzyme. In particular, it is believed to bind to the side chains of Lys52, Glu59, Leu73, Ile82, Leu84, Leu101, and the methyl group of the Thr103 side chain of p38 kinase at the ATP binding site. The pyrimidine ring at the 4-position of the pyrazole ring, as already described for diaryl-imidazoles, brings a suitable hydrogen-bond acceptor functionality. This acceptor bonds to the backbone N–H of the Met106 residue while one edge of this substituent is in contact with bulk solvent. SD06 had been reported to bind to phosphorylated as well as unphosphorylated p38 α (using surface plasmon resonance technology). SD06 inhibits LPS-stimulated TNF- α production in hWB *in vitro* with an IC_{50} of 1.5 μ M. The compound showed efficacy in a number of arthritis animal models (reduction of paw swelling, bone destruction, and cytokine suppression) [71]. In a 3-month toxicity study, SD06 showed no adverse CNS effects in monkeys and rats, despite its ability to cross the blood/brain barrier. Some adverse effects were observed on the skin and in the gastrointestinal tract with prolonged dosing *in vivo*. Pfizer advanced SD06 to Phase I clinical studies and pharmacodynamic effects were reported in a human *ex vivo* model with an EC_{50} value = 50.6 nM for inhibition of LPS-induced TNF- α production, corresponding to an ED_{50} = 11.3 mg. Currently, SD06 is being tested for its anti-TNF- α activity in Phase I clinical trials in healthy volunteers following endotoxin challenge [70].

RO3201195 (Table 9.5, Figure 9.13) is a pyrazole ketone developed at Roche by applying a high-throughput screening (HTS) approach to develop multiple leads

Table 9.5 p38 MAPK inhibitors in clinical development.

Drug name	Therapeutic group	Mechanism of action	Organization
SB242235	Antiarthritic drugs	p38 MAPK inhibitor	GlaxoSmithKline (originator)
RWJ67657	Antiarthritic drugs; Agent for IBD	IL-1 β , TNF- α production inhibitor; p38 MAPK inhibitor	R.W. Johnson (originator)
SB235699	Antipsoriatics; Agent for Atopic dermatitis; Anti-inflammatory agents	p38 MAPK inhibitor	GlaxoSmithKline (originator) Leo
RO3201195	Treatment of RA	IL-1 β , IL-6, TNF- α production inhibitor, p38 MAPK inhibitor	Roche (originator)
SB281832	Antiallergy/asthmatic drugs; Agent for IBD; Treatment of RA	p38 MAPK inhibitor	GlaxoSmithKline (originator)
SCIO323	Antiarthritic drugs	p38 MAPK inhibitor	Scios (originator)
AMG-548	Antiarthritic drugs	TNF- α production inhibitor, p38 MAPK inhibitor	Amgen (originator)
EO1606	Acne therapy; Agent for atopic dermatitis	p38 MAPK inhibitor	Leo (originator)
SD06	Antiarthritic drugs	p38 α MAPK inhibitor	Pfizer (originator)
PS540446	Treatment of RA	p38 MAPK inhibitor	Bristol-Myers Squibb (originator)
KC706	Antipsoriatics; Treatment of RA	p38 MAPK inhibitor	Kemia (originator)
SB203580	Antiarthritic drugs; Agent for IBD	Calcium channel activators stress-activated protein (SAP/Jun) kinase inhibitor. p38 MAPK inhibitor	GlaxoSmithKline (originator)
VX-745	Myelodysplastic syndrome therapy; Treatment of RA	p38 MAPK inhibitor	Kissei Vertex (originator)
CPI1189	Treatment of AIDS, dementia, Alzheimer's dementia, cognition disorders, and neuropathic pain	Antioxidants apoptosis inhibitor; p38 MAPK inhibitor	Centaur (originator) Renovis
BIRB-796 Doramapimod	Antipsoriatics; Agent for IBD; Treatment of RA	p38 MAPK inhibitor	Boehringer Ingelheim (originator) (Continued)

Table 9.5 (Continued)

Drug name	Therapeutic group	Mechanism of action	Organization
SCIO469 Talmapimod	Multiple myeloma; Myelodysplastic syndrome therapy; Treatment of RA	p38 MAPK inhibitor	Scios (originator)
VX-702	Agent for IBD; Treatment of OA, RA, disorders of the coronary arteries, and atherosclerosis	p38 MAPK inhibitor	Kissei Vertex (originator)
SB681323 Dilmapimod	Atherosclerosis therapy; treatment of COPD and RA	p38 MAPK inhibitor	GlaxoSmithKline (originator)
SB856553 Losmapimod	Atherosclerosis therapy; treatment of COPD, RA, and psychiatric disorders	p38 α MAPK inhibitor	GlaxoSmithKline (originator)
GSK610677	COPD	p38 MAPK inhibitor (inhaled)	GlaxoSmithKline (originator)
TAK715	Treatment of RA	TNF- α production inhibitor; p38 α MAPK inhibitor	Takeda (originator)
RO4402257 Pamapimod	Treatment of RA	p38 MAPK inhibitor	Roche (originator)

series from distinct scaffolds. This HTS campaign led to the identification of several pyrazole ketones that were found to inhibit p38 α at low micromolar concentrations. Cocrystallization of RO3201195 with unphosphorylated p38 α revealed a novel binding motif in the ATP binding site that was previously unknown for p38 kinase inhibitors [72]. Particularly, two hydrogen bonds formed between the amine of the inhibitor and the backbone His107 and with the side chain hydroxyl group of Thr106. The latter residue is present in approximately 205 of human kinases and according to the authors an inhibitor with the potential to form a hydrogen bond to Thr106 would confer improved selectivity versus other kinases that lack this residue. In addition, the pyrazole ketones make a hydrogen bond between the benzoyl oxygen and the Met109 backbone NH. This key interaction is observed in all reported structures of ATP-competitive p38 inhibitors. Additional binding energy is generated by the position of the *N*-phenyl ring into the hydrophobic pocket, which is partially defined by the specificity residue Thr106. The glycerol monoether group attached to the meta position of the benzoyl ring of RO3201195 confers good physicochemical properties (solubility and oral bioavailability) while retaining potency against p38 and also affords good inhibition of LPS induced cytokine production in undiluted human whole blood, and efficacy in *in vivo* inflammation models. RO3201195 inhibits p38 with an IC₅₀ = 700 nM. RO3201195 binds to p38 α (both the nonphosphorylated

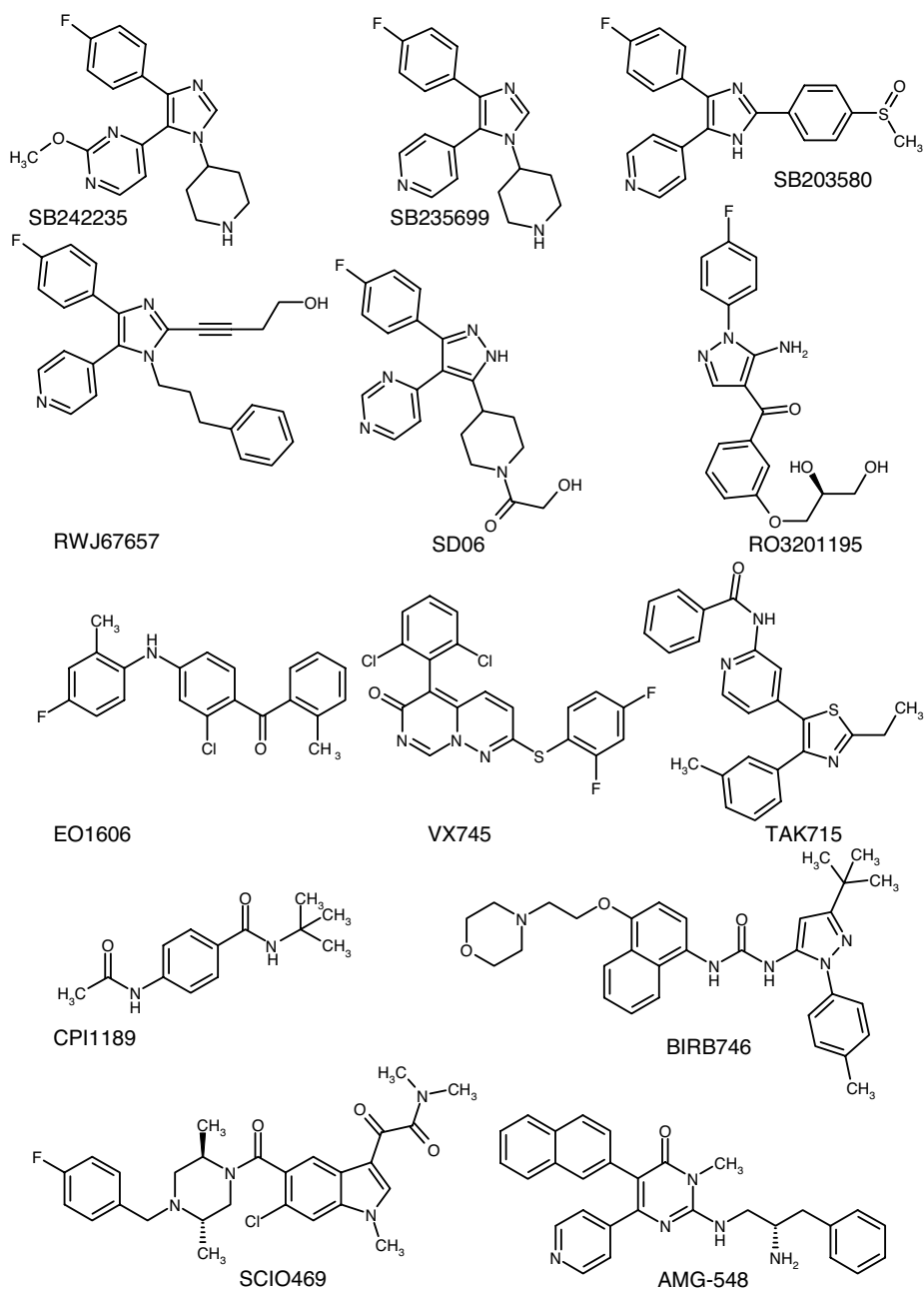


Figure 9.13 Structures of p38 MAPK Inhibitors in clinical development.

and the Thr180 and Tyr182 phosphorylated) and p38 β -isoforms but does not bind to the p38 γ - or the p38 δ -isoform. Based on the range of efficacy in the biological models, the desirable metabolic profile, and the favorable preclinical safety pharmacology, RO3201195 was selected as a clinical candidate for the treatment of rheumatoid arthritis.

AMG-548 [73] (Table 9.5, Figure 9.13), in clinical development as an antiarthritic drug, contains the classical SB203580 diaryl interaction while changing the core heterocycle to a six-membered ring. AMG-548 was in Phase I human trials and data supporting the advancement of this compound has been presented. The pyridinone inhibitor interacts with p38 α through the classical Met109-pyridine hydrogen bond. The C2 carbonyl and Lys53 also form a hydrogen bond. Preclinical data showed that AMG-548 is efficacious in both acute (LPS-induced TNF- α production in mice) and chronic (CIA and adjuvant induced-arthritis (AdA) in Lewis rats) models of arthritis. In these *in vivo* models, AMG-548 ameliorated acute production of pro-inflammatory cytokines (ED₅₀ = 0.5 mg/kg) and inhibited the symptomatic and structural manifestations of severe joint destruction in CIA and also AdA. Pharmacokinetic evaluation in both rat and dog revealed good terminal half-life ($t_{1/2}$) and suitable oral bioavailability for once-daily oral dosing in humans. Evaluation in 14-day rodent toxicology studies and dog QTc studies demonstrated the desired safety multiples with no QTc prolongation in dogs. Based on overall profile of AMG-548, the molecule was advanced to safety assessment and subsequently to Phase I clinical trials. AMG-548 was the first internal small-molecule clinical candidate for Amgen and it progressed from clinical candidate portal to first-in-human (FIH) dosing in less than 1 year. In the FIH study, AMG-548 was dosed orally at 0.3–300 mg (once daily). AMG-548 had linear pharmacokinetics with a mean terminal elimination $t_{1/2}$ of 24 h. The compound demonstrated 30–95% inhibition of *ex vivo* whole blood LPS-induced TNF- α and IL-1 β cytokine production at oral doses of 3, 10, 30, 60, 100, and 300 mg (once daily) in healthy male volunteers. At doses of 60–300 mg, >85% inhibition was observed beyond 24 h, following a single oral dose. These data demonstrate that AMG-548 possesses suitable pharmacodynamics/pharmacokinetics for once-daily oral dosing. AMG-548 was further evaluated in a 14-day multiple dose study in 54 healthy male volunteers. Isolated liver enzyme elevations were observed in nine out of 54 individuals randomized to AMG-548, and one out of 18 individuals randomized to placebo. These hepatic transaminase levels were not associated with increases in bilirubin or alkaline phosphatase. Further development of AMG-548 was suspended due to random liver enzyme elevations that were not dose dependent or exposure dependent.

In March 2005, Takeda reported the discovery of TAK715 (Table 9.5, Figure 9.13) as a potent and orally active antirheumatic agent [74, 75]. The thiazole-benzamide was shown to selectively inhibit p38 α (IC₅₀ = 7.1 nM) and block LPS-induced TNF- α production in THP-1 cells (human monocytic cell line) (IC₅₀ = 48 nM). In an *in vivo* model of acute inflammation in mice, TAK715 inhibited the LPS-induced release of TNF- α by 88% after a 10 mg/kg oral dose. It is reported that the compound has been advanced into Phase II clinical trials. However, TAK715 did not progress to a later development status because it did not meet internal development criteria [76].

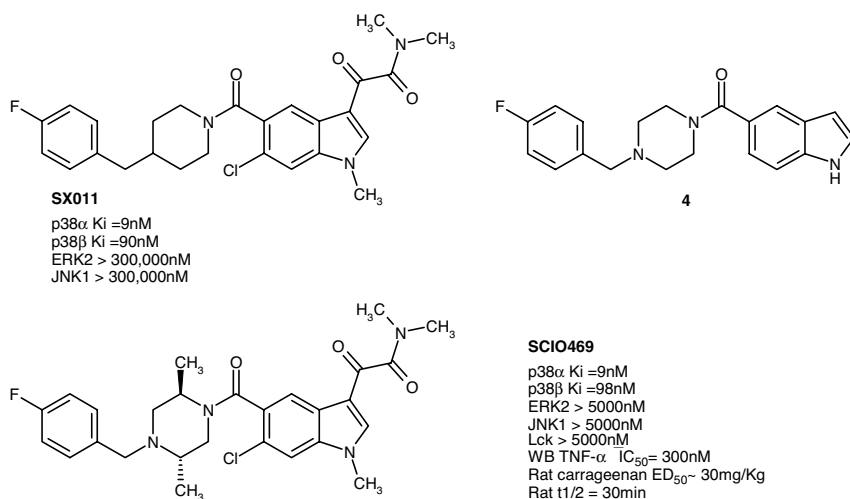


Figure 9.14 Scios compounds. SX011, compound 4, SCIO469.

Scios (a subsidiary of Johnson & Johnson) is developing a series of small-molecule, orally available, p38 inhibitors. Recently, the structure of Talmapimod (SCIO469) (Table 9.5, Figure 9.13) was disclosed revealing that this molecule belongs to a class of indole amides explored by the company in a p38 inhibitors development program started from an HTS hit: an indole carboxamide derivative (**4**, Figure 9.14), with weak inhibitory activity for p38 α [77]. As shown by data of SCIO469 and SX011 (Figure 9.14), substitutions at the 3-position of both the indole and the piperazine ring improved potency dramatically. The carbonyl amide forms the crucial hydrogen bond with NH of Met109 while the polar α -keto amide moiety extends toward solvent, allowing the 6-Cl-indole and the *F*-phenyl moieties to bind into lipophilic pockets. SCIO469 is highly potent against p38 α and p38 β (Figure 9.14), blocking the LPS-induced release of TNF- α from human whole blood, and inhibiting LPS-induced IL-1 β release from human PBMCs in a dose-dependent manner.

A Phase I study investigated the safety, pharmacodynamics, and pharmacokinetics of single ascending oral solution doses from 0.03 to 5 mg/kg SCIO469 in healthy volunteers. The compound was safe and well tolerated, the only reported side effect being mild, transient light-headedness at highest doses, which suggests that SCIO469 crosses the blood/brain barrier. By October 2004, a Phase II study to determine the analgesic efficacy of SCIO469 in acute post-surgical dental pain had also been completed. All SCIO469 treated patients showed a significantly longer time to rescue medication compared with placebo. This study represents the first clinical demonstration of acute analgesic effects by inhibition of p38.

Scios is the first company to disclose clinical exploration of p38 inhibitors in multiple myeloma (MM). In 2004, Scios demonstrated the ability of SCIO469 to strongly reduce p38 phosphorylation in bone marrow stromal cells, and to inhibit the production of IL-6, VEGF, IL-1 β , receptor of activated NF- κ B ligand, and

prostaglandin E2. In combination with proteasome inhibitors, SCIO469 enhanced the reduction in multiple myeloma cell proliferation and potential proteasome inhibitor-induced apoptosis. SCIO469 is at present still under Phase II clinical investigation.

SCIO323 (Table 9.5), the backup candidate to SCIO469, is reported to be highly selective for p38 α with improved efficacy in an autoimmune model of RA, as compared with SCIO469. The structure of SCIO323 has not yet been published.

Vertex Pharmaceutical, Inc. was one of the first companies to disclose, in 2001, a non-pyridinyl-imidazole-based p38 inhibitor. VX-745 (Table 9.5, Figure 9.13), a first-generation p38 inhibitor, is potent against p38 α (IC₅₀ = 10 nM) and blocks the synthesis of TNF- α in human whole blood (IC₅₀ = 177 nM) and PBMCs (IC₅₀ = 56 nM) after LPS stimulation *in vitro*. The compound VX-745 binds to the ATP site of p38 α via a hydrogen bond with the NH of Met109 backbone, while the lipophilic “back pocket” is occupied by the difluorophenyl group [78]. VX-745 was shown to have anti-inflammatory activity in rodent models and to penetrate the blood/brain barrier. The compound was generally well tolerated with the most frequently reported adverse event being elevation in liver transaminases. No CNS side effects were seen in humans, however, the drug was subsequently suspended following the observation of neurological effects in dogs.

VX-702 (Table 9.5), the structure of which has not been disclosed yet, was chosen as a backup compound due to its inability to cross blood/brain barrier. A Phase I safety and pharmacokinetic study showed that VX-702 (2.5–80 mg) was well tolerated. In an *ex vivo* assay primed with LPS, VX-702 inhibited IL-6, IL-1 β , and TNF- α production (IC₅₀ = 59, 122, and 99 ng/ml, respectively). In a Phase IIa study completed in October 2004, VX-702 demonstrated safety and tolerability in patients with acute coronary syndrome (ACS) undergoing percutaneous coronary intervention (PCI). VX-702 significantly reduced serum levels of the inflammatory biomarker C-reactive protein (CRP) in patients undergoing PCI, and CRP remained significantly lowered out to 4 weeks beyond the 5-day dosing period.

In June 2005, Vertex announced initiation of a three-month, double-blinded, randomized, placebo-controlled, Phase II study to assess two doses of VX-702 in rheumatoid arthritis. The compound will be dosed once daily without concomitant methotrexate. In March 2006, in a press release, Vertex reported the results of this 12-week study in patients with moderate to severe RA ($n = 315$), which indicated that VX-702 (5 or 10 mg/kg) was well tolerated. Premature discontinuations for adverse events were low (2, 5 and 10% in the placebo, 5 and 10 mg groups, respectively). No significant effects were observed from liver function tests. Although the structure of VX-702 is not disclosed, a recent review states that VX-702, according to statements from Vertex, is structurally distinct from the earlier inhibitor VX-745. The author supposes that the WO2004072038 [79] covers the preparation of VX-702 and then the product case for VX-702 is likely to be WO09958502 [65] or WO00017175 [80, 81].

Ketone-based p38 inhibitors have been pursued by multiple companies. Leo Pharmaceuticals has explored aminobenzophenone p38 α inhibitors [82–84]. The aminobenzophenone EO1606 (Table 9.5, Figure 9.13) is a potent and selective inhibitor of p38 MAPK (isoforms α and β) and of the upstream kinase MKK6.

The compound was tested in an animal model of noninflammatory acne, the rhino mouse. Its efficacy in this model is comparable to that of the retinoids. The compound is at present in clinical development as agent for atopic dermatitis and acne therapy. The *in vivo* models tested were recently reviewed by Petersen [85]. Starting from Leo's benzophenone-type inhibitors, a rigidisation strategy leads to 3-amino-6,11-dihydro-dibenzo[*b,e*]thiepin-11-one, phenylamino-substituted 6,11-dihydro-dibenzo[*b,e*]oxepin-11-ones, and dibenzo[*a,d*]cyclohepten-5-ones at the University of Tübingen [86].

As reported in Table 9.5, additional compounds are undergoing clinical development. GlaxoSmithKline undertook clinical development of compounds such as SB610677 [87, 88] for which till July 2009 no structure has been disclosed. SB681323 and SB856553 (GW-856553X) meanwhile have got their USAN-names Dilmapi-mod and Losmapimod, respectively. Dilmapi-mod will be discussed together with the VX-745-like compounds below because of their similar SAR.

In 2006, GSK published a patent [89] where the company claims the synthesis and the polymorphs of a compound used to mediate p38 activity. The structure is shown in Figure 9.15 on the left side and belongs to a class of nicotinamides or biphenylamides that GSK had already patented earlier as p38 inhibitors [90]. GSK reports an IC_{50} of <50 nM in their TNF- α hWB assay [89]. Later SB856553 (GW-856553X, Losmapimod) (Figure 9.15) was patented and claimed as a p38 inhibitor for treating psychiatric disorders [91]. A further specification is available on clinicaltrials.org [88] where a Phase II study is referenced evaluating GW856553 for the treatment of major depressive disorder. Moreover, clinical trials are performed with this drug candidate for indications such as chronic obstructive pulmonary disease (COPD), rheumatoid arthritis, and atherosclerosis. A third member of this structural class is shown in the middle of Figure 9.15 and was patented as a single compound together with its synthesis [92]. It might be supposed that one of the structures without a code (Figure 9.15) belongs to SB610677 mentioned above and in the GSK-pipeline (February 2009) [87].

This class of biphenyl amides originally emerged from a research program focusing on the development of Lck kinase inhibitors where p38 α was just used as a crystallographic surrogate for Lck [93]. During a first synthetic optimization, compound 5 (Figure 9.16) was identified. With an IC_{50} = 1.5 μ M, it was already

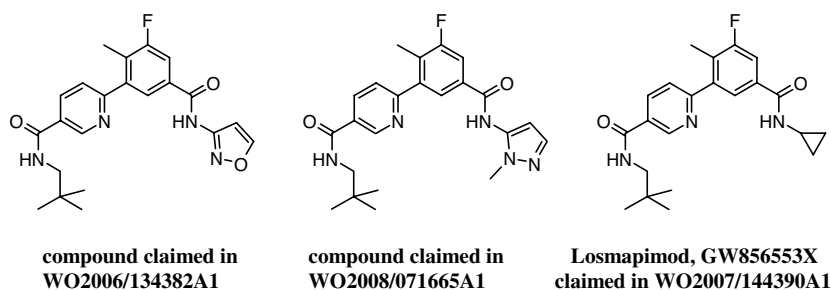


Figure 9.15 Structures of the GSK compounds claimed in several patents.

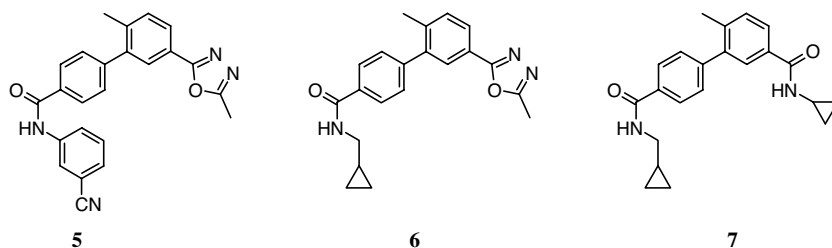


Figure 9.16 Structures of the GSK biphenyl amides.

selective against Lck ($IC_{50} > 16 \mu M$) and JNK ($IC_{50} > 16 \mu M$) [93]. Compound **6** is the result of a second optimization cycle and is a potent and selective inhibitor of p38 α ($IC_{50} = 1.5 \mu M$) with cellular activity, oral bioavailability and activity in an *in vivo* model of joint inflammation [94]. Replacement of the methyl-oxadiazole of compound **6** with a cyclopropylamide resulted in compound **7** (p38 α : $IC_{50} = 75 nM$) with greatly improved properties, including excellent cellular potency, pharmacokinetic properties, and oral activity [95].

Interestingly in the series of compound **7**, the analogues may bind to different conformations of p38 MAPK. Minor changes in substitution of the amide on the right side of the molecule determine whether p38 α is bound in the DFG-in or DFG-out conformation [96]. A binding mode with DFG-in conformation was proposed for the WO2006/134382A1 compound (Figures 9.15 and 9.17) when the compound was docked to the PDB 2BAL [97] crystal structure in our laboratory. The fluorophenyl moiety binds in the direction of hydrophobic pocket I (selectivity pocket) and the

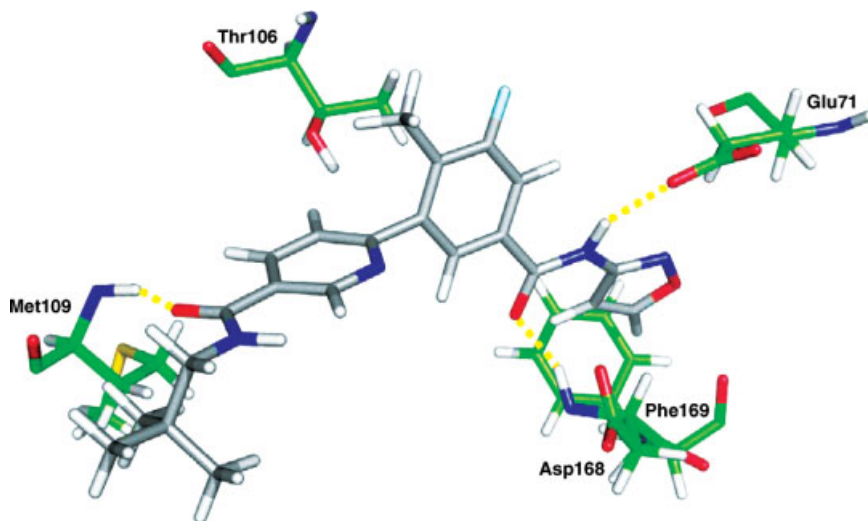


Figure 9.17 The biphenyl amide of WO2006/134382A1 docked to p38 using PDB 2BAL as a template.

amide carbonyl (neopentylamide) accepts an H-bond from backbone N–H of Met109. The compounds in Figure 9.16 are nicotinamides but the additional nitrogen probably is not needed for binding to the kinase. However, physicochemical properties might be improved with the additional nitrogen.

Also Centaur, Bristol-Myers Squibb, and Kemia are developing p38 kinase inhibitors that are being clinically evaluated. Due to the lack of specific information regarding the development status of those compounds, they have not been included in this chapter.

9.9

Medicinal Chemistry Approach on VX-745-Like Compounds

In the past 10 years, Merck developed a very interesting SAR that is illustrated in Figure 9.18, which led to compound **12**, a potent p38 MAP kinase inhibitor, with excellent potency in whole blood and much improved physicochemical properties [98, 99].

The Vertex compound VX-745 [100], which had proceeded in Phase II clinical trial in 1999, could be formally considered as starting point of the Merck SAR. VX-745 and its congeners are particularly interesting in the light of the unprecedented level of selectivity they exhibit for p38 α over a variety of other closely related kinases due to the specific binding mode (peptide flip of Gly110) discussed above. This unexpected

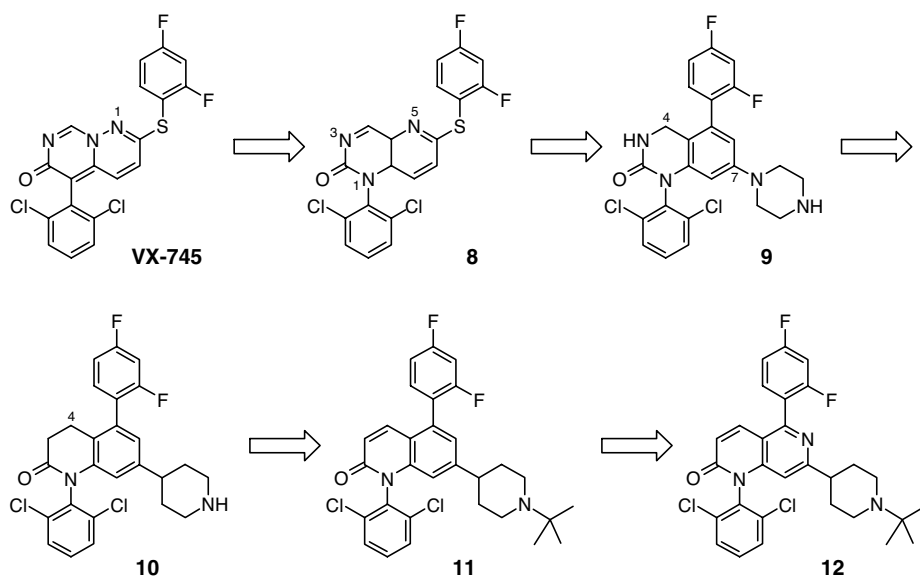


Figure 9.18 Medicinal Chemistry approach at Merck, which led to potent p38 inhibitors formally derived from a Vertex lead (VX-745) by analogue design.

selectivity shown by the Vertex class of inhibitors was the inspiration behind the development of the Merck SAR [101].

Substitution of the central pyrimido-pyridazinone core of VX-745 by the pyrido-pyrimidinone one in compound **8** (Figure 9.18) led to a class of less potent and functionally inactive analogs. The hydrogen-bonding capacity of the urea in compound **8** seemed to be weaker than in VX-745. Hence, the pyrido-pyrimidinone-based inhibitors were not viable at this stage [101]. Improvement was possible by simplification of the core as testified in compound **9**, which shows a more similar polarity to the Vertex compound by having the difluorophenyl moiety shifted, the sulfur omitted and the pyridine part substituted by a benzene ring. As outlined by the superposition of an early imidazole lead and dihydro-quinazolinone **9** (Figures 9.3 and 9.4), a piperazine moiety is most suitably added on C7 in order to derive additional potency by favorable hydrophobic interactions with the possibility of forming a salt bridge with proximal Asp168 [31, 101]. As reported by Stelmach [31], quinazolinone compounds of this class have nanomolar and subnanomolar IC₅₀ values in the p38 enzyme assay and are excellent inhibitors of TNF- α -production but their clearance is high and PK profiles poor. In contrast, in one compound of the series the piperazine was replaced by piperidine and a bulky *t*-butyl substituent added on the piperidine nitrogen, which resulted in compound with excellent p38 and TNF- α inhibition and a dramatically PK profile in the rat [31]. These structural features can be found as well in compounds **10–12**, respectively. Quinazolinone **9** (PDB entry: 1M7Q) and dihydro-quinolinone **10** (PDB entry: 1OVE) were cocrystallized with p38 MAP kinase to reveal a unique binding mode with the peptide flip and the double hydrogen bond formed between the C2 carbonyl and the backbone N–H moieties of Met109 and Gly110 [29].

Unfortunately, clearance of the quinazolinones (compound **9**) remained high, and PK profiles were poor in other animal species. Metabolic studies revealed the benzylic C4 and the two positions α to the piperidine nitrogen as metabolic “hot spots.” Replacement of the dihydro-quinazolinone core (compound **9**) with quinolinone (compound **11**) and naphthyridinone structures (compound **12**) eliminated the lability at the C4-position [30, 102]. The *tert*-butyl piperidines are particularly potent inhibitors of p38 activity and TNF- α release with excellent oral bioavailability in rat, dog, and rhesus monkey [102].

In 2006, Merck published a multikilogram 6-step synthesis [99] for naphthyridinone **12**, which replaced the early [98] 18-step synthesis. This suggests that compound **12** or one which is closely related may have progressed to an advanced development status.

The properties of compound **12** can be summarized as follows: The compound contains a naphthyridone core, which retained the desired selectivity [30, 99]. The higher selectivity of this compound can be explained by the induced peptide flip at the Gly110 [29]. The lipophilic *tert*-butyl piperidine moiety attached to the naphthyridone core greatly improves whole blood and *in vivo* activity. The *tert*-butyl group proved to be optimal for moderating rates of metabolism and improving pharmacokinetic properties [99, 102]. Furthermore, compound **12** shows excellent selectivity against other kinases [99].

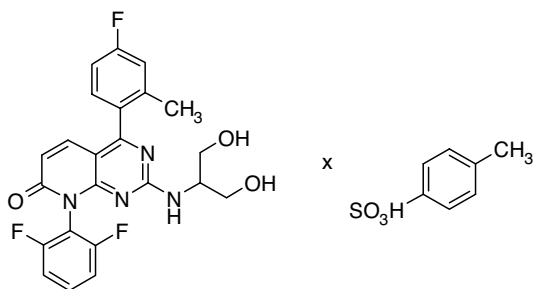


Figure 9.19 Dilmapimod tosylate claimed in WO2007/059500 A2.

Dilmapimod tosylate [103, 104] (SB681323 and GW-681323) (Figure 9.19) is a p38 MAP kinase inhibitor that is currently under development by GlaxoSmithKline. Several Phase I and Phase II clinical trials were performed with the compound or are currently underway for COPD, RA, neuropathic pain, and CHD (coronary heart disease) [88]. The synthesis for this pyrido[2,3-*d*]pyrimidin-7-one class of compounds was published [105] without Dilmapimod as an example and was optimized later [104, 106]. Four polymorphic forms of Dilmapimod tosylate are claimed. The naphthyridinone core of compound **12** (Figure 9.18) was replaced by a pyrido[2,3-*d*]pyrimidin-7-one in Dilmapimod, which means that only one nitrogen was added to the central heterocycle. The two phenyl moieties on the heterocycle were replaced by closely related bioisosteric analogues while the *t*-butyl piperidine was replaced with a more polar dihydroxy-isopropylamine. When comparing the $c \log P$ values of compound **12** ($c \log P = 6.83$) [107] and Dilmapimod ($c \log P = 3.72$) [107], the latter is obviously more in line with Lipinski's rules [108] (see also Chapter 1) and therefore more likely to show preferred ADME characteristics. The metabolic hot spot of the Merck compounds **9** and **10** (Figure 9.18) has been omitted in Dilmapimod as well. Nevertheless, Merck and GlaxoSmithKline are competing in a very narrow patent space.

The development of Roche's Phase II candidate Pamapimod started with lead structure **13** (Figure 9.20). The pyrimido-pyrimidine was discovered in a screening aiming to identify new structural templates for p38 α [109]. Compound **13** is also a potent inhibitor of Lck. Selectivity for p38 versus Lck was obtained by introducing a sp^3 center in α position to the exocyclic nitrogen (compound **14**) in order to inhibit coplanarity and to create unfavorable steric interactions between the inhibitor and Lck kinase. Compound **14** revealed high potency for p38 α ($IC_{50} = 40$ nM) while no longer binding to Lck occurs. Replacement of the pyrimido-pyrimidine core structure with a pyrido-pyrimidine in compound **15** provided for generally more potent structures in this series. Selectivity was improved with an oxygen linker to the difluorophenyl moiety that optimally filled the hydrophobic pocket (R1487). Pamapimod and R1487 are highly potent inhibitors in the enzyme assay with IC_{50} values of 14 and 10 nM, respectively. They showed high potency in the whole blood assay with IC_{50} values of 400 and 200 nM. Both compounds are highly selective, and they were therefore selected as clinical candidates [109, 110]. In a collagen-induced

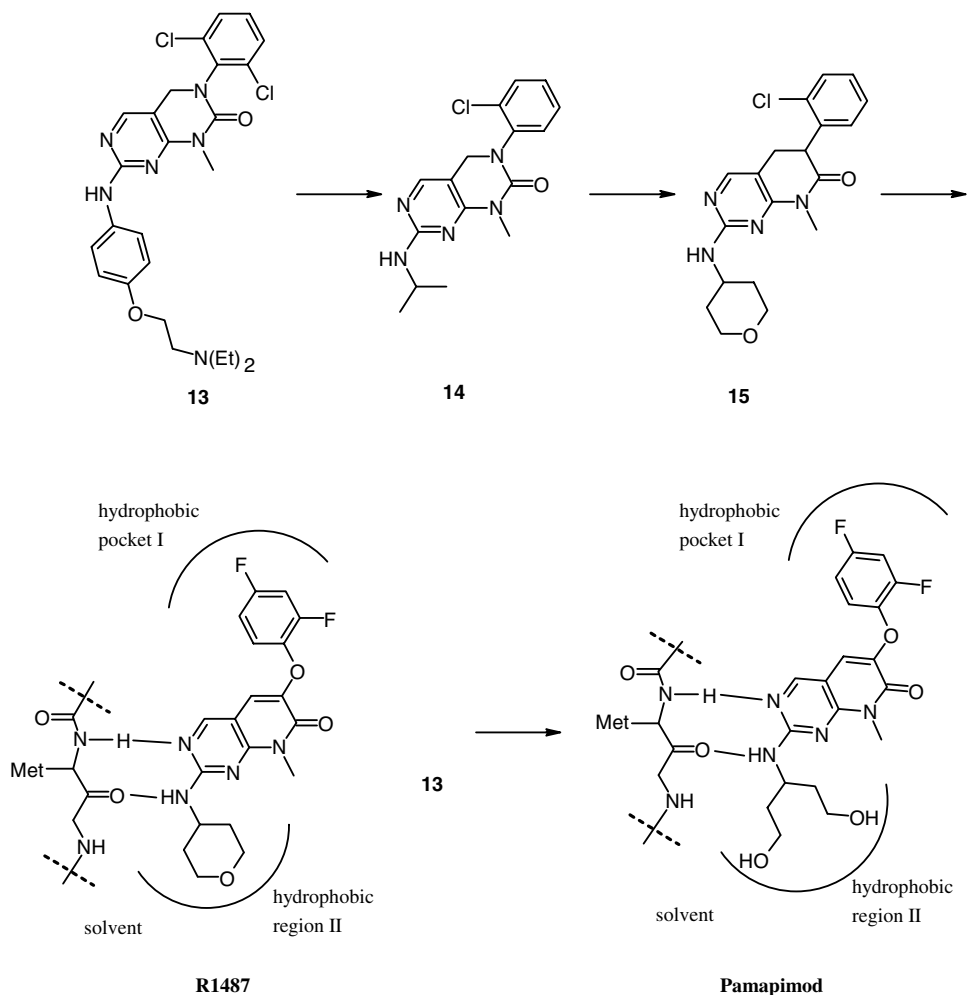


Figure 9.20 Development of Pamapimod.

arthritis model in mice, however, clinical scores were not significantly suppressed by Pamapimod up to a 100 mg/kg dose [110]. Recently published results from clinical Phase II studies showed Pamapimod to be inefficient in reducing clinical signs of RA [111]. Patients were treated 12 weeks either with methotrexate or with Pamapimod. At week 12, ACR20 response of the 300 mg group of Pamapimod was observed with fewer patients (31%) compared to the methotrexate group (45%). Similarly, a greater percentage of patients in the methotrexate group had an ACR50 response at week 12 (23%) compared to the 300 mg group of Pamapimod (13%). Also with the mean DAS28 (disease activity score in 28 joints), the greatest decrease was observed with the methotrexate group. Pamapimod was generally well tolerated, but the overall adverse events were more frequent in the treatment group of Pamapimod than in the

methotrexate group. The adverse events included infections, skin disorders, dizziness, and elevated liver enzymes. Pamapimod probably failed to show efficacy because a dose of 300 mg/day was presumably too low to result in efficacy. It was shown that efficacy observed with Pamapimod was dose dependent and that the best results were obtained with the highest dose of 300 mg/day. Due to the adverse events mentioned above, a higher dosage could not be tested. Side effects seen in the trial with Pamapimod were mainly ascribed to the inhibition of p38 α [111], thus indicating that any inhibitor of p38 α will be affected when applied with effective dosage. Side effects were indeed quite similar to that found in studies of many other compounds, and the important role of p38 MAP kinases in developmental, differentiation, and proliferative processes indicates that the inhibition of p38 MAP kinase might therefore entail several adverse effects. However, to date, it is difficult to predict potential adverse effects under conditions of partial inhibition of p38 activity [112]. Furthermore, the extent of adverse effects such as the degree of liver enzyme abnormalities, dizziness, and skin reactions clearly differs between compounds, and other inhibitors may therefore reveal better toxicity profiles. Perhaps one of the most intriguing results was that of the trend seen in the C-reactive protein (CRP) level. The initial decline in CRP in the 300-mg Pamapimod group was followed by a rapid return to baseline over a period of several weeks [111, 113].

9.10

Conclusion and Perspective for the Future

Some authors think that the era of optimism surrounding the use of p38 MAPK inhibition for the treatment of rheumatoid arthritis might be over [113]. Genovese states in his article that the most interesting science yet to be done will be that which yields a better understanding of why inhibition of p38 MAPK results in only a transient reduction in inflammation. He concludes that elucidating the cause of this phenomenon may yet help us understand how new classes of intracellular enzyme inhibitors may perform when they are evaluated in studies of inflammatory diseases [113].

On the other hand, MAP kinases remain attractive targets for a wide range of other inflammatory diseases despite the setbacks. They regulate the cytokines and other mediators that are known to participate in the pathogenic processes implicated in inflammation. The kinases are expressed at the sites of disease, and functional studies demonstrate that they are highly activated. Preclinical studies confirm remarkable efficacy when MAP kinases are inhibited. Hence, the rationale for MAP kinase blockade in humans is quite clear. Issues related to toxicity and limited efficacy have hampered drug development. A number of alternative strategies have been proposed to overcome some of these problems, including development of allosteric inhibitors or drugs that target other kinases in the cascade. Although the optimism of a few years ago must be tempered, there is still considerable evidence that targeting this signal transduction pathway will offer novel treatment to patients with inflammatory- and immune-mediated diseases [114].

Acknowledgments

The authors would like to thank Verena Schattel for molecular modeling and Solveigh Karcher for discussion of the Pamapimod SAR.

References

- Manning, A.M. and Davis, R.J. (2003) *Nature Reviews. Drug Discovery*, **2**, 554–565.
- Kumar, S., Boehm, J., and Lee, J.C. (2003) *Nature Reviews. Drug Discovery*, **2**, 717–726.
- Griswold, D.E. and Young, P.R. (1996) *Pharmacology Communications*, **7**, 323–329.
- Han, J. et al. (1994) *Science*, **265**, 808–811.
- Lee, J.C. et al. (1994) *Nature*, **372**, 739–746.
- Rouse, J. et al. (1994) *Cell*, **78**, 1027–1037.
- Jiang, Y. et al. (1996) *The Journal of Biological Chemistry*, **271**, 17920–17926.
- Goedert, M. et al. (1997) *The EMBO Journal*, **16**, 3563–3571.
- Kumar, S. et al. (1997) *Biochemical and Biophysical Research Communications*, **235**, 533–538.
- Lechner, C. et al. (1996) *Proceedings of the National Academy of Sciences of the United States of America*, **93**, 4355–4359.
- Li, Z. et al. (1996) *Biochemical and Biophysical Research Communications*, **228**, 334–340.
- Hale, K.K. et al. (1999) *Journal of Immunology*, **162**, 4246–4252.
- Hu, M.C. et al. (1999) *The Journal of Biological Chemistry*, **274**, 7095–7102.
- Lee, J.C. et al. (1999) *Pharmacology & Therapeutics*, **82**, 389–397.
- Derijard, B. et al. (1995) *Science*, **267**, 682–685.
- Ganiatsas, S. et al. (1998) *Proceedings of the National Academy of Sciences of the United States of America*, **95**, 6881–6886.
- Wang, Z. et al. (1998) *Structure*, **6**, 1117–1128.
- Wang, Z. et al. (1997) *Proceedings of the National Academy of Sciences of the United States of America*, **94**, 2327–2332.
- Wilson, K.P. et al. (1996) *The Journal of Biological Chemistry*, **271**, 27696–27700.
- Rana, A. et al. (1996) *The Journal of Biological Chemistry*, **271**, 19025–19028.
- Ono, K. and Han, J. (2000) *Cellular Signalling*, **12**, 1–13.
- Miller, D.S. and Horowitz, S.B. (1986) *The Journal of Biological Chemistry*, **261**, 13911–13915.
- Gribble, F.M. et al. (2000) *The Journal of Biological Chemistry*, **275**, 30046–30049.
- Traut, T.W. (1994) *Molecular and Cellular Biochemistry*, **140**, 1–22.
- Mitchell, R.D. et al. (1995) *Biochemistry*, **34**, 528–534.
- McIntyre, J.A., Castaner, J., and Leeson, P.A. (2005) *Drugs of the Future*, **30**, 771–779.
- Keri, G. et al. (2006) *Current Signal Transduction Therapy*, **1**, 67–95.
- Davies, S.P. et al. (2000) *The Biochemical Journal*, **351**, 95–105.
- Fitzgerald, C.E. et al. (2003) *Nature Structural Biology*, **10**, 764–769.
- Hunt, J.A. et al. (2003) *Bioorganic & Medicinal Chemistry Letters*, **13**, 467–470.
- Stelmach, J.E. et al. (2003) *Bioorganic & Medicinal Chemistry Letters*, **13**, 277–280.
- Norman, P. (2006) *Expert Opinion on Therapeutic Patents*, **16**, 1443–1448.
- Lantos, I. et al. (1984) *Journal of Medicinal Chemistry*, **27**, 72–75.
- Kawai, Y., Yamazaki, H., Tanaka, H., and Oku, T. (1994) WO9419350.
- Otani, Y. et al. (1999) *Transplantation Proceedings*, **31**, 1010–1011.
- Otani, Y. et al. (2000) *The Journal of Heart and Lung Transplantation*, **19**, 377–383.
- Takeyoshi, I. et al. (1999) *Transplantation Proceedings*, **31**, 1935–1936.
- Ohashi, N. et al. (2000) *Arteriosclerosis, Thrombosis, and Vascular Biology*, **20**, 2521–2526.
- Laufer, S.A., Striegel, H.G., and Wagner, G.K. (2002) *Journal of Medicinal Chemistry*, **45**, 4695–4705.

- 40 Laufer, S.A., Zimmermann, W., and Ruff, K.J. (2004) *Journal of Medicinal Chemistry*, **47**, 6311–6325.
- 41 Tong, L. *et al.* (1997) *Nature Structural Biology*, **4**, 311–316.
- 42 Wilson, K.P. *et al.* (1997) *Chemistry & Biology*, **4**, 423–431.
- 43 Gum, R.J. *et al.* (1998) *The Journal of Biological Chemistry*, **273**, 15605–15610.
- 44 Lisnock, J. *et al.* (1998) *Biochemistry*, **37**, 16573–16581.
- 45 Young, P.R. *et al.* (1997) *The Journal of Biological Chemistry*, **272**, 12116–12121.
- 46 Evers, P.A. *et al.* (1998) *Chemistry & Biology*, **5**, 321–328.
- 47 Boehm, J.C. *et al.* (1996) *Journal of Medicinal Chemistry*, **39**, 3929–3937.
- 48 Laufer, S.A. and Wagner, G.K. (2002) *Journal of Medicinal Chemistry*, **45**, 2733–2740.
- 49 de Laszlo, S.E. *et al.* (1998) *Bioorganic & Medicinal Chemistry Letters*, **8**, 2689–2694.
- 50 LoGrasso, P.V. *et al.* (1997) *Biochemistry*, **36**, 10422–10427.
- 51 Wagner, G. and Laufer, S. (2006) *Medicinal Research Reviews*, **26**, 1–62.
- 52 Diller, D.J., Lin, T.H., and Metzger, A. (2005) *Current Topics in Medicinal Chemistry*, **5**, 953–965.
- 53 Hynes, J. Jr. and Leftheris, K. (2005) *Current Topics in Medicinal Chemistry*, **5**, 967–985.
- 54 Adams, J.L. *et al.* (1998) *Bioorganic & Medicinal Chemistry Letters*, **8**, 3111–3116.
- 55 Liverton, N.J. *et al.* (1999) *Journal of Medicinal Chemistry*, **42**, 2180–2190.
- 56 Laufer, S.A. *et al.* (2003) *Journal of Medicinal Chemistry*, **46**, 3230–3244.
- 57 Laufer, S.A., Margutti, S., and Fritz, M.D. (2006) *ChemMedChem*, **1**, 197–207.
- 58 Revesz, L. *et al.* (2000) *Bioorganic & Medicinal Chemistry Letters*, **10**, 1261–1264.
- 59 Ohkawa, S., Naruo, K., Miwatashi, S., and Kimura, H. (2001) WO2001074811.
- 60 Gallagher, T.F. *et al.* (1997) *Bioorganic and Medicinal Chemistry*, **5**, 49–64.
- 61 Adams, J.L. *et al.* (2001) *Bioorganic & Medicinal Chemistry Letters*, **11**, 2867–2870.
- 62 Badger, A.M. *et al.* (2000) *Arthritis and Rheumatism*, **43**, 175–183.
- 63 Thurmond, R.L. *et al.* (2001) *European Journal of Biochemistry*, **268**, 5747–5754.
- 64 Wadsworth, S.A. *et al.* (1999) *The Journal of Pharmacology and Experimental Therapeutics*, **291**, 680–687.
- 65 Salituro, F., Galullo, V., Bellon, S., Bemis, G., and Cochran, J. (1999) WO9958502.
- 66 Salituro, F.G. and Bemis, G. (1999) WO9900357.
- 67 Pargellis, C. *et al.* (2002) *Nature Structural Biology*, **9**, 268–272.
- 68 Regan, J. *et al.* (2002) *Journal of Medicinal Chemistry*, **45**, 2994–3008.
- 69 Dumas, J. *et al.* (2000) *Bioorganic & Medicinal Chemistry Letters*, **10**, 2047–2050.
- 70 Devraj, R.V. (2005) Abstracts of papers presented at 229th ACS National Meeting, San Diego, CA, USA, March 13–17.
- 71 Burnette, B.L. *et al.* (2009) *Pharmacology*, **84**, 42–60.
- 72 Goldstein, D.M. *et al.* (2006) *Journal of Medicinal Chemistry*, **49**, 1562–1575.
- 73 Dominguez, C., Powers, D.A., and Tamayo, N. (2005) *Current Opinion in Drug Discovery & Development*, **8**, 421–430.
- 74 Miwatashi, S. *et al.* (2005) Abstracts of Papers presented at 229th ACS National Meeting, San Diego, CA, USA, March 13–17.
- 75 Miwatashi, S. *et al.* (2005) *Journal of Medicinal Chemistry*, **48**, 5966–5979.
- 76 Graul, A. and Prous, I.J.R. (2007) *Drug News Perspect*, **20**, 57–68.
- 77 Mavunkel, B.J. *et al.* (2003) *Bioorganic & Medicinal Chemistry Letters*, **13**, 3087–3090.
- 78 Ferraccioli, G.F. (2000) *Current Opinion in Anti-Inflammatory and Immunomodulatory Investigational Drugs*, **2**, 74–77.
- 79 Snoonian, J.R. (2004) WO2004072038.
- 80 Salituro, F., Bemis, G., and Cochran, J. (2000) WO2000017175.
- 81 Ding, C. (2006) *Current Opinion in Investigational Drugs*, **7**, 1020–1025.
- 82 Ottosen, E.R. and Rachlin, S. (1998) WO9832730.
- 83 Ottosen, E.R. and Dannacher, H.W. (2001) WO2001005749.

- 84 Ottosen, E.R. *et al.* (2003) *Journal of Medicinal Chemistry*, **46**, 5651–5662.
- 85 Petersen, T.K. (2006) *Basic & Clinical Pharmacology & Toxicology*, **99**, 104–115.
- 86 Laufer, S.A. *et al.* (2006) *Journal of Medicinal Chemistry*, **49**, 7912–7915.
- 87 www.gsk.com (2009).
- 88 www.clinicaltrials.gov (2009).
- 89 Chandi, A., Keel, T.R., Patel, V.K., and Walker, A.L. (2006) WO2006134382.
- 90 Aston, N.M., Bamborough, P., and Walker, A.L. (2003) WO2003068747.
- 91 Corsi, M., Faiferman, I., Merlo Pich, E., Ratti, E., and Wren, P.B. (2007) WO2007144390.
- 92 Patel, V.K. and Walker, A.L. (2008) WO2008071665.
- 93 Angell, R.M. *et al.* (2008) *Bioorganic & Medicinal Chemistry Letters*, **18**, 318–323.
- 94 Angell, R.M. *et al.* (2008) *Bioorganic & Medicinal Chemistry Letters*, **18**, 324–328.
- 95 Angell, R.M. *et al.* (2008) *Bioorganic & Medicinal Chemistry Letters*, **18**, 4428–4432.
- 96 Angell, R.M. *et al.* (2008) *Bioorganic & Medicinal Chemistry Letters*, **18**, 4433–4437.
- 97 Sullivan, J.E. *et al.* (2005) *Biochemistry*, **44**, 16475–16490.
- 98 Doherty, J.B. (2002) WO2002058695.
- 99 Chung, J.Y.L. *et al.* (2006) *Journal of Organic Chemistry*, **71**, 8602–8609.
- 100 Bemis, G.W. (1998) WO9827098.
- 101 Natarajan, S.R. *et al.* (2003) *Bioorganic & Medicinal Chemistry Letters*, **13**, 273–276.
- 102 Bao, J. *et al.* (2006) *Bioorganic & Medicinal Chemistry Letters*, **16**, 64–68.
- 103 Adams, J.L. (2002) WO2002059083.
- 104 Appleby, J.R.G., Humphries, L.A., Blatcher, P., Abu Khalil, A., Kaspavec, J., and Diederich, A. (2007) WO2007059500.
- 105 Kaspavec, J. *et al.* (2003) *Tetrahedron Letters*, **44**, 4567–4570.
- 106 Yan, H. *et al.* (2007) *Tetrahedron Letters*, **48**, 1205–1207.
- 107 Marvin 5.0.6.1, ChemAxon (www.chemaxon.com), Marvin's Calculator Plugins were used for the prediction and calculation of log *P* values. (2008).
- 108 Lipinski, C.A. *et al.* (1997) *Advanced Drug Delivery Reviews*, **23**, 3–25.
- 109 Goldstein, D.M. and Gabriel, T. (2005) *Current Topics in Medicinal Chemistry*, **5**, 1017–1029.
- 110 Hill, R.J. *et al.* (2008) *The Journal of Pharmacology and Experimental Therapeutics*, **327**, 610–619.
- 111 Cohen, S.B. *et al.* (2009) *Arthritis and Rheumatism*, **60**, 335–344.
- 112 Dambach, D.M. (2005) *Current Topics in Medicinal Chemistry*, **5**, 929–939.
- 113 Genovese, M.C. (2009) *Arthritis and Rheumatism*, **60**, 317–320.
- 114 Sweeney, S.E. and Firestein, G.S. (2006) *Annals of the Rheumatic Diseases*, **65**, 83–88.

10

Cellular Protein Kinases as Antiviral Targets

Luis M. Schang

10.1

Introduction

Although most viruses require protein kinases for their replication, very few viruses encode protein kinases, and only in very limited numbers. For example, among all human pathogenic viruses, only the members of the *Rota*-, *Pox*-, and *Herpesviridae* encode for one (rota) or two (pox and herpes) serine/threonine protein kinases (Table 10.1) (reviewed in Ref. [1]). No known human pathogenic virus encodes tyrosine protein kinases. Despite their limited numbers, viral protein kinases are nonetheless most interesting as targets for antiviral drugs. Several novel drugs against human cytomegalovirus (HCMV), such as Go6976, NGIC-I (indolocarbazoles), and maribavir (ribofuranosyl benzimidazole), for example, target the viral serine/threonine protein kinase UL97 (Tables 10.1 and 10.2) [2, 3]. These drugs are in advanced stages of development, maribavir being the most advanced [4]. Unfortunately, although maribavir was well tolerated in a recent Phase III clinical trial, it failed to protect from HCMV-induced disease. Further development of the drug is now under review by ViroPharma. Therefore, the efficacy of inhibitors of viral protein kinases as antiviral drugs is currently being reassessed. Moreover, as for any drug that inhibits a viral protein, resistance to inhibitors of viral protein kinases is promptly selected for [5–7]. In fact, resistance against maribavir is as promptly selected for as is the resistance against the traditional antiviral drugs that target the viral DNA polymerase after activation by the viral kinase [8].

As an alternative to targeting viral protein kinases, the many cellular protein kinases required for viral replication (Table 10.1) are also considered as targets for antiviral drugs. The current interest on cellular protein kinases as pharmaceutical targets, discussed elsewhere in this book, has led to the development of many inhibitors specific for many of them. The existence of these inhibitors has in turn resulted in growing interest in cellular kinases as antiviral targets. This interest was first awakened by the discovery that pharmacological cyclin-dependent kinase (CDK) inhibitors (PCIs) inhibited replication of human herpesviruses. This discovery

Table 10.1 Protein kinases involved in replication or pathogenesis of human viruses.

Family	Examples	Viral PK ^{a)}	Cellular PK ^{b)}
Picornaviridae	Poliovirus, HepA	None	p38JNK, PKR, PKC
Caliciviridae	Norwalk virus	None	PKA
Togaviridae	Rubella virus	None	PKC, PKR, CKII 2, p38MAPK, ERK1, ERK2
Flaviviridae	Western Nile virus Hepatitis C virus	None	CDK2, CDK4, ERK, PKR, PERK, Ras, Raf, Lck
Coronaviridae	SARS virus	None	p38MAPK, PKA, TK
Rhabdoviridae	Rabies virus	None	PKR, CKII, p75 ^{trac}
Filoviridae	Ebola virus	None	PKR, CKII, Proline-directed kinases
Paramyxoviridae	Measles virus	None	PKR, DNAPK, RSV, AKT, GSK3, MAPK, PKC, ERK2, TK
Orthomyxoviridae	Influenza virus ^{c)}	None	CKII, PKC, Raf, MEK, ERK, p38MAPK, PKR
Bunyaviridae	Hantavirus	None	PKR, CKII
Arenaviridae	Hemorrhagic fever	None	“platelet protein kinase,” PKA
Rotaviridae	Human rotavirus	NSP5	IKK, Jak, CKII
Retroviridae ^{d)}	HIV, HTLV-1	None	CDK1, CDK2, CDK4, CDK6, CDK7, CDK9, p38MAPK^{e)} PKG, JNK, JNK2, MEK, IKK JAK3, PKR, Bub1, Pyk2, Mlk3, Lyn, Fyn, Lck, Hck
Polyomaviridae	Polyomavirus	None	CDK2, CHK1, PKC, MAPK, PKC, DNAPK
Papillomaiviridae	HPV16	None	CDK2 , CDK4, FAK, AKT, Raf, ERK2, MEK, PKA, CKII, EGFR
Adenoviridae	Adenovirus	None	CDK2 , MAPK, ERK1, ERK2, PKC, EGFR
Parvoviridae	B19	None	JNK, CDK2, CDK1, PKA, PKC
Herpesviridae	HSV-1/HSV-2 ^{c)}	U _L 13, U _S 3	CDK1, CDK2, CDK4 , PKR, PKA, PKC, CKII, SRPK1, IKK, JNK, TK
	VZV	ORF47, ORF66	CDK1, CDK2 , CDK5, CKII, CKI
	EBV	BGLF4	CDK1, CDK2 , MAPK, PKC, PKR, Src, Syk, Btk
	HCMV	UL97 ^{f)}	CDK2, CDK7, CDK9 , MAPK, MEKK1, CKII, EGFR, Akt, p70 ^{SK6}

Table 10.1 (Continued)

Family	Examples	Viral PK ^{a)}	Cellular PK ^{b)}
	KSHV	vCyc ^{g)} , ORF36	<i>CDK6</i> , <i>CDK2</i> , AKT, GSK3, FAK, MEK, IKK, ERK1, ERK2, PKC, MAPK, KIT, PDGFR
Poxviridae	Vaccinia virus	B1R ^{h)} , F10L ^{h)}	<i>Abl</i> , <i>Src</i> , <i>Erb1</i> , JAK, Lck, IRR
Hepadnaviridae	Hepatitis B virus	None	CDK1, CDK2, CDK4, MEK, SAPK1, SAPK2, PKC, ERK2, JAK1, Src, EGFR

Based on a table by the author [1].

- a) All known viral protein kinases are included.
- b) Only the most important (or better studied) cellular protein kinases are included.
- c) The NP1 protein of influenza virus and the large subunit of HSV-2 ribonucleotide reductase have been reported to be protein kinases, but these activities were later identified as copurifying cellular protein kinases.
- d) Many animal retroviruses encode transforming protein kinases acquired from their hosts.
- e) The involvement in the replication of this virus of the protein kinases in **bold** and *italics* in discussed in the text.
- f) UL97 is the only viral protein kinase currently targeted by (yet preclinical) antiviral drugs.
- g) KSHV encodes only the regulatory subunit (cyclin), which activates cellular CDK catalytic subunit.
- h) Only viral protein kinase known to be essential for viral replication.

actually resulted from basic virology experiments originally aimed at identifying the roles of different cellular proteins in viral replication [9–11]. Fortunately, these experiments coincided in time with the first tests of PCIs as potential anticancer agents, which were yielding some promising results in small preclinical and even clinical trials [12–15]. Thus, it was immediately speculated that PCIs could potentially be developed as novel antiviral drugs [9–11, 16].

The speculations that PCIs could be used as antivirals implied a major departure from the generally accepted approach to ensure specificity and safety by targeting only viral proteins. By the nature of their targets, only infected cells are affected by the latter drugs. This approach has been most successfully used in the development of the 45 existing clinical antiviral drugs and many others under development (Table 10.2). Unfortunately, resistance presents a major challenge to this approach (for selected discussions and examples, see Refs [17–22]). A given cellular protein is, in contrast, often required for multiple viral functions. Drugs targeting such cellular proteins would be functionally equivalent to the current antiviral combination therapies, in which multiple drugs are used to inhibit several viral targets at the same time. Drugs that target cellular proteins required for multiple viral functions could therefore minimize the selection for resistance.

The limited number of potential targets encoded by the viruses with small genomes, such as HPV or even HCV, presents another challenge to the development of traditional antiviral drugs. The former encodes no viral enzymes. The latter

Table 10.2 Targets of current and developing antiviral drugs.

Virus	Target	Drug	Status
HSV-1, HSV-2	DNA polymerase	Idoxuridine	Clinical
HSV-1, HSV-2	DNA polymerase	Trifluridine	Clinical
HSV-1, HSV-2, VZV	DNA polymerase	Acyclovir	Clinical
HSV-1, HSV-2, VZV, EBV, HCMV	DNA polymerase	Valaciclovir	Clinical
HSV-1, HSV-2	DNA polymerase	Penciclovir	Clinical
HSV-1, HSV-2, VZV	DNA polymerase	Famciclovir	Clinical
HSV-1, VZV	DNA polymerase	Brivudin	Clinical
HCMV	DNA polymerase	Ganciclovir	Clinical
HCMV	DNA polymerase	Valganciclovir	Clinical
HCMV	DNA polymerase	Cidofovir	Clinical
HCMV, HSV-1, HSV-2	DNA polymerase	Foscarnet	Clinical
HIV	RT	Zidovudine	Clinical
HIV	RT	Didanosine	Clinical
HIV	RT	Zalcitabine	Clinical
HIV	RT	Stavudine	Clinical
HIV	RT	Abacavir	Clinical
HIV	RT	Emtricitabine	Clinical
HIV	RT	Tenofovir	Clinical
HIV	RT	Nevirapine	Clinical
HIV	RT	Delavirdine	Clinical
HIV	RT	Efavirenz	Clinical
HIV, HBV	RT	Lamivudine	Clinical
HBV	RT	Adefovir dipivoxil	Clinical
HBV	RT	Entecavir	Clinical
HBV	RT	Telbivudine	Clinical
HIV	Integrase	Raltegravir	Clinical
HCV	RNA polymerase ^{a)} / Immunomodulator	Ribavirin/pegylated interferon-2 α	Clinical
HIV	Protease	Saquinavir	Clinical
HIV	Protease	Ritonavir	Clinical
HIV	Protease	Indinavir	Clinical
HIV	Protease	Nelfinavir	Clinical
HIV	Protease	Amprenavir	Clinical
HIV	Protease	Darunavir	Clinical
HIV	Protease	Fosamprenavir	Clinical
HIV	Protease	Lopinavir	Clinical
HIV	Protease	Atazanavir	Clinical
HIV	Protease	Tripanavir	Clinical
HCMV	mRNA ^{b)}	Fomivirsen	Clinical
HIV	Glycoprotein	Enfuvirtide	Clinical
HIV	Glycoprotein ^{c)}	Maraviroc	Clinical
Influenza A/B	Neuraminidase	Oseltamivir	Clinical
Influenza A/B	Neuraminidase	Zanamivir	Clinical
Influenza A	Matrix protein	Amantadine	Clinical
Influenza A	Matrix protein	Rimantadine	Clinical
Poxvirus	Phospholipase?	ST-246	Phase I-EUA application-IND ^{d)}

Table 10.2 (Continued)

Virus	Target	Drug	Status
CMV, EBV	Viral protein kinase	Maribavir	Phase III (disc?) ^{e)}
HIV	Integrase	Elvitegravir	Phase III
HCV	Protease	Telaprevir	Phase III
HCV	Protease	Boceprevir	Phase III
HIV	Glycoprotein	Dextran-2-sulfate	Phase III
HIV	Glycoprotein	BMS-488043	Phase IIa
HIV	Capsid precursor protein	Bevirimat	Phase IIb
HCV	RNA polymerase	Valopicitabine	Phase IIb (disc)

Based on the two tables by Mireille St.Vincent [159].

- The actual molecular target of ribavirin is disputed.
- Fomivirsen is an antisense RNA targeting viral transcripts.
- Maraviroc targets the interaction between HIV glycoproteins and their coreceptors.
- Although poxvirus has been eradicated, ST-246 was used in 2007 in a unique case of vaccinia virus infection of a toddler, under an emergency Investigational New Drug application (IND). The drug was effective and safe in this single case.
- The results of the first Phase III clinical trials of maribavir failed to show antiviral activity; the company is currently reevaluating the drug.

encodes only four viral enzymatic activities, of which three have been targeted *in vitro*, and only two *in vivo*. In contrast, a large number of cellular enzymes are required for the replication of such viruses. The number of potential cellular targets against these viruses is therefore far larger than the number of potential viral ones.

Viral proteins tend to evolve and diverge fast. Drugs targeting them tend therefore to be active against only one or a few closely related viruses. Patients infected with multiple viruses (as occurs generally in HIV/AIDS) must therefore take different drugs against each virus (discussed in Ref. [23]). In contrast, a given cellular protein is often required for replication of many distantly related viruses. Thus, drugs targeting these cellular proteins could be used against multiple viruses, reducing the number of antiviral drugs required and simplifying clinical antiviral treatments.

Drugs targeting cellular proteins can also be used against novel pathogens before their proteins are fully characterized, thus speeding the development of antiviral drugs against emerging pathogens. In contrast, the traditional approach requires the thorough characterization of the viral targets, which precludes its timely use against new and emerging pathogens. For example, the SARS epidemic started in November 2002, and was over by July 2003. The SARS virus was sequenced in April 2003 [24], and proven to be the causative agent in May 2003 [25]. However, the potential targets encoded by it are still being characterized, and consequently no specific inhibitor of any of SARS virus-encoded target has yet been published (several drugs used against other viruses have been tested against SARS, and some of them may be active, but none has been developed against a SARS coronavirus protein).

As a drawback, targeting cellular proteins could lead to unwanted negative side effects, as cellular targets are generally expressed in many uninfected cells. However,

it should be considered that except for anti-infective agents, all clinical drugs target cellular proteins. For example, inhibitors of protein kinases that are expressed by many cells have been successfully tested against many metabolic or inflammatory diseases and cancer. A large body of expertise therefore exists in how to target widely expressed cellular protein kinases without major toxicities.

In this chapter, we will mainly focus on PCIs as an illustration of the potential of cellular protein kinases in general as antiviral targets. We will then expand to other selected protein kinase inhibitors with antiviral activities.

10.2

Antiviral Activities of the Pharmacological Cyclin-Dependent Kinase Inhibitors

10.2.1

Relevant Properties of CDKs and PCIs

CDKs are protein kinases that phosphorylate a serine or threonine immediately before a proline; they also have high degree of sequence homology and all are activated by regulatory subunits, generally cyclins [26]. The human genome encodes for 13 CDKs, 4 related dual-specificity protein kinases (CDC2- and CDK1-like kinases (CLKs)), and 5 related PCTAIRE-motif protein kinases (PMPKs) [27]. All these kinases are classified in the CMGC group, which also includes 39 other protein kinases [27].

The mechanism of activation of CDKs is well understood [28, 29]. As for all protein kinases, the active site resides at a cleft between the amino- and the carboxy-terminal globular domains ("lobes"). Access to the active site is gated by the so-called "T-loop," which is closed in the cyclin-free CDK. Furthermore, free CDKs have lower affinity for ATP than the CDKs bound to their cyclin partners. The free CDK subunit is therefore in a catalytically inactive conformation. Binding by the cyclin partner induces a rotation between the carboxy and the amino-terminal lobes. This conformational change displaces the T-loop, opening the access to the active site, and alters the three-dimensional structure of the catalytic cleft, which then binds ATP with threefold higher affinity. Moreover, the rotation between lobes also repositions the catalytic residues, allowing the nucleophilic attack by the substrate. The cyclin-bound, and properly phosphorylated, CDK subunit is therefore in a catalytically active conformation.

CDK1 and CDK2 are activated by cyclin A, but CDK1 is also activated by cyclin B and CDK2 by cyclin E. CDK4 and CDK6 are activated by the D-type cyclins (D1, D2, and D3). CDK5 is activated by the noncyclin p35, which is expressed only in differentiated neurons thus limiting the activity of CDK5 to these cells. CDK7 is activated by cyclin H and Mat1, whereas CDK8 is activated by cyclin C, and CDK9 is activated by cyclins T and K. The cyclins activating CDK10 are yet unknown, whereas CDK11, CDK12, and CDK13 appear to be activated by L-type cyclins [30–32].

Although 25 cyclins are identified in the human genome by sequence homology [33], many are not known to actually regulate CDK activity. Viruses also encode

cyclins that regulate cellular CDKs, such as the vCyc encoded by several members of the *betaherpesvirinae* subfamily, highlighting the importance of CDKs in viral replication. Even HCMV, which encodes no CDK sequence homologues, encodes for a protein kinase, UL97, that phosphorylates some of the same substrates as CDKs [34]. The activities of CDKs are also regulated by phosphorylation, inhibitory proteins, and subcellular localization.

CDKs mostly regulate progression through the cell cycle, transcription, the neuronal cytoskeleton, apoptosis, and splicing, but have also other cellular functions. CDK1, CDK2, CDK3, CDK4, CDK6, and CDK7 regulate the cell cycle, CDK7, CDK8, and CDK9 regulate transcription, and CDK5 phosphorylates neuronal cytoskeleton proteins (reviewed in Ref. [16]). CDK10 regulates certain transcription factors and may or may not regulate progression through G2 [35–37]. Similar to CDK12, CDK11 also participates in cell cycle regulation, apoptosis, and splicing [30, 31, 38, 39]. Expression and degradation of CDKs, cyclins, and their inhibitory proteins is tightly regulated during the cell cycle or development, as are their regulatory phosphorylations. Dysregulation of any of these events often leads to disease.

Due to their importance in the regulation of the cell cycle, and therefore in cancer, CDKs were among the first protein kinases to be selected as targets for small-molecule (pharmacological) inhibitors. Although the earliest efforts resulted mostly in nonspecific drugs, a number of highly specific PCIs have been developed in the last 10 years (reviewed in Ref. [16, 40–45]). Some of these PCIs are arguably among the most characterized protein kinase inhibitors [42–44, 46].

A number of different core structures have been used to develop PCIs, including purines, pyrimidines, flavonoids, and bis-indoles. The structures of PCIs consequently have only limited commonalities. They are mostly flat heterocycles, most often of less than 300 Da in mass (and always of less than 600 Da). They bind to the ATP binding pocket of their target CDKs, making mostly hydrophobic interactions, and with one exception, inhibit CDKs by competing with the ATP cosubstrate, but not with the peptide cosubstrate. In this chapter, we will focus on the antiviral activities of PCIs, discussing structures, specificities, biochemical, cellular and antitumoral activities, and toxicities, only when strictly necessary. The reader further interested in these aspects is referred to the many reviews published on these topics [45, 47–51].

PCIs are classified as nonspecific, pan-specific and oligo-specific [16, 40, 41, 50, 52]. Mono-specific PCIs may exist but none has yet been published. The nonspecific PCIs inhibit many unrelated protein kinases, including CDKs. These drugs are not likely to be of great pharmacological use and therefore we will not discuss about them in this chapter. The pan-specific PCIs inhibit several CDKs with similar potencies, although they do discriminate CDKs from most other protein kinases (Table 10.3). The oligo-specific PCIs inhibit a subset of CDKs at lower concentrations than others (Table 10.3). No truly mono-specific PCI has been published yet. The experimental evidence supporting the strong preference for a single CDK claimed for some compounds is very limited (for examples, see Ref. [53–58]), and some PCIs that were originally claimed to be mono-specific were later shown to inhibit other CDKs with similar potencies. Some PCIs have been tested only against a limited number of potential targets, or do not fit well into any of these categories.

Table 10.3 Specificity of relevant oligo- and pan-specific PCIs.

Group	Family	Kinase	Oligo-specific				Pan-specific		
			Rosco		Purv		Flavo		Indirubin-3'-monoxime IC ₅₀ (μM)
			IC ₅₀ (μM)	Inhibition at 10 μM (%)	K _d (μM)	IC ₅₀ (μM)	IC ₅₀ (μM)	K _d (μM)	
AGC	AKT	AKT1,	>100	0–2		<20			
		AKT2, AKT3							
	DMPK	ROCK2		<20		43			
		ROCK1,		0					
	GRK	CRIK1							
		BARK1,		0–14					
		BARK2,							
		GRK4,							
		GRK5,							
	NDR PKA	GPRK5,							
		GPRK6,							
		GPRK7			>10			>10	
		NDR2							
		PKA	>50						
	PKB PKC	PKAC	>1000	<20		9	<20	>10	6.3
		PRKACA		7	>10		145–122	>10	
		PRX		0					
		PDK1		1			<20		27
		PKCα	>100	0		>10	<20	6	4
		PKCα1	>100	0		>10			

Table 10.3 (Continued)

Group	Family	Kinase	Oligo-specific				Pan-specific		
			Rosco		Purv		Flavo		Indirubin-3'-monoxime IC ₅₀ (μM)
			IC ₅₀ (μM)	Inhibition at 10 μM (%)	K _d (μM)	IC ₅₀ (μM)	IC ₅₀ (μM)	K _d (μM)	
CAMKL		AMPKα1		<20	>10			6.6	
		AMPKα2		<20					
		CHK1		5					
		MARK2			>10			>10	
		PASK		9					
DAPK		DAPK2,			>10			>10	
		DRAK1							
		DRAK2			>10			5.1	
		DAPK3		0	>10			>10	
		MAPKAP		2					
MAKKAPK		MAPKAPK3		1					
		MAPKAPK5		0					
		MNK2			>10			1.9	
		caMLCK	90						
		skMLCK		0	>10			>10	
PHK		PHKg1		11	>10			>10	
		PHKg2		0	>10			2	
PIM		PIM1		25	>10			0.52	
		PIM2		3	>10			0.65	
PKD		PKD2		0					
		PKD3/		17					
RAD53		PRKN							
		CHK2		13–40					

Table 10.3 (Continued)

Group	Family	Kinase	Oligo-specific				Pan-specific		
			Rosco		Purv		Flavo		Indirubin-3'-monoxime IC ₅₀ (μM)
			IC ₅₀ (μM)	Inhibition at 10 μM (%)	K _d (μM)	IC ₅₀ (μM)	Inhibition at 10 μM (%)	IC ₅₀ (μM)	K _d (μM)
EGFR		ErbB1		8	>10			25-20	>10
		ErbB2		0	>10				>10
		ErbB4		8					
		EphA1		12					
Eph		EphA2,		0-19	>10				>10
		EphA3,							
		EphA4,							
		EphA8,							
		EphB4							
		EphA5		14	>10				4
		EphB1		15	>10				2.2
		EphB2		7					
		EphB3		6					
		EphA7			>10				>10
		EphA6			>10				>10
		FAK		12	>10				>10
Fak				16	>10				>10
Fer				39	>10				>10
FGFR		FPS		6	>10				>10
		FGFR1		13	>10				>10
		FGFR2,							
		FGFR3							

Table 10.3 (Continued)

Group	Family	Kinase	Oligo-specific				Pan-specific		
			Rosco		Purv		Flavo		Indirubin-3'-monoxime IC ₅₀ (μM)
			IC ₅₀ (μM)	Inhibition at 10 μM (%)	K _d (μM)	IC ₅₀ (μM)	Inhibition at 10 μM (%)	IC ₅₀ (μM)	
TKL	Tec	BTK, BMX		0	>10			>10	
		ITK		8					
	Tie Trk	TEK		9					
		TRKA		5	>10			>10	
		TRKB		13					
		TRKC		5					
	VEGFR	VEGFR1		10					
		VEGFR3		9	>10			>10	
		VEGFR2		14	>10			>10	
		IRAK4		27					
Other	RIPK	LIMK1		7	>10			>10	
		MLK1		20–40					
		cRAF		39		>1			>100
		BRAF							>11
	Other	RIPK2			>10			>10	
		Aurora C	>100		>10			>10	
		Aurora B	>100	0					
		Aurora 2	600	0	>10			>10	
		CaMKK2			>10			0.32	
		CaMKK1			>10			0.019	

CDC7/	>1000																																																																																																																																																																																																																																																																																																																																																																																																																																																																																																																																																																																																																																																																																																																																																																																																																																																																																																																																																																																																																																																																																																																																																																																																																																																																																																																																																																																																																			
-------	-------	--	--	--	--	--	--	--	--	--	--	--	--	--	--	--	--	--	--	--	--	--	--	--	--	--	--	--	--	--	--	--	--	--	--	--	--	--	--	--	--	--	--	--	--	--	--	--	--	--	--	--	--	--	--	--	--	--	--	--	--	--	--	--	--	--	--	--	--	--	--	--	--	--	--	--	--	--	--	--	--	--	--	--	--	--	--	--	--	--	--	--	--	--	--	--	--	--	--	--	--	--	--	--	--	--	--	--	--	--	--	--	--	--	--	--	--	--	--	--	--	--	--	--	--	--	--	--	--	--	--	--	--	--	--	--	--	--	--	--	--	--	--	--	--	--	--	--	--	--	--	--	--	--	--	--	--	--	--	--	--	--	--	--	--	--	--	--	--	--	--	--	--	--	--	--	--	--	--	--	--	--	--	--	--	--	--	--	--	--	--	--	--	--	--	--	--	--	--	--	--	--	--	--	--	--	--	--	--	--	--	--	--	--	--	--	--	--	--	--	--	--	--	--	--	--	--	--	--	--	--	--	--	--	--	--	--	--	--	--	--	--	--	--	--	--	--	--	--	--	--	--	--	--	--	--	--	--	--	--	--	--	--	--	--	--	--	--	--	--	--	--	--	--	--	--	--	--	--	--	--	--	--	--	--	--	--	--	--	--	--	--	--	--	--	--	--	--	--	--	--	--	--	--	--	--	--	--	--	--	--	--	--	--	--	--	--	--	--	--	--	--	--	--	--	--	--	--	--	--	--	--	--	--	--	--	--	--	--	--	--	--	--	--	--	--	--	--	--	--	--	--	--	--	--	--	--	--	--	--	--	--	--	--	--	--	--	--	--	--	--	--	--	--	--	--	--	--	--	--	--	--	--	--	--	--	--	--	--	--	--	--	--	--	--	--	--	--	--	--	--	--	--	--	--	--	--	--	--	--	--	--	--	--	--	--	--	--	--	--	--	--	--	--	--	--	--	--	--	--	--	--	--	--	--	--	--	--	--	--	--	--	--	--	--	--	--	--	--	--	--	--	--	--	--	--	--	--	--	--	--	--	--	--	--	--	--	--	--	--	--	--	--	--	--	--	--	--	--	--	--	--	--	--	--	--	--	--	--	--	--	--	--	--	--	--	--	--	--	--	--	--	--	--	--	--	--	--	--	--	--	--	--	--	--	--	--	--	--	--	--	--	--	--	--	--	--	--	--	--	--	--	--	--	--	--	--	--	--	--	--	--	--	--	--	--	--	--	--	--	--	--	--	--	--	--	--	--	--	--	--	--	--	--	--	--	--	--	--	--	--	--	--	--	--	--	--	--	--	--	--	--	--	--	--	--	--	--	--	--	--	--	--	--	--	--	--	--	--	--	--	--	--	--	--	--	--	--	--	--	--	--	--	--	--	--	--	--	--	--	--	--	--	--	--	--	--	--	--	--	--	--	--	--	--	--	--	--	--	--	--	--	--	--	--	--	--	--	--	--	--	--	--	--	--	--	--	--	--	--	--	--	--	--	--	--	--	--	--	--	--	--	--	--	--	--	--	--	--	--	--	--	--	--	--	--	--	--	--	--	--	--	--	--	--	--	--	--	--	--	--	--	--	--	--	--	--	--	--	--	--	--	--	--	--	--	--	--	--	--	--	--	--	--	--	--	--	--	--	--	--	--	--	--	--	--	--	--	--	--	--	--	--	--	--	--	--	--	--	--	--	--	--	--	--	--	--	--	--	--	--	--	--	--	--	--	--	--	--	--	--	--	--	--	--	--	--	--	--	--	--	--	--	--	--	--	--	--	--	--	--	--	--	--	--	--	--	--	--	--	--	--	--	--	--	--	--	--	--	--	--	--	--	--	--	--	--	--	--	--	--	--	--	--	--	--	--	--	--	--	--	--	--	--	--	--	--	--	--	--	--	--	--	--	--	--	--	--	--	--	--	--	--	--	--	--	--	--	--	--	--	--	--	--	--	--	--	--	--	--	--	--	--	--	--	--	--	--	--	--	--	--	--	--	--	--	--	--	--	--	--	--	--	--	--	--	--	--	--	--	--	--	--	--	--	--	--	--	--	--	--	--	--	--	--	--	--	--	--	--	--	--	--	--	--	--	--	--	--	--	--	--	--	--	--	--	--	--	--	--	--	--	--	--	--	--	--	--	--	--	--	--	--	--	--	--	--	--	--	--	--	--	--	--	--	--	--	--	--	--	--	--	--	--	--	--	--	--	--	--	--	--	--	--	--	--	--	--	--	--	--	--	--	--	--	--	--	--	--	--	--	--	--	--	--	--	--	--	--	--	--	--	--	--	--	--	--	--	--	--	--	--	--	--	--	--	--	--	--	--	--	--	--	--	--	--	--	--	--	--	--	--	--	--	--	--	--	--	--	--	--	--	--	--	--	--	--	--	--	--	--	--	--	--	--	--	--	--	--	--	--	--	--	--	--	--	--	--	--	--	--	--	--	--	--	--	--	--	--	--	--	--	--	--	--	--	--	--	--	--	--	--	--	--	--	--	--	--	--	--	--	--	--	--	--	--	--	--	--	--	--	--	--	--	--	--	--	--	--	--	--	--	--	--	--	--	--	--	--	--	--	--	--	--	--	--	--	--	--	--	--	--	--	--	--	--	--	--	--	--	--	--	--	--	--	--	--	--	--	--	--	--	--	--	--	--	--	--	--	--	--	--	--	--	--	--	--	--	--	--	--	--	--	--	--	--	--	--	--	--	--	--	--	--	--	--	--	--	--	--	--	--	--	--	--	--	--	--	--	--	--	--	--	--	--	--	--	--	--	--	--	--	--	--	--	--	--	--	--	--	--	--	--	--	--	--	--	--	--	--	--	--	--	--	--	--	--	--	--	--	--	--	--	--	--	--	--	--	--	--	--	--	--	--	--	--	--	--	--	--	--	--	--	--	--	--	--	--	--	--	--	--	--	--	--	--	--	--	--	--	--	--	--	--	--	--	--	--	--	--	--	--	--	--	--	--	--	--	--	--	--	--	--	--	--	--	--	--	--	--	--	--	--	--	--	--	--	--	--	--	--	--	--	--	--	--	--	--	--	--	--	--	--	--	--	--	--	--	--	--	--	--	--	--

(Continued)

Table 10.3 (Continued)

Group	Family	Kinase	Oligo-specific				Pan-specific		
			Rosco		Purv		Flavo		
			IC ₅₀ (μM)	Inhibition at 10 μM (%)	K _d (μM)	IC ₅₀ (μM)	Inhibition at 10 μM (%)	IC ₅₀ (μM)	Indirubin-3'-monoxime IC ₅₀ (μM)
Phosphatases	VZV ORF47		0						
	Glycogen phosphorylase a					2.5			
	Glycogen phosphorylase b					1–15.5			
	Rosco		Purv		Flavo				Indirubin-3'-monoxime IC ₅₀ > 4.5 μM
1	IC ₅₀ ≥ 7 μM; % inhibition < 80; K _d > 7 μM		IC ₅₀ ≥ 0.7 μM; % inhibition < 80			IC ₅₀ > 1 μM; K _d > 1 μM			2.25 μM ≤ IC ₅₀ < 4.5 μM
1	3.5 μM ≤ IC ₅₀ < 7 μM; 80 ≤ % inhibition < 93; 3.5 μM ≤ K _d < 7 μM		0.35 μM ≤ IC ₅₀ < 0.7 μM; 80 ≤ % inhibition < 93			0.5 μM ≤ IC ₅₀ < 1 μM; 0.5 μM ≤ K _d < 1 μM			0.45 μM ≤ IC ₅₀ < 2.25 μM
1	0.7 μM ≤ IC ₅₀ < 3.5 μM; % inhibition ≥ 93; 0.7 μM ≤ K _d < 3.5 μM		0.07 μM ≤ IC ₅₀ < 0.35 μM; % inhibition ≥ 93			0.1 μM ≤ IC ₅₀ < 0.5 μM; 0.1 μM ≤ K _d < 0.5 μM			

a) Based on a table by Jonathan J. Lacasse [159].

Among the PCIs claimed to have strong preference for only one CDK, CINK4 and faspaplycin were tested against the largest number of potential CDK targets. They preferentially inhibit CDK4, although they also inhibit CDK6, at 3.75- (CINK4) or 10-fold (faspaplycin) higher concentrations [53, 59]. They do not inhibit CDK1, CDK2, or CDK5, but have apparently not been tested against CDK3, CDK7, CDK8, or CDK9. Likewise, the CDK4 inhibitor PD 0332991 does not inhibit CDK1, CDK2, CDK5, or 33 other protein kinases, but it inhibits CDK6 with almost identical potency as it inhibits CDK4 [60]. The *O*⁶-cyclohexylmethylguanine NU6102, referred to as CDK2 mono-specific, actually inhibits CDK1 at concentrations only 1.5-fold higher than CDK2. It does not inhibit CDK4, but it was apparently not tested against other CDKs [61]. No PCI with potential strong preference for a single CDK has yet been reported to have antiviral activities.

The oligo-specific PCIs can be further subclassified into PCIs with preference for CDKs involved mostly in transcription or in cell cycle regulation. Those that inhibit the CDKs involved mostly in cell cycle regulation can be further subclassified according to their preference for CDK1, CDK2, CDK5, and CDK7, or CDK4 and CDK6. The purine-containing PCIs, such as roscovitine [2-(6-benzylamino-9-isopropyl-9*H*-purin-2-ylmethyl)-butan-1-ol], purvalanol [2-[6-(3-chloro-phenylamino)-9-isopropyl-9*H*-purin-2-ylmethyl]-3-methyl-butan-1-ol] (Figure 10.1), the phenylamino-pyrimidines, the *O*⁶-cyclohexylmethylguanines, and the thiazole ureas preferentially inhibit CDK1, CDK2, CDK5, CDK7, or CDK9 [61–67]. The recently described purine-containing CR8 is unique in that it inhibits CDK1, CDK2, CDK5, and CDK9, but not CDK7 [68]. The indolopyrrolocarbazoles and tri-amino pyrimidines, among others, preferentially inhibit CDK4 or CDK6 [53, 59, 69].

The different purine-containing PCIs have common mechanisms of action. They also have a common preference for CDK1, CDK2, CDK5, and CDK7 (except for CR8), although they do differ in their specific degrees of preference for any particular CDK [61–64, 68] (Table 10.3). They all bind to the ATP binding pocket of the cyclin-bound (i.e., active) conformation of CDK2 and compete with the ATP cosubstrate, but not with the peptide cosubstrate. They establish mostly hydrophobic contacts with CDK2, many with residues that make no contacts with ATP, and a few hydrogen bonds, mostly with Leu83 backbone carbonyl and amino groups. A recent study suggests that important transient hydrogen bonds may also form between the inhibitors and the target CDK, which due to their intermittent nature have not been observed in crystal structures [70]. Purine-containing PCIs do not bind with high affinity to the inactive conformation of cyclin-free CDKs [71–73].

Many purine-containing PCIs also inhibit CDK9, although with IC₅₀ approximately 5–10-fold higher than their preferred CDK targets. Some also inhibit ERK1 and ERK2, and DYRK1a, but only at concentrations approximately from 25- to 1000-fold higher. In a kinomic screen, roscovitine bound only to its two known targets included, to one CLK, one PCPK, and CK1ε [74]. However, this first screen apparently used the CDK kinase domains in the absence of their activating cyclin partners [74]. As discussed, noncyclin-bound CDKs adopt the inactive conformation at the kinase domains, whereas roscovitine binds with high affinity only to their active conformations [71, 72]. The observed affinity of roscovitine for its target CDKs was therefore 10-

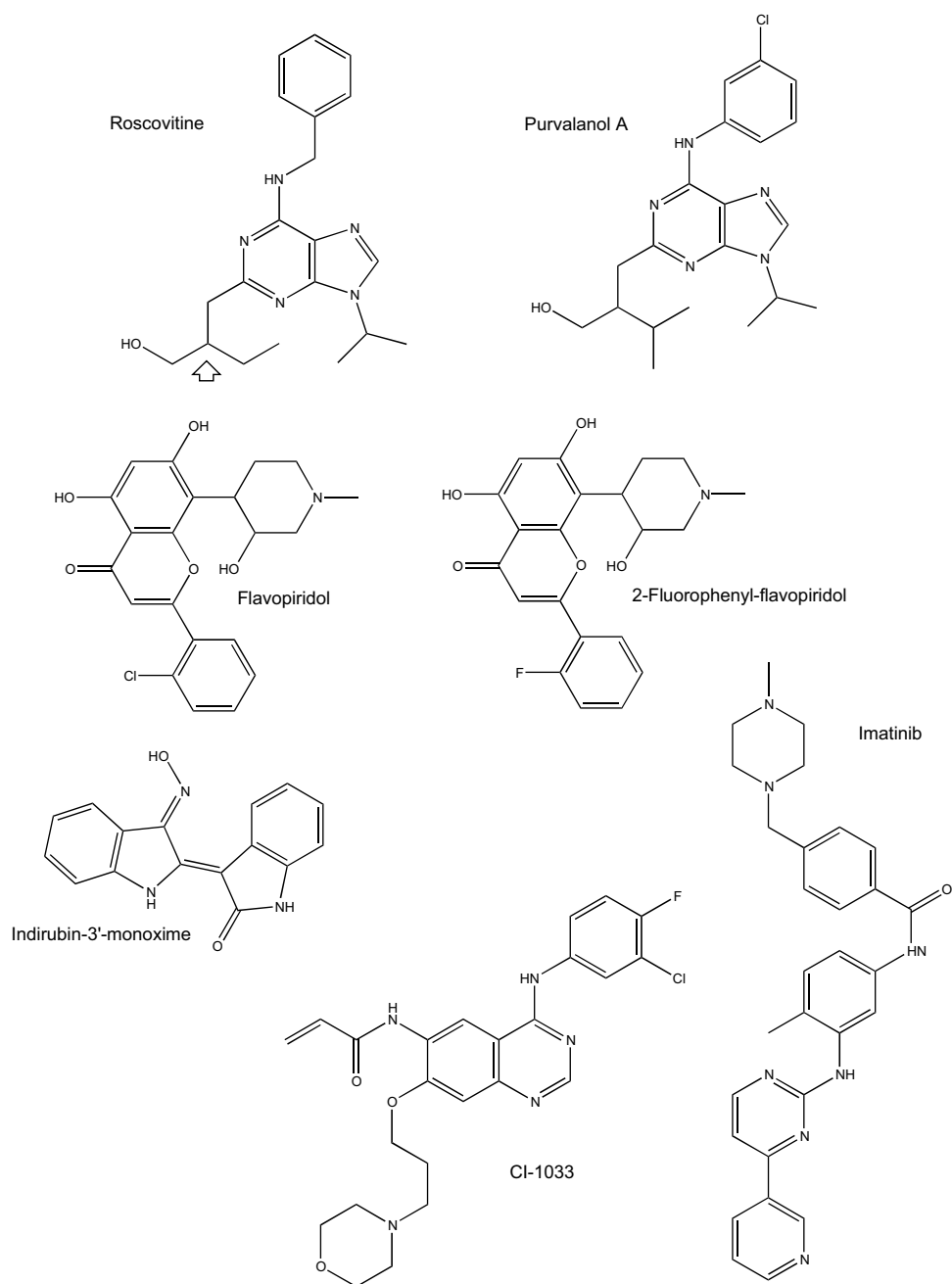


Figure 10.1 Structures of relevant protein kinase inhibitors. The structures of two oligo-specific PCIs with preference for CDK1, CDK2, CDK5, and CDK7, roscovitine and purvalanol A; two pan-specific PCIs, flavopiridol and indirubin-3'-monoxime; and a novel flavopiridol

derivative 2-fluorophenyl-flavopiridol are presented together with those of the c-Abl, KIT, and PDGFR inhibitor imatinib, and the ErbB1 inhibitor CI-1033. The upward arrow in roscovitine indicates the anomeric center that determines the R- and S-isomers.

fold lower than for the native kinases, as expected. An updated version of this screen [75], uses “full-length” CDKs (but still without their cycling partners), resulting in binding affinities approximately fivefold lower than toward the equivalent native CDK-cyclin complexes. This updated and extended screen tested 317 protein kinases, representing 61.1% of the human kinome. Among the 317 protein kinases, roscovitine bound to only 8 with similar K_d as toward cyclin-free CDK2. It is difficult to analyze how the binding affinities of roscovitine to the catalytic domain of these other protein kinases extrapolate to its binding affinities, and inhibitory potency, toward the native versions of these protein kinases. In fact, several of the kinases that bound to roscovitine with K_d similar to that of the cyclin-free CDKs are not inhibited by 10 μ M roscovitine (as tested by Invitrogen; http://www.invitrogen.com/downloads/SelectScreen_Data_193.pdf).

Roscovitine has been tested against more than 246 proteins (mostly protein kinases), and found to inhibit with low IC_{50} only CDK1, CDK2, CDK5, and CDK7 and a closely related protein kinase (CLK2), and CDK9 usually with approximately 5–10-fold higher IC_{50} (in one recent study, the R-stereoisomer of roscovitine inhibited CDK9 phosphorylation of a nonphysiological substrate, pRb, with the same IC_{50} as toward CDK2 [68]). Several other purine-containing PCIs also fail to inhibit, or bind with high affinity to a number of protein serine/threonine or tyrosine kinases, lipid kinases, phosphatases, DNA polymerases, or topoisomerases (Table 10.3). No experimental evaluation of the effects of PCIs on CDK10 or CDK11 has been published. However, the available evidence suggests that these CDKs are not likely inhibited by roscovitine. The short isoform of CDK11 plays a major role in centrosome duplication, and inhibition of CDK11 expression activates the mitotic checkpoint [38]. PCIs such as roscovitine are not known to activate this checkpoint, suggesting that CDK11 is not inhibited by the concentrations of these drugs normally used in cultured cells. Likewise, roscovitine has not been shown to have general effects on alternative splicing, suggesting that it does not inhibit CDK10 or CDK12. However, the effects of PCIs on CDK10, CDK11, and CDK12 have yet to be experimentally tested.

IC_{50} are most often approximately 20-fold lower than the concentrations required to fully inhibit a target enzyme. PCIs compete with ATP, and most often biological effects require almost complete inhibition of the target kinases. It is therefore not surprising that the concentrations of PCIs required to block biological functions [46, 62–64, 68, 73, 74, 76–80] are orders of magnitude above their IC_{50} evaluated against purified kinases and in subphysiological (approximately 100- to 1000-fold lower) ATP concentrations [46, 62–64, 68, 73, 74, 76–80].

The oligo-specific PCIs specific for CDKs involved mostly in transcription include the first PCIs identified, as well as the first PCIs with identified antiviral activities. However, most of these putatively specific early PCIs, such as DRB, have actually little specificity (reviewed in Ref. [16]). Furthermore, the most recent paper on the first PCIs identified to have antiviral activities was published in 2001 [10, 81, 82]. Roscovitine can arguably be classified in this group as well, as it inhibits recombinant CDK7 (expressed in baculovirus), and native CDK7 (highly purified or immunoprecipitated from mammalian cells) with the same IC_{50} as for CDK1 and CDK2

(approximately 0.5 μM) [73, 78, 79]. It also inhibits recombinant, baculovirus expressed, CDK9, but only at approximately 5–10-fold higher concentrations toward a physiological substrate (IC_{50} approximately 2.7–5 μM) [79, 83], or at similar concentrations toward a nonphysiological one [68]. Roscovitine did not bind to cyclin-free CDK9 in a screen against 317 human protein kinases [75]. The R-stereoisomer of roscovitine (seliciclib) was also reported to inhibit CDK9 with IC_{50} approximately 10-fold higher than toward CDK2 [84]. It is difficult to consider how such 5–10-fold differences in IC_{50} may affect inhibition of a specific CDK in cells. In extracts of HSV-1-infected fibroblasts that express very low levels of CDK9, intermediate levels of CDK2 and CDK5 and very high levels of ERK1 and ERK2, purvalanol did not bind to detectable amounts of CDK9 but bound to easily detectable amounts of CDK2, CDK, ERK1, and ERK2 [73].

The pan-specific PCIs include some of the oldest PCIs, such as flavopiridol [2-(2-chloro-phenyl)-5,7-dihydroxy-8-(3-hydroxy-1-methyl-piperidin-4-yl)-chromen-4-one] (Figure 10.1), and some of the newest ones, such as indirubin-3'-monoxime [(1*H*,1'*H*-[2,3'] biindolylidene-3,2'-dione 3-oxime)] (Figure 10.1). Although flavopiridol was among the first PCIs ever discovered, its effects on viral transcription and replication were discovered only in 2000 [85], whereas those of olomoucine and roscovitine had been already discovered in 1997–1998 [9, 11]. Flavopiridol inhibits CDK1, CDK2, CDK4, and CDK6, with IC_{50} of approximately 0.04 μM [86, 87], and CDK9 with IC_{50} of approximately 0.001–0.006 μM [83, 85, 88]. It also inhibits CDK7, but with IC_{50} of only 0.2–0.3 μM [88, 89]. When analyzed against CDK1 or CDK2, flavopiridol competes with ATP and binds to the ATP binding pocket [87, 90]. However, when analyzed against CDK9, the inhibition is noncompetitive [85], even though the binding site is still in the ATP binding pocket [91, 92]. Differing from all other PCI/CDK interactions, including those between deschloroflavopiridol and CDK2, flavopiridol induces major conformational changes on CDK9 [92]. In CDK9 bound to flavopiridol, the access to the active site becomes blocked by a movement of the so-called “G-loop,” which gates access similarly to the T-loop. The CDK9 residues lining the catalytic cleft also get reorganized, maximizing the van der Waals interactions with flavopiridol [92]. As a result, flavopiridol is almost entirely buried into the catalytic cleft, with only 8% of the molecule exposed to the solvent [92]. Such rearrangements of the CDK9 active site, together with the extensive interactions between flavopiridol and CDK9, may underlie the difficulties observed in out-competing inhibition by increasing ATP concentrations [85]. Flavopiridol also binds with high affinity to three of four CLKs tested, and to eight other protein kinases, including the receptor tyrosine kinases EphA5 or EphB1, and CamK2A [74]. It also binds to, inhibits, or modulates the activity of other proteins and even DNA (discussed in Ref. [16, 40]) (Table 10.3). Recent medicinal chemistry work has been directed at designing flavopiridol derivatives with stronger preference for CDK9 over CDK1 or CDK2 [93].

Most biological effects of flavopiridol on cultured cells occur at concentrations below its IC_{50} toward CDK1, CDK2, CDK4, CDK6, or CDK7 (at subphysiological ATP concentrations) (discussed in Ref. [1, 16, 40, 94]). Thus, its major intracellular target may be CDK9 [85]. It could also be concentrated in cells by active transporters,

or its major targets may be some of the many other cellular proteins that it targets [74].

The indirubins are components of a traditional Chinese medicine used against leukemia, Danggui Longhui Wan (for the history, the chemistry, and the biological effects of indirubins, see Ref. [16, 95, 96]). They are specific inhibitors of CDK1, CDK2, CDK5, and CDK9, with IC_{50} of approximately 0.05 μ M (CDK9), 0.1 μ M (CDK5), 0.18 μ M (CDK1), or 0.36 (CDK2) (all in 15 μ M ATP) for indirubin-3'-monoxime [89, 95]. Indirubin-3'-monoxime also inhibits GSK-3 β (IC_{50} 0.022 μ M), but it only inhibits CDK4 with IC_{50} of 3.6 μ M and does not inhibit CDK7 (IC_{50} > 4 μ M) [76]. At high concentrations, it inhibits protein kinase C β 2 (IC_{50} 2.0 μ M), and cAMP-dependent protein kinase (IC_{50} 4.0 μ M), but it does not inhibit 15 other kinases [95]. The indirubins also bind to the ATP binding pocket of the target kinases, and compete with the ATP cosubstrate [95].

10.2.2

Antiviral Activities of PCIs

Olomoucine and roscovitine were among the first PCIs found to inhibit viral replication, that of HCMV and herpes simplex virus type 1 (HSV-1) [9, 11], and their antiviral activities have been continuously studied ever since [73, 78, 89, 97–107]. As a result, the purine-containing oligo-specific PCIs are still the ones for which the antiviral activities have been the most extensively characterized. For example, purine-containing PCIs, including roscovitine, have been found to also inhibit replication of HSV-2 [73], varicella-zoster virus (VZV) [100], Epstein–Barr virus (EBV) [106], HIV [73, 78, 89, 105], and JC virus [108], as well as specific viral functions of human T-lymphotropic virus-1 (HTLV-1) [103], adenovirus [109], and several animal retroviruses [101, 102]. Another, less characterized, purine-containing PCI, CVT-313, has also been shown to inhibit activation of a retroviral promoter [102]. Although no good systems to evaluate replication of Kaposi's sarcoma herpesvirus (KSHV), or its reactivation from latency exist, PCIs have been suggested to inhibit phorbol ester-induced KSHV reactivation *in vitro* [104]. However, as a caveat of these experiments, PCIs could also have inhibited phorbol ester-induced pathways upstream of the reactivation process itself. More recent work is focusing on the pan-specific indirubins as well. Similar to roscovitine, indirubin-3'-monoxime inhibits replication of HIV-1, HCMV [89, 110], and HSV-1 (our own unpublished results). It also inhibits cellular effects of influenza virus [111].

10.2.2.1 Antiviral Activities of PCIs against Herpesviruses

The effects of several PCIs against several herpesviruses are, surprisingly, most similar to those originally described for a single PCI, roscovitine, against a single herpesvirus, HSV-1. Thus, we will use roscovitine and HSV-1 as the major model, highlighting the similarities and the differences with other PCIs and herpesviruses when necessary. The similarities of the effects of PCIs on HSV-1, HCMV, VZV, and EBV are most remarkable because these effects were analyzed using vastly different approaches. Most studies on HSV-1 were performed by infecting immortalized cells

with cell-free virus, whereas the studies with HCMV were performed mostly using primary cells, those with EBV using an inducible promoter to reactivate latent virus, and those with VZV by infecting cultures with previously infected cells. The consistency of the results observed with such different systems raises the level of confidence that the effects of PCIs on herpesvirus replication are independent of technical details.

Roscovotine and related PCIs inhibit replication of EBV, HSV-1, HCMV, and VZV at similar concentrations. Full inhibition is generally achieved at approximately 50 μ M (+/- approximately twofold), concentrations also inhibit cell cycle progression by the respective mock-infected cells [9, 11, 100, 106, 112–114]. When tested, PCIs inhibit herpesvirus replication even at late times after infection, and inhibition is reversible upon removal of the drug [11, 106, 113]. Herpesvirus replication was, in contrast, insensitive to a variety of other protein kinase or cell cycle progression inhibitors, which do not inhibit CDKs [11, 106].

PCIs such as roscovotine inhibit the accumulation of HSV-1 transcripts [11], even in the presence of the HSV-1 transactivators of gene expression [98, 99]. The inhibition of expression of reporter proteins driven by different HSV-1 promoters in the viral genome was reconfirmed in an elegant system using live cells [115]. Similar inhibitory effects have also been described for HCMV [112], EBV [106], and VZV [100]. The concentrations of PCIs that inhibit accumulation of herpesvirus transcripts consistently fail to inhibit the accumulation of representative cellular transcripts.

Surprisingly, however, roscovotine does not inhibit ongoing HSV-1 transcription, it rather prevents its activation [116, 117]. Flavopiridol, in contrast, not only inhibits ongoing HSV-1 transcription to some extent, as expected from inhibition of CDK9, but also, and more efficiently, prevents its activation [117]. Thus, the preferred targets of these PCIs may be exquisitely required to activate transcription from extrachromosomal (episomal) herpesvirus genomes. Supporting this possibility, PCIs also inhibit activation of transcription driven by episomal HSV-1 or EBV promoters in transiently transfected plasmids, but not by the same HSV-1 promoters recombined into the cellular genome [99, 106, 116]. The less specific purvalanol, in contrast, does inhibit to some extent the activation of transcription driven by an HSV-1 promoter recombined into the cellular genome, although not as efficient as it inhibits activation of transcription from the HSV-1 genome [116]. The even less specific PCI flavopiridol inhibits equally well transcription from viral or cellular genomes [116].

The specificity for the activation of transcription from viral genomes, not for specific promoter sequences, may explain in part why PCIs are so similarly active against only distantly related herpesviruses, such as HSV-2 [73], HCMV [9, 112, 113], EBV [106], and VZV [100, 114]. The specificity for viral genomes may also be a major cause of the difficulties encountered when trying to select for resistance against PCIs (as shown or discussed in Ref. [9, 11, 100]), and why HSV-1 mutants resistant to conventional antiviral drugs are still sensitive to PCIs [73]. If PCIs indeed prevent activation of transcription from extrachromosomal genomes in a sequence-independent manner, then no combination of mutations in the extrachromosomal viral genomes would lead to resistance against these drugs.

Roscovitin and related PCIs also inhibit the subcellular localization of herpesvirus proteins, such as the VZV immediate-early protein IE62 [100, 114], and posttranslational modifications and activity of regulatory proteins such as HSV ICP4 or ICP0 [118, 119], and VZV IE63 [114]. They also inhibit herpesvirus DNA replication, even when all required viral replication proteins are expressed [9, 112]. Consequently, they inhibit replication of HSV, HCMV, and EBV even when treatment is started at late times after infection (up to 16, 24, or 48 h for HSV-1, EBV, or HCMV, respectively) [11, 98, 106, 112]. Roscovitin also inhibits even later functions of VZV and HCMV [113, 120]. For HCMV, this effect is likely mediated by downregulation of expression of the structural proteins pp150, gB, and IE2-86, and induction of mislocalization of pp69 [113]. For VZV, these effects are likely mediated by inhibition of phosphorylation of the cytoplasmic tail of the structural protein gI [120]. Roscovitin also inhibits formation of syncytia by HSV-1 [107]. The inhibition of multiple viral functions by PCIs results in two highly desirable features for antiviral drugs, minimization of the selection for resistance and ability to inhibit viral replication at any time after the infection.

Purine-containing PCIs also inhibit herpesvirus reactivation from latency *ex vivo* (for HSV-1, [121]) or in culture (for EBV, [106]). For both viruses, PCIs appear to actually prevent reactivation, in that expression of no viral protein was detected when the reactivation was induced in the presence of these drugs [106, 121]. Thus, in this respect, PCIs also differ from all conventional antiviral drugs, which can only act after the targeted viral proteins are expressed. Therefore, conventional antiviral drugs can only act on already reactivated virus. Whether or not PCIs also inhibit reactivation of latency by HCMV or VZV has been reported, in most likelihood due to the technical difficulties in studying the reactivation of either of these viruses.

However, there are also some important differences in the effects of PCIs on HSV, HCMV, VZV, or EBV replication. For example, roscovitin inhibits activation of transcription of all tested (and likely all) HSV-1, VZV, or EBV genes [11, 98, 106, 116, 122], but it has differential effects on the expression of different HCMV genes [112]. PCIs inhibit to great extent the expression of the so-called IE1-72 HCMV protein, while activating that of IE2-86. These two proteins are expressed from alternatively spliced transcripts from the same transcriptional unit. Roscovitin also has differential effects on the expression of two other alternatively spliced IE genes of HCMV, UL31x1, and UL37 [112]. Expression of UL31x1 is inhibited, whereas that of UL37 is not. In this respect, there are also major differences in the regulation of HSV-1, HCMV, VZV, or EBV gene expression. Most HSV-1 or VZV proteins are expressed from nonspliced transcripts, whereas many HCMV or EBV proteins are expressed from alternatively spliced ones. It is currently unclear why differential splicing by HCMV is affected whereas that by EBV is apparently not. These differential effects on viral alternative splicing strongly suggest that either they are not mediated by inhibition of the CDKs involved in splicing (such as CDK11) or different herpesviruses have differential requirements for these CDKs.

The pan-specific PCI flavopiridol also inhibits the alternative splicing of IE1-72 and IE2-86 [112], but its effects on HCMV replication have apparently not been evaluated.

In our own (unpublished) experiments, flavopiridol was too cytotoxic for the cells in which HSV-1 replicates as to evaluate its true antiviral effects.

Targets of the Activities of PCIs against Herpesviruses The only known common targets for all the PCIs that inhibit herpesvirus replication are CDK1, CDK2, CDK5, CDK7, and at higher concentrations CDK9. Although other yet unknown common targets may also exist, no experimental evidence to support them has been published. Thus, not surprisingly, it has been generally suspected that the cellular protein kinases required for herpesvirus replication are among these known common targets.

The first studies on HCMV and HSV-1 suggested that the most likely target was CDK2. CDK2 localization was dysregulated in HCMV infections, and its kinase activity was activated in infected cells [9, 123, 124]. For HSV-1, the evidence was more indirect. HSV-1 establishes latent infections, in which all viral promoters are silenced, in neurons that express no CDK1, CDK2 or their activating cyclins, but express CDK5, CDK7, and most likely also CDK9. *Ex vivo* induced HSV-1 reactivation from latency occurs only in neurons in which the expression of CDK2 and its activating cyclins E and A is induced by the stress of explantation [121, 125]. In contrast, the expression of CDK1 or cyclin B is not induced, whereas that of CDK7 is downregulated [121, 125]. Furthermore, PCIs inhibit HSV-1 transcription in lytic infections mainly at a level at which neither CDK7 nor CDK9 are known to play limiting roles [116, 117]. The more recent studies on EBV also concluded that the most likely target was CDK2, although CDK1 was not fully excluded [106]. This conclusion was based mostly on the inhibition of accumulation of the physiological CDK inhibitors p21 and p27 in cells in which EBV reactivates, and in the patterns of phosphorylation of known CDK2 substrates under similar circumstances [106]. CDK2 is also proposed to be the major target of the anti-KSHV activities of PCIs. Although the vCyc encoded by KSHV and related viruses directly or indirectly activate CDK6 and CDK2 [126–129], CDK6 is not sensitive to inhibition by roscovitine. Furthermore, CDK2 has been proposed to mediate most of the downstream effects of these vCyc [126, 127, 130, 131].

In contrast, the first study on the effects of roscovitine on VZV suggested that CDK1 was the main target [132]. The phosphorylation inhibited by roscovitine occurs in the cytoplasm (where CDK1 localizes for most of the cell cycle), and can be performed *in vitro* by purified CDK1 [132]. CDK1 was also concluded to be the most likely target for the effects of roscovitine on inhibition of VZV transcription. Roscovitine inhibits phosphorylation of the VZV transcriptional regulator IE63 [114], and induces its nuclear accumulation. VZV IE63 is phosphorylated *in vitro* by purified CDK1 or CDK5, but not by CDK2, CDK7, or CDK9 [114], being perhaps the only protein that is phosphorylated *in vitro* differentially by CDK1 or CDK2. CDK1 and CDK5 are mostly cytoplasmic, thus suggesting that cytoplasmic phosphorylation of VZV IE63 inhibits its nuclear import [114]. However, these studies still do not explain how the nuclear accumulation of a transcription regulator inhibits its (nuclear) transcriptional regulatory activities. One study also suggested that the inhibition of phosphorylation of HSV-1 ICP4 by roscovitine resulted from inhibition of CDK1 [119]. However, this

scenario appears less likely. ICP4 is mostly nuclear, and it does not accumulate in the cytoplasm (where CDK1 is located) in the presence of roscovitine. In contrast to PCIs, kinase inactive ("dominant negative") CDK1 mutants failed to inhibit replication of HSV-1 [133] (which requires ICP4) or HCMV [110]; further supporting the hypothesis that CDK1 is not a major target of the effects of PCIs on the replication of these two viruses. However, these CDK1 mutants did inhibit the accumulation of a late HSV-1 transcript, indicating that CDK1 does play a minor role in HSV-1 replication [133]. Two other studies concluded that it was not possible to differentiate whether CDK1, CDK2, CDK5, CDK7, or perhaps even CDK9, were the kinases to most likely mediate the effects of roscovitine on another HSV-1 protein, ICP0 [118, 134].

CDK7 or CDK9 may also mediate some of the effects of a PCI on HCMV [135]. HCMV infection induced expression of these two CDKs and their activating cyclins, as well as hyperphosphorylation of serines 2 and 5 in the heptad repeats of the carboxy-terminal domain (CTD) of RNA polymerase II. These hyperphosphorylations were partially inhibited by roscovitine [135]. In agreement with current models, the enhanced hyperphosphorylation of the CTD was proposed to provide docking sites for processing factors to regulate the alternative splicing of the primary HCMV transcripts [135]. However, CDK7, CDK9, and hyperphosphorylation of RNA polymerase II were most significantly induced, and roscovitine had the most significant effects on them, at late times after infection [135]. In contrast, roscovitine affected alternative splicing of the IE1-72 and IE2-86 mainly at early times in infection [135].

The possibility that CDK7 or CDK9 were the main targets of the antiherpesvirus activities of PCIs was actually first discussed and explored with HSV-1 [11, 73]. It was in fact from these studies that CDK7 was first identified and characterized as a bona fide target for roscovitine, and CDK8 as resistant to inhibition by this compound [73]. However, neither CDK7 nor CDK9 were expressed in the neurons that supported HSV-1 gene expression during *ex vivo* induced reactivation [121], and CDK9 was expressed only to low levels in cultured cells that support HSV-1 replication [73]. Purvalanol inhibited HSV-1 replication but did not bind to detectable levels of CDK9 in extracts of the infected cells (which express low levels of CDK9), whereas it did bind to CDK2, CDK5, and CDK7 and ERK1 and ERK2 (which are all expressed at high levels in these cells) [73]. Furthermore, the concentrations of roscovitine that fully inhibit activation of HSV-1 transcription do not inhibit cellular transcription [116, 117], which requires CDK7 and CDK9. Similar results have also been obtained with other purine-containing PCIs and HCMV, VZV, or EBV, further suggesting that the effects of PCIs on herpesvirus transcription are not fully mediated by their potential inhibition of CDK7 or CDK9. However, it is still possible that the inhibition of these kinases does contribute to the overall antiviral effects of these drugs.

It is perhaps disappointing that the targets of the antiherpesvirus effects of PCIs remain incompletely defined. However, CDKs are now known to be functionally redundant [32, 136–139]. Several CDKs may be able to provide the cellular functions required for herpesvirus replication and thus inhibition of no single one may inhibit viral replication. The redundancy of CDKs suggests that less specific PCIs (i.e., oligo-specific) may actually be better antiviral drugs than highly mono-specific ones.

Although this possibility remains to be directly tested, no single putatively mono-specific PCI has yet been reported to inhibit replication of any herpesvirus. Likewise, inhibition of a single CDK by either dominant-negative kinase mutants, antisense, or siRNAs has never been proven to inhibit replication of a herpesvirus.

10.2.2.2 Antiviral Activities of PCIs against HIV

CDK9 has been known to be required for HIV replication for many years. CDK9 is the protein kinase recruited by Tat to the TAR-structure in the early transcription complexes to phosphorylate the CTD of RNA polymerase II to stimulate its processivity [140–143]. Thus, CDK9 activates elongation of HIV transcription after the first 30 bases. The activity of CDK9 has likewise been known for many years to be induced by many stimuli that activate HIV replication [144]. CDK9 has consequently been considered as a potential target in HIV therapy also for many years. In fact, the first antiviral activity ever shown for PCIs was the inhibition of HIV transcription and replication by the “CDK9-specific” PCIs [10, 81]. Unfortunately, the last publication on these drugs was published in 2001 [82].

Due in part to the experiments showing that PCIs inhibited transcription and replication of herpesviruses, the effects on HIV functions of the pan-specific PCI flavopiridol started to be studied in 2000 [85]. Since 2001, HIV replication in human primary or immortalized cells has been shown to be inhibited also by several oligo-specific PCIs, including roscovitine and purvalanol, and by the pan-specific flavopiridol and indirubin-3'-monoxime [73, 78, 83, 84, 93, 105, 145–147].

As a potentially important activity for antiviral drugs, PCIs appear to differentially induce death of HIV-infected cells. Wang *et al.* observed in 2001 that purine-containing PCIs preferentially induce killing of chronically infected ACH₂ or monocytic U₁ cells over non-HIV-infected parental CEM or U937 cells [78]. This preferential killing was found to result from the differential induction of apoptosis [78]. Similar results have been more recently reported, albeit not published, for a number of PCIs and HIV-infected cells [145]. Such a differential induction of apoptosis on chronically HIV-infected cells could play a major role in eliminating the reservoirs of HIV in patients simultaneously undergoing standard highly active antiretroviral therapy (HAART)

Similar to their effects on herpesviruses, PCIs also inhibit HIV reactivation from latency in culture [78, 89, 105]. Seliciclib added after induction still inhibits TNF α -induced reactivation of HIV in chronically infected OM 10.1 or U₁ cells [105]. Under this protocol, the effects of roscovitine on reactivation cannot be secondary to any potential inhibition of expression of the TNF α -responsive cellular genes. Indirubin-3'-monoxime also inhibits Tat-induced HIV reactivation in immortalized and chronically infected monocytes. Similar to the effects of other PCIs on herpesviruses, it did so only at higher concentrations than those required to inhibit purified CDKs [89].

As expected, and first demonstrated for HSV-1, PCIs inhibit replication of many unrelated HIV strains, on many different cell types. For example, indirubin-3'-monoxime inhibits replication of R5- or X4-tropic HIV strains in permissive immortalized cells or primary peripheral blood monocytic cells (PBMCs) [89]. They also inhibit equally well replication of multidrug resistant HIV strains or wild-type

HIV. Roscovitine inhibits replication of L10R/M46I/L63P/V82T/I84V and RTMDR/MT-2 [73], for example. These HIV strains are resistant to multiple protease or reverse transcriptase inhibitors (including nucleoside and nonnucleoside ones), respectively. Roscovitine also inhibits replication of HIV strains resistant to AZT, 3TC, TIBO, or proteinase inhibitors (strain PR-V82F/184V) [105]. Indirubin-3'-monoxime inhibits the replication of strains RT MDR and CC101.19, resistant to multiple RT inhibitors or to CCR5 antagonists, respectively [89].

The concentrations of the purine-containing PCIs required to inhibit HIV replication are in the range of 10–15 μ M, approximately the same concentrations that inhibit cell cycle progression in the respective mock- or noninfected cells [73, 78, 105]. HIV replication may perhaps be slightly more sensitive to roscovitine than cell cycle progression [78, 105], but it is not yet clear if such small differences have major biological consequences. Moreover, the potency of PCIs on HIV replication and their toxicity depend on multiple factors, such as specific cell type and duration of treatment (for example, see Ref. [83]). Similar to those of roscovitine, the concentrations of indirubin-3'-monoxime that inhibited HIV replication in cultured immortalized cells had no major effects on cell cycle progression for 48 h [89]. More importantly, indirubin-3'-monoxime did not inhibit cell proliferation or viability of PBMCs, the cells actually infected by HIV *in vivo*, for 28 days at 4 μ M, concentration at which it does inhibit HIV replication [89].

Very recently, a systemic medicinal chemistry approach was undertaken to improve on the anti-HIV activities of flavopiridol [93]. Several substituents were tested in positions 2, 3, and 4 of the 2-chlorophenyl group ("C-ring") of flavopiridol or its D-ring olefin analogue. Several of these compounds maintained anti-HIV potencies very close to, or even higher than that of flavopiridol with decreased cytotoxicity. The 5-methylisoxazole flavopiridol derivative had the highest selectivity index (SI, 184), and potency against HIV replication (IC_{50} , 3.5 nM), although its potency against CDK9 was slightly decreased in comparison to that of flavopiridol (IC_{50} , 19.9 nM, or 9.1 nM, respectively). The 2-fluorophenyl derivative had the second highest SI (36), while maintaining the same potency as flavopiridol toward CDK9 (IC_{50} , 2.8 nM), and slightly increased toward HIV (IC_{50} , 7.5 nM, in comparison to 9.1 nM for flavopiridol). The latter compound was further characterized in uninfected cultured cells. It inhibited the accumulation of cellular transcripts that are highly dependent on CDK9 activity, but not that of transcripts that are more dependent on cell cycle progression (and therefore on CDK2 activity). In contrast, flavopiridol inhibited the accumulation of the transcripts dependent on either CDK2 or CDK9 [93]. The compound was analyzed against a panel of 18 protein kinases. It inhibited CDK9 with the highest potency (IC_{50} , 2 nM), then CDK5/p35 (IC_{50} , 86 nM) and then CDK1/cyclin B and CDK2/cyclin A (IC_{50} , 123 and 350 nM, respectively). It did not inhibit any other of the tested protein kinases, including CDK7/cyclin H/MAT1 (IC_{50} > 10 μ M) [93]. Similar to the recently described purine-containing CR8 [68], and in contrast to the earlier CKD inhibitors, the 2-fluorophenyl flavopiridol derivative can discriminate between CDK1, CDK2, and CDK5 and CDK9 or CDK7. Careful analyses of the potencies against purified CDK9 and the effects on HIV replication indicate that the inhibition of HIV replication by several of these new

flavopiridol derivatives is not likely to be an exclusive result of inhibition of CDK9. For example, the 5-methylisoxazole derivative had an IC_{50} toward CDK9 10-fold higher than that of the 2-fluorophenyl one yet it inhibited HIV replication with a twofold lower IC_{50} [93].

These recent results may raise continuing interest in further using medicinal chemistry to optimize inhibitors of cellular protein kinases to inhibit viral replication and have no ill effects on infected cells.

Targets of the Activities of PCIs against HIV HIV transcription requires CDK9 [10, 81, 147, 148], and flavopiridol and the “CDK9-specific” PCIs potently inhibit elongation of HIV transcription, suggesting that their primary antiviral target is indeed CDK9 [10, 81, 85]. Indirubin-3'-monoxime inhibits expression of full-length HIV transcripts, but not of the first 29 bases of the primary transcript, also strongly suggesting that its anti-HIV effects are mediated by inhibition of CDK9 [89]. However, flavopiridol and the “CDK9-specific” PCIs also inhibit transcription or replication of HIV strains with mutations in Tat or TAR, and which should thus not respond to activation by CDK9 [78, 82], and late HIV replication, which is not inhibited by kinase inactive (“dominant-negative”) CDK9 mutants [81]. Furthermore, flavopiridol inhibits *in vitro* transcription elongation from cellular or viral transcripts at similar concentrations [149], whereas it inhibits HIV replication *in vivo* at concentrations that are too low to inhibit cellular transcription [85]. Thus, the effects of the “CDK9-specific” PCIs on HIV replication do not appear to be entirely mediated by inhibition of CDK9 alone.

The inhibitory effects of oligo-specific PCIs on HIV transcription and replication do not appear to be fully accounted for by their inhibition of CDK9 either. Roscovitine inhibits transcription driven by transiently transfected HIV LTR promoters in the presence or absence of Tat and, similar to the “CDK9-specific” compounds, it also inhibited transcription of HIV Tat-TAR mutants [78].

Thus, PCIs inhibit not only HIV transcription in great part as a result of inhibition of CDK9 but also HIV functions in the absence of the Tat-TAR interactions required to recruit CDK9 to nascent HIV transcripts. Furthermore, no HIV resistance to any PCI has been reported. This would be highly unexpected if their only target was indeed CDK9, which is required for a single HIV function. One would anticipate then that PCIs should have selected for HIV mutants that replicate independently of CDK9. It is possible that other protein kinases inhibited by these drugs participate in HIV, but not cellular, transcription. For example, CDK2 may be required together with CDK7 and CDK9 for initiation and elongation of HIV transcription [150]. It is also possible, and even likely, that PCIs inhibit several HIV functions beyond their inhibition of transcription elongation. However, such potential effects are still only speculative, as they remain to be experimentally evaluated.

In summary, several PCIs have been demonstrated by different groups to inhibit replication of a variety of HIV strains in a variety of immortalized or primary cells. The effects against HIV were not affected by many different mutations that confer resistance to conventional antiviral drugs, including several mutations in the RT

(which could have been considered likely to be a possible target for purine-containing PCIs) [73, 78, 89, 105].

10.2.2.3 Antiviral Activities of PCIs against Other Viruses

Consistent with the hypothesis that PCIs inhibit other retroviral functions beyond transcription, they inhibit replication of human and animal retroviruses not known to require CDK9 [101–103]. Most of these retroviruses, including the HTLV-1 are oncogenic, and thus PCIs could inhibit at once viral functions and pathogenic mechanisms. For HTLV-1, the target was concluded to be CDK2. This kinase associates with HTLV transcription complexes and similar to the PCIs, the physiological CDK2 inhibitory regulator p21 also inhibits HTLV-1 transcription [103]. Likewise, CDK2 was concluded to be the major target for the effects of a PCI against a murine oncogenic retrovirus [102]. The regulatory phosphorylation that is inhibited by PCIs in this model is on Histone H1, which is phosphorylated at this site by CDK2.

Many other viruses are also involved in oncogenesis. For example, human papilloma viruses such as HPV16 are the etiological agents of most cervical cancers. Oncogenesis requires overactivation of the CDKs involved in cell cycle regulation. Thus, it is not surprising that viral oncoproteins regulate CDK activities [131, 151–153]. For example, the oncogenic E7 protein of the HPV16 activates CDK2 [154]. It also induces unscheduled DNA synthesis, chromosome instability and centrosome duplication. All these activities, which most likely contribute to oncogenesis, require CDK2 activity. Consequently, they are all inhibited by PCIs [155–157]. For example, 0.01–1.0, μM indirubin-3'-monoxime inhibits the centrosome reduplication and the chromosome instability induced by HPV16 [157]. These concentrations do not inhibit cellular DNA synthesis (during short time) or the physiological centrosome duplication required for normal cell cycle progression. The inhibition is overcome by overexpression of CDK2 together with its activating cyclins, and is reproduced by overexpression of siRNA specific for CDK2 or kinase inactive ("dominant negative") CDK2 mutants. Thus, it was concluded that the main target of the effects of PCIs against HPV-induced transformation is CDK2 [157].

Similar to HPV, polyomaviruses replication is known to require of CDK activities. For example, the DNA replication functions of the polyomavirus large T antigen (T Ag) protein are activated by CDK2 phosphorylation. It is perhaps surprising that the effects of PCIs on replication of a polyomavirus, JC virus, were tested only in 2008 [108]. Roscovitine inhibited polyomavirus replication and gene expression in susceptible IMR-32 cells at 10 μM , concentration that had no cytostatic or cytotoxic effects on noninfected cells for up to 24 days, or on infected cells for up to 30 days [108]. When tested in simplified models, roscovitine inhibited expression of a reporter gene driven by the late promoter of JC virus, but not of the same reporter driven by the early JC virus promoter. However, even expression driven by the late promoter was inhibited by only 50%, which is unlikely to account for the drastic antiviral effects. The most likely target of inhibition in this system is DNA replication. Roscovitine at 10 μM inhibited large T antigen-dependent DNA replication in transfected cells, without inhibiting cellular DNA replication in the same cells [108]. This concentration of roscovitine had no effect on the levels of ectopically expressed

large T antigen. In contrast, roscovitine did inhibit the CDK-dependent phosphorylation of the large T antigen [108], phosphorylation that is required for its DNA replicative functions.

PCIs are now starting to be tested against viruses that would not be obviously expected to be sensitive to inhibition of CDK activities. For example, influenza virus does not require the cellular proteins that are the most likely mediators of the antiviral effects of PCIs. Its pathogenesis does not include unrestricted cell proliferation either. Nonetheless, 1–10 μM indirubin-3'-monoxime inhibits overexpression of RANTES by infected cells [111]. Although the secretion of cytokines has been often hypothesized to play major roles in the respiratory pathogenesis of influenza virus [158], the effects of PCIs on its pathogenesis have yet to be analyzed. So have the identities of the kinases that mediate inhibition of RANTES expression.

In contrast to the viruses discussed above, PCIs do not inhibit the replication of vaccinia or lymphocytic choriomeningitis virus (LCMV) [73], which are thought to replicate independently of CDKs. However, the pathogenesis of vaccinia virus does include unregulated cell proliferation, and it might thus be inhibited by PCIs, and interesting possibility that remains untested.

10.2.3

PCIs Can be Used in Combination Therapies

Even though PCIs are functionally equivalent to combination antiviral therapies, in that they result in the inhibition of multiple viral functions, they can be further combined with other antivirals. Three different approaches to combination therapies including PCIs have been tested. PCIs have been tested in combination with traditional antiviral drugs that target viral DNA replication, with protein kinase inhibitors targeting viral protein kinases, or even in combination with other PCIs.

When combined with acyclovir, which is activated by the HSV thymidine kinase and inhibits the HSV DNA polymerase (and acts as a chain terminator), roscovitine and purvalanol were most likely additive against wild-type or acyclovir-resistant strains of HSV-1 [73]. When combined with maribavir, which inhibits the HCMV protein kinase, indirubin-3'-monoxime was most likely synergistic [110]. The inhibitory effects of subinhibitory concentrations of maribavir (0.4 μM) were thus enhanced by approximately 500-fold by minimally inhibitory concentrations of indirubin (10 μM) [110]. When combined with each other, PCIs were additive or synergistic [145]. Combinations of any two of nine PCIs of different chemical structures (which individually all inhibit HIV replication) have better selectivity for HIV-infected over uninfected primary T-lymphocytes or macrophages than any of the PCIs by itself [145]. However, these latter studies have yet to be published, and the PCIs combined have different toxicities, which may well result in additive or synergistic toxic effects. Combination of different PCIs have yet to be tested in animals. Therefore, the potential enhanced toxicities remain to be tested before this approach can be pursued any further.

10.2.4

PCIs Inhibit Viral Pathogenesis

The concentrations of PCIs that inhibit viral replication in cultured cells most often also inhibit cell cycle progression. Surprisingly, such concentrations appear to be well tolerated by animals, and even human beings (discussed in Refs [16, 40, 41, 159]). Most cells in the body are arrested for very long periods without ill effects. In contrast, most cultured cells become irreversibly arrested, or even undergo apoptosis, when cell cycle progression is inhibited [160–166]. The true SI of PCIs therefore cannot be evaluated in culture. Even for indirubin-3'-monoxime, which inhibits HIV replication at lower concentrations than those required to inhibit cell cycle progression, the apparent SI is only approximately 4 [89]. In contrast, apparent SI for clinical antivirals is generally ≥ 100 . However, several of the CDKs or cyclins that appear essential in cultured cells are disposable (or redundant) in mice. Single knockouts of CDK2, CDK4, CDK6, cyclins D1, D2, or D3, E1, E2 or A1 result in only limited phenotypes, and even several double or triple knockouts fail to inhibit cell cycle progression (reviewed in Ref. [32, 167]). Thus, it is obvious that cells can cycle (almost) normally in the absence of CDK2, CDK4, or CDK6. The roles of the different CDKs may overlap to such extent that the function of any one of them can be replaced with the activities of the others. Alternatively, certain CDKs may actually be nonessential. In any case, the limited toxicities displayed so far by PCIs in animals and humans are entirely consistent with the nonessential nature of the CDK targets. Such nonessential nature, in turn, supports CDKs as targets for clinical antiviral drugs.

To date, there are no published experimental demonstrations of inhibition of viral replication in animal models by any PCI although preliminary evidence of inhibition of VZV replication in a mouse model was reported at the 2009 International Conference on Antiviral Research [168]. Nonetheless, two PCIs have been demonstrated to inhibit viral-induced pathogenesis, roscovitine and flavopiridol [169–172]. One of the complications of HIV infection, particularly in African-Americans, is the so-called HIVAN (HIV-associated nephropathy), a proliferative and inflammatory kidney disease. The pathogenesis of HIVAN is partially recapitulated in a transgenic mice model, in which HIV Nef is expressed from integrated, defective, HIV provirus. Nef is expressed in epithelial renal cells, among others, producing a kidney proliferative disease with many similarities to HIVAN. The clinical and histological pathology of HIVAN in TG26 mice was inhibited by seliciclib or flavopiridol [169, 170] in the absence of negative side effects. Both these PCIs also corrected the dysregulation of gene expression observed in the HIVAN kidneys [169, 170], and neither affected the expression of other genes. Flavopiridol, but not roscovitine, inhibited the expression of the integrated HIV *nef* transgene [169, 170], which is consistent with their differential effects on expression of viral transgenes in cultured cells [116]. Unfortunately, the integrated proviruses in the TG26 genome are defective and consequently cannot replicate. The effects of PCIs on HIV replication *in vivo*, therefore, still remain to be tested.

Among other diseases, EBV produces a cancer, which is highly prevalent in Southeast Asia, that affects the throat region, nasopharyngeal carcinoma. Nasopharyngeal carcinoma is a late consequence of EBV infection, which does not require ongoing EBV replication. Roscovitine induced apoptosis of cells from nasopharyngeal carcinomas both in culture and in transplanted immunocompromised mice [173]. Based on such positive results, the effects of roscovitine were tested on nasopharyngeal carcinoma patients. Results from the first phase II clinical trials, which were recently published, show that roscovitine inhibited both the tumor growth and the levels of EBV DNA in plasma [171, 172]. These limited trials involved only 20 patients. Nonetheless, they were the first demonstration of the effects of PCIs on virus-induced pathologies and on virus replication in naturally infected human beings. Since nasopharyngeal carcinoma does not require ongoing EBV replication, and most EBV replication occurs in cells that are not in the tumor, the two effects were most likely independent of each other. It appears that the clinical trials of seliciclib (roscovitine) on EBV-induced nasopharyngeal carcinoma are continuing. Therefore, we should know in the near future the actual antiviral effects of PCIs in human beings.

10.3

Antiviral Activities of Inhibitors of Other Cellular Protein Kinases

Many of the protein kinase inhibitors developed against noninfectious diseases target protein kinases that participate in viral pathogenesis (discussed in Ref. [40, 174]). For example, imatinib [4-(4-methyl-piperazin-1-ylmethyl)-N-[4-methyl-3-(4-pyridin-3-yl-pyrimidin-2-ylamino)-phenyl]-benzamide] (Figure 10.1) is a clinical anticancer drug that targets c-abl, and the receptor tyrosine protein kinases Kit [175] and PDGF receptor (PDGFR) [176, 177]. Its major clinical use is against chronic myelocytic leukemia (CML). However, the major targets of imatinib are also either upregulated in KSHV-infected cells [178], or participate in the pathogenesis of KSHV-induced KS [179]. The technical difficulties in analyzing KSHV replication in cultured cells have so far prevented thorough analyses of the potential effects of imatinib (or any other protein kinase inhibitor) in KSHV replication. However, taking advantage of imatinib anticancer activities, its effects on KS have been evaluated in clinical trials [180]. Encouraging, and perhaps not surprisingly, imatinib appears to inhibit the pathogenesis of KS in AIDS patients [180]. However, unexpectedly, imatinib appears to also produce undesirable negative side effects at lower concentrations in KS-AIDS patients than in CML patients [180]. The higher toxicity for KS/AIDS patients does not result from a defect in drug metabolism or excretion. In fact, the plasma levels of imatinib and its major metabolite in all KS/AIDS patients are below those that are well tolerated in CML patients [180]. Imatinib may perhaps have the negative interactions with HAART, but the actual mechanisms of the enhanced toxicity, or even a confirmation of it, await further studies. In any event, the toxicities were not limiting to the therapeutic effects, and, consequently, larger Phase II clinical trials are already ongoing (NCT00090987).

Imatinib was also effective against poxvirus infection in cultured cells and mice models. Although imatinib did not inhibit poxvirus replication in already infected cells, it did inhibit the release of extracellular enveloped virions (EEVs) [181]. These effects are most likely mediated by inhibition of Abl, which together with Src localizes to the actin tails that mobilize vaccinia virions inside the infected cells. Release of EEV was inhibited by 10 μ M imatinib and cell-to-cell spread by 10 μ M PD-166326 (which inhibits Src kinases) [181]. Imatinib was also effective against vaccinia pathogenesis in a mouse model. Mice treated with a continuous infusion of 100 mg/kg per day (via an osmotic pump), were infected with vaccinia virus (2×10^4 PFU; i.p.). Imatinib inhibited infection spread in 4 days, decreasing the number of vaccinia genomes in the ovaries (site of secondary infection) by at least 1000-fold in most animals, and by more than 100 000-fold in approximately half of them [181]. Imatinib also protected against a lethal intranasal infection [181].

Another group of cellular protein kinases that are of interest in the development of anticancer drugs are the receptor protein tyrosine kinases Erbs. Erbs are involved in several human malignancies, such as breast cancer. Some of the many specific inhibitors of this protein kinases are therefore already being clinically tested as potential anticancer agents [182]. Erbs have long been known to be involved also in poxvirus replication and pathogenesis [183–185]. For example, deletion of a vaccinia-encoded ligand for Erb1 (so-called VGF) attenuates vaccinia pathogenesis by approximately 2000-fold [184]. CI-1033 [*N*-[4-(3-chloro-4-fluoro-phenylamino)-7-(3-morpholin-4-yl-propoxy)-quinazolin-6-yl]-acrylamide] (Figure 10.1), one the small molecule Erb1 inhibitors undergoing clinical trials, inhibits vaccinia virus spread in cultured cells, although it does not inhibit replication in the already infected cells [186]. As expected, significantly higher concentrations of CI-1033 are necessary to inhibit viral spread in cultured cells than its *in vitro* IC₅₀ against purified Erb1 (10 μ M and 0.8 nM, respectively). CI-1033 (1 mg/day, i.p. for 8 days starting 6 h before infection) also inhibits vaccinia pathogenesis in a lethal mouse model, even though it does not inhibit viral replication at the primary site of infection [186]. Shorter treatments result in delayed (and reduced) lethality. Unfortunately, this drug is ineffective if treatment is delayed until 2 days postinfection [186]. CI-1033 may have clinical use as preventive, or immediate postexposure, prophylaxis. Thus, it may be useful, together with ring vaccination, in containing any future poxvirus outbreak, should it ever occur.

10.4

Conclusion

Viral and cellular protein kinases are coming of age as targets for antiviral drugs. Both types of protein kinases can be targeted by drugs developed using the broad expertise that currently exists in protein kinase inhibitors. However, the specific approaches are actually very different. To target viral protein kinases, the existing expertise must be used to develop novel drugs against also novel targets. The development of

antiviral protein kinase inhibitors targeting cellular protein kinases, in contrast, only requires testing the antiviral activities of drugs already developed against noninfectious diseases. There are also major differences in the strengths and the limitations of each type of targets.

Viral protein kinases are functionally equivalent to any other virally encoded target. Their specific inhibitors are thus inherently safe, in that these kinases are only expressed in infected cells. However, this approach is limited to viruses encoding functionally important protein kinases, such as HCMV, or the members of the Rotaviridae and Poxviridae families, and selection for resistance is likely to be a limiting factor [5–8]. Moreover, the only viral protein kinase inhibitor that reached clinical trials is currently undergoing reevaluation due to the lack of effectiveness against HCMV in its first Phase III clinical trial.

Cellular protein kinases, in contrast, are equivalent to all other potential cellular targets. They can minimize selection for resistance, and also offer the potential to target multiple viruses with a single drug. Inhibitors of cellular protein kinases can relatively easily be developed against the viruses with small genomes, which encode for few viral targets. They can be active against variants resistant to conventional antiviral drugs, as these variants have mutated viral proteins, which are not targeted by inhibitors of cellular protein kinases. The potential for toxicity could be a limiting factor, but in most cases the toxicity of such inhibitors will be thoroughly tested during their development against noninfectious diseases. As a word of caution, the preliminary clinical trials on imatinib against KS in AIDS patients have highlighted the possibility that the toxicities of inhibitors of cellular protein kinases may actually differ in patients infected with viruses and undergoing standard antiviral therapy from those described in other patients.

Many cellular protein kinases are involved in viral replication and pathogenesis, and many specific protein kinase inhibitors have been developed; many more are still being developed. The protein kinases are thus most promising as potential targets for novel antiviral drugs targeting cellular proteins. The coming years will test the potential of this novel approach to antiviral development.

Acknowledgments

The author wishes to thank colleagues who have so often shared exciting unpublished results. Luis M. Schang is a Burroughs-Wellcome Fund Investigator in the pathogenesis of Infectious Disease. The studies have been supported by CIHR, the Burroughs-Wellcome Fund, PrioNet Canada, and APRI. The laboratory in which the studies have been carried out was equipped with the funds provided by the AHFMR and the Faculty of Medicine and Dentistry of the University of Alberta. Tables 10.2 and 10.3 are based on the original ones by Mireille R. St. Vincent and Jonathan J Lacasse, respectively; the author likes to extend special thanks to both of them.

References

- 1 Schang, L.M. (2004) *Biochimica et Biophysica Acta Proteins and Proteomics*, **1697**, 197–209.
- 2 Zimmermann, A., Wilts, H., Lenhardt, M., Hahn, M., and Mertens, T. (2000) *Antiviral Research*, **48**, 49–60.
- 3 Marschall, M., Stein-Gerlach, M., Freitag, M., Kupfer, R., van den Bogaard, M., and Stamminger, T. (2002) *The Journal of General Virology*, **83**, 1013–1023.
- 4 Trofe, J., Pote, L., Wade, E., Blumberg, E., and Bloom, R.D. (2008) *Annals of Pharmacotherapy*, **42**, 1447–1457.
- 5 Chou, S. (2009) *Antimicrobial Agents and Chemotherapy*, **53**, 81–85.
- 6 Chou, S. and Marousek, G.I. (2008) *Journal of Virology*, **82**, 246–253.
- 7 Chou, S., Wechel, L.C., and Marousek, G.I. (2007) *The Journal of Infectious Diseases*, **196**, 91–94.
- 8 Chou, S. (2008) *Reviews in Medical Virology*, **18**, 233–246.
- 9 Bresnahan, W.A., Boldogh, I., Chi, P., Thompson, E.A., and Albrecht, T. (1997) *Virology*, **231**, 239–247.
- 10 Mancebo, H.S., Lee, G., Flygare, J., Tomassini, J., Luu, P., Zhu, Y. *et al.* (1997) *Genes Development*, **11**, 2633–2644.
- 11 Schang, L.M., Phillips, J., and Schaffer, P.A. (1998) *Journal of Virology*, **72**, 5626–5637.
- 12 Pippin, J.W., Qu, Q., Meijer, L., and Shankland, S.J. (1997) *Journal of Clinical Investigation*, **100**, 2512–2520.
- 13 Drees, M., Dengler, W.A., Roth, T., Labonte, H., Mayo, J., Malspeis, L. *et al.* (1997) *Clinical Cancer Research*, **3**, 273–279.
- 14 Patel, V., Senderowicz, A.M., Pinto, D. Jr., Igishi, T., Raffeld, M., Quintanilla-Martinez, L. *et al.* (1998) *Journal of Clinical Investigation*, **102**, 1674–1681.
- 15 Senderowicz, A.M., Headlee, D., Stinson, S.F., Lush, R.M., Kalil, N., Villalba, L. *et al.* (1998) *Journal of Clinical Oncology*, **16**, 2986–3699.
- 16 Schang, L.M. (2001) *Antiviral Chemistry & Chemotherapy*, **12**, 157–178.
- 17 Balzarini, J., Naesens, L., and Clercq, E.D. (1998) *Current Opinion in Microbiology*, **1**, 535–546.
- 18 De Clercq, E. (2002) *Biochimica et Biophysica Acta*, **1587**, 258–275.
- 19 Liuzzi, M., Kibler, P., Bousquet, C., Harji, F., Bolger, G., Garneau, M. *et al.* (2004) *Antiviral Research*, **64**, 161–170.
- 20 Wei, X., Decker, J.M., Liu, H., Zhang, Z., Arani, R.B., Kilby, J.M. *et al.* (2002) *Antimicrobial Agents and Chemotherapy*, **46**, 1896–1905.
- 21 Briz, V., Poveda, E., and Soriano, V. (2006) *The Journal of Antimicrobial Chemotherapy*, **57**, 619–627.
- 22 Sebastian, J. and Faruki, H. (2004) *Medicinal Research Reviews*, **24**, 115–125.
- 23 Provencher, V.M., Coccaro, E., Lacasse, J.J., and Schang, L.M. (2004) *Current Pharmaceutical Design*, **10**, 4081–4101.
- 24 Marra, M.A., Jones, S.J., Astell, C.R., Holt, R.A., Brooks-Wilson, A., Butterfield, Y.S. *et al.* (2003) *Science*, **300**, 1399–1404.
- 25 Fouchier, R.A., Kuiken, T., Schutten, M., van Amerongen, G., van Doornum, G.J., van den Hoogen, B.G. *et al.* (2003) *Nature*, **423**, 240.
- 26 Meyerson, M., Enders, G.H., Wu, C.L., Su, L.K., Gorka, C., Nelson, C. *et al.* (1992) *EMBO Journal*, **11**, 2909–2917.
- 27 Manning, G., Whyte, D.B., Martinez, R., Hunter, T., and Sudarsanam, S. (2002) *Science*, **298**, 1912–1934.
- 28 Jeffrey, P.D., Ruso, A.A., Polyak, K., Gibbs, E., Hurwitz, J., Massague, J. *et al.* (1995) *Nature*, **376**, 313–320.
- 29 Stevenson, L.M., Deal, M.S., Hagopian, J.C., and Lew, J. (2002) *Biochemistry*, **41**, 8528–8534.
- 30 Chen, H.H., Wang, Y.C., and Fann, M.J. (2006) *Molecular and Cellular Biology*, **26**, 2736–2745.
- 31 Hu, D., Mayeda, A., Trembley, J.H., Lahti, J.M., and Kidd, V.J. (2003) *The Journal of Biological Chemistry*, **278**, 8623–8629.
- 32 Malumbres, M. and Barbacid, M. (2009) *Nature Reviews. Cancer*, **9**, 153–166.

- 33 Murray, A.W. and Marks, D. (2001) *Nature*, **409**, 844–846.
- 34 Hume, A.J., Finkel, J.S., Kamil, J.P., Coen, D.M., Culbertson, M.R., and Kalejta, R.F. (2008) *Science*, **320**, 797–799.
- 35 Bagella, L., Giacinti, C., Simone, C., and Giordano, A. (2006) *Journal of Cellular Biochemistry*, **99**, 978–985.
- 36 Li, S., MacLachlan, T.K., De Luca, A., Claudio, P.P., Condorelli, G., and Giordano, A. (1995) *Cancer Research*, **55**, 3992–3995.
- 37 Bagella, L., Giacinti, C., Simone, C., and Giordano, A. (2006) *Journal of Cellular Biochemistry*, **99**, 978–985.
- 38 Petretti, C., Savoian, M., Montembault, E., Glover, D.M., Prigent, C., and Giet, R. (2006) *EMBO Reports*, **7**, 418–424.
- 39 Li, T., Inoue, A., Lahti, J.M., and Kidd, V.J. (2004) *Molecular and Cellular Biology*, **24**, 3188–3197.
- 40 Schang, L.M. (2002) *The Journal of Antimicrobial Chemotherapy*, **50**, 779–792.
- 41 Schang, L.M. (2005) *Current Drug targets. Infectious Diseases*, **5**, 29–37.
- 42 Meijer, L. (1995) *Progress in Cell Cycle Research*, **1**, 351–363.
- 43 Meijer, L. (1996) *Trends in Cell Biology*, **6**, 393–397.
- 44 Meijer, L. and Kim, S.H. (1997) *Methods in Enzymology*, **283**, 113–128.
- 45 Meijer, L., Jézequel, A., and Roberge, M. (2003) Cell cycle regulators as therapeutic targets, in *Progress in Cell Cycle Research*, vol. 5 (ed L. Meijer) Life in Progress, Station Biologique de Roscoff, Roscoff, France.
- 46 Bach, S., Knockaert, M., Reinhardt, J., Lozach, O., Schmitt, S., Baratte, B. *et al.* (2005) *The Journal of Biological Chemistry*, **280**, 31208–31219.
- 47 Fisher, P., Endicott, J., and Meijer, L. (2003) *Progress in Cell Cycle Research*, **5**, 235–248.
- 48 Knockaert, M., Greengard, P., and Meijer, L. (2002) *Trends in Pharmacological Sciences*, **23**, 417–425.
- 49 Senderowicz, A.M. (2002) *Oncologist*, **7** (Suppl. 3), 12–19.
- 50 Fischer, P.M. and Gianella-Borradori, A. (2003) *Expert Opinion on Investigational Drugs*, **12**, 955–970.
- 51 Dai, Y. and Grant, S. (2003) *Current Opinion in Pharmacology*, **3**, 362–370.
- 52 de la Fuente, C., Maddukuri, A., Kehn, K., Baylor, S.Y., Deng, L., Pumfery, A. *et al.* (2003) *Current HIV Research*, **1**, 131–152.
- 53 Soni, R., Muller, L., Furet, P., Schoepfer, J., Stephan, C., Zumstein-Mecker, S. *et al.* (2000) *Biochemical & Biophysical Research Communications*, **275**, 877–884.
- 54 Misra, R.N., Xiao, H.Y., Kim, K.S., Lu, S., Han, W.C., Barbosa, S.A. *et al.* (2004) *Journal of Medicinal Chemistry*, **47**, 1719–1728.
- 55 Schoepfer, J., Fretz, H., Chaudhuri, B., Muller, L., Seeber, E., Meijer, L. *et al.* (2002) *Journal of Medicinal Chemistry*, **45**, 1741–1747.
- 56 Toogood, P.L. (2001) *Medicinal Research Reviews*, **21**, 487–498.
- 57 Voigt, B., Meijer, L., Lozach, O., Schachtele, C., Totzke, F., and Hilgeroth, A. (2005) *Bioorganic & Medicinal Chemistry Letters*, **15**, 823–825.
- 58 Chassagnole, C., Jackson, R.C., Hussain, N., Bashir, L., Derow, C., Savin, J. *et al.* (2006) *Bio Systems*, **83**, 91–97.
- 59 Soni, R., O'Reilly, T., Furet, P., Muller, L., Stephan, C., Zumstein-Mecker, S. *et al.* (2001) *Journal of the National Cancer Institute*, **93**, 436–446.
- 60 Fry, D.W., Harvey, P.J., Keller, P.R., Elliott, W.L., Meade, M., Trachet, E. *et al.* (2004) *Molecular Cancer Therapeutics*, **3**, 1427–1438.
- 61 Davies, T.G., Bentley, J., Arris, C.E., Boyle, F.T., Curtin, N.J., Endicott, J.A. *et al.* (2002) *Nature Structural Biology*, **9**, 745–749.
- 62 Vesely, J., Havlicek, L., Strnad, M., Blow, J.J., Donella-Deana, A., Pinna, L. *et al.* (1994) *European Journal of Biochemistry*, **224**, 771–786.
- 63 Meijer, L., Borgne, A., Mulner, O., Chong, J.P., Blow, J.J., Inagaki, N. *et al.* (1997) *European Journal of Biochemistry*, **243**, 527–536.

- 64 Gray, N.S., Wodicka, L., Thunnissen, A.M., Norman, T.C., Kwon, S., Espinoza, F.H. *et al.* (1998) *Science*, **281**, 533–538.
- 65 Binarova, P., Dolezel, J., Draber, P., Heberle-Bors, E., Strnad, M., and Bogre, L. (1998) *Plant Journal*, **16**, 697–707.
- 66 Ruetz, S., Fabbro, D., Zimmermann, J., Meyer, T., and Gray, N. (2003) *Current Medicinal Chemistry. Anti-Cancer Agents*, **3**, 1–14.
- 67 Payton, M., Chung, G., Yakowec, P., Wong, A., Powers, D., Xiong, L. *et al.* (2006) *Cancer Research*, **66**, 4299–4308.
- 68 Bettayeb, K., Oumata, N., Echaliier, A., Ferandin, Y., Endicott, J.A., Galons, H. *et al.* (2008) *Oncogene*, **27**, 5797–5807.
- 69 Sanchez-Martinez, C., Shih, C., Zhu, G., Li, T., Brooks, H.B., Patel, B.K. *et al.* (2003) *Bioorganic & Medicinal Chemistry Letters*, **13**, 3841–3846.
- 70 Heady, L., Fernandez-Serra, M., Mancera, R.L., Joyce, S., Venkitaraman, A.R., Artacho, E. *et al.* (2006) *Journal of Medicinal Chemistry*, **49**, 5141–5153.
- 71 De Azevedo, W.F., Leclerc, S., Meijer, L., Havlicek, L., Strnad, M., and Kim, S.H. (1997) *European Journal of Biochemistry*, **243**, 518–526.
- 72 Knockaert, M., Gray, N., Damiens, E., Chang, Y.T., Grellier, P., Grant, K. *et al.* (2000) *Chemistry & Biology*, **7**, 411–422.
- 73 Schang, L.M., Bantly, A., Knockaert, M., Shaheen, F., Meijer, L., Malim, M.H. *et al.* (2002) *Journal of Virology*, **76**, 7874–7882.
- 74 Fabian, M.A., Biggs, W.H., Treiber, D.K., Atteridge, C.E., Azimioara, M.D., Benedetti, M.G. *et al.* (2005) *Nature Biotechnology*, **23**, 329–336.
- 75 Karaman, M.W., Herrgard, S., Treiber, D.K., Gallant, P., Atteridge, C.E., Campbell, B.T. *et al.* (2008) *Nature Biotechnology*, **26**, 127–132.
- 76 Leclerc, S., Garnier, M., Hoessel, R., Marko, D., Bibb, J.A., Snyder, G.L. *et al.* (2000) *The Journal of Biological Chemistry*, **276**, 251–260.
- 77 Bain, J., McLauchlan, H., Elliott, M., and Cohen, P. (2003) *Biochemical Journal*, **371**, 199–204.
- 78 Wang, D., de la Fuente, C., Deng, L., Wang, L., Zilberman, I., Eadie, C. *et al.* (2001) *Journal of Virology*, **75**, 7266–7279.
- 79 Pinhero, R., Liaw, P., and Yankulov, K. (2004) *Biological Procedures Online*, **6**, 163–172.
- 80 Zhang, G.J., Safran, M., Wei, W., Sorensen, E., Lassota, P., Zhelev, N. *et al.* (2004) *Nature Medicine*, **10**, 643–648.
- 81 Flores, O., Lee, G., Kessler, J., Miller, M., Schlieff, W., Tomassini, J. *et al.* (1999) *Proceedings of the National Academy of Sciences of the United States of America*, **96**, 7208–7213.
- 82 Pisell, T.L., Ho, O., Lee, G., and Butera, S.T. (2001) *Antiviral Chemistry & Chemotherapy*, **12** (Suppl. 1), 33–41.
- 83 Biglione, S., Byers, S.A., Price, J.P., Nguyen, V.T., Bensaude, O., Price, D.H. *et al.* (2007) *Retrovirology*, **4**, 47.
- 84 Nelson, P.J., Gherardi, D., Agati, V.D.D., Chu, T.-H.T., Barnett, A., Gianella-Borradori, A. *et al.* (2003) Reversal of collapsing glomerulopathy in mice with the cyclin-dependent kinase inhibitor Cyc202. American Society for Nephrology 36th Annual Meeting and Scientific Exposition
- 85 Chao, S.H., Fujinaga, K., Marion, J.E., Taube, R., Sausville, E.A., Senderowicz, A.M. *et al.* (2000) *The Journal of Biological Chemistry*, **275**, 28345–28348.
- 86 Carlson, B.A., Dubay, M.M., Sausville, E.A., Brizuela, L., and Worland, P.J. (1996) *Cancer Research*, **56**, 2973–2978.
- 87 Losiewicz, M.D., Carlson, B.A., Kaur, G., Sausville, E.A., and Worland, P.J. (1994) *Biochemical & Biophysical Research Communications*, **201**, 589–595.
- 88 Zhou, M., Deng, L., Lacoste, V., Park, H.U., Pumfery, A., Kashanchi, F. *et al.* (2004) *Journal of Virology*, **78**, 13522–13533.
- 89 Heredia, A., Davis, C., Bamba, D., Le, N., Gwarzo, M.Y., Sadowska, M. *et al.* (2005) *AIDS*, **19**, 2087–2095.
- 90 De Azevedo, W.F. Jr., Mueller-Dieckmann, H.J., Schulze-Gahmen, U., Worland, P.J., Sausville, E., and Kim, S.H. (1996) *Proceedings of the*

- National Academy of Sciences of the United States of America*, **93**, 2735–2740.
- 91 de Azevedo, W.F. Jr., Canduri, F., and da Silveira, N.J. (2002) *Biochemical and Biophysical Research Communications*, **293**, 566–571.
 - 92 Baumli, S., Lolli, G., Lowe, E.D., Troiani, S., Rusconi, L., Bullock, A.N. *et al.* (2008) *The EMBO Journal*, **27**, 1907–1918.
 - 93 Ali, A., Ghosh, A., Nathans, R., Sharova, N., O'Brien, S., Cao, H. *et al.* (2009) *ChemBioChem*, **10**, 2072–2080.
 - 94 Sausville, E.A., Zaharevitz, D., Gussio, R., Meijer, L., Louarn-Leost, M., Kunick, C. *et al.* (1999) *Pharmacology & Therapeutics*, **82**, 285–292.
 - 95 Hoessel, R., Leclerc, S., Endicott, J.A., Nobel, M.E., Lawrie, A., Tunnah, P. *et al.* (1999) *Nature Cell Biology*, **1**, 60–67.
 - 96 Meijer, L., Guyard, N., Skaltsounis, L., and Eisenbrand, G. (2006) Indirubin, the red shade of indigo, in *Progress in Cell-Cycle Research*, vol. 1 (ed L. Meijer) Life in Progress, Station Biologique de Roscoff, Roscoff, France.
 - 97 Schang, L.M., Rosenberg, A., and Schaffer, P.A. (2000) *Journal of Virology*, **74**, 2107–2120.
 - 98 Schang, L.M., Rosenberg, A., and Schaffer, P.A. (1999) *Journal of Virology*, **73**, 2161–2172.
 - 99 Jordan, R., Schang, L., and Schaffer, P.A. (1999) *Journal of Virology*, **73**, 8843–8847.
 - 100 Taylor, S.L., Kinchington, P.R., Brooks, A., and Moffat, J.F. (2004) *Journal of Virology*, **78**, 2853–2862.
 - 101 Chao, S.H., Walker, J.R., Chanda, S.K., Gray, N.S., and Caldwell, J.S. (2003) *Molecular Cellular Biology*, **23**, 831–841.
 - 102 Bhattacharjee, R.N., Banks, G.C., Trotter, K.W., Lee, H.L., and Archer, T.K. (2001) *Molecular Cellular Biology*, **21**, 5417–5425.
 - 103 Wang, L., Deng, L., Wu, K., de la Fuente, C., Wang, D., Kehn, K. *et al.* (2002) *Molecular and Cellular Biochemistry*, **237**, 137–153.
 - 104 Ghedin, E., Pumfery, A., De La Fuente, C., Yao, K., Miller, N., Lacoste, V. *et al.* (2004) *Retrovirology*, **1**, 10.
 - 105 Agbottah, E., de la Fuente, C., Nekhai, S., Barnett, A., Gianella-Borradori, A., Pumfery, A. *et al.* (2004) *The Journal of Biological Chemistry*, **280**, 3029–3042.
 - 106 Kudoh, A., Daikoku, T., Sugaya, Y., Isomura, H., Fujita, M., Kiyono, T. *et al.* (2004) *Journal of Virology*, **78**, 104–115.
 - 107 Shin, K.C., Park, C.G., Hwang, E.S., and Cha, C.Y. (2008) *Journal of Korean Medical Science*, **23**, 1046–1052.
 - 108 Orba, Y., Sunden, Y., Suzuki, T., Nagashima, K., Kimura, T., Tanaka, S. *et al.* (2008) *Virology*, **370**, 173–183.
 - 109 Fax, P., Lehmkuhler, O., Kuhn, C., Esche, H., and Brockmann, D. (2000) *The Journal of Biological Chemistry*, **275**, 40554–40560.
 - 110 Hertel, L., Chou, S., and Mocarski, E.S. (2007) *PLoS Pathogens*, **3**, e6
 - 111 Mak, N.K., Leung, C.Y., Wei, X.Y., Shen, X.L., Wong, R.N., Leung, K.N. *et al.* (2004) *Biochemical Pharmacology*, **67**, 167–174.
 - 112 Sanchez, V., McElroy, A.K., Yen, J., Tamrakar, S., Clark, C.L., Schwartz, R.A. *et al.* (2004) *Journal of Virology*, **78**, 11219–11232.
 - 113 Sanchez, V. and Spector, D.H. (2006) *Journal of Virology*, **80**, 5886–5896.
 - 114 Habran, L., Bontems, S., Di Valentin, E., Sadzot-Delvaux, C., and Piette, J. (2005) *The Journal of Biological Chemistry*, **280**, 29135–29143.
 - 115 Yamamoto, S., Deckter, L.A., Kasai, K., Chiocca, E.A., and Saeki, Y. (2006) *Gene Therapy*, **13**, 1731–1736.
 - 116 Diwan, P., Lacasse, J.J., and Schang, L.M. (2004) *Journal of Virology*, **78**, 9352–9365.
 - 117 Lacasse, J.J., Provencher, V.M.I., Urbanowski, M.D., and Schang, L.M. (2005) *Therapy*, **2**, 77–90.
 - 118 Davido, D.J., Leib, D.A., and Schaffer, P.A. (2002) *Journal of Virology*, **76**, 1077–1088.
 - 119 Advani, S.J., Hagglund, R., Weichselbaum, R.R., and Roizman, B. (2001) *Journal of Virology*, **75**, 7904–7912.
 - 120 Ye, M., Duus, K.M., Peng, J.M., Price, D.H., and Grose, C. (1999) *Journal of Virology*, **73**, 1320–1330.
 - 121 Schang, L.M., Bantly, A., and Schaffer, P.A. (2002) *Journal of Virology*, **76**, 7724–7735.

- 122 Taylor, S.L. and Moffat, J.F. (2001) VZV replication *in vitro* is prevented by Roscovitine, and inhibitor of the cell cycle. Proceedings of the Fourth International Conference on VZV, La Jolla, San Diego, CA.
- 123 Bresnahan, W.A., Thompson, E.A., and Albrecht, T. (1997) *The Journal of General Virology*, **78**, 1993–1997.
- 124 Bresnahan, W.A., Albrecht, T., and Thompson, E.A. (1998) *Journal of Biological Chemistry*, **273**, 22075–22082.
- 125 Sawtell, N.M. and Thompson, R.L. (2004) *Journal of Virology*, **78**, 7784–7794.
- 126 Li, M., Lee, H., Yoon, D.W., Albrecht, J.C., Fleckenstein, B., Neipel, F. *et al.* (1997) *Journal of Virology*, **71**, 1984–1991.
- 127 Godden-Kent, D., Talbot, S.J., Boshoff, C., Chang, Y., Moore, P., Weiss, R.A. *et al.* (1997) *Journal of Virology*, **71**, 4193–4198.
- 128 Duro, D., Schulze, A., Vogt, B., Bartek, J., Mitnacht, S., and Jansen-Durr, P. (1999) *Journal of General Virology*, **80**, 549–555.
- 129 Mann, D.J., Child, E.S., Swanton, C., Laman, H., and Jones, N. (1999) *EMBO Journal*, **18**, 654–663.
- 130 Swanton, C., Mann, D.J., Fleckenstein, B., Neipel, F., Peters, G., and Jones, N. (1997) *Nature*, **390**, 184–187.
- 131 Laman, H., Coverley, D., Krude, T., Laskey, R., and Jones, N. (2001) *Molecular and Cellular Biology*, **21**, 624–635.
- 132 Ye, M., Duus, K.M., Peng, J., Price, D.H., and Grose, C. (1999) *Journal of Virology*, **73**, 1320–1330.
- 133 Advani, S.J., Weichselbaum, R.R., and Roizman, B. (2000) *PNAS*, **97**, 10996–11001.
- 134 Davido, D.J., Von Zagorski, W.F., Maul, G.G., and Schaffer, P.A. (2003) *Journal of Virology*, **77**, 12603–12616.
- 135 Tamrakar, S., Kapasi, A.J., and Spector, D.H. (2005) *Journal of Virology*, **79**, 15477–15493.
- 136 Ortega, S., Prieto, I., Odajima, J., Martin, A., Dubus, P., Sotillo, R. *et al.* (2003) *Nature Genetics*, **35**, 25–31.
- 137 Berthet, C., Aleem, E., Coppola, V., Tassarollo, L., and Kaldis, P. (2003) *Current Biology*, **13**, 1775–1785.
- 138 Rane, S.G., Dubus, P., Mettus, R.V., Galbreath, E.J., Boden, G., Reddy, E.P. *et al.* (1999) *Nature Genetics*, **22**, 44–52.
- 139 Malumbres, M., Sotillo, R., Santamaria, D., Galan, J., Cerezo, A., Ortega, S. *et al.* (2004) *Cell*, **118**, 493–504.
- 140 Garber, M.E., Wei, P., KewalRamani, V.N., Mayall, T.P., Herrmann, C.H., Rice, A.P. *et al.* (1998) *Genes & Development*, **12**, 3512–3527.
- 141 Isel, C. and Karn, J. (1999) *Journal of Molecular Biology*, **290**, 929–941.
- 142 Ramanathan, Y., Reza, S.M., Young, T.M., Mathews, M.B., and Pe'ery, T. (1999) *Journal of Virology*, **73**, 5448–5458.
- 143 Karn, J. (1999) *Journal of Molecular Biology*, **293**, 235–254.
- 144 Ghose, R., Liou, L.Y., Herrmann, C.H., and Rice, A.P. (2001) *Journal of Virology*, **75**, 11336–11343.
- 145 Hesselgesser, J., Gibbs, C., and Shibata, R. (2004) Selective killing of HIV-1 infected cells by small molecule cyclin dependent kinase inhibitors. 11th Conference on Retroviruses and Opportunistic Infections. San Francisco, CA, Foundation for Retrovirology and Human Health, NIAID and CDC.
- 146 Nelson, P.J., Gelman, I.H., and Klotman, P.E. (2001) *Journal of the American Society of Nephrology*, **12**, 2827–2831.
- 147 Salerno, D., Hasham, M.G., Marshall, R., Garriga, J., Tsygankov, A.Y., and Grana, X. (2007) *Gene*, **405**, 65–78.
- 148 Chiu, Y.L., Cao, H., Jacque, J.M., Stevenson, M., and Rana, T.M. (2004) *Journal of Virology*, **78**, 2517–2529.
- 149 Chao, S.H. and Price, D.H. (2001) *The Journal of Biological Chemistry*, **276**, 31793–31799.
- 150 Nekhai, S., Zhou, M., Fernandez, A., Lane, W.S., Lamb, N.J., Brady, J. *et al.* (2002) *Journal of Biological Chemistry*, **364**, 649–657.
- 151 Ma, T., Zou, N., Lin, B.Y., Chow, L.T., and Harper, J.W. (1999) *Proceedings of the National Academy of Sciences of the United States of America*, **96**, 382–387.
- 152 van Dyk, L.F., Virgin, H.W., and Speck, S.H. (2000) *Journal of Virology*, **74**, 7451–7461.

- 153 Van Dyk, L.F., Hess, J.L., Katz, J.D., Jacoby, M., Speck, S.H., and Virgin, H.W. (1999) *Journal of Virology*, **73**, 5110–5122.
- 154 He, W., Staples, D., Smith, C., and Fisher, C. (2003) *Journal of Virology*, **77**, 10566–10574.
- 155 Duensing, S., Lee, L.Y., Duensing, A., Basile, J., Piboonyiom, S., Gonzalez, S. *et al.* (2000) *Proceedings of the National Academy of Sciences of the United States of America*, **97**, 10002–10007.
- 156 Nguyen, D.X., Westbrook, T.F., and McCance, D.J. (2002) *Journal of Virology*, **76**, 619–632.
- 157 Duensing, S., Duensing, A., Lee, D.C., Edwards, K.M., Piboonyiom, S.O., Manuel, E. *et al.* (2004) *Oncogene*, **23**, 8206–8215.
- 158 Asai, Y., Hashimoto, S., Kujime, K., Gon, Y., Mizumura, K., Shimizu, K. *et al.* (2001) *British Journal of Pharmacology*, **132**, 918–924.
- 159 Schang, L.M., StVincent, M.R., and Lacasse, J.J. (2006) *Antiviral Chemistry & Chemotherapy*, **17**, 293–320.
- 160 Mgbonyebi, O.P., Russo, J., and Russo, I.H. (1998) *Anticancer Research*, **18**, 751–755.
- 161 Mgbonyebi, O.P., Russo, J., and Russo, I.H. (1999) *Cancer Research*, **59**, 1903–1910.
- 162 Ishida, S., Yamashita, T., Nakaya, U., and Tokino, T. (2000) *Japanese Journal of Cancer Research*, **91**, 174–180.
- 163 Yang, C.T., You, L., Yeh, C.C., Chang, J.W., Zhang, F., McCormick, F. *et al.* (2000) *Journal of the National Cancer Institute*, **92**, 636–641.
- 164 Ramondetta, L., Mills, G.B., Burke, T.W., and Wolf, J.K. (2000) *Clinical Cancer Research*, **6**, 278–284.
- 165 Waheed, I., Guo, Z.S., Chen, G.A., Weiser, T.S., Nguyen, D.M., and Schrupp, D.S. (1999) *Cancer Research*, **59**, 6068–6073.
- 166 Tsao, Y.P., Huang, S.J., Chang, J.L., Hsieh, J.T., Pong, R.C., and Chen, S.L. (1999) *Journal of Virology*, **73**, 4983–4990.
- 167 Santamaria, D. and Ortega, S. (2006) *Frontiers in Bioscience: A Journal and Virtual Library*, **11**, 1164–1188.
- 168 Rowe, J., Greenblatt, R., Liu, D., and Moffat, J.F. (2009) Compounds that target host cell enzymes prevent varicella-zoster virus replication *in vitro*, *ex vivo* and in SCID-HU mice. International Conference on Antiviral Research, Miami, FL
- 169 Gherardi, D., D'Agati, V., Chu, T.H., Barnett, A., Gianella-Borradori, A., Gelman, I.H. *et al.* (2004) *Journal of the American Society of Nephrology*, **15**, 1212–1222.
- 170 Nelson, P.J., D'Agati, V.D., Gries, J.-M., Suarez, J.-R., and Gelman, I.H. (2003) *Journal of Antimicrobial Chemotherapy*, **51**, 921–929.
- 171 Hsieh, W.S., Soo, R., Peh, B.K., Loh, T., Dong, D., Soh, D. *et al.* (2009) *Clinical Cancer Research*, **15**, 1435–1442.
- 172 Yeo, W., Goh, B., Tourneau, C.L., Green, R., Chiao, J.H., and Siu, L.L. (2009) *Journal of Clinical Oncology*, **27**, 6026
- 173 Goh, B., Peh, B.-K., Cui, C.-Y., Soo, T., Loh, T., Green, R. *et al.* (2005) *Journal of Clinical Oncology*, **23**, 3145
- 174 Schang, L.M. (2006) *Current Pharmaceutical Design*, **12**, 1357–1370.
- 175 Demetri, G.D., von Mehren, M., Blanke, C.D., Van den Abbeele, A.D., Eisenberg, B., Roberts, P.J. *et al.* (2002) *The New England Journal of Medicine*, **347**, 472–480.
- 176 Rubin, B.P., Schuetz, S.M., Eary, J.F., Norwood, T.H., Mirza, S., Conrad, E.U. *et al.* (2002) *Journal of Clinical Oncology*, **20**, 3586–3591.
- 177 Cools, J., DeAngelo, D.J., Gotlib, J., Stover, E.H., Legare, R.D., Cortes, J. *et al.* (2003) *The New England Journal of Medicine*, **348**, 1201–1214.
- 178 Moses, A.V., Jarvis, M.A., Raggo, C., Bell, Y.C., Ruhl, R., Luukkonen, B.G. *et al.* (2002) *Journal of Virology*, **76**, 8383–8399.
- 179 Sturzl, M., Roth, W.K., Brockmeyer, N.H., Zietz, C., Speiser, B., and Hofschneider, P.H. (1992) *Proceedings of the National Academy of Sciences of the United States of America*, **89**, 7046–7050.
- 180 Koon, H.B., Bubley, G.J., Pantanowitz, L., Masiello, D., Smith, B., Crosby, K. *et al.* (2005) *Journal of Clinical Oncology*, **23**, 982–989.

- 181 Reeves, P.M., Bommarius, B., Lebeis, S., McNulty, S., Christensen, J., Swimm, A. *et al.* (2005) *Nature Medicine*, **11**, 731–739.
- 182 Baselga, J. (2002) *Journal of Clinical Oncology*, **20**, 2217–2219.
- 183 Kim, M., Yang, H., Kim, S.K., Reche, P.A., Tirabassi, R.S., Hussey, R.E. *et al.* (2004) *The Journal of Biological Chemistry*, **279**, 25838–25848.
- 184 Buller, R.M., Chakrabarti, S., Cooper, J.A., Twardzik, D.R., and Moss, B. (1988) *Journal of Virology*, **62**, 866–874.
- 185 Oppenorth, A., Nation, N., Graham, K., and McFadden, G. (1993) *Virology*, **192**, 701–709.
- 186 Yang, H., Kim, S.K., Kim, M., Reche, P.A., Morehead, T.J., Damon, I.K. *et al.* (2005) *The Journal of Clinical Investigation*, **115**, 379–387.

11

Prospects for TB Therapeutics Targeting *Mycobacterium tuberculosis* Phosphosignaling Networks

Yossef Av-Gay and Tom Alber

11.1

Introduction

Tuberculosis (TB), an infectious disease, is one among the numerous leading causes of death worldwide, killing approximately 1.7 million people annually. In the past decade, the global incidence of TB has risen to approximately nine million cases annually, with 80% of the patients in sub-Saharan Africa or Asia [1]. Drugs to treat TB have been available for the past six decades, yet eradication of the disease is not on the horizon.

Due to the chronic nature of the infection, current therapy for TB takes at least 6 months to treat drug-sensitive infections. Monotherapies are ineffective, necessitating treatment using a cocktail of four or more drugs. A combination of isoniazid (INH), rifampin (RMP), ethambutol (EMB), and pyrazinamide (PZA) are the first-line anti-TB agents. Second-line drugs have also been developed, but they are more expensive, less effective, and more toxic in comparison to first-line drugs. These antibiotics include ethionamide (ETH), streptomycin (STR), cycloserine, *p*-aminosalicylic acid (PAS), capreomycin, amikacin, kanamycin, quinolones (such as ciprofloxacin), and clofazime. This group is used when the first-line drugs become ineffective due to developed resistance or toxicity such as hepatotoxicity resulting from INH treatment.

Current treatment practices have led to a rapidly increasing incidence of drug resistant TB (<http://www.cdc.gov/mmwr/preview/mmwrhtml/00020964.htm>; <http://www.who.int/tb/strategy/en/>). Chromosomal mutations within the *M. tuberculosis* genome [2] have engendered resistance to every anti-TB drug available. Among the new cases, approximately 20% show resistance to multiple drugs [3]. As a result, even current combinatorial therapies are becoming less effective and less capable of reducing the development of further resistance. The emergence of multidrug resistant (MDR; resistant to at least two first-line treatments) and extensively drug-resistant (XDR; additionally resistant to at least three second-line treatments) strains, which account for up to 35% of MDR strains [3], create an urgent need for novel therapies and diagnostics to speed up the treatment and to combat MDR, XDR, and latent TB.

Indeed, after 40 years with no new TB drugs introduced to the market, in the last decade, a combined public–industry effort [4, 5] has resulted in a growing number of drug candidates that are currently in clinical development. These new compounds include Tibotec’s diarylquinone TMC207, which targets the bacterial ATP synthase [6] and nitroimidazopyrans (such as PA-824 and OPC-67683 (Otsuka Pharmaceuticals)) that appear to target synthesis of polypeptides and fatty acids essential for cell wall integrity.

The prospect for continuing emergence of resistance necessitates further development of anti-TB drugs that act by novel mechanisms. Recent evidence suggests that bacterial phosphosignaling systems may provide multiple valid targets for developing new drugs.

11.2

Rationale for Ser/Thr Protein Kinases and Protein Phosphatases as Drug Targets

M. tuberculosis survives for long periods in challenging host environments, including the phagocytic compartment of macrophages. Through a complex set of strategies, *M. tuberculosis* evades the antimicrobial defenses of the host (reviewed in Ref. [7]). These pathogenic strategies include preventing the acidification of phagosome [8], inhibiting phagosome maturation [9, 10], interfering with antigen presentation [11] and cytokine signaling [12], mounting vigorous stress response [13], and expressing resistance mechanisms to counter nitrosative damage [14]. During the acute phase of infection, the bacteria multiply inside the lungs, and the host responds by turning on adaptive immunity to control the bacterial growth. There is growing evidence that the long-term survival of *M. tuberculosis* is associated with adaptation to a phenotypically resistant form in response to exposure to nitric oxide within the activated macrophages or to low-oxygen tension in the granuloma [15, 16], which represent by itself another frontier for tuberculosis therapy. Thus, *M. tuberculosis* responds to host stimuli by mediating appropriate cellular responses during the entire course of the infection.

Four main families of proteins mediate phosphorylation signal transduction pathways in *M. tuberculosis*. These systems provide means of molecular adaptation in response to external stimuli. The classic bacterial signaling machinery comprises the “two-component” systems. Eleven such systems have been identified, each consisting of a histidine kinase and a response regulator [17, 18]. The ATP binding sites of two-component kinases are considered by several experts too shallow to target with inhibitors. The second family was discovered a decade ago [19] and contains 11 “eukaryotic-like” serine/threonine protein kinases (STPKs) called PknA–PknL [20–22]. Antagonizing the protein kinases is a Ser/Thr phosphatase encoded by the *pstP* gene. This PP2C-family enzyme is homologous to the environmental-sensing phosphatase, Rv1663, which regulates transcription through alternative sigma factors. The fourth family encodes a pair of protein tyrosine phosphatases (PTPs), PtpA and PtpB, which are thought to act within host cells to interrupt signaling pathways [23–25].

The Ser/Thr protein kinases afford promising therapeutic targets. Recent interest in drugs that inhibit human protein kinases has led to the development of large, kinase-specific chemical libraries and a wealth of knowledge about how to develop potent, selective inhibitors. The *M. tuberculosis* STPK domains are all <30% identical in sequence to the closest human homologues (CDC2HS and CK2 α), making development of selectivity a relatively low hurdle. Inhibitors that target PknG or PknD in preference to the other *M. tuberculosis* STPKs have been reported [26, 27]. Two of the *M. tuberculosis* STPKs are essential for bacterial growth, and eukaryotic kinase inhibitors block mycobacterial growth *in vitro* [28, 29]. These studies provide traditional genetic and chemical validation for targeting the *M. tuberculosis* STPKs.

While pharmaceuticals that inhibit the human protein kinases have been developed successfully, the protein phosphatases have proven to be more difficult targets for medicinal chemistry. Nonetheless, the general Ser/Thr protein phosphatase, PstP, may be essential for growth, and the protein tyrosine phosphatase, PtpB, may be required to establish latent infections [25].

In this chapter, we review the recent literature about the structure, the function, and the inhibition of these promising targets. An outstanding review of the *M. tuberculosis* Ser/Thr protein kinases has been published recently by Takiff and colleagues [30].

11.3

Drug Target Validation by Genetic Inactivation

In the past decade, mycobacterial researchers developed methods to knock out genes in *M. tuberculosis*, providing powerful tools to explore the genetic determinants of pathogen physiology, infectivity, and virulence. Genetic studies have validated signaling elements as potential drug targets and provided insights into their essentiality to disease. Two of *M. tuberculosis* STPKs, PknA and PknB, were shown to be essential for *M. tuberculosis in vitro* growth [31]. Transposon mutagenesis of the whole *M. tuberculosis* genome also suggested that the deletion of *pknG* might also be lethal [32], but subsequent targeted deletions showed that the *pknG* knockout was viable but severely attenuated in animals [33]. In contrast, *pknB* could be deleted only in a merodiploid [31]. In an elegant study of *M. smegmatis* antisense knockdown strains, Husson and coworkers demonstrated that reduced levels of PknA or PknB attenuate growth rates and cause dramatic changes in cell morphology [34]. Unexpectedly, transposon insertions in the genes for the other eight *M. tuberculosis* STPKs did not attenuate growth in mouse spleen [35]. These results may indicate that the other STPKs are not essential; they serve redundant functions or influence processes (such as persistence or reactivation) that have yet to be surveyed in model organisms.

In vivo infection studies using *M. tuberculosis* mutants deleted for individual STPKs have established roles of specific kinase activities at specific stages of infection. For example, an *M. tuberculosis* mutant deleted for *pknG* displays decreased growth upon infection in immunocompetent mice and causes delayed mortality in SCID mice [33]. Using *M. bovis* BCG and *M. smegmatis* as model systems, Pieters and coworkers reported that PknG prevents phagosome-lysosome fusion [27]. The

relevance of these functions for wild-type *M. tuberculosis* infections and the biological mechanisms of PknG signaling await additional experimentation. In *M. tuberculosis*, PknG kinase acts as a sensor of nutritional stress, and plays a role in regulating glutamine/glutamate levels [33].

In contrast to PknG, Av-Gay and coworkers established that the PknH kinase plays a growth regulatory role during late stages of the infection cycle in mice [36]. Significantly, the *pknH* deletion mutant displayed increased resistance to acidified nitrite treatment and replicated to much higher numbers. Thus, the *pknH* deletion caused a hypervirulent phenotype compared to wild-type H37Rv. These studies supported the model that PknH senses nitric oxide stress produced by inducible nitric oxide synthase in the macrophage. Reduced oxygen tension and increased nitric oxide exposure are two conditions encountered by bacilli *in vivo* that may promote latency [37]. In *M. tuberculosis*, the sensor histidine kinases DosS and DosT sense oxygen tension by monitoring redox conditions and hypoxia, respectively [38]. Mutants lacking DosS and DosT are unable to activate expression of genes regulated by the latency-linked, stress response regulator, DosR. The established roles of some components of the two-component signaling systems in mediating latency [37, 39] and the hypervirulent phenotypes of mutants in a variety of pathways provides a broad scope for the biochemical mechanism of the growth regulating functions of PknH. Identification of the components of metabolic pathways regulated by PknH may help define new downstream drug targets.

Genetic knockout and antisense knockdown studies have been also carried out for PknD [40], PknE, [36, 41] PknF [42], PknI, and PknJ (Av-Gay and coworkers, unpublished results). These kinases seem to be nonessential for growth in culture media *in vitro*.

Whole-genome transposon mutagenesis suggested that the *M. tuberculosis* phosphatases are not essential for growth *in vitro* or *in vivo* [32, 35]. Nonetheless, attempts to make precise deletions of the Ser/Thr phosphatase PstP (Rv0018c) in both *M. smegmatis* and *M. tuberculosis* have failed in multiple laboratories. Although such negative results should be interpreted with caution, it appears that PstP is essential for *M. tuberculosis* growth. The knockout of *ptpB* produced growth attenuation in activated but not resting macrophages [25]. While the *ptpB* deletion mutant survived as well as isogenic wild-type strains in the early stages of infection in guinea pigs, bacterial growth was attenuated after 6 weeks. This phenotype suggested that PtpB antagonizes the adaptive immune response, perhaps by antagonizing interferon- γ signaling [25]. Although these studies hint at roles for the *M. tuberculosis* PTPs in long-term bacterial survival, the phosphatases require further validation to be considered among the most promising pharmaceutical targets.

11.4

STPK Mechanisms, Substrates, and Functions

Genetic and biochemical studies suggest that PknB is the best candidate STPK target for development of a sterilizing inhibitor. PknB was the first bacterial STPK to be

studied in detail, and orthologues are the most widespread of any STPK in other bacterial genera [43]. Thus, inhibitors of *M. tuberculosis* PknB may have applications to treat infections of other species, including *Staphylococcus aureus*. This pathogen is predicted to produce a PknB orthologue as well as more than 30 additional STPKs. In *M. tuberculosis*, PknB was shown to be a functional, autophosphorylated kinase expressed *in vitro* and *in vivo* in alveolar macrophages from a patient with tuberculosis [44]. PknB and the PstP phosphatase encoded in the same operon work as a functional pair [45], and they are thought to control mycobacterial cell growth [20]. The PknB extracellular sensor domain comprises four PASTA repeats that are thought to bind intermediates in cell wall biosynthesis [46]. Nonetheless, the signals that activate PknB or any bacterial STPK are not yet defined.

Dimerization [26] and autophosphorylation of a conserved motif called the activation loop [43, 45] activate PknB, PknD, and other *M. tuberculosis* receptor STPKs. The dimerization interface, on the opposite side of the N-lobe relative to the ATP binding site, comprises a conserved allosteric surface [26] that holds the kinase active sites away from each other in the dimer. A similar activating dimer interface was found in the human double-stranded-RNA-dependent protein kinase, PKR [47, 48]. Consistent with the back-to-back orientation of kinase domains (KDs) in the activated dimers, *M. tuberculosis* STPK autophosphorylation is an intermolecular reaction that is inhibited by mutations in the dimer interface [26].

The crystal structures of the PknB KD complexed with nonhydrolyzable nucleotides provided the first views of bacterial STPKs [43, 49]. The structures showed dramatic similarities between the folds, nucleotide binding sites, nucleotide conformations, and regulatory features of bacterial and eukaryotic STPKs. These similarities support a universal activation mechanism of Ser/Thr protein kinases in prokaryotes and eukaryotes [43]. The back-to-back KD dimer now observed in three different crystal forms of PknB [29] was also observed in the crystal structure of the phosphorylated KD of the *M. tuberculosis* receptor STPK, PknE [50]. The ATP binding site of the activated, nucleotide-free PknE KD adopted a conformation incapable of nucleotide accommodation and provided evidence that nucleotide exchange involves large conformational rearrangements of the ATP binding site. These results suggested that each STPK might adopt multiple conformations that could be targeted by distinct inhibitor classes. The active, back-to-back dimer formed by the PknB and PknE KDs was not seen in the structure of PknG, the first structure of a soluble bacterial STPK [51]. Instead, PknG contained folded N- and C-terminal extensions that may regulate the KD.

The substrates of the *M. tuberculosis* STPKs and phosphatases determine the functions of these proteins and also highlight possible targets for orthogonal inhibitors. Based on the number of phosphoproteins detected in *Corynebacterium glutamicum*, a related actinomycete [52], the upper bound for the number of STPK substrates in *M. tuberculosis* was estimated to approach 800 proteins [21]. Alternatively, the *C. glutamicum* phosphoproteins may reflect the most abundant substrates, or substrates modified with stable phosphates that do not play regulatory functions.

Moreover, if the 11 *M. tuberculosis* STPKs are more specific than the 4 homologous *C. glutamicum* enzymes, the number of authentic substrates in *M. tuberculosis* may be significantly smaller. A computational search of the *M. tuberculosis* genome using the phosphorylation-site sequence in the PknH activation loop revealed 40 potential substrates for this kinase [53]. Some of these candidates were verified to be phosphorylated by the PknH KD *in vitro*.

For the other STPKs, a growing number of candidate substrates have been identified in studies using *in vitro* and *in vivo* assays. These substrates include transcriptional regulators, membrane channels, enzymes, and regulatory proteins (reviewed by Greenstein *et al.*, 2006). Some of these studies, however, have nominated candidates that fail to fulfill characteristics expected for authentic targets of phosphoregulation. The *in vitro* phosphorylation sites identified in PbpA, DacB1, and MmpL7 [40, 53, 54], for example, are predicted to be outside the bacterial cell. In such an extracellular location, it is hard to imagine how the STPK and the PstP catalytic domains, which are intracellular, could perform continuous regulatory functions. It remains to be seen if phosphorylation of extracellular sites occurs prior to protein transport or is a prerequisite for protein secretion. In addition, candidate substrates that are phosphorylated by numerous kinases or are phosphorylated inefficiently *in vitro* may be the targets of nonspecific modifications [55, 56]. Limited selectivity or modest catalytic efficiency could result from the absence of the complete STPK or substrate protein in the native context [57]. Weak phosphorylation, however, may be suppressed in the presence of competing authentic substrates. Moreover, substoichiometric phosphorylation would be incapable of dramatically changing the total metabolic activity of the candidate substrate protein. Efficient phosphorylation of a large excess of substrate, on the other hand, provides more confidence that the target is functionally significant [56, 58, 59].

In our experience, many proteins are weakly phosphorylated by the purified KDs, and incomplete phosphorylation *in vitro* falls short of providing a strong case that the modification plays a regulatory role *in vivo*. Similarly, because PstP rapidly dephosphorylates cognate and noncognate substrates *in vitro*, dephosphorylation by PstP provides only part of the case for functional relevance. Stronger evidence for the function of a particular phosphorylation reaction might include a change in activity upon phosphorylation [58, 60], occurrence of the phosphorylated substrate protein *in vivo* [60] or detection of a phenotype resulting from mutations of the phosphorylation site [34].

To date, a small number of substrates have been shown to be phosphorylated efficiently *in vitro* and to respond to perturbations of STPKs *in vivo*. Importantly, autophosphorylation of the KDs appears to be an authentic regulatory reaction. Supporting this conclusion, mutations of phosphorylation sites in the PknB activation loop inactivated the KD *in vitro*, multiple receptor STPKs are expressed with activation loop phosphates, dephosphorylation with PstP inactivates the KDs, several STPKs are phosphorylated *in vivo*, and expression of catalytically dead and active PknD produced distinct patterns of auto- and transphosphorylation *in vivo* [26, 44, 45, 61]. Consistent with a regulatory network, the PknA and PknB KDs

phosphorylate each other *in vitro* [34]. The sites of these cross-phosphorylations and any regulatory effects on kinase functions remain to be defined.

In vivo studies have implicated several substrates for the *M. tuberculosis* STPKs. Pioneering work by Kang *et al.* identified Wag31, Rv1422 and PknA as substrates for PknB [34]. Effects of expressing (or depleting) *pknA*, *pknB*, and *wag31* in *M. smegmatis* provided evidence that PknA and PknB regulate cell shape in mycobacteria. The transcriptional regulator, EmbR, is an *in vivo* substrate for PknH in *M. tuberculosis* [62, 63], similar to the phosphorylation of the AfsR regulator by the AfsK kinase in *Streptomyces* [64]. Although the apparent effects on activity are modest, all purified *M. tuberculosis* STPK KDs except those of PknG, PknI, and PknJ phosphorylate the FAS II components KasA and KasB *in vitro*, and these fatty-acid biosynthetic enzymes are phosphorylated *in vivo* in *M. bovis* BCG [60]. The PknD kinase efficiently phosphorylates the anti-anti-sigma factor homologue Rv0516c on Thr2 *in vitro* and *in vivo*, and this phosphorylation alters *in vitro* binding to the homologous regulator, Rv2638 [58]. Activation by overexpression of PknD in *M. tuberculosis* altered the expression of more than 100 genes, including genes regulated by sigma F, providing evidence that PknD converts environmental signals into a transcriptional response. Combined with a growing number of studies of STPK functions in other bacteria [65, 66], these studies support the idea that the *M. tuberculosis* receptor kinases regulate diverse physiological processes.

11.5

M. tuberculosis STPK Inhibitors

The sequence motifs and structural similarities shared among the eukaryotic and *M. tuberculosis* STPKs suggested that similar compound classes might inhibit the eukaryotic and prokaryotic family members. This concept, however, received experimental confirmation well before the structure of a bacterial STPK was determined. The initial chemical validation of *M. tuberculosis* STPKs as potential drug targets was provided by analysis of the effects of nonspecific inhibitors of eukaryotic STPKs on mycobacterial growth *in vitro*. The kinase inhibitor 1-(5-isoquinolinesulfonyl)-2-methylpiperazine (H7), a H-series compound developed to bind eukaryotic kinases, not only inhibited the purified PknB in a biochemical assay but also attenuated *M. bovis* BCG and *M. smegmatis* growth *in vitro* [28]. Although H7 concentrations in excess of 100 μ M were needed, which most likely induce off-targets effects and the direct physiological target in the bacteria was not identified experimentally, these studies began to establish the case that STPK inhibitors can sterilize mycobacteria in culture.

A similar approach of surveying available inhibitors of eukaryotic kinases led to the identification of PknB as a target of mitoxantrone and PknD as a target of SP006125 [29, 58]. SP600125, a c-Jun N-terminal kinase inhibitor, shows an IC₅₀ for the purified PknD KD of 30 nM (C. Miecskowski and Tom Alber unpublished results), binds more weakly to other *M. tuberculosis* KDs and inhibits PknD activity *in vivo* [58]. Mitoxantrone, an anthraquinone derivative developed for cancer therapy,

inhibits the PknB kinase domain with an IC_{50} of $0.8 \pm 0.05 \mu M$ and attenuates mycobacterial growth *in vitro* [29]. Mitoxantrone (which also reacts with DNA) showed MIC values of $100 \mu M$ and $400 \mu M$ for *M. smegmatis* and *M. tuberculosis*, respectively. Ectopic expression of PknB in *M. smegmatis* increased the MIC twofold. Because this effect was small, caution is warranted in concluding that PknB is the cellular target of the inhibitor. Overall, these results support the view that a more potent, selective PknB inhibitor may block growth *in vivo* [29].

The first commercial program to develop unique compounds specifically targeting a mycobacterial kinase was carried out by Axxima Pharmaceuticals AG, a German company focusing on developing novel kinase inhibitors for therapeutic treatment of infectious diseases. Using combined screening and medicinal chemistry strategies, Axxima developed AX20017, a tetrahydrobenzothiophene compound that specifically inhibits PknG kinase activity. By inhibiting PknG in *M. bovis* BCG, AX20017 promoted phagolysosome fusion in macrophages, leading to bacterial killing in host cells without affecting the viability of the macrophages [27]. Conceptually, the development of an inhibitor that limits disease processes but does not directly kill *M. tuberculosis in vitro* was unique and challenging to the drug development community. The company produced a series of related compounds targeting PknG, AX14585, and others that were more stable, but development of these kinase inhibitors ceased when the company was sold to GPC Biotech. These tetrahydrobenzothiophene hit compounds are still not potent enough to be active in animal model of infections and require subsequent medicinal chemistry optimization.

The modes of inhibition of mitoxantrone and AX20017 were revealed by the cocrystal structures of these compounds bound, respectively, to the kinase domains of PknB and PknG [29, 51]. Both compounds lodged in the ATP binding sites of the target KDs (Figure 11.1). The two compounds, however, exploited distinct regions of the ATP binding sites that overlapped the position of the adenine ring (Figure 11.2). In particular, AX20017 made contact with the hinge region of PknG [51], while mitoxantrone made contact with residues that recognize the adenine and ribose moieties of the nucleotide and also the “front” of the ATP binding site [29]. Mitoxantrone binding stabilized a conformation of the PknB KD distinct from the nucleotide complex. In the inhibitor complex, the P loop, which recognizes the ATP phosphates, dropped into the active site to make inhibitor contacts (Figure 11.2c). This conformation, which resembles the P loop conformation in the structure of nucleotide-free PknE [50], illustrates the flexibility of the PknB ATP binding site (even in the phosphorylated KD) that can allow recognition of different ligands. Overall, these cocrystal structures illustrate that potency and selectivity can be enhanced by exploiting distinct regions of the ATP binding sites of different KDs.

While PknB currently affords the most promising phosphosignaling target in *M. tuberculosis*, several programs have developed selective inhibitors of the *M. tuberculosis* PTPs, PtpA, and PtpB. Waldmann and coworkers used a new approach inspired by natural-product pharmacophores to discover PTP inhibitors [67–69]. Using this “biology-oriented synthesis” approach, PtpB inhibitors with IC_{50} values as low as 360 ± 12 nM were developed [69]. In contrast, Serono Pharmaceuticals screened libraries of compounds directed against eukaryotic phosphatases for

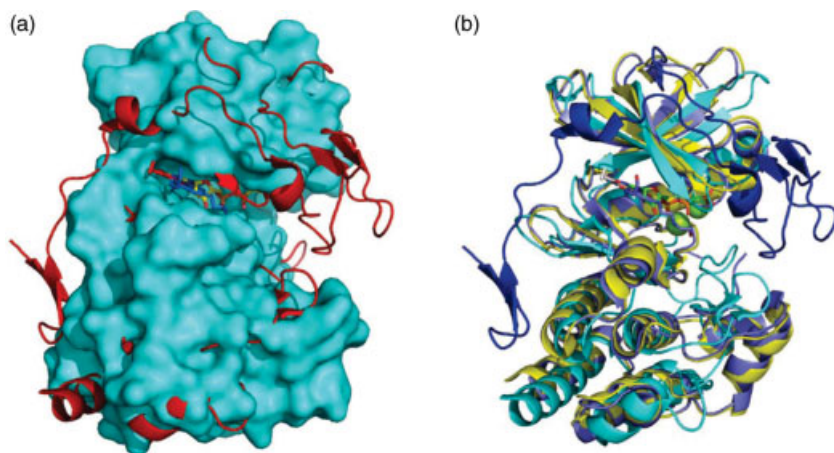


Figure 11.1 Inhibitors occupy the ATP binding site of PknB and PknG. (a) AMPPCP, mitoxantrone and AX20017 (sticks) superimposed on the surface of PknB KD and the ribbon representation of the PknG KD and N-terminal extension. To focus on the shared elements, the C-terminal domains of PknG were omitted. The N-terminal extension of PknG starts on the back of the C-lobe (bottom left) and drapes over the N-lobe, filling the putative binding site for protein substrates.

(b) Superimposed ribbon diagrams of the kinase domains in the AMPPCP (light gray) and inhibitor (medium gray) complexes of PknB and PknG (dark gray), with the N-terminal extension of PknG shown in darker gray. Although the overall folds of the PknB and PknG kinase domains in the complexes are similar, the backbone root mean square deviation (rmsd) is 2.6 Å. Thus, the inhibitors target distinct conformations and surfaces.

inhibitors of the *M. tuberculosis* homologues [70]. Improving potency using medicinal chemistry led to the development of oxalylamino-methylene-thiophene sulfonamide (OMTS), a PtpB inhibitor with an IC_{50} of 440 nM. Remarkably, this compound showed more than 65-fold selectivity for PtpB compared to all human PTPs tested. The cocrystal structure of OMTS bound to PtpB revealed a large change in conformation of the enzyme compared to the product complex and showed two molecules of the inhibitor bound in the active site [70]. The structure supported the idea that the selectivity of OMTS may arise from inhibitor contacts with every residue in the phosphate binding loop, which is conserved in many human phosphatases but differs in three positions in PtpB.

Ellman and coworkers have developed a novel screening method, called substrate activity screening (SAS), and applied it to the *M. tuberculosis* phosphatases to produce the most potent PtpB inhibitor reported to date [70]. Rather than the traditional approach of assaying a compound library for inhibitors, the SAS approach identifies hits in a chemical library of substrates. Because the library compounds must be turned over by the enzyme, false positives due to nonspecific inhibition or denaturation are eliminated and compounds that target the active site are identified. For the PTPs, the substrate library comprises a collection of *O*-aryl phosphates, which are relatively straightforward to synthesize from commercially available building blocks.

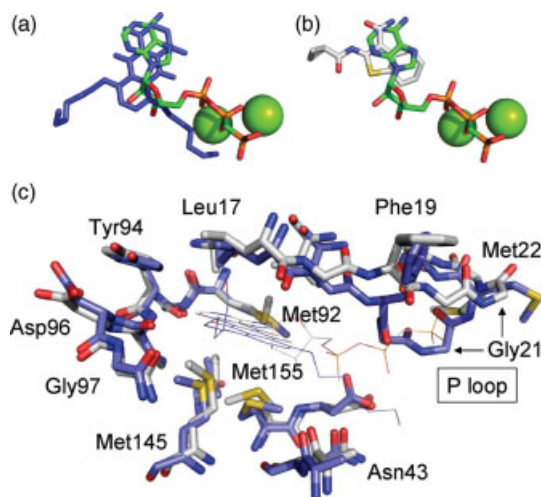


Figure 11.2 Recognition of *M. tuberculosis* STPK inhibitors. (a) Ligands from the superimposed PknB complexes of mitoxantrone (blue, 2FUM) and Mg:AMPPCP (spheres: green, 1O6Y). The inhibitor samples the volume occupied by the adenine and ribose rings of the nucleotide [29, 49]. (b) Nucleotide from the PknB:Mg:AMPPCP complex (spheres: green, 1O6Y) superimposed on the inhibitor from the PknG:AX20017 complex (white and gray atoms, 2PZI). The PknG inhibitor [51] samples a distinct region of the ATP binding site. (c) ATP binding site of PknB

(sticks) adjusts to the binding of AMPPCP (light gray) and mitoxantrone (dark gray). Ligands are shown as lines. The P loop (top right) slumps into the active site in the inhibitor complex, filling the region occupied by the terminal phosphates of the bound nucleotide. Met92, Met155, and Asp156 adopt distinct rotamers in the nucleotide and inhibitor complexes, while the other residues in the binding site adopt similar conformations. The backbone rmsd of the PknB KDs in the superimposed complexes is 0.83 Å.

In the second step of SAS, the best substrates are converted to inhibitors by replacing the labile phosphoryl group with an inhibitory “warhead.” For the PTPs, focusing on the best substrate scaffolds limits the more challenging synthesis of inhibitors to a small set, speeding the overall development process. Using SAS, a PtpB inhibitor with a molecular weight of 433 Da and a K_i value of 220 ± 30 nM was found. This isoxazole inhibitor showed from 35 to >225 selectivity against *M. tuberculosis* PtpA and a panel of four eukaryotic PTPs. The small size of this compound leaves scope for additional modifications to engineer improved properties [70].

A major hurdle for the development of *M. tuberculosis* PTP inhibitors is to demonstrate efficacy *in vivo*. Neither *ptpA* nor *ptpB* are essential for growth in culture, as judged by whole-genome transposon mutagenesis [35] and the growth rate of the *ptpB* deletion mutant [25]. As a result, the PTP inhibitors are expected to have no effects on *M. tuberculosis* growth or viability *in vitro*. The attenuation of the *ptpB* deletion strain in activated macrophages and guinea pigs [25], suggests that cell based or animal assays will be required to establish the validity of these targets and drive further development.

11.6

Conclusions and Prospects

PknB provides the most promising bacterial phosphosignaling target for pharmaceutical development. Promiscuous inhibitors of human kinases are active against PknB, suggesting that the large chemical libraries and deep knowledge about targeting eukaryotic STPKs can be used to develop potent, selective inhibitors. The low sequence identity to the most related human kinase suggests that selectivity will be a low hurdle. High-throughput and secondary assays are well developed, and crystallographic studies to speed inhibitor development are feasible. Genetic studies indicate that *pknB* and *pknA* are essential genes, while the other *M. tuberculosis* STPKs may play interesting adaptive roles with pleiotropic effects on physiology. The scope for inhibitors that target multiple *M. tuberculosis* STPKs to shorten treatment of active TB or enable treatment of latent disease has yet to be explored. PknB orthologues are the most widely distributed bacterial STPKs, suggesting that inhibitors may be active against diverse bacterial pathogens.

Inhibitors of *M. tuberculosis* PtpB have been developed by traditional and novel approaches. These compounds show remarkable selectivity against the human phosphatases. The structures of PtpA and PtpB, as well as a cocrystal structure of the OMTS inhibitor bound to PtpB, indicate that structure-based strategies are accessible to increase potency. Improving potency and demonstrating that the inhibitors limit infection *in vivo* are key steps needed to promote development.

Overall, efforts to discover pharmaceuticals targeting bacterial phosphosignaling are just beginning. Fundamental studies of the functions and structures of these proteins have established the groundwork to make rapid progress in this field.

Acknowledgments

Research in the laboratory of Yossef Av-Gay is funded by the Canadian Institute of Health Research (CIHR) grant # MOP-68857 and the British Columbia TB Veterans Charitable Foundation. Tom Alber acknowledges support from the TB Structural Genomics Consortium and NIH grants GM70962 and AI068135.

References

- 1 WHO (2006) Factsheet No. 104. WHO, Geneva.
- 2 Gagneux, S. and Small, P.M. (2007) Global phylogeography of *Mycobacterium tuberculosis* and implications for tuberculosis product development. *Lancet Infectious Diseases*, **7**, 328–337.
- 3 MMWR (2007) Extensively drug-resistant tuberculosis – United States, 1993–2006. *Morbidity and Mortality Weekly Report*, **56**, 250–253.
- 4 Barry, P.J. and O'Connor, T.M. (2007) Novel agents in the management of *Mycobacterium tuberculosis* disease. *Current Medicinal Chemistry*, **14**, 2000–2008.
- 5 Laughon, B.E. (2007) New tuberculosis drugs in development. *Current Topics in Medicinal Chemistry*, **7**, 463–473.

- 6 Koul, A., Dendouga, N., Vergauwen, K., Molenberghs, B., Vranckx, L., Willebrords, R., Ristic, Z., Lill, H., Dorange, I., Guillemont, J., Bald, D., and Andries, K. (2007) Diarylquinolines target subunit c of mycobacterial ATP synthase. *Nature Chemical Biology*, **3**, 323–324.
- 7 Hestvik, A.L., Hmama, Z., and Av-Gay, Y. (2005) Mycobacterial manipulation of the host cell. *FEMS Microbiology Reviews*, **29**, 87–94.
- 8 Sturgill-Koszycki, S., Schlesinger, P.H., Chakraborty, P., Haddix, P.L., Collins, H.L., Fok, A.K., Allen, R.D., Gluck, S.L., Heuser, J., and Russell, D.G. (1994) Lack of acidification in Mycobacterium phagosomes produced by exclusion of the vesicular proton-ATPase. *Science*, **263**, 678–681.
- 9 Fratti, R.A., Backer, J.M., Gruenberg, J., Corvera, S., and Deretic, V. (2001) Role of phosphatidylinositol 3-kinase and Rab5 effectors in phagosomal biogenesis and mycobacterial phagosome maturation arrest. *The Journal of Cell Biology*, **154**, 631–644.
- 10 Russell, D.G. (2001) Mycobacterium tuberculosis: here today, and here tomorrow. *Nature Reviews. Molecular Cell Biology*, **2**, 569–577.
- 11 Hmama, Z., Gabathuler, R., Jefferies, W.A., de Jong, G., and Reiner N.E., (1998) Attenuation of HLA-DR expression by mononuclear phagocytes infected with *Mycobacterium tuberculosis* is related to intracellular sequestration of immature class II heterodimers. *Journal of Immunology*, **161**, 4882–4893.
- 12 Ting, L.M., Kim, A.C., Cattamanchi, A., and Ernst, J.D. (1999) Mycobacterium tuberculosis inhibits IFN-gamma transcriptional responses without inhibiting activation of STAT1. *Journal of Immunology*, **163**, 3898–3906.
- 13 Schnappinger, D., Ehrt, S., Voskuil, M.I., Liu, Y., Mangan, J.A., Monahan, I.M., Dolganov, G., Efron, B., Butcher, P.D., Nathan, C., and Schoolnik, G.K. (2003) Transcriptional adaptation of *Mycobacterium tuberculosis* within macrophages: insights into the phagosomal environment. *The Journal of Experimental Medicine*, **198**, 693–704.
- 14 Darwin, K.H., Ehrt, S., Gutierrez-Ramos, J.C., Weich, N., and Nathan, C.F. (2003) The proteasome of *Mycobacterium tuberculosis* is required for resistance to nitric oxide. *Science*, **302**, 1963–1966.
- 15 Voskuil, M.I., Schnappinger, D., Visconti, K.C., Harrell, M.I., Dolganov, G.M., Sherman, D.R., and Schoolnik, G.K. (2003) Inhibition of respiration by nitric oxide induces a *Mycobacterium tuberculosis* dormancy program. *The Journal of Experimental Medicine*, **198**, 705–713.
- 16 Wayne, L.G. and Sohaskey, C.D. (2001) Nonreplicating persistence of *Mycobacterium tuberculosis*. *Annual Review of Microbiology*, **55**, 139–163.
- 17 Av-Gay, Y. and Deretic, V. (2004) Two-component system, protein kinases, and signal transduction in *Mycobacterium tuberculosis*, in *Tuberculosis*, vol. 2 (eds S. Cole et al.) ASM Press, Washington DC, pp. 359–366, Chapter 22.
- 18 Zahrt, T.C. and Deretic, V. (2001) Mycobacterium tuberculosis signal transduction system required for persistent infections. *Proceedings of the National Academy of Sciences of the United States of America*, **98**, 12706–12711.
- 19 Av-Gay, Y. and Davies, J. (1997) Components of eukaryotic-like protein signaling pathways in *Mycobacterium tuberculosis*. *Microbial & Comparative Genomics*, **2**, 63–73.
- 20 Av-Gay, Y. and Everett, M. (2000) The eukaryotic-like Ser/Thr protein kinases of *Mycobacterium tuberculosis*. *Trends in Microbiology*, **8**, 238–244.
- 21 Greenstein, A.E., Grundner, C., Echols, N., Gay, L.M., Lombana, T.N., Miecskowski, C.A., Pullen, K.E., Sung, P.Y., and Alber, T. (2005) Structure/ function studies of Ser/Thr and Tyr protein phosphorylation in *Mycobacterium tuberculosis*. *Journal of Molecular Microbiology and Biotechnology*, **9**, 167–181.
- 22 Koul, A., Herget, T., Klebl, B., and Ullrich, A. (2004) Interplay between mycobacteria and host signaling pathways. *Nature Reviews Microbiology*, **2**, 189–202.
- 23 Cowley, S.C., Babakiaff, R., and Av-Gay, Y. (2002) Expression and localization of the *Mycobacterium tuberculosis* protein

- tyrosine phosphatase PtpA. *Research in Microbiology*, **153**, 233–241.
- 24 Grundner, C., Ng, H.L., and Alber, T. (2005) *Mycobacterium tuberculosis* protein tyrosine phosphatase PtpB structure reveals a diverged fold and a buried active site. *Structure*, **13**, 1625–1634.
 - 25 Singh, R., Rao, V., Shakila, H., Gupta, R., Khera, A., Dhar, N., Singh, A., Koul, A., Singh, Y., Naseema, M., Narayanan, P.R., Paramasivan, C.N., Ramanathan, V.D., and Tyagi, A.K. (2003) Disruption of MptpB impairs the ability of *Mycobacterium tuberculosis* to survive in guinea pigs. *Molecular Microbiology*, **50**, 751–762.
 - 26 Greenstein, A.E., Echols, N., Lombana, T.N., King, D.S., and Alber, T. (2007) Allosteric activation by dimerization of the PknD receptor Ser/Thr protein kinase from *Mycobacterium tuberculosis*. *The Journal of Biological Chemistry*, **282**, 11427–11435.
 - 27 Walburger, A., Koul, A., Ferrari, G., Nguyen, L., Prescianotto-Baschong, C., Huygen, K., Klebl, B., Thompson, C., Bacher, G., and Pieters, J. (2004) Protein kinase G from pathogenic mycobacteria promotes survival within macrophages. *Science*, **304**, 1800–1804.
 - 28 Drews, S.J., Hung, F., and Av-Gay, Y. (2001) A protein kinase inhibitor as an antimycobacterial agent. *FEMS Microbiology Letters*, **205**, 369–374.
 - 29 Wehenkel, A., Fernandez, P., Bellinzoni, M., Catherinot, V., Barilone, N., Labesse, G., Jackson, M., and Alzari, P.M. (2006) The structure of PknB in complex with mitoxantrone, an ATP-competitive inhibitor, suggests a mode of protein kinase regulation in mycobacteria. *FEBS Letters*, **580**, 3018–3022.
 - 30 Wehenkel, A., Bellinzoni, M., Grana, M., Duran, R., Villarino, A., Fernandez, P., Andre-Leroux, G., England, P., Takiff, H., Cervenansky, C., Cole, S.T., and Alzari, P.M. (2008) *Mycobacterial Ser/Thr protein kinases and phosphatases: physiological roles and therapeutic potential*. *Biochimica et Biophysica Acta*, **1784**, 193–202.
 - 31 Fernandez, P., Saint-Joanis, B., Barilone, N., Jackson, M., Gicquel, B., Cole, S.T., and Alzari, P.M. (2006) The Ser/Thr protein kinase PknB is essential for sustaining mycobacterial growth. *Journal of Bacteriology*, **188**, 7778–7784.
 - 32 Sassetti, C.M., Boyd, D.H., and Rubin, E.J. (2003) Genes required for mycobacterial growth defined by high-density mutagenesis. *Molecular Microbiology*, **48**, 77–84.
 - 33 Cowley, S., Ko, M., Pick, N., Chow, R., Downing, K.J., Gordhan, B.G., Betts, J.C., Mizrahi, V., Smith, D.A., Stokes, R.W., and Av-Gay, Y. (2004) The *Mycobacterium tuberculosis* protein serine/threonine kinase PknG is linked to cellular glutamate/glutamine levels and is important for growth *in vivo*. *Molecular Microbiology*, **52**, 1691–1702.
 - 34 Kang, C.M., Abbott, D.W., Park, S.T., Dascher, C.C., Cantley, L.C., and Husson, R.N. (2005) The *Mycobacterium tuberculosis* serine/threonine kinases PknA and PknB: substrate identification and regulation of cell shape. *Genes and Development*, **19**, 1692–1704.
 - 35 Sassetti, C.M. and Rubin, E.J. (2003) Genetic requirements for mycobacterial survival during infection. *Proceedings of the National Academy of Sciences of the United States of America*, **100**, 12989–12994.
 - 36 Papavinasasundaram, K.G., Chan, B., Chung, J.H., Colston, M.J., Davis, E.O., and Av-Gay, Y. (2005) Deletion of the *Mycobacterium tuberculosis* pknH gene confers a higher bacillary load during the chronic phase of infection in BALB/c mice. *Journal of Bacteriology*, **187**, 5751–5760.
 - 37 Roberts, D.M., Liao, R.P., Wisedchaisri, G., Hol, W.G., and Sherman, D.R. (2004) Two sensor kinases contribute to the hypoxic response of *Mycobacterium tuberculosis*. *The Journal of Biological Chemistry*, **279**, 23082–23087.
 - 38 Kumar, A., Toledo, J.C., Patel, R.P., Lancaster, J.R. Jr., and Steyn, A.J. (2007) *Mycobacterium tuberculosis* DosS is a redox sensor and DosT is a hypoxia sensor. *Proceedings of the National Academy of Sciences of the United States of America*, **104**, 11568–11573.
 - 39 Park, H.D., Guinn, K.M., Harrell, M.I., Liao, R., Voskuil, M.I., Tompa, M.,

- Schoolnik, G.K., and Sherman, D.R. (2003) Rv3133c/dosR is a transcription factor that mediates the hypoxic response of *Mycobacterium tuberculosis*. *Molecular Microbiology*, **48**, 833–843.
- 40 Perez, J., Garcia, R., Bach, H., de Waard, J.H., Jacobs, W.R. Jr., Av-Gay, Y., Bubis, J., and Takiff, H.E. (2006) *Mycobacterium tuberculosis* transporter MmpL7 is a potential substrate for kinase PknD. *Biochemical and Biophysical Research Communications*, **348**, 6–12.
- 41 Jayakumar, D., Jacobs, W.R. Jr., and Narayanan, S. (2008) Protein kinase E of *Mycobacterium tuberculosis* has a role in the nitric oxide stress response and apoptosis in a human macrophage model of infection. *Cellular Microbiology*, **10**, 365–374.
- 42 Deol, P., Vohra, R., Saini, A.K., Singh, A., Chandra, H., Chopra, P., Das, T.K., Tyagi, A.K., and Singh, Y. (2005) Role of *Mycobacterium tuberculosis* Ser/Thr kinase PknF: implications in glucose transport and cell division. *Journal of Bacteriology*, **187**, 3415–3420.
- 43 Young, T.A., Delagoutte, B., Endrizzi, J.A., Falick, A.M., and Alber, T. (2003) Structure of *Mycobacterium tuberculosis* PknB supports a universal activation mechanism for Ser/Thr protein kinases. *Nature Structural Biology*, **10**, 168–174.
- 44 Av-Gay, Y., Jamil, S., and Drews, S.J. (1999) Expression and characterization of the *Mycobacterium tuberculosis* serine/threonine protein kinase PknB. *Infection and Immunity*, **67**, 5676–5682.
- 45 Boitel, B., Ortiz-Lombardia, M., Duran, R., Pompeo, F., Cole, S.T., Cervenansky, C., and Alzari, P.M. (2003) PknB kinase activity is regulated by phosphorylation in two Thr residues and dephosphorylation by PstP, the cognate phospho-Ser/Thr phosphatase, in *Mycobacterium tuberculosis*. *Molecular Microbiology*, **49**, 1493–1508.
- 46 Jones, G. and Dyson, P. (2006) Evolution of transmembrane protein kinases implicated in coordinating remodeling of gram-positive peptidoglycan: inside versus outside. *Journal of Bacteriology*, **188**, 7470–7476.
- 47 Dar, A.C., Dever, T.E., and Sicheri, F. (2005) Higher-order substrate recognition of eIF2alpha by the RNA-dependent protein kinase PKR. *Cell*, **122**, 887–900.
- 48 Dey, M., Cao, C., Dar, A.C., Tamura, T., Ozato, K., Sicheri, F., and Dever, T.E. (2005) Mechanistic link between PKR dimerization, autophosphorylation, and eIF2alpha substrate recognition. *Cell*, **122**, 901–913.
- 49 Ortiz-Lombardia, M., Pompeo, F., Boitel, B., and Alzari, P.M. (2003) Crystal structure of the catalytic domain of the PknB serine/threonine kinase from *Mycobacterium tuberculosis*. *The Journal of Biological Chemistry*, **278**, 13094–13100.
- 50 Gay, L.M., Ng, H.L., and Alber, T. (2006) A conserved dimer and global conformational changes in the structure of apo-PknE Ser/Thr protein kinase from *Mycobacterium tuberculosis*. *Journal of Molecular Biology*, **360**, 409–420.
- 51 Scherr, N., Honnappa, S., Kunz, G., Mueller, P., Jayachandran, R., Winkler, F., Pieters, J., and Steinmetz, M.O. (2007) Structural basis for the specific inhibition of protein kinase G, a virulence factor of *Mycobacterium tuberculosis*. *Proceedings of the National Academy of Sciences of the United States of America*, **104**, 12151–12156.
- 52 Bendt, A.K., Burkovski, A., Schaffer, S., Bott, M., Farwick, M., and Hermann, T. (2003) Towards a phosphoproteome map of *Corynebacterium glutamicum*. *Proteomics*, **3**, 1637–1646.
- 53 Zheng, X., Papavinasandaram, K.G., and Av-Gay, Y. (2007) Novel substrates of *Mycobacterium tuberculosis* PknH Ser/Thr kinase. *Biochemical and Biophysical Research Communications*, **355**, 162–168.
- 54 Dasgupta, A., Datta, P., Kundu, M., and Basu, J. (2006) The serine/threonine kinase PknB of *Mycobacterium tuberculosis* phosphorylates PBPA, a penicillin-binding protein required for cell division. *Microbiology*, **152**, 493–504.
- 55 Grundner, C., Gay, L.M., and Alber, T. (2005) *Mycobacterium tuberculosis* serine/threonine kinases PknB, PknD, PknE, and PknF phosphorylate multiple FHA

- domains. *Protein Science: A Publication of the Protein Society*, **14**, 1918–1921.
- 56 Villarino, A., Duran, R., Wehenkel, A., Fernandez, P., England, P., Brodin, P., Cole, S.T., Zimny-Arndt, U., Jungblut, P.R., Cervenansky, C., and Alzari, P.M. (2005) Proteomic identification of *M. tuberculosis* protein kinase substrates: PknB recruits GarA, a FHA domain-containing protein, through activation loop-mediated interactions. *Journal of Molecular Biology*, **350**, 953–963.
 - 57 Molle, V., Zanella-Cleon, I., Robin, J.P., Mallejac, S., Cozzzone, A.J., and Becchi, M. (2006) Characterization of the phosphorylation sites of *Mycobacterium tuberculosis* serine/threonine protein kinases, PknA, PknD, PknE, and PknH by mass spectrometry. *Proteomics*, **6**, 3754–3766.
 - 58 Greenstein, A.E., MacGurn, J.A., Baer, C.E., Falick, A.M., Cox, J.S., and Alber, T. (2007) *M. tuberculosis* Ser/Thr protein kinase D phosphorylates an anti-anti-sigma factor homolog. *PLoS Pathogens*, **3**, e49.
 - 59 Skerker, J.M., Prasol, M.S., Perchuk, B.S., Biondi, E.G., and Laub, M.T. (2005) Two-component signal transduction pathways regulating growth and cell cycle progression in a bacterium: a system-level analysis. *PLoS Biology*, **3**, e334.
 - 60 Molle, V., Brown, A.K., Besra, G.S., Cozzzone, A.J., and Kremer, L. (2006) The condensing activities of the *Mycobacterium tuberculosis* type II fatty acid synthase are differentially regulated by phosphorylation. *The Journal of Biological Chemistry*, **281**, 30094–30103.
 - 61 Duran, R., Villarino, A., Bellinzoni, M., Wehenkel, A., Fernandez, P., Boitel, B., Cole, S.T., Alzari, P.M., and Cervenansky, C. (2005) Conserved autophosphorylation pattern in activation loops and juxtamembrane regions of *Mycobacterium tuberculosis* Ser/Thr protein kinases. *Biochemical and Biophysical Research Communications*, **333**, 858–867.
 - 62 Molle, V., Kremer, L., Girard-Blanc, C., Besra, G.S., Cozzzone, A.J., and Prost, J.F. (2003) An FHA phosphoprotein recognition domain mediates protein EmbR phosphorylation by PknH, a Ser/Thr protein kinase from *Mycobacterium tuberculosis*. *Biochemistry*, **42**, 15300–15309.
 - 63 Sharma, K., Gupta, M., Krupa, A., Srinivasan, N., and Singh, Y. (2006) EmbR, a regulatory protein with ATPase activity, is a substrate of multiple serine/threonine kinases and phosphatase in *Mycobacterium tuberculosis*. *FEBS Journal*, **273**, 2711–2721.
 - 64 Umeyama, T., Lee, P.C., and Horinouchi, S. (2002) Protein serine/threonine kinases in signal transduction for secondary metabolism and morphogenesis in *Streptomyces*. *Applied Microbiology and Biotechnology*, **59**, 419–425.
 - 65 Mougous, J.D., Gifford, C.A., Ramsdell, T.L., and Mekalanos, J.J. (2007) Threonine phosphorylation post-translationally regulates protein secretion in *Pseudomonas aeruginosa*. *Nature Cell Biology*, **9**, 797–803.
 - 66 Niebisch, A., Kabus, A., Schultz, C., Weil, B., and Bott, M. (2006) Corynebacterial protein kinase G controls 2-oxoglutarate dehydrogenase activity via the phosphorylation status of the OdhI protein. *The Journal of Biological Chemistry*, **281**, 12300–12307.
 - 67 Bialy, L. and Waldmann, H. (2005) Inhibitors of protein tyrosine phosphatases: next-generation drugs? *Angewandte Chemie – International Edition in English*, **44**, 3814–3839.
 - 68 Correa, I.R. Jr., Noren-Muller, A., Ambrosi, H.D., Jakupovic, S., Saxena, K., Schwalbe, H., Kaiser, M., and Waldmann, H. (2007) Identification of inhibitors for mycobacterial protein tyrosine phosphatase B (MtpB) by biology-oriented synthesis (BIOS). *Chemistry, an Asian Journal*, **2**, 1109–1126.
 - 69 Nören-Müller, A., Reis-Correa, I. Jr., Prinz, H., Rosenbaum, C., Saxena, K., Schwalbe, H.J., Vestweber, D., Cagna, G., Schunk, S., Schwarz, O., Schiewe, H., and Waldmann, H. (2006) Discovery of protein phosphatase inhibitor classes by biology-oriented synthesis. *Proceedings of the*

National Academy of Sciences of the United States of America, **103**, 10606–10611.

- 70 Soellner, M.B., Rawls, K.A., Grundner, C., Alber, T., and Ellman, J.A. (2007) Fragment-based substrate activity

screening method for the identification of potent inhibitors of the *Mycobacterium tuberculosis* phosphatase PtpB. *Journal of the American Chemical Society*, **129**, 9613–9615.

Index

a

- A-420983 179
- A-641593 179
- A-770041 179
- AAL-993 177
- Abelson (Abl) kinase 74ff., 151ff., 177
 - inhibitor 186
- absorption
 - gastrointestinal cell 28
- absorption, distribution, metabolism, and excretion (ADME) issue
- protein kinase inhibitor in early drug discovery 26
- ACE (angiotensin-converting enzyme) inhibitor 90
- activator protein-1 (AP1) 131
- active analogue approach (AAA) 92
- acute myelogenous leukemia (AML) 116
- adenine binding region 104
- adenovirus 327
- AEB071 126
- AEE788 120
- AEW541/NPV-AEW541 120
- affinity chromatography
 - immobilized kinase inhibitor 63
 - kinase inhibitor 97
- AG013736 116
- AG024322 127
- Akt (Akt1)/ PKB (protein kinase B) 129
- Akt/PDK-/Flt3 multiple target inhibitor 117
- allosteric kinase inhibitor 101
- allosteric site 17
- AlphaScreen-based Surefire technology 58
- AMG-548 292
- AMG706 121
- 2-aminobenzimidazole 172
- 2-aminobenzoxazole 172
- 2-aminoquinazoline 176ff.
 - 3-amino-6,11-dihydro-dibenzo[*b,e*]thiepin-11-one 295
 - 3-amino-tetrahydropyrrolo[3,4-*c*]pyrazole 217
 - amino-thiazolo acetanilide quinazolines 208
 - AMN107 118, 170
 - analogue-sensitive kinase allele (ASKA) 71ff.
 - application in molecular biology 76
 - anilinoquinazoline 203
 - antibody-based detection 56
 - antihypertensive drug 90
 - antiviral activity 338
 - PCI 310, 327
 - antiviral target
 - cellular protein kinase 305ff.
 - ARQ197 123
 - ARRY142886 (AZD6244) 126
 - ARRY438162 125
 - N*-aryl-*N'*-pyrazolylurea 287
 - ASKA kinase 71ff.
 - ASKA ligand–kinase pair
 - engineering 71
 - ASKA EGFR 73
 - ASKA Src 72ff.
 - AT9283 128, 220, 250
 - ATP 94
 - competition 47, 102
 - ATP analogues 72
 - ATP binding cassette (ABC) transporter 33ff.
 - ABCB1 (P-gp) 27ff.
 - ABCC2 36
 - ABCG2 36, 119
 - ATP binding site 91ff.
 - ATP concentration 10ff., 48
 - ATP site specificity 236
 - ATP-competitive inhibitor 97, 147, 281

- Aurora kinase 96, 127
 - Aurora A (AurKA, AKA) 99, 151, 175, 196ff., 243
 - Aurora B (AurKB, AKB) 175, 196ff., 243
 - Aurora C (AKC) 196ff., 244
 - biological role 195f.
 - cancer 196
 - X-ray crystal structure 221
- Aurora kinase inhibitor 118ff., 175, 195ff., 242ff.
- clinical trial 248
- *in vitro* phenotype 197
- screening 244
- structure-guided design 244
- treatment for cancer 195ff.
- AV951 116
- AX14585 356
- AX20017 356
- Axitinib (AG013736) 116
- AZD0530 123
- AZD1152 202ff., 219, 249
- AZD2171 116
- AZD6244 126

- b**
- back pocket 146ff.
- back-to-back design strategy 155, 169
- back-to-front design strategy 155, 166
- BAY43-9006 89, 245
- Bcr-Abl (breakpoint cluster region–Abelson murine leukemia viral oncogene homologue) 54, 60, 80, 118
 - inhibitor 91ff.
 - kinase 92
 - tyrosine kinase inhibitor 89, 118
- BCRP (ABCG2) 36, 119
- 5-benzimidazol-1-yl-3-aryloxy-thiophene-2-carboxamides 256
- benzothiophene 166
- benzthiazole PLK1 inhibitor 254
- BEZ235 129
- BGT226 129
- BI1489 245
- BI2536 256f.
- 1*H*,1'*H*-[2,3'] biindolylidene-3,2'-dione 3-oxime 326
- binding affinity 15
- bioactive conformation 92
- biochemical kinase assay 4
 - dependence on the kinase concentration 12
 - identification of substrate 4
 - linearity between signal and kinase concentration 4
 - optimization of reaction buffer 6ff.
 - signal linearity throughout the reaction time 12
 - validation by measurement of IC₅₀ of reference inhibitor 15
- biomolecular interaction analysis
 - surface plasmon resonance (SPR)-based 19
- biosensor
 - genetically encoded 61
- biphenyl amide (BPA) 124
- BIRB-796 15ff, 49, 89, 101, 118ff., 148ff., 166, 245, 277ff.
- BMS354825 118
- BMS387032/SNS032 127
- BMS536924 120
- BMS582949 124
- BMS599626 120
- Bosutinib (SKI606) 123
- BRET (bioluminescence resonance energy transfer) technology 58
- BRK 99
- Btk 77
- Bub1 99
- bump-and-hole approach 70

- c**
- Caco-2 cell 32ff.
- CAL101 130
- CaMKII 99
- cancer
 - treatment with Aurora kinase inhibitor 195ff.
- Canertinib 275
- Captopryl 90
- CARDIAK 99
- casein kinase 2 (CK2) 133
- catalytic site inhibitor 234
- CD117 121
 - inhibitor 121
- CD135 116
- CDC25c 250
- Cediranib (AZD2171) 116, 121
- cell cycle
 - oncology 231
- cell line
 - genetically engineered 60
- cell permeability 52
- cellular kinase assay 45ff.
 - drug discovery application 46
 - measurement of activity 55
- cellular kinase concentration 53
- cellular kinase inhibition 53
- cellular protein kinase 305
 - antiviral target 305ff.
- CEP701 116, 130

- CGP57148B 94
 - CGP79787/CGP79787D 116
 - chemical genetics 71
 - Chemical Validation Library (CVL) 99
 - Cheng–Prusoff equation 10, 48
 - CHIR258/TKI258 116ff.
 - CHIR-265 172
 - 2-(2-chloro-phenyl)-5,7-dihydroxy-8-(3-hydroxy-1-methyl-piperidin-4-yl)-chromen-4-one 326
 - chronic myeloid leukemia (CML) 115
 - CI1033 118, 339
 - CI1040 49, 125f.
 - CL-387785 51
 - Cla4 75
 - combination therapy
 - PCI 336
 - comparative molecular field analysis (CoMFA) 93
 - comparative molecular moment analysis (CoMMA) 93
 - comparative molecular similarity analysis (CoMSIA) 93
 - competition
 - ATP 47
 - conivaptan 125
 - CP547632 116
 - CP690550 130
 - CP724714 120
 - CSK 99
 - CVT-313 327
 - CYC116 116, 250
 - CYC202 127
 - Cyclacel 127
 - cyclin groove inhibitor (CGI) 240
 - cyclin-dependent kinase (CDK) 127, 233f., 310f.
 - CDK1 310ff., 330f.
 - CDK2 71, 92, 236ff., 310ff., 330ff.
 - CDK3 311ff.
 - CDK4 236ff., 310ff.
 - CDK5 236, 310ff., 330f.
 - CDK6 151, 236, 310ff.
 - CDK7 236, 310ff., 330f.
 - CDK8 310ff., 331
 - CDK9 133, 310ff., 331ff.
 - CDK10 310ff.
 - CDK11 310ff.
 - CDK12 310ff.
 - CDK13 310
 - family 48
 - inhibiting 239
 - inhibition of CDK–cyclin association 242
 - property 310f.
 - small-molecule inhibitor 233ff.
 - cyclin-dependent kinase inhibitor (PCI) 305ff., 323ff.
 - combination therapy 336
 - herpes virus 330
 - HIV 332ff.
 - property 310f.
 - specificity 312ff.
 - viral pathogenesis 337
 - cytochrome P450 enzyme (CYP450) 27ff., 283
 - isoform 35
 - measuring inhibition 39
 - cytokine suppressive anti-inflammatory drug (CSAID) 275
 - cytokine suppressive anti-inflammatory drug binding protein (CSPB), *see* p38 MAP kinase
- d**
- dasatinib (BMS354825) 118, 145ff.
 - deep pocket (DP) 17, 146ff.
 - design principle 145ff.
 - deep pocket binder 148
 - deep pocket binding inhibitor 25
 - DELFI (dissociation enhanced lanthanide fluorescent immunoassay) method 57
 - design strategy
 - comparative analysis 180
 - DFG (Asp-Phe-Gly) motif 150
 - DFG-*in* conformation 79, 153
 - DFG-*out* conformation 17ff., 79, 153
 - N,N'*-diarylhurea-based inhibitor 286
 - dibenzo[*a,d*]cyclohepten-5-ones 295
 - 6,11-dihydro-dibenzo-*[b,e]*oxepin-11-ones
 - phenylamino-substituted 295
 - dihydropyrimidopyrimidinone 160
 - Dilmapimod 295ff.
 - Dilmapimod tosylate 299
 - DiscoverX's enzyme fragment complementation technology 59
 - distribution coefficient 30
 - Doramapimod 124
 - drug absorption
 - experimental approach 30
 - drug design
 - kinase inhibitor for signal transduction therapy 87ff.
 - rational, *see* rational drug design
 - drug discovery
 - implication 25
 - drug discovery application
 - cellular kinase assay 46
 - drug metabolism 34
 - experimental approach 34

- phase I and II processes 34
- drug target 350
- validation by genetic inactivation 351

e

- EF-TU 78
- EGFR (epidermal growth factor receptor) 18, 73ff., 89, 118
- inhibitor 91
- EGFR/HER2 kinase inhibitor 119
- EKB569 118
- electrochemiluminescent label 57
- ELISA (enzyme-linked immunosorbent assay)
 - method 56
- enzastaurin 126
- enzyme
 - chemically knock out 70
- enzyme donor (ED) peptide fragment 79
- enzyme fragment complementation (EFC)
 - technology 79
- EO1606 294
- EphB4 (ephrin receptor) 99
- epidermal growth factor receptor, *see* EGFR
- Epstein–Barr virus (EBV) 327ff.
- equilibrium ionization coefficient 31
- ERK1 kinase 51ff., 124
- ERK2 kinase 51ff., 124
- erlotinib (TarcevaTM) 18, 91, 145ff., 164
- extended pharmacophore modeling 99
- Extended Validation Library (EVL) 99
- extracellular enveloped virion (EEV) 339

f

- FGFR (fibroblast growth factor receptor) 92, 120
- flavopiridol 97, 127, 326ff.
- FlexX program 90
- Flt (FMS-like tyrosine kinase)
 - Flt-1 177
 - Flt3 60, 116, 151
 - Flt-4 177
- fluorescent labels in kinases (FLiK) 79
- fluorescent probe 21
- Fms/CSFR 151
- c-Fos 60
- fostamatinib (R935788) 130
- FR167653 278
- FRET biosensor 61
- front-to-back design strategy 155ff.
- fuopyrimidine 160

g

- GAK 99
- gastrointestinal stromal tumor (GIST) 118

- gatekeeper residue 74, 91
- gefitinib (IressaTM) 91ff., 145ff.
- GK00687 168
- Gleevec[®] (Glivec[®], imatinib) 15, 49, 74ff., 89ff., 118ff., 145f., 245, 338f.
- Go6976 305
- GSK690693 129
- GSK1059615 130
- GSK1120212 125
- GSK1363089(XL880) 116
- GW400426 77
- GW572016 18f.
- GW-681323 299
- GW-856553X 295

h

- H7 355
- H-89 15
- Hck 179
- hepatic clearance 37
- hepatocyte growth factor (HGF) 122
- HER2 kinase 73, 120
- HER2 tyrosine kinase inhibitor 54
- herpes simplex virus
 - type 1 (HSV-1) 327ff.
 - type 2 (HSV-2) 327
- herpes virus
 - antiviral activity 327
 - PCI 330
- hesperadin 197, 245ff.
- high-content analysis (HCA) 59
- high-content screening 59
- HIV 327ff.
 - PCI 332ff.
- HIVAN (HIV-associated nephropathy) 337
- HKI-272 51, 119
- HOG1 77
- human cytomegalovirus (HCMV) 305, 327ff.
- human T-lymphotropic virus-1 (HTLV-1) 327
- hybrid design strategy 155ff., 173
- hydrogen bond acceptor (HBA) 180
- hydrogen bond donor (HBD) 180
- hydrophobic back pocket 104
- 7-hydroxy-staurosporine 127

i

- IC₅₀ 13
- IGF1 receptor (IGF1R) 120
- IGFR insulin-like growth factor receptor 120
- IκB 51
- IκB kinase (IKK) 131
- imatinib (Gleevec[®]) 15, 49, 74ff., 89ff., 118ff., 145f., 245, 338f.
- impedance measurement 62

INCB018424 130
 indirubin-3'-monoxime 326ff.
 indolocarbazole 305
 inner centrosome protein (INCENP) 221, 243ff.
 infection 132
 inflammation 131
 – kinase inhibitor 131
 inhibitor
 – effect 54
 – preincubation 22
 inositol polyphosphate 5-phosphatase (SHIP2) 51
 insulin receptor (IR) 120
 insulin receptor kinase (IRK) 151
 investigational new drug (IND) 99
 ionization
 – measurement 30
 Iressa™ 18, 91, 145f.
 1-(5-isoquinolinesulfonyl)-2-methylpiperazine 355

j

JAK (Janus kinase) 130
 – JAK2 kinase 116
 JC virus 327
 JNK (c-Jun N-terminal kinase, MAPK8) 126, 131, 271ff.
 – Jnk2 99

k

Kaposi's sarcoma herpesvirus (KSHV) 327ff.
 KDR 151, 163ff., 178
 Ki23057 121
 kinase
 – analogue-sensitive 69ff.
 – specifically targeting 78
 – untouchable 108
 kinase activity
 – detergent 9
 – ion 9
 – MgCl₂ and MnCl₂ concentration 9
 – phosphatase inhibitor 9
 kinase family selectivity
 – analysis 62
 kinase family-biased master key concept 105
 kinase inhibition 76
 kinase inhibitor
 – affinity chromatography 97
 – cellular efficacy 47
 – dissection of signaling pathway 46
 – immobilized 63
 – infectious disease 131
 – inflammation 131

 – personalized therapy 96
 – screening 45ff.
 – second-generation 105
 – signal transduction therapy 87ff., 115ff.
 – small-molecule, *see* small-molecule kinase inhibitor
 – tool 69ff.
 – unusual 15
 kinase signaling
 – compartmentalization 55
 kinase signaling cascade
 – ultrasensitivity 51
 kinase substrate
 – identification 76
 KinaTor™ technology 97ff.
 c-Kit 80, 118, 121, 151
 c-Kit receptor 121
 KIT 121
 KIT/FLT3 inhibitor 118
 KP3721 117
 KRN383 117

l

L-167782 280
 L-786134 280
 label-free assay 62
 lapatinib (Tykerb™) 15ff., 89ff., 145ff., 169ff.
 large T antigen (T Ag) protein 335f.
 lck (lymphocyte-specific kinase) 92, 151, 175ff.
 LeapFrog 90
 lestaurtinib (CEP701) 116, 130
 ligand efficiency (LE) 180ff.
 ligand-based drug design 92
 Lipinski's rule of five 28
 lipophilicity 31
 – measurement 30
 liver clearance 37
 losmapimod (8565533) 124, 295
 luminex technology 57ff.
 LY294002 51, 73, 254ff.
 LY317615/enzastaurin 126
 LY333531/Ruboxistaurin 126
 Lyn 99

m

Madin-Darby canine kidney cell (MDCK) 32
 magic methyl 154ff.
 MAPK (mitogen-activated protein kinase) 131
 – pathway 60, 121
 maribavir 305
 master key concept 102
 Master Library (ML) 99

MEK 273
 – MEK1 77
 – MEK2 51
 Met (mesenchymal-epithelial transition factor) 99, 122
 metabolic stability
 – measurement 37
 5-methylisoxazole flavopiridol derivative 333
 N-methylpiperidinyl-imidazole 283
 4-(4-methyl-piperazin-1-ylmethyl)-N-[4-methyl-3-(4-pyridin-3-ylpyrimidin-2-ylamino)-phenyl]-benzamide 338
 mHOG1, *see* p38 MAP kinase
 Michaelis–Menten constant 10
 Michaelis–Menten equation 13
 Midostaurin/PKC412 126
 mitoxantrone 355
 mixed lineage kinase (MLK) 274
 MK-0457 (VX-680) 118ff., 198, 214ff., 249
 MK5108 128, 249
 ML3163 278
 MLN8054 202, 219, 250
 MLN8237 128
 morin 254
 Motesanib (AMG706) 121
 MPAQ 160ff.
 MRP2 (ABCC2) 36
 Msk kinase 73
 mTOR 48
 multiple target kinase inhibitor 102
 multiplexing 57ff.
 multitargeted drug 97
Mycobacterium tuberculosis 349ff.
 – phosphosignaling networks 349ff.
Mycobacterium tuberculosis STPK 351
 – inhibitor 355
 MyD88 (myeloid differentiation 88) 131

n

NA-PP1 73ff.
 naphthoylamide 169
 NCI-H460 256
 NCT00090987 338
 Neratinib (HKI272) 119
 Nested Chemical LibraryTM (NCL) technology 99
 3DNET4WTM software 99
 NexavarTM 145ff.
 NF- κ B 51, 131f.
 NGIC-I 305
 nilotinib (AMN107, TasignaTM) 118ff., 145ff., 169

NM-PP1 73ff.
 non-ATP binding site-directed kinase inhibitor 101
 non-ATP competitive inhibitor 148
 NPM-Alk 60
 NPV-AEW541 120
 NPV-AFG210 169
 number of rotatable bond (NROT) 180
 NVP-AEG082 177

o

olomoucine 327
 ON 01910.Na 257
 ON012380 50
 oncology
 – cell cycle 231
 OPC-67683 350
 orthogonal ligand 71
 orthogonal receptor pair 71
 OSI-774 18
 oxalylamino-methylene-thiophene sulfonamide (OMTS) 357

p

P-glycoprotein (P-gp, MDR1, ABCB1) 27ff.
 p21-activated kinase (PAK) Cla4 75
 p38 MAP kinase (p38 MAPK, CSPB, mHOG1, SAPK2) 21, 49, 92ff., 123ff., 271ff.
 – first-generation inhibitor 278
 – inhibitor 89, 101, 118, 275
 – medicinal chemistry approach for the inhibition 271ff.
 p38 α MAP kinase (MAPK14) 20, 49, 151ff., 167ff., 271ff., 287ff.
 – inhibitor 124, 164ff.
 p38 β MAP kinase 272
 – inhibitor 293f.
 p38 γ MAP kinase 281
 p38 δ MAP kinase 281
 P276-00 127
 P1446A-05 127
 PA-824 350
 Pamapimod 300
 pan-kinase inhibitor 99
 pan-tyrosine kinase inhibitor 97
 parallel artificial membrane assay (PAMPA) 32
 partition coefficient (P) 30
 passive diffusion 28
 PCI, *see* cyclin-dependent kinase inhibitor
 PD089828 125
 PD166866 125
 PD168393 73
 PD173074 121

- PD173955 236
 PD180970 97
 PD0183812 237
 PD184352 125
 PD0325901 126
 PD0332991 127, 238f.
 PDGF receptor tyrosine kinase family 168
 permeability
 – measurement 31
 personalized therapy
 – kinase inhibitor 96
 PG-1009247 180
 Ph797804 124
 PHA665752 123
 PHA-680626 245ff.
 PHA-680632 198, 215ff., 245ff.
 PHA-739358 128, 198, 215ff.
 pharmacodynamic (PD) parameter 26
 Phe pocket 146
 phenylaminopyrimidine (PAP) 160
 phospho-p38 60
 phosphohistone 60
 phosphorylation network 69ff.
 PI3K (phosphoinositide 3-kinase) 129ff.
 – inhibitor 73, 252
 PI3K/Akt 133
 PI3 kinase/Akt/mTOR pathway 60
 piperidin-4-yl-imidazoles 283
 PKA (cAMP-activated/dependent protein kinase) 58, 71, 92, 233
 PKB (protein kinase B) 129
 PKC (protein kinase C) 126
 – inhibitor 160
 PKC412 126
 PKI166 120
 PknG 133
 platelet-derived growth factor receptor (PDGFR) 118ff.
 – α (PDGFR α) 80
 PLK 250
 polar surface area (PSA) 180
 polo-box domain (PBD) 251ff.
 polo-like kinase (PLK) 250
 – inhibitor 250ff.
 – PLK1 250f.
 – small-molecule inhibitor 252ff.
 Poloxin 259
 poloxipan 259
 PP2 54
 protein function
 – switch off 69
 protein kinase
 – antiviral target 305ff.
 – cellular 305
 protein kinase inhibitor
 – anticancer drug development 231
 – antiviral activity 338
 – classification 148
 – design 231ff.
 – design principles for targeting 145ff.
 – discovery 231ff.
 protein phosphatase
 – drug target 350
 protein tyrosine phosphatase (PTP) 350ff.
 PS540446 124
 PTEN 51
 PTK787 116
 pure peptide binding site inhibitor 101
 purpurogallin 259
 purvalanol 332
 purvalanol A 252
 PX866 129
 pyrazole acetanilide inhibitor 212
 pyrazolo acetanilide quinazolines 208
 pyrazolopyrimidines 179
 pyridinyl-imidazole inhibitor 278
 pyridodiazines 160
 pyridotriazine 160
 pyridylether 160
 pyrimidinoquinazoline 205ff.
 pyrrolopyrimidine 179
- q**
- quantitative structure–activity relationship (QSAR) model 92f.
 – 3D 92
 – prediction-oriented 99f.
 quercetin 254
- r**
- R112 130
 R763 250
 R788/fostamatinib (R935788) 130
 R1487 299
 Rad51 77
 Rad54 77
 B-Raf kinase 151, 168
 C-Raf 168
 RAF-265 172
 RANTES 336
 rapamycin 50
 rational drug design
 – concept 88
 – kinase inhibitor for signal transduction therapy 87ff.
 RDEA119 125

receptor tyrosine kinase (RTK) 145
 receptor–ligand complex 17
 Red1 77
 reporter displacement assay 22
 residence time 15
 retinoid X receptor (RXR) 78
 retrodesign approach 159
 ribofuranosyl benzimidazole 305
 ribose binding pocket 104
 RIP2 kinase (RICK, RIPK2, RIP2) 54, 99
 RO3201195 288ff.
 Ro5126766 125
 Rock II 6ff.
 roscovitine 325ff.
 R-roscovitine 127
 Rsk1, Rsk2 73
 Ruboxistaurin 126
 rule of five 28
 RWJ67657 283f.

S

SB1518 130
 SB202190 123
 SB203580 49ff., 94, 123, 163, 272ff.
 SB210313 282
 SB235699 282f.
 SB242235 123, 283ff.
 SB610677 295
 SB681323 123, 295ff.
 SB856553 (GW-856553X) 295
 SCIO323 124, 294
 SCIO469 124, 293
 SD06 288
 selectivity pocket 146
 seliciclib 127, 326
 Semaxinib (SU5416) 116
 serine/threonine protein kinase (STPK) 350ff.
 – drug target 350
 – function 352
 – mechanism 352
 – substrate 352
 signal transduction therapy
 – rational drug design of kinase inhibitor 87ff.
 SILAC (stable isotope labeling by amino acids) 62f.
 SKF86002 278ff.
 SKI606 123
 small-molecule inhibitor
 – cyclin-dependent kinase 233
 – structure-guided design 233
 small-molecule kinase inhibitor
 – *in vitro* characterization 3ff.

– pharmacokinetic (PK) behaviour 3
 solubility 31
 – measurement 30
 sorafenib (NexavarTM) 15, 49, 115ff., 145ff., 166
 SP006125 355
 SP600125 126
 SprycelTM 118, 145f.
 SR144528 125
 Src 72, 123
 – kinase 92
 staurosporine 252
 STI-571 55, 94, 236ff.
 stress-activated protein kinase 2 (SAPK2), *see* p38 MAP kinase
 structure-based drug design (SBDD) 89
 – 3D 89
 SU5402 121
 SU5416 116
 SU6668 116
 SU11248 115ff.
 SU11271 123
 SU11274 123
 substrate activity screening (SAS) 357f.
 substrate phosphorylation 54
 – level 51
 sunitinib (SU11248, SutentTM) 115ff., 145ff.
 surface plasmon resonance (SPR) 19
 surface-exposed front area 104
 SX011 293
 Syk (spleen tyrosine kinase) 130ff.

T

TAK715 124, 292
 Tandutinib 116
 TarcevaTM (erlotinib) 18, 91, 145ff., 164
 target
 – fishing 97
 – preincubation 22
 – selection 93
 target family-biased master key concept 102
 TassignaTM 145f.
 TG100-115 129
 TG101348 130
 Tie-2 (tunic internal endothelial cell receptor) kinase 151, 163ff.
 TKI258 116ff.
 TMC207 350
 Tozasertib 249
 transporter assay
 – P-gp interaction 33

- transporter protein 28
 triphosphate binding region 104
 tuberculosis (TB) therapeutics 349ff.
 TykerbTM 145f.
 type II inhibitor 79, 148ff.
 – design strategy 155
 – property 184f.
 tyrphostin 101
- u**
- UCN01 (7-hydroxy-staurosporine) 127
 UDP glucuronosyl transferase (UGT) 35ff.
 ultrasensitivity
 – kinase signaling cascade 51
 uridine 5'-diphosphoglucuronic acid
 (UDPGA) 35
- v**
- validation 93
 vandetanib 116ff.
 varicella-zoster virus (VZV) 327ff.
 vatalanib 116, 177
 VEGF (vascular endothelial growth
 factor) 168
 VEGFR (VEGF receptor) 92, 115, 172f.
 viral pathogenesis
 – PCI 337
 VX509 130
 VX680 (MK-0457) 118ff., 198, 214ff., 249
 VX689 (MK5108) 128, 249
 VX702 124, 294
 VX745 124, 294ff.
 VX-745-like compound 297
- w**
- washout experiment 18
 WHI-P97 130
 WO00017175 294
 WO09958502 294
 WO2004072038 294
 WO2006/134382A1 296
 wortmannin 53, 252
- x**
- xenobiotics 36
 XL019 130
 XL147 130
 XL184 123
 XL418 129
 XL518 125
 XL765 130
 XL880 116
- y**
- Y-27632 15
 Yes 99
- z**
- Zactima/ZD6474 116
 ZD-1839 18
 ZK222584 116
 ZM447439 (ZM) 197ff., 249